Are European bioenergy targets achievable? : an evaluation based on thermoeconomic and environmental indicators

Please check the document version of this publication:

Are European Bioenergy Targets Achievable?
An Evaluation Based on Thermoeconomic and Environmental Indicators

PROEFSCHRIFT

ter verkrijging van de graad van doctor aan de
Technische Universiteit Eindhoven, op gezag van de
rector magnificus, prof.dr.ir. C.J. van Duijn, voor een
commissie aangewezen door het College voor
Promoties in het openbaar te verdedigen op
dinsdag 1 maart 2011 om 16.00 uur

door

Anna Sues Caula

geboren te Barcelona, Spanje

Dit proefschrift is goedgekeurd door de promotor:

Prof.dr. H.J. Veringa

Copromotor:

Dr.ir. K.J. Ptasinski

'We are bad engineers because we have too much energy' – Benjamin Franklin

Dedicated to my family,

Table of Contents

Are European Bioenergy Targets Achievable? An Evaluation Based on Thermoeconomic[1] and Environmental Indicators

Summary

Nowadays, it is globally accepted the need of increasing the share of renewable energy to minimize global warming effects. Biomass is a potential alternative to partly fulfill energy demand and policy targets, although unlike solar or wind energy, its availability is limited and stochastically distributed. Hence, the most effective biomass-to-bioenergy route should be selected which, in turn, would lead to more competitive prices with regard to conventional fossil fuels. However, selection of the best conversion technology generates some controversy as the politicians, industry or the scientific community have their own preferences. Another point of discussion is related to the different biomass sources that can be used for energy purposes. In effect, 1st generation biofuels are currently being questioned for using energy crops which may directly compete with food production. Moreover, some life-cycle studies reveal that several 1st generation biofuels exceed the emissions level of fossil fuels. Conversely, 2nd generation biofuels are now being developed as a possible better alternative to benefit from inedible crops, while operating at higher efficiencies in larger conversion plants.

The motivation of this thesis is to determine the best technology to convert biomass into an optimal energy carrier to ultimately determine: (1) *how feasible is to fulfill the different European Energy Policies when using only forestry and straw residues*, (2) *which would be the potential global CO_2 emissions reduction* and (3) *which would be the average biofuels and bioelectricity prices*. In order to answer these major questions, a multidimensional **3E** model is developed, whose main feature is that integrates 3 key factors: **E**fficiency, **E**conomic and **E**nvironmental impacts.

The 3E model is applied to evaluate five different 2nd generation biofuels (*i.e., Synthetic Natural Gas (SNG), methanol, Fischer-Tropsch fuels, hydrogen and bioelectricity*) for their potential implementation in the European Energy market. For that purpose, *forestry* and *straw* wastes availability of EU-25 countries is firstly calculated and allocated within all regions. The five production chains are then modeled in Aspen Plus and Icarus for efficiency (exergy) and economic evaluation respectively, whereas an LCA is carried out to assess the environmental impact. Simulations are performed at different production scales to identify the optimal plant size for each biofuel. A new taxation system is also proposed to assure actual revenues to governments from fuels taxation, while equalizing biofuels and fossil fuels prices. Eventually, ecocosts are proposed to be added on top of taxed fuel prices to penalize fossil-based CO_2 emissions. Evaluation is finally completed by considering the different motivations of policy makers, industry and scientific community. Hence, different scenarios are analyzed, ranging from maximizing biofuels for road transport in short and long-term future (i.e., ICE and FCV vehicles), optimizing SNG production, maximizing the renewable share in electricity production (i.e., new bio-based BIGCC plants or cofiring) and, ultimately, maximizing CO_2 emissions reduction.

Bioelectricity generation turns out to be the best alternative from a thermoeconomic and environmental point of view. About 290 to 461 Mtn fossil-based CO_2 emissions could be saved

---

[1] The term Thermoeconomic is used in the title of the thesis as part of the optimization process is based on energy efficiency (based on Thermodynamics) as well as on economic evaluation.

annually if all European forest and straw residues were used in either cofiring or new BIGCC plants. The corresponding price difference between bioenergy and fossil alternatives are also the lowest for the bioelectricity scenario. Hence, promoting bioelectricity over biofuels production is a better option from a thermoeconomic and environmental point of view. This decision is translated into an annual extra payment across Europe of ~ 7 Billion €, while the figure is increased to 16 - 56 Billion € when biofuels are produced instead. It is also observed that cofiring is preferred over other biofuels production when the aim is to reduce CO_2 emissions. On the other hand, if bioelectricity is summed to solar and wind energy, about **31%** of the electricity production by 2020 could be renewable, i.e., 10% points higher than the target of Directive 2001/77/EC. In case of prioritizing Fischer-Tropsch fuels, the share of biofuels in transport would be **8.0-9.5%,** which is slightly below the **10%** share target of Directive 2009/28/EC. However, this option involves relatively higher capital investments. ***In any case, there is not enough forest and straw residues in Europe to meet the targets of both Directives 2001/77/EC and 2009/28/EC.***

Individual biofuels comparison reveals that SNG and bioelectricity yield the highest exergetic production efficiencies for wood-fuelled plants (i.e., up to 45.5%). This statement is translated into the lowest biofuel prices per output of energy (i.e., 17-20 and 24 €/GJ for SNG and bioelectricity in the Netherlands). However, SNG prices are about 2-times higher than natural gas in most of the European countries, with the exception of Sweden. If the comparison is established per driving distance, bioelectricity is then the cheapest option, mainly due to the expected higher efficiency of battery electric vehicles. Fischer-Tropsch and methanol can be produced at similar end-user prices, which are relatively close to fossil diesel prices including taxes. However, they emit more CO_2 than the other biofuel options. In particular, methanol even releases more CO_2 emissions than fossil diesel in most of the European countries. When the efficiency analysis is extended to a *well-to-wheel* (WTW) perspective (i.e., from biomass collection to final biofuel use in vehicles), the bioelectricity option is again the most efficient route, with energy ratios in the range of actual oil-based systems (i.e., 17-19%). H_2 attains the second best *WTW* efficiencies values (i.e., 14-15%), but it is also the most expensive biofuel per unit of output energy. Moreover, safety concerns about H_2 distribution queries the viability of this biofuel for the long-term future. SNG and Fischer-Tropsch systems attain similar efficiencies (i.e., 9-11%) whereas methanol is the least efficient (i.e., 5-6%).

An important difference with previous studies from other authors is that we have analyzed different biofuels and bioelectricity for their application in the European market by following a common baseline. In effect, most of the studies differ in the scope, system boundaries, local conditions, conversion technology, financial incentives, and/or efficiency definitions even for the same biofuel pathway. Our analysis has also been extended to incorporate all the stages needed to produce bioelectricity or biofuels with the same quality as the fossil homologues, which incurs in extra heat and/or electricity consumption. Inefficiencies related to heat, steam or electricity production are also added to the analyses. This practice, however, is not carried out by many authors. Production plant scales are also different among studies which could lead to an erroneous selection of the best technology. Consequently, we have presented results for the range of 1 to 5000 MW_{fuel} for all bioelectricity and biofuels options. Nevertheless, possibly, the main contribution of this thesis is the analysis of bioenergy production from a multidimensional point of view, instead of separate thermoeconomic or environmental motivations. Moreover we have estimated the maximal bioenergy production from forest and straw residues and not from edible energy crops.

1

Introduction

This chapter introduces the conformity of some governments and the European Commission to promote energy transition towards more sustainable sources. The research project deals with the fact that biomass availability is limited and, thus, the most convenient biofuel or bioelectricity route should be properly selected. In that sense, the feasibility of producing 2nd generation biofuels via gasification is discussed together with the need of developing a multidimensional model that integrates efficiency, economic and environmental aspects. The evaluation is later extended to determine whether European bioenergy targets can be achieved. Finally, the objective and structure of this thesis is outlined.

1.1. *Current global energy scenario*

Existing environmental and economical problems, such as global warming, ozone layer depletion, dependence on countries with oil reserves and future depletion of fossil fuels, prompt governments to search for urgent solutions. This is of crucial importance for a society with limited natural sources but an exponential rate of human population growth and living standards. In the last 20th century, the world human population has increased from 1.65 billion to almost 6 billion in 1999 and it is projected to reach 8.9 billion by 2050. This growth has been accompanied with a significant increase of fossil fuels consumption, i.e., from 299 EJ in 1980 to 509 EJ in 2007[1]. Consequently, more CO_2 has been released to the atmosphere causing global warming and other severe effects. The Energy Information Administration (EIA) estimated that, in 2005, net CO_2 emissions reached 28×10^9 tones and the same EIA expects that CO_2 emission could exceed 42×10^9 tones by 2030 [1]. Another main disadvantage of fossil fuels, particularly oil and gas, is that their exploitation is controlled by few producer countries. Moreover, prices of fossil fuels are difficult to predict. Some factors, including reservoirs depletion, spot market speculation, and strategy of producing nations, play an important role when fixing the price of fossil fuels, especially for the case of crude oil. For the past years, however, the tendency is an irregular increase of crude oil prices. Natural gas and coal reserves are better distributed geographically, and the prices are better regulated at national level.

Some experts have also estimated that oil, natural gas and coal reserves will last for about 40-45, 100-200 and 400 years, respectively, at present consumption rate, although these numbers are continuously questioned by other scientists. Most of the theories dealing with the estimation of oil reserves have set the oil peak in the timeframe of 1995-2016 [2], including the earliest theory of the geophysicist Dr.M.K.Hubbert. He created his first prediction in 1956 in order to forecast the United States' oil peak production between 1965 and 1970. In 1974 he readjusted his own model and estimated that the production peak would arrive around 1995-2000. Later models based on current data and more complex functions are being developed, but the Hubbert curve profile remains unchanged, although the peak timeframe and the slope of the decline differs from model to model. For instance, the latest model of ASPO (Association for the Study of Peak Oil and Gas) places the oil peak in 2005. If heavy oil, deepwater, polar and natural gas liquids are considered then ASPO expects the oil peak for around 2010-2011.

1.2. *Energy scenarios in Europe: short and long term perspectives*

The economic and environmental problems in EU are somehow similar to those at global scale. In the last 20 years, European primary energy consumption (i.e., 91~ EJ in 2006) has only been surpassed by Asia and the United States (i.e., ~ 158 and 105 EJ respectively) [3], as shown in Figure 1.1. EU has the added drawback that it is a net importer of fossil fuels [4], thus, it is highly dependent on the producer countries.
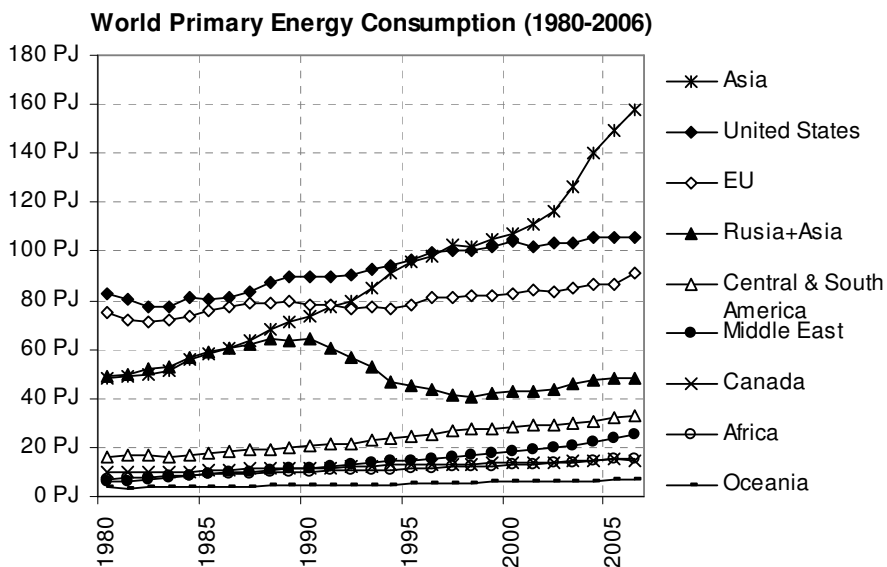
Figure 1.1: *World primary energy consumption in the period 1980-2006. Values have been calculated from U.S. Energy Information Administration agency (EIA) [3].*

This dependency could become even more severe in the coming years as, according to the Mantzos et al prediction, the gross primary energy consumption will increase by 15% between the period of 2000 to 2020 [4]. Similarly, European CO_2 emissions are estimated to raise from 3,671 Mtn/yr in 2000 up to 4,057 Mtn/yr by 2020 [4][2]. Among all sectors, transport and electricity generation account for 30 and 35% of the CO_2 emissions respectively (see Figure 8.15 in Chapter 8) [4]. In order to overcome this situation, the European Commission has launched some Directives with the aim to increase the share of renewable sources in the European Energy market. In particular, 2001/77/EC and 2009/28/EC Directives are addressed to these two most pollutants sectors. Directive 2001/77/EC establishes that renewable electricity should at least achieve 21% of the total power generation in EU-25 countries (or 22.1 % for EU-15). The other Directive 2009/28/EC fixes the biofuels share in transport to reach 5.75% by 2010 and 10% by 2020. Accordingly, Figure 1.2 quantifies the required biofuel and renewable electricity production per country.
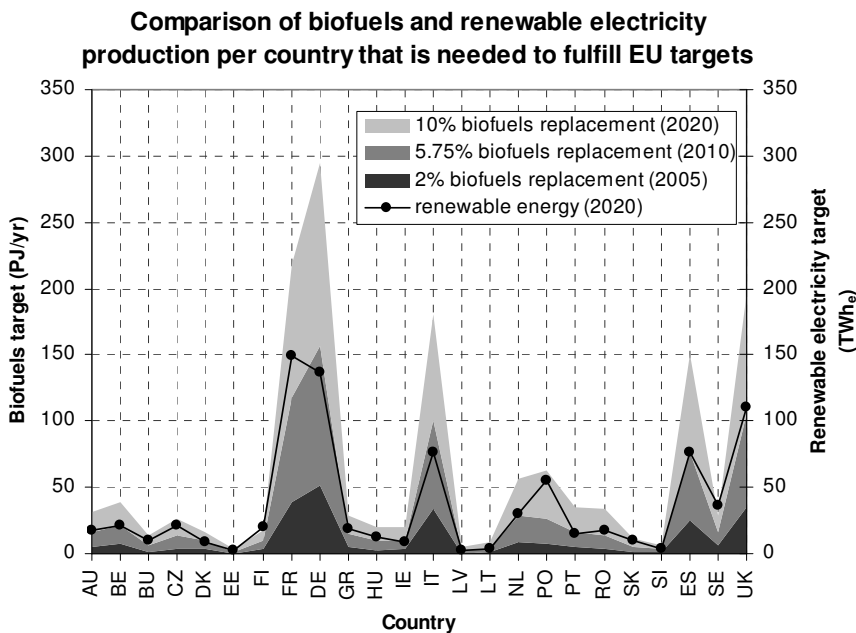
Figure 1.2: European biofuels share target in the road transport sector (i.e., public road transport, private cars and motorcycles, and trucks) and renewable electricity target per country. Values are calculated from Mantzos et al report [4].

Nevertheless, renewable targets for year 2010 will not be achieved under current trends in most of the European countries. In effect, according to *Eurostat database* records [5], in year 2008, Sweden, Germany and Austria were the sole countries that already fulfilled 2010 biofuels' target (i.e., 6.3, 6.5 and 7.1% respectively), as indicated in Figure 1.3. France reached 5.6% whereas the share of the rest of the countries was found in the range of 0.2 to 3.9%. Average EU-27 biofuels share was

---

[2] Those CO_2 emissions account for electricity and steam generation, energy, industry, residential, tertiary and transport sectors.

estimated to be 3.5%. However, all these numbers do not differentiate whether those biofuels are produced following the sustainability criteria of the 2009/28/EC Directive. Concerning renewable electricity generation, more countries would fulfill 2010's targets of the 2001/77/EC Directive [5], being Austria, Sweden and Latvia the leading countries (see Figure 1.4). Average renewable electricity production in 2008 was calculated at 16.6%, which is still below the 21% target.
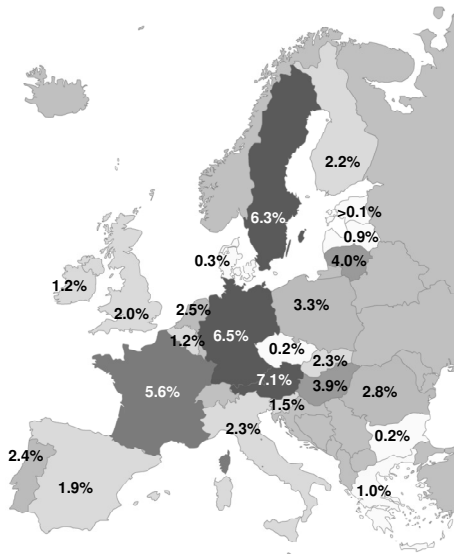
Figure 1.3: *Biofuels share in transport in 2008 It includes biodiesel, bioethanol and Fischer-Tropsch fuels production.*
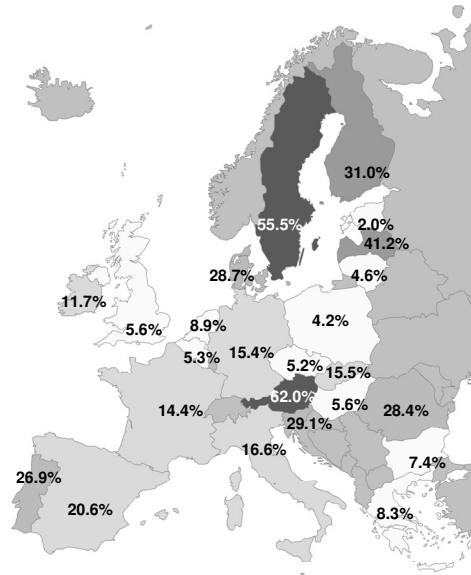
Figure 1.4: *Renewable electricity generation in 2008. It includes hydropower, solar, wind, biomass, hydropower and geothermal sources.*

Although electricity can also be produced from other renewable alternatives (such as hydropower, geothermal, solar or wind energy), biomass is the only available renewable option to produce transport biofuels for *conventional internal combustion engines* (ICE) or more recent *fuel cell vehicles* (FCV). Nevertheless, biomass is still primarily used for bioelectricity or heating purposes rather than for biofuels production. The European Biomass Association (AEBIOM) estimated that, in 2006, bioelectricity generation from solid biomass, biogas and the biodegradable fraction of municipal wastes (MSW) was 89.8 TWh$_e$ (i.e., 0.32 EJ) [6]. Corresponding values for liquid biofuels production were found to reach 0.23 EJ [6]. Assuming that current efficiency of bioelectricity and biofuels plants are in the range of 45-50% [7] and 33-43% [8, 9] respectively, biomass consumption is calculated in the range of 0.75-0.98 EJ and 0.47-0.51 EJ for bioelectricity and biofuels production respectively. Same AEBIOM association claims that there is still a high potential of unused biomass. In effect, according to their figures, European unused biomass potential would be in the range of ~10 % (for Latvia) to ~80% (for Poland or Lithuania) [6]. Denmark and the Netherlands would be on the opposite side, as they are net importers of biomass (i.e., -4%) [6].

1.3. *First versus Second generation technologies*

In general, several biomass streams can be used for energy purposes (e.g., woody materials, agricultural residues, manure, sludge or even municipal solid wastes (MSW)) although not all of them are technically or economically feasible options yet. Alternatively, some companies are also growing edible energy crops (such as rapeseed seed, sugar cane or wheat) or lignocellulosic crops (e.g., miscanthus or poplar) to achieve higher biomass productivity per hectare. Depending on the origin of the biomass source, biofuels are classified in two major groups: the so-called first and second generation technologies (see Figure 1.5).
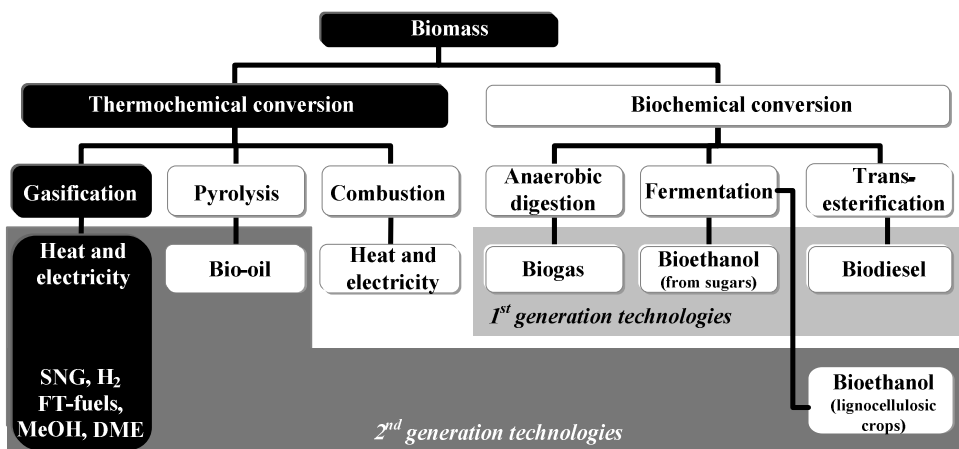
Figure 1.5: *General overview of main 1ˢᵗ and 2ⁿᵈgeneration technologies.*

First generation biofuels are characterized by using sugars or vegetable oils from dedicated edible crops and converting them by biochemical methods. This is the case of bioethanol produced by fermentation, or biodiesel produced from chemical transesterification of vegetable oils. Several 1ˢᵗ generation plants are already operating at commercial scales. In 2006, the global production of bioethanol and biodiesel achieved 39.5 and 5.4 million tones respectively, with Europe covering 10% and 63% of the world's bioethanol and biodiesel supply [6]. However, some life cycle studies reveal that first-generation biofuels frequently exceed the emissions levels of fossil fuels. Moreover, in demographically dense regions like Europe, land is scarce and biofuels can become a competitor for food production.

In order to overcome problems related to land competition as well as mitigate environmental impacts, alternative technologies are now being developed. This is the case of the so-called 2ⁿᵈ generation biofuels that use non-edible feedstock such as lignocellulosic crops or biowastes from different sources (e.g., forest, agriculture, industry or municipalities). In this case, the whole crop (and not only grains) or residues are consumed for biofuels production, which improves land area productivity and reduces GHG's emissions [7]. Moreover, plant production scales are projected to be larger, thus reducing production costs.

Cellulosic bioethanol is obtained in a similar way as bioethanol produced from sugars, but hydrolysis and saccharification steps are needed to convert lignocellulosic materials into a more convenient feedstock for alcoholic fermentation. Hence, the overall process is more complex and energy intensive. Plant capacities are expected to be in the range of 5–110 MW$_{fuel}$ with an overall efficiency of about 45-50% [7].

Alternatively, biofuels can also be produced by thermochemical conversion as shown in Figure 1.5. Among all, *Gasification* is gaining more interest as it offers higher efficiencies compared to combustion, whereas fast pyrolysis is still at a relatively early stage of development [10]. Gasification is a thermal process that converts organic feedstock into a mixture of gases (syngas) using a limited amount of an oxidizing medium. The resulting syngas mainly consists of CO and H$_2$, but other gases can also be present (e.g., CH$_4$, CO$_2$, C$_2$H$_4$, or C$_2$H$_6$). Gasifiers have the added advantage that they can process a wider range of biowastes than biochemical methods, including more heterogeneous and polluted streams like MSW. Moreover, when coupled to downstream catalytic reactors, a wider range of biofuels can also be produced (e.g., *Synthetic Natural Gas* (*SNG*), *methanol*, *Fischer-Tropsch fuels*, *H$_2$*, *DME* or also *bioethanol*). Those biofuels also have better qualities for the transport sector than biochemical-derived fuels (see Table 1-1).

Table 1-1: *Properties of biochemically and thermochemically produced biofuels. Values are also compared with fossil diesel and gasoline. Thermochemical-based biofuels have higher octane and cetane numbers, which is preferable when blending with gasoline or diesel.*

Technology	Fuel	Specific gravity	LHV (MJ/Kg)	Octane number	Cetane number
Biochemical conversion	Bioethanol	0.79	27.0	109	-
	Biodiesel	0.89	37.0	-	55
	Buthanol	0.81	36.0	96-105	-
Thermochemical conversion	Mixed Alcohols	**0.8**	**27-36**	**96-109**	**-**
	Methane (SNG)	**0.42**	**49.5**	**>120**	**-**
	Methanol	**~0.80**	**20.1**	**109**	**-**
	Fischer-Tropsch	**0.77**	**43.9**	**-**	**74.6**
	Hydrogen	**0.07**	**120.0**	**>130**	**-**
	DME	**0.66**	**28.9**	**-**	**>55**
Petroleum refineries	Gasoline	0.72-0.78	43.5	91-100	-
	Diesel	0.85	45.0	-	37-56

However, one of the main disadvantages of gasification is the formation of tars. In general, tars are defined as being a complex mixture of condensable hydrocarbons. When consended, tars can cause obstruction problems in equipments or pipelines, as well as a lost of material. Tars can be removed from the product syngas by either chemical or physical methods. In chemical methods tars are decomposed to smaller molecules. Examples of chemical methods are catalytic cracking, thermal cracking, plasma reactors and catalytic bed materials. Among them, catalytic cracking has the advantage that the heating value of the tars is conserved and converted to other gases [11]. Calcinated dolomite and nickel-based catalyst are commonly used for this purpose. Conversely, physical methods completely remove the tars from the syngas but a new notably-polluted waste stream is then generated. Typical physical devices

are cyclones, filters, electrostatics precipitators and scrubbers. Energy research Centre of the Netherlands (ECN) has also developed a new technology for tars removal, based on syngas scrubbing with oil. The principle is similar to a physical tar removal method but in this case, tars can be recycled back to the gasifier and destructed herein, which in turn, avoids the problematic handling of waste streams [12].

Another major issue for the massive introduction of biofuels into the energy market is the adaptation of current infrastructures. Bioethanol, biodiesel and methanol are blended with fossil fuels in conventional vehicles, but the mixture is limited to certain degree if the engine is not modified. Conversely, Fischer-Tropsch diesel has the same quality than fossil diesel and, hence, it can fuel actual cars without any limitation. Methanol-powered FCV vehicles are also being developed as an alternative to methanol/gasoline blend up to 85% (M85) in actual cars. However, the relatively low efficiency and high capital costs of methanol-fuelled FCV are the two major barriers for their success. Bioelectricity is also seen as an alternative transport fuel in the coming years. *Battery electric vehicles* (BEV) are now under development and they are expected to yield the highest cycle efficiency (i.e., up to 48-60% versus 15-20% for conventional ICE engines. This option involves that electrical charging points should be conveniently spread over municipalities and motorways to assure certain autonomy. Concerning gaseous biofuels, SNG can be used in actual *compressed natural gas* cars (CNG) with prior compression for storage up to ~ 250 bar. Nevertheless, existing gas pipeline would probably need to be enlarged if SNG production is increased to meet the targets of the Directive 2009/28/EC. Similarly, hydrogen pipeline would also need some extension, although the investment costs would be notably higher than those of natural gas pipeline works. Hydrogen has the added drawback that FCV are not economically competitive yet. Examples of initiatives and existing 2nd generation plants in Europe are depicted in Figure 1.6.

1.4. *How sustainable is to produce bioenergy? The need of a multidimensional evaluation model*

There are several challenges for the development and implementation of biofuels in the energy market. Firstly, existing technologies must be adapted and improved to process biomass sources in a more efficient way. In comparison with most of the fossil fuels, biomass has a lower energy density, it is more difficult to grind and its hygroscopic nature hinders the storage. Hence, pre-treatments stages (e.g., drying, size reduction, torrefaction and/or pelletization) are frequently required to facilitate biomass handling and storage, as well as to reduce logistics costs.

On the other hand, there is a wide range of biomass sources that can be converted to a broad range of biofuels with different composition, properties and functionalities. Hence, an additional challenge is to select the most convenient biomass-to-bioenergy conversion technology. Thirdly, biofuels or bioelectricity implementation has to be efficient and sustainable as well. Consequently, an inherent challenge is to develop a reliable model to evaluate the sustainability of any process from thermoeconomic and environmental point of view.

Norrsundet, 1990
Promotor: FosterWheeler Energia Oy
Process : Wood gasification for heat production
Output: 20 MW_{th}
Efficiency: 31% heat

Lahti Plant, 1998
Promotor: FosterWheeler Energia Oy
Process : Coal and biomass gasification
Output: 167 MW_{el} and 240 MW_{th}
Efficiency: 31% electricity and 49% heat

Varkaus, 2000
Promotor: FosterWheeler Energia Oy
Process : Wood and MSW gasification
Output: 40 MW_{th}
Efficiency: n.a

Rudersdof Cement, 2000
Promotor: Lurgi Technology
Process : wood gasification for heat production
Output: 80 MW_{th}
Efficiency: n.a.

Freiberg Plant, 2003
Promotor: CHOREN Industries
Process : Wood gasification for FT-fuels production
Output: 25 kton/yr fuels (betaplant 2007)
200 kton/yr fuels (sigmaplant 2009)
Efficiency: n.a

Güssing Plant, 2001
Promotor: Public institutions
Process : Wood gasification for SNG, FT-fuels, heat and electricity production
Output: 2 MW_{el}, 4.5 MW_{th}, 1 MW_{SNG}, >0.5 MW_{FT}
Efficiency: 25% Electricity & 56% Heat

BIGCC Varnamo Plant, 1999
Promotor: Sydkkraft AB & FosterWheeler
Process : The BIGCC plant has been rebuilt to produce other biofuels.
Output: 6 MW_{el} and 9 MW_{th}
Efficiency: 32% electricity and 51% heat

GoBiGas project, 2006
Promotor: Göteborg Energi's and E.ON
Process : Wood gasification for SNG production
Output: projected 20 MW_{gas}
Efficiency: n.a.

Carbona CHP Plant, 2006
Promotor: Carbona
Process : Wood gasification for heat and electricity production
Output: 5.5 MW_{el} and 11.5 MW_{th}
Efficiency: ~ 30% electricity and 50% heat

Milena Project in Petten, 2001
Promotor: ECN (Energy Research Center)
Process : Wood gasification for SNG production
Output: pilot plant
Efficiency 60-70%

Lausitz, 1995
Promotor: SVZSchwarze Pumpe GmbH
Process : Biomass gasification for methanol, electricity and heat production
Output: 75 MW_{el} and 120 kton/yr of methanol
Efficiency 35%

Greve in Chianti Plant, 1993
Promotor: TPSTermiska Processer
Process : Wood gasification for electricity production
Output: 7 MW_{el}
Efficiency 20%

Figure 1.6: *Overview of some initiatives and existing 2nd generation bioenergy plants in EU.*

A proper model should determine whether biofuels are more beneficial than fossil fuels or other forms of renewable energy. However, sustainability methods are not standardized yet and many of them lack some key factors such as *efficiency*, *economic* and *environmental impacts*. This is the case of the so-called *unidimensional accounting methods* that measure the impact of each factor separately (e.g., *energy* or *exergy analysis*, *Life Cycle Analysis* (LCA) or *Life Cycle Cost* (LCC)). More recently, *multidimensional methods* are considered to be more accurate as they intend to integrate the effect of each factor. In effect, increasing the efficiency of the process has also some benefits on the economic and environmental impact of the conversion route. However, demanding efficiency targets can be translated into extremely high costs, thus, making the process impractical. In any case, conversion factors are needed to integrate parameters with different measuring units. For instance, environmental impact is measured in ppm (or gCO_2eq/MJ for the case of global warming evaluation), production costs are given in $€/GJ_{biofuel}$, and efficiency is commonly calculated as the ratio of energy output divided by the energy input (e.g.., MW_{output}/MW_{input}).

Multidimensional accounting methods such as *Cumulative Exergy Consumption* (CExC) and *Exergetic Life Cycle Analysis* (ELCA) take into account the exergy consumption of the whole production chain, analogous to the LCA for the environmental impact assessment [13, 14]. However, both methods exclude an economic evaluation and decisions are primarily based on efficiency improvement. Alternatively, *Thermo-economics* and *Exergoeconomics* methodologies combine technical and economical aspects but they omit an environmental assessment [15, 16]. More recent *Extended Exergy Accounting* (EEA) method of Sciubba is the only one that combines the three proposed *efficiency*, *environmental impact* and *economic* indicators [17]. In this EEA method, four different exergy sources are indentified in the system and summed up (i.e., feedstock, capital, labor and environmental remediation exergy). Nevertheless, its main limitation is that arbitrary conversion factors are used to translate monetary flows (i.e., capital and labor components) into exergetic flows.

1.5. *Research objectives*

The goal of the research project is dual. Firstly, the creation of a multidimensional model that could be used to assess how sustainable is to produce 2nd generation biofuels in a specific region or country and at any scale. Unlike the previously mentioned methods, this new multidimensional model integrates 3 key parameters for a more accurate evaluation, i.e., efficiency, economic and environmental impact analysis. Secondly, the model is applied to predict the feasibility of producing and implementing different biofuels (i.e., SNG, methanol, Fischer-Tropsch fuels and H_2) or bioelectricity[3] in Europe. The outcome of this analysis gives an overview of which countries are more promising in terms of production and distribution costs as well as CO_2 emissions reduction. Moreover, the accomplishment of the European Energy Policy (i.e., 20% share of renewable energy by 2020) is also discussed. Figure 1.7 depicts the extensive number of combinations that have been analyzed in this thesis to support our conclusions.

---

[3] In this thesis, bioelectricity is often considered as a biofuel when it is to be used in transport.
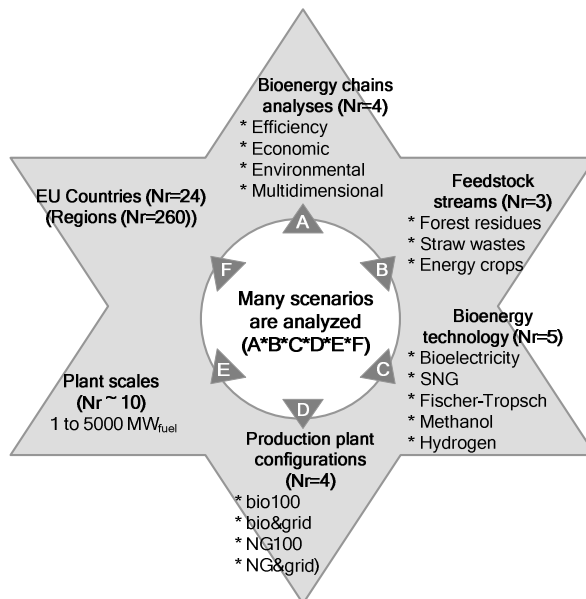
Figure 1.7: *Overview of the number of scenarios (combinations) that have been analyzed.*

It should be mentioned that the initial goal of the project was focused on drawing a *Master Bioenergy* plan for the Dutch province of Friesland. However, we realized that biomass availability in this region is rather limited and, thus, the relatively small scale of the potential new production plants will lead to expensive biofuels or bioelectricity 'end-user' prices. In that sense, borders have been extended to 24 European countries, for which different plant scales have been analyzed. In any case, if Friesland were to import biomass from nearby regions, similar conclusions would be obtained as for the Netherlands country.

1.6. *Outline of the thesis*

The rest of the Chapters of this thesis follow the methodology used to build our multidimensional model. Accordingly, *Chapter 2* is devoted to introduce biomass availability in Europe, its distribution across the different regions and its composition. Different biomass streams are analyzed, and forest and straw residues are selected as potential alternatives for thermochemical conversion technologies. The feasibility of converting lignocellulosic energy crops will be also studied in parallel in following chapters but their real availability is still questioned. This section also includes the calculations of logistics costs for biomass transportation to the processing plants.

Subsequent *Chapter 3* deals with the design of the whole biomass-to-bioenergy conversion routes (i.e., from biomass collection to final biofuel application). The simulation of the processing plants is explained in detail together with the state-of-the art of the most relevant 2nd generation technologies in Europe. Biomass cofiring in existing coal-based power stations is also presented as an option for renewable electricity generation. Mass and energy balances from Aspen Plus simulations are used in *Chapter 4* to calculate the efficiency of biomass-to-bioenergy conversion

plants from an energetic and exergetic point of view. The analysis is further extended to determine the efficiency of the whole biomass-to-bioenergy chains, thus following a *Well-to-Wheel* approach. Plant production capacities are also varied in the range of 1 – 5,000 MW$_{fuel}$ to identify optimal scales. Nevertheless, these values will be confronted in subsequent chapters to verify whether optimal 'energetic' scales correspond to optimal 'economic' or 'environmental' scales.

A *Life Cycle Analysis* (LCA) methodology is applied in ***Chapter 5*** to quantify all emissions from the different bioenergy chains. For that purpose, we have selected the most common environmental indicators, i.e., *global warming potential*, *acidification*, *eutrophication*, *summer* and *winter smog*, *carciogenesis* and *ecotoxicity*. Results are compared with a reference fossil scenario (i.e., coal-based power generation and fossil diesel use in transport) in order to calculate the potential emissions savings. A sensitivity analysis is also performed to identify the more polluting stages.

In ***Chapter 6***, mass and energy balances from Aspen Plus simulations are exported to Aspen Icarus to calculate biofuels and bioelectricity '*ex-work*' prices. In order to get the final '*end-user*' prices, logistics costs from Chapter 2 and distribution costs are added at this stage. A sensitivity analysis is also conducted in this section to underline the factors that notably influence final prices. The gap difference between biofuels and fossil fuel prices is finally addressed by defining a new taxation system. Its goal is to equalize biofuels and fossil fuel prices while maintaining governments' revenues from fuels taxes. Subsequently, '*virtual ecocosts'* are proposed to be added on top of fuel prices to penalize CO_2 emissions.

Results from previous chapter are combined in ***Chapter 7*** to build an own ***multidimensional 3E*** model. A parallelism is also established with methods from other authors. Efficiency, economic and environmental factors are integrated to be able to better select the most convenient technology. This chapter is also accompanied with an excel program (*Multi_model.xls*) that can be used to evaluate bioenergy production in any region, from thermoeconomic and environmental perspectives.

In ***Chapter 8*** the multidimensional model is applied at European scale. Results show the potential biofuel replacement in transport when all available forest and straw residues are converted. This value is confronted with the '10%' replacement target that has been fixed by the European Commission in the Directive 2009/28/EC. Another scenario is focused on maximizing renewable electricity generation by either building new biomass-fuelled BIGCC plants or cofiring. In this case, the Directive 2001/77/EC is taken as a reference, for which 21% of the European electricity should originate from renewable sources. The rest of scenarios maximize SNG, H_2 or methanol production, or combine their production with cofiring practices. The chapter continues with the computation of annual CO_2 savings due to fossil fuels replacement. Final 'end-user' biofuels and fossil prices are also quantified for each scenario together with the total capital investment that would be needed to built all European biomass plants. The application of the ***multidimensional 3E*** model (Chapter 7) ends with the calculation of the '*virtual ecocosts*' to be added on top of fuels prices. Hence, these '*virtual ecocosts*' are somehow the integration of *efficiency*, *economic* and *environmental* impact results. Finally, the main conclusions of this thesis are presented in ***Chapter 9*** together with the recommendations for future work.

2

Review of potential biowastes availability for energy production in Europe

Abstract

Biomass comprises a wide range of materials ranging from woody streams, agricultural residues, green wastes, manure or energy crops. However, not all sorts of biomass sources are suitable for energy production due to their limited accessibility, technological barriers, or economic constraints. The aim of this chapter is to assess the potential availability and delivery costs of the European biowastes for their introduction in the European Energy market. Among all biowastes, woody materials and straw residues are preferred as their low moisture and ash content make these streams especially suitable for downstream thermochemical conversion. Several studies at European level claim that the potential availability of woody and straw residues are in the range of 0.6-2.2 and 1.4-3.4 EJ/yr respectively, whereas their delivery costs are estimated at 0.5-3.8 and 0.8-3.9 €/GJ. However, no distinction is made between availability and contractability as the ratio of both is ultimately determined by politics, economic development or other factors.

2.1. *Introduction*

Biomass is a wide term that refers to all organic matter that derives from the photosynthetic conversion of solar energy, although it also includes other biodegradable materials such as manure and sewage sludge. The term excludes embedded materials in geological formations which have been later transformed into fossils fuels. About 115-120 billion tones of biomass is formed each year by means of photosynthesis in continental ecosystems [18, 19]. This would represent around fivefold of the total energy consumption worldwide (i.e., 400 EJ in 1998 [1]) in the unlike scenario that all biomass sources were converted to energy. Currently, biomass covers less than 14% of the global energy demand, *the majority of which being low grade used*, [20, 21] but some governmental policies have set higher values for the

near future, including European Union, 29 U.S. states and 9 Canadian provinces. The majority of these targets refer to shares of electricity production, primary and/or final energy use in the timeframe of 2005–2020. However, most targets are still far from being achieved in the short term.

In order to predict how feasible will be to fulfill renewable energy policies for near and long-term future, it is particularly important to assess the potential availability of biomass for energy purposes. However, there is some controversy over the origin and exact amount of biomass sources. For instance, non-energy purposes such as food production, technological barriers or need of biomass exploitation at competitive prices bring extra pressure on biomass supply for energy uses. Moreover, unlike solar and wind energy, biomass is normally owned by individuals or holdings, which ultimately decide its final application. In this chapter, biomass availability, quality as well as delivery costs are discussed to select the most suitable feedstock for later production of biofuels and electricity via gasification.

2.2. *Classification and selection of biomass sources for thermochemical conversion*

Biomass resources can be divided into several categories. In the European norm CEN/TC-335, solid biofuels are divided on 4 categories according to their source, i.e., (1) woody biomass, (2) herbaceous biomass, (3) fruit biomass and (4) blends and mixtures. However, this classification does not indicate the origin of the biomass and, hence, it becomes more complex to identify the potential biomass availability in the different economic sectors. Consequently, biomass sources have been re-classified in Table 2-1 under 4 key market sectors, i.e, (A) forest, (B) agriculture and farming, (C) industry and (D) municipalities.

The first group of biomass sources comprises woody streams originated in forests and other wooded land. In this group, two sources of forestry biomass can be retrieved for later energy production. The first subdivision (A.1.1) corresponds to the so-called "*complementary fellings*", which describe the difference between the maximum sustainable harvest level and the actual harvest level needed to satisfy the demand of the round wood industry. The second division of forestry products is further divided into (A.2.1) "*felling residues*" and (A.2.2) "*wood processing residues*". Felling residues comprises the woody materials that are normally left in forests after harvesting operations, including stem tops and stumps, branches, foliage and roots. A fraction of those felling residues stays in the forests in order to protect their biodiversity, whereas the remaining part is seen nowadays as an opportunity for the energy sector. Wood processing residues such as sawdust and bark derive from the wood industry, but unlike the other aforementioned woody sources, their availability and costs is subjected to market fluctuations and, hence, they will not be considered for later calculations. The second group of biomass sources is originated in agricultural and farming activities. In this category, (B.1) "*energy crops*" are often considered as an independent group from agricultural residues such as (B.2) "*crop residues*" and (B.3) "*livestocks wastes*"[22, 23].

Table 2-1: Solid biomass classification for energy production. In grey are market those streams that will be analyzed for later conversion into 2nd generation biofuels and electricity. Fractions of each category are calculated from average values found in literature.

Sector	Resource	Fuel category	Description	EJ/yr
(A) Forest	(A.1)Woodfuel	(A.1.1) **Complementary fellings** from forests	Sustainable exploitation of forests	0.60-2.20[a]
	(A.2) Forestry residues	(A.2.1) **Fellings residues** (i.e., primary residues)	Residues from harvesting and logging activities	
		(A.2.2) **Wood processing residues**	Residues from wood industries (e.g. sawdust)	0.07
(B)Agriculture and Farming	(B.1)Energy crops	(B.1.1) Woody energy crops	e.g., Short rotation crops[b]	0.80-12.0
		(B.1.2) Herbaceus energy crops	e.g., sugar cane, corn	
	(B.2) Crops residues	(B.2.1) Wet crop residues	e.g., greentops from potatoes and beets	n.a.
		(B.2.2) Dry crops residues	**e.g.,straw and prunings**	0.5-3.8[a]
	(B.3)Livestock	(B.3.1) Manure	Organic waste fraction	0.65
(C) Industry	(C.1) Food and beverages industries residues		Organic waste fraction	n.a.
	(C.2) Residues from furniture manufacturing		Excluding forest industry	0.60
(D) Municipality	(D.1) Municipal solid wastes (MSW)		Excluded organic fraction	2.91
	(D.2) Construction and demolition wood		Off-cuts from building construction / demolition	0.25
	(D.3) Parks and gardens residues		Urban wood and cut grass	n.a.
	(D.4) Sewage sludge		Sludge from industries and municipalities	0.21

(a) In later calculations, we use average values of 1.9 and 1.8 EJ/yr for forest and straw wastes.
(b) Lignocellulosic energy crops are studied in parallel, although its real availability is unkown.

In our research, edible energy crops (B.1.2) are disregarded as in demographically dense regions such as Europe, land is scarce and these crops are often questioned for their possible competition with food production. Lignocellulosic energy crops (B.1.1) are studied in parallel to assess its feasibility in regions where biowastes are limited. Wet streams such as (B.2.1) "*wet crop residues*" and (B.3.1) "*manure*" have been also excluded from our analyses as they are predominantly used nowadays for biogas production or composting. In addition, their relatively high moisture and ash content make both streams unsuitable for alternative thermal conversion [24]. The third and fourth subdivision of biomass sources are residues coming from industry and municipalities. Efficiency analyses conducted at the Environmental Energy group at Eindhoven University of Technology have shown that (D.1) "*municipal solid wastes (MSW)*" attains a reasonable energy efficiency when compared to other dry streams like woody and agricultural residues[24]. However, MSW have been finally excluded for later analyses as they are more prone to be reduced in existing landfill and incineration facilities with electricity as by-product. Other residues from municipalities and industries have not been considered either as it has been rather difficult to predict realistic quantities of each material in the different European countries. Green residues from parks and gardens (D.3) have the added disadvantage that their high content in alkalynes could damage the gasifier or other downstream equipments. Apart from their origin, biomass sources have been also analyzed and

classified based on their differences on chemical compositions, heating values, ash and moisture contents. Accessible databases such as Phyllis [25] and EERE (U.S. Department of Energy's Office of Energy Efficiency and Renewable Energy [26]) have listed the composition and properties of many biomass feedstock. Comparison of these biosources reveals that higher heating values moderately vary (standard deviation of 13%), but a larger variation is observed for moisture and ash content (standard deviation of 33% and 55% respectively). Similar trends are observed when comparing larger sources of materials [27]. Since dry streams are preferred for thermal conversion (i.e., the overall energy efficiency is negatively affected by the energy required to evaporate the moisture content of the fresh inlet biowaste), *"complementary fellings"* and *"felling residues"* from the forest ((A.1.1) and (A.2.1)), *"lignocellulosic energy crops"* (B.1.1), as well as *"straw and prunings"* from agricultural residues (B.2.2) are confirmed as the preferred materials for later conversion to 2nd generation biofuels and bioelectricity.

2.3. *Composition of forestry and straw residues*

The ultimate and proximate analysis of the selected woody biomass ((A.1.1), (A.2.1) and (B.1.1)), and lignocellulosic agricultural wastes (B.2.2) is given in Table 2-2. As observed, both streams have a considerable low moisture content which is especially preferred for thermochemical conversion technologies such as gasification. However, straw residues have slightly higher contents of chlorine, sulphur and ash, and hence, it will require more intensive cleaning steps than woody materials. Moreover, the lower density of straw will imply higher costs in the pre-treatment section and logistics.

Table 2-2: Ultimate, proximate analysis of forest and agricultural wastes. Composition values are given in a dry basis (d.b. %).

	Forest biomass[a]	Straw residues
Ultimate analysis		
C (d.b.%)	49.04	45.18
H (d.b.%)	5.74	5.54
N (d.b.%)	1.61	0.84
Cl (d.b.%)	0.10	0.45
S (d.b.%)	0.08	0.15
O (d.b.%)	39.41	40.35
Proximate analysis		
Moisture (w.b.%)	13.80	14.40
Fixed carbon (d.b.%)	19.48	16.86
Volatile matter (d.b.%)	76.50	75.64
Ash (d.b.%)	4.02	7.49
Calorific content and density		
HHV (MJ/kg) (in d.b.)	19.354	17.882
Density (kg/m^3) (in d.b.)	**Average: 420**	**Average: 100**

(a) We assume that lignocellulosic energy crops have a similar composition to forest wastes.

2.4. *Availability of forestry and straw residues in European countries*

Several authors have calculated the potential availability of forestry biomass [22, 28-33] and agricultural wastes [22, 28, 29, 33, 34] for energy purposes. In the following sections, those studies are analyzed and compared, and a final reference value is selected for both biomass streams. These values will be needed in later sustainability analyses to determine how feasible is to fulfill European bioenergy targets, and at which price and environmental cost it could be done (see Chapter 8).

2.4.1.   *Potential Woody residues availability in Europe*

In our calculations, woody residues from forest are assumed to remain constant for the next 20 years, as unlike other regions on the world, were deforestation is proceeding at a rapid pace, European forests are steadily increasing by 0.1% per year [35]. Reference values for forestry biomass availability are taken from the report of the Environmental Energy Agency (EEA)[22] due to its clear definition about the different wood fractions for energy production. Analogous to our classification in Table 2-1, forestry sources in the EEA report are composed of "*complementary fellings*" and "*fellings residues*". *Demolition wood*, a fraction that notably varies with the situation of the building sector, is not taken into account, which is in accordance with our postulates (see subchapter 2.2). The corresponding values of forestry biomass in 24 EU countries (i.e., from France to Belgium) is shown in Figure 2.1 (grey bar) and compared with data from other studies [28-33]. Data for Bulgaria, Greece and Romania are not available in the EEA report and, hence, values from Nikolaou et al [29] are taken instead. Luxembourg is excluded from our analyses due to its relatively small biomass contribution.
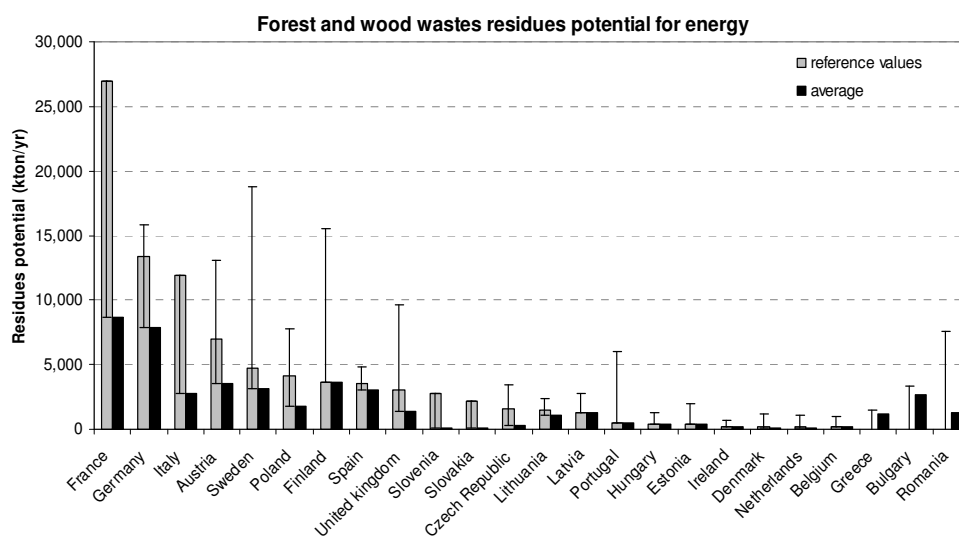
Figure 2.1: *Forest biomass availability in Europe for energy production. Reference values are taken from [22], whereas average and ranges are calculated from [28-32].*

As observed, major differences are observed for countries with largest biomass potential (e.g., France, Italy, Nordic countries, Austria, United Kingdom) but also smaller states like Portugal and Romania show certain divergences. One of the possible explanations could be found in the different definitions of forestry sources for energy production (see Figure 2.2). As shown, in EEA [22] and Asikainen et al reports [31], "*complementary fellings*" (A.1.1) and "*harvesting residues*" (A.2.1) are considered as potential forestry sources for energy production. However, although their definition is similar, the corresponding amounts are notably different for five of the largest biomass suppliers (i.e., France, Sweden, Finland, Italy and Austria). For the case of Sweden and Finland, EEA [22] study presents more conservative values for both categories (i.e., "*complementary fellings*" (A.1.1) and "*harvesting residues*" (A.2.1)), as it considers the over-explotation of Nordic forests by the pulp and paper industry, whereas in Asikainen et al scenario [31] is not clear if that factor has been reflected. Conversely, EEA [22] states that a higher fraction of "*complementary fellings*" can be exploited in France, Austria, and Italy.

Reference	Complementary fellings (A.1.1)	Harvesting residues (A.2.1)	Processing residues (A.2.2)	Woodfuels (e.g., pellets)	Others (e.g., furniture)
EEA	✔	✔	✘	✘	
Siemons	✘	✔	✘	✔	
Nikolaou	✘	✔	✘	✔	
Eubionet	✘	✔	✔	✔	
Asikainen	✔	✔	✘	✘	
Wakker	✔	✔	✔ *	✘	
Kunikowski	✘	✔	✘	✘	
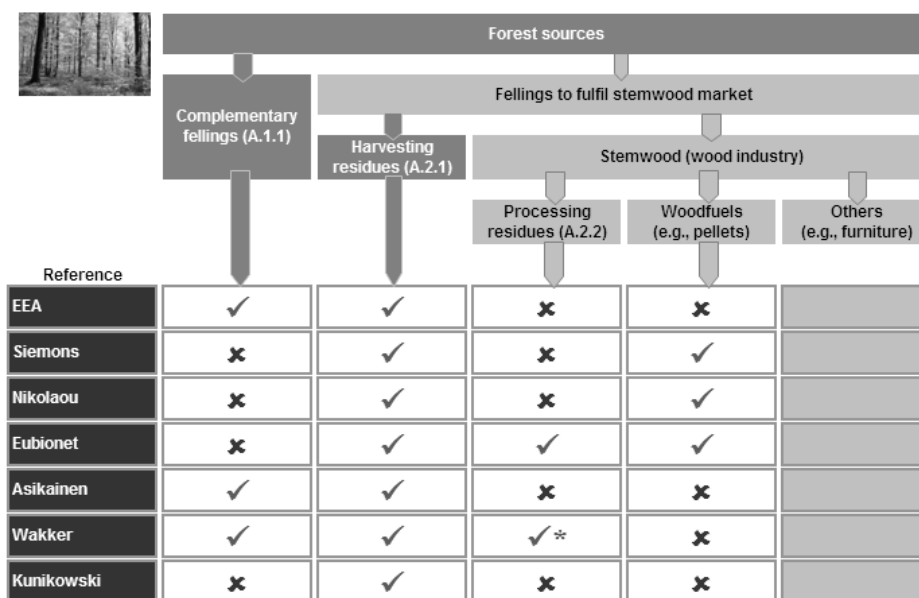
Figure 2.2: Interpretation of available forestry sources for energy uses in different studies. The sign (✔) means that the fraction was included, whereas (✘) indicates that it was excluded.

In accordance with our classification in Table 2-1, Wakker et al [32] have calculated forestry residues as the combination of "*whole-tree chips*" and "*logging residues chips*" which, in turn, could be assimilated to our definitions of "*complementary fellings*" (A.1.1) and "*harvesting residues*" (A.2.1). In addition, they have also presented separate values for the "*wood processing residues*" (A.2.2), but this category has not been included in our comparison of Figure 2.1. When comparing results between Wakker et al [32] and EEA reports [22], major differences are again found in the larger suppliers such as France, Austria and Italy, but also Germany and Poland are listed with notable discrepancies. On the contrary, Nordic countries

reported similar data. Those variations can be again explained by the diverse "*complementary fellings*" definition used in both studies. The rest of studies [28-30, 33] presented in Figure 2.2 state different woody sources for energy production and, hence, more divergences are expected even for smaller states. In the last report from Kunikoski et al [33], reported values are generally lower (except for Nordic countries) as only "*harvesting residues*" are summed up, without any consideration for either "*complementary fellings*" or "*wood processing industries*". Consequently, this report is excluded from the general comparison shown in Figure 2.1. In conclusion, the largest discrepancies among studies are found in France, Sweden and Finland, being also the countries with the largest biomass potential. From Figure 2.1, total forestry sources availability in EU-24 is estimated to be 95 Mtn/yr (i.e., 1.9 EJ/yr).

On the other hand, for a better understanding of forestry biomass availability, those sources have been allocated within European countries at NUTS-2[4] level, which commonly refers to provinces except for smaller countries like the Baltic states or Slovenia (see Figure 2.3).
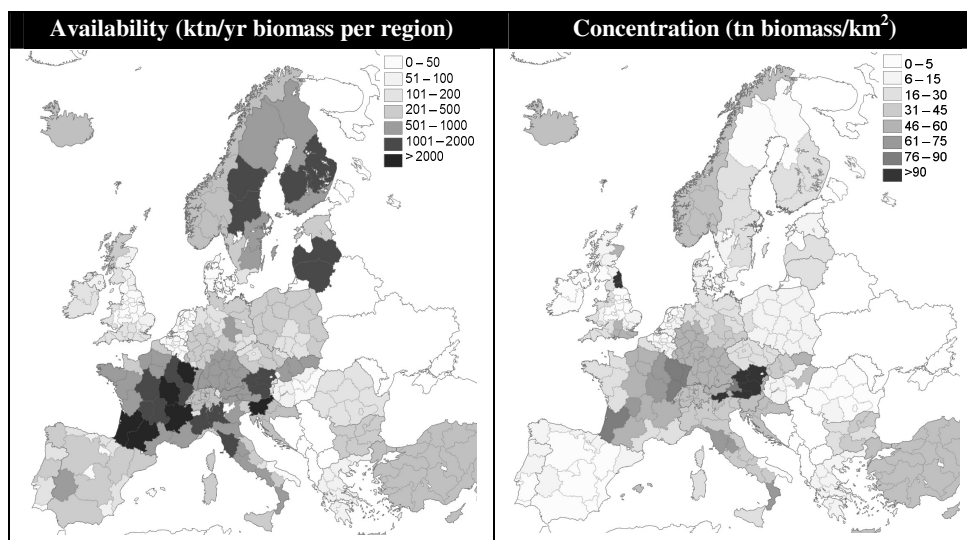
Figure 2.3: Spatial distribution of forestry biomass (i.e., complementary fellings and residues fellings), in terms of its quantity (left graph) and concentration within NUTS-2 regions (right graph). Values have been calculated from EEA report [22], except for Bulgaria, Greece and Romania that have been estimated from Nikolaou et al [29].

The left-hand picture accounts for the total biomass amount that could be deployed per region (represented in ktn/yr). The sum of these regional amounts corresponds to the total national value represented in the grey bars of Figure 2.1. However, this left-hand graph could lead to certain misinterpretation of the most suitable regions. For instance, countries such as Sweden or Finland have a relatively high amount of forestry sources, but they are also spread in a rather broad area. In those cases, logistics costs will be an important share of final production costs. Conversely,

---

[4] NUTS refers to the Nomenclature of Territorial Units for Statistics.

Austria could manage similar biomass quantities in a more compact area. European biomass distribution is, thus, completed by adding the second right-hand picture, which represents the concentration of biomass within regional borders (i.e., tones of biomass per km^2). As observed from both graphs, Central Europe accounts for most of the forestry biomass in relatively condensed areas (darker regions) whereas West-Southern and East-southern Europe are the most "depleted" regions (lighter areas). Nordic countries have considerable biomass availability but its concentration is lower than in Central Europe. Biomass amount and location will be later used to calculate the potential biofuels and biopower production in Chapter 8, as well as the intrinsic logistics costs for transporting biomass to centralized processing plants (see subchapter 2.5.2).

Apart from the differences observed among biomass availability studies, there could be an added source of discrepancy when estimating real forestry biomass amounts. In fact, unlike solar and wind energy, biomass sources are normally owned by individuals or private holdings. As consequence, negotiations must be carried out with the corresponding owners in order to assure biomass accessibility and its final price. In EU-25, this factor is especially sensitive as a considerable high share of the forests is on private hands, notably in Portugal (92%), Austria (82%), Sweden (80%) and Spain (78%). On the other side, there are Eastern countries such as Poland(17%), Czech Republic (16%), Estonia (9%) and Romania (5%)[35]. Assuming that forestry biomass is equally distributed in the national forest areas, it turns out to be that about 61% of the EU-25 available biomass is owned by more than 8.6 million private holdings, whereas the remaining 39% of forestry sources is owned by ~100,000 public holdings.

2.4.2.   *Potential straw residues availability in Europe*

Similar than for the case of forestry biomass, reference values for straw residues availability has been taken from [33] and compared with other studies [22, 28, 29, 32, 34] (see Figure 2.4). In this case, differences among authors are less marked, although France is again the country where we found less consistency. One of the possible sources for divergences is due to the intrinsic definition of agricultural wastes. In fact, some studies [28, 29, 32, 34] includes straw together with other undefined agricultural wastes, whereas in the reference report of Kunikowski et al [33], it is clearly stated that only straw residues coming from maize, cereals and rape crops are considered. In the EEA report [22] straw residues are gathered together with other solid agricultural residues such as stalks and prunings. This extra solid fraction does not represent a significant share and hence, values are quite similar to those presented by Kunikowski et al [33]. From Figure 2.4, it is concluded that reference values of straw residues availability turn out to be 103 Mtn/yr (i.e., 1.8 EJ/yr). Analogous to forestry sources, this value will be used in later calculations in Chapter 8.

Spatial distribution of straw residues supply has been also represented at NUTS-2 level in Figure 2.5, from two perspectives, i.e., biomass availability (ktn per region) and concentration (tone per km^2). Contrary to forestry sources, a higher amount of straw residues is found in southern and Eastern countries, although their concentration is moderate. France is again the country with most straw resources, whereas Nordic and Baltic states do not contribute significantly.
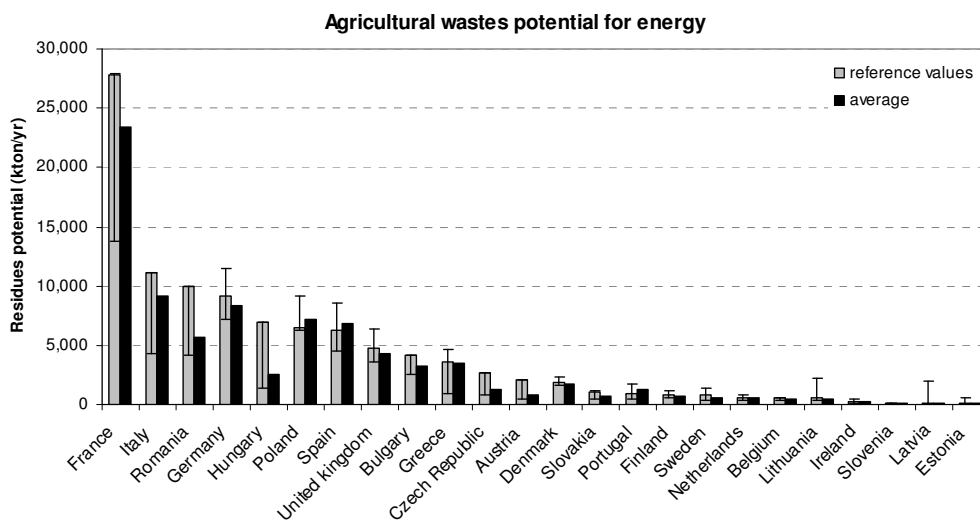
Figure 2.4: *Agricultural and straw wastes potential in Europe for energy. Reference values are taken from [33], whereas average & ranges values are calculated from [22, 28, 29, 32, 34].*
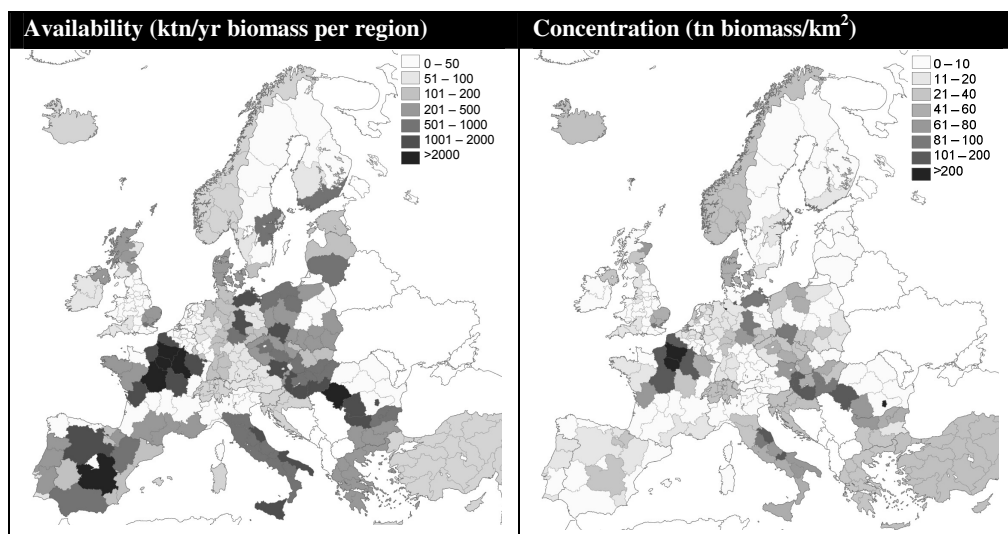
Figure 2.5: *Spatial distribution of straw residues in terms of its quantity (left graph) and concentration within NUTS-2 regions (right graph). Values have been calculated from Kunikowski et al[33].*

2.5. *Biowastes delivery cost*

Biowastes delivery costs are basically composed of two terms, i.e., the costs related to biomass extraction and collection, plus its transport until final biofuel conversion sites. The calculation of both terms is detailed in subsequent sections.

2.5.1.   *Extraction and collection costs*

Knowing exact extraction and collection costs is rather difficult as most of data found in literature also incorporates the logistics costs. An added drawback is that the relative costs for the two forestry fractions (i.e., *"complementary fellings"* and *"harvesting residues"*) are generally rather diverse (see Figure 2.6).   In fact, *"complementary fellings"* are estimated to be supplied at prices equal than stemwood for roundwood industry, whereas corresponding prices of *"harvesting residues"* are expected to be lower. For our analyses, forestry biomass costs have been calculated as the arithmetic mean of the two woody fractions and their corresponding collection costs. In this calculation, logistics costs has been deducted from the values found in literature [28-30, 32], by assuming that they represent about 40% of the total supply cost. According to our results (see Figure 2.8), Baltic and Southern countries report lower collection costs whereas France, UK and Germany are on the opposite side.
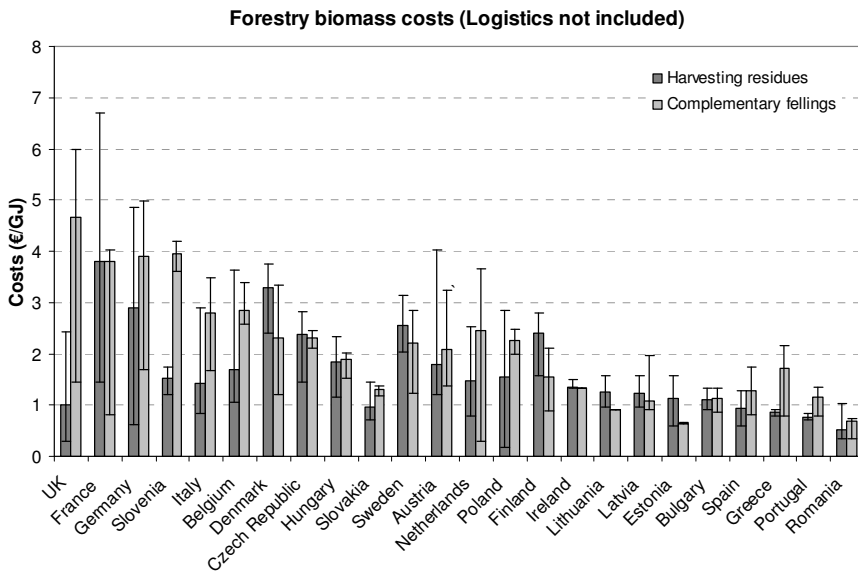
Figure 2.6: Extraction and collection costs for the two fractions of forestry sources. Average and range values have been calculated from [28-30, 32].

Contrary to forestry sources, straw residues collection costs show less variation (see Figure 2.7). In this case, average supply costs are simply calculated from average values found in literature by also deducting the logistics costs. As observed, Southern and Eastern countries have lower supply costs in comparison with Northern countries (see Figure 2.8).
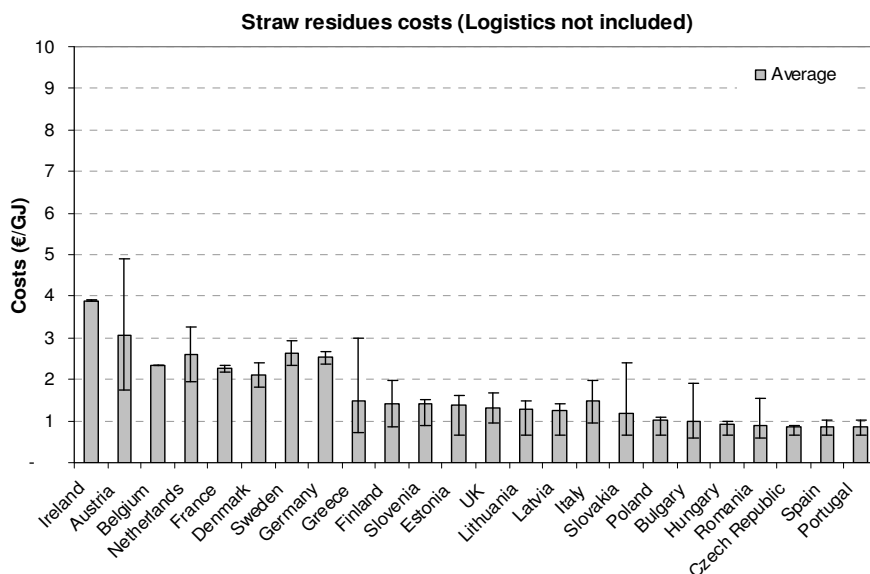
Figure 2.7: *Extraction and collection costs for straw residues. Average and range values have been calculated from [28, 29, 32].*

In all cases, it is assumed that, unlike biowastes availability, supply costs does not vary at national level, although, in reality, there could be slightly differences among the NUTS-2 regions of the same country.
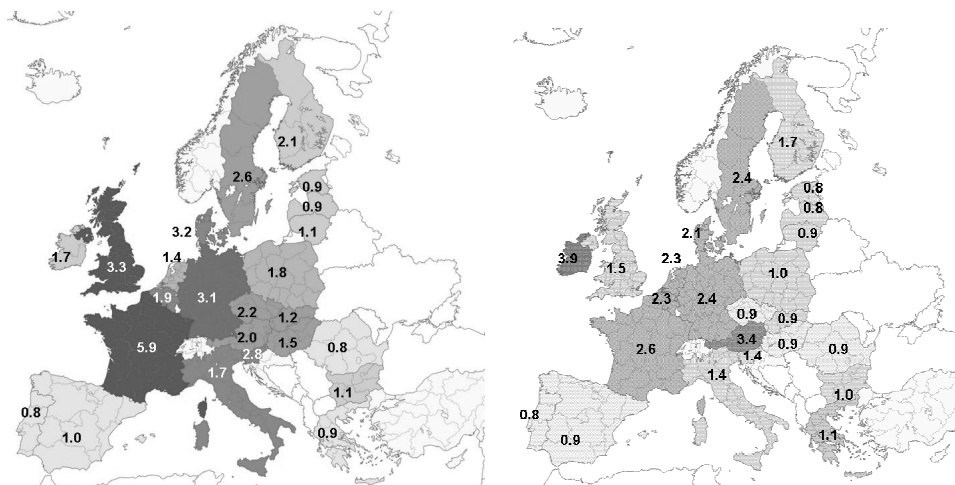
Figure 2.8: *Mean collections costs of the forestry biomass sources (left graph) and straw residues (right graph) in EU-24. Values are given in €/GJ.*

2.5.2.   *Transportation costs to the conversion site*

Transportation costs (l_c) are directly proportional to the distance existing between the collection points and the central biofuel conversion plant. Hence, those costs can be represented by a linear equation (i.e., Eq.(2-1)), where "a" and "b" are country-dependent coefficients and "r" represents the collection distance. Linear equations for transport costs calculations are commonly found in literature [32, 36, 37]. In our case, average logistics costs of a "i" point (L_c), within a certain delimited area ($\pi.r^2$), have been calculated from Eqs.(2-2) and (2-3), and by assuming an homogeneous territorial distribution (see Figure 2.9). Moreover, it is also considered that there are no available biomass sources within a ten-kilometer radius of the conversion plant (i.e., $R_o = 10km$). As shown, average transportation distances are ~ 2/3 of the furthest point (i.e., $r = R$).
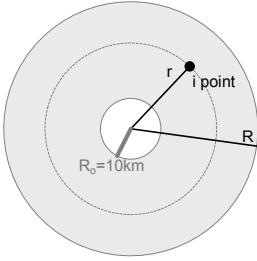
$$l_c(i) = (a + br) \ \ in \ €/tn \tag{2-1}$$

$$L_c(i) = \frac{1}{\pi \cdot R^2} \cdot \int_{r=R_O}^{r=R} 2\pi r \cdot (a + br) dr \tag{2-2}$$

$$L_c(i) = \left[\frac{2b \cdot (R^3 - R_o^3)}{3R^2} + \frac{a \cdot (R^2 - R_o^2)}{R^2} \right] \tag{2-3}$$

Figure 2.9: *Representation of collection distances to the central biofuels conversion site. Corresponding equations are presented aside.*

Coefficients "a" and "b" of the logistics linear equation have been calculated by each of the EU-24 countries, and tabulated in Table 0-1 (see Appendix A). The corresponding values for a particular year (n), biomass amount (tn/yr) and distance (km), are deducted from the sets of equations presented in the scheme of Figure 2.10 (Eqs.(2-4) to (2-22)). The analysis is based on getting a payback time of 3 years and a ROI (Return in Investment) of 11%. General assumptions used in all calculations are summarized in Table 0-2 (see Appendix A). Diesel consumption per truck (S_c) is determined from the Van Laar expression (i.e., Eq.(2-4)) [38], whose parameters are also tabulated in Table 0-2 (see Appendix A). In general, fuel consumption for a fully-loaded truck sums 0.93 MJ/tn.km.

$$S_c = \frac{\left[(m_l + m_v) \cdot g \cdot f_r + 0.5 \cdot C_w \cdot \rho \cdot A \cdot v^2 \right]}{\eta_t \cdot m_l} \ \ in \ MJ/tn.km \tag{2-4}$$

Data input	Parameter	Equations

Data input

v: speed (60 km/h)
t_u: time up/download (2 h/trip)
t_{max}: max daily drive
(18h/day.truck)

Parameter

t_t: total time per trip
N_d: daily trips per truck

Equations

$$t_r = 2r/v$$ (2-5)
$$t_t = roundup(t_u + t_r), \ t_t < t_{max}$$ (2-6)
$$N_d = round \ down(t_{max}/t_t)$$ (2-7)
$$t_{recalculated,t} = N_d \cdot t_t$$ (2-8)

Data input

TB: total biomass (tn/yr)
m_l: truck capacity
r: distance to plant (km)

Parameter

N_a: annual trips
r_t: total annual distance

Equations

$$N_a = roundup(TB/m_l)$$ (2-9)
$$r_t = N_a \cdot 2r$$ (2-10)

Data input

t'_{max}: max annual drive
(250 days/yr.truck)

Parameter

Fleet

N_{trucks}: nr trucks

Equations

$$N_{trucks} = roundup\left[\frac{(N_a/N_d)}{t'_{max}}\right]$$ (2-11)
$$r_{t,recalculated} = N_{trucks} \cdot t_{max} \cdot N_d \cdot 2r$$ (2-12)

Data input

t_{yr}: annual workdays driver
(230 days/yr.driver)
t_{day}: max daily workhours driver
(9 h/day.driver)

Parameter

Labour force

$N_{drivers}$: nr drivers
N_{staff}: nr other staff
t_h: annual hr driver

Equations

$$N_{drivers} = roundup\left(\frac{t_{max} \cdot N_d}{t_{yr} \cdot t_{day}}\right)$$ (2-13)
$$N_{staff} = roundup(0.8 N_{drivers})$$ (2-14)
$$t_h = roundup\left(\frac{r_{t,recalculated} \cdot t_t}{2r \cdot N_{drivers}}\right)$$ (2-15)

Data input

p_d: diesel price (€/lt) eurostat
HHV diesel (36 MJ/lt)
l_p: labour cost (€/h) eurostat
S_c: fuel use (0.93 MJ/tn.km)
m_v: gross weight truck
i_F: inflation fuels, materials 4%
i_M: inflation maintenance 2%
i_L: inflation labour 2%
i_L: inflation taxes 2%
i_I: inflation insurance 2%
n: year
p_c: plant capacity

Parameter

TPC = Variable + Fixed

Variable
F_n: Fuels, materials
M_n: Maintenance
L_n: Labour

Fixed
A_n: Administration
T_n: Local taxes
I_n: Insurance
O_n: Overheads

Data input

Fleet (30 years) = 4*Nr.trucks
Buildings = 8% fleet
Legal expenses = 2% fleet
Contingency = 5% fleet
WC = 15% TCI

Parameter

TCI = FCI + WC

FCI
Direct
Fleet
Buildings
Indirect
Legal expenses
Contingency
WC
Working capital

Profitability analysis

Payback: 3 years
ROI: 11%

Data input

Depreciation time: 10 years
Corporative taxe rate: eurostat

Figure 2.10: *Overview of the transport costs calculation.*

Calculation of annual TPC (total production cost) is made via the sets of expressions Eqs.(2-16) to (2-22), which are annually updated by applying the factor of $(1+i)^{(1+n)}$.

$$F_n = r_{t,recalculated} \cdot p_c \left[\frac{S_c}{HHV} \cdot m_v \cdot p_d + 0.069 \right] \cdot \left(1 + i_F\right)^{(1+n)} \qquad (2\text{-}16)$$

$$M_n = 0.096 \cdot r_{t,recalculated} \cdot p_c \cdot \left(1 + i_M\right)^{(1+n)} \qquad (2\text{-}17)$$

$$L_n = p_c \cdot t_h \cdot N_{drivers} \cdot \left(1 + i_L\right)^{(1+n)} \qquad (2\text{-}18)$$

$$A_n = p_c \cdot 1840 \cdot N_{staff} \cdot \left(1 + i_L\right)^{(1+n)} \qquad (2\text{-}19)$$

$$T_n = 0.03 \cdot FCI \cdot \left(1 + i_T\right)^{(1+n)} \qquad (2\text{-}20)$$

$$I_n = 0.01 \cdot FCI \cdot \left(1 + i_I\right)^{(1+n)} \qquad (2\text{-}21)$$

$$O_n = 0.50 \cdot M_n \qquad (2\text{-}22)$$

For forestry sources, "*a*" and "*b*" coefficients are in the range of **1.05-13.22** €/tn and **0.20-0.34** €/tn.km respectively, whereas for straw residues the corresponding values are found in the ranges of **1.53-18.71** €/tn and **0.23-0.42** €/tn.km. Logistics costs for straw residues are notably higher due to the low density of the feedstock and, hence, more trips are needed to transport the same amount of biomass. Analogous to collection costs (see section 2.5.1), transport costs turned out to be more expensive in Northern countries, in particular Denmark and Sweden. Conversely, Eastern countries account for the lowest logistics costs. Nevertheless, logistics costs represents less than 10% of the final biofuel or electricity price (see Chapter 6).

In order to validate our calculations, results are compared with values found in literature. In Shahab et al study [37], logistics costs for trucks is also given by a linear equation, where "*a*" and "*b*" coefficients are estimated at 5.70 $/tn and 0.137 $/tn.km respectively. Hence, those values are in the range of our calculations (see Table 0-1 in Appendix A). Conversely, Magalhães et al [36] presents values notably lower for "*a*" and "*b*" (i.e., 2.18 and 0.08 €/tn respectively). For Wakker et al [32], is not clear whether fixed costs (i.e., "*a*" coefficient") are included in variable costs (i.e., "*b*" coefficients) or they are calculated aside. In any case, b values of Wakker et al are in the range of 0.012-0.083 €/tn.km, which are also considerable lower than our values.

2.6. *Conclusions*

In this chapter, forestry biomass, straw residues and lignocellulosic crops are selected among all kind of biowastes sources as they are the most suitable feedstock for later biofuel and electricity production via gasification. Basically, two reasons have motivated our preferences, i.e., feedstock availability and higher conversion efficiencies. The forest and straw residues availability in 24 European countries is set in the ranges of 0.6-2.2 and 1.4-3.4 EJ/yr respectively, whereas their supply costs are predicted at 0.5-3.8 and 0.8-3.9 €/GJ. Logistics costs have been calculated aside and compare with other studies. As observed, their contribution do not exceed 10% in final biofuel prices.

3

From biomass-to-bioWatt. Selection of bioelectricity & biofuels conversion technology

Abstract

Nowadays, biomass has a well-known potential for producing energy carriers, such as electricity, heat (steam) and transport biofuels. However, biomass availability is rather limited and stochastically distributed. First generation technologies are now being questioned as they utilize edible crops, thus competing with agricultural practices for food production. Life cycle analyses also reveal that 1st generation biofuels frequently exceed the CO_2 emission levels of fossil fuels. Currently, Second generation technologies are being developed as a possible better alternative to the 1st generation since they can use biowastes from different origins (e.g., forest, agriculture, industry, municipalities). Moreover, 2nd generation biofuels are expected to be produced at higher efficiencies and lower production costs. In this chapter, we present the design and modeling of five different 2nd generation biofuels: SNG, methanol, Fischer-Tropsch fuels, hydrogen and bioelectricity. The five processes have similar operational units (i.e., gasification, cleaning, water-gas-shift reactions, catalytic reactors, final upgrading), although operational conditions and reactors design are different among them. Pre-treatment steps are also considered in order to enhance the low energy density of biomass prior to gasification. All production chains have been modeled in Aspen Plus in order to analyze their technical performance. Mass and energy balances obtained from those simulations are later used for efficiency, economic and environmental impact evaluation.

3.1. *Introduction*

As mentioned in Chapter 1 and 2, biomass availability is rather limited and, hence, selecting the most convenient biomass-to-bioenergy route is of crucial importance. Among all existing second generation technologies, gasification is here selected for the ultimate production of biofuels or electricity from biowastes. In particular, five different conversion routes are designed and analyzed: ***synthetic natural gas (SNG), methanol, Fischer-Tropsch fuels, hydrogen*** and ***electricity***.

Moreover, unlike previous studies, analysis of the biofuels and bio-electricity plants is extended to include the inefficiencies related to cover heat and electricity demand of those processes. In fact, although heat and electricity are co-produced in most of the conversion processes, external fuel is still needed to cover the overall energy demand. The amount and type of this external fuel is compared under the four different plant configurations that are depicted in Figure 3.1.
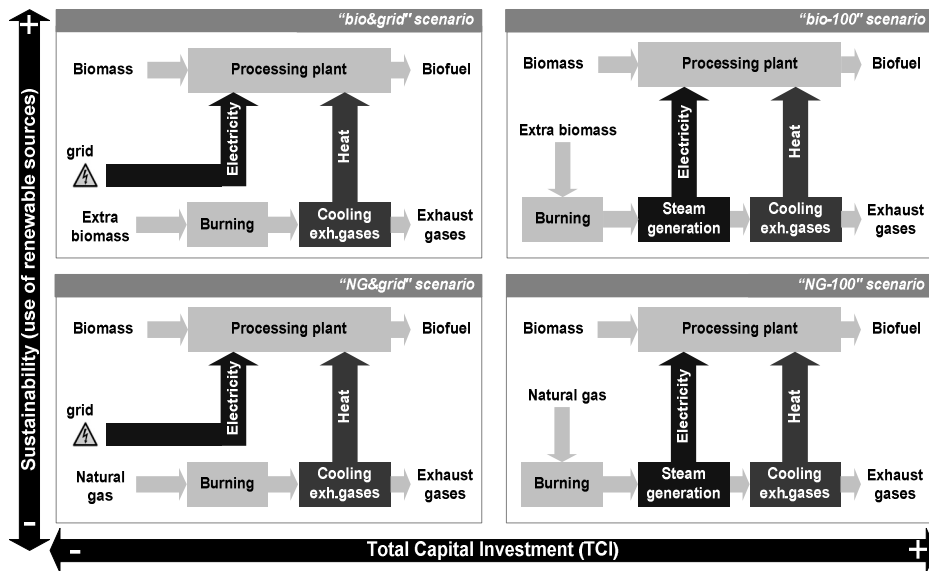
Figure 3.1: *Representation of the 4 different configurations as a function of the fuel used to cover heat and electricity demand of the biofuel processing plant. For the cases "bio-100" and "NG-100", heat and electricity is supplied by burning either extra biomass or fossil natural gas. Conversely, in the "bio&grid" and "NG-grid" options, electricity is taken from the power grid whereas heat is covered by either burning extra biomass or fossil natural gas, respectively. These 4 plant configurations will be applied to the 5 different biofuels plants (i.e., SNG, methanol, Fischer-Tropsch fuels, hydrogen and bioelectricity).*

The "most sustainaible" configuration "***bio-100***" considers that heat and electricity are supplied from burning extra biomass. This option, however, involves higher investments as the pre-treatment section has to be enlarged to treat a higher amount of biomass, and a biomass burner has to be incorporated as well. The least sustainable scenario "***NG-100***" differs from "*bio-100*" in that the extra biomass amount is

replaced by fossil natural gas. Although the pre-treatment section is not modified, a large natural gas burner has to be integrated, which also has considerable impact on the total investment. In the intermediate options "*bio&grid*" and "*NG&grid*", electricity is taken from the grid whereas heat is provided by burning extra biomass and fossil natural gas respectively.

This chapter presents the design and optimization of the five different conversion routes (i.e., SNG, methanol, Fischer-Tropsch fuels, hydrogen and electricity) by means of the Aspen Plus simulation software [39]. Final end-product specifications for SNG, methanol, Fischer-Tropsch fuels, hydrogen are also detailed and compared with the corresponding fossil fuels. Mass and energy balances from all simulations are used in later Chapters 4 to 6. Subsequent subchapters 3.2 to 3.5 give detailed information over the whole conversion chains, i.e., from biomass collection and transport until final biofuel or electricity distribution and use (see Figure 3.2).
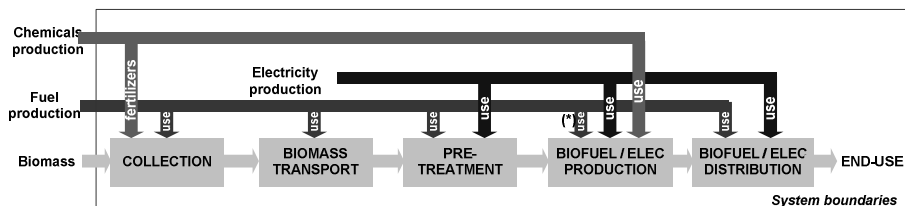
Figure 3.2: *Description of the main stages ranging from biomass collection until final biofuel or electricity production, distribution and use.*

3.2. *Collection and transport*

Biomass collection and transportation costs to centralized biofuels processing plants have been extensively described in previous section 2.5. Selection of biomass collection devices in forest and agrarian fields is out of the scope of our research as the corresponding investment and fuel consumption costs are already included in the given supply cost (see Figure 2.8). Conversely, fuel transport consumption is directly dependent on location of the centralized location plant and, thus, this parameter will be taken into account in the overall Well-to-Wheel efficiency (Ψ_{WTW}) calculation (see Chapter 4).

3.3. *Pre-treatment stages*

Pre-treatment stages are required in order to convert biowastes into a feedstock more effectively for storage, handling and processing. In our design, pre-treatment sections include biowastes *reception*, *conveying*, *size reduction*, *drying* and final *feeding* into the gasifier. In effect, densification practices such as pelletizing, briquetting and more recently torrefaction, increase the bulk density and reliability of the feed, and, in turn, the gasification efficiency [40-42].

The required pre-treatment operations and their extension ultimately depend on the selected biowaste as well as on the specific requirements of the gasifier and its feeding systems. For instance, the gasifier design (fixed, fluidized or entrained bed) especially determines the required degree of size reduction as this reactor is designed for a particular residence time, which is again governed by the particle size. Moreover, due to the short residence times of the reactors (especially for fluidized and entrained beds) fuel size distribution should also be as uniform as possible. Another parameter that notably influences the gasifier performance is the moisture content of the biowaste. Several studies state that higher gasification efficiencies are expected when the inlet biowaste stream is dried up to 10% [43]. Figure 3.3 summarizes the pre-treatment stages applied to each biomass-to-biofuel chain.
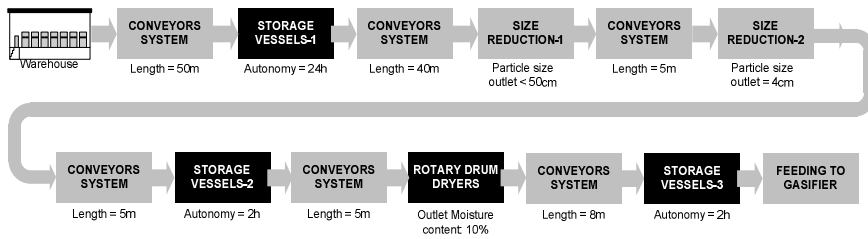
Figure 3.3: *Main pre-treatment stages for biomass-to-biofuels conversion via gasification. Rotary drum dryers and the intermediate vessels are the bottlenecks of the pretreatment chains in terms of maximal operative capacity (i.e., black blocks).*

The rotary drum dryers and the intermediate storage vessels (i.e., black bocks of Figure 3.3) are the bottlenecks of the pre-treatment chains in terms of maximal operative capacity. Hence, for large biomass streams, a series of dryers and vessels units has to be placed in parallel to achieve the desired treated biomass volumes. Maximum capacity of all units has been taken from the library of Aspen Icarus [44], which contains a large list of references from the chemical industry. Conveyors width has been adapted to deliver biomass to the equipments placed either in parallel or in series. Electricity consumption of each unit is calculated from Eqs.(3-1) to (3-4) in Table 3-1, and the results are then included in the calculation of the overall energy efficiency (Ψ_{plant}) of the plant (see Chapter 4, section 4.3).

Table 3-1: *Calculation of electricity consumption in the pre-treatment stages.*

Stage	Equipment type	Electricity consumption (*Adapted from* [43, 45])	
Conveying	Closed-belt conveyor	$W_{in} = 0.00058 \cdot m_{i,in}^{0.82} \cdot L$	(3-1)
Size reduction	Roll crusher	$W_{in} = 0.3 \cdot m_{i,in} \cdot R^*$	(3-2)
	Rotary cutter	$W_{in} = 500 \cdot m_{i,in}$	(3-3)
	Hammer mills	$W_{in} = 40 \cdot m_{i,in} \cdot \ln(R^*)$	(3-4)
Drying	Indirect rotary dryer	15 kWh/tn wet material	
Feeding	Screw feeders	n.a.	

where W_{in} is the power (in Hp), $m_{i,in}$ is the mass flow rate (in lb/hr), L is the length of the conveyor (in ft), and $R*$ is the reduction ratio. Next sections 3.3.1 to 3.3.5 gives more detailed information about each pre-treatment unit.

3.3.1.   Reception and Storage

After transshipment, biomass is sent to the storage facilities. Storage is normally required to assure continuous operation of the whole conversion plant and, hence, different levels of storage capacity have been designed. In the first pre-storage section, feedstock is assumed to be piled up in a roofed stockroom with a capacity of one month. Larger periods are not envisaged in order to avoid severe biological degradation of biowastes containing more than 20% of moisture content. Subsequently, feedstock is sent to a battery of closed silos which are provided with an active removal system (e.g., screw discharges) to avoid biowastes agglomeration and assure an uniform discharge. Silos capacity are calculated by considering one day of autonomy, i.e., the equivalent fresh biowaste amount need to continuously run the plant during 24 hours. This over-sized second storage system assures continuous availability even if the removal system of some silo is blocked. For extra security, additional storage vessels are placed before and after the dryer as the residence time of the sizing, dryer and gasifier is notably different. The autonomy of inter-staged vessels is about two hours each.

3.3.2.   Conveyors systems

Biomass need to be transported among storage facilities, other pre-treatment equipments and the gasifier section. Due to their versatility, reliability and reasonable costs, closed belt conveyors are selected for all the biowastes streams, assuming a speed of 2-5 m/s and a standard belt width in the range of 450-2950 mm. Conveyors are simulated in Aspen Icarus [44] as *DCO-CLOSED-BLT* type, and results are used for later cost analysis (see Chapter 6). Electricity consumption is given by Eq.(3-1).

3.3.3.   Size reduction

Particles size of biowastes streams is adjusted to meet the requirement of the feeding system and the gasifier. Basically, there are three types of sizing equipments, i.e., crushers or impact mills, shredders and cutters. Woody and straw residues are assumed to be received at particles sizes of about 75 x 75 cm and 1 x 100 cm respectively. For both cases, the desired final particle after two-stage sizing is 4 x 4 cm. Roll crushers are firstly used for to crush woody materials into a smaller size which can be further reduced by means of hammer mills. Conversely, two rotary cutters in serie are preferred for fibrous materials such as straw, as successive shear actions are more effective than pressure or physical impact. The features of each equipment are presented in Table 3-2, whereas electricity consumption is calculated from Eqs.(3-2) to (3-4).

Table 3-2: Comparison of different size reduction equipments.

Equipment	Simulated in [44] as:	Capacity	Reduction ratio (R*)	Electricity consumption
Roll crusher	*CR-S-ROLL-MED*	max. 1,330 tn/hr	max. 16	(3-2)
Rotary cutter	Data taken from [43]	max. 180 tn/hr	max. 10	(3-3)
Hammer mills	*CR-REV-HAMR*	max. 408 tn/hr	max. 50	(3-4)

3.3.4.   Drying

Prior to gasification, all biowastes streams are dried to 10% of moisture content. There are several devices available in the market but in our case a rotary indirect drum dryer is selected. Rotary drum drying is the most simple and well proven technology for biomass applications [43]. The selected dryer is built in a completely closed system to prevent odor and hazard problems, although the corresponding investments costs are higher than traditional direct open systems. In our case, hot gases and/or steam produced within the plants are used to evaporate the water at $115^{o}C$ and 1 bar. The evaporated water is removed separately from the heating medium. The rotary indirect drum dryer is simulated in Aspen Icarus using the *INDIRECT* module. Specific electricity production is taken from Pierik et al [43] for an indirect rotary drier, i.e., 15 kWh per tone of wet material and it is calculated for each stream.

3.3.5.   Feeding systems

Different systems have been developed for feeding biomass into a gasifier, i.e., screw feeders, rotary valve feeders, lock-hoppers and screw-piston feeders. A key parameter that influences the choice of a particular system is the gasification pressure against which the feeder has to operate. For instance, reactors operating at pressures up to 25 bar can be coupled to rotary valve feeders, lock-hoppers and screw-piston feeders are preferred for pressures up to 150 bar [43]. Screw feeders can only be applied for moderate pressures due to inherent gas leakage [43]. Hence, in our case, screw feeders are chosen for atmospheric gasifiers and screw-piston feeders for pressurized units.

3.4. *Biofuel production chains*

Once the received biomass has been pre-treated to reduce its particle size and moisture content, it can be converted to biofuel or electricity following the five different paths of Figure 3.4, i..e, **Synthetic Natural Gas** (**SNG**), **methanol**, **Fischer-Tropsch fuels, hydrogen** and **electricity**. In all routes, the gasifier is the core operation unit although the oxidizing agent and the operational conditions are different. For instance, an indirect steam-blown gasifier is applied for SNG and hydrogen production processes as more methane and hydrogen are already produced during this stage. A direct air-blown gasification system is used for electricity generation. For methanol and Fischer-Tropsch routes, air is substituted by pure oxygen to prevent low syngas partial pressures in downstream catalytic reactors (i.e., minimal partial pressures of 20 psig and 600-700 psig for Fischer-Tropsch and methanol production respectively [46]).
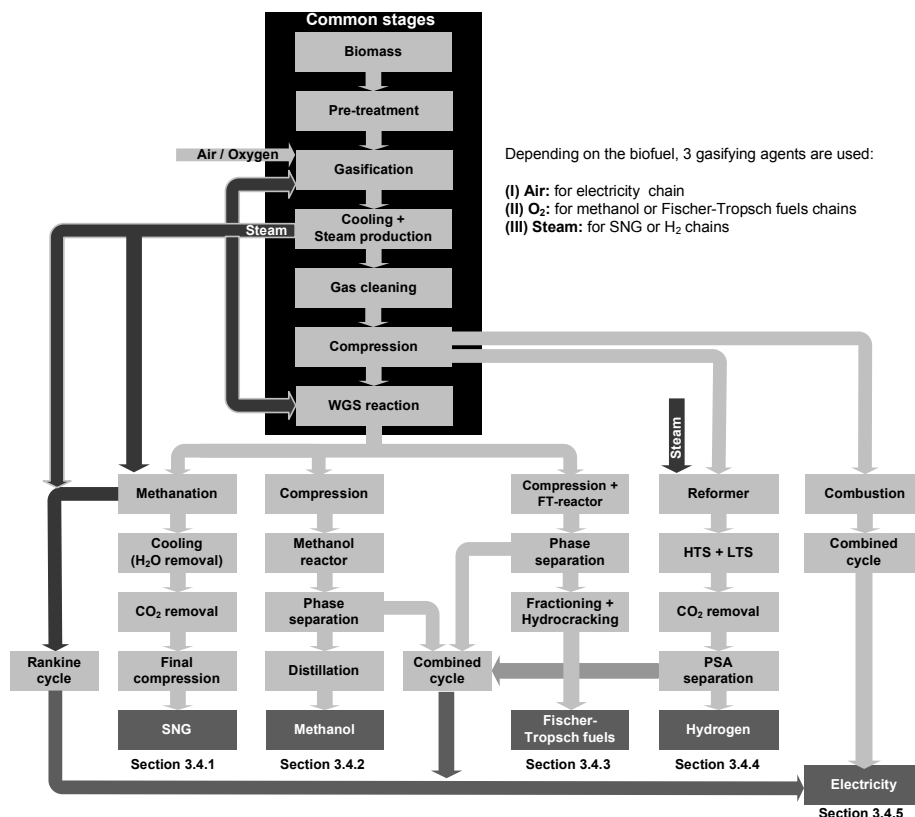
Figure 3.4: Overview of the block diagrams for the 5 biomass conversion routes. The black box refers to the common stages of the 5 chains. Operational conditions of the main equipments are tabulated in Appendix B.

Other common stages of the 5 chains are marked in Figure 3.4 by black boxes, and they comprise: cooling, cleaning compression and final H_2:CO ratio adjustment in a water-gas-shift (WGS) reactor. Cleaning stages are required to avoid deactivation of the catalysts used in downstream reactors as well as to minimize SO_x and NO_x formation when burning remaining unconverted gases. Several compounds have been identified as potential poisons and their corresponding maximum allowed concentration is tabulated in the Table 3-3.

Cleaning stages in all production chains begin with particulates removal after gasification by using a multicyclone, which can remove particles down to 5µm. Syngas is then cooled to 55°C prior to entering the subsequent stages, i.e., sulfur and ammonia removal. Sulfuric acid (H_2S) is captured by means of absorption with an aqueous MDEA (N-methyl-diethanolamine) solution. Amines have been used for acid gas removal (such as H_2S and CO_2) in industry for over 50 years, being MDEA the most widely used amine in existing installations [47, 48]. MDEA is here selected due to its low energy requirement for regeneration and higher selectivity over H_2S compared to CO_2. In fact, at this stage of cleaning, CO_2 removal is not desired as this gas is a reactant for some downstream catalytic reactors. MDEA solvent is also

reported to be less corrosive. The electrolyte package KEMDEA in Aspen Plus [39] is being applied for the kinetics of the reactions whereas an absorber column (RADFRAC) working at 55°C and 1 bar has been used to model the absorber. The sulfur-charged solvent leaving the bottoms of the absorbed is then send to the regeneration column (stripper) which works at higher temperature and pressure, i.e., 110°C and 2 bar. The stripper has also been modeled as a RADFRAC column with a condenser and reboiler. Acid gases (H_2S and CO_2) are released at the top of the column in the same chemical form in which they were absorbed. The regenerated solvent leaves the bottom of the column and it is also used to preheat the inlet stream of the stripping column. A make-up solution (10 wt% MDEA in water) is also fed into the system in order to offset the MDEA losses occurring in the stripping column. Clean syngas leaves the absorber column at around 40°C and it is then send to the ammonia removal unit, where gases are washed with an aqueous H_2SO_4 solution.

Table 3-3: *Specifications for inlet streams prior to some catalytic reactors.*

Sections:	WGS reactor [49, 50]	Methanation reactors [51]	Methanol reactor [50]	FT reactor [52, 53]	Reformer [49, 50]
Catalyst		Ni-based	$Cu/ZnO/Al_2O_3$	Fe/Co	Ni-based
Poisons:					
Ash / dust		<10 mg/Nm^3	< 0 ppm	0 ppb	
Tars		<5 mg/Nm^3	< dew point	0 mg/Nm^3	
S (H_2S + COS)	<0.01 ppm	<0.1 ppm	< 1 ppmV	<10 ppb	<0.25 ppm
N (HCN – NH_3)		<1 ppm	< 1 ppmV	<20 ppb	
Alkalines			< 10 ppb	<10 ppb	
Halogens (HCl)		< 25 ppb	< 10 ppb	<10 ppb	< 1ppm
Heavy metals		<300mg/Nm^3		unknown	
Others	Ar < 1ppm	Hg <0.05			

HCl can be removed by adding Na or Ca based powdered absorbents. These are injected in the gas streams and removed in the de-dusting stage. However, this has not been modeled in Aspen Plus. After cleaning, syngas is compressed and send to the WGS reactor to adjust the H_2:CO ratios at values determined by the desired end-product. Syngas is then converted to biofuel in subsequent catalytic reactors, and upgraded to achieve similar quality as the corresponding fossil fuel. Alternatively, if electricity generation is prefered over biofuel production, compressed syngas is directly send to a combined cycle, thus by-passing the WGS reactor. For the final application of biofuels in end-use devices (e.g., boilers, gas engines, gas turbines and SOFC fuel cells), there are also limitations about the concentration of toxic compounds [54, 55]. This specifications are less restrictive than the corresponding requirements of the catalytic reactors of the production chains (see Table 3-3). Hence, any additional cleaning unit is incorporated in the design of our processes.

On the other hand, heat integration has been carried out in order to minimize the demand of external fuel and electricity. Hence, heat supply and demand is carefully matched so that more high quality heat is left to produce superheated steam, which can be used for electricity generation, in steam gasification, in WGS reactors or for drying. For instance, a considerable amount of heat is recovered after gasification as the syngas needs to be cooled prior to cleaning and compression. Another source of heat

is extracted when cooling down methanation, methanol and Fischer-Tropsch reactors. The five production chains have been modeled in Aspen Plus [39] and mass and energy balances obtained from the simulations are used for later energy efficiency and exergy analysis (see section 4.3). Table 0-3 in Appendix B presents the operational conditions of the main units of each process. Subsequent sections 3.4.1 to 3.4.5 give more detailed information about the five conversion routes as well as the main differences with respect to conventional fossil fuel processes.

3.4.1.   *Synthetic Natural Gas (SNG) for heat & transport sectors*

According to experts from the European Commission, fossil natural gas share in the overall European gross inland energy consumption is predicted to increase from 17% in 1990 to 32% by 2020 (i.e., from 11 to 25 EJ/yr by 2020) [4] and thus being the second most consumed fuel just after oil [4]. One of the motivations of increasing the share of natural gas in the gross inland consumption is that natural gas has a cleaner environmental impact than other fossil fuels. In effect, for an equivalent amount of heat, burning natural gas produces about 30% less carbon dioxide than burning petroleum, and about 45% less than burning coal [56]. However, since the overall natural gas consumption is expected to almost triplicate the coal demand in 2020 [4], by this time, fossil natural gas will have a substantial contribution to global CO_2 emissions. Hence, many European countries are nowadays interested in promoting the production of *SNG* from renewable sources such as biomass. In effect, one of the advantages of the bio-based SNG is that it can benefit from the existing extensive European natural gas pipeline as its quality is similar to fossil natural gas. However, SNG application in the transport sector is still rather limited as the actual fuel-dispensing stations and vehicle fleet are not widely adapted yet. Some examples of SNG applications in transport can be found in Lille (France) and Madrid (Spain), where several public buses are already powered by compressed CNG at 250 bar. In the Netherlands, CNGNet is implementing around 50 tank stations across the country.

The first conversion chain in Figure 3.4 is designed to produce *SNG* with the same quality as the natural gas exploit in the Dutch Groningen fields. The main stages of the SNG production chain are schematically represented in Figure 3.5, whereas detailed Aspen Plus flowsheets are attached in Appendix C. As observed, the main steps are pre-treatment, gasification, conditioning prior to the methanation unit and final upgrading to fulfill the strict specifications for natural gas pipelines, in particular composition, Wobbe-index, calorific value, and relative density. For our scenario, low calorific natural gas distributed from Groningen fields is used as a reference (see Table 3-4). Low calorific natural gas contains more CO_2 and less CH_4 than high calorific natural gas. The H_2 content should not exceed 10 mol%. At this H_2 concentration, produced SNG can be transported through the existing natural gas distribution infrastructure without any adjustment [57]. The index referred to as Wobbe number (W_{index}) is indicative of the combustion energy being delivered to a burner at a constant pressure drop within a burner. The Wobbe index is defined as the ratio of the gross calorific value to the square root of the relative density of a gas. It is calculated from the gas composition according to Eq.(3-5).
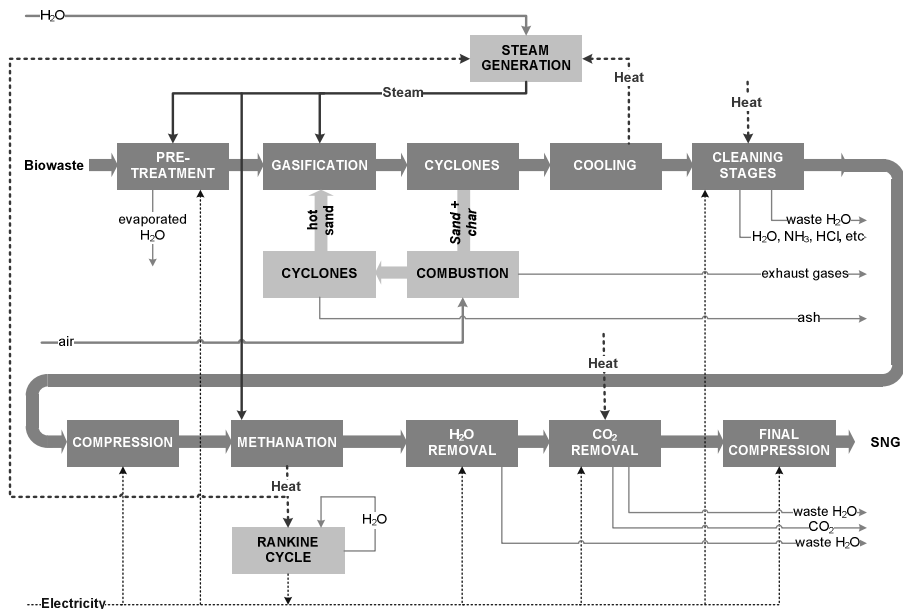
Figure 3.5: *Schematic block diagram for the SNG production. Main inlet and outlet streams are also indicated. Aspen Plus flowsheets are attached in Appendix C.*

$$W_{index} = \frac{HHV \cdot \rho_{gas}}{\sqrt{\rho_{gas} / \rho_{air}}} \tag{3-5}$$

where *HHV* is the gross calorific value (MJ/kg), ρ_{gas} is the density of the gas (kg/m^3) and ρ_{air} is the density of air (kg/m^3).

Table 3-4: *Comparison of Groningen natural gas with average natural gas from US pipelines. Adapted from [51, 58, 59].*

Parameter	Groningen (Netherlands)	US
Gross calorific value	31.6 – 38.7 MJ/Nm^3	35.4 MJ/Nm^3
Wobbe index	43.4 – 44.4 MJ/Nm^3	-
Maximum liquid hydrocarbons	5 mg/Nm^3 below -3°C	-
Aromatic hydrocarbons	0.0025 – 0.1 mol %	-
Hydrocarbon dew point	-	264.9K at 5.5 MPa
Water dew point	- 8 ^{o}C at 70 bar	-
Total sulphur content	< 20 mg/Nm^3	23 – 114 mg/Nm^3
H$_2$S + COS	< 5 mg/Nm^3	< 5.7 mg/Nm^3 (H$_2$S)
NH$_3$	< 1 ppm	-
HCl	< 1 ppm	-
Mercaptans	< 6 mg/Nm^3	4.6 mg/Nm^3
H$_2$O	Dew point <-10°C	64 - 112 mg/Nm^3
CH$_4$	~ 81 mol %	-
CO$_2$	< 3 mol %	1 – 3 mol %
O$_2$	< 0.0005 mol %	0 – 0.4 mol %
Hg	< 0.015 mg/Nm^3	-

An atmospheric steam-blown gasifier is selected for the SNG chain. The Battelle indirect gasifier developed by FERCO corporation is taken as a reference [60], and it consists of 2 physically separate units. The first unit is an atmospheric fluidized bed gasifier in which the biomass is converted into gases and residual char at a temperature of 700ºC. Residual char is burned in a second unit that provides sufficient heat for the gasifier. Heat transfer between reactors is accomplished by circulating sand between the gasifier and the combustor. The amount of residual char is regulated by adding more or less steam into the gasifier. Solids and gases are separated by two cyclones, located at the exit of the gasifier and combustor respectively. The gasifier and the burner are both simulated in Aspen Plus as Gibbs reactors (RGIBBS). Moreover, many authors have used this type of reactor and their simulations show a good agreement with experimental results [61-64]. After gasification, cooling and cleaning stages, outlet gases are compressed to 28 bar and then fed to the methanation section. In this process CO and CO_2 react with H_2 to produce CH_4 according to the reactions (3-6) and (3-7):

$$CO + 3H_2 \leftrightarrow CH_4 + H_2O \quad \Delta H_{298K} = -206 \; kJ/mol \tag{3-6}$$

$$CO_2 + 4H_2 \leftrightarrow CH_4 + 2H_2O \quad \Delta H_{298K} = -165 \; kJ/mol \tag{3-7}$$
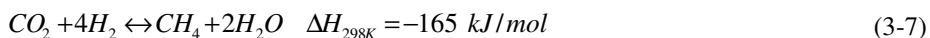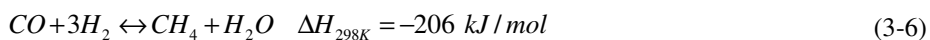
For a common nickel-based catalyst, the operating range is between 260ºC and 450ºC. In order to overcome this limitation, ICI has developed a new high-nickel based catalyst (where nickel oxide is ~ 60%). This new catalyst seems to have the required activity, stability, and physical strength to methanate raw gases at a temperature of 750ºC [49]. This ICI catalyst is selected for our simulation as it also has water-shift activity required to adjust the H_2:CO ratio to the desired value of 3. However, apart from the aforementioned Eqs.(3-6) and (3-7), inlet conditions of the methanation reactors are such that carbon could be formed via the reactions (3-8) and (3-9).

$$CO + H_2 \leftrightarrow C + H_2O \quad \Delta H_{298K} = -131 \; kJ/mol \tag{3-8}$$

$$2CO \leftrightarrow C + CO_2 \quad \Delta H_{298K} = -172 \; kJ/mol \tag{3-9}$$
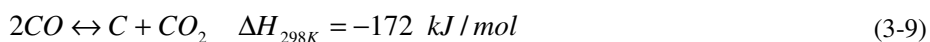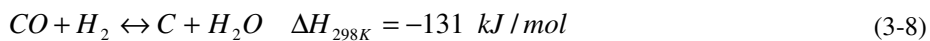
The formation of carbon is undesired, because it results in loss of conversion efficiency, but also in deactivation of the catalyst by carbon deposition. Hence, steam is added into the first catalytic reactor to avoid carbon formation. After methanation, the outlet gases enter an ammonia cooling cycle to remove most of the water. Subsequently, CO_2 is separated from CH_4 by using a MDEA scrubbing system, working at the same conditions as the H_2S removal system. Process conditions of the upgrading stages (H_2O and CO_2 removal) have been adjusted to fulfill the Groningen gas specifications (see Table 3-4), in particular the Wobbe index, considered as the functional parameter and whose target value has been set to 43.5 MJ/Nm³. Under this constraint, the other requirements are also fulfilled, i.e., gross calorific value and concentration of main compounds and toxicity. Heat removal after gasification and methanation is partly employed to cover heat demand of some sections. Remaining heat is then employed to produce electricity in several steam turbines. Superheated steam is generated at 50 bar and 364ºC and expanded to 0.5 bar and 81.3ºC.

3.4.2.   *Methanol as transport fuel*

The second path in Figure 3.4 corresponds to methanol production from biomass. Although the largest application of methanol is found in the production of chemicals (i.e., 40% to synthesize formaldehyde), methanol and its derivatives can also be used as fuel in road transport. In fact, in 1990's, large amount of methanol where used in the U.S. to produce the gasoline additive *methyl tert-butyl ether* (MTBE), although MTBE is no longer marketed in the U.S, whereas its production has declined in Europe. *Dimethylether* (DME) is another methanol-derivative which is seen nowadays as a potential diesel or LPG blending substitute. Methanol is also an alternative fuel for internal combustion and other engines, either in combination with gasoline or directly. Direct (DMFCV) and reformed (RMFCV) methanol fuel cell cars are also under research although their implementation is being questioned due to the limited power that they can produce and the large dimensions and weight of their systems.

A major defender of methanol is the Noble prize G.A.Olah who since 1990's started to advocate the *Methanol Economy* [65]. According to his statements, the *Methanol Economy* is a suggested future economy in which methanol replaces fossil fuels. It offers an alternative to the proposed *hydrogen economy* or *ethanol economy*, although this assertion is also questioned by other experts. In fact, major problems associated to methanol production, distribution and use are: high investments, low energy density (i.e., one half of that of gasoline and 24% less than ethanol), its toxicity and corrosion to some metals. Conversely, the advantages are that the amount of methanol that can be generated from biomass is much larger than bioethanol, and it can also be blended in gasoline up to 85% (M85), thus competing with bioethanol in the energy market. Properties of methanol and other transport fuels are compared in Table 1-1 in Chapter 1. As observed, bioethanol and methanol have the highest octane numbers and Fischer-Tropsch the highest cetane numbers, which is preferable when blending with gasoline or diesel respectively.

The commercialization of methanol from synthesis gas was first developed at BASF Germany in 1922. This process used coal as raw feedstock and a zinc oxide-chromium oxide catalyst with poor selectivity. It also required very extreme conditions with pressures exceeding 300 bar. More selective catalysts discovered in the 1970's, allowed to build larger plants with higher energy and cost efficiency. Current research focuses on shifting the equilibrium to achieve higher conversion per pass.

Nowadays, natural gas is the most economical and widely applied feedstock to produce methanol by autothermal reforming and further catalytic conversion. However, coal is increasingly gaining interest in China, whereas in Europe, Schwarze Pumpe GmbH has reconverted its plant in Lausitz (Germany) to treat a wide variety of biomass and wastes for methanol and power generation (i.e., around 100,000 tones of methanol are manufactured annually). In our case, methanol is produced from biomass via the different stages schematically identified in Figure 3.6. Detailed Aspen Plus flowsheets are attached in Appendix D.
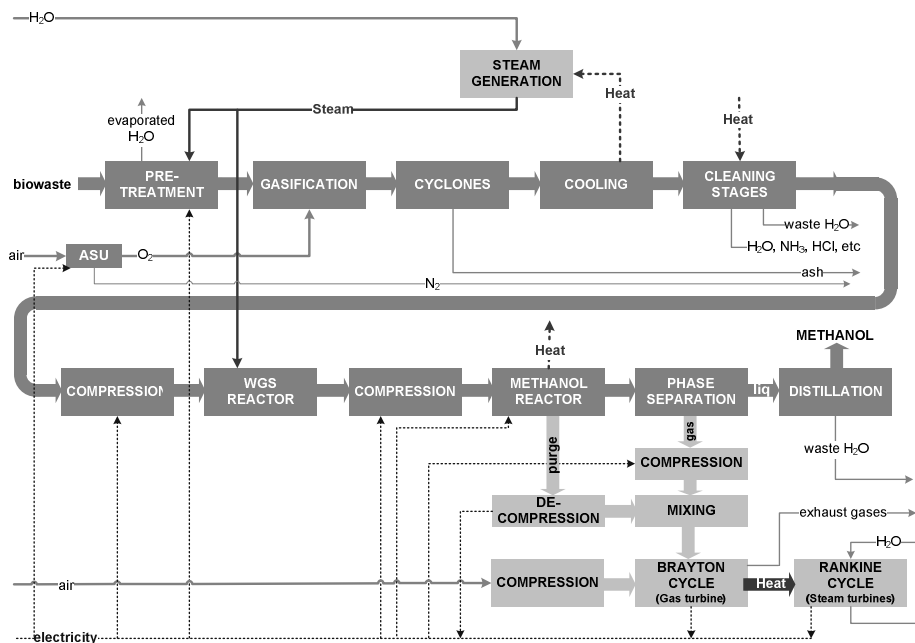
Figure 3.6: Schematic block diagram for the methanol production. Main inlet and outlet streams are indicated. ASU refers to an air separation unit. Detailed Aspen Plus flowsheets are attached in Appendix D.

The main difference with regard to the conventional natural gas-to-methanol process is that syngas is here produced from biomass gasification instead of steam-methane reforming (SMR). Downstream upgrading units are similar and they are required to reach methanol purity above 98.6 mol % (dry basis). In our design, part of the unconverted reactants and purge from the methanol reactor is used to generate electricity. An atmospheric oxygen-blown gasifier is used in this process, working at 1000°C and 1 bar. Energy requirements for the air separation unit (ASU) have been taken from Simbeck et al [66]. In this case, oxygen is preferred as oxidizing agent instead of steam in order to get a higher content of the "building agents" CO and H$_2$ and minimize hydrocarbons formation, such as CH$_4$ or C$_2$H$_6$. An air-blown gasifier could not be used neither as the presence of nitrogen would notably decrease the partial pressure of syngas in downstream methanol synthesis reactor. In effect, syngas partial pressure need to be above ~ 40 bar [46]. After gasification, outlet gases are also cooled down before entering the required cleaning stages. Heat removal is here entirely used for producing pressurized steam. Clean gases are compressed and send to a WGS reactor where the H$_2$:CO ratio is adjusted to 2. The WGS reactor is simulated as a phase equilibrium reactor (REQUIL) from the Aspen Plus library [39], whose main feature is that it calculates the equilibrium by solving stoichiometric chemical and phase equilibrium equations. The reaction taking place is the WGS reaction (3-10).

$$CO + H_2O \leftrightarrow CO_2 + H_2 \quad \Delta H_{298K} = -41 \;\; kJ/mol \qquad (3\text{-}10)$$
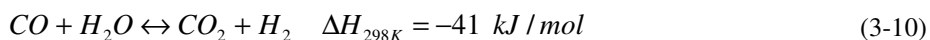
Due to the high catalyst selectivity all gases, except those involved in the WGS reaction, are inert. The reaction is exothermic, independent of pressure and proceeds nearly to completion at controlled temperatures. Subsequently, the outlet stream is further compressed and fed to a catalytic methanol reactor, operated at 77 bar and 200°C. This methanol reactor has been simulated as a stoichiometric reactor (RSTOIC), and the ICI low pressure methanol process is taken as a reference [49, 67, 68]. Table 3-5 presents the possible operation range of the ICI process together with examples of other commercial processes.

Table 3-5: *Heterogeneous catalytic processes for methanol synthesis [68].*

Process	Catalyst	Temperature (^{o}C)	Pressure (bar)
Nissui-Topsoe	$CuO-ZnO-Cr_2O_3$	230 – 260	100 – 150
BASF	$CuO-ZnO-Al_2O_3$	200 – 350	50 – 250
ICI	$CuO-ZnO-Al_2O_3$	220 – 280	50 – 100
Lurgi	$CuO-ZnO$	230 – 250	40 – 50
Mitsubishi Gas Chemical	$CuO-ZnO-Al_2O_3$	250 – 275	50 – 120

In order to establish a uniform temperature in the ICI reactor, gases are fed at various locations along the length of a catalytic bed. Methanol is here produced by hydrogenation of carbon oxides over a Cu/Zn/Al catalyst ($CuO-ZnO-Al_2O_3$), according to the following reactions (3-11) and (3-12).

$$CO + 2H_2 \Leftrightarrow CH_3OH \qquad \Delta H^o_{298K} = -90.6 \ kJ/mol \quad \kappa = 15\% \qquad (3-11)$$

$$CO_2 + 3H_2 \Leftrightarrow CH_3OH + H_2O \qquad \Delta H^o_{298K} = -49.5 \ kJ/mol \quad \kappa = 3\% \qquad (3-12)$$
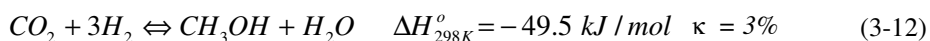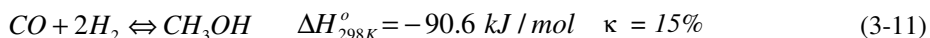
where κ is the conversion degree [69]. As conversion cannot be accomplished in one pass, the unreacted syngas is recycled back to the methanol reactor in order to increase the conversion efficiency. Recycling is carried out via a system consisting of a condenser, a purge valve and a recycle compressor. The condenser works at 45°C and it is used to separate the unreacted syngas from the liquid methanol. About 90% of the unreacted syngas is recompressed to 77 bar and recycled back to the reactor. Compression is required due to the volume decrease occurring in the reactor (Eqs. (3-11) and (3-12)). The remaining 10% is purged and send to a pressurized combustor where it is burned to provide heat the electricity generation cycle. Liquid methanol leaving the condenser of the reactor system is sent to an atmospheric distillation column where it is separated from water and other minor impurities. The distillation column is simulated as a RADFRAC unit.

3.4.3.   Fischer-Tropsch fuels for road transport

The third conversion path in Figure 3.4 is dedicated to produce synthetic diesel and gasoline via a Fischer-Tropsch process. Conversion of coal-derived synthesis gas to aliphatic hydrocarbons over metal catalysts was first discovered by Franz Fischer and Hans Tropsch at the Kaiser Wilhelm Institute in 1923. They discovered that CO hydrogenation over iron, cobalt or nickel catalysts at 180-250°C and atmospheric pressure yielded a product mixture of linear hydrocarbons and some oxygenates. However, Fischer-Tropsch synthesis was not applied at commercial scale until 1930's,

when Germany started producing Fischer-Tropsch liquids from coal to power vehicles. Nowadays, the technology is well proven for feedstock such as coal and natural gas, being Sasol in South Africa and Shell in Qatar the leading plants worldwide. Conversely, Fischer-Tropsch synthesis from biomass has not been scaled up to commercial plants yet, although Choren industries [70] are planning to commission a plant with a capacity of 18 million liter per year by 2010 (i.e., 50 MW$_{fuel}$). Table 3-6 summarizes several existing commercial plants as well as some projected facilities in the coming years.

Table 3-6: *Examples of some operational and under construction Fischer-Tropsch plants.*

Process	Company	Location	Status	Capacity
Coal-to-Liquid (CTL)	Sasol	Secunda (South Africa)	In operation since 1955	150,000 bpd (~ 24,000 m^3/d)
Gas-to-Liquid (GTL)	Sasol Oryx	Ras Laffan (Qatar)	In operation since 2006	34,000 bpd (~ 5,400 m^3/d)
	Royal Dutch Shell	Bintulu (Malaysia)	In operation since 1993	14,700 bpd (~ 2,340 m^3/d)
	Mossgas (PetroSA)	Mossey Bay (South Africa)	In operation since 1992	45,000 bpd (~ 7,200 m^3/d)
	Shell and Qatar Petroleum	Qatar	Under construction	140,000 bpd (~ 22,000 m^3/d)
	Sasol and Chevron	Escravos (Nigeria)	Under construction	34,000 bpd (~ 5,400 m^3/d)
Biomass-to-Liquid (BTL)	Chore industries (alpha plant)	Freiburg (Germany)	Pilot plant in operation	100 lt/d
	Chore industries (beta plant)	Freiburg (Germany)	Under construction	18 million lt/yr
	Chore industries (sigma plant)	Schwedt (Germany)	Projected plant (2013)	270 million lt/yr
	Repotec	Gussing (Austria)	Pilot plant in operation	4,200 tn/yr

Bio-based FT-diesel has similar properties as fossil diesel with regard to their energy content, boiling point, density and viscosity. Hence, synthetic diesel can be fueled in actual vehicles without engine modification. Moreover, since FT-diesel has better auto-ignition behavior than petroleum-based diesel, FT-diesel can also be blended with other lower quality diesels which could not be otherwise utilized as an automotive fuel [71]. Another advantage is that its negligible sulfur and aromatic contents presents a direct improvement on health and environment. The absence of sulfur also maximizes the efficiency of catalysts and particulate traps while it does not influence the lubricating properties of the fuel. However, one of the main drawbacks of synthetic FT-diesel is their use in very cold climates as low temperatures promotes the formation of wax crystals that can obstruct fuel lines and filters in the vehicle's fuel system. In effect, as the temperature decreases, synthetic fuels become cloudy (*Cloud Point*) and, at yet lower temperature (*Pour Point*), it turns into a gel that can no longer be pumped, thus resulting in a possible engine failure. An intermediate point between those states is the so-called *Cold Filter Plugging Point* (*CFPP*), which is commonly applied to determine the performance of any fuel under cold conditions. *CFPP* is higher in the case of FT- diesel than for fossil diesel. One of the primary solutions to overcome this consists of reducing the wax concentration by removing the higher paraffins from the diesel fraction (C23+).

The Fischer-Tropsch process is designed to maximize diesel production (i.e., C12 to C18) although other hydrocarbon fractions are also co-produced. Tail gas (i.e., C1 to C4) is burned to produce electricity that is consumed within the plant, whereas gasoline fraction (i..e, C5 to C11) is sold for its use in conventional vehicles. Upgrading sections are designed to provide a synthetic diesel that meets the *DIN-51606* and *EN-14214* standards specifications. Whenever these standards state different values, the most restrictive has been taken as a design parameter. The characteristics of final FT-diesel are also given in Table 3-7. Appendix F gives detailed information about the calculation of the main parameters.

Table 3-7: *Specifications for fuel-grade biodiesel.*

Parameters	Fossil (EN590)	Biodiesel (DIN51606)	Biodiesel (EN14214)	Produced FT-diesel
Density @ 15°C (g/cm³)	0.82-0.86	0.88-0.90	0.86-0.90	0.80
Viscosity @ 40°C (mm²/s)	2.0-4.5	3.5-5.0	3.5-5.0	3.7
Flashpoint (°C)	>55	>110	>101	111.5
Sulphur (% mass)	0.20	<0.01	<0.01	< 1 ppm
Sulphated Ash (% mass)	0.01	<0.03	0.02	0
Water (mg/kg)	200	<300	<500	~ 100
Carbon Residue (% weight)	0.30	<0.03	<0.03	0
Total Contamination (mg/kg)	Unknown	<20	<24	0
Copper Corrosion 3h/50°C	Class 1	Class 1	Class 1	n.a.
Cetane Number	>51	>49	>51	59.2 CI [a]
Methanol (% mass)	Unknown	<0.3	<0.2	0
Ester Content (% mass)	Unknown	>96.5	>96.5	0
Monoglycides (% mass)	Unknown	<0.8	<0.8	0
Diglyceride (% mass)	Unknown	<0.4	<0.2	0
Tridlycende (% mass)	Unknown	<0.4	<0.4	0
Free Glycerol (% mass)	Unknown	<0.02	<0.02	0
Total Glycerol (% mass)	Unknown	<0.25	<0.25	0
Lodine Number	Unknown	<115	120	0
Phosphor (mg/kg)	Unknown	<10	<10	0
Alcaline Metals Na. K (mg/kg)	Unknown	<5		0

(a): CI is the Cetaned Index

As observed, all requirements are fulfilled with exception of the density, which is slightly below the specified ranges of the norms. This could be partly solved by allowing a higher water content. In effect, water content of the produced FT-diesel is by far lower than the permissible value. Calculated CFPP point is around -60°C, which will fulfill even the arctic conditions stipulated in the EN 590:2004 norm. This could be explained by the fact that waxes are minimized by means of a hydrocracker. Detailed Aspen Plus flowsheets of the Fischer-Tropsch fuels production process are attached in Appendix E.

An atmospheric oxygen-blown gasifier working at 900°C is used this chain (see Figure 3.7). Motivations for using oxygen instead of air for the gasification steps are similar as for the methanol case, although the minimal syngas partial pressure within the Fischer-Tropsch synthesis reactor is less severe (i.e., above 1.5 bar [46]). Outlet gases are again cooled down to 55°C and send to the corresponding cleaning stages.
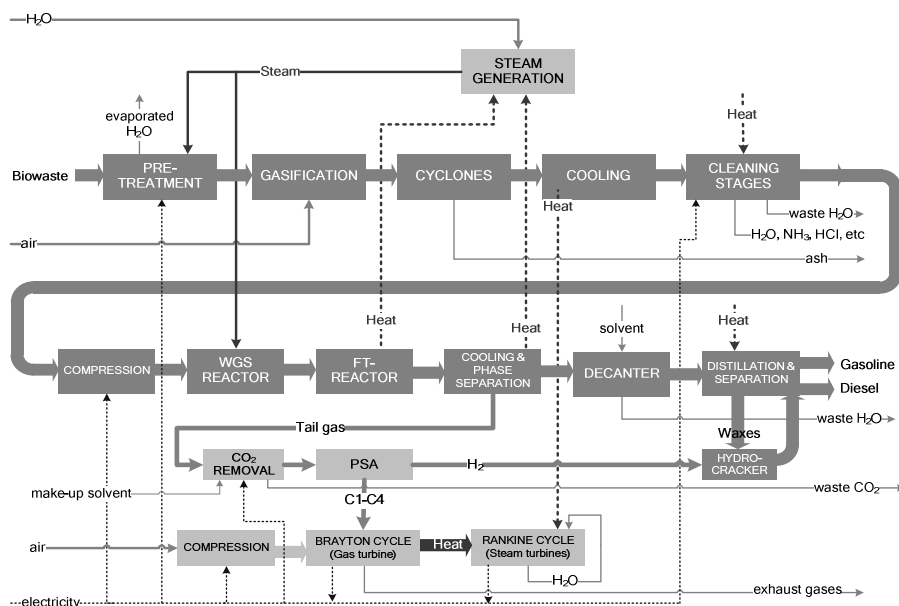
Figure 3.7: *Schematic block diagram for the Fischer-Tropsch fuels production. Main inlet and outlet streams are indicated. ASU refers to an air separation unit, and PSA to a pressure swing adsorption system. Detailed Aspen Plus flowsheets of the Fischer-Tropsch fuels production process are attached in Appendix E.*

In this case, the recovered heat is entirely used in a Rankine cycle to produce electricity. The cycle is working at the same conditions as in the SNG chain. Clean gases are then compressed to 25 bar and send to a WGS reactor to adjust the H$_2$:CO ratio at 2.13. Subsequently, syngas is converted to a mixture of different hydrocarbons in a catalytic Fischer-Tropsch reactor operated at 260°C and 23 bar. The reactor is simulated as a RGIBBS model and conversion of H$_2$ and CO is assumed to reach 80% [72]. Heat removed from the process is used to produce steam required for the WGS reactor and the drying stage. The Fischer-Tropsch synthesis can be described by the set of equations presented in Table 3-8, where the main reactions taking place are hydrocarbons chain formation (Eqs.(3-13) and (3-14)). The most common catalysts for Fischer-Tropsch synthesis are metals of group VIII. Among them, Fe-, Co-, Ni- and Ru- catalysts are considered to have sufficient activity for industrial applications. Table 3-9 summarizes the main characteristics, operation conditions and price relation of these catalysts. The Ru- and Rh- catalyst are the most active but they are also very expensive due to their limited availability and, hence, they are not suitable for large-scale installations. The Ni-catalyst is also notably active but it produces a higher amount of methane and it also forms volatile and very poisonous carbonyls which, in turn, results in metal loss.

Table 3-8: Main Fischer-Tropsch synthesis fuels reactions.

Reaction	Equations	ΔH_{298} (kJ/mol)	Eqs.
Main reactions:			
Paraffins (alkanes)	$nCO + (2n+1)H_2 \leftrightarrow C_nH_{2n+2} + nH_2O$		(3-13)
Methanation (n=1)	$CO + 3H_2 \leftrightarrow CH_4 + H_2O$	- 206	(3-6)
Olefins	$nCO + 2nH_2 \leftrightarrow (-CH_2-)_n + nH_2O$		(3-14)
Water-gas-shift (WGS)	$CO + H_2O \leftrightarrow CO_2 + H_2$	- 41	(3-10)
Side reactions:			
Alcohols	$nCO + 2nH_2 \leftrightarrow C_nH_{2n+2}O + (n-1)H_2O$		(3-15)
Boudouard	$C + CO_2 \leftrightarrow 2CO$	+ 172	(3-16)

Table 3-9: Main catalysts for Fischer-Tropsch synthesis. Relative prices in 2007.

Metal (catalyst)	Price ratio [73]	Advantages	Disadvantages
Iron	1	Low costs High selectivity to olefins Higher WGS promotion	Lower activity than Co Lower lifetime than Co Lower heavy CxHy selectivity (=low diesel output)
Cobalt	235	High activity Longer lifetime than Fe Higher heavy CxHy selectivity	Higher costs than Fe Lower WGS promotion
Nickel	140	High activity	Higher selectivity to methane Forms volatile carbonyls (=loss of metal)
Ruthenium	76000	Higher activity than Fe,Co,Ni	Higher costs than Fe,Co,Ni
Rhodium	824000	The most active catalyst	Excessive costs (=none commercial application)

Therefore, nowadays, Fe- and Co- are the two only practical alternatives for large scale installations. Co- catalyst is selected for our simulation due to its high selectivity towards to linear alkanes, longer life-time and higher activity [74, 75]. However, since Co-catalyst has a limited WGS activity, a specific WGS reactor is placed prior to the Fischer-Tropsch catalytic reactor in order to adjust the H_2:CO ratio. Formation of hydrocarbons is assumed to follow the ideal Anderson-Schulz-Flory equation, characterized by the chain growth probability factor α, whose mathematical representation is given by Eq.(3-17).

$$\log \frac{z_n}{n_a} = n_a \cdot \log \alpha + \log \frac{(1-\alpha)^2}{\alpha} \tag{3-17}$$

where z_n is the mass fraction of a product consisting of n_a carbon atoms. The growth factor α is highly dependent on reaction conditions and the catalyst type. An increase of temperature is translated into a decrease of the α factor, and the same effect is observed when increasing H_2/CO ratio. In our simulation, the factor α is been calculated from Lox and Froment equation (see Eq.(3-18)), which is based on

experiments using a precipitated iron catalyst [76]. This model was used by Prins et al to simulate Co-based catalytic reactions with the assumption that industrial catalysts will follow similar selectivity [72]. The model predicts that the rate determining processes are the adsorption of CO and desorption of hydrocarbon products.

$$\alpha = \frac{R_{propagation}}{R_{propagation} + R_{termination}} = \frac{k_{HC1} \cdot P_{CO}}{k_{HC1} \cdot P_{CO} + k_{HC5} \cdot P_{H_2} + k_{HC6}} \tag{3-18}$$

where R is the rate of either propagation and termination, k_{HC1} is the rate constant for adsorption of CO on an active site (equal to 1.22×10^{-5} mol/g.s.bar), k_{HC5} is the rate constant for desorption of paraffins by hydrogenation of active site (mol/g.s.bar), k_{HC6} is the rate constant for desorption of olefins from active site (mol/g.s), P_{CO} is the partial pressure of CO (bar) and P_{H2} is the partial pressure of H_2 (bar). The rate constants (k_{HC5} and k_{HC6}) follow the Arrhenius law and they are calculated by applying the following experimental relations (3-19)-(3-20).

$$k_{HC5} = A_i \cdot \exp(-E_i/RT) = 423.3 \cdot \exp(-94500/RT) \tag{3-19}$$

$$k_{HC6} = A_i \cdot \exp(-E_i/RT) = 2712508.9 \cdot \exp(-132300/RT) \tag{3-20}$$

where R is the universal gas constant and T is the temperature. Values of the α-factor for all biowastes are in the range of 0.958-0.960. These values are similar to those reported results of Prins and Neira et al [72, 77]. Leaving products from the Fischer-Tropsch reactors behave as two different phases, i.e., an organic liquid phase with heavy hydrocarbons, and a more significant gaseous phase with water and medium/light hydrocarbons. The objective diesel fraction is, however, split between both phases. Two approaches have been analyzed in order to concentrate the diesel fraction in one phase, i.e., expansion to redirect the diesel fraction to the gaseous phase or cooling to condensate diesel together with the liquid fraction. The first approach is an energy-intense process whereas the second approach offers the possibility of effectively removing the water content (see Table 3-7) with little energy consumption.

Accordingly, after the Fischer-Tropsch reactor, products are cooled down to 5°C in order to separate the tail gas from the liquid hydrocarbons and water, thus concentrating the diesel fraction in the liquid phase (see Figure 0.14, Appendix E). Tail gases could be either burned in a combined cycle or recycled back to the reformed in order to obtain more building agents (i.e., CO and H_2) and, ultimately, synthesize extra hydrocarbons. However, the first configuration is selected as previous studies from our own research group concluded that the combined cycle option turned out to be the most economic alternative [77]. Consequently, tail gas is firstly sent to a Selexol unit to remove most of the CO_2. In this case, Selexol is preferred over the conventional amines system as Selexol technology is more suitable for high pressures (i.e., 23 bar). Subsequently, part of the hydrogen contained in the gas stream is removed by means of a Pressure Swing Absorption (PSA) unit. This hydrogen will be

consumed in a downstream hydrocracker, as detailed below. Remaining tail gas is finally sent to the combined Brayton-Rankine cycle, which consists of one gas turbine at 23 bar and one single steam turbine at 50 bar.

The liquid phase containing water and hydrocarbons can be easily separated in a liquid-liquid decanter, in which water and the organic phase are recovered from the top and the bottom part of the equipment respectively [78]. After this operation, waste water is send to a water treatment unit (not included in our design) whereas the organic hydrocarbon fraction is expanded and further upgraded in order to meet the specifications of Table 3-7. Basically, the upgrading section consists of 4 atmospheric distillation columns, several flash vessels, one wax hydrocracker and the necessary auxiliary equipment to accomodate the optimal operations conditions before entering those columns (see Figure 0.14, Appendix E). Following the *chemical rules of thumb*, first distillation column is dedicated to separate the lighter hydrocarbons (C3-C18) from the largest stream (i.e., waxes C19+). In a second column, diesel (C12-C18) is recovered from the bottom part of the equipment, whereas the distillate (C3-C11) is further cooled and split in a flash vessel. The gas phase (C3-C6) is also burned to produce electricity in the combined cycle, whereas the resulting liquid phase (C5-C11) can be sold as synthetic gasoline. Waxes leaving the first distillation column are hydrocracked with the hydrogen recovered in the aforementioned PSA unit. The hydrocracker unit is simulated as a RYIELD reactor whose specifications are taken from Sudiro et al [78]. Unconverted hydrogen is send back to the hydrocracker in order to maximize diesel production. Resulting product streams are diesel (80 wt%), gasoline (15 wt%) and light gases (5 wt%). Those fractions are separated with the subsequent third and fourth column. Light gases are also send to the combined cycle.

3.4.4.   *Hydrogen for Fuel Cell Vehicles (FCV)*

Hydrogen can be produced from different sources, ranging from hydrocarbons, water or even biomass. Nowadays, the main processes for hydrogen production are steam-methane reforming (SMR) and/or catalytic decomposition of natural gas (48%), partial oxidation of heavy crude oils (30%), coal gasification (18%) and electrolysis of water (4%) [79]. Hence, about 96% of the hydrogen is produced from fossil fuels, emitting more than 300 Mtn/year of CO_2. In other to overcome this major environmental problem, recent investigations are focus on developing more sustainable technologies. Hydrogen production from biomass gasification and further catalytic conversion is one of the potential renewable alternatives that is being analyzed in several European projects such as the CHRISGAS (Värnamo, Sweden) [80] and AER GAS-II (Gussing, Austria) [81]. However, bio-based hydrogen synthesis is still far from being commercialized.

In 2005, global fossil hydrogen production already achieved 5×10^{11} Nm^3 per year (i.e., 44.5 Mtn/yr), whose main applications were found in ammonia production (50%), petroleum refining (37%), or methanol and chemicals synthesis (13%) [82]. Recently, hydrogen is also seen as one of the key transport fuels in the long-term, especially for its use in fuel cell vehicles (FCV). For instance, the U.S. Department of Energy (DOE) estimates that, by 2040, the world energy demand of hydrogen use in fuel cell

powered cars and light trucks will be approximately 150 Mtn/year [82]. Meantime, Linde has created the world's first hydrogen filling station using 700 bar technology for the Adam Opel AG, which represents an important milestone in the course of a hydrogen-powered car society. However, hydrogen is still comparatively expensive to produce and deliver, and it also has to overcome some technical barriers for its distribution and end-use. In particular, major concerns are derived from the need of assuring high pressures in the filling stations, i.e., 350-700. Another obstacle is that, unlike natural gas, hydrogen pipelines are less developed in Europe (i.e., 1,500 km of low pressure hydrogen pipelines vs 25,094 km of gas pipelines only in Germany). Hydrogen can also be transported by means of liquid or gas tube trailers. In the first case, hydrogen needs to be liquefied prior to transport, thus incurring in considerably high prodution costs. Gas tube trailers avoid the need of a liquefaction plant, but the amount of transported hydrogen per truck is notably lower. While both truck options are more convenient for small-medium hydrogen demand, they are not considered in our research as total expected biohydrogen production is relatively large. Hence, we assume that, by 2020, a more developed hydrogen pipeline will be already available in Europe.

Figure 3.8 illustrates the block diagram of the projected biomass-to-H_2 process. The Aspen Plus flowsheet is attached in Appendix G. The gasification and downstream cleaning units are similar to those used for the SNG production. A Battelle-type steam-blown gasifier is selected as more hydrogen is obtained when steam is the gasifying medium.
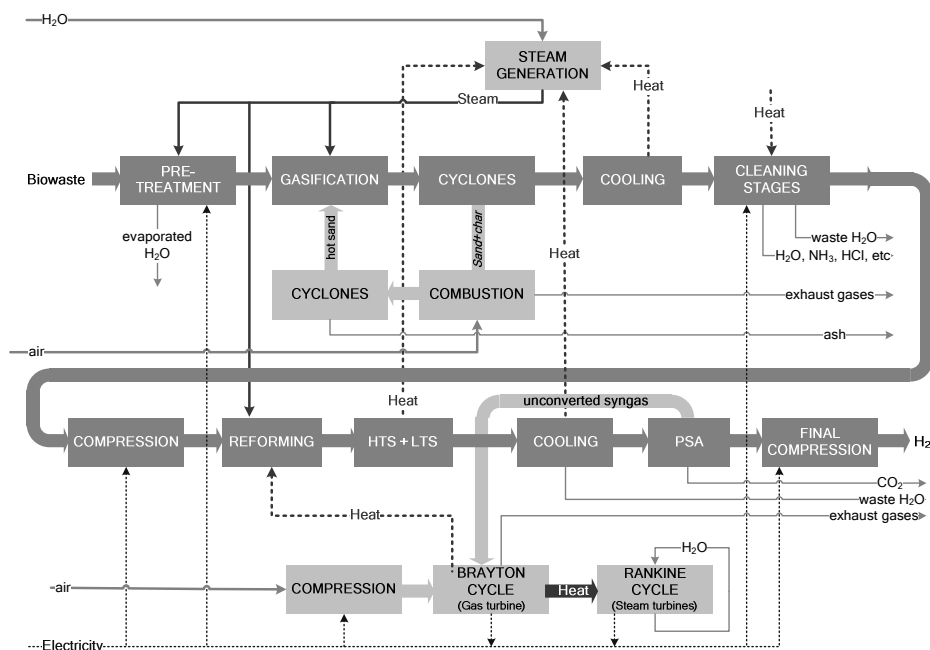

Figure 3.8: *Schematic block diagram for the hydrogen production. Main inlet and outlet streams are indicated. LTS and HTS refer to low and high temperature water-gas-shift reactors, and PSA to a pressure swing adsorption system. Detailed Aspen Plus flowsheet is attached in Appendix G.*

After the cleaning stages, the syngas is compressed and send to a reformer unit that is driven by steam addition over a Ni-based catalyst and operated at 35 bar and 850°C. In the reformer, methane, tars and light hydrocarbons are reconverted to CO and H_2. This process is similar to the catalytic steam reforming of natural gas, but in this case, the steam to carbon ratio is fixed to 3.5 as a small fraction of lighter hydrocarbons are also present. The reforming reactions are strongly endothermic, so the forward reaction is favored by high temperature and low pressure, although elevated pressures benefit economically [50, 83]. The governing reactions are described by the reverse of Eqs.(3-6) and (3-7) and the following reactions (3-21) to (3-22):

$$C_2H_4 + 2H_2O \leftrightarrow 2CO + 4H_2 \qquad \Delta H^o_{298} = +210 \ kJ \, / \, mol \qquad (3\text{-}21)$$

$$C_2H_6 + 2H_2O \leftrightarrow 2CO + 5H_2 \qquad \Delta H^o_{298} = +347 \ kJ \, / \, mol \qquad (3\text{-}22)$$
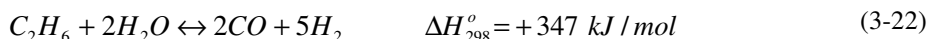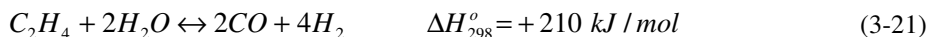
A significant portion of the WGS reaction also takes place (i.e., Eq.(3-10)) and it brings the reformer products to chemical equilibrium [84]. The reformer is modeled as a RGIBBS reactor, where the inlet stream is preheated with the hot stream leaving the unit so as to reduce the external heat supply. Remaining heat is supplied by the hot flue gas leaving the combustor of the combined cycle placed downstream. After reforming, hydrogen content of the syngas can still be increased by using a WGS process. Unlike the reforming reactions, the WGS shift reaction is moderately exothermic, favored by low temperatures and it is not affected by pressure [49, 50]. However, under adiabatic conditions, complete conversion in a single bed catalyst is not possible due to thermodynamic limitations. Therefore, two subsequent high temperature (HTS) and low temperature (LTS) shift reactors with intercooling are placed to assure maximum conversion of CO [49, 50, 85]. Both reactors are simulated as stoichiometric RSTOIC reactors and the operational conditions for the first (HTS) and second (LTS) shift reactor are 435°C and 30 bar, and 220°C and 25 bar respectively, whereas the corresponding catalysts are Fe_3O_4-Cr_2O_3 (HTS) and ZnO-CuO (LTS). Copper catalysts are more prone than iron catalysts to deactivation by sulfur compounds [49]. Hence, the cleaning stages are designed to meet the requirements of the copper catalyst of the LTS.

Subsequently, the hydrogen-rich syngas is cooled down to remove most of the water and, finally, it is purified in a Pressure-Swing-Adsorption unit (PSA). This PSA process is based on the difference in adsorption behaviour between different molecules, i.e., it separates components of a gaseous stream by a selective adsorption over a solid at high pressure, and subsequent desorption unit containing zeolite molecular sieve operated at low pressure. Adsorption and desorption takes place in 2 separate beds, so that the process can be run continuously [50, 84, 85]. About 85% of the H_2 is recovered and a purity of 99% is achieved. However, this system has the limitation that the inlet stream must contain at least 70 mol% of H_2. Therefore, whenever the hydrogen concentration is lower, a recycle is incorporated to achieve the minimum level. Unconverted syngas is burned to produce electricity and heat for the plant. Purified hydrogen is finally compressed to 70 bar for its distribution via low pressure pipelines. Hydrogen is further compressed to 350-700 bar in the filling-stations prior to their use in fuel cell cars, being *Proton Exchange Membrane* (PEM) the most researched fuel cell type.

Fuel cells can be poisoned by different types of compounds [55]. Because of the differences in electrolytes, operating temperatures, catalysts and other factors, the same compound can behave differently in other fuel cells. Nevertheless, the major poisons for all types of fuel cells are sulfur-containing compounds such as hydrogen sulfide (H_2S) and carbonyl sulfide (COS). Sulfur compounds are naturally present in all fossil fuels, and small quantities remain after normal processing and must be almost completely removed before entering the fuel cell. Precisely, in the case of biomass gasification, sulfur compounds are removed in cleaning stages by absorption with a MDEA solution.

3.4.5. Electricity and its potential use in road transport

3.4.5.1. Electricity generation in new BIGCC plants

The fifth conversion path of Figure 3.4 refers to electricity generation by means of an *Integrated Gasification Combined Cycle* (IGCC) process. The concept is similar to the one applied in already existing IGCC (Integrated Gasification Combined Cycle) plants based on coal and, more recently, on biomass (BIGCC). The major benefit of this concept compared to traditional pulverized coal combustion plants is that they attain higher efficiencies, i.e., 40-50% (electrical) or 85-90% (overall) compared to 20-40% (electrical) or 80-88% (overall) for actual coal combustion sites [80]. A higher efficiency is also translated into a 20% reduction of CO_2 emissions per unit of electricity generated [9]. Moreover, since in the IGCC process purities are removed prior to combustion, the overall environmental impact is further reduced. However, the high cost of IGCC is the biggest obstacle to its wider integration into the power market.

The world's first BIGCC demonstration plant was built in Värnamo (Sweden), although it was mothballed after 6 years of operation in 1999, and later reconverted to synthesize other biofuels under the European project CHRISGAS [80]. The power and heat generation of this plant was $6MW_e$ and $9MW_{th}$ respectively, with an electric efficiency (η_{el}) of 32% and a total net efficiency (η_{net}) of 83%. New generation BIGCC plants with better efficiencies are also under development in order to become more cost effective. In particular, emphasis is given to design modified gas turbines that can use gaseous fuels with lower calorific value.

A more detailed block diagram of our BIGCC process is given in Figure 3.9, whereas the corresponding Aspen Plus simulation is included in Appendix H. The process is designed to maximize electricity production at the expense of using all hot streams for that purpose. Hence, residual heat from the Brayton cycle is fully recovered to produce extra superheated steam for the Rankine cycle. Accordingly, generation of low-temperature heat for district heating is here disregarded as, from a thermodynamic point of view, it is the least effective form of biomass use. In effect, other technologies can fulfill district heating requirements in a more effective way (e.g., solar energy or geothermal). Pre-treated biomass is send to a pressurized air-blown gasifier, which operates at 15 bar and at a temperature of 900°C. The advantage of incorporating a gasifier is to convert solid and liquid residual fuels into a form that downstream gas turbines can accept.
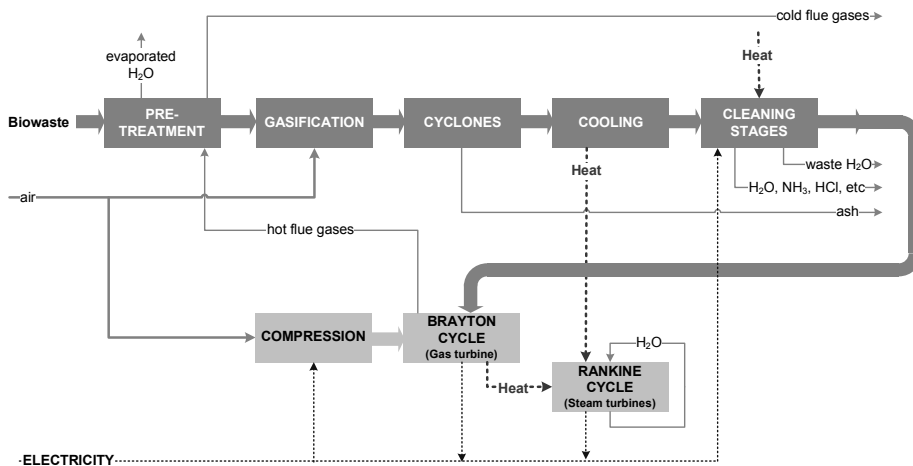
Figure 3.9: *Schematic block diagram for electricity generation following a BIGCC concept. Main inlet and outlet streams are indicated. Aspen Plus simulation is included in Appendix H.*

As for all the previous processes, gases leaving the gasifier are cooled down and send to the corresponding cleaning units in order to remove sulphur and nitrogen compounds, i.e., the precursors of acid rain and photochemical smog. The low temperature and oxygen deficient conditions of the gasifier do not favor NO_x and SO_x generation but the reduced forms NH_3 and H_2S are inevitably produced. Whenever the cleaning stages were not incorporated to the process, these two compounds would be further converted to SO_x and NO_x after combustion, the latter contributing to 75-95% of the total NO_x released. The remaining amount of nitrogen compounds would originate from the injected air. Heat removal from syngas cooling is partly used to provide heat for the reboilers of the cleaning unit and even generate superheated steam that will be expanded in downstream Rankine cycles. Clean syngas is then fed to the Brayton-Rankine combined cycle. As aforementioned, this residual mild-hot stream is further cooled to generate extra superheated steam for the Rankine cycle. Air mass flow entering the combustion chamber is regulated to assure complete combustion and control that the temperature of leaving gases does not exceed 1,300°C. The Rankine cycle operates with 3 turbines with inter-heating, working at different operational onditions. A condenser is incorporated to return saturate water at its initial temperature of 38.9°C.

Maintenance of the gas turbine is critical for the performance of the IGCC process. The lifetime of the turbine can be shortened due to erosion and high temperature corrosion caused by particles impact and impurities present in the flue gas such as alkali metals. The maximum tolerable concentrations set by the turbine manufacturers are taken into account in the cleaning stages of our simulations [86].

3.4.5.2.   *Electricity generation in biomass/coal cofiring plants*

Biomass/coal cofiring is seen nowadays as another alternative for increasing the share of renewable sources in the electricity market. *Cofiring* refers to the combustion of two different feedstock in equal or separate devices, and it is applicable to any traditional combustion system used for power generation (i.e., pulverized fuel firing,

fluidized beds,or grate firing). One of the advantages of cofiring systems is that they represent one of the most economic and shortest-term alternatives for reducing CO_2 emissions in existing coal power plants. In fact, biomass cofiring only requires a relatively modest capital investment, typically in the range of $50-$300 per kW of biomass capacity [87]. However, it does not necessary imply that cofiring is the most environmentally convenient alternative for biomass utilization.

Basically, there are three state-of-the-art systems, i.e., **direct**, **parallel** or **indirect cofiring**. In the direct cofiring systems, combustion of both fuels takes place within the same boiler, thus mixing coal and biomass ashes. Conversely, in the parallel option, biomass and coal are burned in separate boilers with physically independent feeding and ash removal systems. In the third indirect configuration, fossil fuel is burned with previously gasified biomass and, hence, coal and biomass ashes are also removed in different parts of the processes. In fact, ash removal and quality is one the most important constraints for increasing the share of biomass in cofiring systems. Ash melting temperatures of many biomass sources are normally lower than coal due to their high alkali metal, calcium or iron content. This feature may cause several problems such as slagging and fouling in the burners, furnace walls or superheaters. Other problems that may arise are related to the different grindability of biomass and coal, or the diverse combustion behaviour of both fuels [42]. The relatively high chlorine and potassium content, as well as the low bulk density of straw and other herbaceous feedstock may result in higher chances of slagging and fouling together with deposit accumulation and rapid corrosion rates. Nevertheless, straw is still used for energy purposes in some European countries, notably Denmark.
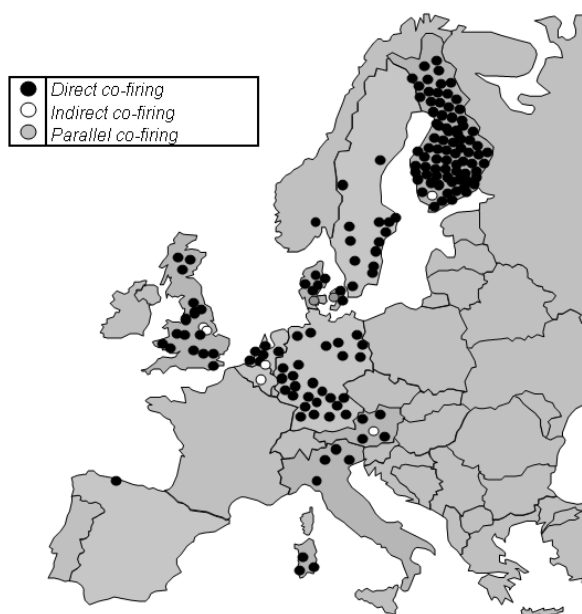
Figure 3.10: *Location of existing cofiring heat and power plants within Europe. The number and type of cofiring option (i.e., direct, indirect or parallel) is taken from the NetBioCof database [88].*

Among all, direct cofiring is by far the most implemented configuration in European coal-fired power plants (see Figure 3.10), accounting for more than 150 plants with total electrical and thermal capacities of 35 GW_{el} and 22 GW_{th}. In direct systems, the maximum share of biomass in the fuel blend is less than 5-10 wt% (i.e., 3-6% on energy basis). Higher ratios would imply boilers modification with the inherent increase in capital investment. Later analyses (see Chapter 8) compare the two alternatives for electricity production from biomass, i.e., building new BIGCC plants or cofiring biomass in existing power stations.

3.5. *Biofuels distribution and final application*

After production, biofuels are distributed as shown in Figure 3.11. Gaseous biofuels such as SNG and Hydrogen are distributed via pipelines, although the infrastructures have to be enlarged or built for the case of hydrogen. Methanol is transport by means of tank trucks that cover a similar distance than the rest of biofuels, i.e., 200 km. FT-fuels are also transported in tank trucks, but we assume that the first 50 km can be covered with existing oil pipelines, in a similar way as in the report of Van Bibber et al [89]. Bioelectricity is simply injected to the national grid system.
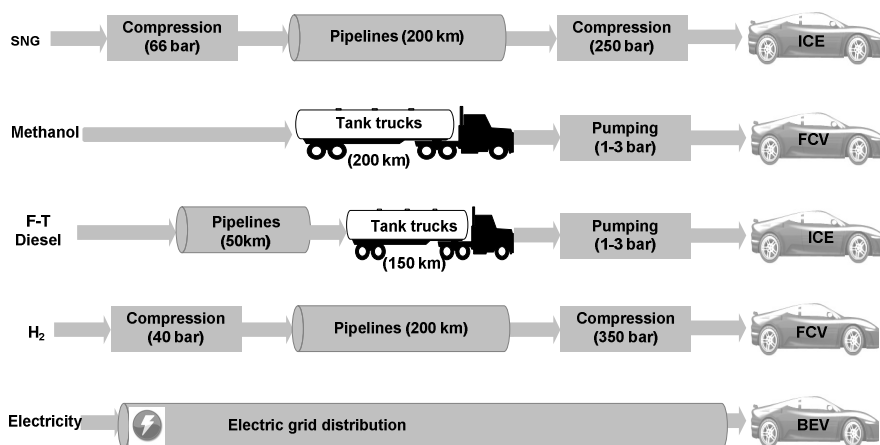
Figure 3.11: Distribution system for each produced biofuel and bio-electricity.

3.6. *Conclusions*

In this chapter, the design and modeling of five 2nd generation biofuels routes have been proposed: SNG, methanol, FT-fuels, hydrogen and bioelectricity. Those 5 processes have several common units (i.e., pre-treatment, gasification, cooling, gas cleaning and H_2/CO ratio adjustment), although the operational conditions are different among them. Specific downstream catalytic reactors synthesize the required biofuel, whereas the final upgrading section assure that the produced biofuel has the same quality as fossil fuels. Moreover 4 different plant configurations have been

defined in order to supply the heat and electricity demand of the production processes. For the '*NG-100*' and '*bio-100*' layouts, heat and electricity is supplied by burning either natural gas or and extra biomass amount whereas for the '*NG&grid*' and '*bio&grid*' options, electricity is simply taken from the local grid. Biomass cofiring in existing coal power plants would be also evaluated in later Chapter 8 for its application in the European energy sector.

4

Extended efficiency analysis of biomass-to-biofuels and bioelectricity chains

Abstract

Biofuels production efficiency based on the 1st Law of Thermodynamics has already been calculated by several authors. However, direct comparison among studies could lead to certain misjudgement as they differ in plant design and scale, inclusion of utilities consumption or even efficiency definition. There are less studies following the exergy approach, which is based on the 2nd Law of Thermodynamics, than on the energy efficiency based on the 1st Law. This method is reported to be more accurate for efficiency evaluation and optimization as it takes into account the degradation of the energy quality. In this chapter, we present the evaluation of biofuels production stage following traditional energy efficiency and the latest exergy methods. Moreover, the analysis is further extended to calculate the overall chain efficiency (i.e., from biomass collection to final biofuel use) from a WTW perspective. Results reveal that bioelectricity is found to attain the highest WTW efficiency (i.e., 17-19%), which is slightly above the one of oil-based vehicles (i..e., ~16-18%). H_2 turns out to be the second best alternative (i.e., 14-15%), whereas MeOH is the least efficient chain (i.e., 4-6%). SNG and FT-fuels systems yield similar efficiencies (i.e., 9-11%).

4.1. *Introduction*

The constraints on energy security and, more recently, the Kyoto protocol incentives have boosted the utmost importance of energy efficiency policies. In January 2007, the European Commission proposed an Energy Policy, in which they endorsed energy efficiency improvement of at least 20% (in comparison with 1990's levels) by the year 2020. However, according to the current trends, this European target would not be fulfilled by 2020. In effect, IEA[5] specialists states that efficiency improvements of all energy sectors averaged 0.9% between 1990 and 2005, and that this efficiency gain was even lower than the 2% of the previous period 1973 to 1990 [90]. Increasing energy efficiency is also motivated by an expected reduction of GHG's emissions and operational costs. However, in some cases, this improvement can also imply substantial capital investment that can even prohibit the modification or erection of a new installation.

Therefore, emerging technologies for renewable sources should be evaluated towards enhancing energy efficiency at a reasonable 'sustainable' cost. For instance, second generation biofuels are expected to achieve higher overall efficiencies than the first generation [7, 91]. In particular, thermochemical conversion technologies (e.g., gasification) can even make use of a wider range of lignocellulosic materials and wastes. Hence, whole crops are consumed for biofuels production, which improves land area productivity and reduces GHG's emissions [7]. Moreover, plant production scales are projected to be higher, although, in general, existing facilities are still more expensive than the first generation alternatives. First generation biofuels also have the added drawback that can only convert edible crops, thus competing with food production.

With regard to the electricity market, advanced integrated gasification combined cycles (IGCC) attain higher efficiencies than combustion schemes (i.e., 35-45% versus 25-30%), but the initial capital investment is again comparatively larger. Solar and wind power achieve lower electrical efficiencies in actual devices. However, an opposite conclusion is drawn when the conversion efficiency of sunlight into chemical bioenergy via photosynthesis is taken into account (i.e., 0.5-1% [92]). Nowadays, commercial photovoltaic cells generate electricity with an efficiency of 10-20%, although values up to 25% have already been recorded in laboratories for crystalline silicone cells. According to the Beltz's law, the theoretical maximum power efficiency of any wind turbine design is 59%, but the most advanced wind turbines do not exceed 35-45%. When inefficiencies of other components are included (e.g., generator, bearings or power transmission), only 10-30% of the wind power is actually converted into usable electricity. On the other hand, hydroelectric power attains the highest electrical efficiency (i.e., 90%) and can be far less expensive than electricity generated from fossil fuels or nuclear energy. However, environmental concerns about the effects of reservoirs limit the development of economic hydropower sources.

---

[5] IEA: International Energy Agency

Consequently, a key challenge is to establish a simple methodology to properly evaluate the energy efficiency of any system. In literature, there are several definitions used for that purpose, although the most commons expressions are based on the *low* or *high heating values* (LHV or HHV) and the *exergy* concept. In general, energy efficiency can be defined as the ratio of energy production divided by energy consumption. The differences among analyses lay on the way of calculating both concepts (see section 4.2.2).

The aim of this chapter is to present the results obtained from the efficiency evaluation of five 2nd generation biofuels chains (i.e., SNG, methanol, Fischer-Tropsch fuels, H_2 and bioelectricity). In order to establish a fair comparison among the five routes, a unified system boundary is defined in Figure 4.1. Accordingly, the analysis is extended from biomass collection to final bioenergy use. Primary energy consumption for utilities and fuels production is also included in the overall calculation in order to follow a *life cycle analysis* approach. Different analyses are here presented chronologically, i.e., from early definitions found in literature to more recent exergetic efficiency and the corresponding results are later compared. Our motivation for comparing these different approaches is that one tool alone does not give enough information to draw conclusions.

4.2. *Methodology: Integration of all stages*

The results for the whole biomass-to-bioenergy chains are split in two sections, as shown in Figure 4.1. Firstly, the biofuels or bioelectricity production stage is presented separately in section 4.3 and compared with other values found in literature. This phase has been evaluated independently as it has the highest potential for improvement. For instance, we have performed an accurate heat integration exercise to reduce the consumption of external fuel and, thus, increase plant's efficiency.
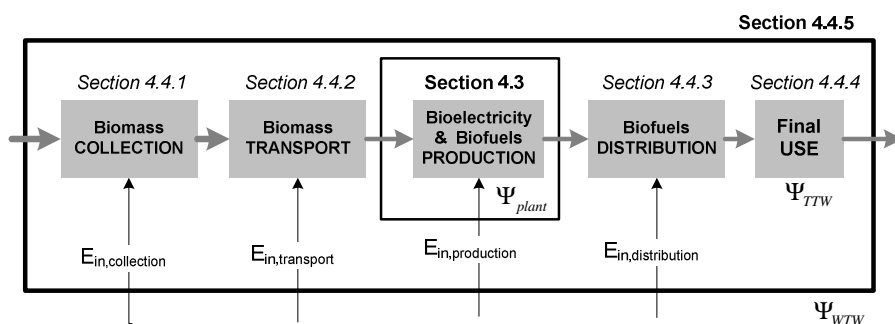
Figure 4.1: Biofuels production stage has been evaluated independently, and it has been later integrated in the analysis of the full biomass-to-bioenergy chain.

Moreover, we have also identified the optimal plant scale for each biofuel and bioelectricity. Results have been integrated in the whole chain in the subsequent section 4.4, to calculate the *well-to-wheel* (WTW) efficiency. The rest of stages (i.e., *collection*, *transport* and *distribution*) merely consume energy. For the sake of simplicity, we assume that tractors and trucks run on a similar diesel engine.

4.2.1.   Mass and Energy Balances

All the analyses start from the mass and energy balances obtained from our model and Aspen Plus simulations [39]. Those balances verify whether all the flows have been included and balanced (see Figure 4.2). These balances are also needed for later mass conversion, energy efficiency and exergy analysis. The energy balance of a control region can be described with the following expression derived from the 1st Law of Thermodynamics, which applies for the principle of energy conservation in a closed control region:

$$\sum_i E_{i,in} - \sum_j E_{j,out} = 0 \tag{4-1}$$

where E_{in}, and E_{out} are the summation of energy flows entering and leaving the system. Eq.(4-1) can be rewritten as the subsequent Eq.(4-2).

$$\left(Q_{in} - Q_{out}\right) + \left(W_{in} - W_{out}\right) + \left(\sum_i m_{i,in} \cdot \left(h + \frac{c^2}{2} + gh_e\right)_{i,in} - \sum_j m_{j,out} \cdot \left(h + \frac{c^2}{2} + gh_e\right)_{j,out}\right) = 0 \tag{4-2}$$[6]

where Q_{in}, Q_{out}, W_{in} and W_{out} are heat and work inlet and outlet flows respectively. Specific enthalpy, kinetic and potential energy associated of mass flows entering and leaving the system are represented by h, c and gk symbols, being g the gravity and h_e the elevation height. Kinetic and potential energy contribution can be neglected, leaving the energy balance as:

$$\left(Q_{in} - Q_{out}\right) + \left(W_{in} - W_{out}\right) + \left(\sum_i m_{i,in} \cdot h_{i,in} - \sum_j m_{j,out} \cdot h_{j,out}\right) = 0 \tag{4-3}$$[6]

Heat is primary consumed in the *production phase* for biomass drying, catalytic reactions or other downstream sections. In our simulations, this heat is supplied by burning natural gas or an extra amount of biomass (i.e., '*NG&grid*' and '*bio&gtrid*' plant configurations in Figure 3.1). Additionally, electricity demand of the processing plants can also be covered by burning a higher amount of natural gas or biomass (i.e., '*NG-100*' and '*bio-100*' options).

According to Hovelius et al, machinery and plant construction represents less than 10% of the total energy expenditure [93]. Hence, this stage is excluded in the energy efficiency evaluation, although it has been considered for the environmental impact evaluation in Chapter 5.

---

[6] The 3rd term in brackets should be divided by 10^3 when using the units of the Nomenclature.
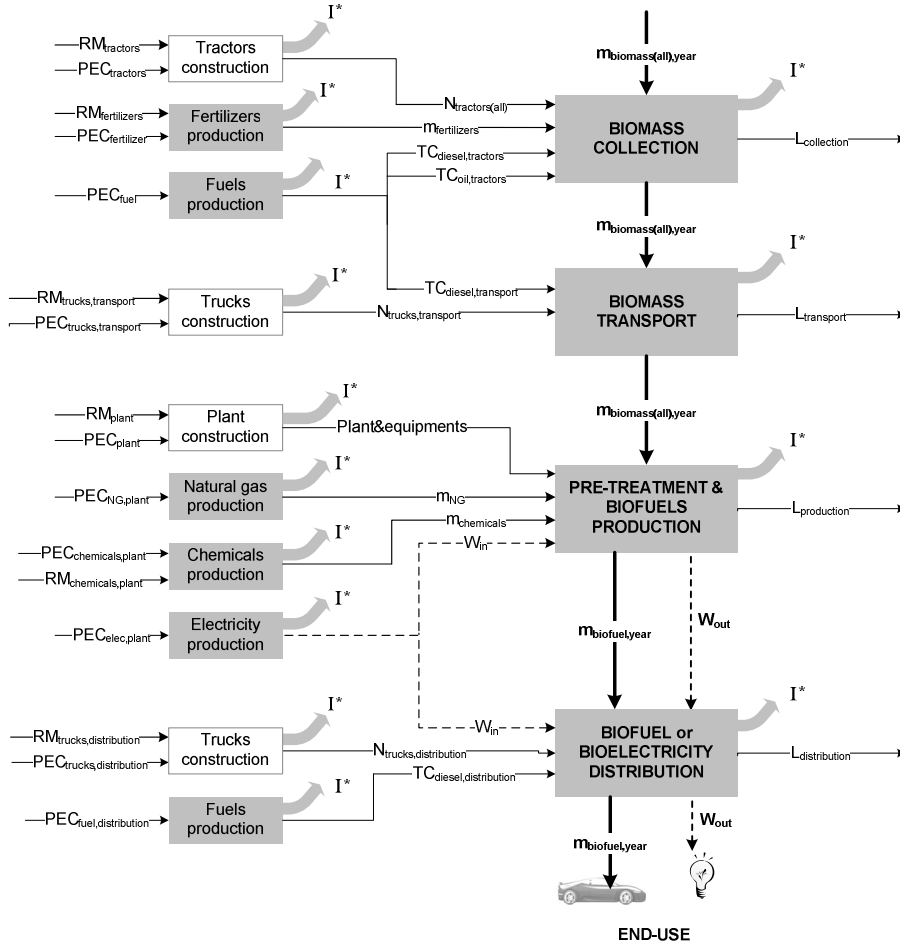
Figure 4.2: Identification of the mass and energy flows within the system boundaries. PEC accounts for primary energy consumption, whereas RM indicates raw materials use. Machinery production (i.e., white boxes) is excluded from the efficiency analysis as the energy expenditure represents less than the 10% of the total.

4.2.2.   Energy efficiency based on HHV

The energy efficiency of a process or system can be simply calculated as the ratio of useful energy divided by the total input. Since there is some controversy about the different energy definition found in literature, results are here presented following the two most common approaches. The first definition ($\Psi_{plant,1}$) indicates the ratio of total energy produced divided by total energy consumed, whereas the second approach ($\Psi_{plant,2}$ or $\Psi_{plant,2el}$) determines the ratio of the produced biofuel or bioelectricity divided by the net input.

$$\Psi_{plant,1} = \frac{m_{biofuel} \cdot HHV_{biofuel} + W_{out} + Q_{out}}{m_{biomass} \cdot HHV_{biomass} + \sum_{i=1}^{n} m_{fuel,i} \cdot HHV_{fuel,i} + W_{in}} \tag{4-4}$$

$$\Psi_{plant,2} = \frac{m_{biofuel} \cdot HHV_{biofuel} + Q_{out}}{m_{biomass} \cdot HHV_{biomass} + \sum_{i=1}^{n} m_{fuel,i} \cdot HHV_{fuel,i} + (W_{in} - W_{out})} \tag{4-5}$$

$$\Psi_{plant,2el} = \frac{(W_{in} - W_{out})}{m_{biomass} \cdot HHV_{biomass} + \sum_{i=1}^{n} m_{fuel,i} \cdot HHV_{fuel,i}} \tag{4-6}$$

where $m_{biomass}$, $m_{biofuel}$ and m_{fuel} is the mass flow of biomass, biofuel or fossil fuels (i.e., natural gas, diesel or lubrication oil), and HHV_i is their high heating values. The output heat flow (Q_{out}) accounts for the produced steam that can be sold. In most cases, this stream is relatively small or even zero, as a significant amount of the produced steam is used for the process itself. This parameter has been calculated by assuming that the output steam is cooled down to a vapor title (x_v) of 0.50[7].

$$Q_{out} = \left(m_{H_2O,v} \cdot Cp_{H_2O,v} \cdot (T - T_{vap}) + m_{H_2O,v} \cdot x_v \cdot \lambda_{vap} \right) \cdot 10^{-6} \tag{4-7}$$

where $m_{H2O,v}$ is the steam mass flow, $Cp_{H2O,v}$ is its specific heat capacity, T is initial temperature of the steam, T_{vap} is the vaporization temperature and λ_{vap} is the latent heat of water. The final WTW efficiency (Ψ_{WTW}) is calculated by means of Eq.(4-31) in the later section 4.4.5.

4.2.3.   Exergetic efficiency

Energy and exergy analyses are used to evaluate and compare the thermodynamic performance of different systems. The previous *energy efficiency analysis* is based on the 1st law of Thermodynamics, which is only concerned with energy conservation and treats all forms of energy as equivalent. Conversely, *exergy* is based on the 1st and 2nd law of Thermodynamics and it considers that, although energy cannot be created or destroyed, it can be degraded in quality. Hence, exergy can be defined as '*the maximum amount of work that can be produced by a system when it is brought into equilibrium with a reference state*[8]'.

The usefulness of an exergy analysis is that it quantifies the potential work that is lost within a process and it may help to identify and allocate the main losses. For example, an exergy analysis can be applied to minimize the use of natural resources. Hence, and in agreement with other authors [94, 95], we propose exergy analysis as a complimentary and more accurate method to evaluate the thermodynamic performance of a system. The main components of exergy are the *kinetic*, *potential*, *physical* and *chemical exergy*, although the kinetic and potential components can be neglected when calculating the exergy content of a process stream.

---

[7] This value has been selected arbitrarily to be able to calculate an approximate useful Q_{out}.
[8] The *reference state* is defined at standard temperature (T_o=25°C) and pressure (P_o=1bar), and the system of reference species covering all chemical elements. Some reference species include CO_2, O_2 and N_2, having a mole fraction of 0.003, 0.2099, 0.7903 in dry air, respectively.

4.2.3.1.   Chemical Exergy

Chemical exergy is defined at the reference state and it results from the deviation of composition in comparison with the components commonly existing in the reference state. The specific chemical exergy of a compound ($\varepsilon_{ch,i}$) is obtained from tabulated values of Szargut et al [96]. Streams of any chemical processes commonly consists of a mixture of different compounds and the corresponding chemical exergy ($\varepsilon_{ch,mix}$) can be calculated as follows:

$$\varepsilon_{ch,\,mix} = \left(\sum_i x_i \cdot \varepsilon_{ch,i} + \left(RT_o \sum_i x_i \cdot \ln(x_i) \right) \cdot 10^{-3} \right) \Big/ M_i \qquad (4\text{-}8)$$

where x_i is the molar fraction of a compound, M_i is the molecular weight, R is the universal gas constant and T_o is the reference temperature, which is set to 25°C in our analyses. The second term of this equation is identical to the specific Gibbs energy of mixing at T_o. The previous Eq.(4-8) can be applied to calculate the chemical exergy of standard or pure chemical compounds. However, these equations are not useful for more complex compounds such as biomass or wastes. In this case, the chemical exergy of biowastes ($\varepsilon_{ch,biowaste}$) is calculated from the statistical correlation (β) by the same author [96]:

$$\varepsilon_{ch,biomass} = z_{org} \left(\beta \cdot LHV_{org} \right) + z_S \left(\varepsilon_{ch,S} - C_S \right) + z_{water} \cdot \varepsilon_{ch,water} + z_{ash} \cdot \varepsilon_{ch,ash} \qquad (4\text{-}9)$$

where z_{org} is the organic mass fraction of biowastes, and z_S, z_{water} and z_{ash} are the mass fraction of sulphur, water and ash respectively. LHV_{org} is the LHV of the organic fraction and it is calculated from the Milne equation by only considering the organic fraction [25]. The coefficient β is defined as ratio of the chemical exergy to the LHV_{org}, and can be calculated from atomic ratios of oxygen, hydrogen and nitrogen depending on the biowaste stream as follows:

$$\beta_{woody} = \frac{1.0412 + 0.2160 \cdot \left(\frac{z_{H_2}}{z_C} \right) - 0.2499 \cdot \left(\frac{z_{O_2}}{z_C} \right)\left[1 + 0.7884 \cdot \left(\frac{z_{H_2}}{z_C} \right) \right] + 0.0450 \cdot \left(\frac{z_{N_2}}{z_C} \right)}{1 - 0.3035 \cdot \left(\frac{z_{O_2}}{z_C} \right)} \qquad (4\text{-}10)$$

$$\beta_{straw} = \frac{1.044 + 0.0160 \cdot \left(\frac{H}{C} \right) - 0.3493 \cdot \left(\frac{O}{C} \right)\left[1 + 0.0531 \cdot \left(\frac{H}{C} \right) \right] + 0.0493 \cdot \left(\frac{N}{C} \right)}{1 - 0.4124 \cdot \left(\frac{O}{C} \right)} \qquad (4\text{-}11)$$

Finally, chemical exergy of diesel and lubrication oil is calculated by the correlation (4-12) of Szargut et al [96], whereas chemical exergy of fertilizers and the exergy expenditure during their production is taken from Hovelius et al [93].

$$\varepsilon_{ch,fuel} = LHV_{fuel} \cdot \left(1.0374 + 0.0159 \cdot \frac{H}{C} + 0.0567 \cdot \frac{O}{C} + 0.5985 \cdot \frac{S}{C} \cdot \left(1 - 0.1737 \cdot \frac{H}{C} \right) \right) \qquad (4\text{-}12)$$

4.2.3.2.   Physical exergy

Physical exergy represents the energetic value due to deviation of temperature and pressure from the reference environment. The specific physical exergy of a compound ($\varepsilon_{ph,i}$) is calculated using enthalpy (h) and entropy (s) data for a given system:

$$\varepsilon_{ph,i} = \Delta h - T_o \Delta s = \left(h - h_o \right) - T_o \left(s - s_o \right) \tag{4-13}$$

where h_o and s_o is the enthalpy and entropy at the reference state (i.e, 25°C and 1 bar). The enthalpy and entropy are calculated from the specific heat capacity (C_p) of a compound. When the specific heat capacity (C_p) is dependent on the temperature, Eq.(62) is rewritten as follows.

$$\varepsilon_{ph,i} = \int_{To}^{T} C_p dT - T_o \int_{To}^{T} \frac{C_p}{T} dT + RT_o \ln\left(\frac{P}{P_o} \right) \tag{4-14}$$

The specific heat capacity (C_p) is calculated from the polynomial correlation of Barin [97] of type $C_p = a + bT + cT^2 + dT^3 + eT^4$. Values of the coefficients a, b, c, d, e for standard compounds are taken from the Aspen Plus library [39].

4.2.3.3.   Total exergy of a stream

The total exergy of a stream (E_i^*) is calculated as the sum of its chemical and physical exergy. Hence, for a stream consisting of a mixture of standard and the total exergy (is obtained via Eq. (4-15).

$$E_i^* = m_i \cdot \left(\varepsilon_{ch,mix} + \sum_i x_i \cdot \varepsilon_{ph,i} \right) \cdot 10^{-3} \tag{4-15}$$

4.2.3.4.   Exergetic efficiency

Different definitions are being used in literature to calculate the *exergy efficiency* of a process. Rational efficiency defined by Kotas [98] is selected in this chapter to compare the performance of all chains. Hence, the exergetic efficiency of a processing plant (Ψ^*_{plant}) is here calculated as the ratio of the desired exergy output (E^*_{out}) by the used exergy (E^*_{in}). Analogous to the previous energy efficiency in section 4.2.2, two defintions are given:

$$\Psi^*_{plant,1} = \frac{E^*_{out}}{E^*_{in}} = \frac{E^*_{biofuels} + E^*_{surplussteam} + W_{out}}{E^*_{biomass} + E^*_{chemicals} + \sum_{i=1}^{n} E^*_{fuels,i} + W_{in}} \tag{4-16}$$

$$\Psi^*_{plant,2} = \frac{E^*_{out}}{E^*_{in}} = \frac{E^*_{biofuels} + E^*_{surplussteam}}{E^*_{biomass} + E^*_{chemicals} + \sum_{i=1}^{n} E^*_{fuels,i} + \left(W_{in} - W_{out} \right)} \tag{4-17}$$

$$\Psi^*_{plant,2el} = \frac{E^*_{out}}{E^*_{in}} = \frac{\left(W_{in} - W_{out}\right)}{E^*_{biomass} + E^*_{chemicals} + \sum_{i=1}^{n} E^*_{fuels,i}}$$

(4-18)

where $E^*_{biofuels}$, E^*_{fuels}, $E^*_{biomass}$, $E^*_{surplus\ steam}$, and $E^*_{chemicals}$ are the total exergy of biofuels, fossil fuels, biomass, surplus steam and chemicals respectively.

4.2.3.5.   Exergy losses of a process (irreversibilities)

Unlike ideal processes, exergy is consumed during real processes and the corresponding exergy consumption rate is proportional to the entropy created due to process irreversibilities (I^*). Identifying irreversibilities within a process or system is compulsory when intending to optimize its thermodynamic performance. For that purpose, the Eq.(4-19) has been applied in each part of the process, ranging from biowastes pre-treatment to final upgrading of the biofuels:

$$I^* = \sum_{in} E^*_i - \sum_{out} E^*_j + E_{in}^{*Q} - E_{out}^{*Q} + W_{in} - W_{out}$$

(4-19)

where E_{in}^{*Q} is calculated from fuel burning and E_{out}^{*Q} is the exergy of surplus steam.

4.3. *Biofuel or bioelectricity production*

4.3.1.   Evaluation for a given biomass input

Results obtained from energy ($\Psi_{plant,1}$) and exergy efficiency ($\Psi^*_{plant,1}$) are here presented for a given biomass availability of 456 ktn/yr (i.e., ~ 57 tn/hr) in Figure 4.3 and Figure 4.4. This amount has been chosen as it corresponds to medium plant sizes and it would be available in all European countries with the exception of Ireland and Estonia. As aforementioned in Chapter 3, heat integration is performed in order to decrease the energy demand of the process. However, in some routes, external fuel is still needed to drive some units of the plant, including reformers, cleaning, pre-treatment or upgrading sections. This leads to the study of 4 plants configurations, as explained in Figure 3.1. For the '*NG-100*' and '*bio-100*' layouts, heat and electricity is supplied by burning either natural gas or and extra biomass amount whereas for the '*NG&grid*' and '*bio&grid*' options, electricity is simply taken from the local grid. It should be noticed that only two plant configurations ('*bio-100*' and '*bio&grid*') are defined for the FT-fuels process as the heat demand of the plant can be covered by burning some by-products that have a lower market value. Similarly, the bioelectricity plant only has one possible configuration ('*bio-100*') because the heat and electricity demand of the process is fully matched by heat integration. Accordingly, efficiency values for the '*NG&grid*' and '*bio&grid*' configurations will be always larger than their corresponding counterparts '*NG-100*' and '*bio-100*' as they do not include the inefficiencies related to electricity production. It should be mentioned that, although the '*NG-100*' and '*bio-100*' provide a better comparison because of including all inefficiencies, the '*NG&grid*' and '*bio&grid*' options are still evaluated separately to compare our results with literature (see section 4.3.3).
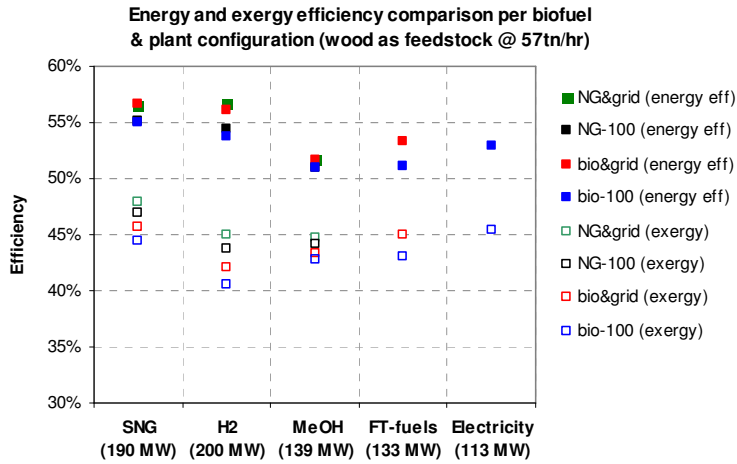
Figure 4.3: *Energy ($\Psi_{plant,1}$) & exergy ($\Psi^*_{plant,1}$) efficiency per biofuel & plant configuration, when woody streams (i.e., forest residues or lignocellulosic energy crops) are converted.*
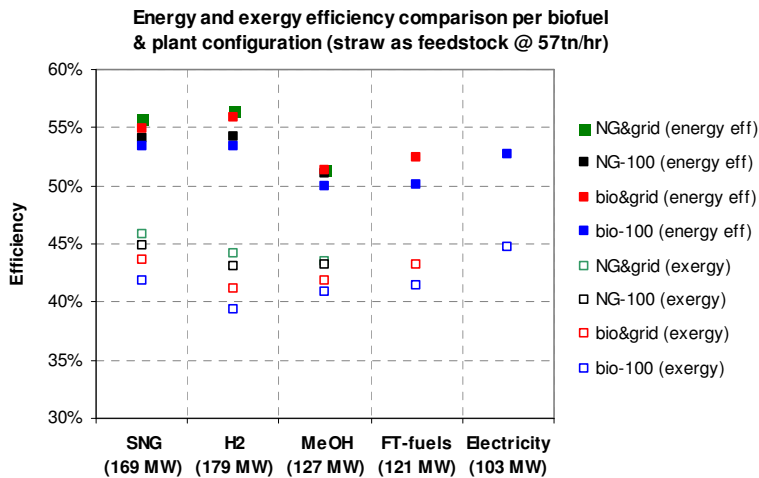
Figure 4.4: *Energy ($\Psi_{plant,1}$) and exergy ($\Psi^*_{plant,1}$) efficiency per each biofuel and plant configuration, when straw residues are converted.*

Exergy results ($\Psi^*_{plant,1}$) are lower than traditional energy efficiency ($\Psi_{plant,1}$) values. This is explained by the fact that the β-factor used to calculate the chemical exergy of biomass (see Eq.(4-9)) is always higher than 1, thus increasing the input ($E^*_{biomass}$) in the exergetic efficiency calculation (see Eqs. (4-16) to (4-18)). Another major difference is that the consumption of chemicals ($E^*_{chemicals}$) is also included in the exergy analysis. Conversely, their contribution is neglected in the energy efficiency equation as the calorific value of those chemicals is zero. Moreover, produced biofuels exergy ($E^*_{biofuels}$) is generally lower than their calorific content ($E_{biofuels}$). Disparity between exergy and energy effiency definitions has also some consequences on the ranking of biofuels, especially for those routes which are intense on heat and

electricity consumption. This is the case of hydrogen[9] which is found to be the least exergetic biofuel when heat and electricity demand is covered by biomass burning, whereas less differences are found when natural gas is used instead. Our previous calculations indicates that hydrogen would be the second most exergetically efficient biofuel if inefficiencies related to heat and electricity production were excluded from the evaluation [99], although this would not be a proper comparison.

On the other hand, hydrogen is the most efficiency biofuel when the comparison in based on traditional energy ratios ($\Psi_{plant,1}$) and for those configurations that exclude electricity production (i.e., '*bio&grid*' and '*NG&grid*'). A possible explanation for this 'new ranking' would be the relatively higher HHV value of hydrogen in comparison with its chemical exergy (i.e., 141 MJ_{HHV}/kg versus 118 MJ_{exe}/kg). Following the bio-100 plant configuration (see blue values in Figure 4.3 and Figure 4.4), bioelectricity production turns out to be the most exergetically efficiency route, but this position is relegated to SNG for the traditional energy efficiency ratio. It is also observed that MeOH yield lower rates than FT-fuels irrespective of the configuration and efficiency definition. Comparison among feedstock reveals that wood-fuelled plants are slightly more efficient than straw.

As detailed in sections 4.2.2 and 4.2.3, a second definition is applied for energy ($\Psi_{plant,2}$) or exergy efficiency ($\Psi*_{plant,2}$) calculation. Following this approach, lower efficiency values are obtained for all configurations and biomass streams. The extent of this decrease is found to be: ~2.5%-point for SNG, ~3.5%-point for H_2, ~6.0%-point for MeOH and FT-fuels, and ~10%-point for bioelectricity plants. Differences for bioelectricity production are particularly large because, unlike other biofuels chains, power is the only energy output. Conversely, the efficiency decrease is less marked for SNG and H_2 chains as their relatively higher biofuel output (i.e., 169-190 MW_{SNG} and 179-200 MW_{H2}) mitigates the effect of including the net power input in the denominator of Eqs.(4-5) and (4-17). Consequently, SNG becomes the most exergetic and energetically efficient route whereas bioelectricity is relegated to the lowest position. Moreover, exergy efficiency of hydrogen is now higher than MeOH.

4.3.2.   *Effect of plant scale on the production efficiency*

The analysis is further extended to determine the optimal plant size for biofuels and bioelectricity production. Accordingly, simulations have been scaled from 1 MW to 2000 MW and the corresponding energy ($\Psi_{plant,1}$) and exergy efficiency ($\Psi*_{plant,1}$) results are presented in Figure 4.5 to Figure 4.9. As observed, optimal '*efficiency*' scales are smaller for electricity and SNG processes (i.e., ~50 MW_{el} and ~200 MW_{SNG} respectively) than for the rest of the biofuels (i.e., ~ 300 MW_{H2} and ~500 MW_{fuel} for MeOH and FT-fuels). These trends are in line with the economic appraisal of Chapter 6 (see section 6.2.1.3). However, the optimal '*economic*' scales are notably larger for H_2, MeOH and FT-fuels as they need to compensate their relatively high capital investment (i.e., 500 MW_{H2} and 1000 MW_{fuel} for MeOH and FT-fuels). Electricity and SNG plants are found to be already profitable at smaller sizes (i.e., 100 and 200 MW_{fuel} respectively).

---

[9] Reforming and final compression @ 70 bar prior to H_2 distribution are some of the most energy intensive stages.
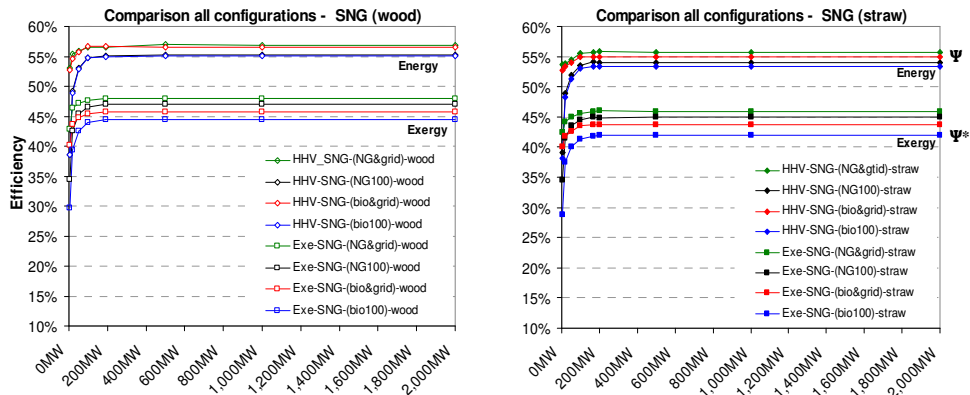
Figure 4.5*: Effect of plant scale on the energy ($\Psi_{plant,1}$) and exergy ($\Psi^*_{plant,1}$) efficiency of wood (left graph) and straw (right graph) fuelled SNG plants.*
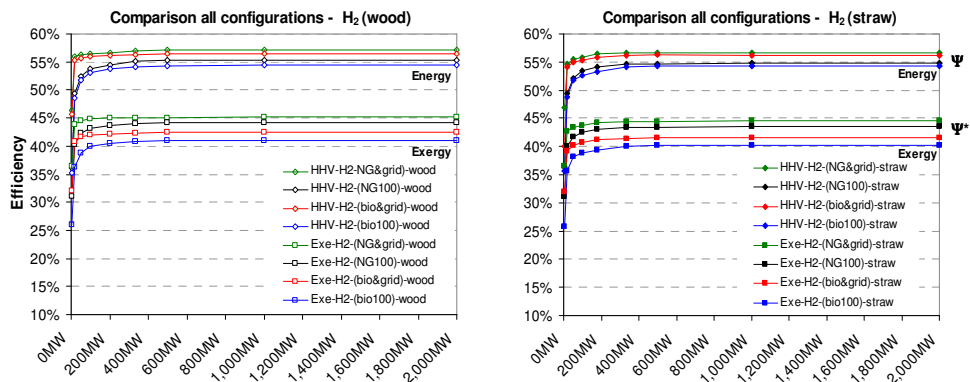
Figure 4.6*: Effect of plant scale on the energy ($\Psi_{plant,1}$) and exergy ($\Psi^*_{plant,1}$) efficiency of wood (left graph) and straw (right graph) fuelled H_2 plants.*
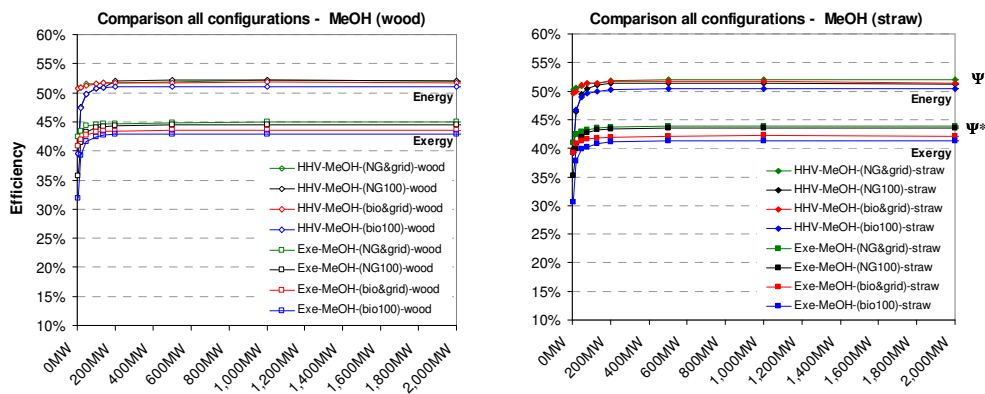

Figure 4.7*: Effect of plant scale on the energy ($\Psi_{plant,1}$) and exergy ($\Psi^*_{plant,1}$) efficiency of wood (left graph) and straw (right graph) fuelled MeOH plants.*
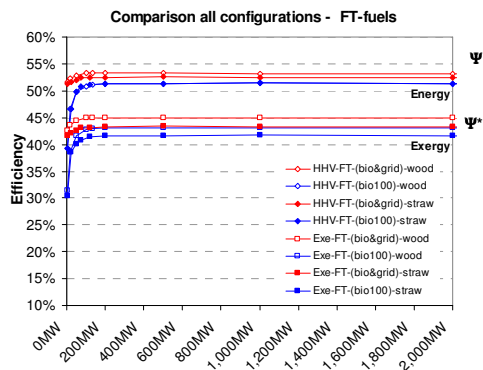
Figure 4.8: *Effect of plant scale on the energy ($\Psi_{plant,1}$) and exergy ($\Psi^*_{plant,1}$) efficiency of wood and straw FT-fuels plants.*
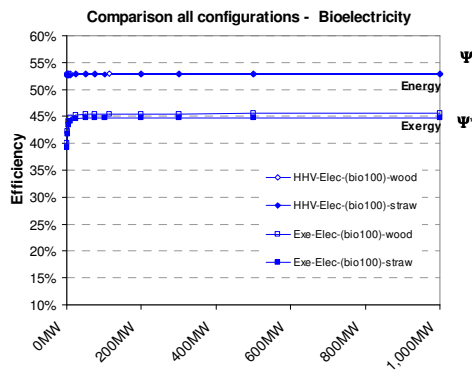
Figure 4.9: *Effect of plant scale on the energy ($\Psi_{plant,1}$) & exergy ($\Psi^*_{plant,1}$) efficiency of wood and straw fuelled-bioelectricity plants.*

The ranking of biofuels efficiency is similar as in the former section 4.3.1, although absolute values have changed, with the sole exception of wood-fuelled SNG and bioelectricity plants. In effect, the previous fixed biomass input of 57 tn/hr means that SNG and bioelectricity can operate at their optimal production scales (i.e., 190 MW_{SNG} and 113 MW_{el}). Hence, differences among the rest of the fuels are lower. Following the '*bio-100*' configuration, bioelectricity and SNG wood-fuelled plants attain exergetic efficiencies ($\Psi^*_{plant,1}$) of around 45.4% and 44.4% respectively. Corresponding values for FT-fuels and MeOH are rather similar (i.e., 43.1% and 42.9% respectively), whereas H_2 is again penalized by the compression requirements of the pipelines distribution system (i.e., 41%). Straw-based processes run at about 1-2% lower exergetic efficiency, being the largest differences found for the MeOH and FT-fuels plants. The rest of the plant configurations always imply smaller exergetic efficiencies, as shown in Figure 4.5 to Figure 4.9. Concerning energy efficiencies ($\Psi_{plant,1}$), differences among '*bio-100*' and the rest of plant configurations are less remarkable. For the 'bio-100' option, wood-based SNG and H_2 lead to the most efficient processes (i.e., 55.0 and 54.3%). However, similar efficiencies are obtained for the 'bio&grid' and 'NG&grid' configurations (i.e., ~ 57.0% for both biofuels). Bioelectricity plants run at 53.0% efficiency, whereas MeOH anf FT-fuels values are again rather close for the'*bio-100*' case (i.e., 51.4% and 51.0% respectively). Differences with straw-fuelled plants are in the range of 0.3-1.5 %, thus being less significant than those resulting from the exergetic evaluation.

For a complete evaluation, Eq.(4-19) has been applied to determine the main exergy losses (i.e., irreversibilities) within all biofuels and biofuels production chains. Corresponding figures are depicted in Figure 4.10 to Figure 4.14 only for wood-fuelled plants, although similar conclusions are drawn when straw is converted instead. Results show that the gasifier is the main contributor to the exergy losses, except for bioelectricity process where the combined cycle is the section with largest relative exergy losses. The electricity co-production cycle in other biofuel chains also represents an important share of exergy losses.
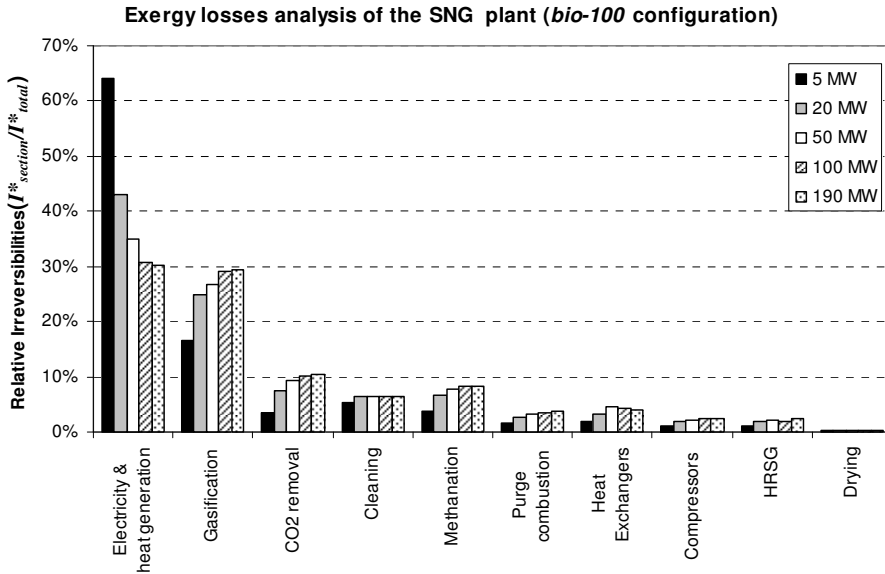
Figure 4.10: *Relative Irreversibilities (I*$_{section}$/I*$_{total}$) of the wood-to-SNG conversion plant. Total irreversibilities (I*$_{total}$) from plant scales of 5 to 190MW$_{HHV,SNG}$ are: 15MW$_{ex}$, 34 MW$_{ex}$, 73MW$_{ex}$, 135 MW$_{ex}$ and 254 MW$_{ex}$.*
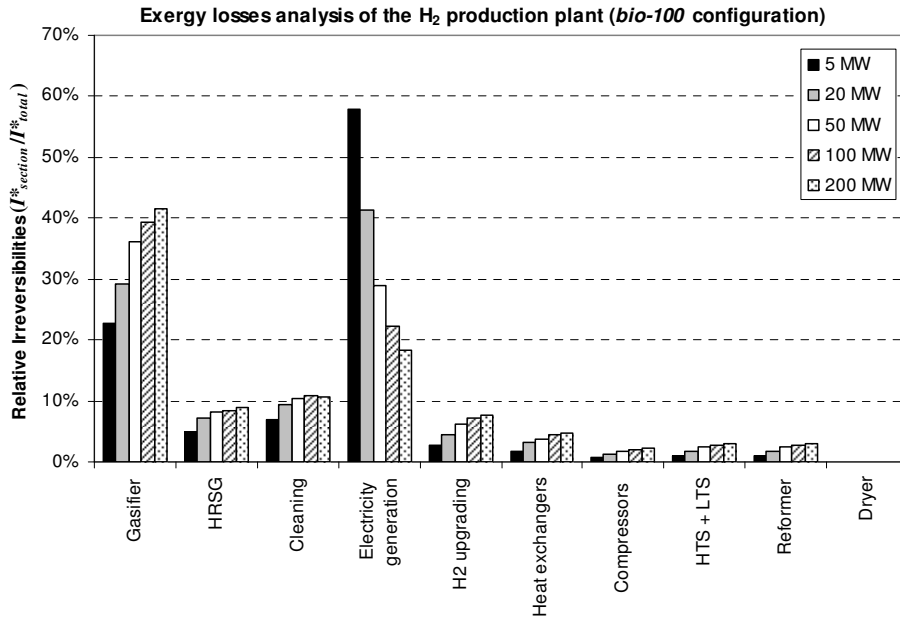
Figure 4.11: *Relative Irreversibilities (I*$_{section}$/I*$_{total}$) of the wood-to-H$_2$ conversion plant. Total irreversibilities (I*$_{total}$) from plant scales of 5 to 200 MW$_{HHV,H2}$ are: 18MW$_{ex}$, 38MW$_{ex}$, 82MW$_{ex}$, 155MW$_{ex}$ and 298MW$_{ex}$.*

Exergy losses analysis of the MeOH plant (bio-100 configuration)
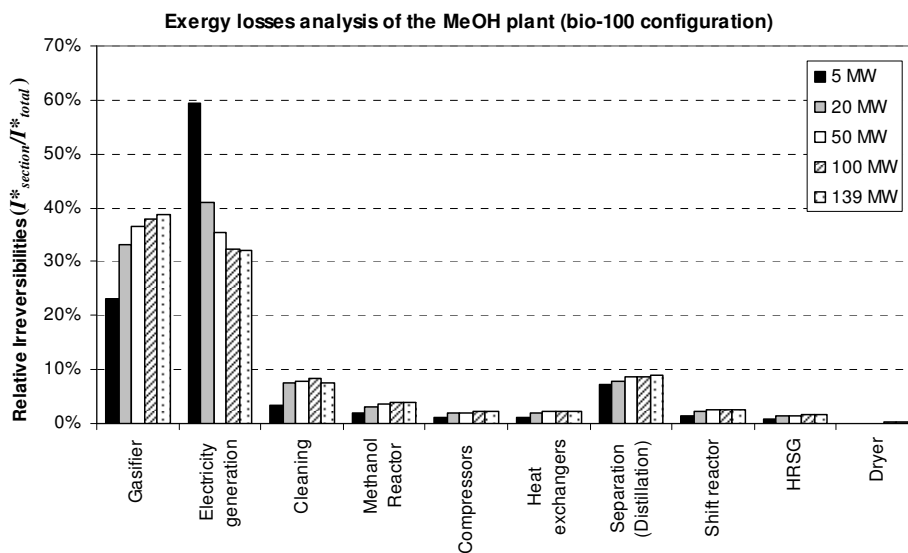
Figure 4.12: Relative Irreversibilities ($I^*_{section}/I^*_{total}$) of the wood-to-MeOH conversion plant. Total irreversibilities (I^*_{total}) from plant scales of 5 to 139 $MW_{HHV,MeOH}$ are: 17 MW_{ex}, 43 MW_{ex}, 95 MW_{ex}, 180 MW_{ex} and 246 MW_{ex}.

Exergy losses analysis of the FT plant (bio-100 configuration)
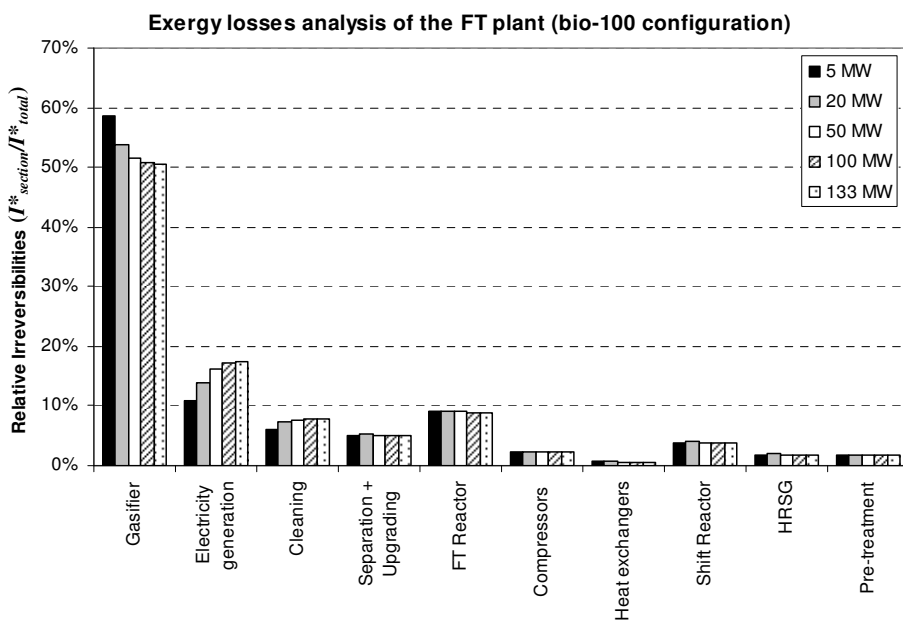

Figure 4.13: Relative Irreversibilities ($I^*_{section}/I^*_{total}$) of the wood-to-FT fuels conversion plant. Total irreversibilities (I^*_{total}) from plant scales of 5 to 133 $MW_{HHV,FT}$ are: 17 MW_{ex}, 43 MW_{ex}, 92 MW_{ex}, 173 MW_{ex} and 227 MW_{ex}.

Exergy losses analysis of the bioelectricity plant (bio-100 configuration)
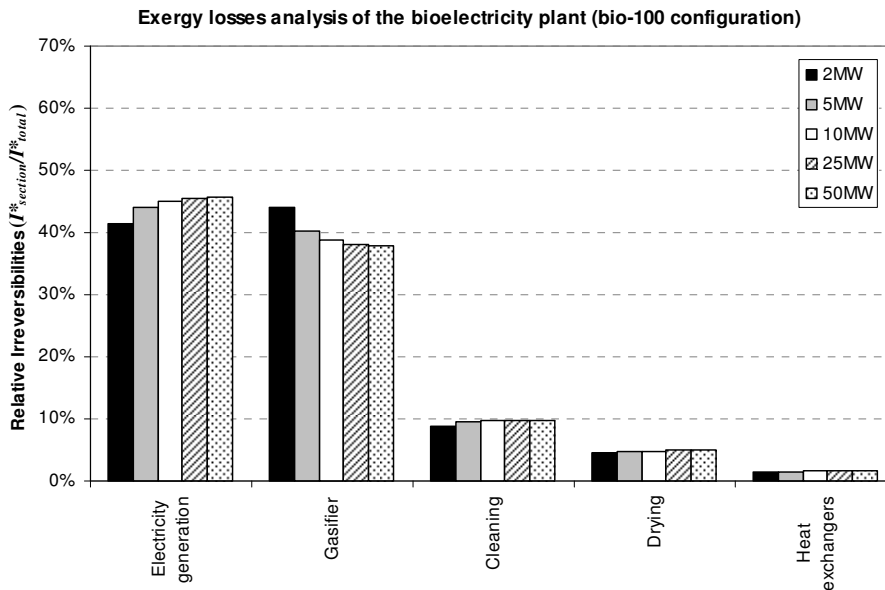
Figure 4.14: *Relative Irreversibilites ($I^*_{section}/I^*_{total}$) of the wood-to-bioelectricity conversion plant. Total irreversibilities (I^*_{total}) from plant scales of 2 to 50 MW_{el} are: 4 MW_{ex}, 10 MW_{ex}, 19 MW_{ex}, 46 MW_{ex} and 91 MW_{ex}.*

However, irreversibilites of these cycles can be still reduced by operating at different pressures of temperatures and improving heat integration. Cleaning stages (H_2S, NH_3 and CO_2 removal) are also an important source of irreversibilities which could be reduced by changing their operational parameters. Irreversibilities originated in the cleaning stages are more important for biowastes with a higher sulphur content (i.e., straw).

4.3.3.   Present efficiency results divergences with other studies

The present results are confronted with previous studies of other authors for woody streams. However, it is difficult to make a straight comparison as values found in literature correspond to processes that may differ in operational conditions, plant scale and/or configuration, gasifier design, heat and electricity consumption, as well as biomass composition. The efficiency definition is also different among studies. In effect some authors give the results according to our first or second definitions (i.e., Eqs.(4-4) or (4-5)), while others only apply the ratio of the calorific value of biofuel and biomass (i.e., $\Psi_{plant,3}=HHV_{biofuel}/HHV_{biomass}$). This third expression can lead to certain misunderstanding as it does not include heat and electricity consumption of the processing plant (i.e., values are notably higher than the first two definitions). The relatively large range of the values found in literature is a reflection of all these different assumptions and definitions (see Figure 4.15). Hence, the usefulness of our study is that all biofuels chains have been evaluated with a common baseline and efficiency definition. Moreover, the analysis has been extended to incorporate all the stages needed to produce a biofuel with the same quality as the fossil homologue, which incurs in extra heat and/or electricity consumption. Inefficiencies related to

utilities heat, steam or electricity production are also added to the efficiency calculation. This practice, however, is not carried out by some authors. Values for straw-fuelled plants have not been found in literature. Concerning SNG production, values from Duret et al [100] are in line with our calculated energy efficiency ($\Psi_{plant,1}$) for a similar '*bio&grid*' configuration (i.e., 54-58% versus 57%). Gassner et al [101] claim a higher efficiency (i.e., 63-69%) although they do not include the required final compression of SNG prior to its distribution via pipelines.
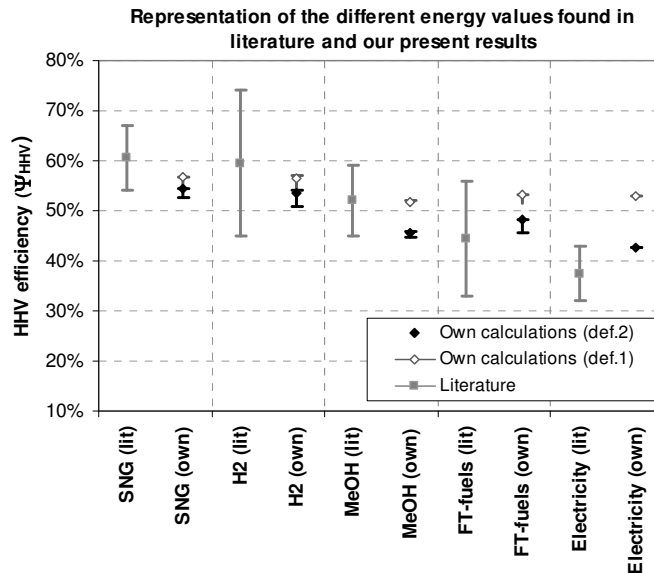
Figure 4.15: *Representation of the different energy efficiency values (Ψ_{HHV}) found in literature with our own data [7-9, 51, 52, 83, 84, 91, 100-105]. The range is relatively large for the same biofuel as different assumptions, plant design and definitions are used.*

Moreover, they assume that cleaning and CO_2 removal are neutral in thermal and electrical energy consumption whereas, according to our irreversibility analysis, both stages significantly contribute to efficiency losses (see Figure 4.10). Mozaffarian et al [51] calculated a calorific ratio ($\Psi_{plant,3}$) of 67%, which is closer to Gassner et al. However, this numer is not comparable with our results as they have not taken into account utilities consumption. Published values for hydrogen efficiency are even more diverse among them than those of SNG. Values from Katofsky et al [84] are at the same level that our calculations for the '*bio&grid*' configuration (i.e., 54-58% versus 56%), whereas estimations from Hamelinck et al [102] are more deviated (i.e., 56-63%). Both authors has a similar process scheme as our simulations (i.e., indirect gasifier design, upgrading stages and electricity co-production) although they do not include the final H_2 compression stage up to ~ 70 bar. Hamelinck et al also presume that efficiencies up to 74% can be reached with a pressurized oxygen-blown IGT (Institute of Gas Technology) gasifier and ceramic membranes for upgrading. Inefficiencies related to oxygen production should be added to the overall energy efficiency computation for a fair comparison. Wright et al [91] present a more conservative efficiency value for hydrogen production (i.e., 50%) because, unlike the

previous authors, this value corresponds to the second efficiency definition ($\Psi_{HHV,2}$). Same author claim similar $\Psi_{HHV,2}$ efficiencies for MeOH and FT-fuels plants (i.e., 46 and 47% respectively) which are in line with our estimates (i.e., 46% and 48% respectively). Boerrigter [103] find that biomass-to-FT fuels conversion can be done with a 56% efficiency, although he does not specify the efficiency definition used and whether the upgrading section is included. Other authors of the Utrecht University [52, 104] state a wider $\Psi_{HHV,1}$ efficiency range for different gasifier designs and growth probability chain factors (i.e., 33-50%), whereas Vogel et al [105] presume that entrained flow gasifiers could reach notably higher efficiencies than the CFB concept (i.e., ~70% versus ~40% respectively). Müller-Langer et al [7] also present a rather wide range of efficiency values for either FT-fuels or MeOH (i.e, 40-52%), whereas Williams and Hamelinck et al [83, 102] give similar results for MeOH production (i.e., 54-58% and 52-59% respectively).

Comparison of bioelectricity plants is more accurate as, unlike biofuels, electricity generation does not include any extra upgrading section. In effect, plants integrate a gasification unit with a conventional combined cycle. Moreover, values are normally based on the same first efficiency definition $\Psi_{plant,1}$. As observed in Figure 4.15, our results are rather high as we incorporate a pressurized gasifier, which is reported to yield higher efficiencies than atmospheric units. Our values are in line with studies from Marbe and Zheng et al [8, 9] (i.e., 42% versus 38-43%). Same author Marbe also calculated efficiencies of 33-38% for atmospheric gasifier.

Less studies are found for the exergy concept than for the energy ratio based on the 1st Law of Thermodynamics, as shown in Figure 4.16. In general, major differences are found for SNG and H$_2$ fuels because, as previously mentioned, cleaning, upgrading, final compression or even utilities production are frequently not included in the studies of other authors. Analogous to the energy efficiency (Ψ_{plant}) calculation of the SNG chain, Gassner et al [101] present higher exergy values (Ψ^*_{plant}) than our estimates (i.e., 63-69% versus 46% respectively). In case that heat is simply supplied by steam from nearby producers, our exergy value is increased up to 54% [24]. The remaining 10-15%-point difference with Gassner et al could be explained by the fact that we have also included the energy consumption of the cleaning, CO_2 removal and final compression units, which according to the irreversibility analysis, are significant sources of exergy losses (see Figure 4.10).

With regard to H$_2$ production, Toonsen et al [106] present exergy efficiencies in the range of 46%-51% for systems without heat recovery, and 63-66% when produced heat is included in the exergy calculation. However, they also claim that real values will be in between these two ranges as not all produced heat can be recovered. Moreover, they have not included inefficiencies related to the final compression stage of H$_2$ to 70 bar. According to Ptasinski [107], exergy efficiencies ($\Psi^*_{plant,1}$) for H$_2$, MeOH and FT-fuels are 66%, 56% and 36%. The first two values are comparatively higher than our present results (i.e., 43-45 and 44-45% respectively) whereas the FT-fuels value is more conservative that our estimate (i.e., 45%). Differences are found again on the way of producing utilities (e.g., heat, steam or electricity), cleaning, heat integration and the final upgrading stage. FT-fuels exergy values from Boissonnet et al [108] are in line with our results (i.e, 40-47%) as, analogous to our process, electricity

is also co-produced. Concerning bioelectricity generation plants, Brown et al [109] give an exergetic efficiency ($\Psi^*_{plant,1}$) of 33% for a system operating a mildly pressurized gasifier (i.e., 2.5 bar). Our system incorporates a 15-bar pressurized gasifier, which allows to reach slightly higher exergetic efficiencies (i.e, 35.5%).
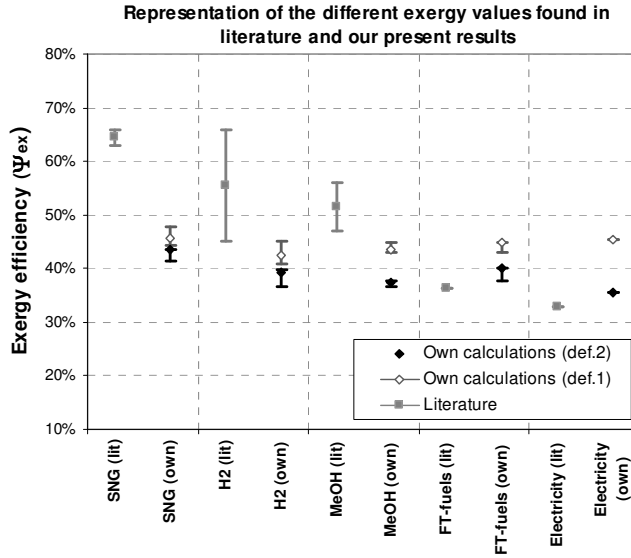
Figure 4.16: *Representation of the different exergy efficiency values (Ψ_{ex}) found in literature with our own data [101, 106-109]. Direct comparison is rather difficult as biofuel as different assumptions, plant design and definitions are used.*

4.4. *Full biomass-to-bioenergy chain evaluation*

4.4.1.   *Biomass collection and transport to the processing plant*

In the first stage, biomass is collected by means of tractors or similar equipment. For the sake of simplicity, we have assumed that the machinery is equal for either forest residues, straw or lignocellulosic energy crops. Annual fossil diesel ($TC_{diesel,biowaste}$ or $TC_{diesel,ecrop}$) and lubrication oil consumption ($TC_{oil,biowaste}$ or $TC_{oil,ecrop}$) is calculated by the algorithm of sections 5.2.2.1 and 5.2.2.2 in Chapter 5. In case of growing lignocellulosic energy crops in a virtual region (VEC), fertilizers are also applied to enhance biomass productivity up to 13.4 tn/ha [110]. Table 5-1 specifies the dosing of those fertilizers (q_i). Energy consumption during fertilizers production is taken from Helikson [111], who estimated an expenditure (e_i) of about 83.7 MJ/kg $_{N\text{-Fertilizer}}$, 27.9 MJ/kg $_{P\text{-Fertilizer}}$ and 9.3 MJ/kg $_{K\text{-Fertilizer}}$. Total energy consumption of the '*biomass collection*' stage can be written as follows:

$$E_{in,collection(biowastes)} = \frac{TC_{diesel,biowastes} \cdot \rho_{diesel} \cdot HHV_{diesel}}{\Psi_{PEC,diesel}} + \frac{TC_{oil,biowastes} \cdot \rho_{oil} \cdot HHV_{oil}}{\Psi_{PEC,oil}} \qquad (4\text{-}20)$$

$$E_{in,collection(ecrops)} = \frac{TC_{diesel,ecrops} \cdot \rho_{diesel} \cdot HHV_{diesel}}{\Psi_{PEC,diesel}} + \frac{TC_{oil,ecrops} \cdot \rho_{oil} \cdot HHV_{oil}}{\Psi_{PEC,oil}} + E_{in,fertilizers} \quad (4\text{-}21)$$

$$E_{in,fertilizers} = \frac{A_{T,ecrops}}{4} \cdot \left(q_N \cdot e_N + q_P \cdot e_P + q_K \cdot e_K \right) \quad\quad (4\text{-}22)$$

where $\Psi_{PEC,i}$ is the energy efficiency of producing diesel or lubrication oil, ρ_i is the density and HHV_i is the high heating value. We assumed that existing European refinery plants operates with an average efficiency ($\Psi_{PEC,i}$) of ~ 80%. $E_{in,collection}$ values are included in the general equation (4-31) of the later section 4.4.5, in order to calculate the overall energy efficiency of a biomass-to-bioenergy chain (Ψ_{WTW}). Energy consumption for biomass transportation ($E_{in,transport}$) is calculated with a similar procedure, although in this case, lubrication oil is negligible.

$$E_{in,transport} = \frac{\left(TS_{diesel,\log 1} + TS_{diesel,\log 2} \right) \cdot \rho_{diesel} \cdot HHV_{diesel}}{\Psi_{PEC,diesel}} \quad\quad (4\text{-}23)$$

Similarly, the set of equations (4-24) to (4-27) are applied to calculate the exergy use for biomass collection, fertilizers application and biomass transport to the processing plant. Values for fertilizers production (ε_i) are calculated from Hovelius et al [93].

$$E_{in,collection(biowastes)}^* = \frac{TC_{diesel,biowastes} \cdot \rho_{diesel} \cdot \varepsilon_{diesel}}{\Psi_{PEC,diesel}^*} + \frac{TC_{oil,biowastes} \cdot \rho_{oil} \cdot \varepsilon_{ch,oil}}{\Psi_{PEC,oil}^*} \quad\quad (4\text{-}24)$$

$$E_{in,collection(ecrops)}^* = \frac{TC_{diesel,ecrops} \cdot \rho_{diesel} \cdot \varepsilon_{diesel}}{\Psi_{PEC,diesel}^*} + \frac{TC_{oil,ecrops} \cdot \rho_{oil} \cdot \varepsilon_{ch,oil}}{\Psi_{PEC,oil}^*} + E_{in,fertilizers}^* \quad\quad (4\text{-}25)$$

$$E_{in,fertilizers}^* = \frac{A_{T,ecrops}}{4} \cdot \left(q_N \cdot \varepsilon_N + q_P \cdot \varepsilon_P + q_K \cdot \varepsilon_K \right) \quad\quad (4\text{-}26)$$

$$E_{in,transport}^* = \frac{\left(TS_{diesel,\log 1} + TS_{diesel,\log 2} \right) \cdot \rho_{diesel} \cdot \varepsilon_{ch,diesel}}{\Psi_{PEC,diesel}^*} \quad\quad (4\text{-}27)$$

where $\varepsilon_{ch,diesel}$ and $\varepsilon_{ch,oil}$ are the chemical exergy of diesel and lubrication oil, while $\Psi^*_{PEC,diesel}$ and $\Psi^*_{PEC,oil}$ are the exergetic efficiency of producing diesel and lubrication oil respectively (i.e., ~ 80%).

4.4.2.   Biofuels and bioelectricity production

Energy ($E_{in,production}$) or exergy ($E^*_{in,production}$) consumption during biofuels or bioelectricity production is also included in the final well-to-wheel efficiency (Ψ_{WTW} and Ψ^*_{WTW} respectively). Total energy consumption of this stage has been calculated in previous section 4.3 from Aspen Plus simulations, and it equals the denominator of Eqs.(4-5) or (4-16).

4.4.3.   Biofuels and bioelectricity distribution

Biofuels are finally distributed to dispensing filling stations, whereas bioelectricity is simply injected in the existing national grids. We assume that bioelectricity distribution incurs in 10% of energy losses. Gaseous biofuels, such as SNG and H_2, are compressed and transported via pipelines, and the corresponding electricity consumption ($W_{in,distribution}$) is retrieved from Aspen Plus simulations. Conversely, liquid MeOH and FT-fuels are distributed by means of dedicated tank trucks. Fuel and exergy use is then calculated with the following equations (4-28) and (4-29):

$$E_{in,transport} = \frac{TS_{diesel,distribution} \cdot \rho_{diesel} \cdot HHV_{diesel}}{\Psi_{PEC,diesel}} \qquad (4\text{-}28)$$

$$E_{in,transport}^* = \frac{TS_{diesel,distribution} \cdot \rho_{diesel} \cdot \varepsilon_{ch,diesel}}{\Psi_{PEC,diesel}^*} \qquad (4\text{-}29)$$

where $TS_{diesel,distribution}$ account for the diesel consumption, and it can be calculated by applying the algorithm of Figure 5.4 in Chapter 5.

4.4.4.   Biofuels and bioelectricity application

Biofuels are finally used in vechicles such as: advanced internal combustion engines (ICE), fuel cell vehicles (FCV) and battery electric vehicles (BEV)[10]. The tank-to-wheel efficiency ($\Psi_{TTW,i}$) of each car system has been taken into account to evaluate the overall well-to-wheel efficiency. This tank-to-fuel efficiency represents the efficiency of converting chemical energy contained in the fuels into kinetic energy of work, and it can be defined by Eq.(4-30):

$$\Psi_{TTW} = \frac{Energy\ to\ wheels}{Energy\ biofuel} = \frac{\left[m_v \cdot g \cdot f_r + 0.5 \cdot \rho_{air} \cdot C_w \cdot A_{car} \cdot (v + v_o)^2 + m_v \cdot a \right]}{FE} \qquad (4\text{-}30)$$

where m_v is the vehicle mass, g is the gravity, f_r is the rolling resistance coefficient, ρ_{air} is the air density at normal conditions, C_w is the drag coefficient, A_{car} is the frontal area of a car, v is the velocity of the car, v_o is the head wind velocity, a is the acceleration and FE is the fuel economy (i.e., consumed MJ_{fuel} per 1 km). For the sake of simplicity, idling or increased fuel consumption due to acceleration have not been taken into account in our calculations (i.e., $a = 0 m/s^2$). Head wind velocity has also been neglected ($v_o = 0 m/s$). Values for FE have been taken from the report of Weiss et al [112], and they predicted to be by year 2020: 0.92 MJ_{FT}/km, 1.03 MJ_{SNG}/km, 1.33 MJ_{MeOH}/km, 0.81 MJ_{H2}/km and 0.51MJ_{el}/km. Results from Eq. (4-30) are compared with values from other authors in Table 4-1. Although our results are generally more conservative, they are used in section 4.4.5   to calculate overall well-to-wheel efficiency ($\Psi_{WTW,i}$).

---

[10] SNG and FT-fuels are used in ICE cars, whereas H_2 and MeOH are fuelled in FCV.

Table 4-1: *Comparison of tank-to-wheel efficiencies (Ψ_{TTW}) with values from other authors. These values are predicted for year 2020.*

Vehicle	Literature values (Ψ_{TTW}) [112, 113]	Own calculations (Ψ_{TTW})
Gasoline conventional ICE cars:	16.7 – 17.1 %	15.4 %
Diesel conventional ICE cars:	19.4– 20.2 %	17.9 %
Advanced diesel hybrid-ICE cars:	30.9 %	26.2 % [a]
MeOH FCV cars:	26.6 %	18.9 % [a]
MeOH hybrid-FCV cars:	31.1– 22.7 %	n.a.
CNG (methane) conventional ICE car:	16.9 %	23.3 % [a]
CNG (methane) hybrid-ICE car:	27.3 %	n.a.
GH_2 FCV car:	36.3 %	30.9 % [a]
GH_2 hybrid-FCV car:	36.0 %	n.a.
BEV electric cars:	60.3 %	48.9 % [a]

(a): These more conservative values are used for later $\Psi_{WTW,i}$ calculations

4.4.5.   Well-to-Wheel efficiency

The final well-to-wheel (Ψ_{WTW}) efficiency has been calculated by applying Eq.(4-31), which considers all energy consumption of all the stages and the efficiency of vehicles in Table 4-1.

$$\Psi_{WTW} = \Psi_{WTT} \cdot \Psi_{TTW} = \frac{E_{biofuels}}{E_{in,collection} + E_{in,transport} + E_{in,production} + E_{in,distribution}} \cdot \Psi_{TTW} \qquad (4\text{-}31)$$

The calculation has only been applied to the '*bio-100*' configuration as it already takes into account the energy consumed during electricity generation. Energy consumption for biofuels production ($E_{in,production}$) and distribution ($E_{in,distribution}$) is independent of the country where the biofuel's plant is to be built. Conversely, the collection and transport stages are notably influenced by the biomass availability (tn/ha) of each region, as explained in subsequent Chapter 5. For the sake simplicity, results are only given for those countries with high biomass availability per hectare (e.g., Austria, Germany or France). As observed in Table 4-2, biowastes and lignocellulosic energy crops achieve similar figures, being the bioelectricity chain the most efficient one (i.e., ~17-19%). Growing energy crops could become an alternative for those locations where biomass is scarce (e.g., Ireland or Estonia). Notwithstanding this option, soil depletion studies should confirm the feasibility of growing energy crops. The well-to-wheel efficiency (Ψ_{WTW}) of the bioelectricity system would be in line with the actual figure for fossil diesel production and use (i.e, ~16-18[11]%).

Hydrogen is the second best alternative from an energetic point of view, whereas overall efficiencies of SNG and FT-fuels systems are rather close (i.e., ~10-11%). In effect, the higher efficiency of FT-diesel cars (see Table 4-1) is counteracted by the large energy consumption of its production and distribution chain. The global efficiency of the MeOH route is the lowest among all biofuels (i.e., 5-6%) as it incurs

---

[11] This number is obtained by assuming that the efficiency of producing and distribution fossil diesel is ~ 80%, and the actual ICE car efficiency is ~ 20-22%.

in the highest energy expenditure. Moreover, the expected efficiency of FCV-MeOH vehicles ($\Psi_{TTW,}$) should be improved to equal the rest of the biofuels (see Table 4-1). Due to the lack of data, vehicle's energy efficiency of Table 4-1 (Ψ_{TTW}) is also applied in the extended exergy analysis.

Table 4-2: *Comparison of overall well-to-wheel efficiency ($\Psi_{WTW,i}$) per each biofuel system. For this calculation, own calculated Ψ_{TTW} values are used (i.e., right column of Table 4-1). Numbers in brackets correspond to the Ψ_{WTW} that would be obtained if using Ψ_{TTW} data from literature [112, 113] (i.e., middle column of Table 4-1).*

↓ Biofuels	Energy analysis (Ψ_{WTW})		Exergy analysis (Ψ^*_{WTW})	
	Wood & straw	Energy crops	Wood & straw	Energy crops
Electricity	17 - 18% (21 - 23%)	19% (23%)	14 - 16% (17 - 19%)	16% (19%)
Hydrogen	14 - 15% (15 - 17%)	15% (17%)	8 - 10% (10 - 12%)	11% (12%)
SNG	10 - 11% (7 - 8%)	11% (8%)	7 - 9% (4 - 6%)	9% (6%)
FT-fuels	9 - 10% (10 - 12%)	10% (12%)	7 - 9% (9 - 10%)	8% (11%)
MeOH	5 - 6% (7 - 8%)	6% (8%)	4 - 6% (7 - 9%)	5% (9%)

Following this evaluation, a similar ranking is observed, although new exergy values (Ψ^*_{WTW}) are generally lower than the previous energy results (Ψ_{WTW}). In this case, overall exergy efficiency of the bioelectricity system is found to be in the range of 14-16%. SNG and MeOH positions are swapped when applying Ψ_{TTW} efficiencies of literature [112, 113] (i.e., middle column of Table 4-1). However, Ψ_{TTW} reported values for MeOH-fuelled cars (i.e., 26.6%) are rather optimistic as these cars are still under development. Fuel economy (*FE*) values of Weiss et al can also be used to calculate the total driving distance that could be covered from 1 tone of biomass. Those results are depicted in Figure 4.17 which again identifies the bioelectricity chain as the optimal alternative from an energetically point of view.

For a better comprehension, Figure 4.18 represents the relative energy consumption per stage (i.e., from biomass collection to the final biofuel use in cars). It should be mentioned that this picture only represents the '*bio-100*' configuration of wood-fuelled chains, but similar values are calculated for straw residues and lignocellulosic energy crops. Figure 4.18 can be read by knowing that the relative energy consumption of one stage is the difference between its value in the graph and the preceding stage (e.g., the corresponding value of bioelectricity distribution equals 17 minus 14%). As observed, biofuel production and final-use incurs in the largest energy consumption (i.e., 57-77% and 14-22% respectively). The biofuel distribution stage becomes significant for the liquid biofuels MeOH and FT-fuels, with relative expenditure in the range of 7 and 17% respectively. The slope of the last stage (i.e., '*final use in cars*') would be less pronounce if Ψ_{TTV} values from literature were to be applied [112, 113] (i.e., middle column of Table 4-1).
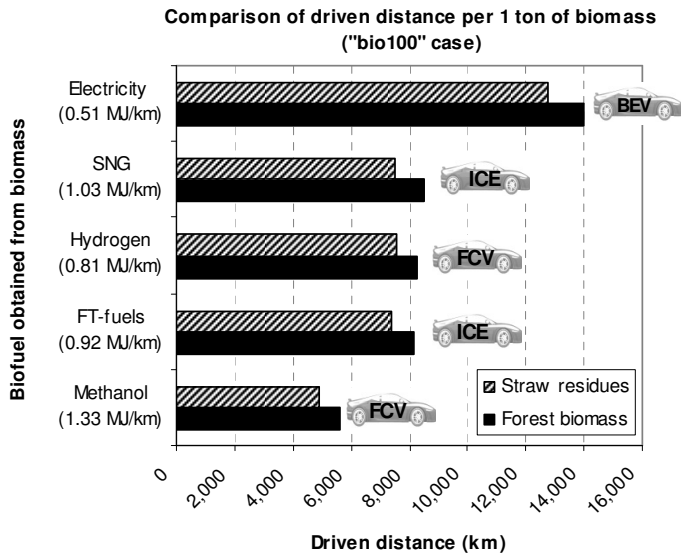
Figure 4.17: *Comparison of the driven distance when converting 1 tone of biomass into the five different biofuels. Car fuel expected consumption by 2020 [112]is indicated in brackets by each biofuel. Methanol and Hydrogen are fuelled in FCV (fuel cell vehicles), Fischer-Tropsch fuels in advanced ICE cars (internal combustion engines), whereas electricity drives BEV (battery electric vehicles). Values presented in this figure accounts for the "bio100" case, in which extra biomass is consumed to cover heat and electricity demand of the biofuels plants.*
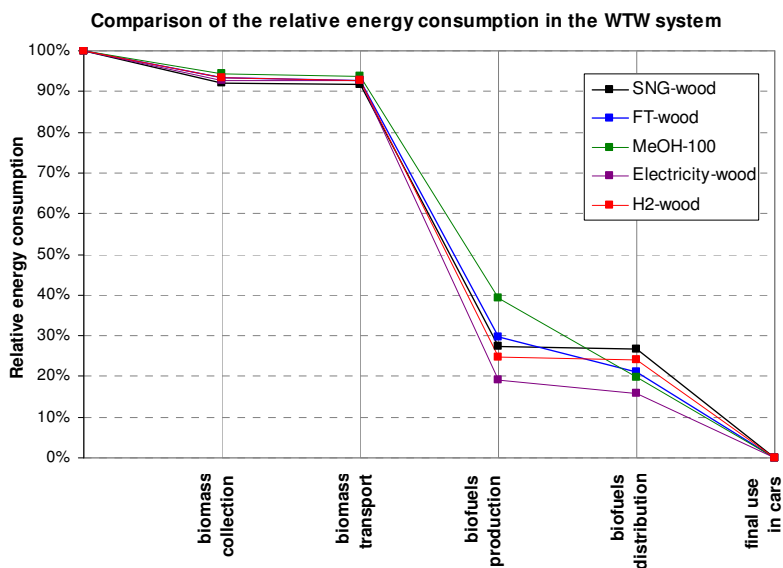
Figure 4.18: *Comparison of the relative energy consumption of each stage in the whole well-to-wheel (WTW) system. The absolute value of one stage is the difference between its value in the graph and the preceding stage.*

4.5. *Conclusions*

In this chapter we have presented the exergy and exergy efficiency evaluation for five different biomass-to-biofuels and bioelectricity conversion routes. Firstly, the appraisal has been only focused on the production plant as it is the stage with the highest potential for improvement. Secondly, the evaluation has been extended following a *Well-to-Wheel* (WTW) approach, in which energy expenditure of all stages as well as vehicle's efficiency has been integrated. The usefulness of this study is that it has been conducted following a common baseline. In effect, production plants include all the required upgrading units to distribute biofuel with the same quality as the corresponding fossil homologues. Moreover, inefficiencies related to utilities production and consumption have also been included for a fair comparison among biofuels. This practice led to the design of four different plant configurations (i.e., '*bio100*', '*bio&grid*', '*NG100*' and '*NG&grid*') which provide different ways of covering heat and electricity requirements of the conversion processes. Results have also been presented following two different production efficiency definitions. The first one ($\Psi_{plant,1}$ or $\Psi^*_{plant,1}$) correspond to the ratio of the total output (i.e., biofuels and co-production of steam and power) divided by all inputs (i.e., biomass, chemicals and utilities), whereas the second relation ($\Psi_{plant,2}$ or $\Psi^*_{plant,2}$) is the ratio of produced biofuels and surplus steam divided by the net input.

According to the exergy efficiency ($\Psi^*_{plant,1}$) results for the production stage and the '*bio100*' configuration, wood-fuelled bioelectricity plants attain the highest rates, closely followed by SNG production (i.e., 44.4% and 45.4% respectively). FT-fuels and MeOH plants operate at similar exergetic efficiencies (i.e., 43.1 and 42.9%) whereas H_2 production yields the lowest figure (i.e., 41.0%). However, bioelectricity generation is relegated to the lowest position when the comparison is made according to the second efficiency definition ($\Psi^*_{plant,2}$), i.e., 35.5%. In this case, SNG becomes the most exergetically efficient process (i.w., 41.9%) and less differences are also found among the rest of biofuels, with ratios between 36.7 % and 37.5%. When inefficiencies related to electricity production are not included (i.e., '*NG&grid*'configuration), H_2 achieve higher exergetic efficiencies than MeOH.

Different trends are observed for the conventional energy efficiency evaluation (Ψ_{plant}). SNG becomes the most energetically efficient process irrespective of the plant configuration and energy definition, i.e., 55.0-56.7% based on $\Psi_{plant,1}$. H_2 plants attain similar values than SNG (i.e., 54.3-56.4%), thus exceeding bioelectricity, FT-fuel and MeOH alternatives (i.e., 53.0%, 51.4-53.2% and 51.0-52.1% respectively). A possible explanation for this new ranking can be found in the relatively higher calorific value of H_2 in comparison with its chemical exergy. Moreover, analogous to the exergy evaluation, bioelectricity is the least exergetic process when the appraisal is made following the second efficiency definition ($\Psi_{plant,2}$), i.e., 42.6%. Corresponding values for straw-fuelled plants are about 1-2 and 0.3-1.5 %-point lower for exergy and energy calculations respectively. It is also observed that electricity co-production and gasification stages contribute to the largest efficiency losses.

When the analysis is extended to the overall WTW chain, bioelectricity generation seems to be the most convenient solution (i.e, Ψ_{WTW} equals 17-19%), mainly due to the relatively higher efficiency of BEV cars. H_2 becomes the second best alternative (i.e., 14-15%), whereas SNG and FT-fuels chain attain similar values (i.e., 9-11%). MeOH is the least efficiency route (i.e., 5-6%) due to its relatively low production and car's utilization efficiency. Among all stages, biofuels production and vehicles operation are the main contributors to the efficiency losses of the whole WTW chain.

5

Well-to-Wheel Environmental impact analysis of biomass-to-biofuels and bioelectricity chains

Abstract

Several authors have already conducted LCA of different 1st and 2nd generation biofuels. However, direct comparison among studies could lead to certain misjudgment as they differ in scope, system boundaries, and/or methodology for even the same biofuel pathway. Moreover, there is still some controversy about the benefit of producing biofuels when the appraisal is extended to emissions other than CO_2. Hence, in this chapter, we present the environmental evaluation of the five proposed biofuels following a standard procedure and for seven different environmental impacts, i.e., GWP, acidification, eutrophication, ecotoxicity, carciogenesis, summer and winter smog. Moreover different biomass feedstock, including lignocellulosic energy crops, are evaluated for 25 different locations. Results are also confronted with the reduction targets of the European Parliament, which establish that biofuels should at least reduce 60% of the GHG's emissions in comparison with the fossil alternatives. According to our values, bioelectricity production is the preferred option for either electricity or transport applications. SNG is the second best alternative per output of energy, whereas this position is relegated to H_2 when the analysis is based on the driving distance. It is also observed that, in general, biofuels production release lower carciogenesis emissions but higher acidification and ecotoxicity pollutants than fossil diesel. The rest of environmental impacts depend on the feedstock and plant configuration. In most countries, European reduction targets are met with the production of bioelectricity, SNG or H_2, whereas MeOH normally exceeds CO_2 emissions of fossil diesel.

5.1. *Introduction*

Energy sources are the drivers of our society but current energy consumption, in particular fossil fuels, is no longer sustainable. In effect, environmental and economic problems, such as global warming or the perspective of oil reserves depletion, have prompted governments to search for more renewable alternatives. Nowadays, biofuels production is generally more expensive than fossil fuels exploitation. Hence, one of the main motivations for ongoing biofuels development is their expected lower environmental impact. Nevertheless, there are major concerns about the real environmental benefit of some biofuels. For instance, when taking into account emissions from fertilizers production, biomass transport and/or conversion treatments, life cycle analyses (LCA) reveal that some first-generation biofuels frequently exceed the emission of fossil fuels. Conversely, second generation biofuels are expected to release lower CO_2 emissions as they make profit of biowastes (thus avoiding the use of fertilizers) in more efficient installations [7, 114].

In order to overcome this controversy, public authorities of several countries, such as United Kingdom [115] and the Netherlands [116], have imposed minimum sustainability targets for biofuels to be eligible for economic incentives (e.g., tax reduction). On 17th December 2008, the European Parliament also adapted a clear position on sustainability criteria for biofuels [117]. The proposal defined increasing minimum targets for GHG's emissions reduction in comparison with fossil fuels:

• At least 35 % ➔ From year 2010 (for plants that came into operation after 2008)
• At least 35 % ➔ From year 2013 (for plants that came into operation before 2008)
• At least 50 % ➔ From year 2017 (any plant)
• At least 60 % ➔ From year 2018 (for plants that come into operation after 2017)

Many authors have already conducted LCA analyses for different feedstock and biofuels chains. However, results from these studies are often difficult to compare as they differ in the scope, system boundaries, geographical conditions and/or selected technology, even for the same biofuel pathway. Hence, the aim of this chapter is to establish a common framework to evaluate the global warming reduction potential of five second-generation biofuels with regard to fossil fuels. Our results will be finally confronted with the aforementioned European targets by year 2018.

For that purpose, the appraisal is conducted for 24 European countries and for an extra "virtual" region, in which lignocellulosic energy crops are grown for subsequent biofuels conversion. Comparison of both cases will determine whether it is more convenient to process biowastes, such as forest or straw residues, or use energy crops that can be obtained in a reduced area when applying fertilizers. In all scenarios, LCA methodology is applied to cover the whole biomass-to-bioenergy conversion system. Bioelectricity production is compared with coal based-power generation, whereas a Well-to-Wheel (WTW) perspective is applied to analyze the potential benefit of biofuels replacement in the transport sector. The appraisal is conducted for the optimal plant scales of each biofuel (i.e., ~100 $MW_{electricity}$, 200 MW_{SNG}, 500 MW_{H2}, 1000 MW_{FT} and 1000 MW_{MeOH}), which result from the economic evaluation of Chapter 6.

5.2. *LCA methodology: from cradle-to-grave*

LCA is a holistic procedure for estimating the environmental burden of a technological system on a cradle-to-grave basis. In the last decades, it has become widely accepted as an effective tool for environmental management, particularly in the context of decision making support. According to the ISO-14040 [118], LCA is defined as *''the compilation and evaluation of the inputs, outputs and potential environmental impacts of a product throughout its life cycle'',* and it consists of 4 main procedures: (1) goal and scope definition, (2) inventory analysis, (3) impact assessment, (4) interpretation and action.

5.2.1.   *LCA: Goal and scope definition*

The first component of the LCA analysis is the *goal* and *scope* definition in accordance with the norm ISO-14041 [119]. In our case, the goal of the study is to evaluate the potential emissions savings of five different second generation biofuels in comparison with the corresponding fossil fuel alternatives. The analysis is applied to either the electricity or transport sector. Bioelectricity generation is judged against coal-power production, whereas biofuels performace (i.e., SNG, FT-fuels, methanol or H_2) is compared to conventional fossil diesel. Accordingly, the functional unit (f.u.)[12] for both sectors is fixed to **1 MW$_{electricity}$** and **1 km** of driving distance.
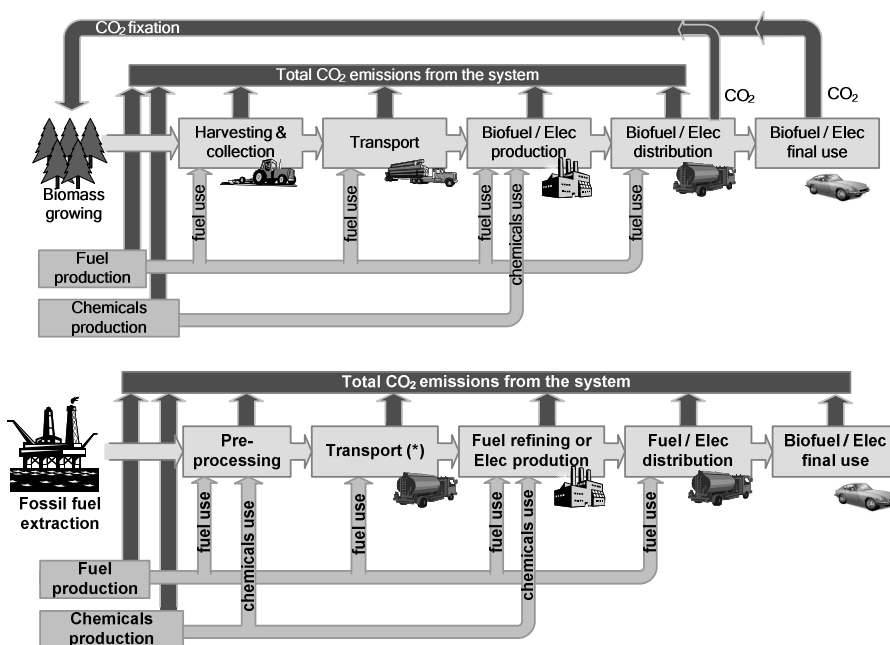
Figure 5.1: *Indication of the stages that contribute to CO_2 emissions within bioenergy (top picture) and fossil fuels system (bottom picture). CO_2 emissions that are released during machinery production are also included, but car manufacturing is excluded. Transport(*) between fossil fuel pre-processing and refining is not always necessary.*

---

[12] A functional unit is needed to standardize the comparison among different systems

System boundaries for the biofuels and fossil fuels systems are depicted in Figure 5.1 As observed, LCA evaluation is extended from biomass collection to final fuel use in vehicles or electric devices. Emissions from fuels and chemicals production, trucks manufacture, plants and machinery building are also included in the global balance. Conversely, private cars are assumed to be already available, thus their manufacturing is excluded from the appraisal. In case of growing energy crops, emissions originated during fertilizers and pesticides fabrication are also added to the general computation. CO_2 emissions released from biomass and biofuel consumption are equal to the amount fixed by trees or straw. Hence, it is assumed that the last "*final-use*" stage does not contribute to net emissions.

5.2.2.   LCA: Inventory analysis

The inventory analysis involves data collection and calculation procedures to quantify relevant inputs and outputs from the system in the form of mass and energy flows. These data is also needed for the subsequent '*impact assessment*' stage. The main streams of each stage are indicated in Figure 5.2.

5.2.2.1.   Biomass harvesting and collection

Diesel ($C_{diesel,operation}$) and lubrication oil ($C_{oil,operation}$) consumption per each harvesting operation is calculated by means of Eqs.(5-1) and (5-2) respectively [120]:

$$C_{diesel,operation} = P_T \cdot \left(2.64 \frac{P_T}{P_{max}} + 3.91 - 0.203 \sqrt{738 \frac{P_T}{P_{max}} + 173} \right) \quad (5\text{-}1)$$

$$C_{oil,operation} = 0.00059 \cdot P_{max} + 0.02169 \quad (5\text{-}2)$$

where P_T corresponds to the total power required per operation, and P_{max} is the maximum available power per machinery. Both parameters depend on the operation that needs to be carried out (e.g., seeding, coppicing, fertilizers application, etc). Specific P_T and P_{max} values are also taken from Heller et al [120]. For the sake of simplicity, it is assumed that the same tractor will be used for all the harvesting operations, although in real applications, there could be specialized equipments. The number of harvesting operations is assumed to be one for biowastes (i.e., coppicing and collection is done together) and four for the case of lignocellulosic energy crops (i.e., seeding, two fertilizers application, coppicing+collection) as nitrogen fertilizers cannot be spread at the same period than phosphorous and potassium fertilizers. The level of fertilizers' application is tabulated in Table 5-1 together with other assumptions. It has also been assumed that water is entirely supplied by rainfall, thus any energy for watering has not been included in the balance.

Materials and energy are also consumed during the manufacture of tractors or similar machinery, thus contributing to the total emissions computation, although the share of this phase is below 2%. The number of tractors ($N_{tractors,all}$) is directly dependent on the area (A_T) that has to be covered in order to collect enough biomass to fed one production plant.
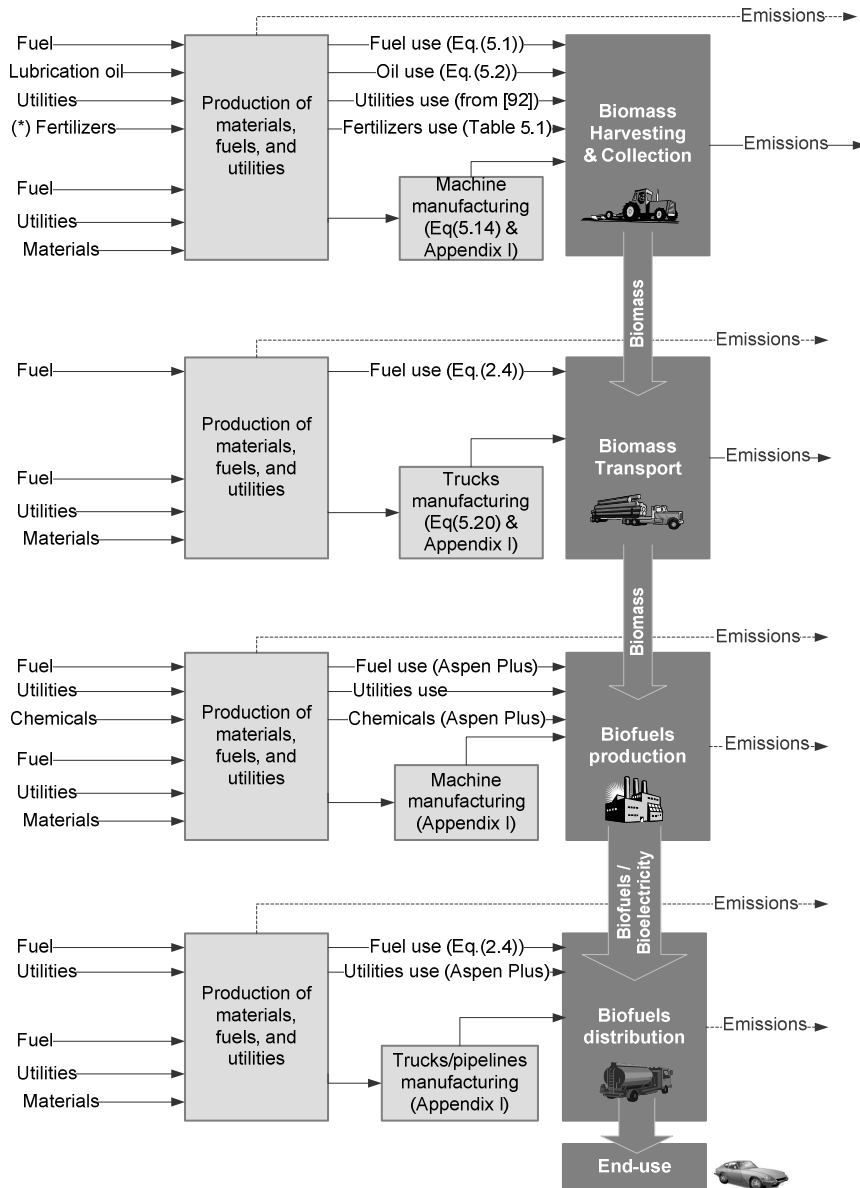
Figure 5.2: *Inventory of main input and output streams of the biomass-to-biofuel pathway.*

In our model, this total area (A_T) is composed of several NUTS-2[13] regions ($A_{NUTS2,i}$), each one modeled as a concentric circle divided by multiples of six (e.g., French FR-61 region in Figure 5.3). This division assures that each tractor always covers the same area ($A_{subarea,j}$) from rows (1) to (k-1), i.e., 28 km^2 (see Figure 5.3). The last row of circles (k) has always smaller subareas ($A_{subarea,k}$), because it is calculated as the

_____

[13] NUTS-2 refers to the Nomenclature of Territorial Units of Statistics, which is a standard geocode for referencing the subdivisions of countries in several regions. In Europe, this 2nd level of division normally refers to provinces.

difference of the total area (A_T) and the summation of the subareas ($A_{subarea,j}$) of the previous rows (see Eq.(5-6)). In any case, one tractor can easily cover the maximum subarea of 28 km^2 annually. This value has been calculated by taking into account the maximum number of working hours per tractor ($h_{tractor}$), the tractor speed ($v_{tractor}$), the tractor plough width (w_{plough}) and its efficiency ($\psi_{tractor}$). Those parameters are defined in Table 5-1. For energy crops, the total application area ($A_{T,ecrop}$) is multiplied by a factor of four (see Eq.(5-4)) because four different collection activities need to be performed (i.e., cutting and collection are done together, but seeding and fertilizers application are staggered in three different periods). In that case, more tractors will be needed, as shown by Eq.(5-10). Conversely, only one operation is performed for biowastes (i.e.,collection).
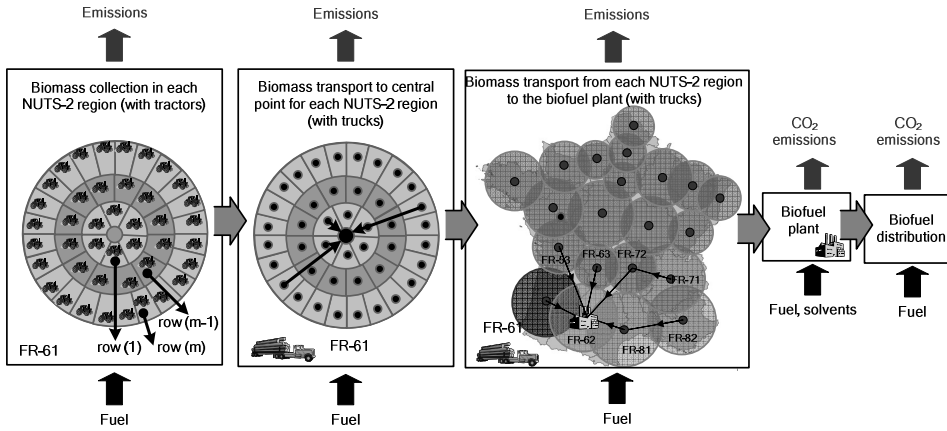
Figure 5.3: *Identification of the stages that requires external fossil fuel.*

Accordingly, the number of required tractors in operation ($N_{tractors,all}$), the total number of tractors to be built ($TN_{built-tractors,all}$), and the total consumed fuel (TC_{diesel}) and lubrication oil (TC_{oil}) per year can be calculated by the set of equations (5-3) to (5-15).

$$A_{T,biowaste} = \sum_{i=1}^{n\ regions} A_{NUTS2,i} = \sum_{i=1}^{n\ regions} \frac{m_{biowaste(NUTS2,i),year}}{\eta_{biowaste(NUTS2,i)}} \qquad (5\text{-}3)$$

$$A_{T,ecrop} = = 4 \cdot \frac{m_{ecrop(all),year}}{\eta_{ecrop}} \qquad (5\text{-}4)$$

$$A_{NUTS2,i} = \sum_{j=1}^{k-1} 6 \cdot j \cdot A_{subarea,j} + 6 \cdot k \cdot A_{subarea,k} \qquad (5\text{-}5)$$

$$A_{subarea,k} = \frac{A_{NUTS2,i} - \sum_{j=1}^{k-1} 6 \cdot j \cdot A_{subarea,j}}{6 \cdot k} \qquad (5\text{-}6)$$

$$N_{tractors,biowaste(NUTS\,2,i)} = 6 \cdot (1 + 2 + \ldots + k) \cdot N_{operations} = 6 \cdot \frac{k \cdot (k+1)}{2} \qquad (5\text{-}7)$$

$$N_{tractors,biowaste(all)} = \sum_{i=1}^{n\,regions} N_{tractors,biowaste(i)} \qquad (5\text{-}8)$$

$$TN_{built-tractors,biowaste(all)} = N_{tractors,biowaste(all)} \cdot \mathrm{int}\left(\frac{l_{project}}{l_{tractor}}\right) \qquad (5\text{-}9)$$

$$N_{tractors,ecrops(all)} = 6 \cdot (1 + 2 + \ldots + k) \cdot N_{operations} = 6 \cdot \frac{k \cdot (k+1)}{2} \cdot 4 \qquad (5\text{-}10)$$

$$TN_{built-tractors,ecrops(all)} = N_{tractors,ecrops(all)} \cdot \mathrm{int}\left(\frac{l_{project}}{l_{tractor}}\right) \qquad (5\text{-}11)$$

$$TC_{diesel,biowaste} = 6 \cdot \frac{k \cdot (k+1)}{2} \cdot C_{diesel,operation} \cdot A_{T,biowaste} \qquad (5\text{-}12)$$

$$TC_{oil,biowaste} = 6 \cdot \frac{k \cdot (k+1)}{2} \cdot C_{oil,operation} \cdot A_{T,biowaste} \qquad (5\text{-}13)$$

$$TC_{diesel,ecrops} = 6 \cdot \frac{k \cdot (k+1)}{2} \cdot C_{diesel,operation} \cdot A_{T,ecrop} \qquad (5\text{-}14)$$

$$TC_{oil,biowaste} = 6 \cdot \frac{k \cdot (k+1)}{2} \cdot C_{oil,operation} \cdot A_{T,ecrop} \qquad (5\text{-}15)$$

Table 5-1: *Main assumptions for LCA calculations of biomass harvesting & collection phase.*

Parameter	Value
Forest residues yield in tn/ha (η_{wood}):	Country specific (see Chapter 2)
Straw residues yield in tn/ha (η_{straw}):	Country specific (see Chapter 2)
Lignocellulosic energy crops yield (η_{ecrops}):	13.4 tn/ha (for willow [110])
Amount N-fertilizer used:	100 kg/ha (in the 4th year) [110]
Amount P-fertilizer used:	22.4 kg/ha (in the 1st year) [110]
Amount K-fertilizer used:	39.2 kg/ha (in the 1st year) [110]
Pesticides and/or herbicides:	Negligible
Tractor plough width (w_{plough}):	2.2 m
Energy crops growth rate:	7 years [110]
Tractor speed ($v_{tractor}$):	7.5 km/hr
Tractor lifetime ($l_{tractor}$):	12,000 hr (~ 8 years)
Project lifetime ($l_{project}$):	30 years
Farmer (or tractor) working hours per year ($h_{tractor}$):	2000 hr/yr
Tractor efficiency ($\psi_{tractor}$)	85 % (for more than 51 ha) [121]

where $m_{biowaste,year}$ is the required biowaste amount per year (tn/yr), $\eta_{biowaste}$ is the biomass production per hectare (see Chapter 2), $N_{operation}$ is the number of activities per area (e.g., seeding, coppicing, harvesting, etc.), and 'k' is the total number of rows of subareas (see Figure 5.3). Values of other parameters are given in Table 5-1.

Emissions originated during tractors construction are calculated from the study of Heller et al [120]. Alternatively, the database of the SimaPro program [122] is used to calculate the emissions from fuels, utilities and fertilizers production and consumption (see Appendix I for detailed calculations).

5.2.2.2.   *Biomass transport to the processing plant*

Biomass transport comprises two stages: (1) transport of collected biomass to a central location of the NUTS-2 region (named as "*log-1*"), and (2) final transport to the biofuels processing plant (named as "*log-2*"), as shown in Figure 5.3. The second stage "*log-2*" can be avoided in those regions where there is enough biomass to supply one biofuel plant (e.g., French FR-61 region for the case of producing SNG). Diesel consumption per truck ($S_{diesel,trip}$) is determined from the Van Laar expression (i.e., Eq.(2-4)) [38], whose parameters are tabulated in Table 0-2 (see Appendix A). In general, fuel consumption for a fully-loaded truck sums 0.93 MJ/tn.km. In this case, lubrication oil expenditure is not significant.

$$S_{diesel,trip} = \frac{\left[(m_l + m_v)\cdot g \cdot f_r + 0.5 \cdot C_w \cdot \rho \cdot A_{truck} \cdot v^2\right]}{\eta_t \cdot m_l} \tag{2-4}$$

Analogous to the previous section, the number of required trucks in operation ($N_{trucks,total}$), and the total number of trucks to be built ($TN_{trucks,total}$) are also calculated in order to include the emissions released during their manufacture.
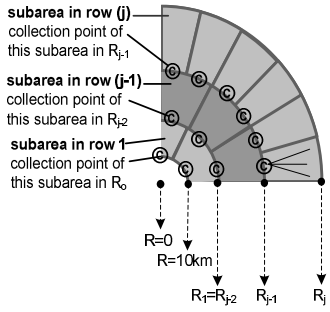
$$N_{trucks,total} = N_{trucks,\log 1} + N_{trucks,\log 2} \tag{5-16}$$

$$TN_{trucks,total} = \left(N_{trucks,\log 1} + N_{trucks,\log 2}\right)\cdot \text{int}\left(\frac{l_{project}}{l_{truck}}\right) \tag{5-17}$$

An algorithm has been created for that purpose, as shown in Figure 5.4 and Figure 5.5. One of the main restrictions is that one driver could not work more than 10 hours per day ($t_{trip,max}$) and he has to return to the departure point after his workday. This condition means that the maximum driving time ($t_{driving,max}$) is 8 hours, as about 2 hours (t_{fix}) are spent for biomass uploading, transshipment and resting time of the driver (see Eq.(5-19)). For a truck speed of 60 km/hr, the maximum allowed driving distance of one truck is then 240 km (d_{max}). Hence, when the total driving time ($t_{trip,calc}$) exceeds 10 hours ($t_{trip,max}$), extra trucks are needed to cover the remaining driving time and distance (see Figure 5.5). In that case, total driving distance (d_i) is divided in "z" interstages, as done in Eqs.(5-27) and (5-28). This division is not needed for the 1st

biomass transport stage "**log-1**" as the largest radius distance R_m of all NUTS-2 regions (i.e., Upper Norrland Sweden "SE08") is smaller than 240 km. Conversely, this division will be required for the "**log-2**" transport part as total driving distance will be frequently larger than R_{max}, notably when producing FT-fuels or methanol.

Another condition, for the '*log-1*' phase, is that the tractor leaves the collected biomass to the closest point of the central point of the NUTS-2 region. Accordingly, the trip distance of a subarea located in a (j) row will be R_{j-1} (see Figure 5.4). Total diesel consumption during '*log-1*' phase ($TS_{diesel,log1}$) is calculated by summing the fuel expenditure of all subareas and NUTS-2 regions (see Eq.(5-25)). Alternatively, diesel consumption during "*log-2*" phase ($TS_{diesel,log2}$) is equal to the total number of trips ($N_{trips,all}$) multiplied by the specific fuel expenditure ($S_{diesel,trip}$) of each trip (see Eq.(5-32)). Moreover, the total number of trucks for both phases ($N_{trucks,log1}$ and $N_{trucks,log2}$) are calculated based on the premise that the maximum working days for one truck ($t_{max,truck}$) is limited to 250 days in order to comply with their maintenance (see Eqs.(5-24) to (5-31)). Values of truck performance (e.g., speed (v_{truck}), payload (m_l), etc) can be found in Appendix A.

$$N_{trips,suabarea(j)} = roundup\left(\frac{m_{biomass,subarea(j)}}{m_l}\right) \quad (5\text{-}18)$$

$$t_{trip,calc(j)} = t_{fix} + t_{driving} = 2 + \frac{R_{j-1} \cdot 2}{v_{truck}} \quad (5\text{-}19)$$

$$t_{total,subarea(j)} = t_{trip,calc(j)} \cdot N_{trips,subarea(j)} \quad (5\text{-}20)$$

$$t_{total,row(j)} = 6 \cdot j \cdot t_{total,subarea(j)} \quad (5\text{-}21)$$

$$t_{total,NUTS-2(i)} = \sum_{j=1}^{m} 6 \cdot j \cdot t_{total,subarea(j)} \quad (5\text{-}22)$$

$$t_{total,log-1} = \sum_{i=1}^{n} t_{total,NUTS-2(i)} \quad (5\text{-}23)$$

$$N_{trucks,log-1} = \sum_{i=1}^{n\ regions} roundup\left(\frac{t_{total,NUTS2(i)}}{t_{max,truck}}\right) \quad (5\text{-}24)$$

$$TS_{diesel,log-1} = \sum_{i=1}^{n\ regions}\left(S_{diesel,trip} \cdot \sum_{j=1}^{m} N_{trips,subarea(j)}\right)_i \quad (5\text{-}25)$$

Figure 5.4: *Set of equations to calculate the number of required trucks ($N_{trucks,log1}$) and consumed diesel ($TS_{diesel,log-1}$) for the "**log-1**" stage.*

$$N_{trips,NUTS2(i)} = \left(\text{int} \left(\frac{m_{biomass(i)}}{m_l} \right) + 1 \right) \quad \text{(5-26)}$$

$$N_{\text{int} erstages(i)} = roundup \left(\frac{\left(2 + d_i \cdot 2/v_{truck} \right)}{10} \right) = z_i \qquad 3 \le z \le 0 \quad \text{(5-27)}$$

$$d_{st(i)} = d_i / z_i \qquad \text{(5-28)}$$

$$t_{trip,\log-2(i)} = z_i \cdot \left(2 + \frac{d_{st(i)} \cdot 2}{v_{truck}} \right) \cdot N_{trips,NUTS2(i)} \quad \text{(5-29)}$$

$$t_{total,\log-2} = \sum_{i=1}^{n} t_{total,NUTS-2(i)} \qquad \text{(5-30)}$$

$$N_{trucks,\log-2} = \sum_{i=1}^{n\,regions} \left(\text{int} \left(\frac{t_{trip,\log-2(i)}}{t_{\max,truck}} \right) + 1 \right)_i \quad \text{(5-31)}$$

$$TS_{diesel,\log-2} = S_{diesel,trip} \cdot \sum_{i=1}^{n\,regions} N_{trips,NUTS2(i)} \qquad \text{(5-32)}$$
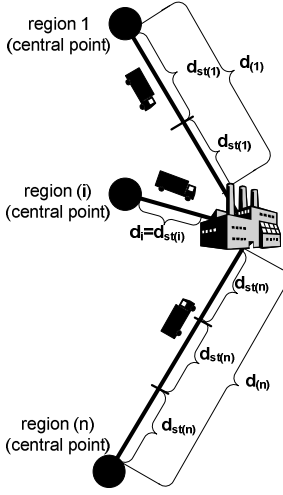
Figure 5.5: *Set of equations to calculate the number of required trucks ($N_{trucks,log2}$) and consumed diesel ($TS_{diesel,log-2}$) for the "**log-2**" stage.*

5.2.2.3.   Biomass-to-biofuels or bioelectricity conversion

Inventory data for biofuels or bioelectricity production is retrieved from Aspen Plus [39] simulations (see Chapter 3), whereas emissions from chemicals production (e.g., MDEA solution) are calculated from the SimaPro database [122]. CO_2 emissions originated from biomass or syngas burning are not included in the global balance, as the same amount of CO_2 had previously been fixed during the biomass growing phase.

Analogous to previous sections, emissions released during plant construction are also included in the general balance. Those emissions account for materials production and the on-site energy consumption for equipments and plant assembly. The amount and type of required materials for biofuels and bioelectricity plants construction have been calculated by scaling the reference values found in the reports of Spath et al [123] and Fiaschi et al [124] respectively (See Appendix I). The inaccuracy of this calculation is not significant as the plant construction phase represents less than 0.5% of the total CO_2 emissions.

5.2.2.4.   Bioelectricity and biofuels distribution and final use

It is assumed that bioelectricity can be distributed via the existing power grid, incurring in ~10% energy losses. Nevertheless, no emissions are attributed to that phase. Gaseous biofuels such as SNG or H_2 are transported by means of a network of

pipelines, whose construction is also taken into account in the LCA analysis [122]. Energy consumption and emissions for biofuels compression to the required distribution pressure (i.e., 66 and 70 bar for SNG and H_2 respectively) are retrieved from Aspen Plus simulations. Conversely, liquid methanol is entirely distributed in tank trucks with a net capacity of 20.4 tn per trip. The number of required trucks as well as the total diesel consumption is calculated following the same algorithm in Figure 5.5. Liquid FT-fuels are first introduced into a 50 km dedicated pipeline and finally transported using similar tank trucks than for methanol. For all biofuels, the total distribution distance is fixed at 200 km.

5.2.3. LCA: Impact assessment and Interpretation

The last stages of the LCA analysis are the '*impact assessment*' and '*interpretation*'. Those sections evaluate and compare the environmental burdens associated with the mass and energy flows that have been quantified in the previous inventory compilation. For that purpose, the inventory flows are classified according to seven selected impact categories from the Eco-Indicator'99 methodology [125]:

- Global warming potential (in kg-eq CO_2/f.u.)
- Acidification (in kg-eq SO_2/f.u.)
- Eutrophication (in kg-eq PO_4/ f.u.)
- Summer smog (in kg-eq C_2H_4/f.u.)
- Winter smog (in kg-eq PM_{dust}/f.u.)
- Ecotoxicity (in kg-eq Pb/f.u.)
- Carciogenesis (in kg-eq PAH/ f.u.)

The environmental impact of each released compound is translated into the previous seven categories by means of the characterization factors of Table 0-5 in Appendix I. Punctual emissions from fertilizers application, tractors, trucks and plant construction phase are normalized over the entire lifetime of the project, i.e., 30 years, as shown in Eqs.(5-33) to (5-37):

$$L_{total} = L_{collection} + L_{transport} + L_{production} + L_{distribution} \tag{5-33}$$

$$L_{collection} = L_{fuel} + L_{oil} + L_{utilities} + \frac{L_{fertilizers-NPK}}{30} + \frac{L_{tractors\ construction}}{30} \tag{5-34}[14]$$

$$L_{transport} = L_{fuel} + \frac{L_{trucks\ construction}}{30} \tag{5-35}$$

$$L_{production} = L_{fuel} + L_{chemicals} + L_{utilities} + \frac{L_{plant\ construction}}{30} \tag{5-36}$$

$$L_{distribution} = L_{fuel} + L_{utilities} + \frac{L_{inf\ rastructure\ construction}}{30} \tag{5-37}$$

---

[14] $L_{fertilizers}$ equal 0 for forest and straw wastes. There are 3 types of fertilizers for energy crops.

where L_i represent emissions per functional unit (f.u.). Results from the impact assessment analyses are finally compared with a fossil baseline scenario in subsequent sections 5.3 and 5.4, in order to determine the feasibility of producing biofuels or bioelectricity from an environmental point of view.

5.3. *LCA results for bioelectricity generation*

Figure 5.6 and Figure 5.7 represent the Global Warming Potential (GWP) of producing bioelectricity from forest residues and straw respectively (i.e., black lines). Those emissions originates from the use of fossil energy for biomass collection, transport, chemicals production and use, tractors, trucks and plant construction. As previously mentioned, a 25th "virtual" region is appended in which energy crops are grown (VEC) for the same energy purposes. Results are given in g-eq CO_2 per functional unit of 1 $MJ_{electricity}$, and they can be compared with the reference value of ~400 g-eq $CO_2/MJ_{electricitiy}$[15] for coal-based power generation. As observed, bio-electricity production emits less CO_2 than the coal alternative irrespective of the location and/or feedstock. Energy crops release similar emissions (i.e., ~10 g-eq $CO_2/MJ_{electricitiy}$) as those countries with high biomass availability per hectare (e.g. Austria for forest residues or Hungary for straw). In effect, although fertilizers production and application has an important share on the total CO_2 balance, they increase the biomass yield production per hectare (i.e., η_{ecrops} = *13.4 tn/ha* versus $\eta_{biowastes}$ < *2 tn/ha*). Consequently, less fuel is consumed to collect the same amount of biomass, as tractors have to cover a smaller area, which offsets CO_2 emissions from fertilizers.

Same Figure 5.6 and Figure 5.7 also provide GWP emissions breakdown per stage (see grey bars for "*biomass collection*", dashed bars for "*biomass transport to the processing plant*", black bars for "*electricity production*", and white bars for "*electricity distribution*"). In general, biomass collection is the stage with the largest impact on total GWP emissions (i.e., 86% for energy crops, 86-98% for forest residues and for 73-97% straw) as tractors consume a relatively high fuel amount per tone of biomass. Moreover, unlike trucks, tractors have to collect biomass over a rather extensive area. Tractors engines also pollute more due to their lower efficiency and the heavier type of diesel fuel (i.e., 4.233 and 3.870 kg-eq CO_2/kg fuel for tractors and trucks respectively). Conclusions for CO_2 emissions breakdown are in line with other studies [120, 126, 127]. Differences among coal-based and bioelectricity production is dependent on the location, being France one of the preferred locations due to its high biomass availability per hectare.

In addition, results are also compared with other renewable and fossil alternatives for electricity generation (see Figure 5.8) [120, 124, 128-132]. Values for forest and straw options correspond to our calculations in Figure 5.6 and Figure 5.7.

---

[15] This value includes coal extraction, transport and power generation. It has been calculated by using SimaPro database.
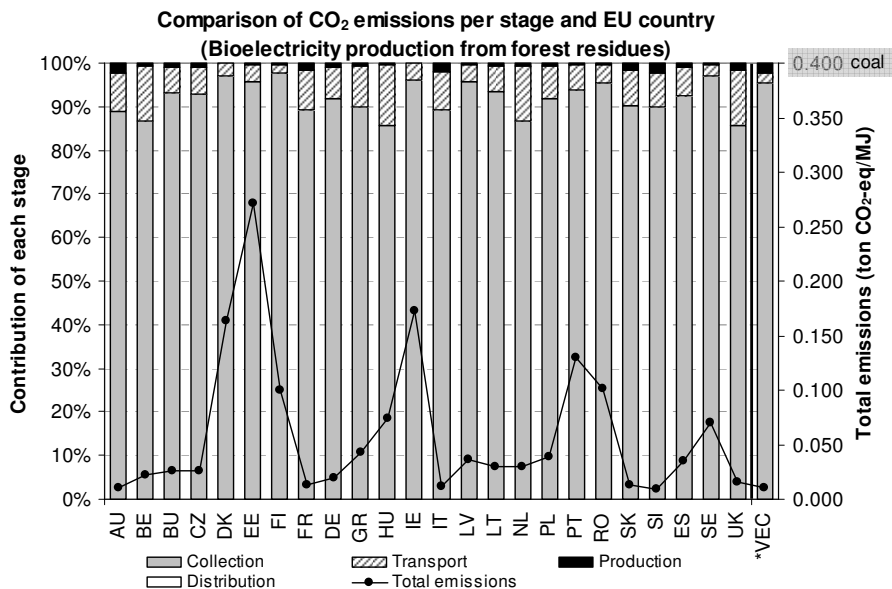
Figure 5.6: *Comparison of total emissions (straight line) and the contribution of each stage (bars). The analysis is extended to 24 EU countries and a virtual region with energy crops (*VEC). Results are compared with coal-based power generation (i.e., 0.400 tn CO₂/MJ).*
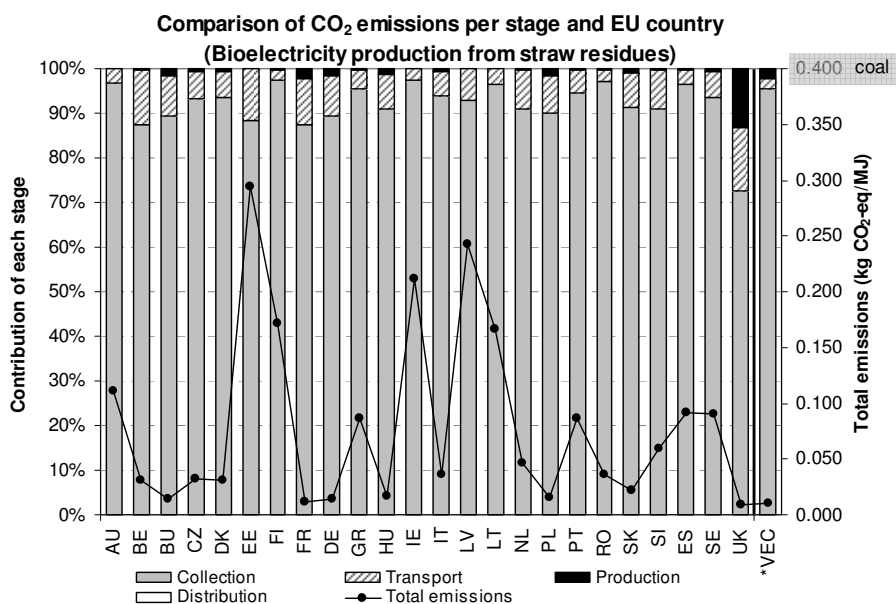

Figure 5.7: *Comparison of total emissions (straight line) and the contribution of each stage (bars). The analysis is extended to 24 EU countries and a virtual region with energy crops (*VEC). Results are compared with coal-based power generation (i.e., 0.400 tn CO₂/MJ).*

As observed, bioelectricity production in locations where biomass is widely available (i.e., minimum values in Figure 5.8) yield similar results to solar (photovoltaic) energy (i.e., 0.004-0.043 kg-eq CO_2/MJ_{elec}) and coal plants with carbon capture 'CC' (i.e., 0.031 kg-eq CO_2/MJ_{elec}). Nuclear, wind and hydropower release the lowest CO_2 emissions (i.e., 0.0001-0.008 kg-eq CO_2/MJ_{elec}), whereas gas, oil and, especially, coal-based power are on the opposite site (i.e., 0.123-0.375, 0.206-0.226 and 0.219-0.400 kg-eq CO_2/MJ_{elec} respectively).
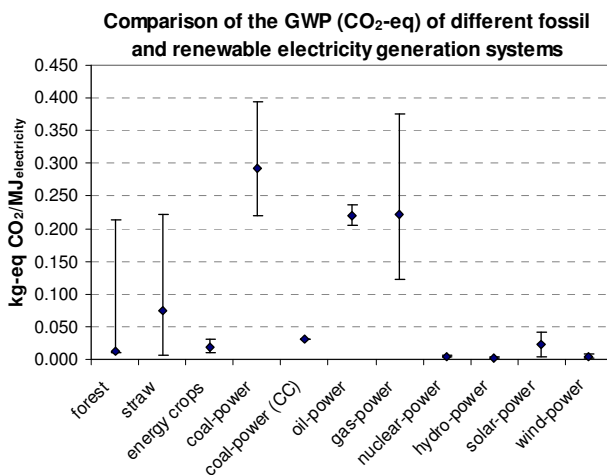
Figure 5.8: *Comparison of emissions released from bioelectricity (owns calculations) and other renewable and fossil alternatives [120, 124, 128-132].*

Additionally, Figure 5.9 compares other environmental impacts with regard to coal-based power and bioelectricity generation. Major differences are observed for the *ecotoxicity* and *carciogenesis* indicators which are reduced up to 90 and 40 times respectively when coal is replaced by biomass in France (FR). *Acidification*, *summer* and *winter smog* indicators are reduced in the range of 10-20 times, whereas *eutrophication* impact is slightly larger for bioelectricity production. This could be explained by the fact that nitrogen content in biomass is notably higher than in coal, and released nitrogenous compounds (i.e., NO_x, NH_3 or N_2) are the main contributors to the eutrophication effect (see Table 0-5 in Appendix I.1). Unfortunately, it is rather difficult to compare our results from Figure 5.9 with literature as reported values are less consistent than published values for CO_2 emissions. For instance, Carpentieri et al stated that environmental indicators, other than GWP, turn out to be larger for the bioelectricity option [127]. Conversely, Mann et al claimed completely the opposite [133], which is closer to our results with the exception of the previously commented *eutrophication* indicator.

For a complete picture, "***virtual ecotaxes***" ($\gamma_{eco,i}$) are applied to each environmental indicator to get a single *environmental score*. This method also penalizes those environmental impacts that have a more severe effect on human's health and the environment (see Figure 5.10). Those virtual ecotaxes have been defined by researchers of the Delft University of Technology (the Netherlands), and they are based on the concept of "***marginal prevention costs***" (*e.g. costs required to bring*

back the environmental burden to a sustainable level, by either end-of-pipe measures or by system integrated solutions) [134]. Applied ecotaxes values are tabulated in Table 5-2, although they are susceptible to variation. In effect, in the last Copenhagen Climate Change summit COP15, there were not clear agreements for the costs of CO_2 emissions, whereas the other environmental impacts were barely discussed.

Table 5-2*: Ecotaxes values from Delft University of Technology (the Netherlands) [134].*

Environmental indicator	Ecotax $\gamma_{eco,i}$ (year 2007)
GWP	*13.5 €/tn-eq CO_2*
Acidification	*7.55 €/kg-eq SO_2*
Winter smog	*14.5 €/kg-eq PM_{dust}*
Ecotoxicity	*802 €/kg-eq Pb*
Eutrophication	*3.6 €/kg-eq PO_4*
Carciogenesis	*14.5 €/kg-eq PAH*
Summer smog	*3.5 €/kg-eq C_2H_4*

According to Figure 5.10, we should paid about 0.750 €/$MJ_{electricity}$ to compensate for the environmental burdens related to coal-based electricity production. Values for bioelectricity production in France (FR) are notably smaller: 0.023, 0.029 and 0.025 €/$MJ_{electricity}$ for forest residues, energy crops and straw chains respectively. Different values are calculated for the rest of the locations, although they are always much lower than the coal alternative. Figure 5.10 also shows that *ecotoxicity* and *acidification* contribute to 30% and 60% of the total environmental score (*given in €/MJ_{el}*) for coal-based electricity generation, whereas for bioelectricity the relevance of this indicators is reversed, i.e., 50-70% for *acidification* and 10-23% for *ecotoxicity*.
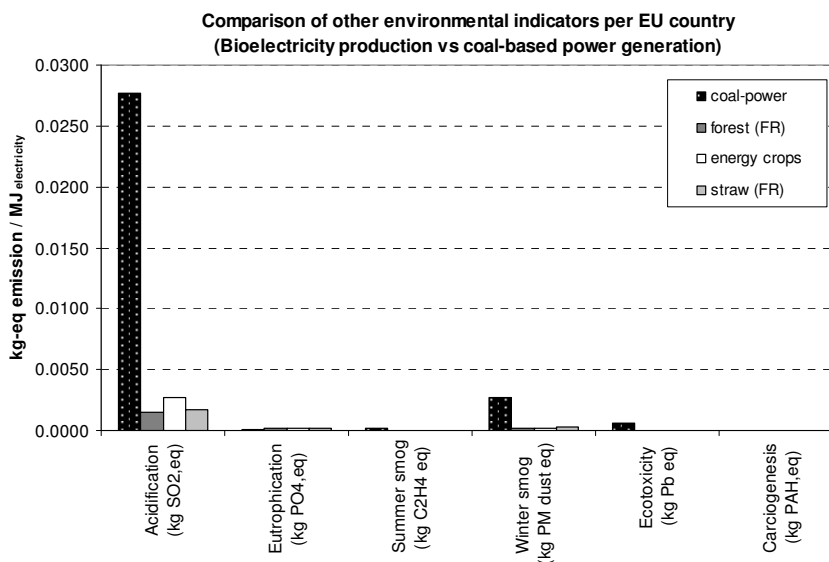
Figure 5.9: *Comparison of other environmental indicators for bioelectricity and coal-based power generation (black bars). All indicators are smaller when electricity is produced from biomass, in France (FR), with the exception of the Eutrophication parameter.*

Normalized environmental score by applying ecotaxes
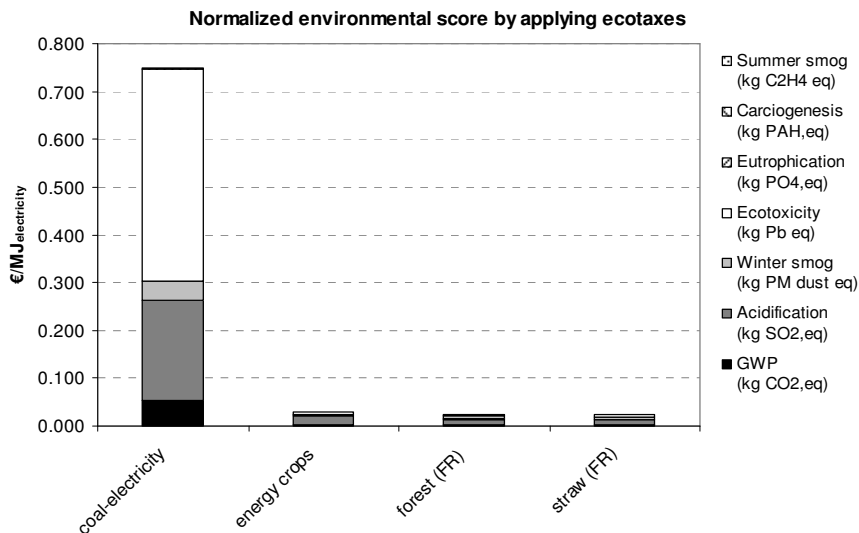
Figure 5.10: Environmental impact is translated into a single score (in €/MJ$_{el}$) by applying the following ecotaxes [134]: 0.135 €/kg-eq CO$_2$ (GWP), 7.55 €/kg-eq SO$_2$ (acidification), 14.5 €/kg-eq PM$_{dust}$ (winter smog), 802 €/kg-eq Pb (ecotoxicity), 3.6 €/kg-eq PO$_4$ (eutrophication), 14.5 €/kg-eq PAH (carciogenesis), and 3.5 €/kg-eq C$_2$H$_4$ (summer smog).

5.4. *LCA results for biofuels in the transport sector with a WTW perspective*

Analogous to previous section 5.3, CO$_2$ emissions (GWP) for each biofuel system, feedstock and location are compared in subsequent Figure 5.11 to Figure 5.14, and previous Figure 5.6 and Figure 5.7 for bioelectricity. For a given country and plant configuration, it is observed that SNG and electricity production releases the lowest emissions per output of energy (*MJ$_{fuel}$*), whereas MeOH is the most polluting option. In countries where biomass availability per hectare is low, those differences are even more marked as the collection area for large biofuels plants (i.e., FT-fuels and/or MeOH) can even transcend national borders. Moreover, unlike electricity or gaseous biofuels, FT-fuels and MeOH are distributed by means of tank trucks which consume a significant amount of fossil diesel (see section 3.5).

As expected, the '*NG-100*' configuration (in which heat and electricity demand of the biofuel plant is covered by burning natural gas) releases the highest CO$_2$ emissions in most cases. The '*NG&grid'* configuration is less pollutant than "*NG-100*' as electricity is taken by the grid instead of burning more natural gas, and this grid system consists of a mixture of "green" and fossil sources. The environmental burden of the '*bio-100*' and '*bio&grid*' configurations is even lower as an extra amount of biomass substitutes the consumption of natural gas and electricity from the grid (see section 3.1). However, opposite conclusions are drawn for those countries with low biomass availability per hectare (e.g., straw-based chain for Finland, Ireland and Baltic states,

and wood-based chain for Ireland and Estonia). Similar to bioelectricity generation, straw conversion turns out to be more environmentally favorable than forest residues in Denmark, Hungary, Romania and Spain. In the United Kingdom, this statement is only valid for electricity, SNG and H_2 production as Fischer-Tropsch and MeOH plants requires straw from longer distances.
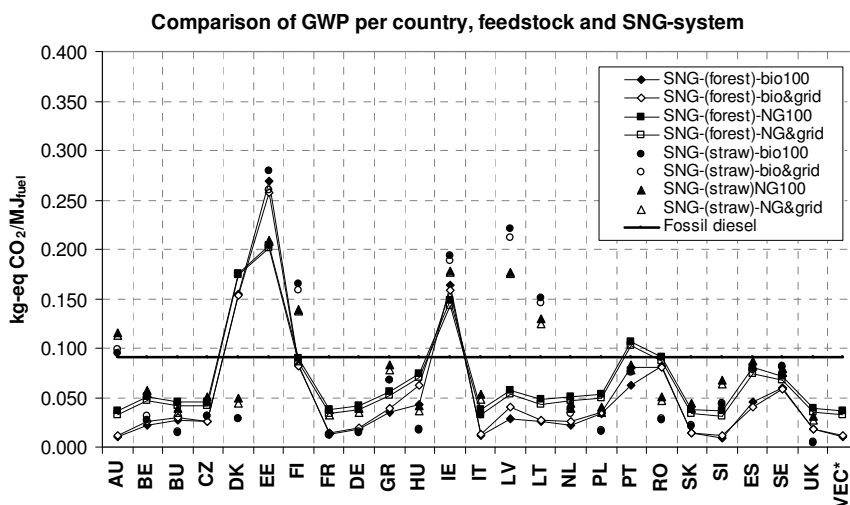
Figure 5.11: *Comparison of GWP (CO_2 emissions) per European country, feedstock and SNG plant configuration.*
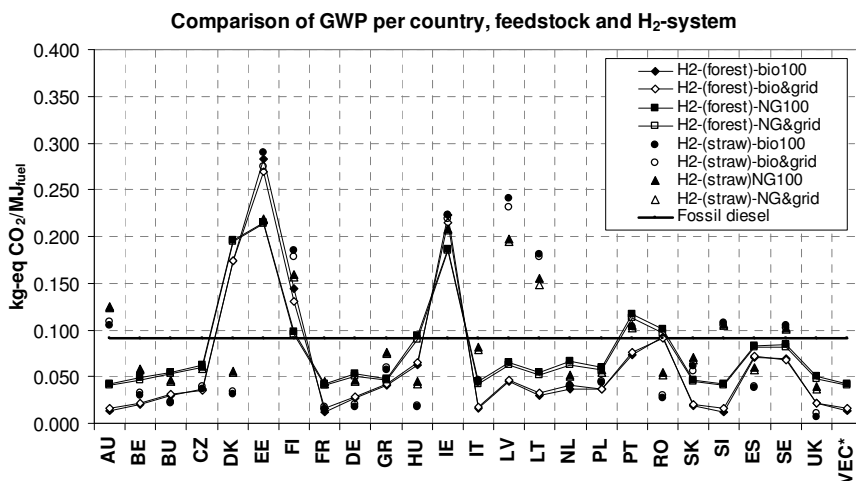
Figure 5.12: *Comparison of GWP (CO_2 emissions) per European country, feedstock and H_2 plant configuration.*

Comparison of GWP per country, feedstock and FT-fuels system
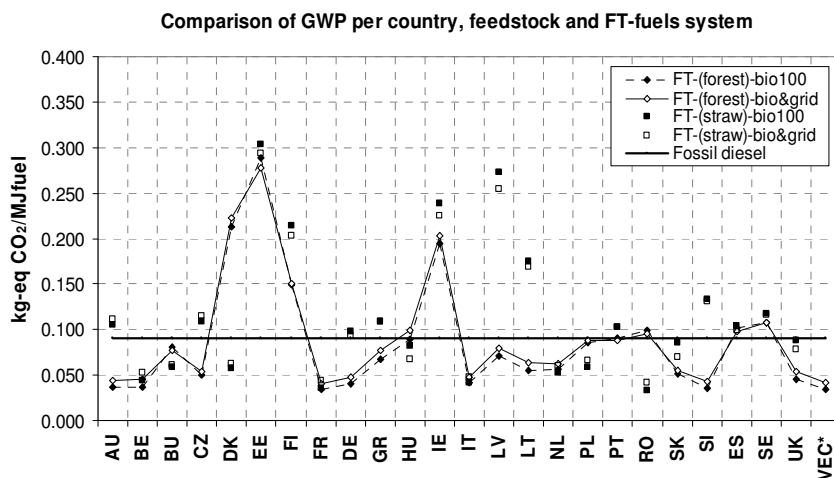
Figure 5.13: Comparison of GWP (CO_2 emissions) per European country, feedstock and FT-fuels plant configuration.

Comparison of GWP per country, feedstock and MeOH-system
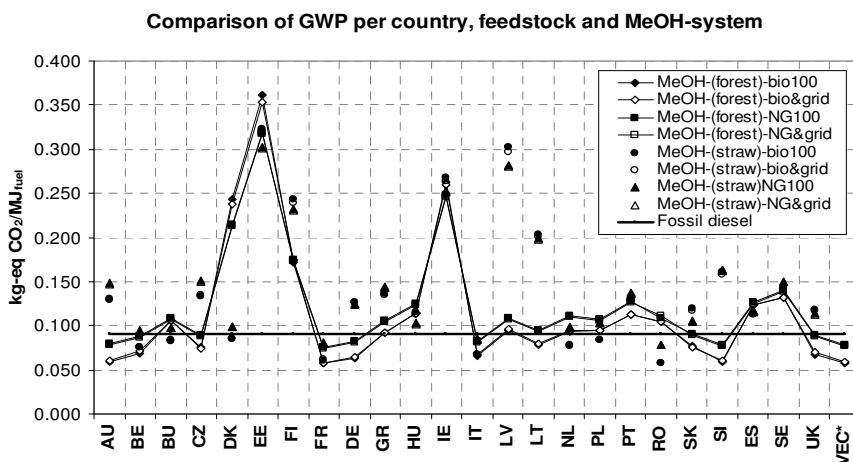
Figure 5.14: Comparison of GWP (CO_2 emissions) per European country, feedstock and MeOH plant configuration.

When values are compared to fossil diesel (i.e., ~0.90 kg-eq $CO_2/MJ_{fossil\ diesel}$), it is observed that biofuels production in some locations yield higher CO_2 emissions, notably FT-fuels and MeOH. In particular, Estonia and Ireland become the worst locations irrespective of the feedstock or biofuel produced.

For a complete picture, Figure 5.15 and Figure 5.16 depict the contribution of each stage of the biomass-to-biofuel chain on the total CO_2 emissions computation. Values are given for two locations with disparate biomass availability per hectare (i.e., France and Finland).

Contribution of CO$_2$ emissions per stage
(Biofuels production from forest residues)
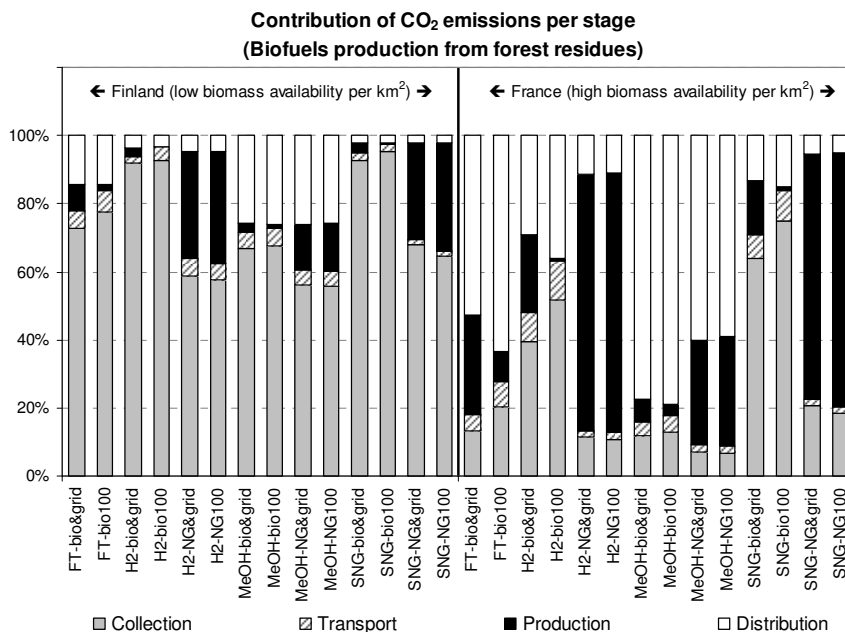
Figure 5.15: Contribution of each stage of the wood-to-biofuel chain on the total CO$_2$ emissions. Values are given for two locations with different biomass availability.

Contribution of CO$_2$ emissions per stage
(Biofuels production from straw residues)
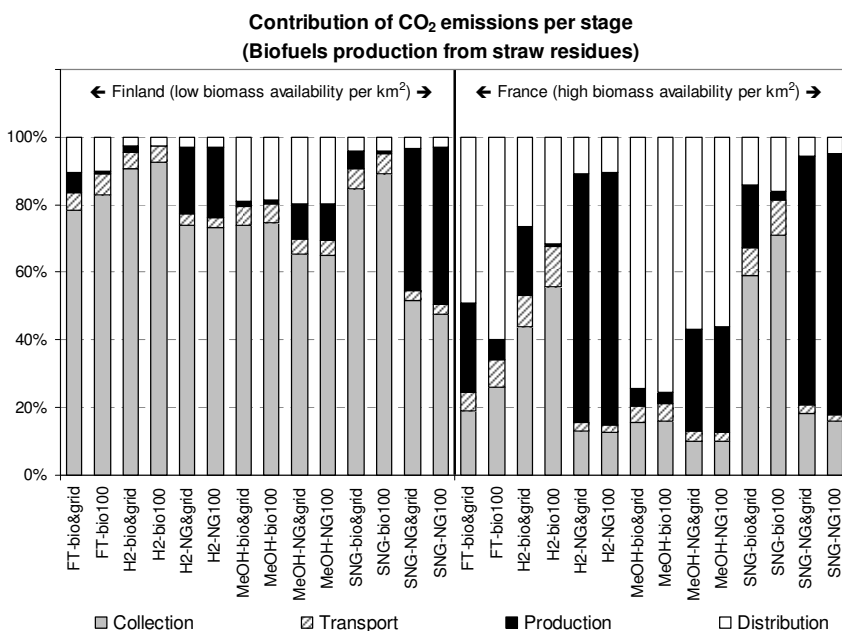
Figure 5.16: Contribution of each stage of the straw-to-biofuel chain on the total CO$_2$ emissions. Values are given for two locations with different biomass availability.

As observed, biofuel distribution (white bars) becomes more important for liquid FT-fuels and MeOH as, aforementioned, they are distributed by tank trucks that consume fossil diesel. Biofuel production (black bars) becomes significant when natural gas is used to provide heat and electricity for the processing plant (i.e., '*NG-100*' and '*NG&grid*' configurations). Biomass collection (grey bars) is the main contributor to total CO_2 emissions for the Finland case. This stage is gradually more important for '*bio&grid*' and '*bio-100*' configurations as an extra biomass amount is needed to replace natural gas and grid-power. The collection stage is to some extent more important for the straw-based alternative due to the low density of this feedstock.

Biofuels are also compared according to the functional unit of "*1 km of driving distance*" in subsequent Figure 5.17 to Figure 5.19. Values are obtained by applying expected car efficiencies by 2020 to previous figures (i.e., $1.03MJ_{SNG}$/km, $1.33MJ_{MeOH}$/km, $0.92MJ_{FT}$/km, $0.81MJ_{H2}$/km and $0.51MJ_{elec}$/km [112]). In this baseline, electric vehicles (BEV) release again the lowest amount of CO_2 per driving distance, irrespective of the location, feedstock and/or plant configuration. In effect, for the French case, emissions are in the range of 6-7 g-eq CO_2/km for forest residues and straw respectively, whereas for Finland, emissions are increased up to 51-88 g-eq CO_2/km. Energy crops would produce even lower emissions, i.e., 5 g-eq CO_2/km.
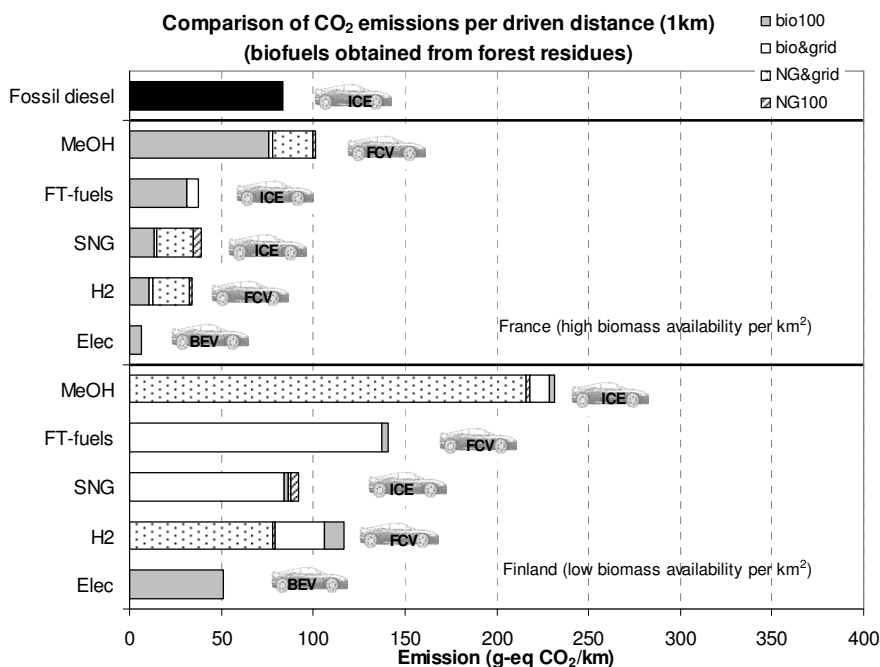
Figure 5.17: *Comparison of CO_2 emissions that are released per 1 km, for two locations with different biomass availability per hectare. Biofuels are obtained from forest residues.*
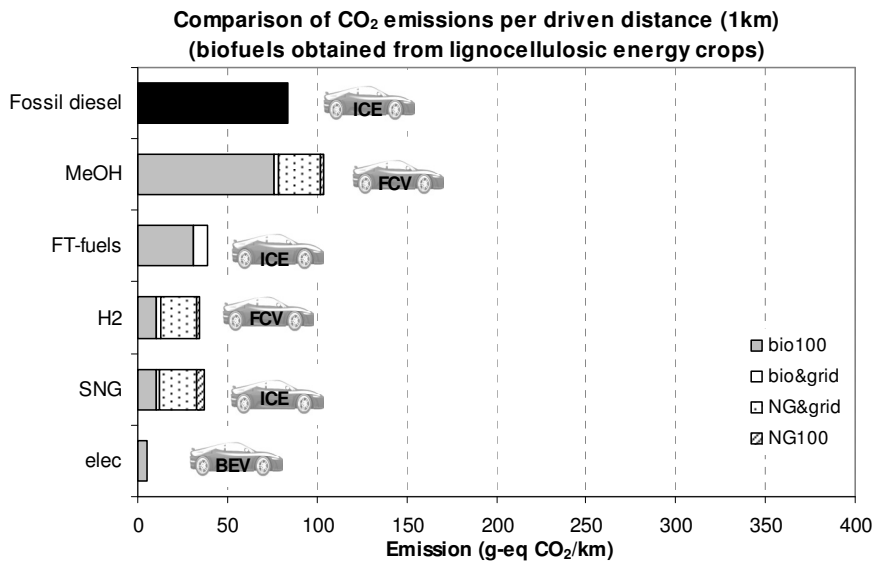
Figure 5.18: *Comparison of CO$_2$ emissions that are released per 1 km. Biofuels are obtained from energy crops in a 'virtual' region (VEC).*
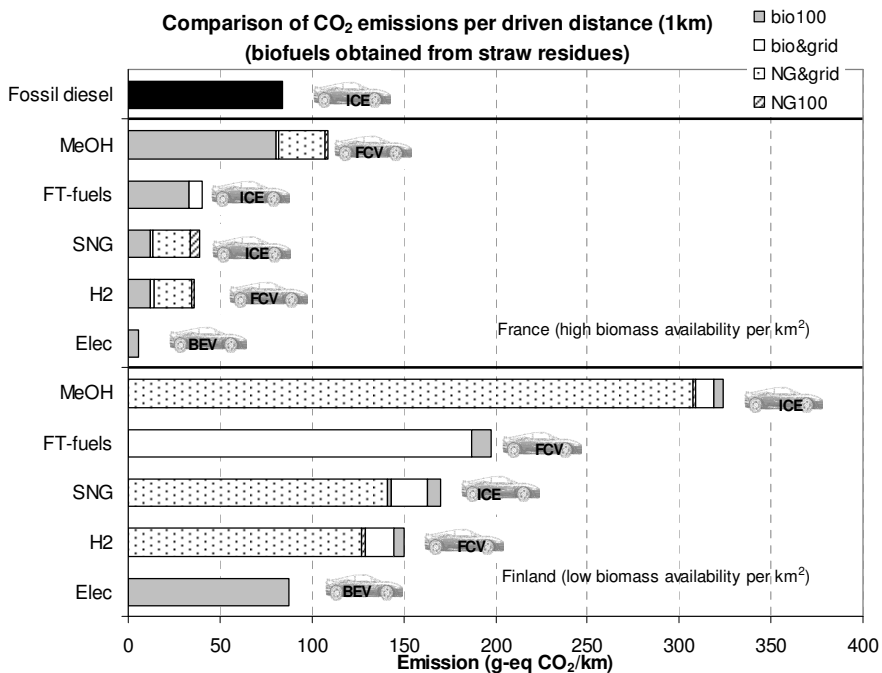
Figure 5.19: *Comparison of CO$_2$ emissions that are released per 1 km, for two locations with different biomass availability per hectare. Biofuels are obtained from straw residues.*

The rest of biofuels are also compared according to the plant configuration: '*bio-100*' (grey bars), '*bio&grid*' (white bars), '*NG&grid*' (dotted bars) and '*NG-100*' (dashed bars). Values of each configuration are added on top of the previous one. Comparisons among configurations reveal that, although SNG releases less CO_2 per MJ_{fuel} (see previous Figure 5.11 and Figure 5.12), H_2 is a better fuel than SNG when emissions are recalculated for the driving distance of 1 km (see Figure 5.17 to Figure 5.19). The main explanation for this fact can be found in the expected higher efficiency of H_2-FCV vehicles versus conventional CNG cars (i.e., 0.51 vs 1.03 MJ_{fuel}/km expenditure for H_2 and SNG fuelled cars respectively). MeOH is again the worst option from an environmental point of view, as not only the emissions per energy output were already the highest (see Figure 5.14), but also MeOH-fuelled FCV vehicles are the least efficient (i.e., 1.33 MJ_{MeOH}/km). The '*bio-100*' configuration (grey bars) is the preferred alternative for France and the virtual energy crop region (VEC), closely followed by the '*bio&grid*' configuration (white bars). Opposite conclusions are drawn for Finland, for which the '*NG&grid*' (dotted bars) becomes the best solution to minimize CO_2 emissions in this location.

Results are also compared with the proposal of the European Parliament that establishes a gradual GHG's emissions reduction for biofuels [117] (see section 5.1). In particular, we have adopted the measure that biofuels should reduce at least 60% of the GHG's emissions with regard to fossil fuels by 2018, as we estimate that 2nd generation technologies will be available after 2020. Table 5-3 compiles the list of countries and plant configurations that would fulfill the '60% target'. As expected, countries with large biomass availability per hectare would have more options to comply with the European proposal (e.g., France, Italy, Germany or United Kingdom). Results for energy crops (VEC region) are rather similar to those regions. Conversely, countries such as Estonia or Ireland would be limited to bioelectricity production to reduce CO_2 emissions to a certain extent. Table 5-3 also identifies that MeOH production would not comply with the '*60% target*', irrespective of the plant configuration, country or feedstock, whereas FT-fuels production would be limited to only 5 countries (i.e., Austria, Belgium, France, Romania, Slovenia) or the virtual 'energy crops' region (VEC).

Table 5-3: *Identification of those countries and plant configurations that would meet European Parliament targets concerning GHG's emission reduction of biofuels [117].*

Countries → / Chain ↓	AU	BE	BU	CZ	DK	EE	FI	FR	DE	GR	HU	IE	IT	LV	LT	NL	PL	PT	RO	SK	SI	ES	SE	UK	EC
TRANSPORT SECTOR (Comparison with fossil diesel)																									
SNG-bio100(wood)	✓	✓	✓	✓	✗	✗	✗	✓	✓	✗	✗	✗	✓	✗	✓	✓	✓	✗	✗	✓	✓	b.t.	b.t.	✓	✓
SNG-bio&grid(wood)	✓	✓	✓	✓	✗	✗	✗	✓	✓	b.t.	b.t.	✗	✓	b.t.	✗	✓	✓	b.t.	b.t.	✓	✓	b.t.	b.t.	✓	✓
SNG-NG100(wood)	b.t.	b.t.	b.t.	b.t.	✗	✗	b.t.	b.t.	b.t.	b.t.	b.t.	✗	b.t.	✗	b.t.	b.t.	b.t.	b.t.	b.t.	b.t.	b.t.	b.t.	b.t.	b.t.	b.t.
SNG-NG&grid(wood)	✓	b.t.	b.t.	b.t.	✗	✗	b.t.	✓	b.t.	b.t.	b.t.	✗	✓	b.t.	b.t.	b.t.	✓	✗	✗	✓	b.t.	b.t.	b.t.	✓	✓
SNG-bio100(straw)	✗	✓	✓	✓	✓	✗	✗	✓	✓	b.t.	✓	✗	✓	✗	✓	✓	✓	b.t.	✓	✓	b.t.	b.t.	✗	✓	
SNG-bio&grid(straw)	✗	b.t.	b.t.	✓	b.t.	✗	b.t.	b.t.	b.t.	b.t.	b.t.	✗	b.t.	✗	✓	✓	b.t.	✗	b.t.	b.t.	b.t.	b.t.	b.t.	✓	
SNG-NG100(straw)	✗	b.t.	b.t.	b.t.	✗	✗	b.t.	b.t.	b.t.	b.t.	b.t.	✗	b.t.	✗	✗	✓	b.t.	b.t.	b.t.	b.t.	✗	b.t.	b.t.	b.t.	✗
SNG-NG&grid(straw)	✗	b.t.	✓	b.t.	✓	✗	b.t.	✓	b.t.	b.t.	b.t.	✗	✓	✗	b.t.	b.t.	✓	b.t.	✓	b.t.	b.t.	b.t.	b.t.	✓	✗
H2-bio100(wood)	✓	✓	✓	✓	✗	✗	✗	✓	✓	b.t.	b.t.	✗	✓	b.t.	✓	✓	✓	b.t.	b.t.	✓	b.t.	b.t.	✗	✓	✓
H2-bio&grid(wood)	b.t.	b.t.	b.t.	b.t.	✓	✗	b.t.	b.t.	b.t.	b.t.	b.t.	✗	✓	✗	b.t.	b.t.	b.t.	b.t.	b.t.	b.t.	b.t.	b.t.	b.t.	b.t.	✓
H2-NG100(wood)	✓	b.t.	b.t.	b.t.	✗	✗	✗	b.t.	b.t.	b.t.	✗	✗	✓	✗	b.t.	b.t.	✓	✗	✗	✓	✗	b.t.	b.t.	✓	✓
H2-NG&grid(wood)	✓	b.t.	✓	✓	✓	✗	b.t.	✓	✓	b.t.	b.t.	✗	✓	✗	b.t.	b.t.	b.t.	b.t.	✓	b.t.	b.t.	b.t.	b.t.	✓	
H2-bio100(straw)	✗	b.t.	b.t.	✓	✗	✗	b.t.	b.t.	b.t.	b.t.	✗	✗	b.t.	✗	✗	✗	b.t.	b.t.	✗	b.t.	b.t.	b.t.	✗	b.t.	b.t.
H2-bio&grid(straw)	b.t.	b.t.	b.t.	b.t.	✗	✗	b.t.	b.t.	b.t.	b.t.	✗	✗	b.t.	✗	✗	✗	b.t.	b.t.	b.t.	b.t.	b.t.	b.t.	✗	b.t.	b.t.
H2-NG100(straw)	✗	b.t.	b.t.	✗	✗	✗	✗	✗	✗	✗	✗	✗	✗	✗	✗	✗	✗	✗	✗	✗	✗	✗	✗	✗	✗
H2-NG&grid(straw)	✗	b.t.	b.t.	b.t.	✗	✗	b.t.	✗	b.t.	✗	✗	✗	b.t.	✗	✗	✗	b.t.	b.t.	✗	b.t.	✗	b.t.	✗	b.t.	✗
MeOH-bio100(wood)	b.t.	✗	✗	✗	✗	✗	✗	b.t.	b.t.	✗	✗	✗	b.t.	✗	b.t.	b.t.	b.t.	b.t.	✗	b.t.	b.t.	✗	✗	b.t.	b.t.
MeOH-bio&grid(wood)	b.t.	✗	✗	✗	✗	✗	b.t.	b.t.	b.t.	✗	✗	✗	b.t.	✗	b.t.	b.t.	b.t.	b.t.	✗	b.t.	b.t.	✗	✗	b.t.	b.t.
MeOH-NG100(wood)	✗	✗	✗	✗	✗	✗	✗	✗	✗	✗	✗	✗	✗	✗	✗	✗	✗	✗	✗	✗	✗	✗	✗	✗	✗
MeOH-NG&grid(wood)	✗	✗	✗	✗	✗	✗	✗	✗	✗	✗	✗	✗	✗	✗	✗	✗	✗	✗	✗	✗	✗	✗	✗	✗	
MeOH-bio100(straw)	✗	✗	✗	✗	✗	✗	✗	✗	✗	✗	✗	✗	✗	✗	✗	✗	✗	✗	✗	✗	✗	✗	✗	✗	✓
MeOH-bio&grid(straw)	✗	✗	✗	✗	✗	✗	✗	✗	✗	✗	✗	✗	✗	✗	✗	✗	✗	✗	✗	✗	✗	✗	✗	✗	
MeOH-NG100(straw)	✗	✗	✗	✗	✗	✗	✗	✗	✗	✗	✗	✗	✗	✗	✗	✗	✗	✗	✗	✗	✗	✗	✗	✗	✗
MeOH-NG&grid(straw)	✗	✗	✗	✗	✗	✗	✗	✗	✗	✗	✗	✗	✗	✗	✗	✗	✗	✗	✗	✗	✗	✗	✗	✗	
FT-bio100(wood)	✓	b.t.	b.t.	b.t.	b.t.	b.t.	✗	✓	b.t.	b.t.	b.t.	✗	b.t.	b.t.	b.t.	b.t.	✓	b.t.	✗	b.t.	✓	✗	b.t.	b.t.	✓
FT-bio&grid(wood)	b.t.	b.t.	b.t.	b.t.	b.t.	b.t.	b.t.	b.t.	b.t.	b.t.	b.t.	✓	b.t.	b.t.	b.t.	b.t.	✓	b.t.	b.t.	b.t.	b.t.	✗	✗	b.t.	b.t.
FT-bio100(straw)	✗	b.t.	b.t.	b.t.	b.t.	b.t.	✗	✓	✗	b.t.	b.t.	b.t.	✗	✗	b.t.	✗	✓	✓	✓	b.t.	b.t.	✗	✗	b.t.	
FT-bio&grid(straw)	✗	b.t.	b.t.	b.t.	b.t.	b.t.	✓	b.t.	✗	b.t.	b.t.	b.t.	✗	✗	b.t.	✗	✓	b.t.	b.t.	b.t.	b.t.	✗	✗	b.t.	
Elec-bio100(wood)	✓	✓	✓	✓	✓	b.t.	✗	✓	✓	✓	✓	✓	✓	✓	✓	✓	✓	✓	✓	✓	✓	✓	✓	✓	✓
Elec-bio100(straw)	b.t.	✓	✓	✓	✓	✗	✓	b.t.	✓	✓	✓	✓	✓	b.t.	✗	✓	✓	b.t.	b.t.	✓	✓	b.t.	✓	✓	
ELECTRICITY SECTOR (Comparison with coal power plants)																									
Elec-bio100(wood)	✓	✓	✓	✓	✓	b.t.	✗	✓	✓	✓	✓	✓	✓	✓	✓	✓	✓	✓	✓	✓	✓	✗	✓	✓	✓
Elec-bio100(straw)	✓	✓	✓	✓	✓	✓	✓	✓	✓	b.t.	✓	b.t.	✓	b.t.	✗	✓	✓	✓	✓	✓	✓	✓	✓	✓	

(a): b.t: refers below the targets of year 2018 (i.e., 60% of GHG's reduction)
(b): the '✓' sign indicates that the targets of year 2018 could be fulfilled
(c): the '✗' sign indicates that the corresponding chain pollutes more than the fossil fuel option.

Own results are also compared with studies from other authors in Figure 5.20, although system boundaries, methodology, assumptions or even technology commonly differ. Values are also compared with the production of fuels from fossil sources such as natural gas (NG) or coal. It should be mentioned that our calculations are extended to those countries where the biomass availability per hectare is far lower than the average value found in literature. Hence, our maximum values for biowastes (see black lines in Figure 5.20) normally exceed the predictions of other authors (grey lines). Conversely, minimum values for biowastes and energy crops are more in line with other authors as the biomass availability is more similar as well. MeOH is the only exception as Pehnt et al [135] found that CO_2 emissions would be about 55 g-eq CO_2/km, which is far from our estimate of 76-108 g-eq CO_2/km. In our model, one of the main contributors to CO_2 emissions is the distribution of MeOH via tank trucks. This stage is, however, not clearly included in Penht et al study [135], which could explain those large divergences with regard to our results.

Emissions from SNG production and use in transport have barely been quantified by other authors. Felder et al come to the same conclusion that SNG releases lower CO_2 emissions than fossil diesel [136], but they do not give a final specific figure per driven distance or energy output. For the rest of biofuels, results are comparable with those of literature, being H_2 one of the favorite alternatives from an environmental point of view. Same analysis has already been done in Figure 5.8 for electricity, whose values can be translated to transport applications by applying the estimated fuel consumption of electric cars (i.e., 0.51 MJ_{elec}/km).
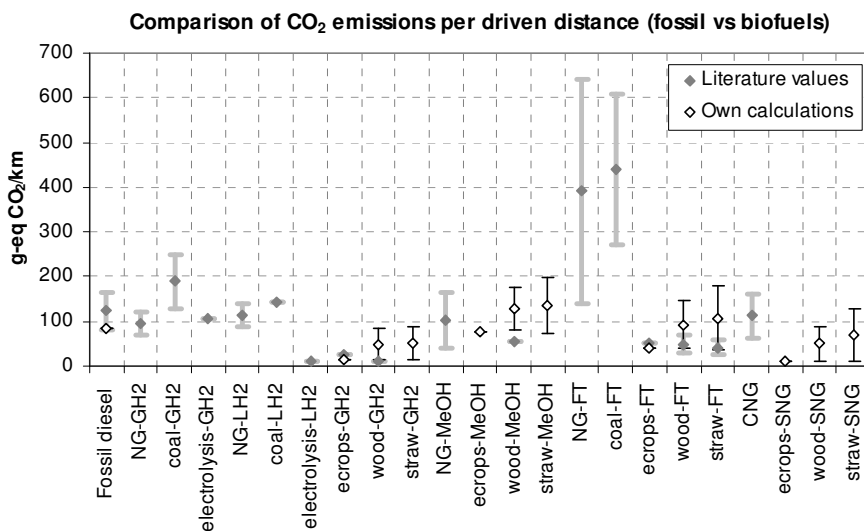

Figure 5.20: *Comparison of own calculations (black dots) with values retrieved from literature (grey dots). For certain fossil alternatives, the variation found in different studies is noticeable (e.g., FT-fuels from natural gas).*

Analogous to the previous section 5.3 for the electricity market, other environmental impacts are also analyzed in Figure 5.21 to Figure 5.25. In general, environmental impacts from MeOH production, irrespective of the plant configuration, are higher than diesel due to the relatively high fossil fuel consumption for its distribution. *Carciogenesis* effect is again negligible for either fossil or bioenergy systems, whereas the *ecotoxicity* indicator is increased when biomass replaces fossil diesel in locations similar to France. The rest of the factors directly depend on the feedstock and the plant configuration. For instance, the *euthrophication* and *winter smog* impacts of the '*bio-100*' and '*bio&grid*' configurations are always lower than the reference values of fossil diesel (i.e., 0.100 g-eq PO_4/km and 0.099 g-eq PM_{dust}/km respectively), with the exception of the MeOH pathway. Conversely, '*NG&grid*' and '*NG-100*' plant configurations release higher emissions for certain cases (e.g., MeOH and straw-based H_2 chains). As mentioned in previous section 5.3, *eutrophication* impact is even lower for coal-based power generation (see Figure 5.9).

Worse conclusions are drawn from the acidification effect of biofuels production than any other environmental parameter. In effect, '*bio-100*' and '*bio&grid*' configurations of the wood-based SNG pathway are the only alternatives that would release lower emissions than the reference value of fossil diesel (i.e., 0.642 g-eq SO_2/km). Fertilizers application for energy crops growing are partly responsible for the high acidification impact of this feedstock, irrespective of the biofuel being produced (see Table 0-6 in Appendix A). Thus, systems fed with energy crops always release higher acidification emissions than fossil diesel. Concerning bioelectricity production, emissions from forest residues conversion are also slightly lower than diesel-fuelled cars (i.e., 0.370 g-eq SO_2/km respectively).

Comparison of other environmental indicators per EU country
(SNG production from forest residues, energy crops or straw)

Legend:
- ■ fossil-fuel
- SNG-bio100-wood (FR)
- SNG-bio&grid-wood(FR)
- SNG-NG100-wood(FR)
- SNG-NG&grid-wood(FR)
- □ SNG-bio100-Ecrops
- SNG-bio&grid-Ecrops
- SNG-NG100-Ecrops
- SNG-NG&grid-Ecrops
- SNG-bio100-straw (FR)
- SNG-bio&grid-straw (FR)
- SNG-NG100-straw (FR)
- SNG-NG&grid-straw (FR)

Figure 5.21: *Comparison of other environmental indicators for SNG production in France (FR), a virtual "energy crops" region and fossil diesel. Values are given per driving distance.*

Comparison of other environmental indicators per EU country
(H_2 production from forest residues, energy crops or straw)
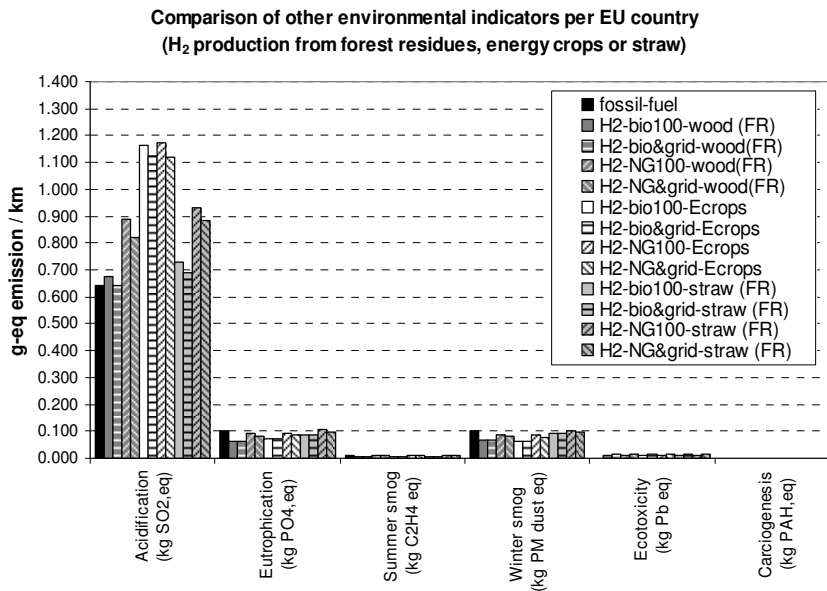
Figure 5.22: *Comparison of other environmental indicators for H_2 production in France (FR), a virtual "energy crops" region and fossil diesel. Values are given per driving distance.*

Comparison of other environmental indicators per EU country
(FT-fuels production from forest residues, energy crops or straw)
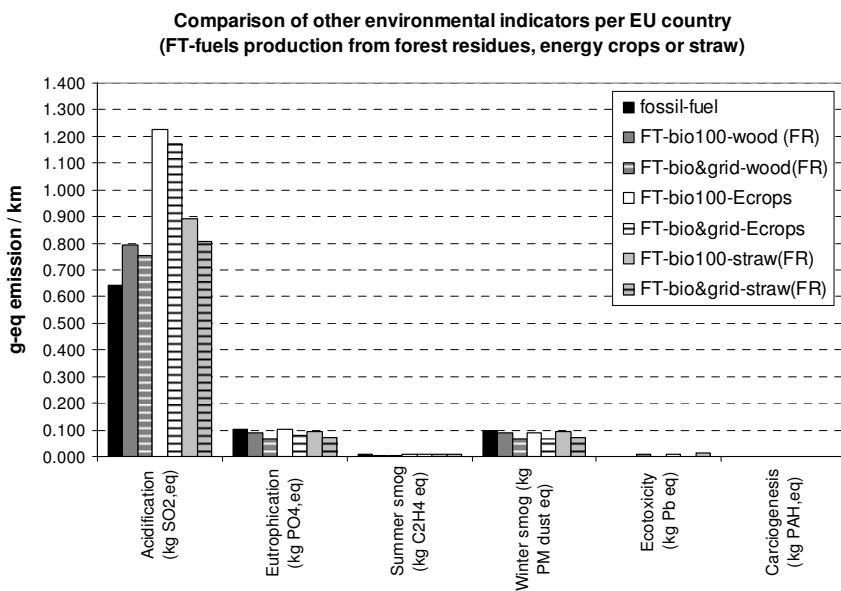
Figure 5.23: *Comparison of other environmental indicators for FT-fuels production in France (FR), a virtual "energy crops" region and fossil diesel. Values are given per driving distance.*

**Comparison of other environmental indicators per EU country
(MeOH production from forest residues, energy crops or straw)**
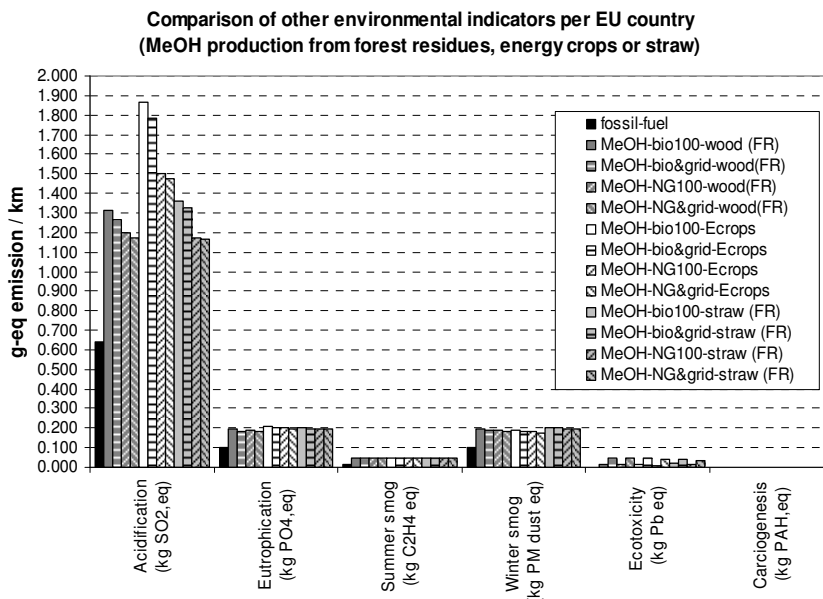
Figure 5.24: Comparison of other environmental indicators for MeOH production in France (FR), a virtual "energy crops" region and fossil diesel. Values are given per driving distance.

**Comparison of other environmental indicators per EU country
(Bioelectricity production vs fossil alternatives)**
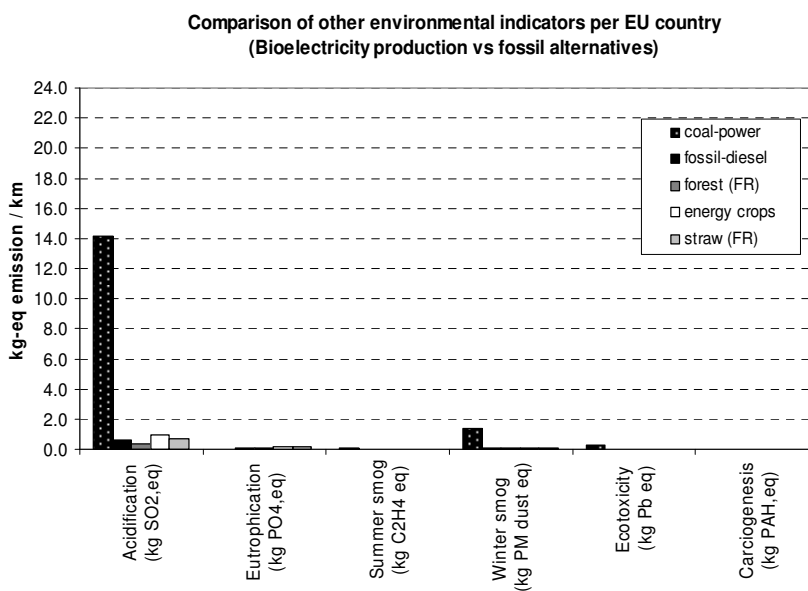
Figure 5.25: Comparison of other environmental indicators for bioelectricity production in France (FR) a virtual "energy crops" region, coal-based electricity and fossil diesel. Values are given per driving distance.

The quantification of these set of environmental impacts is less analyzed in literature than CO_2 emissions, which limits the possibility to compare with our results. As aforementioned, studies from other authors are conducted under different premises, plant scales and/or configurations, or transport distances. Moreover, some reports also include the stage of manufacturing the cars, which notably influences some environmental impacts. Felder et al have conducted an extensive analysis to compare the use of wood-based SNG for either heating or transport applications, by using the Eco-Indicator 99' and Eco-scarcity methods [136]. Direct comparison of values is rather difficult as their results are given in different units. Nevertheless, they come to the conclusion that SNG involves lower CO_2, NO_x and SO_2 emissions than conventional petrol/diesel vehicles, but higher particulates emissions. This statement is in line with our '*bio&grid*' and '*bio-100*' configurations for wood-fuelled SNG chains, with the exception that particulates emissions are also lower in our evaluation.

Concerning H_2 production, Koroneos et al have quantified acidification, eutrophication and winter smog emissions to be ~ 0.290 g-eq SO_2/MJ, ~0.028 g-eq PO_4/MJ and 0.140 g-eq PM_{dust}/MJ respectively, although they do not specify their biomass source [137]. Moreover, their study is only limited to the production process, thus excluding biomass collection and transport, and H_2 distribution. Our corresponding values for the production phase are higher for the acidification and eutrophication indicators but about two times lower for the winter smog (i.e., 0.559 g-eq SO_2/MJ, 0.067 g-eq PO_4/MJ and 0.069 g-eq PM_{dust}/MJ). Hence, reverse conclusions are drawn if the values are compared to the reference case of fossil diesel. For Koroneos et al, H_2-fuelled cars would lead to a decrease of acidification and eutrophication impacts, whereas we got higher impacts than diesel (see Figure 5.22). Unfortunately we have not found other studies to confront these divergences. Koroneos et al also state that, although production of H_2 from natural gas reforming release higher CO_2 emissions than the biomass chain, the acidification, eutrophication and winter smog impacts are lowered with natural gas conversion [137].

Patyk et al [138] and Pehnt [135] come to the same conclusion that bio-based MeOH production account for higher acidification, eutrophication, summer and winter smog impacts than fossil diesel. As shown in Figure 5.24, this statement is in line with our calculations, although values from Pehnt are notably lower [135]. Those differences could be attributed to the assumed fuel consumption of cars. Analogous to the H_2 case, Pehnt also concluded that MeOH production from fossil natural gas release lower acidification, eutrophication and summer smog emissions, while the GWP is still worse than the biomass chain [135].

Contradictory statements are found in literature for Fischer-Tropsch fuels production. Specialists from Choren Industries GmbH claim that acidification, eutrophication and summer smog impacts are reduced in comparison with fossil diesel [139]. Jungbluth et al have extended the analysis to different types of feedstock (i.e., wood, straw and lignocellulosic energy crops) and gasifiers designs (i.e., allothermal and authothermal CFB, and entrained beds) [140]. According to their values, all feedstock improve acidification emissions (i.e., 0.120-0.350, 0.237-0.528 and 0.466 g-eq SO_2/MJ for straw, wood and energy crops respectively versus 0.642 g-eq SO_2/MJ for fossil diesel) whereas eutrophication and summer smog impacts are aggravated by more than 4%

and 10% respectively for wood or straw, and 300% and 170% for energy crops. Our results are closer to Jungbluth et al [140], with the exception of the acidification impact (see Figure 5.23). Edwards et al also presume that acidification and eutrophication emissions would be significant for bio-based chains but they have not quantified those impacts [141].

There is some controversy about the real environmental benefits of the 2nd generation biofuels over the 1st generation. In fact, the biomass origin and its cultivation practices notably influence the overall emissions balance of 1st generation alternatives [142]. In any case, recent publications state that, analogous to our results for 2nd generation biofuels, 1st generation bioethanol and biodiesel also release higher acidification and eutrophication impacts than fossil fuels [142-146].

Finally, and analogous to the previous electricity market analysis in section 5.3, ecotaxes of Table 5-2 are also applied to biofuels to compute the effect of different environmental impacts (see Figure 5.26). In this case, liquid MeOH and FT-fuels turn out to be the most environmentally costly options for transport applications (i.e., 0.037-0.048 and 0.020-0.034 €/km respectively), being the '*ecotoxicity*', one of the most influencing impacts for either fossil or biofuels. Conversely, electricity and SNG production from forest residues would implied the lowest scores (i.e., 0.014-0.027 and 0.012-0.021 €/km respectively).
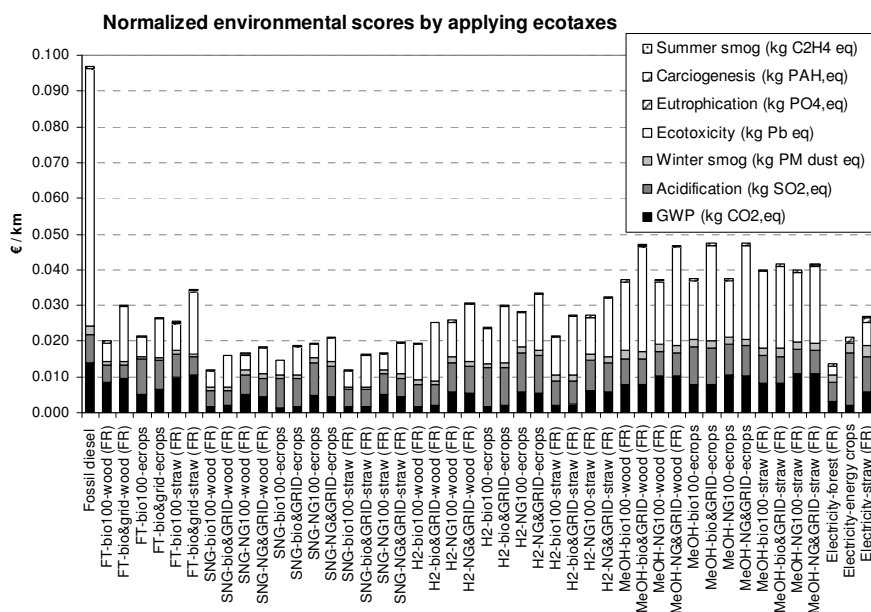

Figure 5.26: *Environmental impact is translated into a single score (in €/MJ$_{el}$) by applying the following ecotaxes $\gamma_{eco,i}$ [134]: 0.135 €/kg-eq CO_2 (GWP), 7.55 €/kg-eq SO_2 (acidification), 14.5 €/kg-eq PM_{dust} (winter smog), 802 €/kg-eq Pb (ecotoxicity), 3.6 €/kg-eq PO_4 (eutrophication), 14.5 €/kg-eq PAH (carciogenesis), and 3.5 €/kg-eq C_2H_4 (summer smog). CO_2 emissions come exclusively from the use of fossil fuel.*

5.5. *Sensitivity analysis*

A sensitivity analysis is conducted in this last section to identify the parameters that have the largest effect on the results, as well as to minimize the impact of inaccurate data on the conclusions. Accordingly, each parameter has been varied independently of all others so that the magnitude of its effect can be properly assessed. Figure 5.27 depicts the sensitivity analysis for FT-fuels production in two locations with disparate biomass availability per hectare. Previous calculations have shown that biomass collection is one of the stages with major impact on CO_2 emissions (see Figure 5.16 and Figure 5.17). In particular, it has been observed that increasing biomass production per hectare significantly reduce emissions. This can be done by applying fertilizers, as for the case of growing energy crops in a virtual region. However, it is rather difficult to know the impact of varying fertilizers dosing on the biomass productivity per hectare. Consequently, this factor is excluded from the sensitivity analysis.

Another alternative to decrease the impact of the biomass collection stage is to optimize the fuel consumption of tractors. In fact, and analogous to private cars, specialists presume that the efficiency of tractors will be improved by 2020. Similar expectations are drawn for the fuel consumption of trucks. Both parameters are varied by $\pm 30\%$ (i.e., fuel consumption in the range of 23-43 lt/ha and 0.65-1.20 MJ/tn.km for tractors and trucks respectively) in Figure 5.27. As observed, diesel consumption of trucks has a notably lower impact than in tractors, irrespective of the location (i.e., France or Finland). Conversely, fuel expenditure in tractors can even become the most relevant factor in countries where biomass is not densely available (e.g., Finland). Biofuel distribution is notably important for the case of liquid biofuels such as FT-fuels or MeOH as they are transported by means of tank trucks, which are fuelled with fossil diesel. Hence, the transport distance is also varied in the range of $\pm 30\%$ (i.e., $\pm$ 60 and 100km for France and Finland respectively). For France, this parameter becomes the most relevant one, whose deviation lies in the extent of ± 2 g-eq CO_2/km. Similar variation is calculated for Finland, although tractors efficiency is still the most influencing parameter on total CO_2 emissions. In the SNG, H_2 and electricity chains, the effect of the distribution distance is relegated to even lower positions as they make use of existing pipelines or grid systems. The last set of factors that have been included in the sensitivity analysis are related to the construction of tractors, trucks and production plants. Materials and energy use has been calculated by scaling the values of other authors, which entails certain inaccuracy. Calculations are also varied in the range of $\pm 30\%$, but it is observed that these parameters barely have an impact on total CO_2 emissions.

Additionally, the plant scale of the different biofuel systems has also been assessed to confront the optimal size from an economic point of view, i.e., ~100 $MW_{electricity}$, 200 MW_{SNG}, 500 MW_{H2}, 1000 MW_{FT} and 1000 MW_{MeOH} (see Chapter 6). In effect, plant scale has a direct impact on energy efficiency (see Chapter 4) and, thus, in total emissions. Figure 5.28 and Figure 5.29 summarizes the results for the same two different locations.

**Sensitivity analysis for the FT-bio100 configuration
(with wood as feedstock) - France**

■30% ■20% □10% □-10% ■-20% ■-30%

**Sensitivity analysis for the FT-bio100 configuration
(with wood as feedstock) - Finland**

■30% ■20% □10% □-10% ■-20% ■-30%
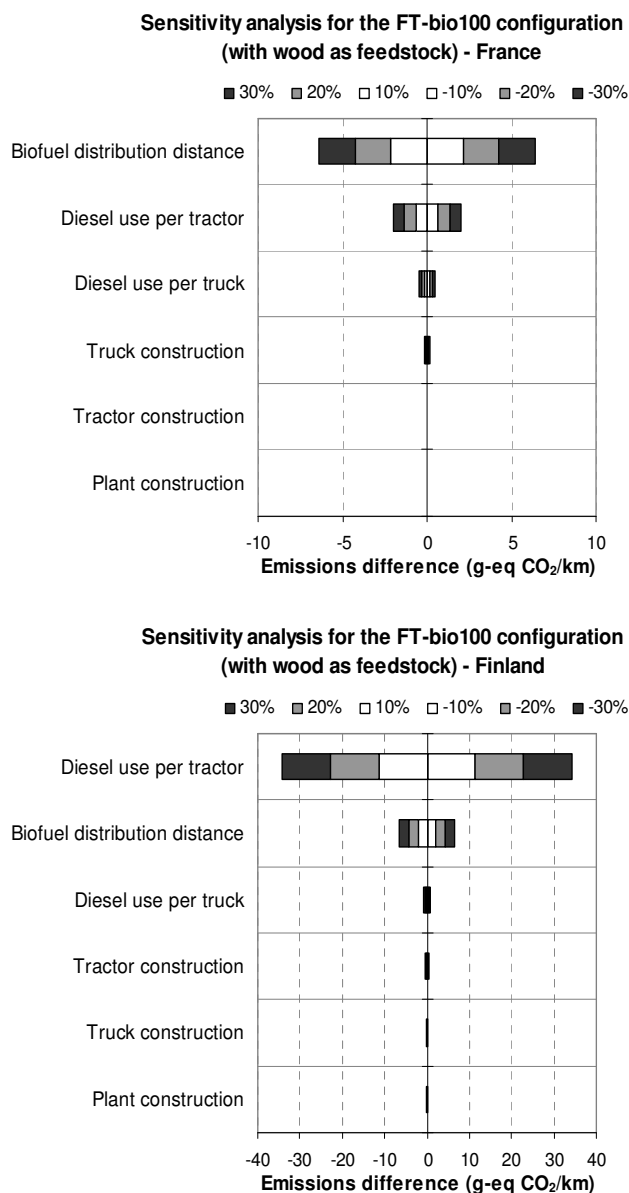
Figure 5.27: *Sensitivity analysis of several parameters on the total CO_2 emissions. The chain under analysis is the production of FT-fuels production from forest residues.*

The plant scale also dictates the transport distance between biomass collection areas and the processing plant. As expected, optimal 'environmental' scales are shifted to smaller scales. In that sense, optimal sizes are found to be around 200 MW_{fuel} for either MeOH or FT-fuels, between 100-200 MW_{fuel} for H_2, and about 100 MW_{fuel} for SNG. It should be mentioned that the effect of plant scale is less marked for France than for Finland.

**Effect of pant scale on total CO$_2$ emissions (France)**
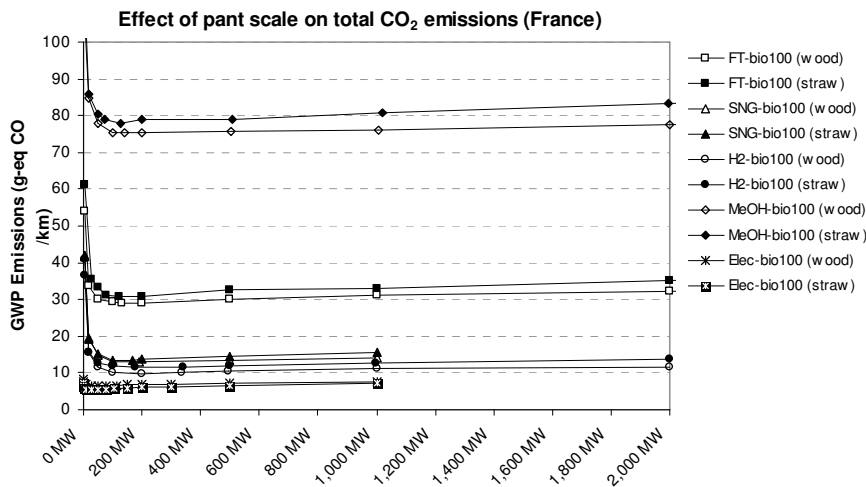
Figure 5.28: *Effect of plant scale of total CO$_2$ emissions in France (i.e., a location with low biomass availability per hectare).*

**Effect of pant scale on total CO$_2$ emissions (Finland)**
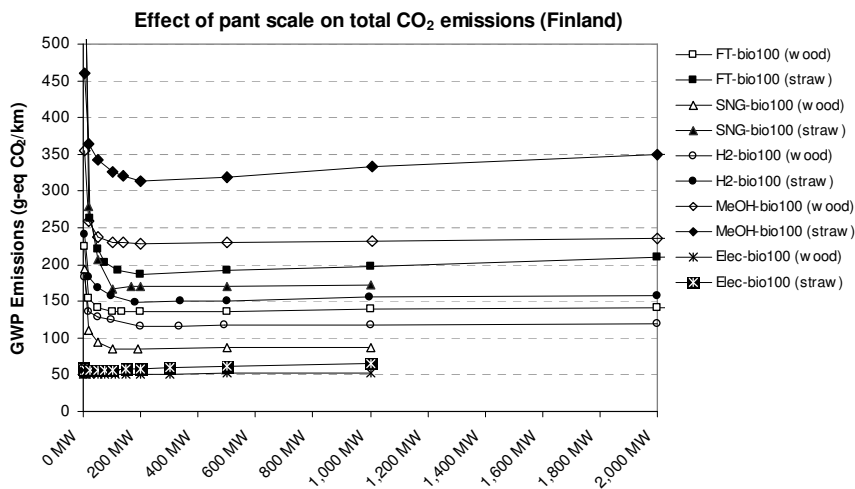
Figure 5.29: *Effect of plant scale of total CO$_2$ emissions in France (i.e., a location with low biomass availability per hectare).*

The optimal value for electricity production is about 25 MW$_{el}$, although the variation is not significant for the range of 10-150 MW$_{el}$. Another important remark is that, even at optimal scales, MeOH production is still more pollutant than fossil diesel in most of the European countries.

5.6. *Conclusions*

An environmental impact analysis has been conducted in this chapter to confront the GHG's emissions targets of the European Parliament [117]. The study has been extended to different biofuels plant configurations and locations to identify which would be the best option from an environmental point of view. Moreover, the analysis covers two very distinct sectors, i.e., electricity and transport.

According to the results, bioelectricity releases notably lower CO_2 emissions than coal power generation, irrespective of the location, plant configuration or feedstock (i.e., 10, 9-271 and 9-295 g-eq CO_2/MJ for energy crops, forest and straw residues versus 400 g-eq CO_2/MJ for coal). In most locations, bioelectricity chains also emit less CO_2 than oil or natural gas-fueled power installations. Growing energy crops in regions with low biowastes availability would be an interesting option as they release the minimum amount of CO_2 emissions. However, this practice increases the *acidification* and *eutrophication* impacts in comparison with forest or straw residues. In effect, production and application of fertilizers account for a significant amount of ammonia, SO_2, NO_x, nitrates or phosphates emissions. The rest of environmental impacts (i.e., *ecotoxicity*, *summer* and *winter smog*) are reduced when coal is replaced by any source of biomass, with the only exception of the *eutrophication* impact. Virtual *ecotaxes* of Table 5-2 are also applied to estimate the environmental costs that should be added on top of fuel prices to penalize the emissions released during their production and distribution. This calculation also takes into account that, although CO_2 emissions are by far the largest in quantity, there are other environmental impacts that are more harmful to human's health. As expected, the corresponding values for coal-based power generation (i.e., 0.750 €/MJ_{el}) are notably larger than those for bioelectricity (i.e., 0.023, 0.025 and 0.029 €/MJ_{el} for forest residues, straw and energy crops respectively).

Alternatively, biofuels and bioelectricity production is also analyzed for the transport sector. In this case, the functional unit (f.u.) is fixed to '*1 km*' of driving distance. Energy crops are again the preferred feedstock for minimizing CO_2 emissions, although regions with high biomass density per hectare yield similar values (e.g., France). Results also show that electricity and SNG production release the lowest CO_2 emissions per energy output (i.e., 10 g-eq CO_2/MJ_{el} and 10 g-eq CO_2/MJ_{SNG} for energy crops, and 9-10 g-eq CO_2/MJ_{el} and 13-14 g-eq CO_2/MJ_{SNG} for France). However, H_2 becomes the second best alternative if the predicted fuel consumption of vehicles (FE) by 2020 is applied. In any case, electric cars release always the lowest CO_2 emissions per driven distance (i.e., 5 g-eq CO_2/km for energy crops, and 6-7 g-eq CO_2/km for France). Conversely FT-fuels, and particularly MeOH, production normally release the highest CO_2 emissions per either energy output or driven distance. There are even certain locations where the production of these liquid biofuels emits more CO_2 than fossil diesel. The amount of other environmental impacts is also analyzed for the transport sector. Results reveal that the *acidification* impact is normally larger for biofuels than for fossil diesel. The sole exceptions are SNG and bioelectricity generation from forest residues in the '*bio-100*' configuration mode. *Cargiogenesis* effect is almost negligible for either fossil or biofuels whereas

ecotoxicity is larger for all bioenergy systems. The rest of parameters (i.e., *eutrophication*, *winter* and *summer smog*) directly depend on the feedstock and plant configuration.

Results of the CO_2 emissions are also compared with European targets in Table 5-3. According to the European Parliament, new biofuels technologies should at least reduce 60% of the GHG's emissions in comparison with fossil alternatives. As observed, countries with a large biomass reserve per hectare would fulfil this target with either SNG, electricity or H_2 production, whereas FT-fuels generation is reserved to the 'top-4' (i.e., Austria, Belgium, France and Slovenia) countries or the 'virtual region with energy crops (VEC). Moreover, our sensitivity analysis also reveals that plant scales and fuel consumption in tractors are the most influencing parameters on total CO_2 emissions. Biofuels distribution also plays an important role for liquid biofuels such as MeOH or FT-fuels.

In brief, bioelectricity production for either transport or electricity applications seems to be the best option from an environmental point of view, as most of the environmental impacts are minimized.

6

Economic analysis of biomass-to-biofuels and bioelectricity chains in European countries

Abstract

Biofuels price calculation has already been done by many authors. However, direct comparison among studies is rather inaccurate as they use different biomass prices, locations, plant scales and/or financial assunmptions. Hence, in this chapter, we present the economic evaluation of the five proposed biofuels following a standard procedure and under different plant scales and locations. Results reveal that wood-based biofuel are cheaper than straw-based chains, with the exception of France. In any case, SNG is always the most economical biofuel per unit of output energy (i.e., 14-33 €/GJ), followed by electricity (i.e., 20-40 €/GJ), FT-fuels (i.e., 21-41 €/GJ) and methanol (i.e., 22-42 €/GJ). The excessive distribution costs of H_2 renders this biofuel into the most expensive alternative (i.e., 24-43 €/GJ,. However, price differences between biofuels and their corresponding fossil competitors are the largest for bio-based SNG, thus hindering its possible penetration into the European energy market. Conversely, there are some locations where FT-fuels or H_2 prices are lower than fossil diesel after taxation. Similar observation is found for bio-electricity generation. A new taxation system is proposed to equalize biofuels and fossil fuels prices and maintain government's revenues from fuels taxes. Additionally, 'virtual' eco-costs are also calculated to charge CO_2 emissions that are released during biofuels or fossil fuels production and distribution stages. The summation of taxed fuel prices and ecocosts is the lowest for SNG when the comparison is made per output of energy (i.e., €/GJ_{fuel}). Conversely, bioelectricity is the preferred option when the comparison is made per driving distance (i.e., €/km).

6.1. *Introduction*

Biofuels have many advantages over conventional fossil fuels. In effect, as stated in previous chapter 5, they contribute to a net reduction of GHG's gases emissions, while decreasing the dependence on fossil sources. However, one of the main constraints for biofuels implementation is their higher price in comparison with conventional fuels. This tendency could change in the future when more restrictive emissions limits and taxes will be agreed. Moreover, fossil fuel prices are expected to increase considerably in the coming years due to reservoirs depletion and market speculation.

Some authors have already performed economic evaluations for a wide range of either 1st or 2nd generation biofuels, with prices lying in the range of 4.5 to 30 €/GJ [51, 52, 83, 103, 104, 147-157]. However, it should be noticed that these analyses are not performed on the same basis and, hence, side-by-side comparison of the different biofuels is rather difficult and inaccurate. In fact, these analyses are done at different plant sizes, while using inconsistent feedstock costs, diverse financial incentives as well as different methodologies to calculate capital and operating costs. Consequently, it becomes rather difficult to state which biofuels could be more economically attractive for their implementation into the energy market.

Hence, the aim of this chapter is to evaluate the commercial viability of producing five 2nd generation biofuels (i.e., SNG, methanol, Fischer-Tropsch, hydrogen and electricity) with the technology options discussed in previous chapter 3. For that purpose, we assume that biofuels production systems will be at a competitive level of technological maturity by 2020. Apart from the chosen technology, biofuels costs are strongly dependent on plant scales and local conditions. These two factors are included in our model by extending the economic appraisal to several plant sizes (i.e., from 1 to 5000 MW_{fuel}) and 24 European countries. This evaluation has the inherent objective of determining the optimal plant scale for each biofuel as well as the best plant location within Europe. Moreover, LCA analyses of previous chapter 5 have been included in the economic analysis by calculating an ecocost α_{CO2} (i.e., €/tn CO_2). This ecocost is a 'virtual' value that should be added on top of taxed prices to penalize CO_2 emissions. Hence it does not correspond with actual Carbon credits.

6.2. *Biofuels final end-user price*

Biofuels expected final '*end-user*' price have been calculated by adding the estimated price of each step of the value chain:

- **Production price**: price at which the investment of production plants is profitable.
- **Distribution price:** market price for distributing biofuels via pipelines or trucks.
- **Logistics price**: market price of outsourcing the services of collecting and transporting biomass to the biofuels processing plants.

It should be mentioned that the '***Production price'*** strongly depends on the '***Total Capital Investment' (TCI)***, which is different for each biofuel system and plant size,

as well as on the '***Total Production Costs' (TPC)***, which also depend on regional labor market conditions (see Table 6-1). '***Logistics price'*** is mainly a function of regional transportation infrastructures and average distance transported, which also increases with the plant size. Conversely, as concluded by literature review [32, 158-161] '***Distribution costs'*** merely depend on the type of biofuel.

Table 6-1: *List of dependencies of main components on the biofuel final 'end-user' price.*

Parameter			Biofuel type	Plant size	Region
Biofuel final 'end-user' price			●	●	●
↪	Production price 'ex-works'		●	●	●
	↪	Total Capital Investment (TCI)	●	●	
	↪	Total Production Costs (TPC)	●	●	●
↪	Logistics Price		●	●	●
↪	Distribution Price		●		

Accordingly, the global economic analysis has been modeled for each *biofuel system*, *plant size* and *regional parameters* (see Figure 6.1). Moreover, it has been repeated for both, wood and straw feedstock. This model is the base to determine the optimal plant size at which biofuel 'ex-work' prices are minimal.
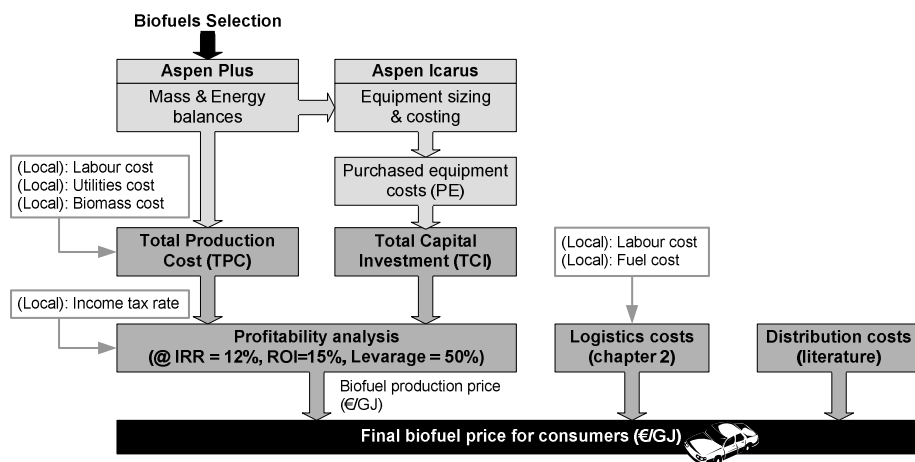

Figure 6.1: *Economic evaluation model, which is applied for the 5 different biofuels, under the 4 different plant configurations (see Figure 3.1) and for 24 European countries.*

6.2.1. *Biofuel 'ex-works' price calculation*

Biofuels production prices have been calculated by establishing an ***Investor's Rate of Return*** (IRR) of 12% for the required investment to implement each production plant. This figure is in accordance with European financial market standards for mid-term ventures within the renewable energy industry. For innovative ventures in the energy industry, and following same market standards, it is assumed that the '*Liability over Assets ratio'* (*Leverage)* of the venture can be up to 50% (i.e., half of the ***TCI*** is

covered by liabilities with financial institutions). Other assumptions used for the calculation of the biofuels production 'ex-work' prices are listed in Table 6-2.

Table 6-2: *List of assumptions that have been used for the economic appraisal.*

Parameter	Assumptions
Bank interest rate:	5%
Inflation rate:	2%
Income tax rate:	National values have been taken from eurostat database [5]
Depreciation:	Linear method, calculated over 10 years.
Start-up-time:	3 years after start of construction
Economic lifetime:	30 years
Nr. shifts:	5 shifts per day
Load factor:	8000 h/year
Utilities prices:	National values have been taken from eurostat database [5]
Biomass costs:	National values have been calculated in chapter 2

6.2.1.1.   Total Capital Investment (TCI)

The first component of the economic evaluation of a conversion plant is the '***Total Capital Investment'*** (**TCI**), which is calculated by means of factored estimation [45]. The expected accuracy is in the range of ±20-30%, although for comparable plants of different capacities, the accuracy can become close to ±10%. The application of this method requires the determination of the purchased equipment cost (PE) of all the components units of the conversion system. As shown in Table 0-11 of Appendix J, the rest of the direct (DFC) and indirect fixed costs (IFC) are estimated as percentages of this PE. This Table 0-11 also gives the corresponding percentages of the Fixed Capital Investment (FCI), whose values lay in the range proposed by several authors [45, 162]. Purchased equipments costs (PE) of standard components units are calculated by means of the Aspen Icarus simulation program [44]. However, its library has a limited range of specific reactors and, hence, PE costs of gasifiers, catalytic reactors, tar crackers, Selexol and even air separation unit (ASU) have been retrieved from values found in literature (see Table 0-12 in Appendix J). William's equation (6-1) is applied to adjust the prices to the correct size, and the resulting price is multiplied by a cost index factor in order to update literature values to our reference year 2010. Although there are several published indexes that permit fairly accurate estimates, the '*Chemical Engineering Plant Cost Index (CE Index)[16]*'' has been used in our calculations.

$$Cost_{actual} = Cost_{ref} \cdot \left(\frac{Size_{actual}}{Size_{ref}} \right)^{R_f} \cdot \left(\frac{CE\ Index_{actual}}{CE\ Index_{ref}} \right) \qquad (6-1)$$

---

[16] These indexes are monthly published in the '*Chemical Engineering Journal'*.

where "R_f" is the scaling factor which is specific for each component (see Table 0-12 in Appendix J), although it generally lies between 0.4 and 0.8. Moreover, since various equipments have a limited maximum size, multiple units are placed in parallel whenever the size exceeds this technological limit.

Figure 6.2 summarizes the required TCI when using the same amount of biomass input (i.e., 57 tn/hr of either forest or straw residues) and for the 5 proposed biofuels under the 4 different plant configurations of Figure 3.1. The usefulness of this figure is to compare the required TCI for a given biomass availability. Hence, in general, wood-fuelled biofuels plants require less investment as its efficiency is higher than straw conversion plants (see Chapter 4). Moreover, the pre-treatment section for forest residues is smaller in size, in particular the storage and conveying facilities, as wood density is about 4 times higher than straw. Whenever extra biomass is burned to provide heat and/or electricity to cover the energy demand of the processing plant (i.e., 'bio-grid' and 'bio-100' configurations), the corresponding TCI are consequently larger as the biomass pre-treatment section needs to be enlarged. Additionally, burners, HRSG systems and turbines also need to be incorporated or enlarged in both configurations. Comparison among biofuels shows that SNG production involves lower TCI, followed by electricity generation, whereas Fischer-Tropsch fuels and methanol plants are on the opposite side. However, as indicated by later analysis (see section 6.2.3), TCI values in Figure 6.2 do not correspond with their optimal scales, with the exception of wood-fuelled SNG and electricity plants, and straw-fuelled power plants. The rest of biofuels systems need larger plant scales in order to achieve more competitive biofuels prices. Consequently, TCI for optimal biofuels plant scales is given in subsequent Figure 6.3. Similar trends are observed, although differences among biofuels are more remarkable.
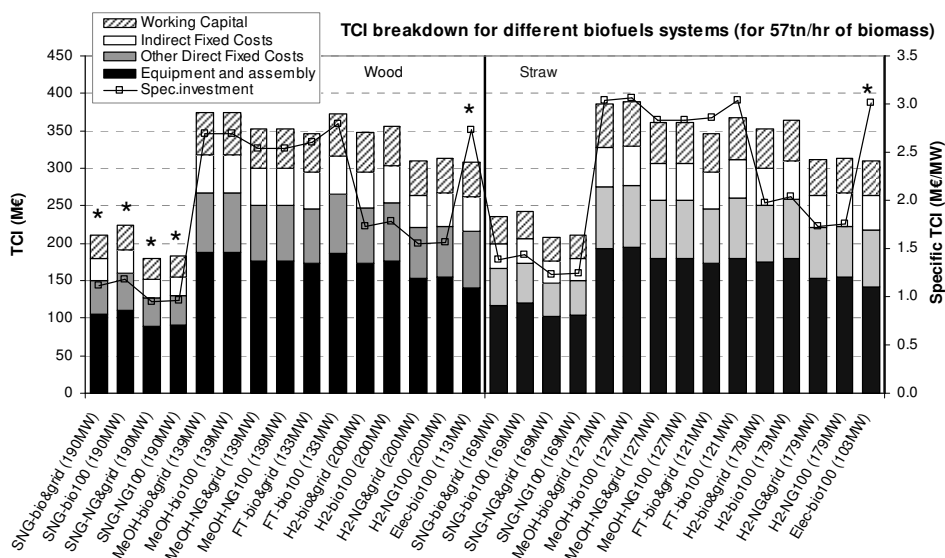

Figure 6.2: *TCI breakdown when using same amount of wood (left side) and straw (right side) for 5 biofuels and 4 different plant configurations in Figure 3.1. The "*" sign indicates optimal plant scales. Lines represent the specific TCI.*
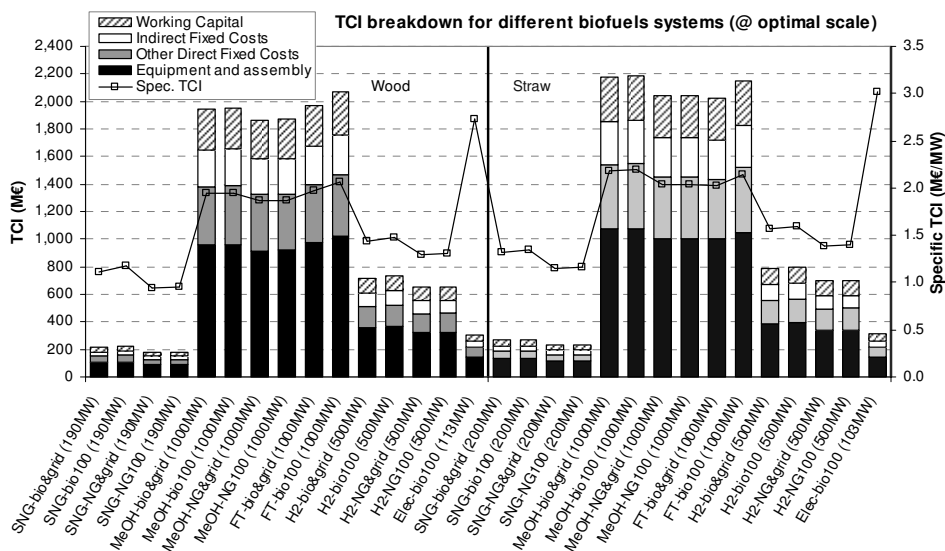
Figure 6.3: *TCI breakdown at optimal plant scales(bars).Lines represent the specific TCI.*
Values are given for 5 different biofuels and 4 different plant configurations in Figure 3.1.

For a complete picture, Appendix J contains the total purchased equipment (PE) breakdown costs per each operation unit. As aforementioned, proper determination of PE is of crucial importance because the rest of the parameters of the TCI are calculated based on that value. An added remark is that gasification accounts for 22-45% of the PE in all biofuels systems, followed by catalytic reactors (i.e., 14-29%) and heat and electricity generation (i.e., 8-27% for biofuels production but up to 64% in the bioelectricity production chain). Hence, reducing gasifier's purchasing price would notably decrease the TCI, and consequently the final biofuel price.

6.2.1.2.   Total Production Costs (TPC)

The second major component of any economic analysis corresponds to the '*Total Production Costs*' (TPC), which include the costs related to: operating the plant, selling the products, recovering the capital investment and contributing to corporate functions such as management and R&D. These costs are further itemized into the several categories presented in Table 0-13. Depreciation is calculated separately in the Profitability analysis (i.e., section 6.2.1.3) as it changes from year to year. Mass and energy balances from Aspen Plus simulations are used to determine raw materials and utilities costs, which represent up to 40% of the TPC in large plant scales. Labor requirements (i.e., workers and supervisors per shift) are calculated as a function of the number and type of components units of the whole processing plant [45]. Operating labor costs are especially sensible to plant sizes and regional GDP data, and they can account for 45% of TPC in small facilities. Analogous to the TCI calculation, the rest of the items are calculated by factored estimation, as shown in the same Table 0-13. TPC values at different plant sizes follows similar trends as efficiency numbers in Chapter 4. In effect, larger scales imply relatively smaller specific TPC (i.e., TPC divided by total biofuel production).

6.2.1.3.   *Optimal plant size determination per each biofuel system*

For all systems, biofuels production price is iterated to give an IRR of 12%[17], and the resulting values are summed to logistics to obtain biofuel '*ex-works*' price. The ultimate goal of this calculation is to identify the optimal plant size that will lead to more competitive biofuels prices. Distribution costs are then added to the 'ex-works' price to obtain the final biofuel '*end-user*' price in section 6.2.3. These distribution cost do not influence the optimal plant size as they are assumed to be constant for a fixed distance of ~ 200 km.

6.2.2.   *Distribution costs*

Distribution costs of each biofuel are calculated from literature data [32, 158-161]. As observed, hydrogen distribution is by far more expensive than other biofuels (see Table 6-3). Moreover, an extra cost should be added in case hydrogen pipelines would need be enlarged to serve hydrogen demand. Hydrogen transportation by trucks is ignored as overall costs are even higher (i.e., 16 €/GJ for trucks vs 10 €/GJ for pipelines [158]). Due to lack of clear information, distribution costs for methanol are assumed to be equal to bioethanol. Fischer-Tropsch distribution costs are slightly lower than methanol as it combines transport by pipelines from plant to bulk and trucks to cover the remaining distance. Electricity distribution costs are assumed to be 10% of the production price.

Table 6-3: Biofuels distribution costs that have been calculated from literature [32, 158-161].

Biofuel	Distribution cost
SNG	3.61 €/GJ
Fischer-Tropsch	3.44 €/GJ
Methanol	4.32 €/GJ
Hydrogen	10 €/GJ
Electricity	~ 10% production price

### 6.2.3.   *Biofuels 'end-user' prices comparison*

For a complete picture, the comparison among final '*end-user*' prices is divided in three sections. Firstly, and analogous to the TCI calculation in section 6.2.1.1, we compare the resulting prices for the case where biomass availability was limited to a certain value (i.e., 57 tn/hr of either forest or straw residues). This biomass amount corresponds to medium plant sizes and it would be available in all European countries with the exception of Ireland and Estonia. Results for Germany are depicted in Figure 6.4. Other countries show similar trends although with different quantitative values (see Appendix J). Biofuel 'end-user' price is the sum of 'ex-work' (i..e., grey bars) and distribution values (i.e., dashed bars).

---

[17] Following all premises and assumptions of Table 6-2, the payback period (PB) is slightly below 5 years and the return on investment (ROI) is found to be ~ 15% (i.e, moderate risk).

According to both figures, SNG is identified as the cheapest option (i.e., 23.9-25.2 and 25.1-27.3 €/GJ for wood and straw-based bio-SNG), whereas FT-fuels and methanol are the most costly option (i.e., 38.0-40.1 and 39.2-41.7€/GJ for wood and straw-based biofuels). However, it should be mentioned that each biofuel has different application in the energy market (e.g., lighting, heating or transport), thus, direct comparison could lead to confusing conclusions. To overcome this possible misinterpretation, biofuels are compared with their corresponding fossil competitor (see black straight lines in the same Figures). In this case, the price difference between bio-SNG and its fossil homonym is notably higher (i.e., bio-SNG values are about 2-fold larger). Conversely, less divergences are found for the rest of biofuels. In particular, German bio-electricity is ecomically more competitive than fossil-based power generation (i.e., 32.9 €/GJ$_{el}$ versus 33.6 €/GJ$_{el,2007}$). This observation, however, is only valid for some European countries, as discussed later in Figure 6.9. There are already some small-scale bioelectricity plants operating in Germany although larger scales, which would benefit from the mentioned reduced price of 32.9 €/GJ$_{el}$, are not yet well-proven. On the other hand, and analogous to TCI conclusions, straw-based biofuels are always more expensive than the corresponding wood-fueled options.

Figure 6.4 also includes the biofuel expenditure per km in case they were used in conventional (*FT-fuels*) or adapted vehicles such as *ICE (for SNG), FCV (for H₂ and MeOH)* or *battery electric vehicles (BEV)*. Fuel consumption in chapter 4 has been used for that calculation (i.e., 1.03MJ$_{SNG}$/km, 1.33MJ$_{MeOH}$/km, 0.92MJ$_{FT}$/km, 0.81MJ$_{H2}$/km and 0.51MJ$_{elec}$/km [112]). As observed, high efficiency BEV vehicles lead to less fuel expenditure (i.e., 1.6 ¢€/km), whereas methanol is again the most expensive alternative (i.e., 5.2-5.5 ¢€/km). However, manufacturing car companies state that *BEV* and *FCV* vehicles are at least 2-fold more expensive than conventional diesel cars. For an average annual driving distance of 20,000 km, it means that the FT-fuels and bio-electricity price difference will be compensated after more than 40 years of operation. This figure will correspond to the case that actual fossil diesel prices do not change within the coming years. If fossil diesel prices are doubled, the time period would be reduced to ~ 15 years. Following same calculations, the time period would be increased to more than 20 years if the comparison is made between diesel and H₂. Hence, it of crucial importance to reduce the capital costs of alternative cars in order to make alternative biofuels more attractive for consumers. Moreover, since the presented FT-fuels values in Figure 6.4 do not correspond with their optimal plant scale, the compensation period will be larger than 40 years.

Secondly, the analysis has been extended to different plant configurations, sizes and locations within Europe. However, for a better clarity, the effect of plant scale on biofuel prices has been represented only for one configuration (i.e., '*bio&grid*' in Figure 3.1) and one country in subsequent Figure 6.5 and Figure 6.6. In effect, optimal plant sizes are found to be equal irrespective of the plant configuration (i.e., '*bio&grid*', '*bio-100*', '*NG&grid*' or '*NG-100*') and location. Corresponding exergetic efficiency values are also represented in the same figure to point out the effect of this parameter on the biofuel prices. According to the results, electricity and SNG production is more profitable at lower sizes (i.e., 100 and 200 MW$_{fuel}$ respectively), followed by H₂ (i.e., 500 MW$_{H2}$), whereas methanol and FT-fuels generation require larger plants (i.e., 1000 MW$_{fuel}$).

Comparison of biofuel end-user prices for a given availability (i.e., wood residues @ 57 tn/hr) - Germany

Comparison of biofuel end-user prices for a given availability (i.e., straw residues @ 57 tn/hr) - Germany
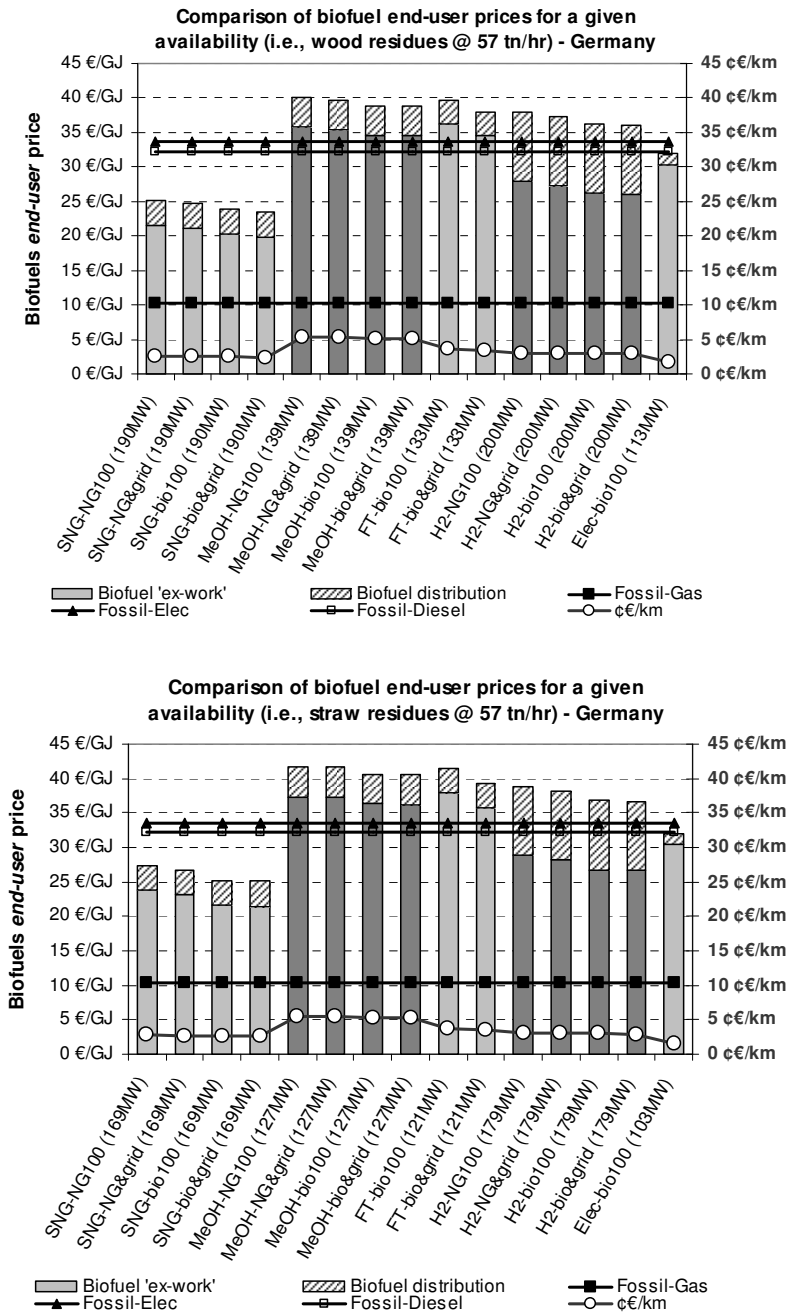
Figure 6.4: *Comparison of wood and straw biofuels and fossil fuels prices in €/GJ$_{fuel}$ for a given forestry wood amount (i.e., 57 tn/hr). Values are also compared with the cost of biofuel per km in case they were used in ICE (FT-fuels, SNG), FCV (H$_2$, MeOH) or BEV vehicles. In this graph, fossil fuels prices include taxes but biofuels are not taxed. In later section 6.4, a new taxation system is proposed to charge both types of fuels.*
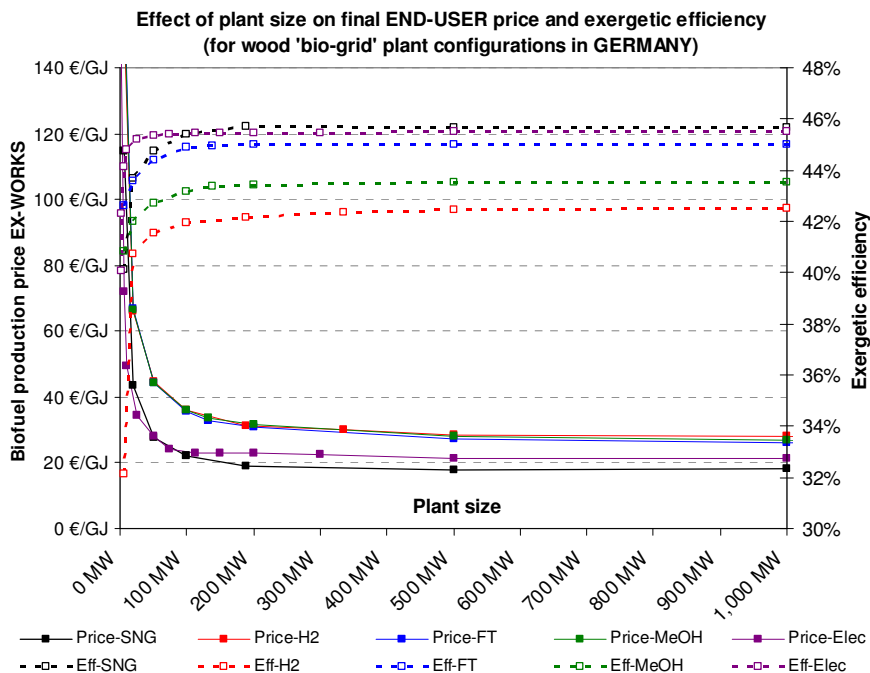
Figure 6.5: *Effect of plant scale on biofuel 'end-user' price and exergetic efficiency. Values correspond to wood-based biofuel chain in Germany, and they include distribution costs.*
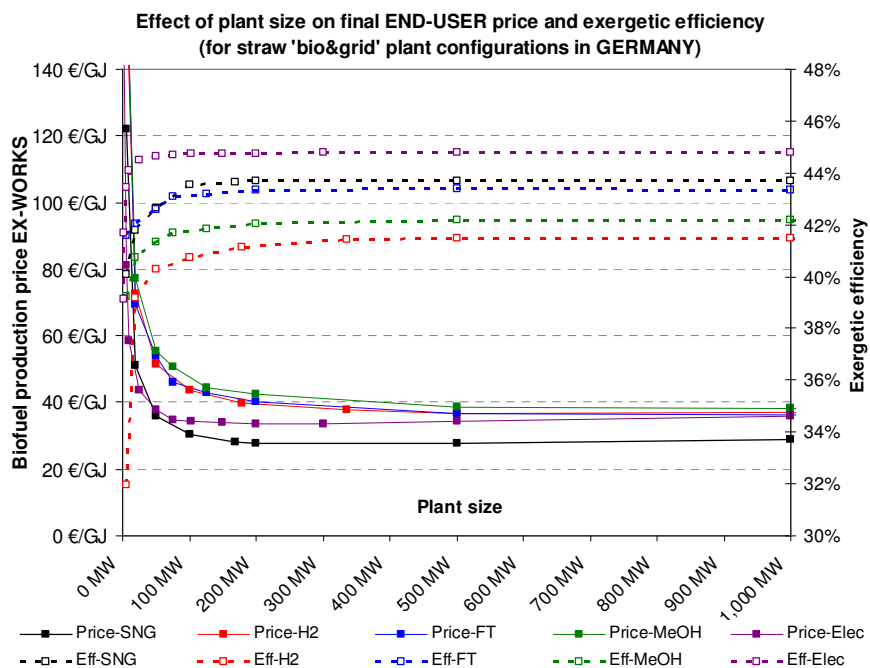

Figure 6.6: *Effect of plant scale on biofuel 'end-user' price and exergetic efficiency. Values correspond to straw-based biofuel chain in Germany, and they include distribution costs.*

Larger scales imply higher prices, notably for straw-based biofuels, as more biomass needs to be transported (see Figure 6.5 and Figure 6.6). Notwithstanding, the effect of logistics is almost negligible for large facilities such as Methanol and Fischer-Tropsch processing plants (i.e., the slope of the curve after the optimal plant size is not very pronounced). Comparison among biofuels reveals that SNG and electricity prices are again on the lowest side (i.e., 23.4 and 30.4 €/GJ respectively for Germany). Conversely, FT-fuel, methanol and H_2 are more expensive and yield close values (i.e., 31.5, 32.4 and 33.2 €/GJ respectively). H_2 price is much higher than SNG due to its intensive distribution costs. Similar conclusions can be drawn in terms of exergetic efficiency, as indicated in Chapter 4. In effect, SNG and electricity production ($\Psi^*_{plant,1}$) is more efficient (i.e., 45.7 and 45.4% for wood-fuelled plants), followed by FT-fuels and MeOH (i.e., 45.0 and 43.5% respectively). Hydrogen efficiency (i.e., 42.5%) is notably penalized by the compression requirements of the pipelines distribution system. Same evaluation is done for straw residues in Figure 6.6, where it is observed that prices are again higher due to lower efficiencies and larger pre-treatment and logistics costs.

Additionally, fuel expenditure in vehicles (expressed in ¢€/km) is also calculated for each biofuel and plant configuration working at optimal scales. As expected, differences among biofuels are now less noticeable (i.e., 1.6 and 2.9 ¢€/km for bio-electricity and FT-fuels respectively for Germany). In line with previous calculations, overpriced BEV vehicles will be now amortized in more than 55 years with actual diesel prices, or 20 years when doubling diesel prices.

In the third stage, biofuels prices at optimal plant scales are compared among European countries in order to identify those locations where biofuels production is economically more attractive. Results from this evaluation are summarized in Figure 6.7 and Figure 6.8 for wood and straw-based respectively. In this case, all plant configurations have been represented in order to identify if there are any country where burning natural gas is cheaper than burning an extra biomass amount to cover heat and/or electricity demand of the biofuels processing plants. Results show that the '*bio&grid*' configuration is the cheapest alternative for all countries with the exception of Greece, where it is economically more convenient to burn natural gas to cover the heat demand of the processing plants. The '*bio-100*' and '*NG-100*' options (in which electricity consumption is also covered by burning a larger quantity of biomass or natural gas respectively) are always more expensive due to the low prices of fossil-based electricity. On the other hand, an analogous to previous Figure 6.5 and Figure 6.6, SNG is again the cheapest alternative for all the analyzed European countries, followed by electricity, FT-fuels, methanol and H_2.

When wood is used for biofuels production (see Figure 6.7), the lowest biofuels prices are found in most of the Eastern countries, the Baltic states, Greece, Portugal and even in the Netherlands. One plausible explanation is that biomass costs are relatively low in those countries (see Figure 2.6 in Chapter 2). The wood market has the peculiarity that the countries with the highest forest residues potential turn out to be the most expensive locations for biofuels production (e.g., France, Germany, Italy, Slovenia or Sweden). This fact will negatively influence average European biofuels prices in Chapter 8. Corporate's taxes also play an important role in biofuels price definition.
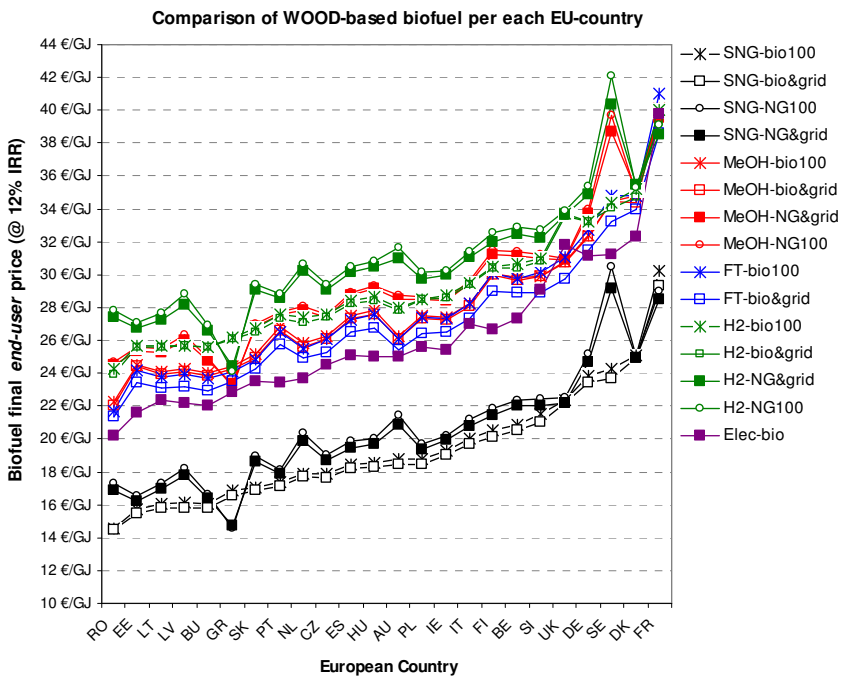
Figure 6.7: *Final end-user prices for wood-based biofuels (@ optimal plant scales).*
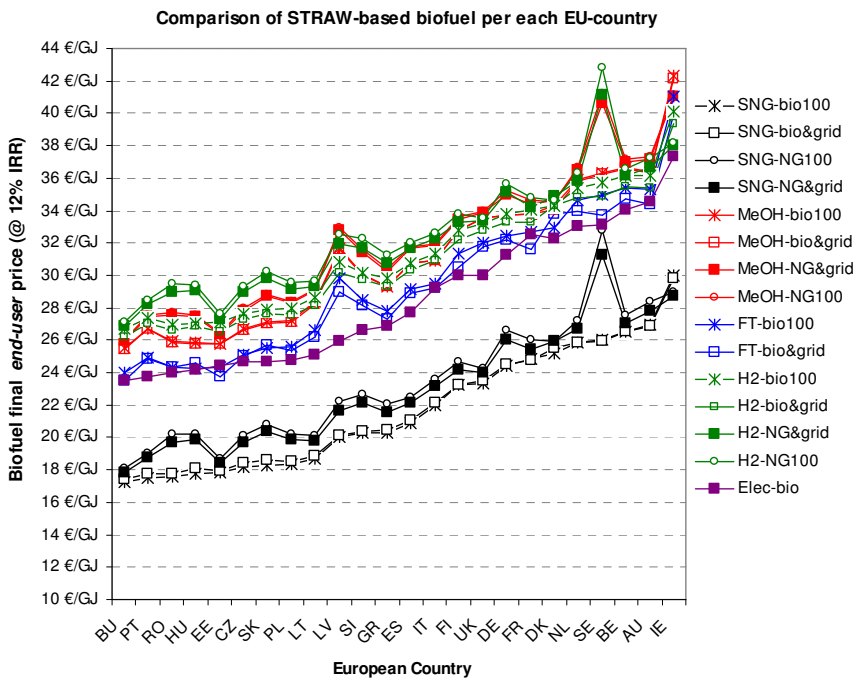

Figure 6.8: *Final end-user prices for straw-based biofuels (@ optimal plant scales).*

In effect, although forest residues have similar prices in Spain and Portugal, the high Spanish corporate's tax (i.e., 35%) is compensated by increasing 'ex-works' prices. Similar consequences occur for the Dutch and Belgian scenarios, having corporative taxes in the range of 26% and 34% respectively. Conversely, labor costs do not have a significant influence on final prices (see section 6.3).

Eastern, Baltic and Southern countries, with the exception of Italy, are again the preferred locations to produce cheaper biofuels when straw is used as sole feedstock, although some positions have changed (see Figure 6.8). However, in this case, France is not the worst location as its position has been relegated to Ireland and Austria. In effect, French straw prices are in line with other countries, whereas its forest residues are the most expensive in Europe (see Figure 2.8 in Chapter 2). The main causes for this new ranking are the same ones than for the wood case, i.e., deviations in biomass costs and corporative taxes.

For a complete evaluation, minimal biofuel prices (i.e., *'NG&grid'* configuration for Greece and *'bio-grid'* for the rest of the countries) are compared with the corresponding fossil competitors to find out the 'green' market potential within country borders (see Figure 6.9 and Figure 6.10). Unlike fossil fuels, produced biofuels are assumed to be exempt of taxation, although, nowadays, this is only valid for certain *renewability* promotors such as Germany. Hence, values of both Figures correspond to the minimal expected biofuels prices. Since methanol and hydrogen are intended for the transport sector, their values are compared with fossil diesel prices. As observed, proposed road biofuel alternatives (i.e., FT-fuels, methanol or hydrogen) are always more expensive for all countries when the evaluation is established with diesel prices before taxation (see blue squares in Figure 6.9 and Figure 6.10). Conversely, if the comparison is made with diesel prices after taxation (see grey squares in same Figures), it is observed that there are some countries where wood-based alternatives are more profitable. In effect, France, Belgium, Slovenia and Scandinavian countries are the only locations where FT-fuels production turns out to be more expensive than petroleum refining. Methanol values need to be somehow penalized due to the low efficiency of the FCV (i.e., 1.33 MJ_{MeOH}/km versus 0.92 MJ_{diesel}/km). In that sense, fuel expenditure will be more costly in methanol-fuelled vehicles than in conventional fossil diesel cars. When a similar procedure is applied to hydrogen, results reveal that fuel expenditure in H_2-FCV will be much cheaper in all countries with the exception of France. However, and, analogous to previous calculations in Figure 6.4, the current high cost of FCV vehicles makes this alternative not globally profitable as fuel savings will not pay off car price differences within 55 years.

The list of 'potential' green locations is reduced when the same analysis is applied to straw-based biofuels in Figure 6.10. As observed, FT-fuels production is now only profitable for Eastern countries, Italy, Germany or UK. In case of shifting to hydrogen generation, the list can be extended to include Greece, Spain, France and Denmark, whereas methanol is again dismissed for any location.
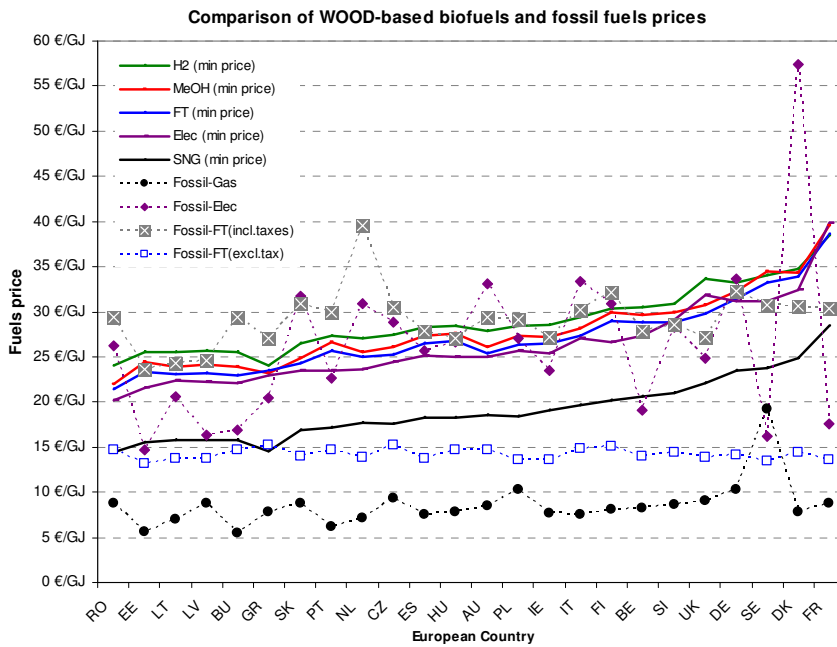
Figure 6.9: *Comparison of minimal wood-based biofuel prices (i.e., 'bio&grid' configuration) with their corresponding fossil alternative. Fossil-diesel values are given before and after taxation.*
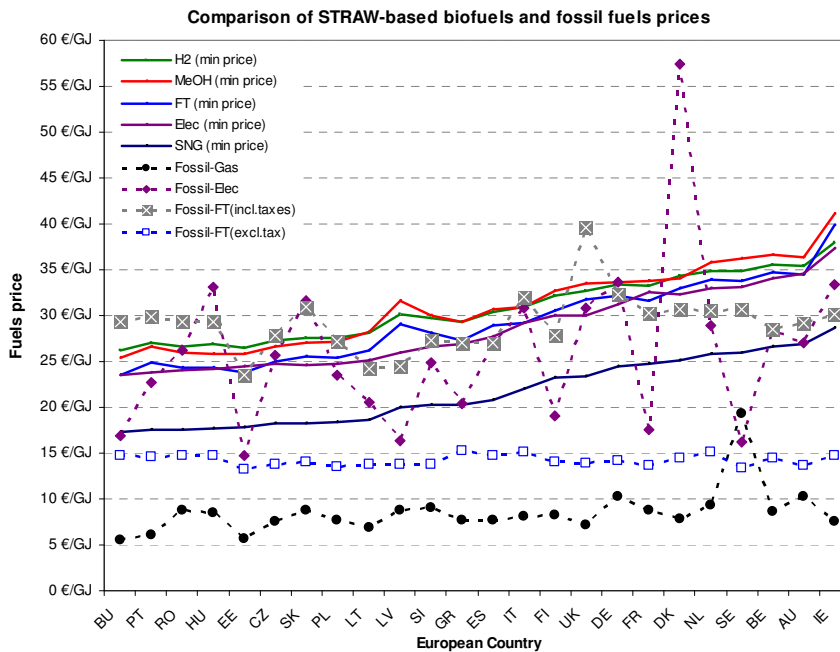
Figure 6.10: *Comparison of minimal straw-based biofuel prices (i.e., 'bio&grid' configuration) with their corresponding fossil alternative. Fossil-diesel values are given before and after taxation.*

Concerning the natural gas market, bio-based SNG production, from either forest or straw residues, is always more expensive than fossil gas exploitation (see black dots in Figure 6.9 and Figure 6.10). Hence, if the aim is to reduce gas import from suppliers countries such as Russia or Algeria, states would need to subsidy SNG production to not charge the final consumer. In particular, Sweden[18] is the location where the price difference is the lowest, thus requiring less public funds. The main reason of this peculiarity is that Swedish fossil natural gas is notably costly (i.e., 19.3 €/GJ versus European average price of 8.6 €/GJ).

According to both Figure 6.9 and Figure 6.10, it would seem that FT-fuels production is a better option than SNG for the introduction of biomass into the European energy market. However, it should be mentioned that the required initial TCI for optimal FT-fuels plants is by far more intensive than for SNG, as shown in previous Figure 6.3. Consequently, it would become more difficult to find private and/or public funds to built those large plants.

Finally, the relatively low prices of fossil electricity give an intermediate situation for bio-power generation in BIGCC plants. In effect, there are less locations than in the FT-fuel scenario where bio-electricity prices are lower than the fossil alternative (see purple rhombus in Figure 6.9 and Figure 6.10). The 'green' locations for straw-based electricity production are: Romania, Hungary, Czech Republic, Slovakia, Italy, UK, Germany and especially Denmark. In case of converting forest residues, the list is extended to also include: Portugal, Netherlands, Spain Austria, Ireland and Belgium. Moreover, bio-electricity has the added advantage that the required initial investments are one of the lowest among the 5 analyzed biofuels (see previous Figure 6.3).

6.2.4.   Results validation with literature studies

Calculated biofuels 'end-user' prices are compared with values from other authors in Figure 6.11 [52, 83, 84, 101-104, 148, 151, 152, 163-168]. The appraisal has been limited to wood-based biofuels as no relevant data was found for straw conversion chains. Our prices correspond to the '*bio&grid*' configuration plants working at their optimal plant scales, as done in Figure 6.7 to Figure 6.8. However, literature values are a bit inconsistent as their calculations have been performed at different plant scales and various feedstock costs. In effect, plant sizes are in the ranges of: 100-260 MWth for SNG, 18-132 MW_{el} for electricity, 260-2000MW$_{th}$ for FT-fuels, 400-530 MW_{th} for MeOH, and 350-530 MW$_{th}$ for H$_2$ production, whereas biomass costs diverge in ± 50%. Moreover, in some studies, it is not clear whether reported values refer to '*ex-work*' prices or to production costs. In any case, distribution costs have been added to their numbers to harmonize all results.

As observed in Figure 6.11, our prices (i.e., black lines) lie in the range of literature values (i.e., grey bars) with the exception of the methanol alternative, which seems at the high side in our calculations. However, according to McKeough et al [163], 'end-use' costs are higher for Methanol than for FT-fuels, which is in line with our results.

[18] This could be one of the motivations for the GoBiGas project in the Göteborg area.
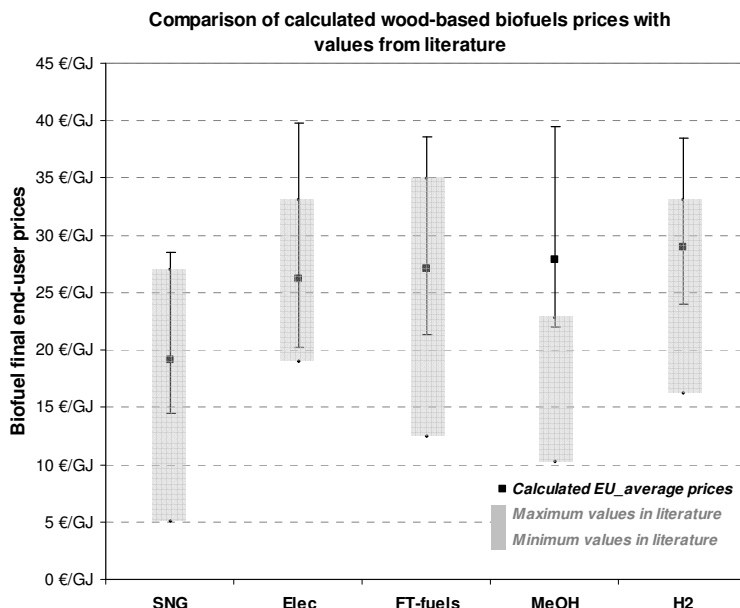
Figure 6.11: *Comparison of calculated biofuel 'end-user' prices for the 'bio-grid' configuration with values found in literature for: SNG [101, 163, 167], electricity [152, 164-166], MeOH [83, 84, 102, 148, 151], FT-fuels [52, 103, 104, 163] and H₂ [83, 84, 102, 168]. Distribution costs have been added to the production costs reported in literature for a harmonized appraisal.*

6.3. *Sensitivity Analysis for 'end-user' prices*

As shown, the economic model presented in this chapter can be used to calculate biofuels prices for any configuration, location and/or plant scale. However, this model does not identify which parameter has the major impact on final 'end-user' prices in order to conduct more profitable negotiations. To overcome this limitation, a sensitivity analysis is carried out for the eight most influencing parameters: (1) *biomass price*, (2) *labor costs*, (3) *corporative tax rates*, (4) *loans interest*, (5) *leverage* (6) *IRR*, (7) *Fixed Capital Investment (FCI)* and (8) *fossil fuel prices*.

Governmental policies and actions may play an important role in some cases. For instance, public subsidies could help to automate biomass collection, thus minimizing overall costs. However, market competition can also increase prices, especially in those countries where biomass availability is limited. Jobs creation can also be recompensed by states although the extent of the public aid will notably vary across Europe. Similarly, having dedicated public funds for renewable energy activities could lower loan interest rates while allowing higher debt capital to supplement equity (i.e., higher leverage percentage). Other Governmental support such as production purchase guarantee would reduce the risk of ventures and, thus, the required IRR in financial markets.

All parameters are varied in the range of ± 10 to 30% and corresponding values for SNG and FT-fuels '*bio&grid*' configurations are presented in Figure 6.12. Other biofuels alternatives are not represented as they follow similar trends. As observed, FCI is the most influencing factor irrespective of the biofuel and location. Major differences are even found for large facilities such as FT-fuels and methanol production. Hence, efforts should be addressed to develop more efficient equipments rather than subsidizing other parameters. For countries where biomass prices are high (e.g., Germany), this parameter turns out to be the second candidate for improvement. Conversely, the effect of biomass price is relegated to the third place in those locations where biomass is cheaper (e.g., the Netherlands). Labor costs are less significant in large FT-fuels or methanol plant scales. Another conclusion that can be drawn from Figure 6.12, is that fossil fuel prices barely influences biofuels 'end-user' prices. Therefore, in case fossil fuels prices soar in the coming years, biofuels could become a more economically attractive energy option.
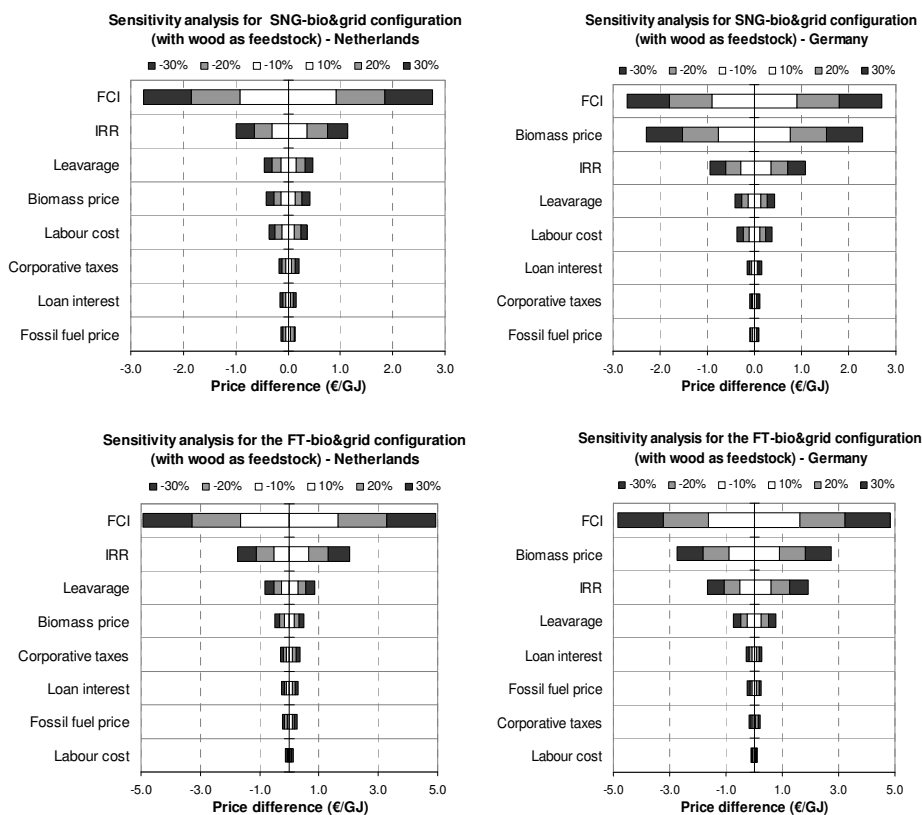

Figure 6.12: Sensitivity analysis for SNG and FT-fuels 'bio&grid' configurations. The analysis is duplicated for two locations (i.e, Germany and the Netherlands), as they have very different biomass prices. Hence, the starting point has a significant influence in the sensitivity analysis.

6.4. *Biofuels taxation to maintain actual Income from fossil fuel taxes*

Biofuel prices of previous sections do not include taxes, which is a substantial income to public finances. In order to assure actual revenues from fuel taxation (CI_{actual}), a new taxation system is proposed in this section. Basically, extra taxes are added to fossil fuels in order to promote biofuels production, which are also taxed. The analysis also takes into account that final fossil and biofuel prices must be equal (see Appendix J.4 for detailed calculations). Accordingly, new fossil fuel (TD_{new}) and biofuel taxes (TB) are defined in Eqs.(6-2) and (6-3).

$$TD_{new} = TD + \lambda \cdot \left(\frac{\alpha_{biofuel}}{\alpha_{fossil}} - 1 \right)$$

(6-2)

$$TB = \frac{\alpha_{fossil} \cdot (1 + TD_{new})}{\alpha_{biofuel}} - 1 = \frac{\alpha_{fossil} \cdot (1 + TD - \lambda)}{\alpha_{biofuel}} - (1 - \lambda)$$

(6-3)

where α_{fossil} and $\alpha_{biofuels}$ are the fuel prices excluding taxes, TD is the actual fuel taxes, and λ is the biofuel replacement in the energy sector. Both equations can be applied to any fossil-biofuel system. In any case, the new taxes for fossil fuels are always positive ($TD_{new} > 0$). The value is equal to previous taxes ($TD_{new} = TD$) in case there is no biofuel production ($\lambda=0$) or fuels prices are equal ($\alpha_{fossil}/\alpha_{biofuels} = 1$). Conversely, biofuels taxes (TB) could be either positive or negative (i.e., they are subsidized by the taxes of fossil fuels), as given by Eq.(6-3).
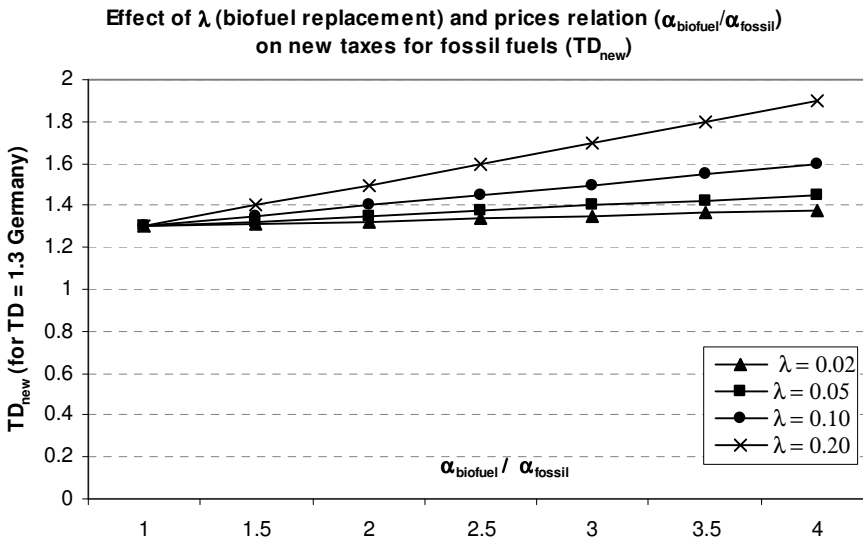

Figure 6.13: *Effect of biofuel replacement (λ) and price ratio ($\alpha_{biofuel}/\alpha_{fossil}$) on new fossil fuel taxes (TD_{new}). Germany is taken as an example (i.e., TD=1.3), but similar trends are obtained for all EU countries.*
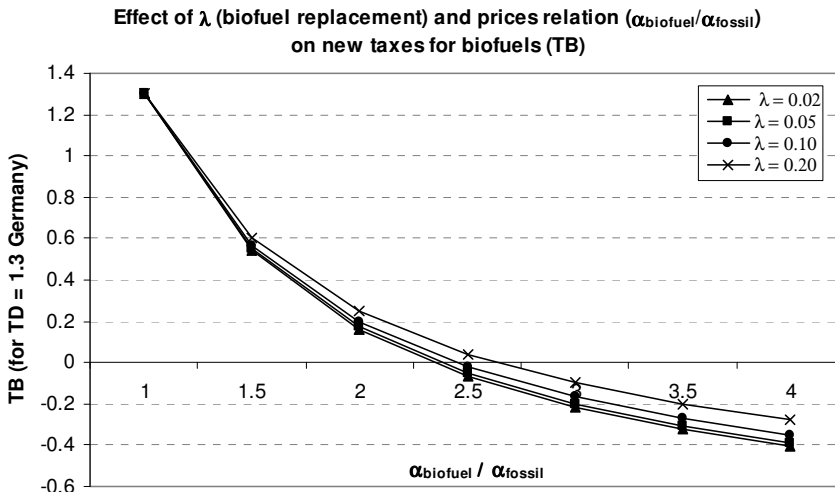
Figure 6.14: *Effect of biofuel replacement (λ) and price ratio (α_{biofuel}/α_{fossil}) on new biofuel taxes (TB). Germany is taken as an example (i.e., TD=1.3), but similar trends are obtained for all EU countries.*

The biofuel tax (*TB*) is especially dependant on the price ratio ($\alpha_{biofuel}/\alpha_{fossil}$), as shown in Figure 6.14. In effect, for price ratios above ~ 2.4, biofuel tax is negative. However, the price ratio is found to be always below 2.4 in all the scenarios analyzed in this chapter. Figure 6.15 represents the corresponding values for fossil and bio-based FT-diesel and within a biofuel replacement in the range of 2.5-20% for Germany. In any case, end-user would incur the price difference between actual fuel prices (i.e., straight line in Figure 6.15) and total final prices. For a 10% biofuel replacement (i.e., established target in the EU Directive 2009/28/EC), the final user would have to pay 1.3 €/GJ (i.e. 5¢€/liter) more, which is translated into ~ 24 €/year.
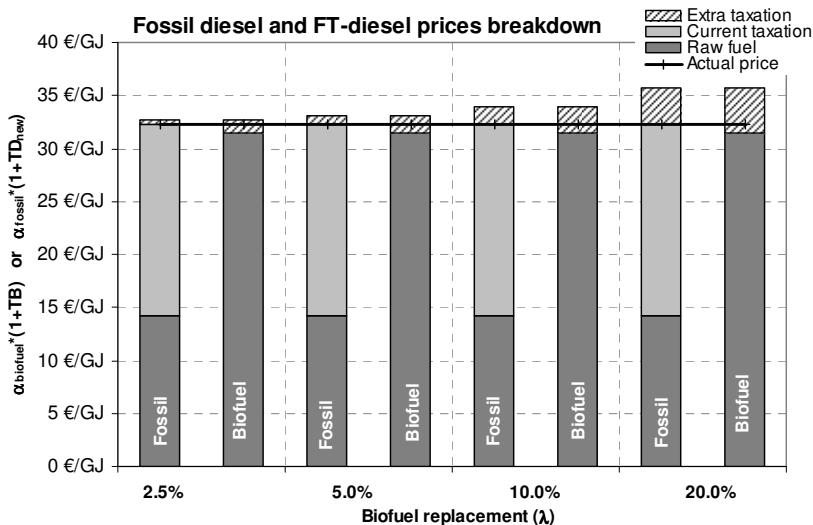

Figure 6.15: *New proposed taxation system for Germany.*

6.5. *Ecocosts for environmental impact inclusion*

The proposed taxation system in previous section 6.4 has the disadvantage that it does not take into account that fossil fuels systems generate more CO_2 emissions than bioenergy routes. Hence, environmental impact results from Chapter 5 are integrated into the economic evaluation by adding an ecocost (α_{CO2} in €/GJ). This ecocost (α_{CO2}) is a 'virtual' value to be added on top of 'end-user' prices and, thus, it does not correspond with the established Carbon credits that are levied from companies exceeding CO_2 emissions limits. Ecocost (α_{CO2}) is calculated by means of Eq.(6-4), whereas final 'integrated' end-user prices are given by Eqs.(6-5) and (6-6).

$$\alpha_{CO2} = \gamma_{eco,CO2} \cdot \left(l_{CO_2,fossil} \cdot (1-\lambda) + l_{CO_2,biofuel} \cdot \lambda \right) \tag{6-4}$$

$$\alpha_{biofuel,\text{int}} = \alpha_{biofuel} \cdot (1+TB) + \alpha_{CO2} \tag{6-5}$$

$$\alpha_{fossil,\text{int}} = \alpha_{fossil} \cdot (1+TD_{new}) + \alpha_{CO2} \tag{6-6}$$

$$\alpha_{fossil,\text{int}} = \alpha_{biofuel,\text{int}} \tag{6-7}$$

where $\gamma_{eco,CO2}$ is a 'virtual' ecotax value (in €/tn CO_2), $l_{CO2,i}$ are the CO_2 emissions originated by the use of fossil fuels in bioenergy and fossil systems (in tn CO_2/GJ). Those emissions have been calculated in previous Chapter 5. As observed from the sets of Eqs. (6-4) to (6-7), a higher biofuel replacement (λ) imply that the ecocost (α_{CO2}) will be smaller because emissions from biofuel systems ($l_{CO2,biofuel}$) are generally lower than the fossil ones ($l_{CO2,fossil}$). Conversely, the monetary part ($\alpha_{biofuel}(1+TB)$ or $\alpha_{fossil}(1+TD_{new})$) will be larger as biofuels prices are normally higher than the fossil prices.

Similarly, ecocosts from other emissions (e.g., acidification or eutrophication) could also be added on top of the final 'end-user' price. However, the value of their corresponding ecotax (see $\gamma_{eco,i}$ values in Table 5-2) is still less agreed than the one for CO_2 emissions ($\gamma_{eco,CO2}$). The value of the CO_2 ecotax ($\gamma_{eco,CO2}$) fluctuated substantially in the last years, and it seems to follow the economic cycles rather than environmental motivations. For instance, in the year 2007, experts fixed its value to 13.5 €/ton CO_2 [134], whereas in the last Copenhagen summit in 2009, with serious climate problems and economic crisis, the tax was decreased to about 5 €/ton CO_2. Figure 6.16 shows the effect of different ecotax values on the 'integrated' final end-user price ($\alpha_{biofuel,int}$) for the '*bio100*' plant configuration in Germany and for a biofuel replacement (λ) of 10%. The left-hand graph displays the prices in terms of energy output (i.e., €/GJ$_{fuel}$), whereas the right-hand one incorporates the fuel expenditure in cars (FE) to give the end prices in terms of euros per driving distance (i.e., €/km). It is observed that SNG is again the cheapest option per output of energy. Same conclusion was already obtained before fuel's taxation (see Figure 6.7 and Figure 6.8). Conversely SNG is relegated to the fourth position when the fuel expenditure (*FE*) in cars is taken into account (see right-hand graph of Figure 6.16). In this case, electricity cars account for the lowest 'integrated' end-user price.

Increasing biofuel replacement affects the final price value, but the biofuels ranking is the same, thus, confirming electricity as the best option from a thermoeconomic and environmental point of view. Values for other countries can be found in Appendix J.5.
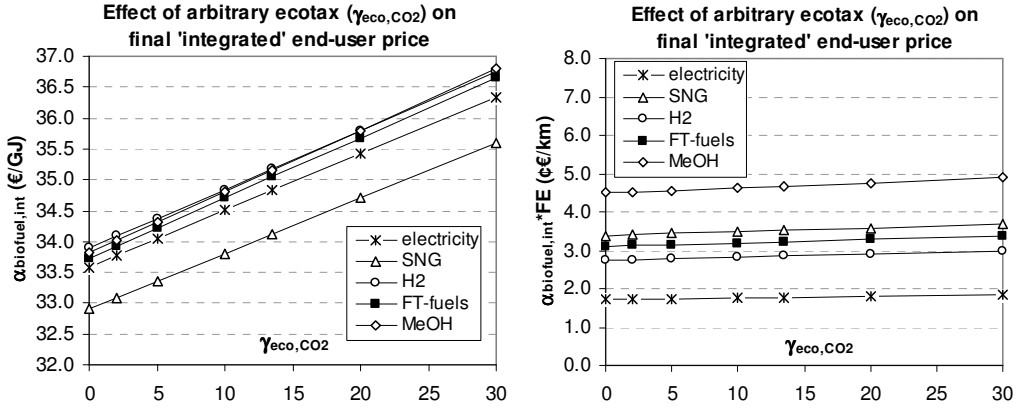

Figure 6.16: *Effect of the arbitrary definition of the ecotax ($\gamma_{eco,CO2}$) on the 'integrated' final 'end-user prices ($\alpha_{biofuel,int}$ or $\alpha_{fossil,int}$). The calculation has been applied to biofuels production in Germany, and for a biofuel replacement (λ) equal to 10% (i.e., target of the EU Directive 2009/28/EC). Wood is used as feedstock for biofuels production with the 'bio100' plant configuration. Similar trends are observed for straw and other plant configurations.*

Similarly to previous section 6.4, final 'integrated' end-user prices at filling stations will be also equal for either biofuels or fossil fuels. Table 6-4 compares the two new proposed taxation systems. In the case of incorporating ecocosts, governments will receive a higher revenue (CI_{new}) from taxation (i.e., $CI_{actual} + CI_{ecocosts}$), as given by Eq.(6-8). The part of ecocosts could be used to promote technologies for CO_2 sequestration or use in other industries[19].

$$CI_{new} = CI_{actual} + CI_{eco\cos t} =$$
$$\left[\alpha_{fossil} \cdot TD_{new} \cdot (1-\lambda) \cdot DC + \alpha_{biofuel} \cdot TB \cdot \lambda \cdot DC \right] + DC \cdot \alpha_{CO2} \qquad (6\text{-}8)$$

where *DC* is the annual diesel consumption (GJ/yr). These two new taxation systems will be applied in Chapter 8 to calculate corresponding prices with the specific biofuel replacement (λ) presented in Table 8-7.

---

[19] The new taxation and ecocosts system presented in this section is based on the potential replacement of fossil fuels by biofuels (λ) in terms of their calorific values (i.e., $GJ_{biofuel}/GJ_{fossil}$) and, thus, it is a measure of the dependence on fossil fuels reserves. Alternatively, this (λ) factor can be redefined in terms of CO_2 savings (λ_{CO2}) and replaced in Eqs.(6-4) to (6-8):

$$\lambda_{CO2} = \lambda \cdot \left(1 - \frac{l_{CO_2,biofuel}}{l_{CO_2,fossil}} \right) \quad \text{(for } l_{CO2,biofuel} = 0, \text{ the } \lambda_{CO2} \text{ is equal to the previous } \lambda).$$

Hence, this new approach is more concerned about the environmental problems.

Table 6-4: Comparison of the final biofuel and fossil fuel 'end-user prices' for the two systems in sections 6.4 and 6.5.

Parameter ⇩	Current situation (No production of biofuels, λ=0)	Biofuels production (λ > 0)	
		New monetary taxes' system (section 6.4)	Monetary taxes and ecocosts system (section 6.5)
Biofuel end-user price	n/a	$\alpha_{biofuel} \cdot (1+TB)$	$\alpha_{biofuel} \cdot (1+TB) + \alpha_{CO2}$
Fossil end-user price	$\alpha_{fossil} \cdot (1+TD)$	$\alpha_{fossil} \cdot (1+TD_{new})$	$\alpha_{fossil} \cdot (1+TD_{new}) + \alpha_{CO2}$
Revenues from taxes	Equal to CI_{actual} (see Eq.(0-22))	Equal to CI_{actual} (see Eq.(0-22))	$CI_{actual} + CI_{ecocosts}$ (see Eq.(6-8))

6.6. *Conclusions and Discussion*

In this chapter, we have evaluated the economic implications of producing 5 different types of biofuels, under the 4 different plant configurations of Figure 3.1 (i.e., '*bio&grid*', '*bio-100*', '*NG&grid*' and '*NG-100*') and within 24 European countries. The '*NG-100*' is dismissed for later appraisal in Chapter 8 as not only is the most expensive option, but also its environmental impact is the worst by far (see Chapter 5). Conversely, the '*bio&grid*' configuration turns out to be the cheapest option irrespective of the biofuel type and plant location. However, this option does not necessarily imply the largest fossil CO_2 emissions savings (see Chapter 5).

For a given biomass input of 57 tn/hr (i.e., ~260 MW_{th} or 240 MW_{th} input of either forestry residues or straw respectively), SNG becomes the cheapest alternative per unit of output energy (see Figure 6.4), followed by electricity, hydrogen, FT-fuels and methanol. When the comparison is translated into fuel expenditure, BEV electric vehicles imply lower costs per driven distance (i.e., 1.6¢€/km). However, capital costs of BEV are at least 2 times higher than conventional diesel cars. Hence, for an average driving distance of 20,000 km/year, FT-fuels and bio-electricity price difference would be paid off after more than 40 years with actual fossil diesel prices, but within 15 years if diesel prices are doubled.

The previous ranking of 'end-user' prices changes when biofuels are produced at their optimal plants scales, which are: ~100 MW_{el} for electricity, 200 MW_{fuel} for SNG, 500 MW_{fuel} for hydrogen, 1000 MW_{fuel} for FT-fuels and methanol. In this case, hydrogen is the most expensive biofuel per unit of output energy, whereas SNG and electricity are still the most economic energy carriers (see Figure 6.7 and Figure 6.8). Similar trends are observed for wood and straw feedstock, although straw-based biofuels are always more expensive, except for France. In effect, the extremely high prices of French wood makes straw conversion more profitable. Plant location also influences final 'end-user' prices, being biomass costs and corporate's taxes some of the most relevant local parameters. In general, Eastern and Southern European countries turn out to be the cheapest locations, whereas France, Italy, Germany and Scandinavian countries are on the opposite side. However, later sensitivity analyses reveal that the FCI (which has been kept equal irrespective of the location) has even a major impact on the final price than biomass costs and/or corporative taxes. Therefore, it is more

cost-effective to focus on improving existing technology rather than on negotiating biomass prices.

For a complete picture, biofuels prices are also compared with their corresponding fossil competitors in order to determine their potential market opportunity. This analysis also overcomes the possible misinterpretation of comparing fuels with different energy applications (e.g., SNG for heating, and FT-fuels, methanol or hydrogen for the transport sector). In this case, SNG is almost double the price of fossil natural gas, thus increasing gas expenditure in all countries. In Sweden, the situation is somehow better as the price difference is only 18% for wood-based SNG. There is also a considerable price difference when bio-based FT-fuels, methanol or hydrogen are compared with fossil diesel before taxation.

For methanol, the situation is even worse as the low efficiency of MeOH-fuelled FCV increases the fuel expenditure. However, when biofuels are compared with fossil diesel after taxation, price differences are reduced and, for some countries, FT-fuels and H_2 become even cheaper than fossil diesel. For instance, France is the only country where bio-H_2 consumption is more costly than fossil diesel. Same conclusion applies for FT-fuels production in France, Belgium, Slovenia and Scandinavian countries. The list of countries is extended when straw is used as feedstock.

In summary, although SNG is the cheapest biofuel in terms of energy output, the price difference with natural gas is notably higher than the one between FT-fuels and fossil diesel, thus hindering the introduction of SNG into the energy market. One plausible explanation could be that FT-fuels production involves similar downstream units to petroleum refining. In effect, after biomass gasification and syngas conversion to a mixture of hydrocarbons, the upgrading stages (e.g., distillation, fractioning and wax hydrocracking) are rather comparable for both processes. Moreover, fuels distribution is done with similar tank truck systems. Conversely, bio-SNG production involves a more complex process than natural gas exploitation, and this is reflected in the large price differences between these two fuels. However it should be mentioned that TCI is by far higher for FT-fuels or H_2 chains than for SNG. Hence, it would be more difficult to find the required private and/or public capital to build large FT-fuels or H_2 plants.

Similar argument can be applied for the case of electricity generation, as there are also some countries where bio-electricity is cheaper than conventional power generation. In fact, most conventional and bio-based power generation plants incorporate an equivalent combined cycle, which accounts for about 60-64% of the purchased equipment costs.

Finally, in the last stage of this chapter, a new taxation system is proposed to assure actual revenues to governments from fuel's taxation. Additionally, environmental impact results from the LCA analysis of Chapter 5 are integrated into the economic evaluation by adding a 'virtual' ecocost on top of fuels prices. The goal is to charge the CO_2 emissions while making biofuel and fossil fuels prices equal for the consumers. In this case, SNG is again the cheapest fuel per output of energy (i.e.,

€/GJ$_{fuel}$), whereas bioelectricity is the most economical option when the comparison baseline is the fuel expenditure per driving distance (i.e., €/km).

Hence, it can be concluded that using biomass sources in the electricity sector seems the most economically beneficial alternative as not only yields mean end-user prices, but also its relatively low TCI aids the attraction of public and/or private capital. However, if the motivation is to comply with the European Directive 2009/28/EC, then FT-fuels production should be preferred over methanol or hydrogen. Results from this Chapter are used in later Chapter 8, in which European biomass is transported to nearby regions to maximize the number of plants, and thus bioenergy production, that would operate at optimal scales.

7

# Multidimensional 3-E Sustainability model

Abstract

Nowadays, it is globally accepted the need of shifting to more sustainable energy carriers. However, Sustainability is rather difficult to evaluate and quantify from a scientific point of view. In effect, many different definitions exist as society, governments, scientists or industry normally have opposing motivations. In general, a sustainable process 'should efficiently use materials and energy, guarantee energy security, be respectful with the environment and economically feasible'. Unidimensional accounting methods such as energy or exergy efficiency calculation, life cycle analysis (LCA) or life cycle cost evaluation (LCC) have already been extensively applied to independently calculate efficiency, environmental and economic parameters respectively, but they are questioned for not including all these parameters at once. Bidimensional methods such as thermo or exergo-economics, cumulative exergy calculation (CExC) and exergetic life cycle analysis (ELCA) seem to be more accurate as they already combine two different parameters. The more recent multidimensional extended exergy accounting (EEA) aims to improve bidimensional alternatives by integrating thermo-economic and environmental results. However, arbitrary conversion factors are still needed in the EEA method, which somehow queries its accuracy. In this chapter we propose a new multidimensional 3E model that combines same parameters as in the EEA approach. Efficiencies are integrated into the economic as well as the environmental evaluations so as to give final biofuel end-user prices and potential CO_2 savings. Environmental impact values can be further combined into the economic calculation by applying 'virtual' ecocosts. Additionally, a program based on our multidimensional 3-E model is also created to evaluate the production and use of biofuels or bioelectricity in any specific region.

7.1. *Introduction*

Energy sources are the drivers of our society but current energy consumption, in particular fossil fuels, is no longer sustainable. In order to shift this situation, countries are defining policies towards a more sustainable development, although there is still a lack of well-defined indicators to quantify any achievement. Several definitions exist about sustainability, but, in a general, it is defined as "*the capacity to maintain a certain process or state indefinitely*". Applied to the human community, sustainability has been expressed as "*meeting the needs of the present without compromising the ability of future generations to accomplish their own needs*" (U.S. Environmental Protection Agency). However, from a scientific point of view, sustainability is rather difficult to evaluate and quantify. In fact, there are several "barriers" for sustainability evaluation. For instance, there is no concise standard definition approved by the scientific community yet, and many divergent definitions and criteria can be found in literature.

We propose that *sustainability* should be measured following *efficiency*, *environmental* and *economic* indicators since there is a strong relationship among these three parameters. For instance, an efficient process normally uses less resources and causes less pollution. This is also translated into lower operational and maintenance costs. However, demanding efficiency targets can also incur in excessive investment costs, thus, making the process impractical. Consequently, a *sustainable process should efficiently use materials and energy, guarantee energy security, be respectful with the environment and economically feasible*. In general, most of the *sustainability* definitions of other authors can be accommodated into our concept, and an example is given in Table 7-1. As observed, the six *"Cramer"* sustainability criteria for biomass conversion can be gathered into our three key factors. These six criteria have been set by the current Dutch minister of Housing, Spatial Planning and the Environment, Jacqueline Cramer [116].

Own definition Sustainability   *Sustainability Criteria by the Dutch minister Jacqueline Cramer*
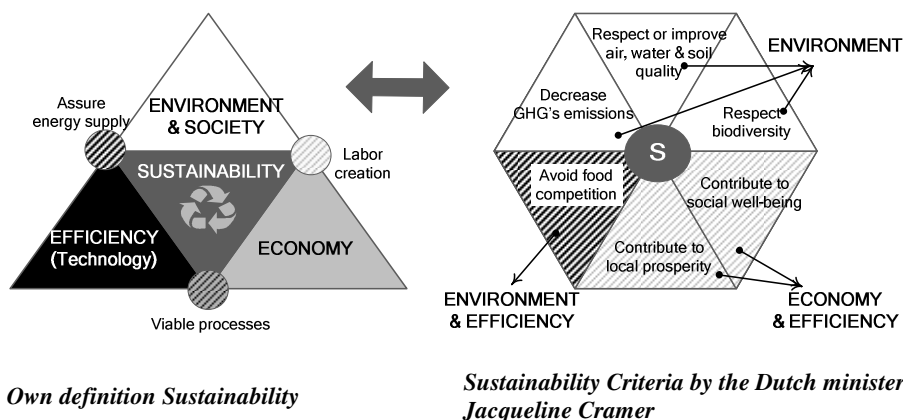
Figure 7.1: *Analogies between our definition for sustainability and the sustainability criteria set by the Dutch minister of Housing, Spatial Planning and the Environment, Jacqueline Cramer [116].*

An added "barrier" is that most parameters have different units of measurement. For instance, environmental impact is measured in ppm (or gCO_2eq/MJ for the case of global warming evaluation), whereas production costs are given in $€/GJ_{biofuel}$, and efficiency is commonly calculated as the ratio of energy output divided by the energy input (e.g.., MW_{output}/MW_{input}). Hence, these parameters cannot be integrated into one value unless conversion factors are applied. This unique value would facilitate communication among scientists, legislators, economists and/or society.

In this chapter we present a multidimensional *sustainability* model (3E) that combines the previously calculated efficiency, environmental and economic indicators. Independent calculations of each parameter have been carried out in the previous Chapters 4, 5 and 6 respectively. The ultimate goal of this model is to select the preferred biomass-to-bioenergy route for a specific country or region. In particular, this model is applied in the subsequent Chapter 8 in order to quantitatively discuss whether European bioenergy targets of Directive 2009/28/EC can be achieved by year 2020. For a complete picture, we have also drawn an analogy between our model and former unidimensional and multidimensional accounting methods of other authors.

7.2. *Previous Unidimensional and Multidimensional accounting methods*

As mentioned, using traditional unidimensional methods such as *exergy* or *energy efficiency*, *Life Cycle Analysis* (LCA) and *Life Cycle Cost* (LCC) does not seem to be the ultimate methodology for *sustainability* evaluation. More recently, multidimensional methods are considered to be more accurate as they intend to integrate several parameters, as shown in Table 7-1.

Table 7-1: Comparison of unidimensional and multidimensional accounting methods.

Accounting method	Methodology	Efficiency $(MW_{output}/MW_{inputs})$	Environmental impact (ppm)	Economic analysis $(€/GJ_{biofuel})$
Uni-dimensional	*Traditional energy efficiency*[a] (see Chapter 4)	✓		
	Exergy analysis[b] (see Chapter 4)	✓		
	LCA (Life Cycle Analysis) (see Chapter 5)		✓	
	LCC (Life Cycle Cost) (see Chapter 6)			✓
Multi-dimensional	*TE (Thermoeconomics)* [b] [169]	✓		✓
	Exergoeconomics[b] [15]	✓		✓
	CExC (Cumulative exergy)[b] [13]	✓	✓	
	ELCA (Exergetic Life Cycle Analysis)[b] [14]	✓	✓	
	EEA (Extended Exergy Accounting) [b] [17]	✓	✓	✓
	Own 3E model [b] (see Chapter 7 and 8)	✓	✓	✓

(a) Efficiency calculation is based only on the 1st law of Thermodynamics
(b) Efficiency calculation is based on the 1st and 2nd law of Thermodynamics (i.e., exergy).

Nevertheless, unidimensional accounting methods are needed to proceed with the calculations of the multidimensional alternatives. In the seventies and eighties, specialists realized the strong relationship between Thermodynamics and Economics, and they came up with the concepts of *Thermoeconomics* and *Exergoeconomics*. *Thermoeconomics* is based on the proposition that "*the role of energy in biological evolution should be defined and understood not in terms of the 2nd Law of Thermodynamics but in terms of such economic criteria as "productivity," "efficiency," and especially the costs and benefits of the various mechanisms for capturing and utilizing available energy to build biomass and do work*"[169]. The main feature of this analysis is the assignment of costs to the exergy content of an energy carrier (i.e., *exergy costing*). Those values represent the total costs required to produced the stream. Hence, *Thermoeconomics* identifies the location and the cost sources, their magnitude and compares their effects on the product costs. In that sense, exergy losses are also economically quantified by charging a uniform cost per exergy unit, which equals the average cost per exergy unit of the produced fuels in the plant. Nevertheless, process optimization is still based on the thermodynamic model, as the cost information is not always available or reliable. Thermoeconomic's supporters claim that this bidimensional method offers the advantage of better understanding and monitoring the main cost sources of any process [15, 16]. Hence, the search for potential costs reduction is simplified. However, there is still some controversy about the real benefit of this new methodology as most of the conclusions can already be obtained with traditional energy and economic analyses.

In some studies, the Thermoeconomics concept has been misused for analyses exclusively based on the 1st Law of Thermodynamics. Moreover, in some cases thermodynamics and economic calculations are even conducted separately. In order to avoid confusion, Tsasaronis [15] proposed the new term of *Exergoeconomics* to give '*a more precise and unambiguous characterization of the combination of an exergy analysis with an economic one using exergy costing*'. In later studies, he even used both concepts indistinctly [16]. In brief, both methods converge on considering exergy and economic aspects but they lack on environmental impact assessment.

In 1987, Szargut [13] proposed the concept of *Cumulative Exergy Consumption* (*CExC*) to calculate the exergy consumption of any system following the *Life Cycle Analysis* (LCA) perspective. According to his definition, "*the Cumulative Exergy Consumption of a product is the sum of the exergy of natural resources consumed in all links of the technological network that starts with these resources and leads to the product under consideration*". For that purpose, both energy flows and non-energetic materials consumption (e.g., metals for vehicles construction) are computed. System boundaries can be as extended as desired but, in general, four levels are proposed (see Figure 7.2). Most authors stay to the second level as the extra primary energy consumption in the third and fourth level adds less than the 6-10% of the total energy. The benefit of the CExC is that, unlike traditional LCA, it can be used to optimize the performance of the system and not merely quantify its emissions.

Subsequently, Cornelissen [14] developed the concept of *Exergetic Life Cycle Analysis* (*ELCA*), which is especially intended for quantifying depletion of natural sources and calculate the efficiency of using all resources. However, since the calculation of natural sources depletion is somehow complex and its relevance is also

being questioned, the ELCA methodology is less often applied than the previous LCA and CExC concepts. Alternatively, other publications use the ELCA accounting method to estimate the dependency on non-renewable sources to produce bioenergy or other forms of renewable energy [170]. ELCA and CExC studies are mostly focused on the calculation of exergy flows and thus, they are normally accompanied by separate LCA assessments to enclose the environmental burden of the process [170, 171]. In any case, the many disadvantages of these accounting methods is that they do not include any economic assessment, which is an important factor for the proper evaluation of different energy systems.
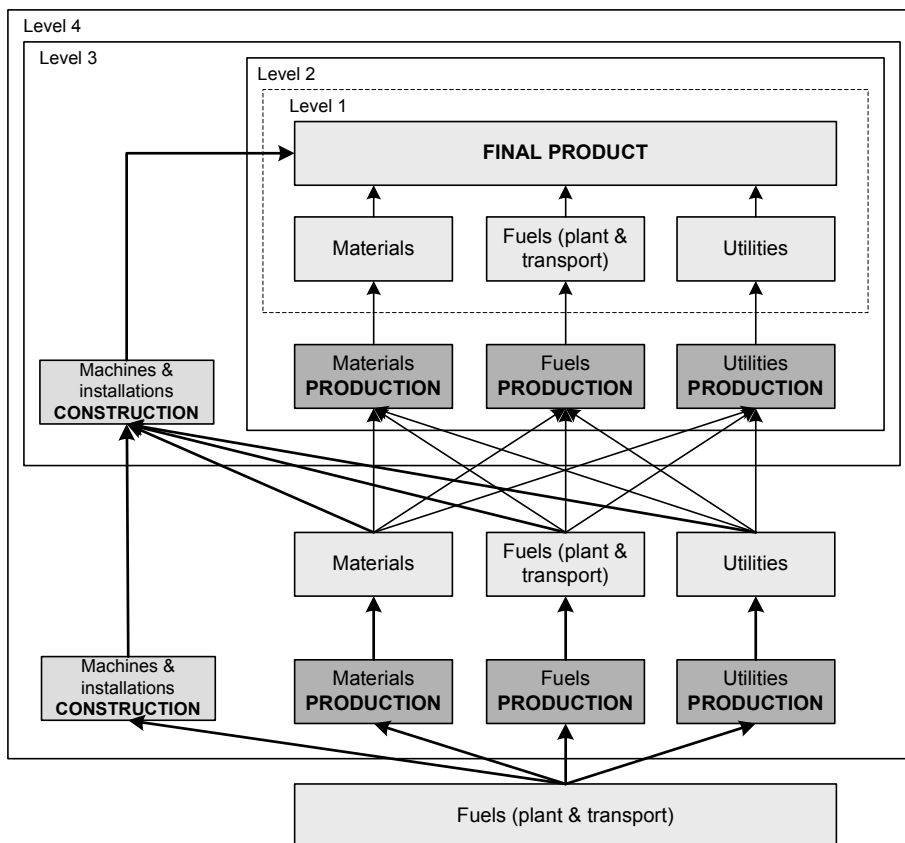

Figure 7.2: *Schematic representation of the four levels for extended exergy analysis such as CExC and ELCA methodologies.* **Level 1** *comprises the consumption of materials and energy carriers (i.e., fuels and/or utilities) in the production plant. Fuels consumption for transportation is also included.* **Level 2** *adds the materials and energy expenditure for the production and transport of materials and energy carriers of the 1st level.* **Level 3** *also evaluates the fabrication of machines and installation for the 1st level.* **Level 4** *also takes into account the fabrication of machines and installations that are used to build the machines and installations used in the 1st level. Materials and energy expenditure for the production of materials and energy carriers of the 3rd level is also included in this last stage.*

The more recent *Extended Exergy Accounting* (EEA) method proposed by Sciubba [17] is the only one that combines the three proposed *efficiency*, *environmental impact* and *economic* indicators. The extended exergy (EE^{ex}) of a system is calculated as the

summation of the feedstock exergy (FE^{ex}), the capital equivalent exergy (CEE^{ex}), the labor equivalent exergy (LEE^{ex}) and the environmental remediation exergy (ERE^{ex}), i.e., the exergy needed to neutralize the impact of waste flows.

$$EE^{ex} = FE^{ex} + CEE^{ex} + LEE^{ex} + ERE^{ex} \qquad (7\text{-}1)$$

The FE^{ex} and ERE^{ex} components can be simply calculated from mass and energy balances, as done in chapter 4, whereas a '*conversion capital*' factor (K_{cap}) is needed to translate monetary flows (i.e., capital investment and labor) into the corresponding exergy values CEE^{ex} and LEE^{ex}. In effect, the main challenge of this EEA method is to set a proper conversion K_{cap} factor, which represents the cost of producing one unit of exergy. Sciubba [17] proposes that this factor equals the annual exergy input of a country divided by the economic variable M2[20], which is published by the European Central Bank. Alternatively, Ptasinski et al [172] calculated separate conversion factors K_{cap} for the exploitation, transformation and distribution of fuels within the energy sector. In their study, the M2 value is replaced with the annual monetary of the feedstock (FE^{ϵ}), which accounts for feedstock, water and utilities consumption costs, fuel expenditure for transportation, freight costs, and storage. The FE component of the EEA analysis is calculated with the former bidimensional *CExC* method proposed by Szargut [13].

In our model, exergy and energy efficiency calculations are conducted following the 2nd level of the CExC approach of Szargut [13] (see Figure 7.2). Those calculations have allowed us to allocate the largest exergy losses within the whole biomass-to-bioenergy chains, as detailed in Chapter 4. Economic and environmental impact evaluation has been done following traditional LCA and LCC accounting methods to cover the full life span of the five different bioenergy systems (see Figure 7.3 in section 7.3). In our case, the economic appraisal does not include the costs related to plant, machines or vehicles dismantling due to the lack of reliable data. The impact of this dismantling stage is also presumed to be negligible in comparison with the costs of biofuels production and distribution. Thermoeconomics and Exergoeconomics methodologies are not applied as optimization is based on improving energy and exergetic efficiencies. Moreover, our sensitivity analysis in Chapter 6 already identified that *Fixed Capital Investment (*FCI) and *biomass price* are the most influencing parameters when aiming to reduce final end-user price of the biofuels or bioelectricity (see Figure 6.12). Finally, we opt for creating an own model instead of using the EEA methodology as the calculation of the capital conversion factor K_{cap} and the ERE (*environmental remediation exergy*) is somehow questioned.

---

[20] According to the European Central Bank, M2 is the summation of the: *Currency in circulation + Overnight deposits + Deposits with an agreed maturity up to 2 years + Deposits redeemable at a period of notice up to 3 months*. In the EEA methodology, the choice of M2 applies for a specific control volume (e.g., industrial sector).

7.3. *Integration of the Efficiency, Economic and Environmental indicators: Building the 3E Model*

Our model starts with calculating mass and energy balances from Aspen Plus simulations, which are later used to calculate exergetic and energy efficiencies of the five biofuels conversion routes (i.e., SNG, MeOH, FT-fuels, H_2 and bioelectricity), as shown in the left-hand sequence of Figure 7.3. Aspen Plus simulations are coupled to Aspen Icarus in order to calculate the biofuels production price "ex-works". This price is determined by fixing and investor internal rate of return (IRR) of 12%, and with 50% of capital leverage (i.e., 50% of the TCI is borrowed from banks). Final end-user price is obtained by adding logistic and distribution costs. Those calculations are iterated for different plants sizes (i.e., from 1 to 5000 MW_{fuel}) and 24 European countries in order to determine the optimal plant scale and location for each biofuel. In the last stage, environmental impact of each configuration is integrated into the economic evaluation by calculating an ecocost (in €/GJ) that is added on top of taxed fuels (i.e., α_{CO2}). In that sense, all results are combined to a final monetary value. From the left-hand sequence of Figure 7.3, separate values of efficiency (Chapter 4), emissions (Chapter 5), and final 'end-user' biofuels and bioelectricity (Chapter 6) are obtained per each European country. In the right-hand sequence of Figure 7.3, the model is applied to a more complex region such as Europe to determine the maximum fossil energy replacement, as done in Chapter 8.

Iteration for 5 biofuels, 24 countries and different plant scales
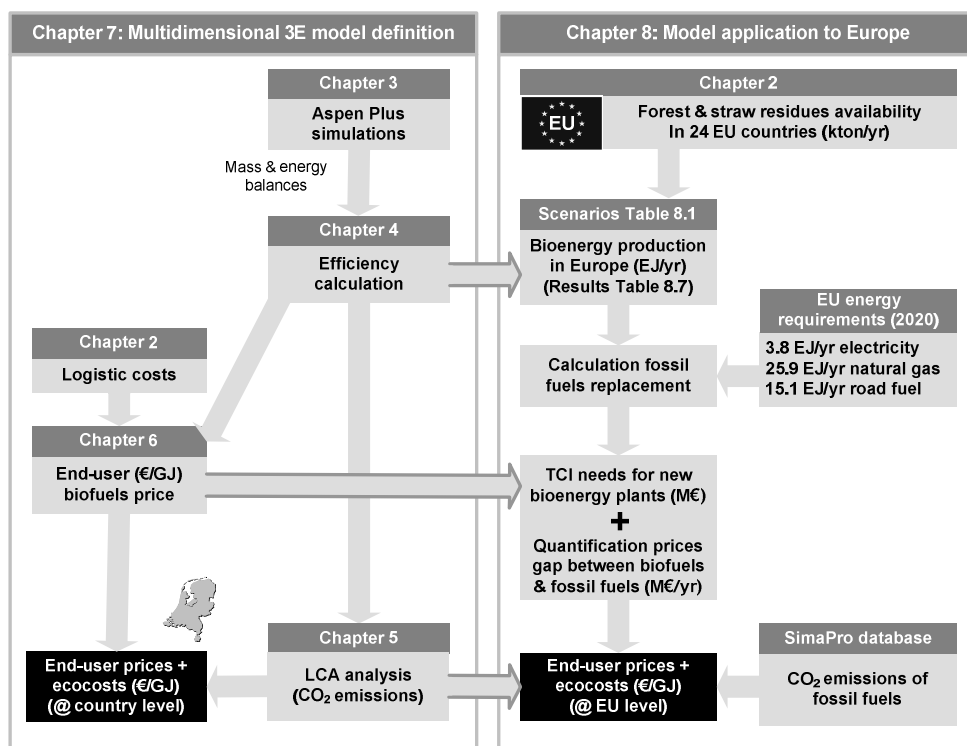
Figure 7.3: *Schematic representation of our model.*

Optimal biofuels plant scales are deducted from the iteration of our model in section 3.1. This parameter, together with biomass availability across Europe, fixes the number of plants that could be built in each scenario in Table 1, which in turn, allows the calculation of total capital investment (TCI). Subsequently, price differences between bioenergy and a fossil reference scenario (see Table 8-6) are quantified in Billion € per year.

7.4. *Building a program in order to apply the 3-E multidimensional model to any region*

Finally, a basic program is created in an excel format (*Multi_model.xls*) which combines the concept of Figure 7.3 and the results from previous Chapter 4, 5 and 6. The ultimate goal of this program is to determine the final biofuel '*end-user*' prices and CO_2 emissions savings for any specific region. The characteristics of the new specific region under study are introduced by the *program user*, as indicated by the grey boxes of Figure 7.4. This required information comprises: biomass amount and availability, biomass transport, economic, regional and biofuel distribution variables (see Figure 0.28 in J.5). Ecotaxes values of Table 5-2 [134] can also be subjected to revision by the *program user*. The user starts by selecting the biofuel type (i.e., *SNG*, *MeOH*, *FT-fuels*, H_2 or *bioelectricity*), the plant configuration (i.e., '*bio100*', '*bio&grid*', '*NG100*', '*NG&grid*') and the biomass source (i.e., forest residues, straw or lignocellulosic energy crops). The program also contains some '*fixed input data*' that cannot be modified by the program user, as given in Figure 0.29 in J.5. The main reason for fixing some parameters is that they barely influence final results and their *flexibility* would considerably complicate the program.

Annual biofuel production is calculated in first place from the efficiency results of Figure 4.5 to Figure 4.9. Specific emissions per output of energy (i.e., g-eq/$MJ_{biofuel}$ or $MJ_{bioelectricity}$) or driven distance (i.e., g-eq/km) are subsequently calculated by applying the algorithms of Chapter 5 (see Eqs.(5.1) to (5.37)). As explained in Chapter 5, those emissions are notably influenced by variables such as biomass availability per hectare, which is introduced by the '*program user*'. Diesel consumption for biomass collection has also a major impact in total CO_2 emissions. However, this parameter cannot be arbitrarily selected by the '*program user*' as fuel consumption of tractors is a rather standard value. Alternatively, the '*program user*' can still choose the '*truck capacity*' and '*biofuel distribution distance*'.

Regional (e.g., biomass and fossil fuel prices, labor costs or corporate taxes) and economic variables (i.e., inflation and bank interest rates) are also introduced by the '*program user*' in order to perform the economic calculations. For that purposes, same methodology of Chapter 6 is applied. Investment costs are extrapolated by using William's correlation of Eq.(6.1), whereas production costs are assumed to follow a linear relationship. Figure 0.26 and Figure 0.27 of Appendix J.3 can be used as a reference.
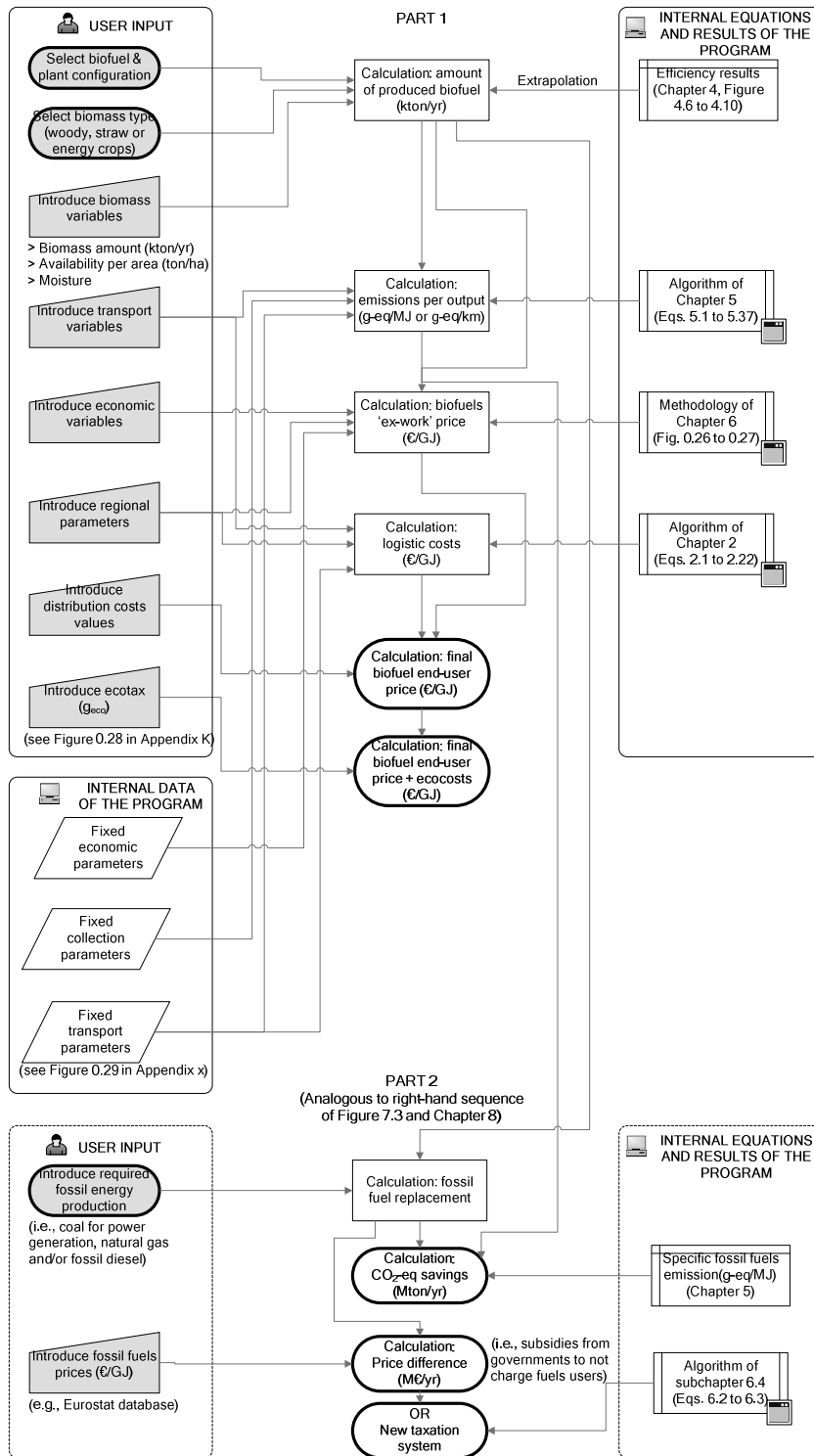
Figure 7.4: *Flowchart of the multidimensional 3-E excel program.*

Subsequently, logistics costs are calculated from regional and transport variables and by applying the algorithm of Chapter 2. Those costs are added to previously calculated '*ex-works*' prices and biofuels distribution costs, which can also be modified by the '*program user*'. Emissions can be integrated into the final biofuel '*end-user*' prices by either accepting proposed ecotaxes in Table 5-2, or introducing new values.

The second part of the program (i.e., bottom part of Figure 7.4) is the real essence of the 3E multidimensional model, and it is devoted to quantify:

- The maximum fossil fuel replacement that can be achieved from a given biomass amount (in %).
- Total CO_2 emissions reduction (in Mton CO_2/year).
- Final biofuel prices including taxes and ecocosts (in $€/GJ_{fuel}$).
- And especially, the annual extra payment that consumers will pay because bioenergy is more expensive than fossil fuels production (in Billion $€$/yr).

7.5. *Conclusions*

Current environmental and economic problems prompt governments to search for more sustainable energy options. However, sustainability is rather difficult to evaluate and quantify as different parameters are involved (e.g., efficiency, economic and/or environmental impact). Moreover, those parameters are normally expressed in different units. In this chapter, an own multidimensional sustainability 3E model has been proposed. It combines efficiency, environmental and economic parameters that have been previously calculated in Chapters 4, 5 and 6 respectively. Efficiency of biomass-to-biofuels conversion routes have been calculated following a *cumulative exergy consumption* approach (CExC), whereas traditional unidimensional *life cycle analysis* (LCA) and *costs* (LCC) are applied for environmental impact and biofuels '*end-user*' price calculations. Additionally, we have also created a program based on our multidimensional 3-E model that could be used to evaluate the production and use of biofuels in a specific region. This program also predicts the potential fossil fuel replacement of a specific location and its consequences from an environmental and economic point of view (e.g., CO_2 emissions savings, a new taxation system to equalize biofuels and fossil fuels prices and maintain income from fuel's taxation, and ecocosts). The multidimensional 3-E model is applied to Europe in subsequent Chapter 8.

8

Redrawing Europe borders for maximal biofuels and biopower implementation

Abstract

Biomass availability is rather limited in Europe and, hence, it is of crucial importance to determine the optimal biomass-to-energy conversion pathway. This selection is somehow complex as there could be antagonist motivations coming from industrial stake-holders, politicians, scientists or the society. The aim of this chapter is to present different biomass-to-biofuels alternatives that follows various economical, environmental and/or social drivers. Results are also compared with European Directives 2001/77/EC and 2009/28/EC. In General, maximizing bio-electricity over other biofuels turns out to be the most economic and environmental friendly option, especially when using part of the biomass in existing coal power plants. Combined with other renewable sources, about 31% of the electricity production by 2020 could be "green", i.e., 10 %-points higher than the renewable target of Directive 2001/77/EC. If biomass is directed to SNG production, fossil natural gas imports could be reduced by 1.63 EJ/yr in 2020, although this alternative involves higher costs and less CO_2 savings than the previous bio-electricity solution. In case of promoting Fischer-Tropsch fuels, the share of biofuels in transport will be 9.5%, which is slightly below the 10% share target of Directive 2009/28/EC. Hydrogen is disregarded as a feasible option for transport due to several technological barriers, although it would lead to substantial CO_2 savings. Conversely, methanol results in the worst environmental solution as CO_2 emissions are normally larger than those of conventional fossil fuels.

8.1. *Introduction*

As mentioned in previous Chapter 2, forestry biomass and agricultural residues are stochastically distributed in Europe, leading to definite areas where the concentration of biomass differs substantially (see Figure 2.3 and Figure 2.5). In some cases, those areas do not correspond with the established country borders and, hence, new "bio-borders" are here suggested to maximize the amount of biofuels that can be later produced in Europe. This "re-drawing" is especially sensitive for the processes that require a relatively large scale in order to operate at a more competitive price (e.g., Fischer-Tropsch or methanol plants). SNG and hydrogen production are profitable at medium plant sizes, thus giving a combined national and "bio-borders" scenario. Similarly, since logistics costs have a major impact in electricity final price, borders follow also a combined scenario. Once determined the "bio-border" for different biofuels and biopower production, the next step is to identify which alternative is the best for the European energy market. Answering this question is somehow complex as the society, the scientific community, industry, or the politicians have their own motivations. In this chapter, biofuels or bioelectricity implementation within European countries is discussed under the several preferences presented in Table 8-1.

Table 8-1: Rank of biofuels and biopower implementation according to different preferences from the society, scientific community and politicians. Numbers identify the priority.

Preferences	Electricity	SNG	F-T fuels	Methanol	Hydrogen
(I) Maximizing renewable electricity production[a]	❶ cofiring +new plants[e]				
(II) Potential replacement in existing infrastructure	❶ cofiring	❸ new plants	❷ new plants		
(III) Maximizing biofuels replacement in transport[b]		❷ new plants	❶ new plants		
(IV) Maximizing only FT-diesel (Oil companies)	❷ cofiring		❶ new plants		
(V) Maximizing SNG to reduce natural gas imports	❷ cofiring	❶ new plants			
(VI) Maximizing potential CO_2 reduction[c]	❶ cofiring	❷ new plants			
(VII) Potential replacement in FCV[d]	❷ cofiring				❶ new plants
(VIII) Maximizing methanol production	❷ cofiring			❶ new plants	

(a): According to the European Directive **2001/77/EC**, about 21% of the electricity should be produced from renewable sources by 2010 in EU-25 (22.1% for EU-15).

(b): According to the European Biofuels Directive (**2009/28/EC**), the share of biofuels in transport should achieve the target of 10% by 2020

(c): The EU countries have committed to reduce greenhouse gas emissions during the first Kyoto commitment period 2008-2012 by 5% compared to the 1990 reference year (COM 2006).

(d): It refers to the potential introduction of fuel cell vehicles (FCV) in the long-term.

(e): "New plants" refers to new BIGCC plants that will operate on 100% biomass (i.e., no cofiring)

The analysis covers the estimation of total bioenergy production from forestry and straw residues (see subchapters 8.2 to 8.10.1), and its hypothetical exclusive use in road transport (see subchapter 8.10.2). Moreover, the analysis is completed by calculating the CO_2 emissions in all scenarios, so as to identify which would be the best alternative from an environmental point of view (see subchapter 8.10.3). However, since maximizing bioenergy production and/or CO_2 savings is not always the most economic option, the analysis is extended to include the economic implications of each option, i.e., required investments and biofuel consumer price (see subchapter 8.10.4). In the last part of this chapter, results are compared with renewable energy targets established in the European Directives and White Papers.

8.2. *(I) Maximizing renewable electricity generation: Cofiring and biopower plants implementation*

When looking at the introduction of biomass in a short-term perspective, *direct cofiring* in existing coal-fueled power plants turns out to be one of the most feasible alternatives as it requires little or no extra investment and, hence, reduction of GHG's and sulfur emissions are comparatively rapid and inexpensive. Direct cofiring refers to burning biomass and coal in the same furnace using same or separate mills. This cofiring option is the cheapest and the most implemented in Europe, accounting for ~ 160 units with a total capacity of approx. 35 GW_{el} and 22 GW_{th} [88] (see section 3.4.5). Possibly, one of the most representative examples can be found in the Amer plant (the Netherlands) that have two operative direct cofiring units and an indirect cofiring station that makes use of wood-syngas obtained in a separate atmospheric CFB gasification unit. However, direct cofiring has certain limitations, i.e., only about 10wt% (i.e., ~6% in energy basis) of coal can be safely replaced with biomass if no modifications are made in the furnace. Most of the challenges related to increasing the share of biomass originates from the differences between biomass and coal fuel properties. In particular, ash characteristics have a key role in boiler design because deposit formation, erosion and corrosion should be minimized and defluidisation avoided. Another alternative is to build new biomass BIGCC (Biomass Integrated Gasification Combined Cycles) power plants that could fully operate on biomass. As mentioned in chapter 3, one of the advantages of this technology is that high efficiencies are attained and a substantial higher amount of biomass can be used, although building new BIGCC plants requires extra investment.

For an optimal utilization of biomass sources, three "*short-term scenarios*" are here analyzed (see Table 8-7 and Table 8-8). In the first two cases (**scenario A1** and **A2**), it is assumed that 10 wt% of the coal consumed in power plants is substituted by the corresponding amount of biomass (either forestry biomass **(A1)** or straw residues**(A2)**), and the remaining part is used in new BIGCC plants operating at the optimal scale of about 103-113 MW_{el} (see Figure 8.1 and Figure 8.2). For both scenarios, overall electrical efficiency (η_{el}) of cofiring plants is negatively affected by 2-4% when introducing 10 wt% of wood or straw respectively. Assuming that average EU-24 thermal electricity efficiency is reported to reach 45.2% by year 2020 [4], net electrical efficiencies (η_{el}) of wood and straw-fueled cofiring plants are estimated to

reach 43.2 and 41.2% respectively. Electrical efficiencies of new bio-based BIGCC
stations attain lower values, i..e, 42% and 36% for wood and straw (see Chapter 4). In
the third case (**scenario A3**), biomass sources are fully consumed in potential new
BIGCC plants (see Figure 8.3). Hence, in this case, no cofiring is envisaged and
energy efficiencies of coal plants are not affected (i.e., 45.2% [4]). Table 8-7 presents
the share of renewable electricity generated in these 3 scenarios, whereas subsequent
Table 8-8 extends the comparison to renewable and fossil energy. In both tables, "*x*"
and "*y*" represent the biomass fraction that is used in cofiring plants, as defined in
Eqs.(8-1) to (8-5). The 3 scenarios are labeled with *I-bio100-A1*, *I-bio100-A2* and *I-
bio100-A3*, where "*I*" accounts for the rank of Table 8-1, "*bio100*" means that no
extra fuel is needed to cover the energy demand of the plant, and index *A1* to *A3*
indicates the 3 scenarios.

$$TW = Total\ Wood = Wood\ for\ cofiring\ +\ Wood\ for\ new\ biopower\ plants \qquad (8\text{-}1)$$

$$TW = TW_{cof} + TW_{new} = TW \cdot x + TW \cdot (1 - x) \qquad (8\text{-}2)$$

$$x = fraction\ of\ wood\ consumed\ in\ cofiring\ power\ plants \qquad (8\text{-}3)$$

$$TS = Total\ Straw = Straw\ for\ cofiring\ +\ Straw\ for\ new\ biopower\ plants \qquad (8\text{-}4)$$

$$TS = TS_{cof} + TS_{new} = TS \cdot y + TS \cdot (1 - y) \qquad (8\text{-}5)$$

$$y = fraction\ of\ straw\ consumed\ in\ cofiring\ power\ plants \qquad (8\text{-}6)$$

In scenarios *I-bio100-A1* and *I-bio100-A2*, replacement of 10wt% of coal correspond
to "*x*" and "*y*" fractions equal to 26 wt% (i.e., 26 wt% of available wood (*A1*) or straw
(*A2*) is consumed in cofiring plants (see Table 8-7)). By definition, in scenario
bio100-A3, "*x*" and "*y*" fractions are both 0%. In all cases, final electricity outcome
(renewable + fossil) should at least equal 3.77 EJ/yr, which accounts for the predicted
coal-based electricity generation by 2020 [4]. In *I-bio100-A1* and *I-bio100-A2*
scenarios, total power outcome is higher than 3.77 EJ/yr (i.e., 4.58 and 4.41 EJ/yr
respectively). This is because coal replacement is limited and the rest of biomass is
still used to generate electricity in new BIGCC plants. Consequently, the natural gas
fraction that would be consumed to generate electricity is discounted (i.e., natural gas
production would be 24.44 and 24.73 EJ/yr for scenarios *I-bio100-A1* and *I-bio100-
A2* instead of 25.90 EJ/yr, as given in Table 8-7 and Table 8-8).

According to results from Table 8-7, the share of renewable electricity produced from
biomass (i.e., 34.3%) is larger for the third scenario *I-bio100-A3,* in which no cofiring
is planned. In effect, notably less coal (i.e., 2.48 EJ/yr) is needed to fulfill total power
outcome of 3.77 EJ/yr (see Table 8-8), although net bio-electricity production is lower
(i.e., 1.29 EJ/yr). This could be explained by the fact that, as aforementioned, biomass
is more effectively converted in cofiring plants (i.e., η_{el} of 43.2 and 41.2% for wood
and straw) than in new BIGCC power sites (i.e., η_{el} of 42 and 36 %). However, this
would be the picture for year 2020 as, nowadays, electrical efficiencies of coal-power
plants are lower than bio-based BIGCC [4]. When comparing the ratio of fossil +
renewable "*outputs/inputs*" in Table 8-8, the conclusion is somehow different as
scenarios *I-bio100-A1* and *I-bio100-A3* attain higher ratios (i.e., 40.8% and 41.1%
respectively), whereas the second option *I-bio100-A2* is now slightly less profitable

(i.e., 39.4%). However, from an environmental point of view, *I-bio100-A3* is still the preferred alternative although it will also require extra investment. For a complete overview, the number of potentially new BIGCC power plants (i.e., plants that run on 100% biomass), have been allocated within the EU-24 countries in subsequent Figure 8.1 to Figure 8.3 for the three options *I-bio100-A1*, *I-bio100-A2* and *I-bio100-A3*. In the first scenario *I-bio100-A1*, when summing wood and straw-fuelled plants (i.e., left and right graphs), it is observed that all countries at least could built one new BIGCC plant with the exception of Ireland and Estonia. The second case *I-bio100-A2* is less limited as Ireland is the only country that does not have enough biomass to plan a new BIGCC at optimal scale. The third case *I-bio100-A3* is similar to the second one as Ireland is again the only state depleted of new BIGCC plants. This fact confirms *I-bio100-A3* as the best alternative for maximizing green electricity production.
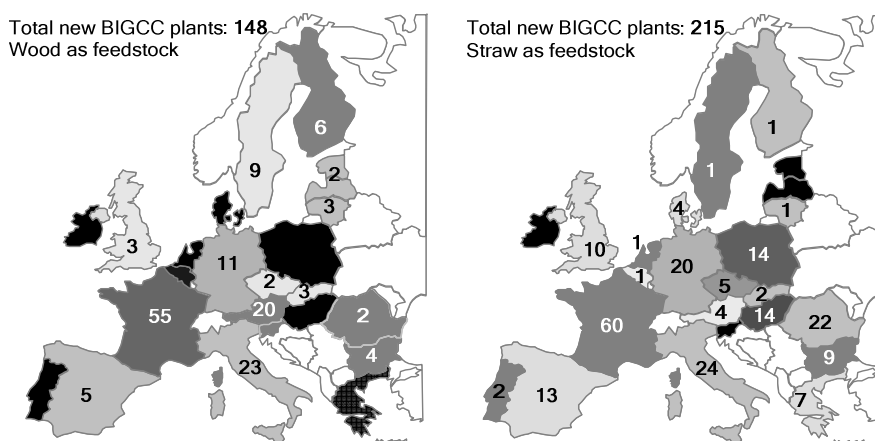

Figure 8.1: *Number of new BIGCC power plants that can be built using the wood left after cofiring and all available straw (**Scenario I-bio100-A1**). The left graph accounts for plants that can be built on wood, whereas the right graph corresponds to the straw-fueled plants*
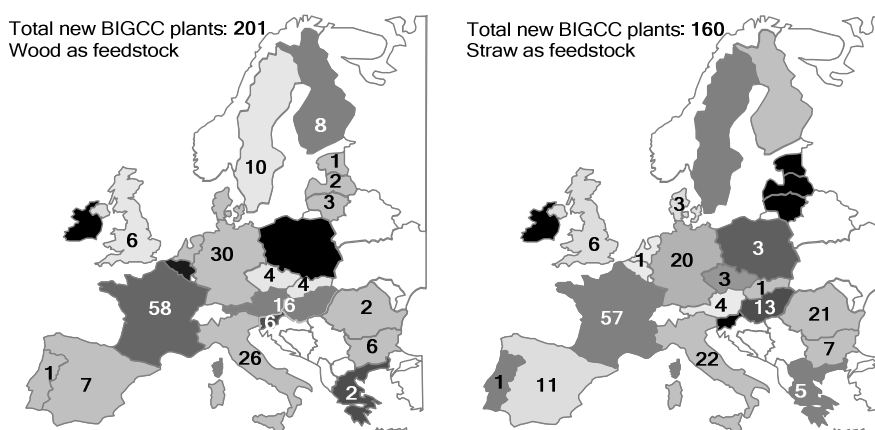

Figure 8.2: *Number of new BIGCC power plants that can be built using the straw left after cofiring and all available wood (**Scenario I-bio100-A2**). The left graph accounts for plants that can be built on wood, whereas the right graph corresponds to the straw-fueled plants*
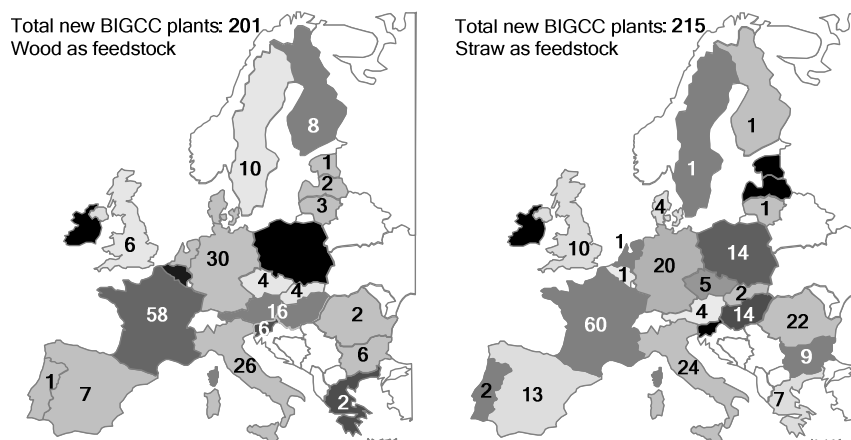
Figure 8.3: *Number of new BIGCC power plants that can be built if all available wood and straw is used in those plants (**Scenario I-bio100-A3**). The left graph accounts for plants that can be built on wood, whereas the right graph corresponds to the straw-fueled plants*

8.3. *(II)Potential replacement in actual infrastructure Cofiring and Fischer-Tropsch fuels plants*

This second scenario of Table 8-1 refers to maximize the introduction of biomass into the energy market with minor changes in the actual infrastructure. In this case, about 10 wt% of coal consumed in existing coal-fired power plants is replaced by the corresponding biomass amount (i.e., wood or straw). The remaining biomass fraction is then used for new bio-based Fischer-Tropsch plants which would operate at the optimal scale of 1000 MW$_{fuel}$ (see Chapter 6). Synthetic diesel produced in those FT-plants has the same quality of fossil diesel (see Chapter 3) and, hence, engines of actual cars do not have to be adapted. Moreover, since the produced bio-diesel has the same qualities of fossil diesel, it could benefit from the existing infrastructure for its distribution to final fuel-dispensing stations.

Taking into account the aforementioned premises, two scenarios are analyzed in order to maximize synthetic diesel production. Analogous to subchapter 8.2, scenario *A1* represents the situation where all available straw is used for new Fischer-Tropsch plants, and the wood fraction left after cofiring is converted to FT-diesel (i.e., in Eqs.(8-3) to (8-6) "*x*" equals 26% and "*y*" is 0%). Conversely, in scenario *A2*, all available wood is preferred for diesel production, whereas straw is primarily used in cofiring and the residual part is then converted to biofuel (i.e., in Eqs.(8-3) to (8-6) "*x*" equals 0% and "*y*" is 26%). For both scenarios, electricity consumption in Fischer-Tropsch plants is supplied by burning an extra biomass amount (i.e., case "*bio100*" in subchapter 3.1, Figure 3.1), resulting in the *II-bio100-A1* (i.e., wood cofiring) and *II-bio100-A2* (i.e., straw cofiring) scenarios. In a "*semi-renewable*" perspective, the electricity is taken from the grid, so more biomass is available for biofuels production. This is the so-called "*bio&grid*" case (previously detailed in subchapter 3.1) which, in

turn, is further divided in **II-biogrid-B1** (i.e., wood cofiring) and **II-bio&grid-B2** (i.e., straw cofiring). All scenarios, FT-diesel production as well as the potential biofuel replacement in road transport are summarized in Table 8-7 and Table 8-8.

As observed in Table 8-7, from a *fully-renewable "bio-100"* perspective, **II-bio100-A2** turns out to be the best alternative as about 6.8 % of transport fuel could be replaced by bio-derived FT-diesel contrary to only 6.6 % for the **II-bio100-A1** option (see Table 8-7). The *semi-renewable "bio-grid"* case follows similar trends as the potential biofuels replacement attains 8.1 % in the **II-bio&grid-B2** option but only 7.6% in the **II-bio&grid-B1** scenario. Consequently, it is more convenient to use all available forestry biomass for FT-diesel production and dedicate part of straw residues to cover 10 wt% coal replacement in cofiring stations (i.e., **II-bio&grid-B2**). From an economic point of view, this selection is also preferred as production costs of wood-derived FT-diesel are notably lower than when using straw (see section 6.2.3). On the other hand, when comparing "*bio-100*" and "*bio-grid*" cases it is observed that about 1.0-1.3% of potential replacement is lost when an extra amount of biomass is dedicated to cover the electricity demand of the Fischer-Tropsch plant. Electricity consumption in "bio-grid" cases is deducted from power generated in cofiring plants. Net electricity production is indicated by an "*" sign in Table 8-7. Higher differences are observed for the case of operating straw-fueled Fischer-Tropsch plants as corresponding efficiencies are lower than wood-to-biodiesel conversion.

The share of biofuels in road transport could be yet extended if remaining of either wood or straw left after cofiring and Fischer-Tropsch plants are dedicated to operate new SNG plants at the optimal scales of ~200 MW$_{SNG}$. Since the produced bio-SNG has the same quality of fossil natural gas (see Chapter 3) it could be safely introduced in gas-powered vehicles such as some municipal buses or garbage trucks. Potential SNG production in the four scenarios are also indicated in Table 8-7. As expected, more SNG can be obtained in those options where less FT-diesel was produced. This is the case for **II-bio100-A1** and **II-bio&grid-B1** scenarios, where annual bio-SNG plants accounts for 0.16 and 0.17 EJ respectively, versus 0.16 and 0.10 EJ for **II-bio100-A2** and **II-bio&grid-B2**. Fossil natural gas replacement by bio-based SNG is, in all cases, below 1%.

The share of biomass utilization for the 4 different scenarios is depicted in Figure 8.4. Biomass consumed in cofiring plants accounts for 13 wt% of total biomass. This value is the mean average of "*x*" and "*y*" fractions, and it corresponds to 10 wt% of coal replacement. "*Leftovers*" represent the biomass fraction that is not used in any case and it is composed of small biomass quantities scattered in a broad area. Hence, collection and transport of leftovers would not be feasible from an economic and environmental point of view. This non-valuable fraction should be minimized in order to maximize biofuels production. In effect, this is the case of the two aforementioned optimal cases **II-bio100-A2** and **II-bio&grid-B2**, where more biomass is dedicated to Fischer-Tropsch fuels production.
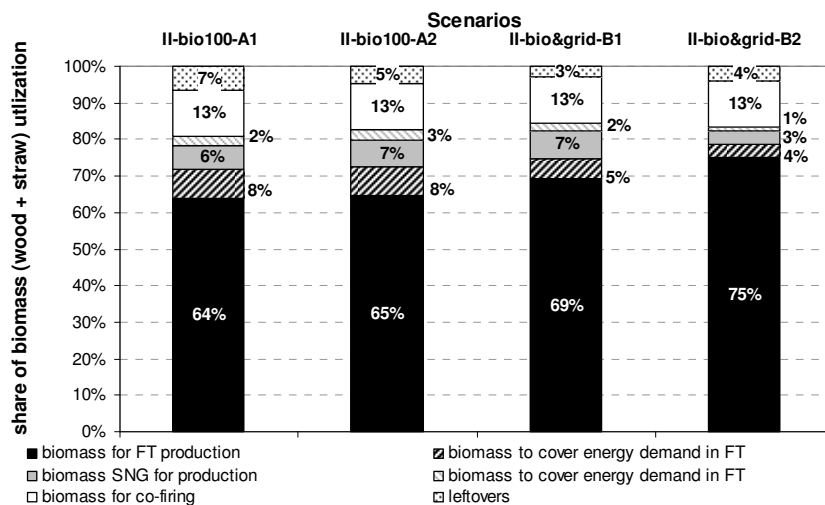
Figure 8.4: *Share of biomass utilization in the 4 different scenarios.*

When comparing the overall energy (i.e., electricity, gas and transport fuels) production, power consumption in "*bio&grid*" cases has to be deducted from the electricity generated in cofiring plants. Net electricity production is indicated by an "***" sign in Table 8-7. The "*total renewable energy*" ratio indicates that the two "*bio-grid*" cases **II-bio&grid-B1** and **II-bio&grid-B2** attain the highest values (i.e., 3.4% vs 3.1% for "*bio-100*" options). Hence, **II-bio&grid-B2** is confirmed to be the most renewable alternative as not only is the biofuel replacement higher (i.e, 8.1%), but also more green energy is produced (i.e., 3.4% of total energy). This gain is also accompanied with a reduction of production costs when wood is primarily used for Fischer-Tropsch production, thus confirming **II-bio&grid-B2** as the best alternative.

For a complete picture, new Fischer-Tropsch and SNG plants of the optimal scenarios **II-bio100-A2** and **II-bio&grid-B2** are located within different European regions (see Figure 8.5 and Figure 8.6). In both cases, country borders are crossed in order to maximize biofuels generation. These new defined "bio-regions" are indicated by different colours. In comparison with previous subchapter 8.2, the number of new Fischer-Topsch plants is notably lower than the corresponding one for new BIGCC (see Figure 8.1 to Figure 8.3) since a larger amount of feedstock is needed to produce synthetic diesel at plant scales of 1000 MW$_{FT}$. As observed in Figure 8.5 and Figure 8.6, there are few countries that have enough biomass to built own Fischer-Tropsch plants, i.e., Spain, France, Italy, Austria, Germany, Poland, Sweden, Finland, Hungary, Romania and United Kingdom. The rest of European countries need to import biomass from nearby regions in order to concentrate enough feedstock to operate at optimal scales.
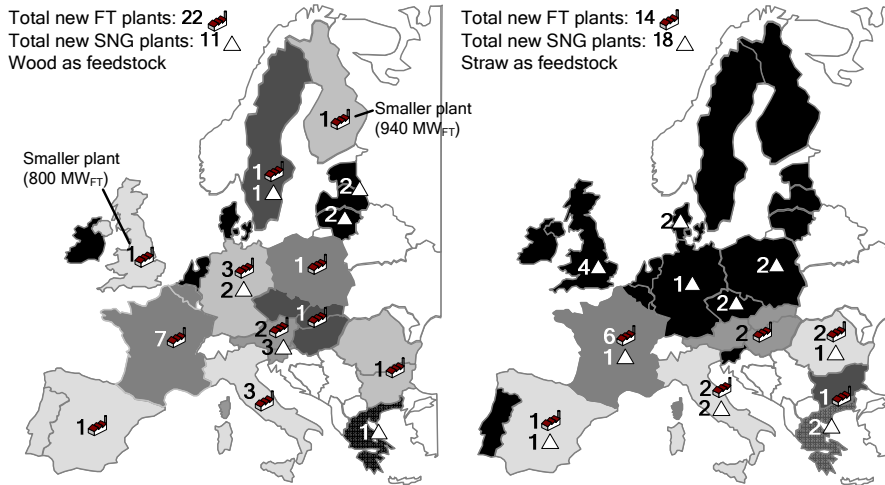
Figure 8.5: *Number of wood (left graph) and straw fueled (right graph) FT-plants that can operate (@ the optimal size scale of 1000 MW$_{fuel}$, except indicated elsewhere) using the straw left after cofiring but all the forestry biomass available in Europe (**Scenario II-bio100-A2**).*
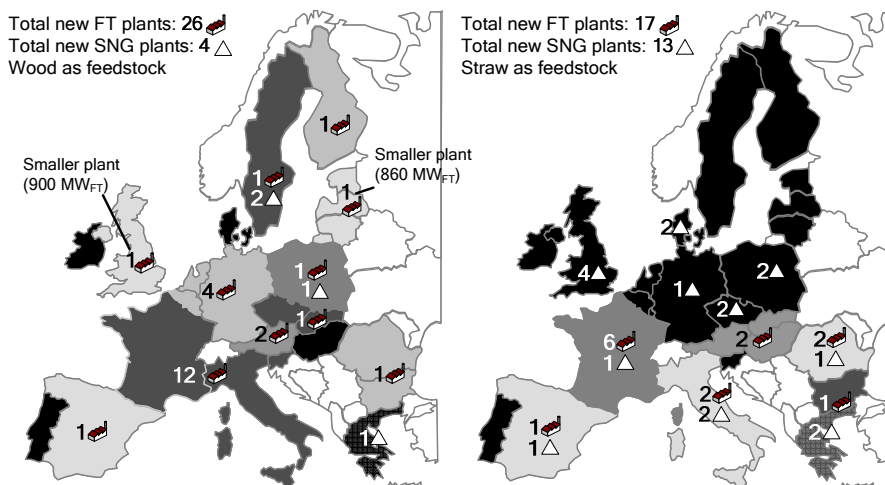

Figure 8.6: *Number of wood (left graph) and straw fueled (right graph) FT-plants that can operate (@ the optimal size scale of 1000 MW$_{fuel}$, except indicated elsewhere) using the straw left after cofiring but all the forestry biomass available in Europe (**Scenario II-bio&grid-B2**).*

In order to complete the analysis of this subchapter, the potential biomass replacement in coal-fueled power plants has been extended from 10 wt% to the theoretical maximal absorption of biomass in cofiring plants, i.e., 80 wt%. This value symbolizes that forest and straw residues could replace about 80 wt% of the coal in power stations, although this operation would have a detrimental effect on the energy efficiency. Moreover, exceeding 10 wt% of coal replacement in existing burners would lead to severe operational problems if the furnace is not modified to accept more biomass. Replacing more than 30% of coal by forest and straw residues is also rather unrealistic as it means that a large amount of biomass has to be transported from far distances to

cover the demand of large coal-consumers such as Poland or Germany. On the other hand, increasing coal replacement directly diminishes biodiesel production and, in turn, potential fossil fuel replacement in the road transport sector (see Figure 8.7).

Cofiring ↓	Biofuels replacement	
	II-biogrid-B2	II-bio100-B2
0%	9.5%	8.0%
10%	8.1%	7.6%
20%	7.0%	6.0%
30%	5.5%	4.8%
40%	4.8%	4.0%
50%	3.3%	2.7%
60%	1.5%	1.3%
70%	0.8%	0.6%
80%	0.0%	0.0%
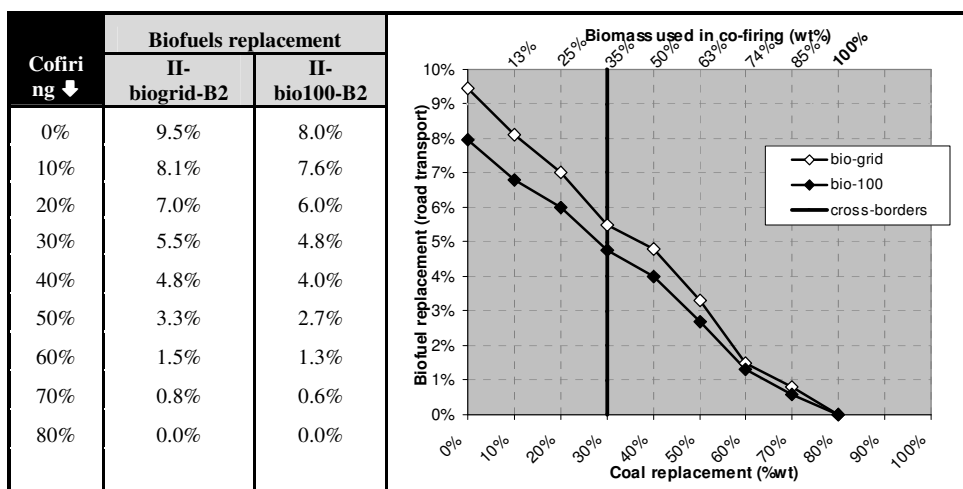
Figure 8.7: *Potential biofuels replacement vs biomass replacement in coal cofiring stations. For cofiring values exceeding 30%, national biosources do not satisfy the demand of biomass and, thus, it has to be imported from nearby countries.*

8.4. *(III) Maximizing biofuels share in the transport sector: Fischer-Tropsch implementation*

The third scenario of Table 8-1 aims to maximize the introduction of biofuels in the road transport sector. This approach is in line with the European Biofuels Directive (**2003/30/EC**) that establishes a 10% fossil fuel replacement in the road transport by 2020 [173]. Consequently, all available woody and straw sources are firstly dedicated to new Fischer-Tropsch fuels plants, which also operate at optimal scale of 1000 MW_{fuel}, whereas leftovers are converted in new SNG plants. Analogous to section 8.3, the share of renewable energy in "*bio-100*" and "*bio-grid*" cases are analyzed and compared in Table 8-7 (see **III-bio100-A3** and **III-bio&grid-B3** labels). As observed, scenario **III-bio&grid-B3** produces ~ 0,23 more EJ/yr of FT-diesel than **III-bio100-A3.** However, if the electricity consumption is included in **III-bio&grid-B3** (i.e., -0.04 EJ/yr), the difference would be then reduced to ~ 0.19 EJ/yr. As expected, more bio-based SNG is produced in the option where less FT-diesel is obtained. That is the case of **III-bio&grid-B3** scenario where extra 0.05 EJ/yr of SNG is calculated. Hovever, the overall renewable energy share is still higher for **III-bio&grid-B3** (i.e. 3.3% vs 3.0%) and, hence, **III-bio&grid-B3** becomes the best option. Similar conclusions can be drawn from Table 8-8, as the overall renewable + fossil energy input/output ratio is again higher for **III-bio&grid-B3.**

For a complete picture, results can be contrasted in Table 8-7 with the optimal previous scenarios of subchapter 8.3, in which straw cofiring was envisaged (i.e., *II-bio100-A2* and *II-bio&grid-B2*). As shown, the increase of biofuel potential replacement is estimated in the range of 0.4 % and 1.4 % for the "*bio-grid*" and "*bio-100*"cases respectively. Nevertheless, all scenarios are slightly behind the European Biofuels Directive (2003/30/EC) [173]. New Fischer-Tropsch plants for *III-bio100-A3* and *III-bio&grid-B3* scenarios are located within EU-24 map in Figure 8.8 and Figure 8.9. As shown for the "*bio-grid*" cases, about 60 new plants can be built when summing wood and straw-fueled cases. The corresponding number for the cofiring approach (i.e., *II-bio100-A2* and *II-bio&grid-B2*) was only 43. In any case, Ireland is the only country that does not have enough feedstock to justify the construction of any plant. The rest of the countries can share biomass in order to maximize the number of new FT-plants.
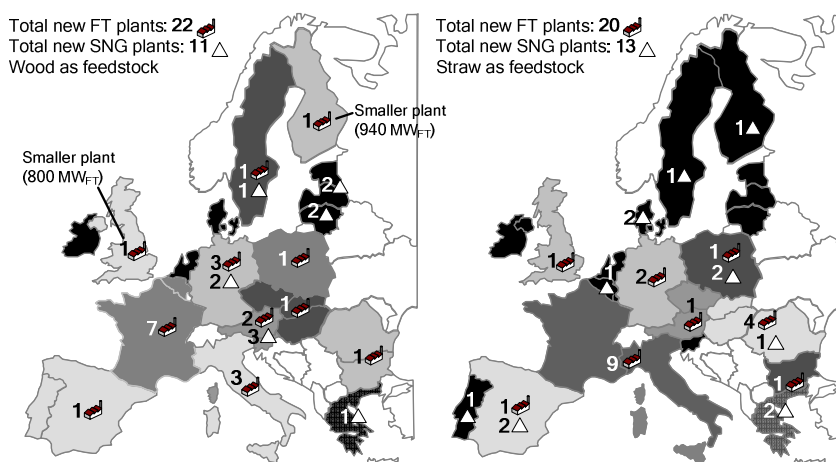

Figure 8.8: *Nr of wood (right graph) and straw (left graph) fueled FT-plants that operate at the optimal size scale of 1000 MW$_{fuel}$, if all biomass used in those plants (**Scenario III-bio100-A3**).*
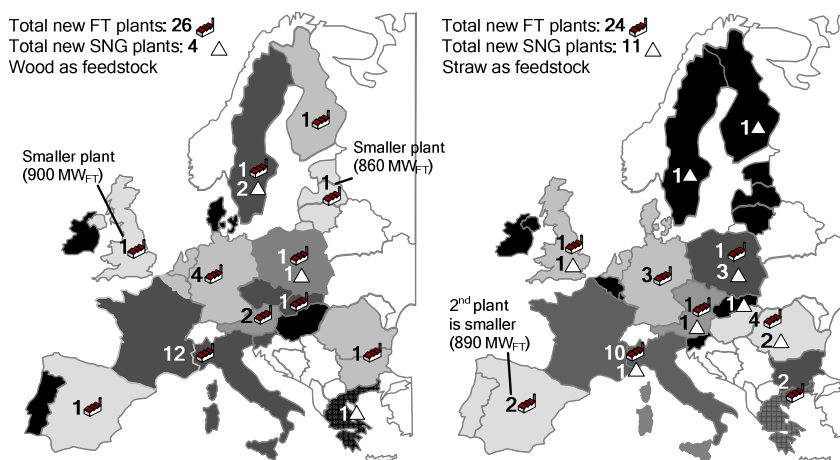

Figure 8.9: *Nr of wood (right graph) and straw (left graph) fueled FT-plants that operate at the optimal size scale of 1000 MW$_{fuel}$, if all biomass used in those plants (**Scenario III-bio&grid-B3**).*

8.5. *(IV) Maximizing Fischer-Tropsch production in accordance with Oil companies preferences*

The fourth case of Table 8-1 is similar to the previous one detailed in subchapter 8.4, with the sole difference that biomass leftovers are here preferably used in cofiring power plants instead of producing SNG. In fact, this scenario is more representative of Oil companies' directives as this industry is barely involved in the natural gas market. The number of Fischer-Tropsch plants that can be built following the "*bio-100*" and "*bio-grid*" cases is equal than in subchapter 8.4, i.e., ***III-bio100-A3*** and ***III-bio&grid-B3*** (see Figure 8.8 and Figure 8.9). Hence, the corresponding production of FT-diesel is 1.20 and 1.40 EJ/year respectively (see Table 8-7, labels ***IV-bio100-A3*** and ***IV-bio&grid-B3***). Similarly, if the electricity consumption is included the difference is then reduced to only 0.19 EJ/year. Even though, ***IV-bio&grid-B3*** continues to be the best alternative in terms of renewable energy production. When comparing the results with previous subchapter 8.4, it is observed than using leftovers for cofiring instead of SNG production turns out to be slightly less renewable for the ***IV-bio100-B3*** option, as only 2.9% ratio is now achieved.

On the other hand, for both scenarios ***III-bio100-A3*** and ***IV-bio&grid-B3***, biomass leftovers for cofiring plants represents ~ 4.5 wt% of average coal replacement in EU-24, which is far from the 10 wt% share that can accept burners without any modification. The corresponding total biomass fraction (i.e., "x and y" in Eqs. (8-3) to (8-6)) used for cofiring is in this case 5.7%. Figure 8.12 depicts the countries where 10 wt% replacement is fulfilled (*white*), the countries whose values are below 10 % (*black*) and the countries which would need to import biomass from nearby countries to fulfill the 10% share (*dashed*).

Share of coal replacement by biomass (either straw or wood) < 10%
Share of coal replacement by biomass (either straw or wood) ≥ 10%
Biomass has to be imported from nearby countries to achieve 10% coal replacement
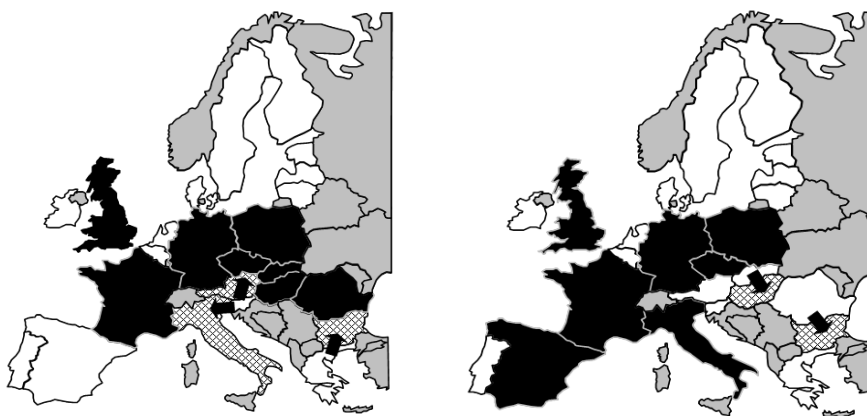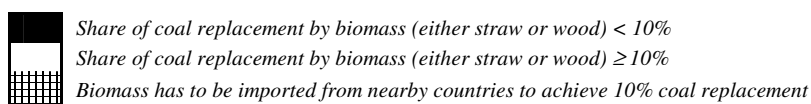
Figure 8.10: *Representation of the percentage of potential coal replacement when using the biomass left after supplying Fischer-Tropsch plants.*

8.6. *(V) Maximizing SNG production to reduce Natural Gas imports*

The fifth case of Table 8-1 is only focused on maximizing the production of SNG at the optimal scale of ~ 200 MW$_{SNG}$. The quality of the produced SNG is similar to the specification of the fossil natural gas exploited in the northern Dutch Groningen fields (see Chapter 3). Therefore, it is assumed that bio-based SNG could partially decrease the demand of imported natural gas and, in turn, decrease the dependency on suppliers such as Russia or Algeria. For this analysis, all available wood and straw residues are primarily converted in SNG plants, whereas the leftovers are used in cofiring stations. Since the heat and electricity demand of SNG plants is not covered from own resources, three new scenarios are here identified (see Chapter 3). In the most renewable one ("*bio-100*"), heat and electricity is supplied by burning an extra amount of biomass. In the intermediate scenario ("*bio-grid*"), heat demand is offset by also combusting an extra biomass amount, whereas electricity is taken from the grid. In the least renewable scenario ("*NG-grid*"), the extra biomass amount needed for heat supply is replaced by fossil natural gas but electricity is also consumed from the grid. The 3 scenarios are labeled as **V-bio100-A3**, **V-bio&grid-B3** and **V-NG&grid-B3**.

Analogous to previous subchapters, the electricity consumption for SNG process is deducted in cases **V-bio&grid-B3** and **V-NG&grid-B3**, where resulting net electricity production is identified by a "*" sign in Table 8-7.   In addition, fossil natural gas consumption for **V-NG&grid-B3** is also deducted. Net fossil natural gas production is also indicated by an "*" sign. When comparing SNG production in the three scenarios, major difference is observed for **V-NG&grid-B3** (i.e., 2.16 EJ in versus 1.63 and 1.55 EJ for **V-bio&grid-B3** and **V-bio100-A3** respectively). This could be explained by the fact that the SNG process requires a considerable external heat supply to operate the cleaning and upgrading sections, whereas the electricity demand is moderate. Despite this observation, renewable energy ratio is still more favorable for the third scenario **V-NG&grid-B3** (i.e., 8.0% renewable SNG and 4.8 % overall renewable energy). For the calculation of the 8.0% of renewable SNG ratio, natural gas consumption of the SNG process (i.e., 0.89 EJ/yr) is included in the denominator of Eq.(8-12). For a better understanding, the different shares of SNG and fossil natural gas production are depicted in Figure 8.11. This picture also includes the scenarios of the subsequent section 8.7, in which cofiring is prioritized over maximizing SNG.

Despite of the higher renewability shares of the **V-NG&grid-B3**, this third scenario is not preferred in case natural gas imports need to be minimized as overall volumes are larger (i.e., 23.76 plus 0.89 EJ/yr). The remaining biomass fraction is then used in cofiring power plants. However, the potential coal replacement for the 3 scenarios **V-bio100-A3**, **V-bio&grid-B3** and **V-NG&grid-B3**   is rather insignificant (i.e., 1.9%, 1.7% and 1.5% respectively). The corresponding utilization of biomass (i.e., "x and y" in Eqs. (8-3) to (8-6)) is 2.4%, 2.2%, and 1.9% respectively. In fact, unlike Fischer-Tropsch fuels, SNG requires a moderate biomass amount and, thus, is more feasible to optimize European biomass availability for SNG production.
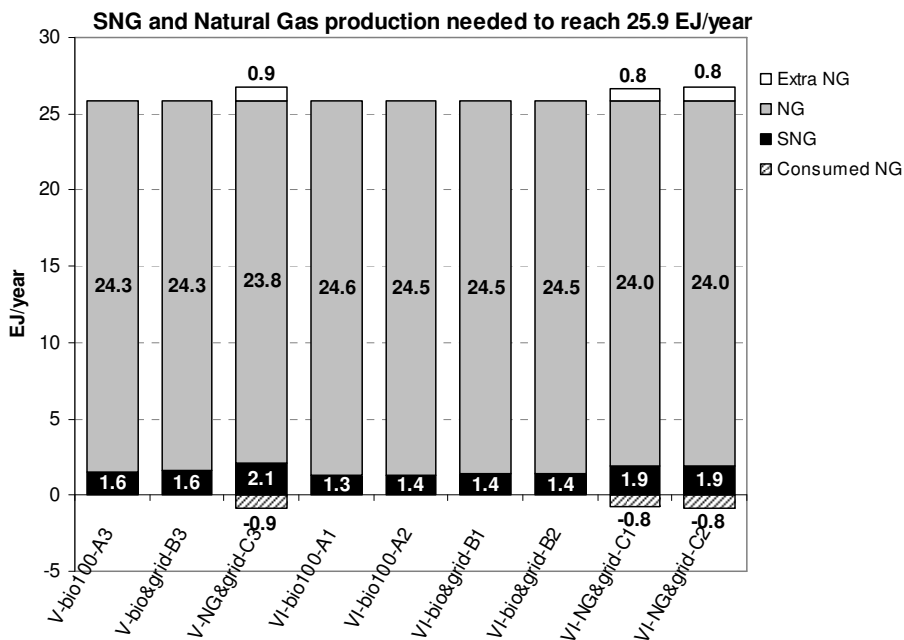
Figure 8.11: *Share of SNG and natural gas production for "V" and "VI" scenarios.*

The number of bio-based SNG plants is allocated within the EU-24 borders in subsequent Figure 8.12 to Figure 8.14. As shown, all countries, with the exception of Ireland, could build alt least one SNG plant.
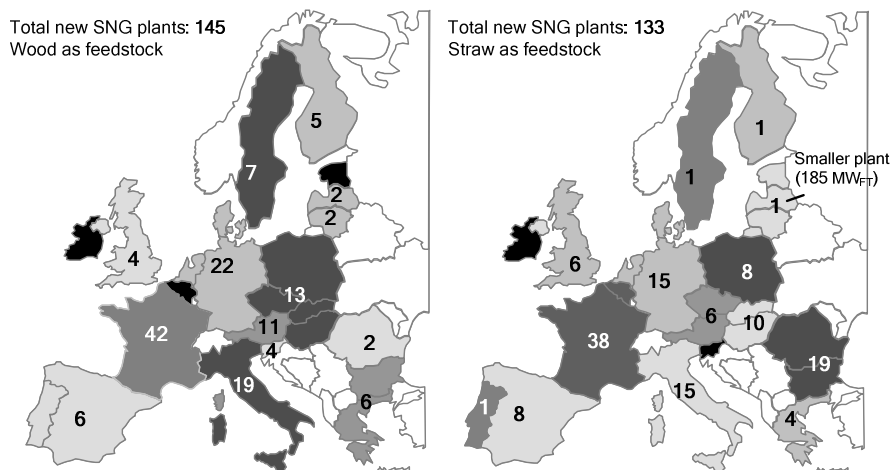

Figure 8.12: *Number of SNG plants that run on wood (left graph) and straw (right graph) at the optimal size scale of ~200MW$_{SNG}$, if all biomass is used in those plants (**Scenario V-bio100-A3**).*
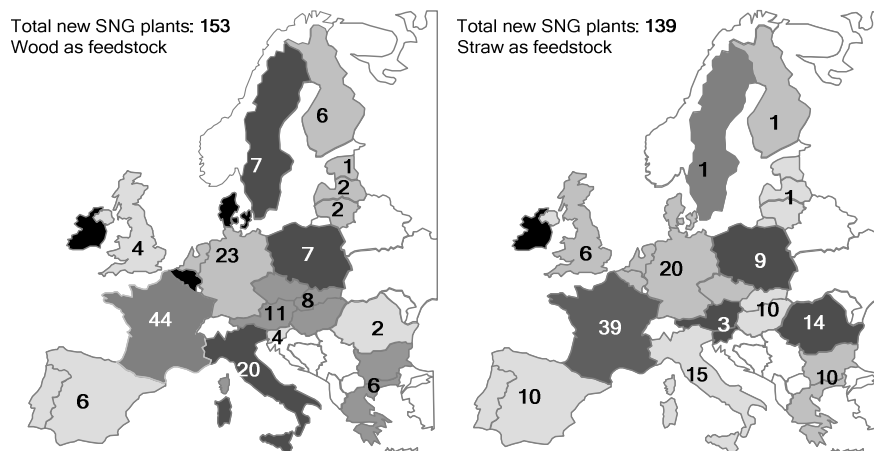
Figure 8.13: *Number of SNG plants that run on wood (left graph) and straw (right graph) at the optimal size scale of ~200MW$_{SNG}$, if all biomass is used in those plants (**Scenario V-bio&grid-B3**).*
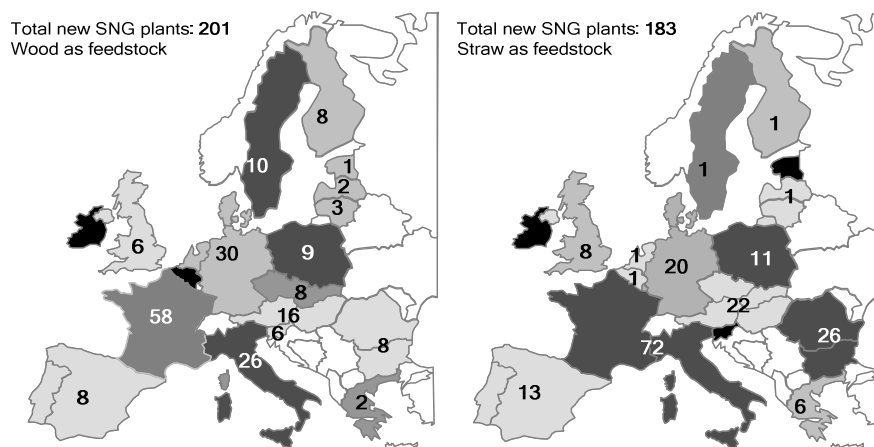

Figure 8.14: *Number of SNG plants that run on wood (left graph) and straw (right graph) at the optimal size scale of ~200MW$_{SNG}$, if all biomass is used in those plants (**Scenario V-NG&grid-C3**).*

8.7. (VI) Maximizing CO$_2$ potential reduction: Cofiring and SNG plants implementation

Electricity and steam generation accounts for most of the CO$_2$ emissions in Europe, followed by the transport sector [4]. Moreover, both sectors are predicted to remain the two major contributors for the coming 20 years (see Figure 8.15). Among all fossil sources consumed during thermal electricity production, coal and natural account for most of the CO$_2$ emissions [4]. Further to Figure 8.15, our initial hypothesis establishes that major CO$_2$ reduction could be achieved in the electricity market when substituting firstly coal and secondly natural gas for more renewable sources such as wood or straw. However later analyses (see subchapter 8.10.3) will either confirm or confront our hypothesis.

Contribution of CO₂ emissions per sector
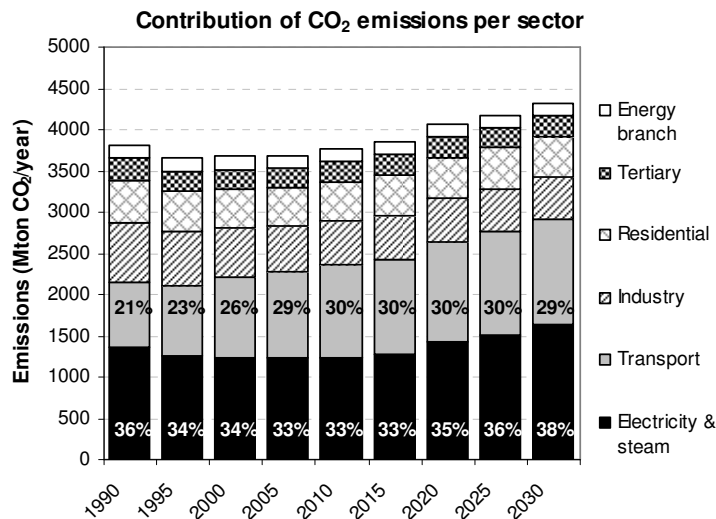
Figure 8.15: Contribution of each economic sector on the total CO_2 emissions in EU-24. Values are calculated from Mantzos et al [4].

Following our initial hypothesis, the highest coal replacement would occur if all biomass is dedicated to new BIGCC power plants. In fact, this was the third scenario in subchapter 8.2. However, as mentioned, this alternative was accompanied with a considerable high investment needed to built new power plants. An intermediate situation is here presented as the sixth approach of Table 8-1. It differs from the previous one detailed in section 8.6 in that biomass sources are preferably used in cofiring plants, whereas the remaining fraction is then processed in SNG plants. In this case, six possible scenarios are analyzed, which correspond to "*bio100*", "*bio&grid*" and "*NG-grid*" cases and their subdivision based on using either wood or straw in cofiring. Results are summarized in Table 8-7 and Table 8-8 (see labels **VI-bio100-A1** to **VI-NG&grid-C2**). Similarly, to previous subchapter 8.6, electricity consumption in SNG process is included for cases "*bio&grid*" and "*NG&grid*" cases, and likewise the natural gas demand for "*NG&grid*".

According to Table 8-7, the most renewable options are the "*NG-grid*" cases (i.e., **VI-NG&grid-C1** and **VI-NG&grid-C2**), which account for general renewable shares of 4.6% and 4.5% respectively, and SNG renewable ratios of 7.0% and 7.6% respectively. Analogous to previous section 8.6, "*NG&grid*" processes are again the least favored ones when the aim is to reduce natural gas import (See Figure 8.11). Comparison among "*bio100*", "*bio&grid*" and "*NG-grid*", reveals that straw cofiring is always preferred over wood cofiring, although the electricity outcome is lower. Fossil + renewable energy input/outputs in Table 8-8 follows opposite trends. Finally, the number of new SNG plants that can be operated from the biomass left after cofiring is presented in Figure 8.16 to Figure 8.19. As observed, the "*NG-grid*" cases run more SNG plants (see Figure 8.19), and they also achieve highest fossil natural gas replacement (i.e.,6.4 and 6.9%).
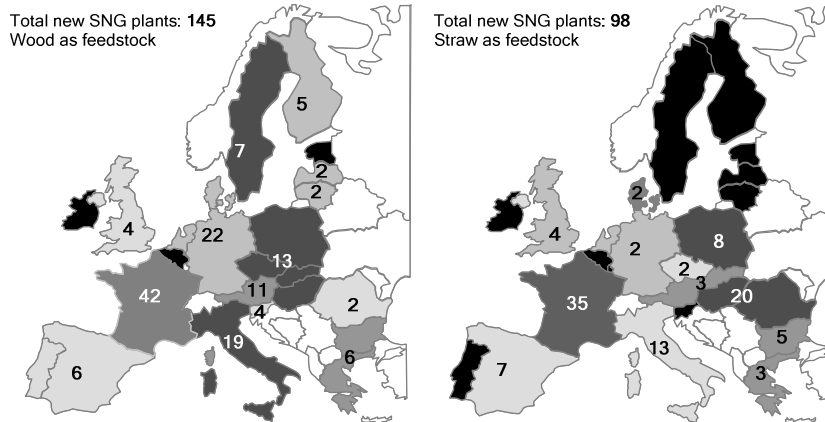
Figure 8.16: *Number of wood (left graph) and straw fueled (right graph) SNG plants that can be built using straw left after cofiring but all forest biomass in EU-24 (**Scenario VI-bio100-A2**).*
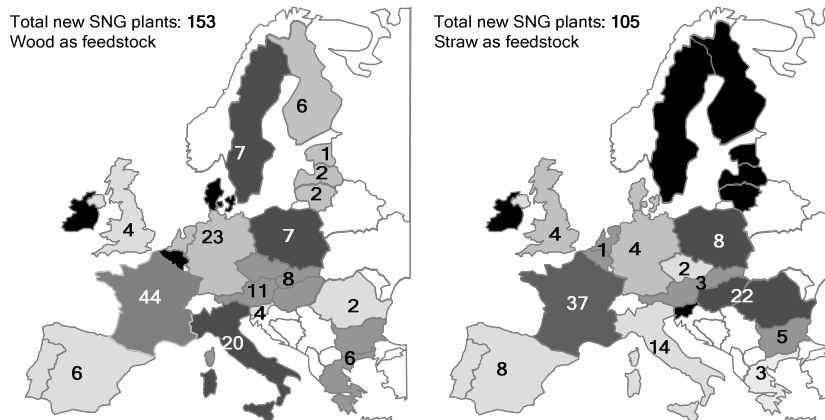
Figure 8.17: *Number of wood (left graph) and straw fueled (right graph) SNG plants that can be built using straw left after cofiring but all forest biomass in EU-24 (**Scenario VI-bio&grid-B2**).*
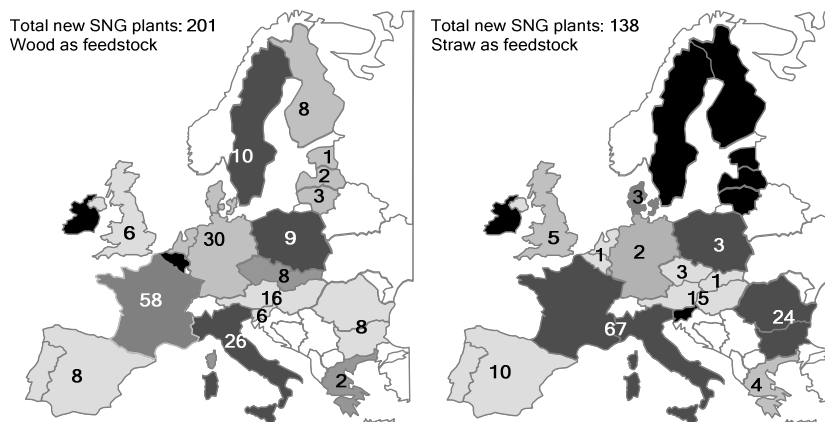

Figure 8.18: *Number of wood (left graph) and straw fueled (right graph) SNG plants that can be built using straw left after cofiring but all forest biomass in EU-24 (**Scenario VI-NG&grid-B2**).*

8.8. *(VII) Replacement potential in future vehicles: Introduction of Hydrogen FCV*

The analysis of this seventh category of Table 8-1 is somehow different to the six previous cases because the introduction of hydrogen in the energy market is predicted for a long-term future. Therefore, is highly probable that biomass would have been already consumed in other processes. Consequently, real biomass availability for hydrogen production would be notably lower than the one indicated in Chapter 2. However, in order to determine the theoretical maximal hydrogen potential, biomass accesability is assumed to remain equal than in Chapter 2 (i.e., 1.9 and 18 EJ/yr of wood and straw respectively).

For a complete analysis, the same three scenarios presented in section 8.6 are here discussed and named as *VII-bio100-A3*, *VII-bio&grid-B3* and *VII-NG&grid-C3*. For all cases, biomass is primarily used in hydrogen plants operating at optimal scales of ~500 MW_{H2}, whereas leftovers can be then burned in cofiring plants, as done in subchapter 8.6. Electricity and natural gas consumed in biomass-to-H_2 conversion process is also taken into account for the corresponding cases *VII-bio&grid-B3* and *VII-NG&grid-C3*. Results from this approach are tabulated in Table 8-2 and Table 8-3. More bio-based H2 is generated in the third scenario VII-NG&grid-C3 because biomass is only dedicated to biofuel production (i.e., heat is covered by natural gas combustion whereas electricity is taken from the grid). Biomass leftovers are then used in cofiring stations. In this case, coal replacement is ~ 3.6% for the first two alternatives *VII-bio100-A3* and *VII-bio&grid-B3*, whereas is ~0.1% lower in the third case *VII-NG&grid-C3* (see Table 8-2). Corresponding biomass utilization in cofiring plants is 4.6wt%, 4.6wt% and 4.5wt% for *VII-bio100-A3*, *VII-bio&grid-B3* and *VII-NG&grid-C3* respectively. When adding the renewable electricity and H_2 production, *VII-NG&grid-C3* becomes again the most renewable scenario (i.e., 4.7%). Similar conclusions can be drawn when comparing the fossil+renewable energy ratios in Table 8-3 (i.e., 44.1%). Hence, from an energetic point of view, *VII-NG&grid-C3* is confirmed to be the best alternative.

Table 8-2: Overview of bio-electricity and H_2 production and share of total renewable energy produced. (*) means that consumed electricity has been deducted from total production.

Scenario VII	Biomass use [a]	Net electricity (EJ/yr) produced from:						% renewable electricity	H₂ production (EJ/yr) from:			% renewable energy [b]
		wood (new plants)	straw (new plants)	wood (cofiring)	straw (cofiring)	wood+straw (cofiring & new plants)	Coal 2020		wood	straw	total	
bio100-A3	x&y ~4.6	0.00	0.00	0.04	0.04	0.08	3.69	2.0	0.73	0.73	1.46	3.3
bio&grid-B3	x&y ~4.6	0.00	0.00	0.04	0.04	0.08	3.72 3.69*	2.0	0.78	0.78	1.56	3.5
NG&grid-C3	x&y ~4.5	0.00	0.00	< 0.04	< 0.04	0.07	3.73 3.69*	1.9	1.09	1.07	2.16	4.7

Table 8-3: *Overview of input, output & overall ratios for the 3 scenarios.*

| Scenario VII | Biomass use [a] | Total input | | | | Total input | Output electricity | Input for electricity | Output/input electricity % | Output H_2 | Input H_2 | Output/input H_2 % | Average output/input |
		wood	straw	fossil NG	coal 2020								
bio100-A3	x&y ~4.6	1.9	1.8	0.0	8.3	12.0	3.77	8.43	44.7	1.47	3.53	41.6	43.4
bio&grid-B3	x&y ~4.6	1.9	1.8	0.0	8.3	12.0	3.77	8.49	44.4	1.55	3.53	44.0	44.1
NG&grid-C3	x&y ~4.5	1.9	1.8	1.4	8.4	13.4	3.77	8.52	44.2	2.16	4.91	44.0	44.1

(a): The "x" and "y" parameters represent the forest and straw fraction that is used in cofiring stations. Values are calculated from Eqs.(8-1) to (8-5). In this case, both values are ~0 as the biomass fraction used in cofiring is rather insignificant.

(b): % total renewable energy accounts for total energy produce from biomass divided by the sum of fossil coal (i.e., 3.77 EJ/yr), natural gas (i.e., 25.9 EJ/yr) and transport fuels (i.e., 15.1EJ/yr) needed by 2020 (i.e., sum = 44.8 EJ/yr).

$$\% \ total \ renewable \ energy = \frac{Electricity + H_2 \ from \ wood \ \& \ straw}{3.77 + 25.9 + 15.1 \ EJ \ / \ yr} \tag{8-7}$$

Analogous to all sections, the number of new bio-based Hydrogen plants is depicted in Figure 8.19 to Figure 8.21. As expected, more plants can be erected for the third scenario **VII-NG&grid-C3** (i.e., 150 plants), as in this case, biomass is only used for H_2 production. Ireland and Estonia do not have enough sources to operate any H_2 plant, whereas Belgium, Netherlands and Portugal always to need to import biomass from nearby countries.
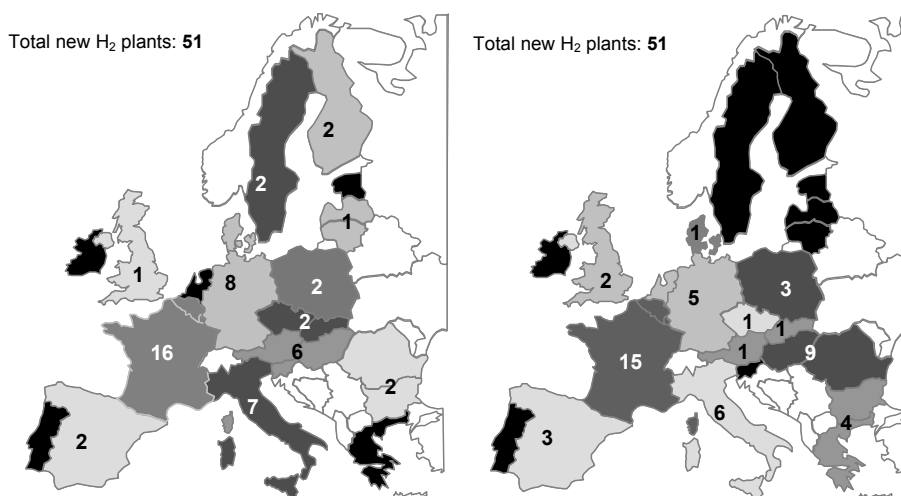

Figure 8.19: *Number of Hydrogen plants that could be built (@ the optimal size scale of 500MW$_{H2}$) if all biomass is used in those plants (**Scenario VII-bio100-A3**).*
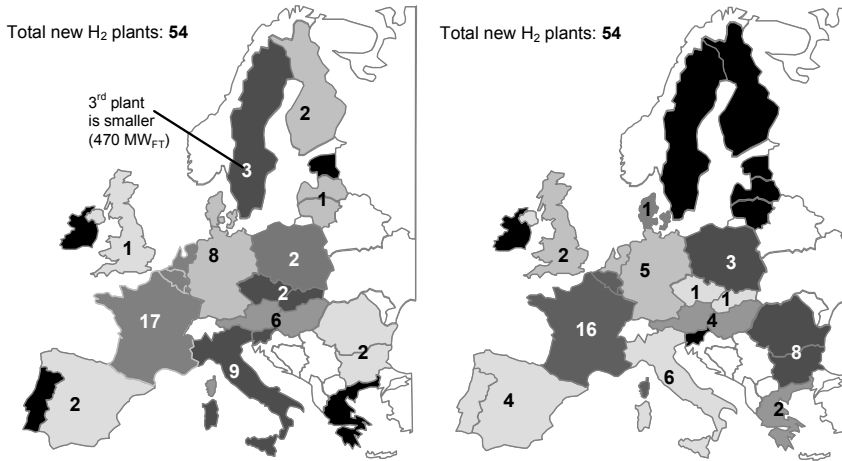
Figure 8.20: *Number of Hydrogen plants that could be built (@ the optimal size scale of 500MW$_{H2}$) if all biomass is used in those plants (**Scenario VII-bio&grid-B3**).*
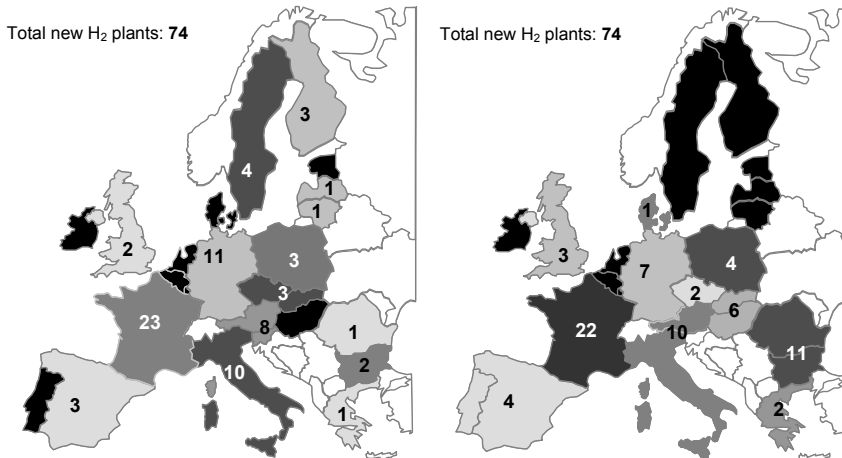
Figure 8.21: *Number of Hydrogen plants that could be built (@ the optimal size scale of 500MW$_{H2}$) if all biomass is used in those plants (**Scenario VII-NG&grid-C3**).*

8.9. *(VIII) Maximizing Methanol production*

As mentioned in subchapter 3.4.2, methanol can be either blended with gasoline in ICE cars (i.e., M85 mixture) or neat used in fuel cell cars. The timeframe of both alternatives is somehow different as commercial methanol-fueled fuel cell cars are predicted to enter the market not earlier than year 2020. In any case, methanol production is here optimized to maximize the number of FCV vehicles that could run on methanol. Results from this approach are summarized in Table 8-4 and Table 8-5. In this case, biomass leftovers are also sent to cofiring stations, and they have the potential to replace 5.1wt%, 5.0wt% and 4.0 wt% of coal in ***VIII-bio100-A3***, ***VIII-bio&grid-B3*** and ***VIII-NG&grid-C3*** scenarios respectively. This replacement consumes 6.4wt%, 6.3wt% and 5.1wt% of total biomass availability respectively. Hence, maximal biomethanol production (i.e., 1.46 EJ/yr) is produced in the third

option *VIII-NG&grid-C3*, where more renewable energy is also generated (i.e., 3.3%), as shown in Table 8-4. Hence, the last scenario *VIII-bio&grid-B3* is the best alternative from an energetic point of view. Similar trends are observed in Table 8-5, in which total renewable + fossil energy ratios are compared.

Table 8-4: *Overview of bio-electricity & methanol produced, and share of total renewable energy. (*) means that consumed electricity has been deducted from total production.*

Scenario VIII	Biomass use [a]	Net electricity (EJ/yr) produced from:						% renewable electricity	Methanol (EJ/yr) produced from:			% renewable energy [b]
		wood (new plants)	straw (new plants)	wood (cofiring)	straw (cofiring)	wood+straw (cofiring & new plants)	Coal 2020		wood	straw	total	
bio100-A3	x&y ~6.4	0.00	0.00	0.05	0.05	0.10	3.67	2.7	0.60	0.58	1.18	2.8
bio&grid-B3	x&y ~6.3	0.00	0.00	0.05	0.05	0.10	3.68	2.7	0.65	0.58	1.23	2.9
NG&grid-C3	x&y ~5.1	0.00	0.00	0.05	0.05	0.10	3.68	2.6	0.75	0.72	1.46	3.3

Table 8-5: *Overview of input, output & overall ratios for the 3 methanol scenarios.*

Scenario VIII	Biomass use [a]	Total input				Total input	Output electricity	Input for electricity	Output/input electricity %	Output methanol	Input methanol	Output/input methanol %	Average output/input
		wood	straw	fossil NG	coal 2020								
bio100-A3	x&y ~6.4	1.9	1.8	0.0	8.4	11.9	3.77	8.47	44.5	1.18	3.51	33.6	40.9
bio&grid-B3	x&y ~6.3	1.9	1.8	0.0	8.4	12.0	3.77	8.49	44.4	1.23	3.52	34.9	40.8
NG&grid-C3	x&y ~5.1	1.9	1.8	1.3	8.3	13.2	3.77	8.44	44.7	1.46	4.85	30.2	38.7

(a): The "x" and "y" parameters represent the forest and straw fraction that is used in cofiring stations. Values are calculated from Eqs.(8-1) to (8-5). In this case, both values are ~0 as the biomass fraction used in cofiring is rather insignificant.

(b): % total renewable energy accounts for total energy produce from biomass divided by the sum of fossil coal (i.e., 3.77 EJ/yr), natural gas (i.e., 25.9 EJ/yr) and transport fuels (i.e., 15.1EJ/yr) needed by 2020 (i.e., sum = 44.8 EJ/yr).

$$\% \ total \ renewable \ energy = \frac{Electricity + Methanol \ from \ wood \ \& \ straw}{3.77 + 25.9 + 15.1 \ EJ \, / \, yr} \tag{8-8}$$

On the other hand, Figure 8.22 and Figure 8.24 illustrate the number of new biomethanol plants. Similarly to previous subchapters, more plants can be erected for the third scenario *VII-NG&grid-C3* (i.e., 61 plants), as in this case, biomass is only dedicated to biofuel production. In comparison with Fischer-Tropsch plants, which also operates at the optimal scale of 1000 MW$_{fuel}$, it is observed that the number of new biofuels plants is rather similar for *bio-100* and *bio&grid* cases (i.e., only 1 plant difference in bio-100, and extra 3 plants in bio&grid). In effect, efficiencies (i.e., biomass consumption) of both conversion processes are quite close. Ireland, Belgium and Netherlands do not have enough biomass to build any methanol plant.
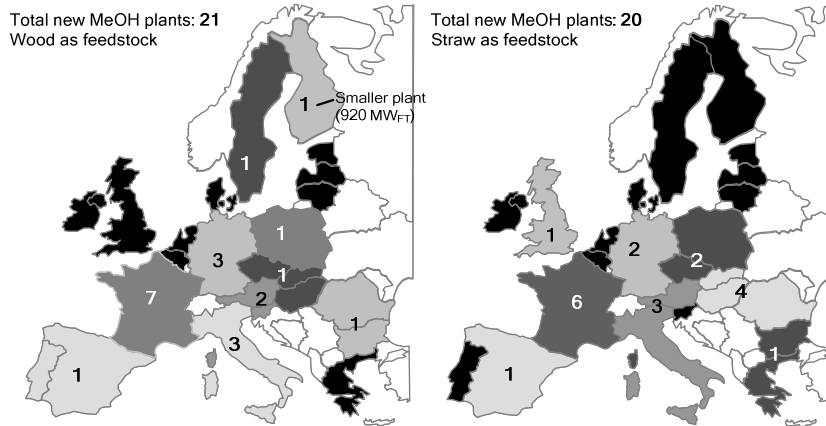
Figure 8.22: *Number of Methanol plants that could be built (@ the optimal size scale of 1000MW$_{fuel}$) if all biomass is used in those plants (**Scenario VIII-bio100-A3**).*
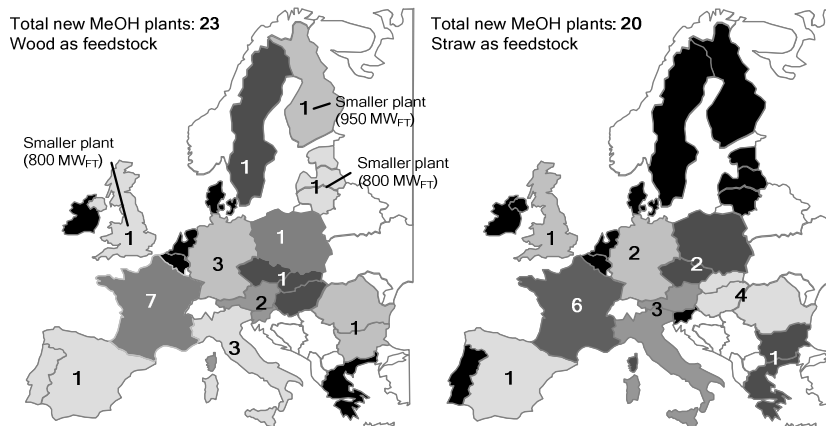

Figure 8.23: *Number of Methanol plants that could be built (@ the optimal size scale of 1000MW$_{fuel}$) if all biomass is used in those plants (**Scenario VIII-bio&grid-B3**).*
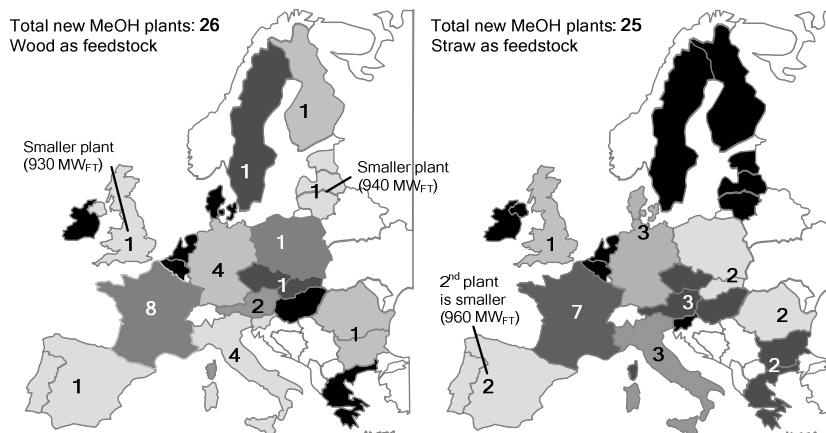

**Figure 8.24:** *Numbe of Methanol plants that could be built (@ the optimal size scale of 1000MW$_{fuel}$) if all biomass is used in those plants (**Scenario VIII-NG&grid-C3**).*

8.10. *Comparison & Conclusions*

8.10.1.   *Total bioenergy production from forest and straw residues*

As aforementioned, results of all scenarios are gathered in subsequent Table 8-7 and Table 8-8. All cases are compared to achieve the same energy production in the timeframe of year 2020, whose values have been stipulated in the report of Mantzos et al [4]. Basically, biomass is used to reduce the fossil fuel input in three key sectors of Table 8-6 for 24 European countries.

Table 8-6: *Reference 'fossil' scenario. It is defined as the expected fossil fuel consumption in EU by 2020. The sum of bioenergy and fossil fuels production in all scenarios (see Table 8-1) always comply with EU fuel consumption in 2020. Values are calculated from [4].*

- Electricity production from coal (i.e., **3.77 EJ/year**). This figure means that about **8.34 EJ** of coal is consumed annually.

- Natural gas consumption for several uses (e.g., electricity, heating, or other industrial applications), which accounts for **25.90 EJ/year**

- Fossil fuel consumption in the road transport that sums **15.10 EJ/year**. This figure includes public road transport, private cars and motorcycles, and trucks.

According to the results from Table 8-7, the first scenario "*I*", which is intended to maximize renewable electricity, lead to the lowest "*total renewable share*" (i.e., 3.0-3.1%), followed by the scenarios where Fischer-Tropsch fuels are produced (i.e., "*II*", "*III*" and "*IV*"). This could be explain by the fact that bioenergy production from wood and straw is the lowest for the electricity case but, unlike other biofuels whose final use will imply extra inefficiencies, electricity is the final energy outcome. In effect, when taking into account that a diesel-fuelled car has an efficiency of about 22%, and natural gas-fuelled power plants work at less than 60% efficiency, the conclusion is then different, as more "useful" renewable energy is produced in the "*I*" case that accounts for maximizing renewable electricity production. From previous Table 8-2 and Table 8-4, can be concluded that methanol give similar figures than Fischer-Tropsch whereas H_2 is slightly worse than SNG. In effect, the results follow the efficiency ranking presented in Chapter 3. Moreover, an added penalty for large scale processes such as Fischer-Tropsch and Methanol is that, since both processes consumes a relatively large amount of biomass, it is more difficult to allocate biomass for those plants than for medium sizes like electricity, SNG and H_2 processes. Hence, the fraction of unused biomass (i.e., leftovers) is relatively larger for Fischer-Tropsch and methanol than for the rest of biofuels and bio-electricity.

Another general observation is that, as expected, renewable energy production for the "*bio-grid*" and "*NG-grid*" cases is always larger, as biomass is only dedicated to produce biofuels and not to cover the energy demand of the processes. However, later environmental analysis (see subchapter 8.10.3) will confront if this statement is also accompanied with higher CO_2 savings. In fact, although more biofuels are produced in the "*bio-grid*" and "*NG-grid*" cases, production plants consume some fossil fuel to cover heat and electricity demand, thus resulting, in higher CO_2 than the "*bio-100*"

case that uses entirely biomass. Another interesting remark is that maximum biofuel replacement in 2020 (i.e., **9.5%**) is accomplished in the "*III-bio&grid-B3*" case. This value is slightly behind the target established in the more recent European Directive **2009/28/EC**. However, it should be noticed that this value of 9.5% would decrease for successive years as biomass availability will not grow, contrary to the energy demand that is predicted to steadily increase. On the other hand, fossil natural gas can be replaced by bio-based SNG up to **8.1%** in the "*V-NG&grid-C3*" option. This value takes into account that extra fossil natural gas is consumed by the process itself. The share of renewable energy is lower for natural gas than for the road transport fuel as the natural gas consumption is far larger (i.e., 25.9 EJ/year of natural gas versus 15.1EJyear of road transport fuel).

Subsequently, Table 8-8 summarizes the inputs of forest and straw residues, together with fossil fuel energy (i.e., coal, natural gas and fossil transport fuel). It is assumed that fossil natural gas and oil is extracted at 80% of efficiency. Hence, the primary energy consumption for fossil natural gas and transport fuel is 32.4 and 18.9 EJ/year respectively, in case of requiring 25.9 and 15.1 EJ/yr of fossil natural gas and fossil transport fuel respectively. Biomass input (i.e., 1.8 and 1.9 EJ/yr for forest and straw respectively) is distributed to produced bio-electricity and/or biofuels. Results show that "*output/input*" electricity ratios are higher when minimizing cofiring as the introduction of biomass in existing boilers has a negative influence on the efficiency. Similarly, "*output/input*"ratios for natural gas and fuel transport are diminished when using more biomass, as efficiencies of biofuels plants are notably lower than 80%. Global average "*output/input*"ratios do not significantly change among all scenarios as the contribution of fossil energy is by far larger than the bioenergy.

Table 8-7: Overview of biofuels & electricity produced, and % of renewable energy as function of scenario.(*) means that electricity consumed has been deducted from total production.

	I. Maximal renewable electricity production			II. Potential replacement in existing infrastructure				III. Maximum biofuel for transport		IV. Maximum FT-diesel (Oil industry)	
Case biofuel plant	bio-100 (a)	bio-100 (a)	bio-grid (b)	bio-100 (a)	bio-100 (a)	bio-grid (b)	bio-grid (b)	bio-100 (a)	bio-grid (b)	bio-100 (a)	bio-grid (b)
Scenario (use of biomass %)	A1 (d) x=26 y=0	A2 (e) x=0 y=26	A3 (f) x=0 y=0	A1 (d) x=26 y=0	A2 (e) x=0 y=26	B1 (d) x=26 y=0	B2 (e) x=0 y=26	A3 (f) x=0 y=0	B3 (f) x=0 y=0	A3 (f) x & y ~5.7	B3 (f) x & y ~5.7
wood (new plants)	0.48	0.65	0.65	0.00	0.00	0.00	0.00	0.00	0.00	0.00	0.00
straw (new plants)	0.64	0.47	0.64	0.00	0.00	0.00	0.00	0.00	0.00	0.00	0.00
wood (cofiring)	0.21	0.00	0.00	0.21	0.00	0.21	0.00	0.00	0.00	0.05	0.05
straw (cofiring)	0.00	0.19	0.00	0.00	0.19	0.00	0.19	0.00	0.00	0.05	0.05
wood+straw (cofir+new)	1.33 (m)	1.32 (m)	1.29	0.21	0.19	0.21	0.19	0.00	0.00	0.09	0.09
coal 2020	3.24 (m)	3.09 (m)	2.48	3.56	3.58	3.59 / 3.56*	3.61 / 3.58*	3.77	3.81 / 3.77*	3.68	3.72 / 3.68*
% renewable electricity (h)	29.1%	29.9%	34.3%	5.7%	5.1%	5.6%	5.1%	0.0%	0.0%	2.5%	24%
wood (gas)				0.08	0.06	0.11	0.02	0.06	0.02		
straw (gas)				0.07	0.10	0.06	0.07	0.07	0.06		
wood+straw (gas)				0.16	0.16	0.17	0.10	0.13	0.08		
Fossil gas 2020	24.44 (m)	24.73 (m)	25.90	25.74	25.74	25.73	25.80	25.77	25.82	25.90	25.90
% renewable gas (i)	0%	0%	0%	0.6%	0.6%	0.7%	0.4%	0.5%	0.3%	0.0%	0.0%
wood (transport)				0.43	0.63	0.46	0.74	0.63	0.74	0.63	0.74
straw (transport)				0.58	0.40	0.69	0.48	0.58	0.69	0.58	0.69
wood+straw (transport)				1.00	1.03	1.15	1.23	1.20	1.43	1.20	1.43
fossil oil 2020	15.10	15.10	15.10	14.10	14.07	14.05	13.87	13.90	13.67	13.90	13.67
% renewable transport fuel (j)	0%	0%	0%	6.6%	6.8%	7.6%	8.1%	8.0%	9.5%	8.0%	9.5%
% total renewable energy (k)	3.1%	3.1%	3.0%	3.1%	3.1%	3.4%	3.4%	3.0%	3.3%	2.9%	3.4%

Table 8-7: *[Continuation] Overview of biofuels & electricity produced, and % of renewable energy as function of scenario.*

	A3 (f)	B3 (f)	C3 (f)	A1 (d)	A2 (e)	B1 (d)	B2 (e)	C1 (d)	C2 (e)
% total renewable energy (k)	3.6%	3.7%	4.8%	3.5%	3.5%	3.6%	3.6%	4.5%	4.6%
% renewable transport fuel (j)	0%	0%	0%	0%	0%	0%	0%	0%	0%
Net transport fuel (EJ/yr) produced from: fossil oil 2020	15.10	15.10	15.10	15.10	15.10	15.10	15.10	15.10	15.10
wood + straw									
straw									
wood									
% renewable gas (i)	6.0%	6.3%	8.0% (l)	5.2%	5.2%	5.4%	5.5%	7.0% (l)	7.6% (l)
Net natural gas (EJ/yr) produced from: fossil gas 2020	24.35	24.27	24.65 / 23.78*	24.55	24.55	24.49	24.48	24.81 / 24.05*	24.87 / 24.01*
wood + straw	1.55	1.63	2.14	1.35	1.35	1.41	1.44	1.85	1.89
straw	0.76	0.79	1.04*	0.76	0.56	0.79	0.60	1.04	0.79
wood	0.79	0.84	1.10*	0.59	0.79	0.62	0.84	0.81	1.10
% renewable electricity (h)	1.1%	1.0%	0.8%	5.7%	5.1%	5.6%	5.1%	5.6%	5.1%
Net electricity (EJ/yr) produced from: coal 2020	3.73	3.75 / 3.73*	3.76 / 3.73*	3.56	3.58	3.57 / 3.56*	3.59 / 3.58*	3.57 / 3.56*	3.60 / 3.58*
wood+straw (cofir+new)	0.04	0.04	0.03	0.21	0.19	0.21	0.19	0.21	0.19
straw (cofiring)	0.02	0.02	< 0.02	0.00	0.19	0.00	0.19	0.00	0.19
wood (cofiring)	0.02	0.02	< 0.02	0.21	0.00	0.21	0.00	0.21	0.00
straw (new plants)	0.00	0.00	0.00	0.00	0.00	0.00	0.00	0.00	0.00
wood (new plants)	0.00	0.00	0.00	0.00	0.00	0.00	0.00	0.00	0.00
Scenario (use of biomass) (%)	x & y ~ 2.4	x & y ~ 2.2	x & y ~ 1.9	x = 26 / y = 0	x = 0 / y = 26	x = 26 / y = 0	x = 0 / y = 26	x = 26 / y = 0	x = 0 / y = 26
Case biofuel plant	bio-100 (a)	bio-grid (b)	NGgrid (c)	bio-100 (a)	bio-100 (a)	bio-grid (b)	bio-grid (b)	NGgrid (c)	NGgrid (c)
Ranking table 8.1	V. Maximum SNG production			VI. Maximum potential CO$_2$ reduction					

(a): "*bio-100*": it refers to the case where the electricity demand of biofuels plants is covered by burning an extra amount of biomass.

(b): "*bio-grid*": it refers to the case where electricity consumed to operate biofuels plants is taken from the national grid.

(c): "*NG-grid*": it refers to the case electricity consumed to operate biofuels plants is taken from the power grid, and the heat demand is covered by burning natural gas.

(d): A1, B1, C1: accounts for the scenarios where the forestry wood left after cofiring is used for biofuels production, but all the straw residues available in Europe.

(e) A2, B2, C2: accounts for the scenarios where all forestry wood is used for biofuels production but only straw left after cofiring can be used for biofuels production.

(f) A3, B3, C3: accounts for the scenarios where no cofiring is planned and, hence, all available forestry wood and straw residues are used in new biofuels or BIGCC plants.

(g): "*x*" and "*y*" represent the forest and straw fraction that is used in cofiring stations. Values are calculated from Eqs.(8-1) to (8-5).

(h): % renewable electricity it is defined in Eq.(8-9) as the ratio of electricity produced from wood and straw divided from 3.5 EJ/yr (i.e., electricity produced from coal without cofiring). Since in I-bio100-A1 and I-bio100-A2 scenarios, total electricity production exceeds 3.77 EJ/yr, Eq.(8-9) is reformulated to include in the denominator the total electricity produced Eqs.(8-10) to (8-11).

$$\% \ renewable \ electricity = \frac{Electricity \ from \ wood \ \& \ straw}{3.77 \ EJ \ / \ yr} \tag{8-9}$$

$$\% \ renewable \ electricity_{I-bio100-A1} = \frac{SNG \ from \ wood \ \& \ straw}{4.5 \ EJ \ / \ yr} \tag{8-10}$$

$$\% \ renewable \ electricity_{I-bio100-A2} = \frac{SNG \ from \ wood \ \& \ straw}{4.3 \ EJ \ / \ yr} \tag{8-11}$$

(i): % renewable gas: it is defined as the ratio of SNG produced from wood and straw divided from 25.9 EJ/yr (i.e., natural gas consumption by 2020).For *NG&grid* cases, natural gas consumption is included in the denominator of Eq.(8-12)

$$\% \ renewable \ gas = \frac{SNG \ from \ wood \ \& \ straw}{25.9 \ EJ \ / \ yr + NG \ consumption} \tag{8-12}$$

(j): % renewable fuel: it is defined as the ratio of FT-fuels produced from wood and straw divided from 15.1 EJ/yr (i.e., transport fuel consumption by 2020)

$$\% \ renewable \ transport \ fuel = \frac{FT_{fuels} \ from \ wood \ \& \ straw}{15.1 \ EJ \ / \ yr} \tag{8-13}$$

(k): % total renewable energy accounts for total energy produce from biomass divided by the sum of fossil coal (i.e., 3.77 EJ/yr), natural gas (i.e., 25.9 EJ/yr) and transport fuels (i.e., 15.1EJ/yr) needed by 2020 (i.e., sum = 44.8 EJ/yr).

$$\% \ total \ renewable \ energy = \frac{Electricity + SNG + FT_{fuels} \ from \ wood \ \& \ straw}{3.77 + 25.9 + 15.1 \ EJ \ / \ yr} \tag{8-14}$$

(l): Renewability share in "*NG&grid*" scenarios is notably larger as the numerator of the Eq. (8-12) is more sensible to an increase of biofuels production than the denominator is sensible to an increase of the fossil natural gas consumption, i.e:

$$\% \ renewable \ gas = \frac{x_{SNG}}{x_{NG} + x_{SNG} + x_{EXTRA \ NG}} = \frac{x_{SNG}}{25.9EJ + x_{EXTRA \ NG}} \tag{8-15}$$

(m): Electricity production from coal and biomass sources is higher than 3.77 EJ/yr (see Table 8-8). This is because coal replacement is limited (i.e., maximum of 10% $^{wt}/_{wt}$) and the rest of biomass is still used to produce electricity in new BIGCC plants. Consequently less natural gas needs to be produced, that will be later used in gas combined cycle plants. Gas power plants are assumed to work at 55% of electricity (Ψ_{el}).

Table 8-8: *Overview of total input, output and overall ratios for all scenarios. In this case, the ratios do not distinguish between renewable and fossil energy.*

Ranking table 8.1	I Maximizing renewable electricity production			II Potential replacement in existing infrastructure				III Maximizing biofuel for transport		IV Maximizing FT-diesel (Oil industry)	
Case biofuel plant	bio-100 (a)	bio-100 (a)	bio-100 (a)	bio-100 (a)	bio-100 (a)	bio-grid (b)	bio-grid (b)	bio-100 (a)	bio-grid (b)	bio-100 (a)	bio-grid (b)
Scenario (use of biomass)	A1 (d) x = 26 y = 0	A2 (e) x = 0 y = 26	A3 (f) x = 0 y = 0	A1 (d) x = 26 y = 0	A2 (e) x = 0 y = 26	B1 (d) x = 26 y = 0	B2 (e) x = 0 y = 26	A3 (f) x = 0 y = 0	B3 (f) x = 0 y = 0	A3 (f) x & y ~ 5.7	B3 (f) x & y ~ 5.7
Total input — wood	1.90	1.90	1.90	1.90	1.90	1.90	1.90	1.90	1.90	1.90	1.90
Total input — straw	1.80	1.80	1.80	1.80	1.80	1.80	1.80	1.80	1.80	1.80	1.80
Total input — coal	7.51	7.51	5.48	8.20	8.58	8.28	8.65	8.34	8.43	8.25	8.34
Total input — fossil gas	30.54	30.91	32.38	32.18	32.17	32.16	32.25	32.21	32.27	32.38	32.38
Total input — fossil oil	18.88	18.88	18.88	17.62	17.59	17.44	17.34	17.37	17.09	17.37	17.09
Total input	60.6	61.0	60.4	61.7	62.0	61.6	61.9	61.6	61.5	61.7	61.5
Output electricity	4.58	4.41	3.77	3.77	3.77	3.77	3.77	3.77	3.77	3.77	3.77
Input for electricity	11.21	11.21	9.08	8.69	9.07	8.77	9.14	8.34	8.43	8.46	8.55
Output/input electricity	40.8%	39.4%	41.1%	43.4%	41.6%	43.0%	41.2%	45.2%	44.7%	44.6%	44.1%
Output NG & SNG	24.44	24.73	25.90	25.90	25.90	25.90	25.90	25.90	25.90	25.90	25.90
Input for NG & SNG	305.4	30.91	32.38	32.51	32.58	32.49	32.42	32.55	32.45	32.38	32.38
Output/input NG & SNG	80.0%	80.0%	80.0%	79.7%	79.5%	79.7%	79.9%	79.6%	79.8%	80.0%	80.0%
Output transport fuel	15.10	15.10	15.10	15.10	15.10	15.10	15.10	15.10	15.10	15.10	15.10
Input for transport fuel	18.88	18.88	18.88	20.49	20.41	20.29	20.41	20.73	20.61	20.86	20.58
Output/input transport fuel	80.0%	80.0%	80.0%	73.7%	74.0%	74.4%	74.0%	72.8%	73.3%	72.4%	73.4%

Table 8-8: *[Continuation] Overview of total input, output & overall ratios for all scenarios.*

Ranking table 8.1		Case biofuel plant	Scenario (use of biomass)		Total input for electricity, SNG and transport fuel production					Total input	Output electricity	Input for electricity	Output/input electricity	Output NG & SNG	Input for NG & SNG	Output/input NG & SNG	Output transport fuel	Input for transport fuel	Output/input transport fuel
					wood	straw	coal	fossil gas	fossil oil										
V	Maximizing SNG production	bio-100	**A3** (f)	x & y ~ 2.4	1.90	1.80	8.30	30.44	18.88	61.3	**3.77**	8.39	44.9%	**25.90**	34.07	76.0%	**15.10**	**18.88**	80.0%
		bio-grid	**B3** (f)	x & y ~ 2.2	1.90	1.80	8.34	30.34	18.88	61.3	**3.77**	8.42	44.8%	**25.90**	33.98	76.2%	**15.10**	**18.88**	80.0%
		NG-grid	**C3** (f)	x & y ~ 1.9	1.90	1.80	8.36	30.81	18.88	61.7	**3.77**	8.43	44.7%	**25.90**	34.46	75.2%	**15.10**	**18.88**	80.0%
VI	Maximizing potential CO₂ reduction	bio-100 (a)	**A1** (d)	x = 26, y = 0	1.90	1.80	8.20	30.69	18.88	61.5	**3.77**	8.69	43.4%	**25.90**	33.89	76.4%	**15.10**	**18.88**	80.0%
			A2 (e)	x = 0, y = 26	1.90	1.80	8.58	30.68	18.88	61.8	**3.77**	9.07	41.6%	**25.90**	33.92	76.4%	**15.10**	**18.88**	80.0%
		bio-grid (b)	**B1** (d)	x = 26, y = 0	1.90	1.80	8.23	30.61	18.88	61.4	**3.77**	8.72	43.2%	**25.90**	33.82	76.6%	**15.10**	**18.88**	80.0%
			B2 (e)	x = 0, y = 26	1.90	1.80	8.61	30.58	18.88	61.8	**3.77**	9.10	41.4%	**25.90**	33.81	76.6%	**15.10**	**18.88**	80.0%
		bio-100 (a)	**C1** (d)	x = 26, y = 0	1.90	1.80	8.24	31.01	18.88	61.8	**3.77**	8.73	43.2%	**25.90**	34.21	75.7%	**15.10**	**18.88**	80.0%
			C2 (e)	x = 0, y = 26	1.90	1.80	8.62	31.04	18.88	62.2	**3.77**	9.11	41.4%	**25.90**	34.27	75.6%	**15.10**	**18.88**	80.0%

8.10.2.   *Potential biofuel use in the European fleet by 2020.*

Although electricity and natural gas have other applications than road transport, in this section, we intend to calculate how many cars could be fuelled in case of using all the bioenergy produced from forest and straw residues. For that calculation, car consumption values for year 2020 (i.e, $MJ_{fuel\ consumed}$/km) have been taken from Weiss et al [112], and assuming that a passenger cars drives on average 20,000 km per year.
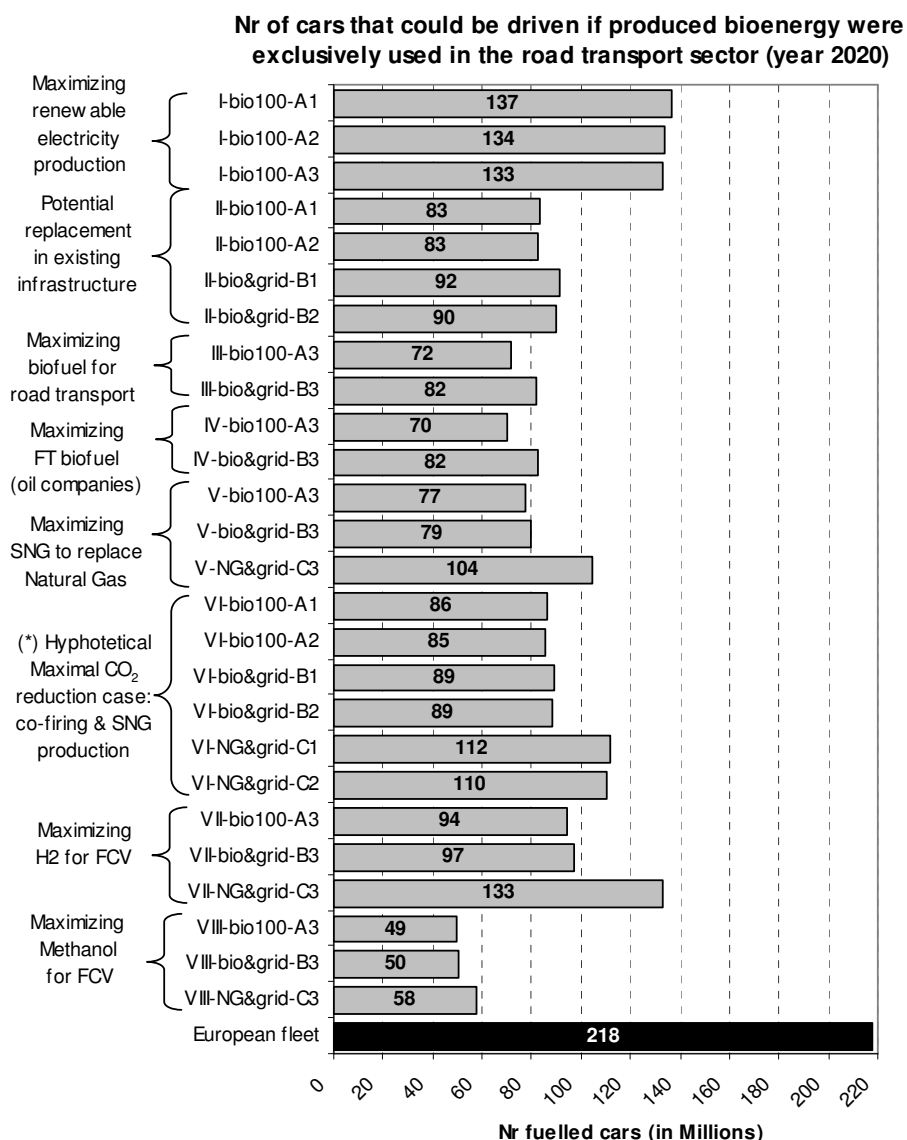

Figure 8.25: *Comparison of number of cars that could be driven if all produced bioenergy (i.e., electricity and biofuels from biomass) were used for the road transport sector. Values are given in million cars.*

The set of equations (8-16) to (8-20) are used for this calculation. Hydrogen and methanol are used in fuel cell vehicles (FCV), SNG and Fischer-Tropsch are fuelled in advanced internal combustion engines (ICE), whereas electricity drives battery electric vehicles (BEV).

$$BEV\ cars = Nr.plants \cdot \frac{113\ MJ/s}{1\ plant} \cdot \frac{3600s}{1\ hr} \cdot \frac{8000\ hr}{1\ yr} \cdot \frac{1\ yr \cdot 1\ car}{20,000\ km} \cdot \frac{1\ km}{0.51\ MJ} \qquad (8\text{-}16)$$

$$ICE_{FT}\ cars = Nr.plants \cdot \frac{1000\ MJ/s}{1\ plant} \cdot \frac{3600s}{1\ hr} \cdot \frac{8000\ hr}{1\ yr} \cdot \frac{1\ yr \cdot 1\ car}{20,000\ km} \cdot \frac{1\ km}{0.92\ MJ} \qquad (8\text{-}17)$$

$$ICE_{SNG}\ cars = Nr.plants \cdot \frac{200\ MJ/s}{1\ plant} \cdot \frac{3600s}{1\ hr} \cdot \frac{8000\ hr}{1\ yr} \cdot \frac{1\ yr \cdot 1\ car}{20,000\ km} \cdot \frac{1\ km}{1.03\ MJ} \qquad (8\text{-}18)$$

$$FCV_{Methanol}\ cars = Nr.plants \cdot \frac{1000\ MJ/s}{1\ plant} \cdot \frac{3600s}{1\ hr} \cdot \frac{8000\ hr}{1\ yr} \cdot \frac{1\ yr \cdot 1\ car}{20,000\ km} \cdot \frac{1\ km}{1.33\ MJ} \qquad (8\text{-}19)$$

$$FCV_{H2}\ cars = Nr.plants \cdot \frac{500\ MJ/s}{1\ plant} \cdot \frac{3600s}{1\ hr} \cdot \frac{8000\ hr}{1\ yr} \cdot \frac{1\ yr \cdot 1\ car}{20,000\ km} \cdot \frac{1\ km}{0.81\ MJ} \qquad (8\text{-}20)$$

According to the Figure 8.25, electricity is the favored biofuel for the road transport by year 2020, as up to 137 million cars could be driven (i.e., more than 50% of the actual European fleet could run on bioelectricity). This observation was somehow expected as not only is electricity rather effectively produced, but also BEV vehicles run on less fuel (i.e., 0.51 MJ/km [112]). However, the electricity option means that electric cars should be ready by 2020 at a competitive price for the final user. Moreover, the grid infrastructure should also be further developed to absorb the electricity production and distribution to the final charging points. Hydrogen is the second best alternative as 94 to 133 million cars could be fueled, whereas SNG and Fischer-Tropsch are in the intermediate range. However, hydrogen implementation is still predicted for a long-term future as the hydrogen distribution system for large capacities is not well defined yet, and hydrogen-fuelled FCV are still under development. SNG faces similar problems for its distribution, although the European natural gas pipeline is more developed than the hydrogen pipeline. An added advantage is that there are already commercial vehicles that fully run on compressed natural gas, especially in countries such as Argentina, Brazil or Italy. Conversely, Fischer-Tropsch cars could benefit from the existing distribution infrastructure, as well as actual cars without any modification in the engine. Methanol is the worst option as only 49 to 58 millions cars could be fuelled. Moreover, methanol-fuelled FCV are the least developed and major concerns are derived from the low autonomy of these cars. An alternative would be to blend methanol in actual ICE cars.

8.10.3. CO_2 Emissions and Savings

In Table 8-7, it has been observed that the share of produced bioenergy was the largest in the *VI-NG&grid-C1/C2* and *V-NG&grid-C3* scenarios that involved major SNG production, whereas the electricity options *I-bio100-A1/A2/A3* were some of the least renewable. This conclusion is here confronted by calculating CO_2 emissions of each scenario and comparing them with the corresponding emissions of a reference fossil scenario in which no bioenergy is produced (i.e., production **3.77 EJ/yr** of electricity from coal, **25.9 EJ/yr** of natural gas and **15.1 EJ/yr** of fossil fuel for road transport). Analogous to Chapter 5, an LCA is applied to calculate all the emissions from "cradle-to-grave". Figure 8.26 identifies the main stages of the LCA together with the points were CO_2 emissions are produced.
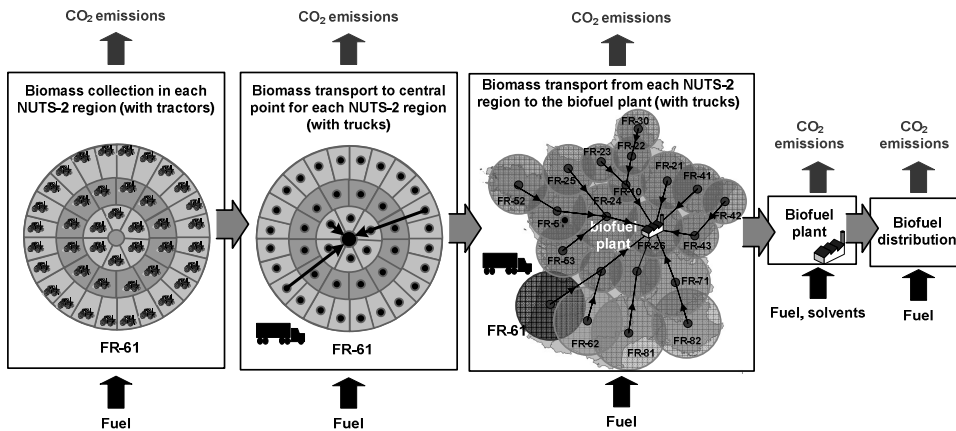
Figure 8.26:Identification of CO_2 emissions in all stages of the LCA analysis. Calculations are done at NUTS-2 level. The French FR-61 region and France are used as an example. Biomass is firstly collected in all European NUTS-2 regions, then transported to a central point of the same region and finally transported to the biofuel plant, located in other nearby region.

In our model, biomass of each European NUTS-2 region (see Figure 2.3 and Figure 2.5) is firstly collected by means of tractors or similar devices from forests. Each region (e.g., French FR-61 in Figure 8.26) is modeled as a concentric circle divided by multiples of six. This division assures that each tractor always covers the same area, i.e., 28 km^2, which can be easily done in one-year time (see Chapter 5 for calculations). Biomass is then transported to a central point (i.e., R=0) of the same region by means of trucks, whose capacity is different for wood and straw (see Appendix A). This central gathering point is somehow similar to the function of forestry Associations in many NUTS-2 regions (e.g., Catalonia ES-51). These first two stages are equal for all the scenarios in Table 8-7, as irrespective of the final biofuel, biomass has to be always collected and gathered to a central location. In the third stage, collected biomass is send to the different biofuels plants. The destination of biomass is made on minimizing the transport distance and to achieve the needed volume to operate biofuels plants at optimal scales. Total radius of each NUTS-2 region is taken as transport distance, as shown in Figure 8.26. Finally, extra CO_2 emissions originate during biofuel conversion processes and their final distribution to the dispensing fuelling stations. Distribution distances and energy consumption is

detailed in subchapter 3.5. Results for each scenario are summarized in Figure 8.27, where dashed bars represents the "*CO₂ emissions from fossil fuels*". Those emissions are originated during the production, transport and consumption of fossil fuels, and they are needed to cover European energy requirements (i.e., 3.77 EJ/yr of coal-based electricity, 25.9 EJ/yr of natural gas and 15.1 EJ/yr of road fuels). Biofuels and bio-electricity partly substitutes those fossil fuels, thus diminishing CO_2 emissions (i.e., dark grey bars in Figure 8.27). However, bioenergy production is not CO_2 "neutral" as few fossil fuels are still consumed for biomass collection and transport, biofuels production and distribution. These emissions are labeled as "*CO₂ emissions from bioenergy*" and represented by light grey bars in Figure 8.27.
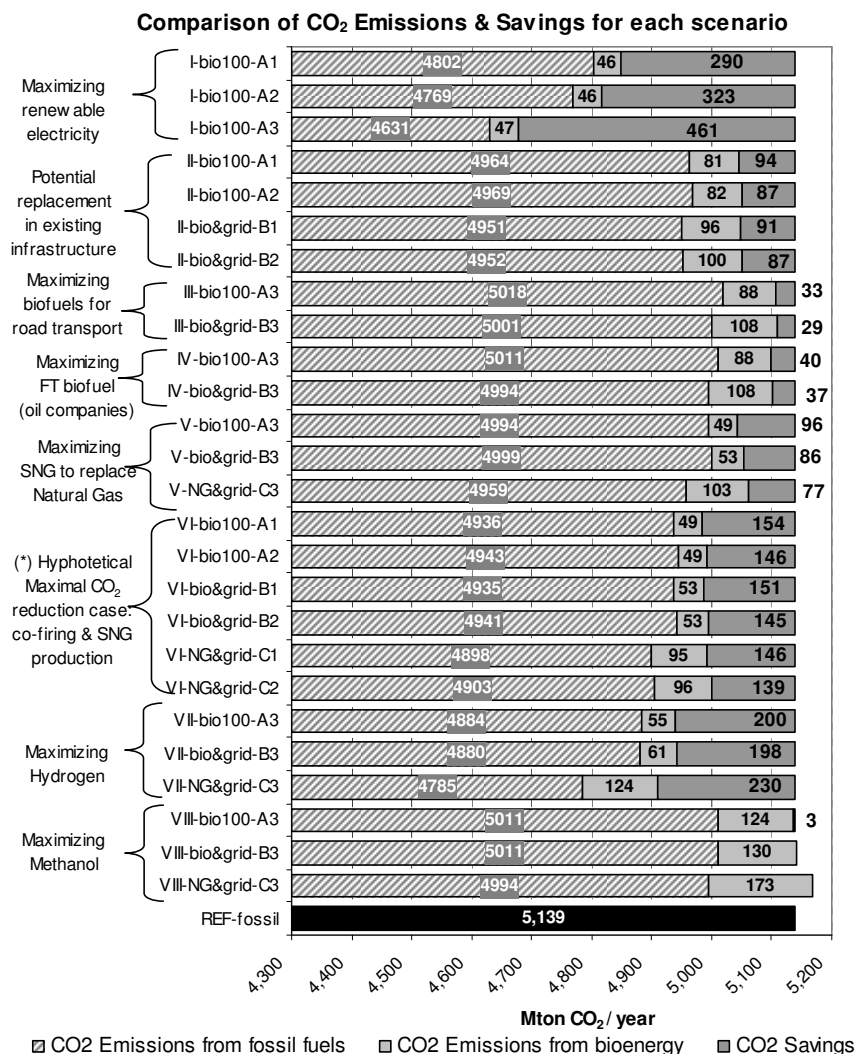
Figure 8.27: *CO₂ emissions from fossil fuels consumption (dashed bars) and from bioenergy production (light grey bars), CO₂ and savings (dark grey bar) for each scenario of Table 8-7. CO₂ savings are calculated as the difference between the fossil reference case (i.e., 5139 Mtn CO₂/yr) and the CO₂ emissions of each scenario. CO₂ emissions of the bioenergy systems originate from the consumption of fossil energy (see Chapter 5).*

Finally, emissions of the reference fossil scenario of Table 8-6 (i.e., **5139 Mtn CO_2/yr**) are indicated by a black bar in the same figure. All LCA equations are detailed in Chapter 5. As observed, contrary to the results from Table 8-7, maximizing renewable energy (i.e., ***I-bio100-A1/A2/A3***) turns out to be the best alternative in terms of CO_2 savings. In particular, the ***I-bio100-A3*** scenario, in which biomass was entirely fed in new bio-based BIGCC plants, lead to the maximal CO_2 reduction (i.e., **461 Mtn CO_2/yr**). In effect, this scenario is the one that needs less coal (i.e., **5.48 EJ/yr**) to fulfill energy production targets (see Table 8-8). Reducing coal consumption has a greater influence on CO_2 emissions as its global warming effect is notably larger than most of the fossil fuels. When cofiring is combined with new bio-based BIGCC plants, CO_2 savings are rather similar (i.e., **290 and 323 Mtn CO_2/yr** when cofiring either wood or straw respectively). Although both cofiring options ***I-bio100-A1/A2*** results in less CO_2 reduction that the fully bio-based BIGCC alternative ***I-bio100-A3***, the required investment is far lower and, thus, cofiring becomes more realistic.

The second best alternative accounts for prioritizing cofiring and using the remaining of biomass to built new bio-based SNG plants (i.e., ***VI-bio100-A1*** to ***VI-NG&grid100-C2***). In this case, CO_2 savings are in the range of **139-154 Mtn CO_2/yr**, being ***VI-bio100-A1*** the leading alternative within the "***VI***" group. Maximizing SNG production (i.e., "***V***" group) results in worse values than the former mentioned combination of cofiring/SNG (i.e., "***VI***" group). This observation can also be extended to those scenarios involving Fischer-Tropsch production (i.e., "***II***", "***III***" and "***IV***" groups). In effect, larger CO_2 savings (i.e., **87-94 Mtn CO_2/yr**) are obtained in the "***II***" scenario, where more cofiring is envisaged (i.e., 10wt% coal replacement).

Hydrogen and methanol scenarios (i.e., ***VII*** and ***VIII*** respectively) are compared separately as their use needs further development of actual fuel cell cars. In order to estimate the corresponding CO_2 savings, we assume that, by 2020, part of the fossil diesel could be substituted by either hydrogen or methanol, although fuel consumption is different (i.e., 0.51 and 1.33 MJ/km for hydrogen and methanol FCV respectively, whereas 0.92 MJ/km for advanced diesel ICE cars). It is observed that introducing hydrogen-fuelled FCV has a considerable CO_2 reduction potential (i.e., 198-230 Mtn CO_2/year). In effect, although hydrogen production does not differ significantly from the rest of the biofuels, fuel car consumption is notably lower than in conventional ICE cars and, thus, more fossil diesel can be proportionally substituted. Conversely, the picture for methanol-powered FCV is completely different due to the low efficiency of those cars. Hence, CO_2 emissions are almost negligible for the "***VIII-bio100-A3***" case (i.e., 3 Mtn CO_2/year), whereas for the last two cases "***VIII-bio&grid-B3***" and "***VIII-NG&grid-C3***" they are even negative.

In general, although less bioenergy is produced in all "*bio-100*" cases (see Table 8-7), global CO_2 savings are larger. This could be explained by the fact that, in the "*bio-100*" configurations, the biofuel conversion plants do not consume fossil fuel to cover the energy demand of the process, as an extra biomass amount is used instead. In effect, CO_2 minimization during biofuels production can offset the extra emissions originated in transporting a larger amount of biomass to the conversion plant. Conversely, the "*NG-grid*" cases turns out to be less favorable, although the share of

renewable energy was the highest in Table 8-7. For a better understanding, Figure 8.28 gives the contribution of each stage on the total CO_2 compute. As observed, one of the main problems of Fischer-Tropsch and methanol production is that biofuel distribution is made by trucks that consume fossil diesel. Therefore, CO_2 emissions are notably larger than for other gaseous biofuels and/or bioelectricity.

Contribution of each stage on total CO_2 emissions, which come from fossil fuel consumption

Category	Case	Value
Maximizing renewable electricity production	I-bio100-A1	97%
	I-bio100-A2	97%
	I-bio100-A3	97%
Potential replacement in existing infrastructure	II-bio100-A1	55%
	II-bio100-A2	55%
	II-bio&grid-A1	47%
	II-bio&grid-A2	45%
Maximizing biofuel for road transport	III-bio100-A3	51%
	III-bio100-B3	42%
Maximizing FT biofuel (oil companies)	IV-bio100-A3	51%
	IV-bio&grid-B3	42%
Maximizing SNG to replace Natural Gas	V-bio100-A3	91%
	V-bio&grid-B3	85%
	V-NG&grid-C3	44%
(*) Hyphotetical Maximal CO_2 reduction case: co-firing & SNG production	VI-bio100-A1	91%
	VI-bio100-A2	91%
	VI-bio&grid-B1	86%
	VI-bio&grid-B2	85%
	VI-NG&grid-C1	48%
	VI-NG&grid-C2	47%
Maximizing Hydrogen	VII-bio100-A3	82%
	VII-bio&grid-B3	74%
	VII-NG&grid-C3	36%
Maximizing Methanol	VIII-bio100-A3	36%
	VIII-bio&grid-B3	35%
	VIII-NG&grid-C3	26%

☐ Biomass collection & pre-transport   ■ Transport to biofuel plant
▨ Biofuels production   ⊠ Biofuels distribution

Figure 8.28: *Contribution of each stage in total fossil CO_2 emissions. In order to know exact CO_2 emissions from each stage, percentage values have to be multiplied by "CO_2 emissions from bioenergy" of Figure 8.27 (i.e., light grey bars).*

8.10.4.   Economic implications

From an economic point of view, it is important to firstly know the required investment for each alternative, and whether this investment could be covered by private, public capital, and/or bank credits. Following Figure 8.29 summarizes the total investment that would be needed for each alternative in order to achieve the bioenergy production targets previously established in Table 8-7.

Required TCI (Total Capital Investment) per scenario
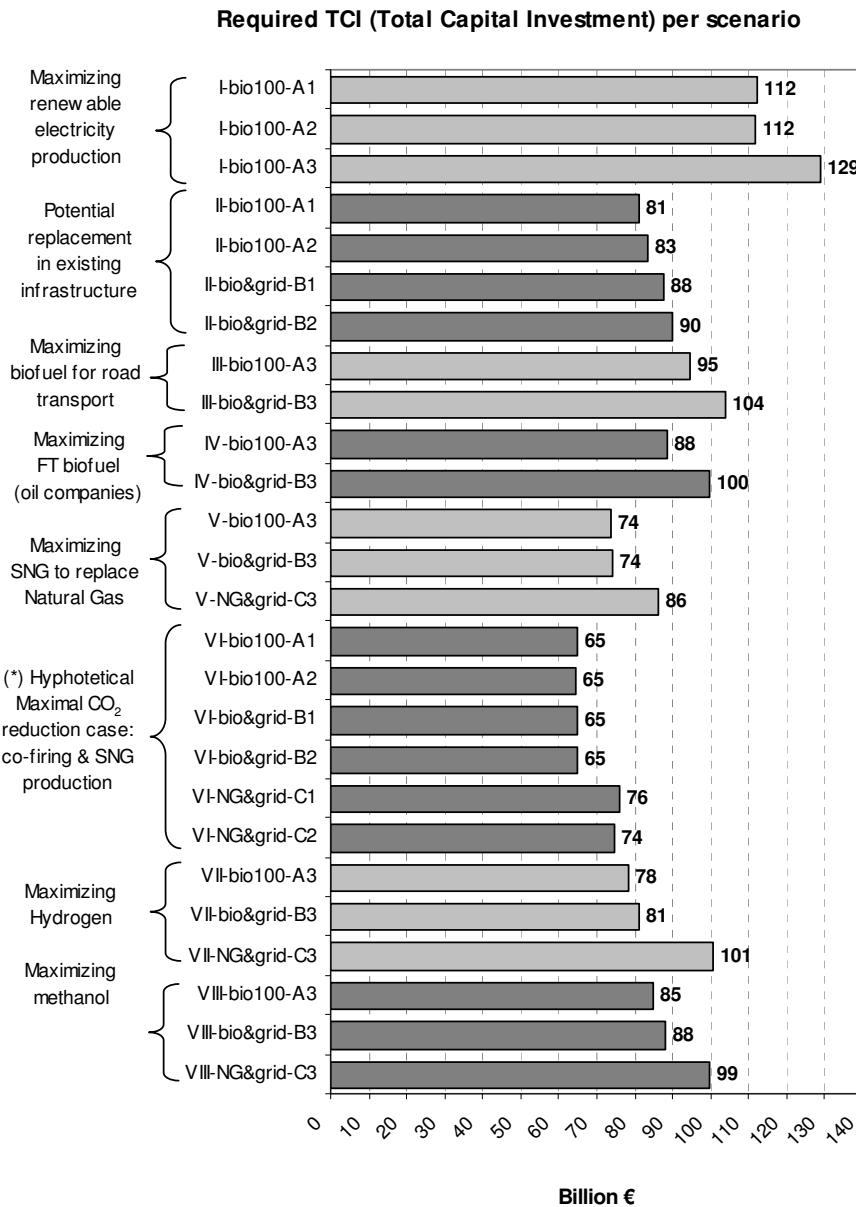
Figure 8.29: *Required TCI (Total Capital Investment) for each scenario. TCI of existing coal-based power plants is not included.*

As observed, the third "*I*" case (which aims to maximize renewable electricity production) accounts for the largest TCI. In effect, although individual TCI for BIGCC power generation plants is far lower than for the rest of the biofuels (see Chapter 6), in this case the number of plants that can be built is larger than for other biofuels (with exception of some SNG cases) and thus, total TCI is the largest. Apart from this TCI, an investment should be added for biofuels distribution. This parameter is especially sensible for the hydrogen case as existing pipelines should be enlarged to accommodate bio-based hydrogen production. Own rough estimates lead to 15.6-20.5 Billion €$_{2020}$ investment for the EU-pipeline. Moreover, filling stations have also to be incorporated in the European map, which accounts for extra 26 Billion €$_{2020}$ [174]. Hydrogen FCV price difference with regard to conventional cars would add an extra 0.2-0.3 Billion €$_{2020}$. Same calculations should be done for the rest of the biofuels, although hydrogen distribution turns out to be always the most expensive system. Conversely, Fischer-Tropsch and electricity could benefit form the existing infrastructure with minor investments. Knowing the TCI for each alternative does not, however, determine the best option as other costs are associated to biofuels production and distribution. Hence, another important economic measure is to determine the final biofuel price that would be paid by the user and compare it with the price of conventional fossil fuels. Nowadays, biofuels prices are still higher than fossil prices and, hence, one question immediately arises: ***who should paid the difference?*** Some experts claim to charge that difference on the surplus of CO_2 emissions of conventional fossil fuels, whereas others manifest that governments should motivate biofuels development by the introduction of subsidies. In section 6.4, we proposed a new taxation system to assure actual revenues from fuel's taxation while equalizing biofuels and fossil fuels prices. Additionally, in section 6.5, ecocosts were suggested to be added on top op taxed fuel's prices to penalize CO_2 emissions. Both systems are applied in this chapter.
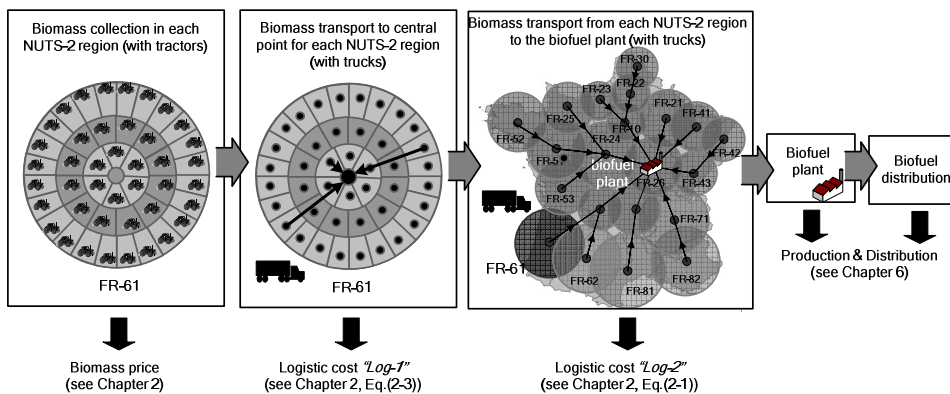
Figure 8.30: *Identification of all costs for the calculation of the final biofuel price.*

Several concepts have to be included for the calculation of the final biofuel price, as shown in Figure 8.30. Similarly to the LCA analysis, all stages are analyzed to include all the costs that would determine the final price. Biomass price has been discussed already in Chapter 2 (see Figure 2.8), whereas production and distribution costs have been presented by each country and at different plant scales in Chapter 6 (see Table 0-14 and Table 0-15 in Appendix J.5 for production costs and Table 6-3

for distribution costs). Logistics costs consist of two items: biomass transport to a central location in the NUTS-2 region and transport to the biofuels production plants. Both concepts are calculated by Eqs.(2-3) and (2-1) respectively. The first term of logistic costs "*Log-1*" is equal for each scenario as all biomass needs to be collected, whereas the second term "*Log-2*" is dependent on each scenario (see Appendix L).

Table 8-9: *Final average biofuel and fossil fuels prices for each scenario of Table 8-7. These values correspond to the application of a new taxation system (of section 6.4) and ecocosts (of section 6.5). Exact values for each are enclosed in Appendix L, Table 0-20 to Table 0-25.*

Prices given in €/GJ$_{fuel}$ Scenario ↓	Fuels prices including new taxation (see section 6.4)			Fuels prices including new taxation & ecocosts [b] (see section 6.5)		
	$\alpha_{FTfuels}$ (1+TB)	α_{SNG} (1+TB)	$\alpha_{bioelec}$ (1+TB)	$\alpha_{FTfuels}$ (1+TB) + α_{CO2}	α_{SNG} (1+TB) + α_{CO2}	$\alpha_{bioelec}$ (1+TB) + α_{CO2}
Fossil scenario, λ=0 (see Table 8-6)	30,4[a]	8,5[a]	27,6[a]	31,7[a]	9,7[a]	32,9[a]
I-bio100-A1	30,4[a]	8,5[a]	30,9	31,7[a]	9,7[a]	34,7
I-bio100-A2	30,4[a]	8,5[a]	31,0	31,7[a]	9,7[a]	34,8
I-bio100-A3	30,4[a]	8,5[a]	30,9	31,7[a]	9,7[a]	34,7
II-bio100-A1	32,5	8,6	27,7	33,7	9,8	32,7
II-bio100-A2	32,6	8,6	27,7	33,8	9,8	32,8
II-bio&grid-B1	32,7	8,6	27,7	33,9	9,8	32,8
II-bio&grid-B2	32,8	8,6	27,7	34,0	9,8	32,8
III-bio100-A3	32,8	8,6	27,7	34,0	9,8	33,0
III-bio&grid-B3	33,0	8,6	27,7	34,2	9,8	33,0
IV-bio100-A3	32,8	8,5[a]	27,7	34,0	9,7[a]	32,9
IV-bio&grid-B3	33,0	8,5[a]	27,7	34,2	9,7[a]	32,9
V-bio100-A3	30,4[a]	9,5	27,7	31,7[a]	10,7	33,0
V-bio&grid-B3	30,4[a]	9,6	27,7	31,7[a]	10,7	32,9
V-NG&grid-C3	30,4[a]	10,0	27,7	31,7[a]	11,1	33,0
VI-bio100-A1	30,4[a]	9,2	27,7	31,7[a]	10,4	32,8
VI-bio100-A2	30,4[a]	9,2	27,7	31,7[a]	10,3	32,8
VI-bio&grid-B1	30,4[a]	9,2	27,7	31,7[a]	10,3	32,8
VI-bio&grid-B2	30,4[a]	9,2	27,7	31,7[a]	10,4	32,8
VI-NG&grid-C1	30,4[a]	9,5	27,7	31,7[a]	10,6	32,8
VI-NG&grid-C2	30,4[a]	9,5	27,7	31,7[a]	10,6	32,8
VII-bio100-A3	33,3	8,5[a]	27,7	34,4	9,7[a]	32,9
VII-bio&grid-B3	33,4	8,5[a]	27,7	34,5	9,7[a]	32,9
VII-NG&grid-C3	34,2	8,5[a]	27,7	35,4	9,7[a]	32,9
VIII-bio100-A3	32,8	8,5[a]	27,7	34,0	9,7[a]	32,9
VIII-bio&grid-B3	32,9	8,5[a]	27,7	34,1	9,7[a]	32,9
VIII-NG&grid-C3	33,5	8,5[a]	27,7	34,7	9,7[a]	32,9

(a): In those cases, there is no biofuel/bioelectricity production and, thus, average fuel prices are equal to the ones of the reference 'fossil' scenario (see Table 8-6).

(b): The ecotax value ($\gamma_{eco,CO2}$) is fixed to 13.5 €/ton CO_2 (see Eq.(6-4) in section 6.5).
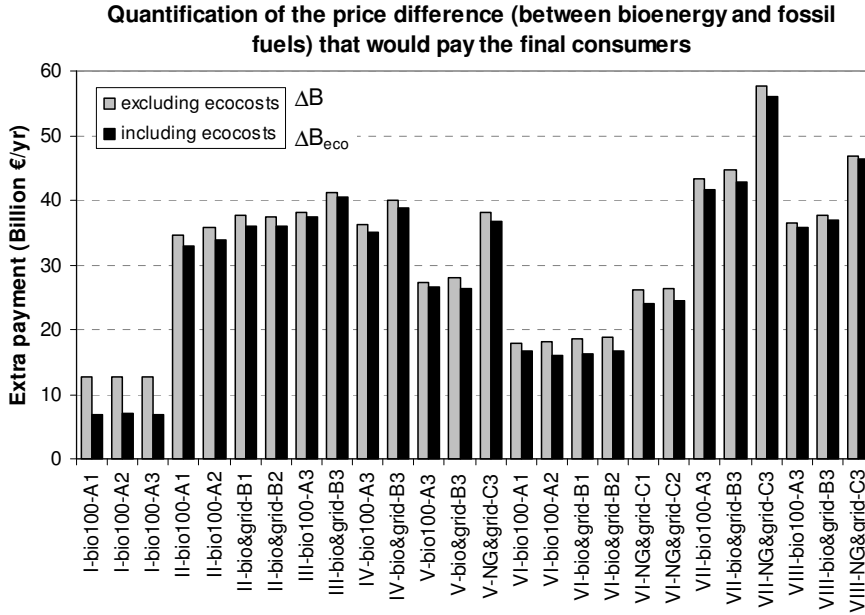
Figure 8.31: *Comparison of annual extra payment that would have to pay final users in EU due to differences of biofuel/fossil fuels mixtures and the reference fossil case. Grey bars refers to fuels prices including new taxes (i.e., $\alpha_{biofuel}(1+TB)$), whereas black bars also include ecocosts ($\alpha_{biofuel}(1+TB)+ \alpha_{CO2}$).*

Final average EU fuel prices (including new taxes and ecocosts) are summarized in Table 8-9. Corresponding values per country can be found in Appendix L (see Table 0-20 to Table 0-25). As observed in Table 8-9, average electricity price is notably higher in the first three "*I*" scenarios in which biomass is completely used to maximize renewable electricity production. In effect, bio-based electricity generation, especially when produced in new BIGCC plants, is more expensive than conventional coal power production. Conversely, electricity prices differences of cofiring plants are more moderate. The annual extra payment across Europe for the '*I*' scenario accounts for ~12.6 Billion € (as shown by grey bars in Figure 8.31), or ~ 6.8 Billion € in case of incorporating ecocosts (see black bars in same Figure 8.31). This extra payment (ΔB_i) is calculated as the difference of biofuel/fossil mixtures prices minus the reference 'fossil' scenario of Table 8-6, as done in the sets of Eqs.(8-21) to (8-26). When including ecocosts, the annual extra payment (ΔB_{eco}) is lowered because the reference fossil scenario is notably penalized for its higher CO_2 emissions.

- Annual payment (reference fossil scenario, λ=0):

$$B_{fossil} = \alpha_{coal-elec} \cdot \left(1+TD_{ce}\right)\cdot 3.77 + \tag{8-21}$$
$$\alpha_{fossil-diesel} \cdot \left(1+TD_{fd}\right)\cdot 15.1 + \alpha_{fossil-gas} \cdot \left(1+TD_{fg}\right)\cdot 25.9$$

- Scenarios of Table 8-1 (bioenergy/fossil mix, λ>0):

$$B_{bioenergy} = \alpha_{bioelec} \cdot (1 + TB_{be}) \cdot 3.77 +$$
$$\alpha_{FTfuels} \cdot (1 + TB_{FT}) \cdot 15.1 + \alpha_{SNG} \cdot (1 + TB_{SNG}) \cdot 25.9 \tag{8-22}$$

- Annual EU extra payment (grey bars in Figure 8.31):

$$\Delta B = (\alpha_{bioelec} \cdot (1 + TB_{be}) - \alpha_{coal-elec} \cdot (1 + TD_{ce})) \cdot 3.77 +$$
$$(\alpha_{FTfuels} \cdot (1 + TB_{FT}) - \alpha_{fossil-diesel} \cdot (1 + TD_{fd})) \cdot 15.1 + \tag{8-23}$$
$$(\alpha_{SNG} \cdot (1 + TB_{SNG}) - \alpha_{fossil-gas} \cdot (1 + TD_{fg})) \cdot 25.9$$

- Annual payment (reference fossil scenario, λ =0) including ecocosts:

$$B_{fossil,eco} = (\alpha_{coal-elec} \cdot (1 + TD_{ce}) + \alpha_{CO2,ce}) \cdot 3.77 +$$
$$(\alpha_{fossil-diesel} \cdot (1 + TD_{fd}) + \alpha_{CO2,fd}) \cdot 15.1 + \tag{8-24}$$
$$(\alpha_{fossil-gas} \cdot (1 + TD_{fg}) + \alpha_{CO2,fg}) \cdot 25.9$$

- Scenarios of Table 8-1 (bioenergy/fossil mix, λ>0) including ecocosts:

$$B_{bioenergy} = (\alpha_{bioelec} \cdot (1 + TB_{be}) + \alpha_{CO2,be}) \cdot 3.77 +$$
$$(\alpha_{FTfuels} \cdot (1 + TB_{FT}) + \alpha_{CO2,FT}) \cdot 15.1 + \tag{8-25}$$
$$(\alpha_{SNG} \cdot (1 + TB_{SNG}) + \alpha_{CO2,SNG}) \cdot 25.9$$

- Annual EU extra payment (black bars in Figure 8.31) including ecocosts:

$$\Delta B_{eco} = (\alpha_{bioelec} \cdot (1 + TB_{be}) + \alpha_{CO2,be} - \alpha_{coal-elec} \cdot (1 + TD_{ce}) - \alpha_{CO2,ce}) \cdot 3.77 +$$
$$(\alpha_{FTfuels} \cdot (1 + TB_{FT}) + \alpha_{CO2,FT} - \alpha_{fossil-diesel} \cdot (1 + TD_{fd}) - \alpha_{CO2,fd}) \cdot 15.1 + \tag{8-26}$$
$$(\alpha_{SNG} \cdot (1 + TB_{SNG}) + \alpha_{CO2,SNG} - \alpha_{fossil-gas} \cdot (1 + TD_{fg}) - \alpha_{CO2,fg}) \cdot 25.9$$

Analogous to bioelectricity cases, average natural gas prices are gradually higher when more bio-based SNG is introduced in the gas mix (see Table 8-9, scenarios "*V*" and "*VI*"). This observation is especially sensible for the "*NG&grid*" scenarios as more SNG is produced and its price is, in some countries, up to 2-fold more expensive than fossil natural gas (see Figure 6.9 and Figure 6.10 in Chapter 6). Natural gas and SNG prices difference (*ΔB*) represents about 17.9 to 38.2 Billion € per year, and 15.9 to 36.8 Billion € per year when ecocosts are charged (*ΔB_eco*). Moreover, prioritizing cofiring over extra SNG production is a better solution (i.e., "*VI*" scenario) than maximizing SNG (i.e., "*V*" scenario). In any case, extra payments are always larger for "*IV*" and "*V*" scenarios than for the "*I*" scenario in which bioelectricity is maximized.

Average road fuel prices in Table 8-9 are again higher for those cases where more biofuel is produced, i.e., "*II*" and "*III*" scenarios for Fischer-Tropsch, "*VII*" for hydrogen, and "*VIII*" for methanol production. Fuel prices for Fischer-Tropsch (i.e., $\alpha_{biofuel}(1+TB)$) are slightly lower than methanol and/or hydrogen options (see Table 8-9). However, the difference is reduced when ecocosts are charged ($\alpha_{biofuel}(1+TB) + \alpha_{CO2}$) as Fischer-Tropsch emits more CO_2 than hydrogen. Annual extra payment for road biofuel/fossil mixtures are notably larger than for the SNG alternatives "*IV*" and "*V*" or the bioelectricity "*I*" scenario.

8.10.5. *Comparison with EU Energy Policy and previous studies*

There are some Directives regarding renewable energy production and, hence, fossil fuel replacement within the European Union. The most recent Directive 2009/28/EC repeals previous Directives 2001/77/EC and 2003/30/EC. This new Directive reaffirms a mandatory target of 10% biofuel share in transport by 2020, although it does not specify whether this target has to be achieved by 1st or 2nd generation fuels or a combination of both. Nevertheless, the Directive 2009/28/EC underlines that this target could be achieved upon the introduction and commercialization of 2nd generation biofuels, similar to what we propose in this chapter.

Following our results, maximum biofuels replacement (i.e., 9.5% in Table 8-7) is achieved in "***III-bio&grid-B3***" and "***IV-bio&grid-B3***" scenarios in which all biomass is used to produce Fischer-Tropsch fuels. However, it should be mentioned that the value of 9.5% can only be fulfilled if all available forest and straw residues (i.e., 1.9 and 1.8 EJ/yr) can be purchased. In effect, this assumption is overly optimistic as 61% of the EU-25 available biomass is owned by more than 8.6 million private holdings, whereas the remaining 39% of forestry sources is owned by ~100,000 public holdings (see subchapter 2.4.1). Moreover the value of 9.5% excludes attaining other bioenergy targets (e.g., production of bio-power in order to contribute to the target of 22.1% of renewable electricity, as stated in the White Paper 1997). Consequently, the 10% biofuels share target requires the introduction of energy crops in the bioenergy balance. Another major question arise: ***Is there enough available land to grow energy crops***? The answer is somehow difficult as the predicted energy crops availability is rather inconsistent among studies, which values are found in the range of 0.8 to 12.0 EJ/yr (see Table 2-1). Table 8-10 presents a rough estimation of the percentage of European land area that will be needed to fulfill the 10% biofuels share target for different levels of forestry and straw purchase. For our calculations, we have assumed that rapeseed would be grown as energy crops for 1st generation biodiesel production, which together with Fischer-Tropsch fuels from forest and straw will lead to the 10% biofuels target.

Table 8-10: *Required EU-land as a function of forestry and straw biomass that can be bought for the production of Fischer-Tropsch fuels. Biodiesel from rapeseed is calculated in order to achieve the 10% biofuels share target difference in transport (Directive 2009/28/EC).*

Purchased forest wood & straw	Biofuels replacement by FT	Remaining biofuel target	Rapeseed needed (EJ)	Biodiesel produced (EJ)[(a)]	Required EU-land (km²)[(b)]	Required EU-land (%)
100%	9.5%	0.5%	0.15	0.08	19,995	0.5%
50%	4.8%	5.3%	1.52	0.79	209,945[(c)]	4.9%
20%	1.9%	8.1%	2.35	1.22	323,916[(c)]	7.5%
10%	1.0%	9.1%	2.63	1.37	361,906[(c)]	8.4%
5%	0.5%	9.5%	2.77	1.44	380,901[(c)]	8.8%

(a): About 0.520 MJ$_{diesel}$ is produced per 1 MJ of rapeseed.
(b): Crop yield of rapeseed plantation is ~ 3.09 tn/ha.
(c): Values exceeding the '*Blair House Agreement*' (BHA) of 1992 [176].

Another study published by the '*Biofuels Research Advisory Council*' (BIOFRAC) [177] is even more positive than the Directive 2009/28/EC as it claims that biofuel production from biomass can meet up to 25% of the EU's automotive fuel needs. This

prediction is translated in that 14.3-22.7% of European land should be dedicated to biodiesel production for a forestry and straw biomass purchase viability in the range of 5-100% (see subsequent Table 8-11). It should be noticed, however, that certain values of Table 8-10 and Table 8-11 exceed the limitations of the '*Blair House Agreement*' (BHA) of 1992 [176]. In effect, the BHA restricts the maximum EU oilseeds area for food use to ~ 5 Million ha. This agreement also limits the amount of rapeseed that could be produced as a byproduct from industrial oilseed crops (i.e., rapeseed, sunflower and/or soybeans) grown on set-aside land to the equivalent of 1 Mtn of soy meal per year. This value equals approximately 900,000 ha of oilseed production across the EU [174]. Hence, biodiesel production should be accompanied with bioethanol generation from other feedstock, like proposed lignocellulosic crops.

Table 8-11: Required EU-land as a function of forestry and straw biomass that can be bought for the production of Fischer-Tropsch fuels. Biodiesel from rapeseed is calculated in order to achieve the 25% biofuels share target difference in transport [177].

Purchased forest wood & straw	Biofuels replacement by FT	Remaining biofuel target	Rapeseed needed (EJ)	Biodiesel produced (EJ)[a]	Required EU-land (km^2)[b]	Required EU-land (%)
100%	9.5%	15.5%	4.50	2.34	619,839[c]	14.3%
50%	4.8%	20.3%	5.88	3.06	809,790[c]	18.7%
20%	1.9%	23.1%	6.71	3.49	923,760[c]	21.4%
10%	1.0%	24.1%	6.98	3.63	961,750[c]	22.2%
5%	0.5%	24.5%	7.12	3.70	980,745[c]	22.7%

(a): About 0.520 MJ$_{diesel}$ is produced per 1 MJ of rapeseed.
(b): Crop yield of rapeseed plantation is ~ 3.09 tn/ha.
(c): Values exceeding the '*Blair House Agreement'* (BHA) of 1992 [176].

For a complete overview, Figure 8.32 indicates those European countries that could achieve their national biofuels targets depending only in Fischer-Tropsch production from forest and straw (i.e., "*IV-bio&grid-B3*" scenario). Values are compared with the Commission targets of 5.75 % and 10% biofuels share by year 2005 and 2010 respectively. Moreover, this comparison also includes the most optimistic estimation from BIOFRAC (i.e., 25% biofuels replacement by 2020). As observed, about half of countries are available to fulfill 2010 targets without the need of growing energy crops, whereas the 25% biofuels replacement is exclusive of 5 countries.

As aforementioned, SNG, methanol and hydrogen can also be used in road transport, although their application is estimated for a long-term future. Among them, SNG has a better perspective as the required distribution infrastructure is more developed. In effect, there is already an extensive European gas pipeline where SNG could already be injected. Certified gas compression units, storage and filling systems are also available to meet the necessary criteria for safe and emission-free vehicle refueling [174]. The main drawback is, however, that gas-powered vehicles are still more expensive than conventional ICE. In any case, natural gas use for transportation is limited to public transport (e.g., municipal buses) and private cars, which represent less than 35% of fossil fuel consumed in road transportation. Hence, biofuel shares of Figure 8.32 will not be improved in case of producing SNG instead of Fischer-Tropsch. Hydrogen and methanol alternatives are even more restrictive as, once technological barriers will be overcome, their application is limited to private cars, thus accounting for less than 33% of the road transportation market.
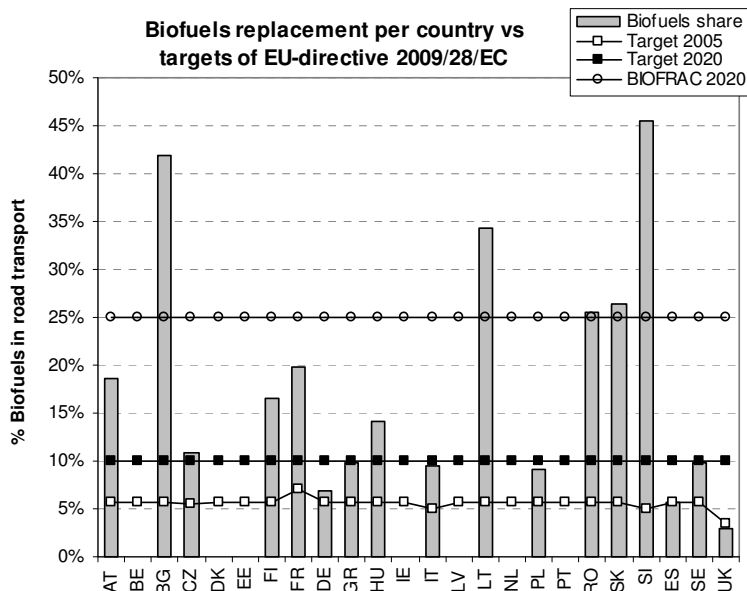
Figure 8.32: *Fischer-Tropsch share in road transport per country (i.e., VI-bio&grid-B3 scenario). Values are compared with European Directive 2009/28/EC targets for year 2005 (i.e., 5.75%) and year 2020 (i.e., 10%), and the estimation from BIOFRAC (i.e., 25%).*

On the other hand, although natural gas have major application in other sectors (e.g., heating, electricity and/or chemicals), the Directive 2009/28/EC does not fix any specific target concerning "green" gas production. Notwithstanding, some initiatives are found at national levels. For instance, the Dutch "***Platform New Gas***" has defined an ambitious plan to replace 20% of the natural gas by green gas by 2030, whereas substitution target of 50% has been suggested for 2050 [178]. However, Netherlands would need to import biomass from nearby regions as the country does not have enough forest and straw residues to produce the required SNG amount (i.e., 0.38 EJ of SNG by 2030). Moreover, according to the European Directive **2001/77/EC**, 21.0% of electricity should be produced from renewable sources by 2010. Although the corresponding real value for 2007 was already 15.5% [5], the '*Directorate General for Energy and Transport*' states that, under current trends, only 18-19% of the RES-electricity target will be accomplished by the end of 2010 [179]. If any of the "*I*" scenarios of Table 8-7 were applied in 2010, the share of renewable electricity would have been 31.2%, i.e., 10 points higher than the target in the Directive 2001/77/EC. Similar conclusions are drawn for year 2020, as 30.8% of the electricity could be generated from renewable sources.

Finally, in terms of economic and environmental implications of 2nd generation biofuels production, all the studies found in literature present values for stand-alone biofuels and not as a combination of biofuel/fossil fuel mixtures in order to comply with the European energy consumption by 2020 (i.e., 3.77 EJ/yr of electricity from solids, 25.9 EJ/yr of natural gas and 15.1 EJ/yr of road transport fuels). Hence, it is difficult to compare our results from those studies from an European perspective. Comparison of stand-alone biofuels can be found in Chapter 5 and 6.

8.10.6.   *Conclusions and Discussion*

The aim of this chapter was to present optimal conversion of all available forestry and straw residues for energy purposes. Biomass availability (i.e., 1.9 and 1.8 EJ of wood and straw respectively) was supposed to be equal to the biomass that could be ultimately purchased. However, as mentioned, this hypothesis could be difficult to carry out in practice as an important share of biomass is on private hands, thus, requiring intensive negotiations. Moreover, biofuels are produced at optimal scales, which are still far larger than actual pilot and demonstration plants, although some studies claim that they could be feasible by 2020. Hence, the relevance of our results lays on determining the maximal biofuels capacity within EU-24 by 2020, and whether this bioenergy production can comply with existing European Energy policies (i.e., Directive **2001/77/EC** and **2009/28/EC**). Moreover, analyses are conducted under different "*I*" to "*VIII*" scenarios which takes into account the motivations of various sectors, ranging from policy-makers, industry, scientists and the society.

From an economic and environmental perspective, maximizing renewable electricity production (i.e., scenario "*I*") is by far the best alternative as it leads to the largest CO_2 savings (i.e., 290-461 Mtn CO_2/yr). In effect, this option is the one that replaces more coal, which is one of the main contributors to CO_2 emissions in Europe [4]. However, analogous to other biofuels, bioelectricity is still more expensive than fossil-based power generation. An advantage is that this price difference is the lowest for the bioelectricity case (i.e., ~7 Billion €/yr for bio-electricity versus 16 to 56 Billion €/yr for other biofuels, when including ecocosts). Among the three "*I*"scenarios, combination of cofiring plus new BIGCC plants (i.e., "*I-bio100-A1*" and "*I-bio100-A2*") are suggested as the most feasible ones since CO_2 savings are done at a more competitive cost. Both alternatives would be also suitable for the society as we would benefit from lower pollution at a rational price, and without the need of changing the existing infrastructure. Following this alternative, the share of renewable electricity (including also wind, solar, hydropower and geothermal energy) would be ~ 31% by 2020, i.e., 10 points higher than the 2010-target established in the Directive 2001/77/EC.

Whenever the politics strategy will be to diminish the import of fossil natural gas, the "*V-bio&grid-B3*" scenario would be the best solution (i.e., 1.63 EJ/yr of fossil natural gas could be avoided). Scenario "*VI-bio&grid-B2*" would lead to lower fossil gas-independence (i.e., 1.44 EJ/yr) but higher CO_2 savings would be achieved as it also combines biomass cofiring in coal power plants (i.e., 145 Mtn CO_2/yr versus 86 Mtn CO_2/yr). Prices differences between bio-SNG and natural gas are notably larger than the electricity case (i.e., annual extra payment for SNG scenarios is in the range of 18-38 Billion €, when including ecocosts). An advantage is that SNG could be injected in existing gas pipelines, thus, minimizing the impact for its distribution. In case SNG were to be used as transport biofuel, existing filling stations should be modified, and final consumers would need to buy a CNG car which, currently, is about more expensive.

The most recent Directive **2009/28/EC** reaffirms the compromise to achieve 10% biofuels share in transportation. As aforementioned, SNG can be technically used for

that purpose as there are already some commercial CNG vehicles. However, the higher operational cost of this option is still too high to attract major industrial stakeholders (e.g., car manufacturers, fuel suppliers, infrastructure providers, fleet managers etc). This led us to study Fischer-Tropsch, methanol or hydrogen as potential biofuels for the transport sector. Hydrogen and methanol face similar distribution and end-use problems although even more severe. In particular, the hydrogen alternative has to solve the problem of its distribution as existing pipelines could not absorb the demand, and some safety concerns are even jeopardizing its development. Moreover H_2-FCV cars are still under development and the most optimistic specialists postpone its commercialization by year 2020 or 2030. Unfortunately, by this time, biomass will be probably consumed in other energy applications. Nevertheless, hydrogen results presented in this chapter show that it could be an interesting environmental option if the infrastructure and FCV vehicles were already there. In effect, CO_2 emissions reductions are quite substantial (i.e., 198-230 Mtn CO_2/yr). However, final hydrogen end-users prices are generally higher than the Fischer-Tropsch fuels.

On the other hand, methanol can be distributed using normal tank trucks, thus avoiding the problems of building pipelines. However, FCV-methanol prototypes are expected to arrive later than H_2-FCV vehicles. In Europe, methanol can also be blended with conventional gasoline up to 3%, but this option does not significantly contribute to the replacement of fossil fuels. Despite these facts, our results shows that methanol scenario "*VIII-bio100-A3*" barely induces any CO_2 savings (i.e., only 3 Mtn CO_2/yr), whereas the other two scenarios "*VIII-bio&grid-B3*" and "*VIII-NG&grid-C3*" have even negative reductions. Hence, we suggest not advocating for methanol as a biofuel for transport. Moreover, if conventional ICE cars are to be changed, electric cars (BEV) seems to be a more promising solution as, not only are they more efficient, but, as aforementioned, the CO_2 reduction potential is higher at lower costs.

Another option is the promotion of Fischer-Tropsch fuels for road transport. In effect, this solution will be customer-friendly as conventional cars could be used without any modification of engines. Moreover, it could benefit from existing distribution and filling stations infrastructure, while decreasing the dependence on oil imports from OPEC countries. According to our results, "*III-bio&grid-B3*" and "*IV-bio&grid-B3*" scenarios yield 9.5% biofuels share in road transport (i.e., 1.43 EJ/yr of Fischer-Tropsch fuels). In particular, "*IV-bio&grid-B3*" is a better alternative from an environmental perspective, as CO_2 savings are larger (i.e., 37 vs 30 Mtn CO_2/yr). Corresponding annual extra payment is found in the range of 39-41 Billion €, when including ecocosts. In comparison with Directive 2009/28/EC, there is a gap of 0.5% biofuels share that should be covered with other biofuels (e.g., biodiesel and/or bioethanol from feedstock other than forest or straw residues). In case of growing rapeseed for biodiesel production, about 0.5% of EU land will be needed for that purpose.

9

Conclusions and Outlook

9.1. *Main Conclusions and Discussion*

The European Commission has published some Directives for the promotion of renewable sources. In particular, Directive 2001/77/EC has established that by the end of 2010, about 21% of the EU-25 electricity generation should come from renewable alternatives. Recently, Directive 2009/28/EC adds the target of replacing 5.75% of the fossil fuels consumed in transport by biofuels in 2010. The figure is increased to 10% for year 2020. However, according to current trends, both targets are not going to be met in 2010, and experts query whether there is enough biomass to fulfill the targets of 2020. Accordingly, this research is intended to answer the key questions:

(Q1) Are European bioenergy targets achievable?
And if they are, *(Q2) how much it would cost to society and the environment*?

Answering these questions is somehow complex as there are many factors involved. For instance, biomass availability in Europe is rather limited and not all sources are eligible for biofuels or bioelectricity generation. Current technologies also need to be improved as efficiencies and production costs are not optimal yet. Another major issue is to select the best biofuel. In effect, although the governments, scientists, industry or the society have their own motivations, the selection should be based on objective parameters. Hence, an inherent goal of this thesis is to develop a ***multidimensional model*** to be able to evaluate bioenergy from thermoeconomic and environmental perspectives.

- *Biomass availability across Europe*

The first step of the model starts with biomass selection and quantification. The list is narrowed down from more than 10 different streams to forest and straw residues, as they are more effectively converted in gasifiers and their availability is also more stable. Average forest and straw residues availability in 24 European countries is estimated to be 1.9 and 1.8 EJ/yr respectively, with supply costs in the range of 0.8-5.9 and 0.8-3.9 €/GJ. Logistics costs are calculated aside but they represent less than 10% of the biofuel prices.

- *Efficiency evaluation of biomass-to-bioenergy chains*

Mass and energy balances from Aspen simulations are used to calculate the energy and exergy efficiency of the conversion plants. Inefficiencies related to utilities production and consumption are also included for a fair comparison among biofuels. Results are given with two different definitions as they are both found in literature. These two definitions can lead to opposite conclusions.

Table 9-1: *Comparison of energy and exergy efficiencies according to 2 different definitions and for the biofuels production stage and the WTW approach.*

stage	Definition	SNG	H_2	FT-fuels	MeOH	Electricity
Production plant (bio100 scenario)	$\Psi_{plant,1}{}^{(a)}$	55.0%	54.3%	51.4%	51.0%	53.0%
	$\Psi_{plant,2}{}^{(b)}$	52.6%	51.0%	45.7%	44.8%	42.6%
	$\Psi^*_{plant,1}{}^{(a)}$	44.4%	41.0%	43.1%	42.9%	45.4%
	$\Psi^*_{plant,2}{}^{(b)}$	41.9%	37.3%	37.5%	36.7%	35.5%
WTW	Ψ_{WTW}	10-11%$^{(c)}$ (7-8%$^{(d)}$)	14-15%$^{(c)}$ (15-17%$^{(d)}$)	9-10%$^{(c)}$ (10-12%$^{(d)}$)	5-6%$^{(c)}$ (7-8%$^{(d)}$)	17-19%$^{(c)}$ (21-23%$^{(d)}$)
	Ψ^*_{WTW}	7-9%$^{(c)}$ (4-6%$^{(d)}$)	8-10%$^{(c)}$ (10-12%$^{(d)}$)	7-9%$^{(c)}$ (9-10%$^{(d)}$)	4-6%$^{(c)}$ (7-9%$^{(d)}$)	14-16%$^{(c)}$ (17-19%$^{(d)}$)

(a): In the 1st definition, efficiency is calculated as the 'total outputs' divided by the 'total inputs' (See Eqs. (4-4) & (4-16)).

(b): In the 2nd definition, efficiency ratio is calculated as the 'produced biofuel or bioelectricity' divided by the 'net input' (see Eqs.(4-5)(4-6)(4-17)(4-18)).

(c): Well-to-wheel efficiencies when applying calculated tank-to-wheel efficiencies (Ψ_{TTW}) by Eq.(4-30).

(d): Well-to-wheel efficiencies when applying tank-to-wheel efficiencies (Ψ_{TTW}) from literature.

For instance, according to the 1st exergy definition ($\Psi^*_{plant,1}$) and the '*bio-100*' configuration, wood-based bioelectricity generation is the most exergetically efficient process closely followed by SNG (see Table 9-1). However, bioelectricity becomes the worst option when the 2nd exergy or energy definition ($\Psi^*_{plant,2}$ or $\Psi_{plant,2}$) is applied. SNG is the most efficient conversion process for the 2nd exergy and all energy definitions. FT-fuels and MeOH plants operate at similar efficiencies, although MeOH always yields slightly lower ratios than FT-fuels. Different trends are observed for H_2 when the exergetic base is changed for the conventional energy evaluation. In effect, it is a relatively low efficient process from an exergetic point of view, whereas H_2 attains the second best position when the evaluation is made on a HHV basis.

Corresponding values for straw-fuelled plants are about 1-2 and 0.3-1.5 %-point lower for exergy and energy calculations respectively. On the other hand, electricity co-production and gasification stages contribute to the largest efficiency losses (i.e., irreversibilities). Optimal '*efficiency*' scales are found to be smaller for bioelectricity and SNG processes (i.e., ~50 MW$_{el}$ and ~200 MW$_{SNG}$ respectively) than for the rest of the biofuels (i.e., ~ 300 MW$_{H2}$ and ~500 MW$_{fuel}$ for MeOH and FT-fuels).

The analysis is also extended to cover all stages, thus following a WTW approach. In this case, bioelectricity generation seems to be the most convenient solution (i.e, Ψ_{WTW} equals 17-19%), mainly due to the relatively higher efficiency of BEV cars. Conversely, SNG and MeOH are on the lowest side. Biofuels production and vehicles

operation are the main contributors to the efficiency losses of the whole WTW chain. Efficiency results are used in subsequent economic and environmental impact assessments.

- *Environmental impact evaluation (LCA) of biomass-to-bioenergy chains*

An LCA is applied to compute the emissions of different biomass-to-bioenergy routes, for two very distinct sectors (i.e., electricity and transport) and 24 European countries. The option of growing non-edible lignocellulosic crops is also added to the study. Bioelectricity generation release lower CO_2 emissions than coal-based power plants, although biomass availability per hectare notably influences the final number (i.e., 10, 9-271 and 9-295 g-eq CO_2/MJ for energy crops, forest and straw residues versus 400 g-eq CO_2/MJ for coal). In effect, growing energy crops in regions with low biomass availability would be an interesting option as they release the lowest amount of CO_2 emissions. However, this practice would increase *acidification* and *eutrophication* impacts in comparison with forest or straw residues.

Biolectricity use in transport is also the preferred option over other biofuels when the comparison is made per driving distance (i.e., 5 g-eq CO_2/km for energy crops, and 6-7 g-eq CO_2/km for forest and straw residues in France). Conversely FT-fuels, and particularly MeOH production normally releases the highest CO_2 emissions, and there are even some locations where emissions exceeds the levels of fossil diesel. According to the European Parliament, new biofuels technologies should at least reduce 60% of the GHG's emissions in comparison with fossil alternatives. Countries with a large biomass reserves would fulfill this target with either SNG, electricity or H_2 production, whereas FT-fuels generation is reserved to the 'top-4' countries (i.e., Austria, Belgium, France and Slovenia) or the 'virtual region with energy crops (VEC). The sensitivity analysis reveals that plant scales and fuel consumption in tractors are the most influencing parameters on total CO_2 emissions. Biofuels distribution also plays an important role for liquid biofuels such as MeOH or FT-fuels.

- *Economic evaluation(LCA) of biomass-to-bioenergy chains*

New 'optimal' plant scales are determined in the economic assessment part. They are notably larger for H_2, MeOH and FT-fuels as they need to compensate for their relatively high capital investment (i.e., 500 MW_{H2} and 1000 MW_{fuel} for MeOH and FT-fuels). Electricity and SNG plants are found to be profitable at smaller sizes (i.e., 100 and 200 MW_{fuel} respectively). In this case, hydrogen is the most expensive biofuel per unit of output energy, whereas SNG and electricity are the most economic energy carriers (i.e., 27.1 €/GJ_{H2}, 17.7 €/GJ_{SNG} and 23.7 €/GJ_{el} for the '*bio-&grid*' configuration in the Netherlands). FT-fuels and MeOH prices are rather close (i.e., 24.9 €/GJ_{FT} and 25.6 €/GJ_{MeOH} respectively). Similar trends are observed for wood and straw feedstock, although straw-based biofuels are always more expensive, except for France. Plant location also influences final 'end-user' prices. Nevertheless, the sensitivity analysis shows that the FCI has even a major impact on the final price than biomass costs and/or corporative taxes.

Biofuels prices are also compared with their direct fossil competitor. SNG is almost double the price of fossil natural gas, thus increasing gas expenditure in all countries.

There is also a considerable price difference when bio-based FT-fuels, methanol or hydrogen are compared with fossil diesel before taxation. When biofuels are compared with fossil prices after taxation, differences are reduced and, for some countries, FT-fuels and H_2 become even cheaper than fossil diesel. In same Chapter 6, a new taxation system is proposed to equalize biofuels and fossil fuels prices as well as to maintain actual revenues to governments from fuels' taxation. Addditionally, ecocosts are suggested to be added on top of taxed prices to penalize CO_2 emissions.

- *Multidimensional 3E model application to Europe*

Previous efficiency, economic and environmental impact results are combined in an own multidimensional 3E model in Chapter 7. This model is also implemented in an excel file (Multi_model.xls) to facilitate its utilization. Efficiency, economic and environmental results are integrated to give a final monetary value (i.e., the summation of the taxed fuel prices and *ecocosts*). The 3E model is finally applied at European scale to answer the previous two questions (*Q1*) and (*Q2*) of this thesis. For that purpose, we assume that bioelectricity or biofuels would be used to partly replace:

- Electricity production from coal (i.e., **3.77 EJ/year**). This figure means that about **8.34 EJ/yr** of coal is consumed.
- Natural gas consumption (e.g., electricity, heating, or other industrial applications), which accounts for **25.90 EJ/year**
- Fossil fuel consumption in the road transport, which sums **15.10 EJ/year**. This figure includes public road transport, private cars, motorcycles, and trucks.

Seven scenarios are proposed, ranging from maximizing renewable electricity, maximizing biofuels production and/or combining biomass cofiring with biofuels plants. Major CO_2 savings are computed for the scenarios that prioritize bioelectricity generation. In particular, building new bio-based BIGCC plants (scenario *I-bio100-A3*) accounts for the highest CO_2 savings (i.e., 461 Mtn CO_2/yr). In effect, this option is the one that replaces more coal, which is one of the main contributors to CO_2 emissions in Europe [4]. Nevertheless, combining cofiring with new BIGCC plants (i.e., *I-bio100-A1 and I-bio100-A2* scenarios) are suggested as the most feasible options because CO_2 savings are done at more competitive final prices. For both scenarios, the share of renewable electricity (including also wind, solar, hydropower and geothermal energy) would be ~ 31% by 2020, i.e., 10-% points higher than the 2010-target established in the Directive 2001/77/EC. An added advantage is that the annual quantified price difference (*ΔB*) is the lowest when maximizing bioelectricity (scenarios "*I*") instead of biofuels production (i.e., 7 Billion €/yr for bioelectricity versus 16 to 56 Billion €/yr for other biofuels, when including ecocosts).

Nevertheless, if the goal is to comply with the 10% biofuels replacement target in the transport sector, Fischer-Tropsch fuels seem to be the best option. Scenarios *III-bio&grid-B3* and *IV-bio&grid-B3* yield 9.5% biofuels share in road transport (i.e., 1.43 EJ/yr of Fischer-Tropsch fuels). In particular, *IV-bio&grid-B3* is a better option from an environmental perspective, as CO_2 savings are larger (i.e., 37 vs 30 Mtn CO_2/yr). Corresponding annual extra payment is found in the range of 39-41 Billion €, when including ecocosts. In comparison with Directive 2009/28/EC, there is a gap of 0.5-% biofuels share that should be covered with other biofuels (e.g., biodiesel and/or

bioethanol from feedstock other than forest or straw residues). In case of growing rapeseed for biodiesel production, about 0.5% of EU land would be needed.

In brief, bioelectricity production, for either transport or electricity applications seems to be the best option from an thermoeconomic and environmental perspective, although it would not be possible to fulfill all bioenergy targets of Directives 2001/77/EC and 2009/28/EC with actual forest and straw availability in Europe. However, the values presented in this thesis assume that all forest and straw residues (i.e., 1.9 and 1.8 EJ/yr respectively) could be purchased at stables prices. This presumption is rather optimistic as ~ 61% of European forests are on private hands, thus requiring extensive negotiation for biomass acquisition. Moreover, the biomass market is not developed yet, which means that a growing interest in this renewable energy source will probably be accompanied with an increase of biomass prices.

9.2. *Outlook*

If European bioenergy targets are to be met, biomass consumption will have a substantial impact on the energy market. Consequently, existing infrastructures will need some adaptation. This subject, however, is out of the scope of this thesis due to its complexity. Hence, we proposed to address the extension of actual infrastructures in subsequent studies. In particular, since bioelectricity seems to be one of the best alternatives from a thermoeconomic and environmental point of view, we would like to draw the attention to improve national grids and optimize the allocation of charging points. These proposals are accompanied by the need of improving existing BEV cars and significantly reduce their capital costs.

On the other hand, although biomass transport has a relatively minor impact on final biofuel prices, it has a direct impact on total CO_2 emissions of the full biomass-to-bioenergy chains. This fact is especially significant for biofuels options requiring large plant scales (e.g., Fischer-Tropsch and methanol). Several pre-treatment options are being proposed to increase energy density of biomass, thus reducing fuel consumption for transport. Coupling of pelletization and/or torrefaction practices prior to biomass transport could also be studied in parallel. Torrefaction has the added advantage that biomass is transformed into a hydrophobic feedstock which is more easy to storage and grind. Moreover, several authors claim that it improves gasification efficiency and reliability [40, 42]. However, the analysis should also include an economic evaluation to predict the increased production cost and if it can be accepted by the consumers.

Finally, we would also like to suggest determining in more detail the real availability and potential acquisition of biomass since there is a great divergence in the studies of several authors. In particular, it is rather difficult to predict the biomass amount that could be purchased at reasonable prices. In addition, it would be also very useful to develop a model to predict biomass prices as a function of its penetration into the European energy market. Knowing all this information will allow other researchers to better estimate how feasible will be to fulfill European bioenergy targets.

Nomenclature

Symbols

a: car acceleration (m/s^2).

A_{car}: frontal area of a car (m^2).

A_i: Arrenhius constant (mol/g.s.bar).

$A_{NUTS2,i}$: area of the NUTS-2 region 'i' that will be covered to collect the biomass herein (ha).

$A_{subarea,j}$: subarea in which is divided each NUTS-2 or 'virtual' region (28 km^2).

$A_{subarea,k}$: subarea in which is divided the last 'k' row of each NUTS-2 or 'virtual' region (<28 km^2).

$A_{T,biowaste}$: total area that has to be covered to collect enough biowaste to feed one conversion plant (ha).

$A_{T,ecrop}$: total area that has to be covered to collect enough energy crops to feed one conversion plant (ha).

$A_{T,ecrops}$: total area that has to be covered to collect enough energy crops to fed one conversion plant. It has been calculated in Chapter 5 (ha).

A_{truck}: frontal area of a truck (m^2).

$B_{bioenergy}$: annual payment for the mix of bioenergy/fossil fuels consumption (i.e., electricity, natural gas and diesel) in Europe (Billion €/yr).

B_{fossil}: annual payment for the mix of fossil fuels consumption (i.e., electricity, natural gas and diesel) in Europe (Billion €/yr).

c: specific kinetic energy (kJ/kg).

$C_{diesel,operation}$: consumption of diesel per tractor and operation (lt/ha).

CE Index $_{actual}$: Chemical Engineering Plant Cost Index of the year of the study. These indexes are monthly published in the '*Chemical Engineering Index*'.

CE Index $_{ref}$: Chemical Engineering Plant Cost Index of the year 2010.

CI_{actual}: actual annual income from fossil fuel taxation (€/GJ).

CI_{new}: new annual income that is calculated from the new taxation system of fossil fuels and biofuels (€/GJ).

$C_{oil,operation}$: consumption of lubrication oil per tractor and operation (lt/ha).

C_p: specific heat capacity (J/kg.K).

$C_{pH2O,v}$: specific heat capacity of steam (J/kg.K).

C_S: calorific value of biomass (J/kg).

C_w: drag coefficient (-).

DC: Annual fossil diesel consumption (GJ/yr).

d_i: distance from the central point of a NUTS-2 region and the processing plant (km).

$d_{st(i)}$: division of the 'd_i' distance per 'z' interstages (km).

$E^*_{biofuels}$: total exergy flow of the produced biofuel (MW).

$E^*_{biomass}$: total exergy flow of biomass stream (MW).

$E^*_{chemicals}$: total exergy flow of chemicals being consumed in the process (MW).

E^*_{fuels}: total exergy flow of fossil fuels being consumed in the process (MW).

E^*_i: total exergy of an "i" mass flow (MW).

$E^*_{surplus\ steam}$: total exergy flow of the produced steam that it is not consumed in the process (MW).

$E_{i,in}$: total energy flow entering a system (MW).

$E_{i,out}$: total energy flow leaving a system (MW).

E_i: Activation energy (J/mol).

$E_{in}*^Q$: total exergy flow of an inlet heat flow (MW).

$E_{in,collection}$: input energy for the biomass collection stage (MW).

$E_{in,distribution}$: input energy for the biofuels or bioelectricity production stage (MW).

$E_{in,fertilizers}$: input energy for the fertilizers production (MW).

$E_{in,transport}$: input energy for the biomass transport stage (MW).

e_K: specific energy expenditure for K-fertilizers production (MJ/kg).

e_N: specific energy expenditure for N-fertilizers production (MJ/kg).

$E_{out}*^Q$: total exergy flow of an outlet heat flow (MW).

$E_{out,production}$: output energy from the biofuels or bioelectricity production stage (MW).

e_P: specific energy expenditure for P-fertilizers production (MJ/kg).

E_{useful}: useful energy from the last chain stage (MW).

FE: fuel economy (MJ/km).

f_r: rolling resistance coefficient (-).

g: gravity (9.8 m/s^2).

$H/C, O/C, N/C$: atomic ratios in the biomass.

h: specific enthalpy of a stream (kJ/kg).

h_e: elevation height needed to calculate the potential energy (m).

HHV: High heating value (MJ/kg).

$HHV_{biofuel}$: high heating value of the produced biofuel (MJ/kg)

$HHV_{biomass}$: high heating value of biomass (MJ/kg)

HHV_{diesel}: high heating value of fossil diesel (MJ/kg)

$HHV_{fuel,i}$: high heating value of fossil fuels (i.e., natural gas, diesel or lubrication oil) (MJ/kg)

HHV_{oil}: high heating value of lubrication oil (MJ/kg)

h_o: specific enthalpy of a stream at the reference state of 1 bar and 25°C (kJ/kg).

$h_{tractor}$: farmer (or tractor) working hours per year (hr/yr).

$I*$: Irreversibilities (exergy losses).

j: number of subareas in which a NUTS-2 or virtual region is divided (-).

k: total numbers of rows in which are divided each NUTS-2 region (biowastes) and the 'virtual' region (energy crops).

k_{HC1}: Rate constant for adsorption of CO on an active site (mol/g.s.bar).

k_{HC5}: Rate constant for desorption of paraffins by hydrogenation of active site (mol/g.s.bar).

k_{HC6}: Rate constant for desorption of olefins from active site (mol/g.s).

L: length of the conveyor (m).

L_c: average logistics costs of a "i" point within a certain delimited area ($\pi.r^2$). They are calculated in Eqs.(2-2) and (2-3) in Chapter 2 (€/tn).

$L_{chemicals}$: total emissions from the chemicals production, distribution and application (kg-eq component/f.u.).

$l_{CO2,biofuel}$: CO$_2$ emissions originated by the use of fossil fuels in bioenergy systems (in tn CO$_2$/GJ).

$l_{CO2,fossil}$: CO$_2$ emissions originated by the use of fossil fuels (in tn CO$_2$/GJ).

$L_{collection}$: total emissions of the collection stage (kg-eq component/f.u.).

$L_{distribution}$: total emissions of the distribution stage (kg-eq component/f.u.).

$L_{fertilizers}$: total emissions from the fertilizers production, distribution and application (kg-eq component/f.u.).

L_{fuel}: total emissions from the fuel production, distribution and use (kg-eq component/f.u.).

$LHV_{biomass}$: lower heating value of biomass (MJ/kg).

LHV_{fuel}: low heating value of a fuel (i.e., diesel or lubrication oil) (MJ/kg).

LHV_{org}: low heating value of the organic fraction (MJ/kg).

$L_{infrastructure\ construction}$: total emissions from the construction of the infrastructure (kg-eq component/f.u.).

L_{oil}: total emissions from the lubrication oil production, distribution and use (kg-eq component/f.u.).

$L_{plant\ construction}$: total emissions from the conversion plant construction (kg-eq component/f.u.).

$L_{production}$: total emissions of the production stage (kg-eq component/f.u.).

$l_{project}$: lifetime of the project (30 years).

L_{total}: total emissions of the whole LCA analysis (kg-eq component/f.u.).

$l_{tractor}$: lifetime of the one tractor (-~8 years).

$L_{tractors\ construction}$: total emissions from the tractors construction (kg-eq component/f.u.).

$L_{transport}$: total emissions of the transport stage (kg-eq component/f.u.).

l_{truck}: lifetime of the one truck (-~7 years).

$L_{trucks\ construction}$: total emissions from the trucks construction (kg-eq component/f.u.).

$L_{utilities}$: total emissions from the utilities production, distribution and use (kg-eq component/f.u.).

$m_{biofuel}$: mass flow rate of produced biofuel (kg/s).

$m_{biomass,subarea(j)}$: amount of biomass in subarea "j" (tn/yr).

$m_{biomass}$: mass flow rate of a biomass stream (kg/s).

$m_{biowaste(NUTS2,i)}$: collected biowaste in the NUTS-2 region 'i' (tn/yr).

$m_{ecrop,all(year)}$: collected energy crops in the 'virtual' region (tn/yr).

$m_{fuel,i}$: mass flow rate of fossil fuels (i.e., natural gas, diesel or lubrication oil) (kg/s).

$m_{H2O,v}$: mass flow rate of steam (kg/s).

$m_{i,in}$: mass flow rate of an inlet compound "i" (kg/s). In Eqs.(3.1) to (3.4), this parameter is given in lb/hr.

M_i: molecular weight (kg/mol).

$m_{j,out}$: mass flow rate of an outlet compound j (kg/s).

m_l: biomass load in the truck (tn).

m_v: gross weight of one truck (tn).

m_v: weight of one car (kg).

n: number of NUTS-2 regions that are needed to fed one processing plants (-).

n_a: number of atoms.

n_i: total molar flow rate of a stream (mol/s).

$N_{interstages(i)}$: number of interstages in which the transport distance (i.e., from the collection point to the processing plant) is divided to comply with the limitations of maximum driving hours per driver and day (-).

$N_{operations}$: number of operations that are done by tractors (e.g., coppicing, fertilizers application, seeding, etc). This parameter equals '1' for biowastes and '4' for energy crops (-).

$N_{tractors,biowastes(all)}$: total number of tractors that are needed to collect biowastes in all NUTS-2 regions (-).

$N_{tractors,biowastes(NUTS2,i)}$: number of tractors that are needed to collect biowastes in NUTS-2 region 'i' (-).

$N_{tractors,ecrops(all)}$: total number of tractors that are needed to collect energy crops in the 'virtual' region (-).

$N_{trips,NUTS2(i)}$: number of trips that have to be done annually to transport all biomass of the NUTS-2 or virtual region to the conversion plant(-).

$N_{trips,subarea(j)}$: number of trips that have to be done annually to transport all biomass of subarea "j" to the central location of the NUTS-2 or virtual region (-).

$N_{trucks,log1}$: total number of required trucks for the '*log-1*' stage (-).

$N_{trucks,log2}$: total number of required trucks for the '*log-2*' stage (-).

$N_{trucks,total}$: total number of required trucks to transport all biomass (-).

P: pressure (bar).

P_{CO}: partial pressure of CO (bar).

P_{H2}: partial pressure of H_2 (bar).

P_{max}: total power required per tractor and operation (kW). Values are taken from [124].

P_o: reference pressure (1 bar).

P_T: total power required per tractor and operation (kW). Values are taken from [124].

Q_{in}: inlet heat flow (MW).

q_K: dosign of K-fertilizers (kg/ha).

q_N: dosign of N-fertilizers (kg/ha).

Q_{out}: outlet heat flow (MW).

q_P: dosign of P-fertilizers (kg/ha).

$R*$: particle reduction rate (-).

R: universal gas constant (8.314472 J/mol.K).

R_f: Scaling factor (see Table 0-12 in Appendix J).

R_{j-1}: distance from the collection plant to the central point (i.e., R=0) of a NUTS-2 or virtual region (km).

$R_{propagation}$: rate of propagation (mol/g.s).

$R_{termination}$: rate of termination (mol/g.s).

s: specific entropy of a stream (kJ/kg.K).

$S_{diesel,trip}$: consumption of diesel per truck, payload and distance (MJ/tn.km).

s_o: specific entropy of a stream at the reference state of 1 bar and 25°C (kJ/kg.K).

T: Temperature (K)

TB_i: new biofuel taxes ratio based on the new taxation system of section 6.4 (-).

$TC_{diesel,biowaste}$: total consumption of diesel to collect all biowastes (lt/yr).

$TC_{diesel,ecrops}$: total consumption of diesel to collect all energy crops (lt/yr).

$TC_{oil,biowaste}$: total consumption of lubrication oil to collect all biowastes (lt/yr).

$TC_{oil,ecrops}$: total consumption of lubrication oil to collect all energy crops (lt/yr).

TD_i: actual fossil fuel taxes ratio (-).

TD_{new}: new fossil fuel taxes ratio based on the new taxation system of section 6.4 (-).

$t_{driving}$: driving time per trip and truck(hr).

t_{fix}: required time for uploading and downloading biomass (2 hr).

$t_{max,truck}$: maximum driving time per truck (hr).

$TN_{built-tractors,biowastes(all)}$: total number of tractors that will be built for the whole lifetime of the project to collect all biowastes (-).

$TN_{built-tractors,ecrops(all)}$: total number of tractors that will be built for the whole lifetime of the project to collect all energy crops (-).

$TN_{trucks,total}$: total number of required trucks that that will be built for the whole lifetime of the project to (-).

T_o: reference temperature (298.15 K).

$TS_{diesel,distribution}$: total diesel consumption to distribute FT-fuels or MeOH (kg/yr).

$TS_{diesel,log1}$: total diesel consumption to perform '*log-1*' transport, as detailed in Figure 5.4 of Chapter 5 (kg/yr)

$TS_{diesel,log2}$: total diesel consumption to perform '*log-2*' transport, as detailed in Figure 5.5 of Chapter 5 (kg/yr).

$t_{total,log-1}$: total required time to transport all biomass in all regions to the central point of each region (hr).

$t_{total,log2}$: total required time to transport all biomass from all regions to the conversion plant (hr).

$t_{total,NUTS-2(i)}$: total required time to transport all biomass from the NUTS-2 region (hr).

$t_{total,row(j)}$: total required time to transport all biomass from row 'j' (hr).

$t_{total,subarea(j)}$: total required time to transport all biomass from subarea 'j' (hr).

$t_{trip,calc(j)}$: calculated driving time per trip to transport biomass from subarea 'j' to the central point of the NUTS-2 or virtual region (hr).

$t_{trip,log-2}$: required time per trip in the 'log-2' stage (hr).

T_{vap}: temperature of water evaporation (K).

v: velocity of a car (m/s).

v_o: head wind velocity (m/s).

$v_{tractor}$: tractor speed (km/hr).

v_{truck}: truck speed (km/hr).

W_{index}: Wobbe index (MJ/Nm^3).

W_{in}: work input for a process (MW). In Eqs.(3.1) to (3.4) this parameter is given in Hp.

W_{out}: work output from a process (MW).

w_{plough}: tractor plough width (m).

x_i: molar fraction of compound i.

x_v: vapor title (-).

z: number of interstages that are needed to assure that the driving distance does not exceed 240 km. It is calculated by Eq.(5-27) in Figure 5.5 (-).

z_i: mass fraction of compound i (-).

z_n: mass fraction of a product consisting of n_a atoms (-).

z_{org}: organic mass fraction of biomass (-).

Greek symbols

α: Chain growth probability factor (-).

$\alpha_{biofuel}$: 'end-user' biofuel price excluding taxes (€/GJ).

$\alpha_{biofuel,int}$: 'end-user' biofuel price including taxes and ecocosts (€/GJ).

$\alpha_{CO2,i}$: ecocosts that should be added on top of taxed fuels to penalize for CO_2 emissions occurring during their production, distribution and use (€/GJ).

α_{fossil}: 'end-user' fossil fuel price excluding taxes (€/GJ).

$\alpha_{fossil,int}$: 'end-user' fossil fuel price including taxes and ecocosts (€/GJ).

α_i: price of the 'i' biofuel (€/GJ).

β_{straw}: ratio of the chemical exergy to the LHV of the organic fraction of straw (-).

β_{wood}: ratio of the chemical exergy to the LHV of the organic fraction of woody biomass (-).

ΔB: annual EU extra payment due to the price difference between the reference fossil scenario in Table 8-6 and bioenergy/fossil misture (Billion €/yr).

ΔB_{eco}: annual EU extra payment due to the price difference between the reference fossil scenario in Table 8-6 and bioenergy/fossil misture (Billion €/yr). It includes ecocosts.

ε_K: specific exergy expenditure for K-fertilizers production (MJ/kg).

ε_N: specific exergy expenditure for N-fertilizers production (MJ/kg).

ε_P: specific exergy expenditure for P-fertilizers production (MJ/kg).

$\varepsilon_{ch,biomass}$: specific chemical exergy of biomass (kJ/kg).

$\varepsilon_{ch,diesel}$: specific chemical exergy of fossil diesel (kJ/kg).

$\varepsilon_{ch,fuel}$: specific chemical exergy of fuel (i.e., diesel or lubrication oil) (kJ/kg).

$\varepsilon_{ch,i}$: specific chemical exergy of compound i (kJ/mol).

$\varepsilon_{ch,mix}$: specific chemical exergy of a mixture of compounds (kJ/kg).

$\varepsilon_{ch,oil}$: specific chemical exergy of lubrication oil (kJ/kg).

$\varepsilon_{ph,i}$: specific physical exergy of compound i (kJ/mol).

$\gamma_{eco,i}$: virtual ecotax that is neede to calculate ecocosts (€/tn-eq emissions).

κ: conversion degree in the methanol synthesis reactor, in Eqs (3-11) and (3-12) (-).

$\eta_{biowaste(NUTS2,i)}$: biowaste productivity per hectare in the NUTS-2 region 'i' (tn/ha).

η_{ecrop}: energy crops productivity per hectare in the 'virtual' region (tn/ha).

η_i: mass conversion yield (kg biofuel/kg biomass).

η_t: truck efficiency (-).

λ: fraction of biofuel replacement in the energy sector (-).

λ_{vap}: latent heat of water evaporation (J/kg).

ρ: density of the air (kg/m^3).

ρ_{air}: density of air (kg/m^3).

ρ_{diesel}: density of diesel (kg/m^3).

ρ_{gas}: SNG gas density (kg/m^3).

ρ_{oil}: density of lubrication oil (kg/m^3).

τ: extra taxes for fossil fuels in a 'virtual' new taxation system (-).

$\Psi_{PEC,diesel}$: efficiency of producing fossil diesel (i.e., ~ 80%).

$\Psi_{PEC,oil}$: efficiency of producing lubrication oil (i.e., ~ 80%).

$\Psi^*_{PEC,diesel}$: exergetic efficiency of producing fossil diesel (i.e., ~ 80%).

$\Psi^*_{PEC,oil}$: exergetic efficiency of producing lubrication oil (i.e., ~ 80%).

$\Psi^*_{plant,1}$: energy efficiency according to Eq.(4-5) (%).

$\Psi^*_{plant,2}$: energy efficiency according to Eq.(4-6) (%).

$\Psi^*_{plant,2el}$: exergy efficiency for bioelectricity production according to Eq.(4-7) (%).

$\Psi^*_{plant,1}$: exergy efficiency according to Eq.(4-17) (%).

$\Psi^*_{plant,2}$: exergy efficiency according to Eq.(4-18) (%).

$\Psi^*_{plant,2el}$: exergy efficiency for bioelectricity production according to Eq.(4-19) (%).

$\psi_{tractor}$: tractor efficiency (%).

Ψ_{TTW}: energy efficiency of vehicles (%).

Ψ_{WTW}: overall well-to-wheel efficiency of the biofuels chains (%).

Ψ^*_{WTW}: overall well-to-wheel exergetic efficiency of the biofuels chains (%).

Acronyms

ASPO: Association for the Study of Peak Oil and Gas.

ASU: Air separation unit.

BEV: Battery electric vehicle.

BHA: Blair House Agreement.

BIGCC: Biomass integrated gasification combined cycle.

bio&grid: Plant configuration where the heat demand of the conversion process is supplied by burning an extra biomass amount, while electricity is taken from the grid.

bio-100: Plant configuration where the heat and electricity demand of the conversion process is supplied by burning an extra biomass amount.

BTL: Biomass-to-liquid.

CC: Carbon Capture.

CFB: Circulating Fluidized Bed

CFPP: Cold filter plugging point.

CNG: Compressed natural gas.

COM: Annual manufacturing costs (see Table 0-13 in Appendix J).

CR-S-REV-HAMR: Hammer mill model of the Aspen Icarus library.

CR-S-ROLL-MED: Roll crusher model of the Aspen Icarus library.

CTL: Coal-to-liquid.

DC: Direct current.

DCO-CLOSE-BLT: Closed belt conveyors model of the Aspen Icarus library.

DFC: Direct fixed costs (see Table 0-11 in Appendix J).

DME: Dimethyleter.

DMFCV: Direct methanol fuel cell vehicles.

DPC: Direct production costs (see Table 0-13 in Appendix J).

f.u.: functional unit.

FCV: Fuel cell vehicle.

FR-61: French region that corresponds to Aquitaine.

FR-61: French region that corresponds to Aquitaine.

FT: Fischer-Tropsch

FXC: Fixed charges (see Table 0-13 in Appendix J).

GDP: Gross domestic product.

GE: General expenses (see Table 0-13 in Appendix J).

GH_2: Hydrogen in gas phase.

GHG: Greenhouse gases.

GTL: Gas-to-liquid.

GWP: Global Warming Potential.

HRSG: Heat recovery steam generation process.

HTS: High temperature shift reactor.

ICE: Internal combustion engine.

IEA: International Energy Agency

IFC: Indirect fixed costs (see Table 0-11 in Appendix J).

IGCC: Integrated gasification combined cycle.

IGT: Institute of Gas Technology.

IRR: Investor's rate of return.

KEMDEA: Kinetic electrolyte package in Aspen Plus for modeling MDEA absorption.

LCA: Life Cycle Analysis.

log-1: It refers to the stage where collected biomass is transported to a central location of a NUTS-2 region (see section 5.2.2.2 in Chapter 5 for further details).

log-2: It refers to the stage where gathered biomass in the central location is transported to the final processing plant (see section 5.2.2.2 in Chapter 5 for further details).

LTS: Low temperature shift reactor.

M85: Methanol blend up to 85% (in weight basis).

MDEA: N-methyl-diethanolamine solution

MeOH: Methanol.

NG&grid: Plant configuration where the heat demand of the conversion process is supplied by burning natural gas, while electricity is taken from the national grid.

NG: Natural Gas.

NG-100: Plant configuration where the heat and electricity demand of the conversion process is supplied by burning natural gas.

NUTS-2: Nomenclature of Territorial Units of Statistics at 2nd level.

PAH: Polycyclic aromatic hydrocarbon.

PE: Purchased equipment cost.

PEC: Primary energy consumption.

PEM: Proton exchange membrane

PM: Particulate Matter.

PSA: Pressure swing adsorption.

RADFRAC: Distillation column model of the Aspen Plus library. It performs rigorous rating and design calculations for single columns.

REQUIL: Equilibrium reactor of the Aspen Plus library. It performs chemical and phase equilibrium by stoichiometric calculations.

RGIBBS: Equilibrium reactor with Gibbs energy minimization. It performs chemical and phase equilibrium by Gibbs energy minimization.

RM: Raw materials.

RMFCV: Reformed methanol fuel cell vehicles.

ROI: Return on investment.

RSTOIC: Stoichiometric reactor of the Aspen Plus library. It models stoichiometric reactor with specified reactor extent or conversion.

RYIELD: Yield reactor of the Aspen Plus library. It models reactor with specified yield.

SMR: Steam methane reforming.

SNG: Synthetic Natural Gas.

SOFC: Solid oxide fuel cell.

TCI: Total capital investment (see Table 0-11 in Appendix J).

TPC: Total production cost (see Table 0-13 in Appendix J).

TTW: Tank-to-Wheel

VEC: Virtual region where Energy Crops are grown.

WC: Working capital (see Table 0-11 in Appendix J).

WGS: Water-gas-shift reactor.

WTW: Well-to-Wheel.

References

1. EIA, *International Energy Outlook 2008*, Energy Information Administration. Office of Integrated Analysis and Forecasting. U.S. Department of Energy. Washington DC, Editor. 2008.

2. Meng, Q.Y. and R.W. Bentley, *Global oil peaking: Responding to the case for [`]abundant supplies of oil'*. Energy, 2008. 33(8): p. 1179-1184.

3. EIA, *Total Primary Energy Consumption (Quadrillion Btu).All Countries, 1980-2006 for the International Energy Annual 2006*, Energy Information Administration. Office of Integrated Analysis and Forecasting. U.S. Department of Energy. Washington DC, Editor. 2006.

4. Mantzos, L., et al., *European Energy and transport Trends to 2030 (Appendix2)*, in *Summary Energy Balances and Indicators*. 2003, European Comission. Directorate General for Energy and Transport: Luxembourg (Luxembourg).

5. Eurostat, *Environment and Energy statistics*.

6. *European Biomass Statistics 2009*, European Biomass Association (AEBIOM).

7. Muller-Langer, F., et al. *Analysis and evaluation of the 2nd generation of transport biofuels*. in *15th European Biomass Conference & Exhibition*. 2007. Berlin (Germany).

8. Marbe, A., S. Harvey, and T. Berntsson, *Biofuel gasification combined heat and power--new implementation opportunities resulting from combined supply of process steam and district heating*. Energy, 2004. 29(8): p. 1117-1137.

9. Zheng, L. and E. Furinsky, *Comparison of Shell, Texaco, BGL and KRW gasifiers as part of IGCC plant computer simulations.* Energy Conversion and Management, 2005. 46(11-12): p. 1767-1779.

10. Bridgwater, A.V., *Renewable fuels and chemicals by thermal processing of biomass.* Chemical Engineering Journal, 2003. 91(2-3): p. 87-102.

11. Basu, P., *Combustion and Gasification in Fluidized Beds*. 2006, 473 pages: CRC Press.

12. Boerrigter, H., et al. *Tar removal from biomass product gas; development and optimizationf of the OLGA tar removal technology*. in *14th European Biomass Conference and Exhibition*. 2005. Paris (France): ETA Renewable Energies and WIP Renewable Energies.

13. Szargut, J., *Analysis of cumulative exergy consumption.* International Journal of Energy Research, 1987. 11(4): p. 541-547.

14. Cornelissen, R.L. and G.G. Hirs, *The value of the exergetic life cycle assessment besides the LCA.* Energy Conversion and Management, 2002. 43(9-12): p. 1417-1424.

15. Tsatsaronis, G. and M. Winhold, *Exergoeconomic analysis and evaluation of energy-conversion plants--I. A new general methodology.* Energy, 1985. 10(1): p. 69-80.

16. Tsatsaronis, G., *Thermoeconomic analysis and optimization of energy systems.* Progress in Energy and Combustion Science, 1993. 19(3): p. 227-257.

17. Sciubba, E., *Beyond thermoeconomics? The concept of Extended Exergy Accounting and its application to the analysis and design of thermal systems.* Exergy, An International Journal, 2001. 1(2): p. 68-84.

18. Whittaker, R.H. and G.E. Likens, *Primary Productivity of the Biosphere*. Ecological Studies. Vol. 14. 1975, New York (USA): Springer-Verlag.

19. Mengije, W. and D. Suzhen, *A potential renewable energy resource development and utilization of biomass energy*, FAO Corporate Document Repository. Natural Resources Management and Environmental Department Editor, Food and Agriculture Organization of the United Nations (FAO).

20.   Martinot, E. *Renewables 2007. Global status report.* Renewable Energy Policy
        Network for the 21st Century (REN21)   2007   [cited; Available from:
        http://www.martinot.info/RE2007_Global_Status_Report.pdf.

21.   Faaij, A.P.C., *Energy from biomass and waste*, in *Department of Science,
        Technology and Society* 1997, Utrech University (the Netherlands): Utrecht (the
        Netherlands).

22.   EEA, *How much bioenergy can Europe produce without harming the environment?*
        2006, European Environment Agency (EEA): Copenhagen (Denmark).

23.   Rettenmaier, N., et al., *Status of Biomass Resource Assessments. Version 1*. 2008,
        Biomass Energy Europe (BEE): Freiburg (Germany).

24.   Sues, A., M. Jurascik, and K.J. Ptasinski, *Exergetic Evaluation of 5 Biowastes-to-
        Biofuels Routes via Gasification* Energy, 2009. Submitted for revision.

25.   Energy Research Centre the Netherlands (ECN), *Phyllis database*. 2008, ECN.

26.   EERE, *Biomass Feedstock Composition and Property Database*, U.S. Department of
        Energy's Office of Energy Efficiency and Renewable Energy.

27.   Prins, M.J., *Thermodynamic analysis of biomass gasification and torrefaction*, in
        Chemistry and Chemical Engineering.Laboratory of Environmental Technology.
        2005, Eindhoven University of Technology: Eindhoven (the Netherlands).

28.   Siemons, R., et al., *Bio-Energy's role in the EU Energy Market. A view of
        developments until 2020*. 2004, BTG biomass technology group BV: Enschede (the
        Netherlands).

29.   Nikolaou, A., M. Remrova, and I. Jeliazkov, *Biomass availability in Europe*, in *Lot
        5: Bioenergy's role in the EU Energy Market*. 2003, Centre for Renewable Energy
        Sources (CRES). BTG Czech Republic s.r.o. ESD Bulgaria Ltd: Pikermi Attiki
        (Greece).

30.   Eubionet2. *Import and Export possibilities and fuel of biomass in 20 European
        countries. Country summary reports*.   2001   [cited; Available from:
        http://eubionet2.ohoi.net/.

31.   Asikainen, A., et al., *Forest Energy Potential in Europe (EU27)*, in *Working Papers
        of the Finnish Forest Research Institute*. 2008, Finnish Forest Research Institute,
        Joensuu Research Unit: Helsinki (Finland).

32.   Wakker, A., et al., *Biofuel and bioenergy implementation scenarios: VIEWLS WP5,
        modelling studies* 2005, Energy Research Centre of the Netherlands (ECN).
        Chalmers University of Technology: Petten (the Netherlands).

33.   Kunikowski, G., et al., *Residue biomass potential inventory results*, in *Renewable
        fuels for advanced power-trains*. 2006, ECBREC Baltic Renewable Energy Centre,
        Central Petroleum Laboratory (European RENEW project): Warsaw (Poland).

34.   de Wit, M. and A.P.C. Faaij, *Biomass Ressources Potential and Related Costs*, in
        REFUEL Work Package 3. 2008, Copernicus Institute. Utrecht University: Utrecht
        (the Netherlands).

35.   MCPFE and UNECE/FAO. *State of Europe's Forests 2003. The MCPFE Report on
        Sustainable Forest Management in Europe*. in *4th Ministerial Conference on the
        Protection of Forests in Europe*. 2003. Vienna (Austria): Ministerial Conference on
        the Protection of Forests in Europe.

36.   Magalhães, A., et al., *Techno-economic assessment of biomass pre-conversion
        processes as a part of biomass-to-liquids line-up.* Biofuels, Bioproducts and
        Biorefining, 2009. 3(6): p. 584-600.

37.   Shahab, S., et al., *Large-scale production, harvest and logistics of switchgrass
        (<I>Panicum virgatum L.</I>) - current technology and envisioning a mature
        technology.* Biofuels, Bioproducts and Biorefining, 2009. 3(2): p. 124-141.

38.   van Laar, P.A., *Het specifiek energiegebruik van transportmodaliteiten*. 1993,
        Faculteit   der   Werktuigbouwkunde   en   Maritieme   Techniek,   Vakgroep
        Transporttechnologie: Technische Universiteit Delft.

39.   Aspen Technology Inc, *Aspen Plus*. 2005: Cambridge, Massachussets (USA).

40. Prins, M.J., K.J. Ptasinski, and F.J.J.G. Janssen, *More efficient biomass gasification via torrefaction.* Energy, 2006. 31(15): p. 3458-3470.

41. Uslu, A., A.P.C. Faaij, and P.C.A. Bergman, *Pre-treatment technologies, and their effect on international bioenergy supply chain logistics. Techno-economic evaluation of torrefaction, fast pyrolysis and pelletisation.* Energy, 2008. 33(8): p. 1206-1223.

42. van der Stelt, M., *Chemistry and Reaction Kinetics of Biowaste Torrefaction*, in *Chemical Reaction and Engineering. Environmental Technology group*. 2011, Eindhoven University of Technology: Eindhoven.

43. Pierik, J.T.G. and A.P.W.M. Curvers, *Logistics and pre-treatment of biomass fuels for gasification and combustion.* . Contribution to the Joule project. Vol. ECN-C-95-038. 1995, Petten (the Netherlands): Energy Research Center of the Netherlands (ECN).

44. Aspentech, *Aspen Icarus Process Evaluator.* 2004: Cambridge, Massachusetts, U.S.A.

45. Peters, M.S., K.D. Timmerhaus, and R.E. West, *Plant Design and Economics for Chemical Engineers*. Fifth edition ed. Science/Engineering/Math. 2002: McGraw-Hill.

46. Wender, I., *Reactions of synthesis gas.* Fuel Processing Technology, 1996. 48(3): p. 189-297.

47. Shiveler, G. *Retrofit of a H2S Selective Amine Absorber Using MellapakPlus Structured Packing*. in *AIChE Meeting*. April 2005. Atlanta, Georgia (USA).

48. Kohl, L.A. and R.B. Nielsen, *Gas Purification*. Fifth edition ed. Gulf Professional Publishing. 1997: Gulf Professional Publishing.

49. Twigg, M.V., *Catalysis Handbook*. 1989: Wolfe Publishing Ltd.

50. Hamelick, C.N. and A.P.C. Faaij. *Future prospects for production of methanol and hydrogen from biomass*. 2001 [cited; Available from: http://copernicus.geog.uu.nl/downloads/nws/e2001-49.pdf.

51. Mozaffarian, M. and R.W.R. Zwart. *Feasibility of biomass / waste-related SNG production technologies* 2003 [cited; Available from: http://www.ecn.nl/docs/library/report/2003/c03066.pdf.

52. Tijmensen, M.J.A., et al., *Exploration of the possibilities for production of Fischer Tropsch liquids and power via biomass gasification.* Biomass and Bioenergy, 2002. 23(2): p. 129-152.

53. Boerrigter, H., H. den Uil, and H.P. Calis. *Green Diesel from Biomass via Fischer-Tropsch synthesis: New Insights in Gas Cleaning and Process Design*. in *Pyrolysis and Gasification of Biomass and Waste, Expert Meeting*. 2002. Strasbourg (France).

54. Paasen, S.V.B., M.K. Cieplik, and N.P. Phokawat. *Gasification of non-woody biomass* 2006 [cited; Available from: http://www.ecn.nl/docs/library/report/2006/e06032.pdf.

55. Dayton, D.C., *Fuel Cell Integration: A Study of the Impacts of Gas Quality and Impurities*. 2001, National Renewable Energy Laboratory: Golden, CO.

56. www.naturalgas.org (2004) *Natural Gas and the Environment*. Volume,

57. Okken, J.P.A., *Waterstof energie-toepassingen; een compilatie van mogelijke technieken in de toekomstige Nederlandse energiehuishouding.* . 1992, Netherlands Energy Research Foundation (ECN): Petten.

58. *SNG specifications for grid injection*. [cited; Available from: http://www.biosng.com/existing-infrastructure/sng-specifications/.

59. Woodcock, K.E. and M. Gottlieb, *Gas, Natural.* Kirk Othmer Encyclopedia of Chemical Technology, 2004. 12(June): p. 365-386.

60. Paisley, M.A. and R.P. Overend. *The SilvaGas Process from Future Energy Resources - A Commercialization Success*. in *12th European Conference and Technology Exhibition on Biomass for Energy, Industry and Climate Protection*. 2002. Amsterdam (the Netherlands): Ferco Energy Resources Corporation.

61. Nikoo, M.B. and N. Mahinpey, *Simulation of biomass gasification in fluidized bed reactor using ASPEN PLUS.* Biomass and Bioenergy. In Press, Corrected Proof.

62.   Shen, L., Y. Gao, and J. Xiao, *Simulation of hydrogen production from biomass gasification in interconnected fluidized beds.* Biomass and Bioenergy, 2008. 32(2): p. 120-127.

63.   Schuster, G., et al., *Biomass steam gasification - an extensive parametric modeling study.* Bioresource Technology, 2001. 77(1): p. 71-79.

64.   Baratieri, M., et al., *Biomass as an energy source: Thermodynamic constraints on the performance of the conversion process.* Bioresource Technology, 2008. 99(15): p. 7063-7073.

65.   Olah, G.A., *Beyond Oil and Gas: The Methanol Economy13.* Angewandte Chemie International Edition, 2005. 44(18): p. 2636-2639.

66.   Simbeck D.R., Dickenson R.L., and O. E.D., *Coal gasification systems: a guide to status, application and economics*. 1983, Palo Alto, CA: EPRI.

67.   Fitzpatrick, T. *LCM, the low cost methanol technology*.   [cited; Available from: http://www.methanol.org/pdfFrame.cfm?pdf=Synetix_Methanol_Production.pdf.

68.   Sunggyu, L., *Methanol Synthesis Technology*. 1st edition ed. 1990, Boca Raton, FL.: CRC Press, Inc.

69.   Ptasinski, K.J., C. Hamelinck, and P.J.A.M. Kerkhof, *Exergy analysis of methanol from the sewage sludge process.* Energy Conversion and Management, 2002. 43(9-12): p. 1445-1457.

70.   Bienert, K., *The status of the Choren Carbo V gasification*, in *2nd European Summer School on Renewable Motor Fuels*. 2007, Choren Industries: Warsaw (Poland).

71.   Opdal, O.A., *Production of synthetic biodiesel via Fischer-Tropsch synthesis. Biomass-To-Liquids in Namdalen, Norway.* 2006.

72.   Prins, M.J., K.J. Ptasinski, and F.J.J.G. Janssen, *Exergetic optimisation of a production process of Fischer-Tropsch fuels from biomass.* Fuel Processing Technology, 2005. 86(4): p. 375-389.

73.   E. van Steen, M.C., *Fischer-Tropsch Catalysts for the Biomass-to-Liquid (BTL)-Process.* Chemical Engineering & Technology, 2008. 31(5): p. 655-666.

74.   Bartholomew, C.H., *Recent technological developments in Fischer-Tropsch catalysis.* Catalysis Letters, 1990. 7(1): p. 303-315.

75.   Chaumette, P., et al., *Higher alcohol and paraffin synthesis on cobalt based catalysts: Comparison of mechanistic aspects.* Topics in Catalysis, 1995. 2(1): p. 117-126.

76.   Lox, E.S. and G.F. Froment, *Kinetics of the Fischer-Tropsch reaction on a precipitated promoted iron catalyst. 2. Kinetic modeling.* Ind. Eng. Chem. Res., 1993. 32(1): p. 71-82.

77.   Neira, M.F., *Upgrading of Wood-Based Fischer-Tropsch Transportation Fuel Production:Process Analysis and Optimization.*, in *Chemical Reaction and Engineering. Environmental Technology group*. 2010, Eindhoven University of Technology: Eindhoven (the Netherlands).

78.   Sudiro, M. and A. Bertucco, *Production of synthetic gasoline and diesel fuel by alternative processes using natural gas and coal: Process simulation and optimization.* Energy. In Press, Corrected Proof.

79.   Hassmann, K. and H.M. Kühne, *Primary energy sources for hydrogen production.* International Journal of Hydrogen Energy, 1993. 18(8): p. 635-640.

80.   Albertazzi, S., et al., *The technical feasibility of biomass gasification for hydrogen production.* Catalysis Today, 2005. 106(1-4): p. 297-300.

81.   Puchner, B., et al. *Biomass Gasification with a CO2-Absorptive Bed Material to Produce a Hydrogen Rich Gas*. in *14th European Biomass Conference & Exhibition, Biomass for Energy, Industry and Climate Protection*. 2005. Paris (France): ETA Florence and WIP Renewable Energies.

82.   Dupont, V., *Steam reforming of sunflower oil for hydrogen gas production.* Helia, 2007. 30(46): p. 103-132.

83.   Williams, R.H. and R.E. Katofsky, *Methanol and hydrogen from biomass for transportation with comparisons to methanol and hydrogen from natural gas and*

coal 1995, Center for Energy and Environmental Studies. Princeton University: Princenton (USA).

84. Katofsky, R.E., *The production of fluid fuels from biomass*. 1993.
85. Koroneos, C., A. Dompros, and G. Roumbas, *Hydrogen production via biomass gasification--A life cycle assessment approach.* Chemical Engineering and Processing, 2007. In Press, Corrected Proof.
86. Spliethoff, H., *Status of Biomass Gasification for Power Production.* IFRF Combustion Journal, 2001. Article number 200109: p. 1-25.
87. *Integrated European Network for Biomass Co-firing. First state-of-the-art report*. 2006, NetBioCof: Bremerhaven (Germany).
88. Koppejan, J., *Database of Biomass Cofiring initiatives*. 2005, IEA Bioenergy Task 32.
89. van Bibber, L., et al., *Baseline Technical and Economic Assessment of a Commercial Scale Fischer-Tropsch Liquids Facility*. 2007, National Energy Technology Laboratory (NETL): Pittsburgh (PA, USA).
90. Tanaka, N., *Worldwide Trends in Energy Use and Efficiency. Key Insights from IEA Indicator Analysis*, in *In support of the G8 Plan of Action*. 2008, International Energy Agency (IEA): Paris (France).
91. Wright, M.M. and R.C. Brown, *Comparative economics of biorefineries based on the biochemical and thermochemical platforms.* Biofuels, Bioproducts and Biorefining, 2007. 1(1): p. 49-56.
92. Hermann, W.A., *Quantifying global exergy resources.* Energy, 2006. 31(12): p. 1685-1702.
93. Hovelius, K. and P.-A. Hansson, *Energy- and exergy analysis of rape seed oil methyl ester (RME) production under Swedish conditions.* Biomass and Bioenergy, 1999. 17(4): p. 279-290.
94. Moran, M.J., *Availability analysis: a guide to efficient energy use* ed. A.S.o.M. Engineers. 1990, New York: AsME. 260 pages.
95. Cornelissen, R.L., *Thermodynamics and sustainable development, the use of exergy analysis and the reduction of irreversibility*, in *Laboratory of Thermal Engineering, Department of Mechanical Engineering*. 1997, University of Twente, Netherlands.
96. Szargut, J., D.R. Morris, and F.R. Steward, *Exergy analysis of thermal, chemical, and metallurgical processes*. 1988, Berlin: Springer. 322 pages.
97. Barin, I., *Thermochemical data of pure substances: part I and II.* 1989, Weinheim, Germany: VCH Verlagsgesellschaft GmbH.
98. Kotas, T.J., *The exergy method of thermal plant analysis*. 1995, Malabar, Florida: Krieger.
99. Sues, A., M. Jurascík, and K. Ptasinski, *Exergetic evaluation of 5 biowastes-to-biofuels routes via gasification.* Energy, 2010. 35(2): p. 996-1007.
100. Duret, A., C. Friedli, and F. Maréchal, *Process design of Synthetic Natural Gas (SNG) production using wood gasification.* Journal of Cleaner Production, 2005. 13(15): p. 1434-1446.
101. Gassner, M. and F. Maréchal, *Thermo-economic process model for thermochemical production of Synthetic Natural Gas (SNG) from lignocellulosic biomass.* Biomass and Bioenergy, 2009. 33(11): p. 1587-1604.
102. Hamelinck, C.N. and A. Faaij. *Future prospects for production of methanol and hydrogen from biomass*. 2001 [cited; Available from: http://copernicus.geog.uu.nl/downloads/nws/e2001-49.pdf.
103. Boerrigter, H., *Economy of Biomass-to-Liquids (BTL) plants*. 2006, ECN (Energy research Centre of the Netherlands). Unit ECN Biomass, Coal & Environmental Research: Petten (the Netherlands).
104. Hamelinck, C.N., et al., *Production of FT transportation fuels from biomass; technical options, process analysis and optimisation, and development potential.* Energy, 2004. 29(11): p. 1743-1771.

105.   Vogel, A., F. Muller-Langer, and M. Kaltschmitt. *Technical and economic assessment of existing and future BTL-plants. State of knowledge 2008*. in *16th European Biomass Conference & Exhibition. From research to Industry Markets*. 2008. Valencia (Spain): ETA-Florence Renewable Technologies, and WIP-Renewable Technologies.

106.   Toonssen, R., N. Woudstra, and A.H.M. Verkooijen, *Exergy analysis of hydrogen production plants based on biomass gasification.* International Journal of Hydrogen Energy, 2008. 33(15): p. 4074-4082.

107.   Ptasinski, K.J., *Thermodynamic efficiency of biomass gasification and biofuels conversion.* Biofuels, Bioproducts and Biorefining, 2008. 2(3): p. 239-253.

108.   Boissonnet, G., et al. *Process simulation, thermal and economic assessment of several technical options for BTL production*. in *16th European Biomass Conference & Exhibition. From research to Industry Markets.* 2008. Valencia (Spain): ETA-Florence Renewable Technologies, and WIP-Renewable Technologies.

109.   Brown, D., et al., *Thermo-economic analysis for the optimal conceptual design of biomass gasification energy conversion systems.* Applied Thermal Engineering, 2009. 29(11-12): p. 2137-2152.

110.   Mann, M.K. and P.L. Spath. *Life Cycle Assessment of a Biomass Gasification Combined-Cycle System*. Life Cycle Assessment 1997 [cited; Available from: http://www.nrel.gov/docs/legosti/fy98/23076.pdf.

111.   Helikson, H., *Energy Efficiency & Environmental News: The Energy and Economics of Fertilizers*. 1991, North Carolina Division of Pollution Prevention and Environmental Assistance: Gainesville (Florida, U.S.).

112.   Weiss, M.A., et al., *On the road 2020. A life-cycle analysis of new automobile technologies*. 2000, Energy Laboratory. Massachussets Institute of Technology: Cambridge, Massachussets (U.S.A).

113.   Ruselowski, G.e.a., *Volume 2: Well-to-Wheel Energy Use and Greenhouse Gas Emissions of Advanced Fuel/Vehicle Systems. North American Analysis.* 2001, General Motors. Global Alternative Propulsion Center (GAPC). Argonne National Laboratory. BP. Exxon Mobil and Shell.

114.   Kaltschmitt, M., G.A. Reinhardt, and T. Stelzer, *Life cycle analysis of biofuels under different environmental aspects.* Biomass and Bioenergy, 1997. 12(2): p. 121-134.

115.   Elghali, L., et al., *Developing a sustainability framework for the assessment of bioenergy systems.* Energy Policy, 2007. 35(12): p. 6075-6083.

116.   Cramer, J., et al., *Testing framework for sustainable biomass. Final report from the project group "Sustainable production of biomass"*, in *Creative Energy. Energy Transition*. 2007.

117.   *Proposal for a directive of the european parliament and of the council on the promotion of the use of renewable sources*. 2008, Commission of the european communities.

118.   *ISO 14040. Environmental management. Life cycle assessment. Principles and framework*. 1997.

119.   *ISO 14041. Environmental management. Life cycle assessment. Goal and scope definition and inventory analysis*. 1998.

120.   Heller, M.C., G.A. Keoleian, and T.A. Volk, *Life cycle assessment of a willow bioenergy cropping system.* Biomass and Bioenergy, 2003. 25(2): p. 147-165.

121.   *http://www.deere.com/es_MX/ag/homepage/tips/hectareas_hora.html.*   [cited; Available   from: http://www.deere.com/es_MX/ag/homepage/tips/hectareas_hora.html.

122.   PRé_Consultants, *SimaPro LCA software*. 2007: Amersfoort (the Netherlands).

123.   Spath, P. and M.K. Mann, *Life Cycle Assessment of Hydrogen Production via Natural Gas Steam Reforming*. 2001, NREL National Renewable Laboratory: Golden, Colorado (US).

124.   Fiaschi, D. and L. Lombardi, *Integrated Gasifier Combined Cycle Plant with Integrated CO2 – H2S Removal: Performance Analysis, Life Cycle Assessment and*

Exergetic Life Cycle Assessment. Int. J. Applied Thermodynamics, 2002. 5(1): p. 13-24.

125. *Eco-indicator'99*, PRé Consultants

126. Styles, D., F. Thorne, and M.B. Jones, *Energy crops in Ireland: An economic comparison of willow and Miscanthus production with conventional farming systems.* Biomass and Bioenergy, 2008. 32(5): p. 407-421.

127. Carpentieri, M., A. Corti, and L. Lombardi, *Life cycle assessment (LCA) of an integrated biomass gasification combined cycle (IBGCC) with CO2 removal.* Energy Conversion and Management, 2005. 46(11-12): p. 1790-1808.

128. Iannone, F. and D. Zaninelli. *Life cycle assessment applications to electrical energy production: a possible sustainability analysis tool.* in *Power Engineering Society General Meeting, 2007. IEEE.* 2007.

129. Gagnon, L., C. Bélanger, and Y. Uchiyama, *Life-cycle assessment of electricity generation options: The status of research in year 2001.* Energy Policy, 2002. 30(14): p. 1267-1278.

130. Varun, I.K. Bhat, and R. Prakash, *LCA of renewable energy for electricity generation systems--A review.* Renewable and Sustainable Energy Reviews, 2009. 13(5): p. 1067-1073.

131. Rafaschieri, A., M. Rapaccini, and G. Manfrida, *Life Cycle Assessment of electricity production from poplar energy crops compared with conventional fossil fuels.* Energy Conversion and Management, 1999. 40(14): p. 1477-1493.

132. Pehnt, M., *Dynamic life cycle assessment (LCA) of renewable energy technologies.* Renewable Energy, 2006. 31(1): p. 55-71.

133. Mann, M.K. and P. Spath. *A Comparison of the Environmental Consequences of Power from Biomass, Coal, and Natural Gas.* in *internet-based InLCA/LCM.* 2002. Portland (Oregon, US): American Center for Life Cycle Assessment (ACLCA).

134. *The Model of the Eco-costs / Value Ratio (EVR). An LCA based decision support tool for the de-linking of economy and ecology.* 2007, Delft University of Technology

135. Pehnt, M., *Assessing future energy and transport systems: the case of fuel cells.* The International Journal of Life Cycle Assessment, 2003. 8(6): p. 365-378.

136. Felder, R. and R. Dones, *Evaluation of ecological impacts of synthetic natural gas from wood used in current heating and car systems.* Biomass and Bioenergy, 2007. 31(6): p. 403-415.

137. Koroneos, C., et al., *Life cycle assessment of hydrogen fuel production processes.* International Journal of Hydrogen Energy, 2004. 29(14): p. 1443-1450.

138. Patyk, A. and A.G. Reinhardt. *Life cycle analysis of biofuels for transportation used in fuel cells and conventional technologies under European conditions.* 2001 [cited; Available from: http://www.p2pays.org/ref/35/34357.pdf.

139. Baitz, M., et al., *Comparative Life Cycle Assessment for SunDiesel (Choren Process) and Conventional Diesel Fuel.* 2004, PE-Europen GmbH: Leinfelden-Echterdingen (Germany).

140. Jungbluth, N., et al. *RENEW: Renewable fuels for advanced powertrains. Sixth Frame-work Programme: Sustainable Energy Systems, Deliverable: D 5.2.15.* 2007 [cited; Available from: Retrieved from www.esu-services.ch/renew.htm.

141. Edwards, R., et al., *Well-to-Wheels analysis of future automotive fuels and powertrains in the European context.* 2007, EUCAR, CONCAWE and JRC/IES.: Petten (the Netherlands).

142. Reinhardt, J. *Environmental impacts of various options of biofuels for transportation.* in *Seminar on Bioenergy: Food, Fuel or Forest ?* 2007. Wageningen (the Netherlands): Institute for Energy and Environmental Research Heidelberg (IFEU, Germany).

143. Luo, L., E. van der Voet, and G. Huppes, *Life cycle assessment and life cycle costing of bioethanol from sugarcane in Brazil.* Renewable and Sustainable Energy Reviews. 13(6-7): p. 1613-1619.

144.   Kim, S. and B.E. Dale, *Life cycle assessment of various cropping systems utilized for producing biofuels: Bioethanol and biodiesel.* Biomass and Bioenergy, 2005. 29(6): p. 426-439.

145.   Spirinckx, C. and D. Ceuterick, *Biodiesel and fossil diesel fuel: Comparative life cycle assessment.* The International Journal of Life Cycle Assessment, 1996. 1(3): p. 127-132.

146.   Halleux, H., et al., *Comparative life cycle assessment of two biofuels ethanol from sugar beet and rapeseed methyl ester.* The International Journal of Life Cycle Assessment, 2008. 13(3): p. 184-190.

147.   Phillips, S., et al., *Thermochemical Ethanol via Indirect Gasification and Mixed Alcohol Synthesis of Lignocellulosic Biomass*, in *Innovation for Our Energy Future*. 2007, NREL National Renewable Energy Laboratory: Springfield (USA).

148.   Komiyama, H., et al., *Assessment of energy systems by using biomass plantation.* Fuel, 2001. 80(5): p. 707-715.

149.   Hamelinck, C.N., G.v. Hooijdonk, and A.P.C. Faaij, *Ethanol from lignocellulosic biomass: techno-economic performance in short-, middle- and long-term.* Biomass and Bioenergy, 2005. 28(4): p. 384-410.

150.   Hamelinck, C.N., *Outlook for advanced biofuels*, in *Faculteit Scheikunde (Chemical Engineering*. 2004, Utrecht University: Utrecht (the Netherlands).

151.   Larson, E.D. and R.E. Katofsky, *Production of Methanol and Hydrogen from Biomass*. 1992, Princeton University, Center for Energy and Environmental Studies: Princeton (USA).

152.   Craig, K.R. and M.K. Mann, *Cost and Performance Analysis of Biomass-Based Integrated Gasification Combined-Cycle (BIGCC) Power Systems*. 1996, National Renewable Energy Laboratory: Golden, Colorado (USA).

153.   Demirbas, A., *Progress and recent trends in biodiesel fuels.* Energy Conversion and Management. In Press, Corrected Proof.

154.   Haas, M.J., et al., *A process model to estimate biodiesel production costs.* Bioresource Technology, 2006. 97(4): p. 671-678.

155.   Davila-Vazquez, G., et al., *Fermentative biohydrogen production: trends and perspectives.* Reviews in Environmental Science and Biotechnology, 2008. 7(1): p. 27-45.

156.   Tsagarakis, K.P. and C. Papadogiannis, *Technical and economic evaluation of the biogas utilization for energy production at Iraklio Municipality, Greece.* Energy Conversion and Management, 2006. 47(7-8): p. 844-857.

157.   Walla, C. and W. Schneeberger, *The optimal size for biogas plants.* Biomass and Bioenergy, 2008. 32(6): p. 551-557.

158.   *Platinum and hydrogen for fuel cell vehicles*.   [cited 2010 20th April]; Available from:
        http://www.dft.gov.uk/pgr/roads/environment/research/cqvcf/platinumandhydrogenforfuelce3838?page=4.

159.   Seiffert, M., et al., *BioSNG – Demonstration of the production and utilization of synthetic natural gas (SNG) from solid biofuels. Specific Targeted Research or Innovation Project*. 2009, German Biomass Research Centre (DBFZ). Technical University of Viena (TUV). Repotec. Paul Scherrer Institute (PSI). : Viena (Austria).

160.   *International resource costs of biodiesel and bioethanol*.   [cited 2010 20th April]; Available   from:
        http://www.dft.gov.uk/pgr/roads/environment/research/cqvcf/platinumandhydrogenforfuelce3838?page=4.

161.   Jørgen Koch, H., *Automotive Fuels for the Future. The Search for Alternatives.* 1999, IEA (International Energy Agency): Paris (France).

162.   Seider, W.D., J.D. Seader, and D.R. Lewin, *Product and process design principles : synthesis, analysis and evaluation*. 2nd edition ed. 2003: Wiley.

163.   McKeough, P. and E. Kurkela. *Detailed comparison of efficiencies and costs of producing FT liquids, Methanol, SND and hydrogen from biomass*. in *15th European*

Biomass Conference & Exhibition. 2007. Berlin (Spain): EtaFlorence Renwable Technologies and WIP Renewable Energies.

164. Klimantos, P., et al., *Air-blown biomass gasification combined cycles (BGCC): System analysis and economic assessment.* Energy, 2009. 34(5): p. 708-714.

165. Varela, M., R. Sáez, and H. Audus, *Large-scale economic integration of electricity from short-rotation woody crops.* Solar Energy, 2001. 70(2): p. 95-107.

166. Hamelinck, C.N., R.A.A. Suurs, and A.P.C. Faaij, *International bioenergy transport costs and energy balance.* Biomass and Bioenergy, 2005. 29(2): p. 114-134.

167. Mozaffarian, M., et al., *Green Gas as SNG Synthetic Natural Gas a renewable fuel with conventional quality*, in *Science in Thermal and Chemical Biomass Conversion*. 2004, ECN: Vancouver Island, BC, Canada.

168. Spath, P., A. Aden, and T. Eggeman, *Biomass to Hydrogen Production. Detailed Design May and Economics Utilizing the Battelle Columbus Laboratory Indirectly-Heated Gasifier*. 2005, National Renewable Energy Laboratory (NREL): Golden (Colorado, USA).

169. Corning, P.A., *Thermoeconomics: Beyond the Second Law.* Journal of Bioeconomics, 2002. 4(1): p. 57-88.

170. Talens Peiró, L., et al., *Life cycle assessment (LCA) and exergetic life cycle assessment (ELCA) of the production of biodiesel from used cooking oil (UCO).* Energy, 2010. 35(2): p. 889-893.

171. Lombardi, L., *Life cycle assessment (LCA) and exergetic life cycle assessment (ELCA) of a semi-closed gas turbine cycle with CO2 chemical absorption.* Energy Conversion and Management, 2001. 42(1): p. 101-114.

172. Ptasinski, K.J., M.N. Koymans, and H.H.G. Verspagen, *Performance of the Dutch Energy Sector based on energy, exergy and Extended Exergy Accounting.* Energy, 2006. 31(15): p. 3135-3144.

173. *Directive 2003/30/EC. Promotion of the use of biofuels and other renewable fuels for transport* May 2003, European Parliament and the Council.

174. Steenberghen, T. and E. López, *Overcoming barriers to the implementation of alternative fuels for road transport in Europe.* Journal of Cleaner Production, 2008. 16(5): p. 577-590.

175. van Thuijl, E. and E. Deurwaarder, *European biofuel policies in retrospect*. 2006, Energy Research Centre (ECN): Petten (the Netherlands).

176. Lieberz, S. and K. Ramos, *Oilseeds and Products Biodiesel in Germany. An Overview.*, in *Global Agriculture Information Network*. 2002, United States Department of Agriculture (USDA): Washington (DC, USA).

177. Potocnik, J., *Biofuels in the European Union. A vision for 2030 and beyond.* 2006, Biofuels Research Advisory Council. Directorate General for Research Sustainable Energy Systems: Luxembourg (Luxembourg).

178. Zwart, R.W.R., et al. *Production of Synthetic Natural Gas (SNG) from Biomass*. 2006 [cited; Available from: http://www.ecn.nl/docs/library/report/2006/e06018.pdf.

179. Howes, T., *Biomass Action Plan - EC Energy & Transport DG*. 2010, European Comission. Directorate General for Energy and Transport

180. Vogtländer, J.G., *Corrugated Board Boxes and Plastic Container Systems: An analysis of costs and eco-costs*. 2004, FEFCO.

181. Boerrigter, H. and R.W. Zwart. *High efficient co-production of Fischer-Tropsch (FT) transportation fuels and Substitute Natural Gas (SNG) from biomass* 2004 [cited; Available from: http://www.ecn.nl/publications/default.aspx?nr=c04001.

182. Bechtel, *Aspen Process Flowsheet Simulation Model of a Battelle Biomass-Based Gasification, Fischer-Tropsch Liquefaction and Combined-Cycle Power Plant*. 1998, U.S. Department of Energy. Office of Fossil Energy. Federal Energy Technology Center: Morgantown, West Virginia (U.S.).

List of Publications

Refereed journal publications, 2010
A. Sues Caula, H.J. Veringa, *Are European Bioenergy Targets Achievable? (Part A): Extended efficiency analysis of biomass-to-biofuels and bioelectricity chains.* **In Progress.**

A. Sues Caula, H.J. Veringa, *Are European Bioenergy Targets Achievable? (Part B): Well-to-Wheel Environmental impact analysis of biomass-to-biofuels and bioelectricity chains.* **In Progress.**

A. Sues Caula, H.J. Veringa, *Are European Bioenergy Targets Achievable? (Part C): Economic analysis of biomass-to-biofuels and bioelectricity chains in European countries.* **In Progress.**

A. Sues Caula, H.J. Veringa, *Are European Bioenergy Targets Achievable? (Part D): Multidimensional 3E Sustainability model and its application to Europe.* **In Progress.**

2009
A. Sues Caula, M. Jurascik, K.J. Ptasinski, Exergetic evaluation of 5 biowastes-to-biofuels routes via gasification, Energy Int. J., 35(2), 996-1007, (2009).

M. Jurascik, A. Sues Caula, K.J. Ptasinski, Exergy analysis of synthetic natural gas production method from biomass, Energy Int. J., 35(2), 880-888, (2009).

M. Jurascik, A. Sues Caula, K.J. Ptasinski, Optimization of biomass-to-synthetic natural gas conversion technology based on exergy analysis, Energy Environ. Sci., 2(7), 791-801, (2009)

Books and book chapters and edited books, 2009
K.J. Ptasinski, A. Sues Caula, M. Jurascik, *Biowastes-to-biofuels routes via gasification*, in Biomass Gasification: Chemistry, Processes and Applications; Editors: J-P. Badeau & A. Levi (Eds.), pp. 87-197, Nova Publishers, Book Chapter 9781607417156 (2009).

Refereed proceedings, 2010
A. Sues Caula, H.J. Veringa, *Selection of the best Biomass-to-Bioenergy route for its implementation in the European Energy sector. An Integrated Efficiency, economic and Environmental Analyasis*, in Proc. The 3rd International Multi-Conference on Engineering and Technological Innovation (IMETI 2010): Editors: N.Callaos, H.W. Chu, A.Tremante, C.D. Zinn, Orlando, U.S. pp.324-329, volume I (2010).

2008

A. Sues Caula, M. Jurascik, K.J. Ptasinski, *Exergetic analysis of 5 biowastes-to-biofuels routes for Friesland province (The Netherlands)*, in Proc. 21st Int. Conf. on Efficiency, Cost, Optimization, Simulation and Environmental Impact of Energy Systems (ECOS 2008); Krakow, Poland, pp. 1233-1240, (2008).

M. Jurascik, A. Sues Caula, K.J. Ptasinski, *Exergy analysis of synthetic natural gas production from biomass*, in Proc. 21st Int. Conf. on Efficiency, Cost, Optimization, Simulation and Environmental Impact of Energy Systems (ECOS 2008); Editors: -, Krakow, Poland, 1303-1310, (2008).

A. Sues Caula, M. Jurascik, K.J. Ptasinski, *DSS Decision Support System Biowastes-to-biofuels for the province of Friesland. An exergetic efficiency comparison of five conversion routes*, in Proc. 16th Eur. Biomass Conf. & Exh. from Research to Industry Markets; Valencia, Spain, pp. 1, (2008).

M. Jurascik, A. Sues Caula, K.J. Ptasinski, *Optimization of biomass to SNG conversion technology*, in Proc. 16th Eur. Biomass Conf. & Exh. from Research to Industry Markets; Valencia, Spain, pp. 1, (2008).

2007

M. Jurascik, A. Sues Caula, K.J. Ptasinski, *Optimization of biomass (waste)-to-biofuels conversion technology*, in Netherlands Process Technology Symposium; Veldhoven, Netherlands, pp. 1, (2007).

A. Sues Caula, M. Jurascik, K.J. Ptasinski, *DSS (Decision Support System) biowaste-to-biofuels in the region of Friesland*, in Netherlands Process Technology Symposium; Editors: -, Veldhoven, Netherlands, pp. 1, (2007).

Non-refereed proceedings
2008

A. Sues Caula, M. Jurascik, K.J. Ptasinski, H.J. Veringa, *Biowaste-to-biofuels via gasification: Exergetic efficiency of 5 conversion routes*, in Netherlands Process Technology Symposium (NPS-8); Editors: -, Veldhoven, Netherlands, pp. 1, (2008).

M. Jurascik, A. Sues Caula, K.J. Ptasinski, *Exergy analysis of synthetic natural gas production method from biomass*, in Workshop Biomass Gasification Technologies (BIOGASTECH); Editors: -, Gebze, Turkey, pp. 1, (2008).

Appendix A.   Logistics costs

Table 0-1: *Coefficients "a" and "b" for the calculation of linear transport costs (l_c), where $l_c=a+br$ and "r" is the collection distance. Values are given for the reference year of 2007.*

Nr	Code	Country	Forestry biomass		Straw residues	
			a	b	a	b
EU-1	AT	Austria	10.776	0.303	15.256	0.375
EU-2	BE	Belgium	12.516	0.320	17.702	0.399
EU-3	BG	Bulgaria	1.742	0.195	2.533	0.225
EU-4	CZ	Czech Republic	3.907	0.222	5.598	0.262
EU-5	DK	Denmark	13.227	0.337	18.707	0.420
EU-6	EE	Estonia	3.451	0.197	4.952	0.236
EU-7	FI	Finland	10.863	0.299	15.937	0.370
EU-8	FR	France	9.966	0.299	14.117	0.367
EU-9	DE	Germany	10.848	0.318	15.308	0.390
EU-10	GR	Greece	7.290	0.255	10.353	0.311
EU-11	HU	Hungary	3.641	0.225	5.221	0.265
EU-12	IE	Ireland	1.047	0.201	1.531	0.229
EU-13	IT	Italy	9.558	0.303	13.547	0.369
EU-14	LV	Latvia	2.662	0.193	3.838	0.228
EU-15	LT	Lithuania	2.908	0.194	4.185	0.230
EU-16	NL	Netherlands	10.900	0.311	15.433	0.383
EU-17	PL	Poland	3.515	0.214	5.043	0.253
EU-18	PT	Portugal	5.124	0.244	7.311	0.290
EU-19	RO	Romania	2.299	0.201	3.323	0.234
EU-20	SK	Slovakia	3.384	0.229	4.860	0.268
EU-21	SI	Slovenia	5.395	0.235	7.688	0.282
EU-22	ES	Spain	6.895	0.251	9.799	0.305
EU-23	SE	Sweden	12.735	0.332	18.012	0.412
EU-24	UK	United Kingdom	10.650	0.348	15.091	0.419

Table 0-2: *General assumptions made to calculate linear transportation costs for EU-24.*

Section	Parameter	Value	Units
Vehicle design	η_t (truck efficiency)	0.4	-
	f_r (rolling resistance model)	0.01	-
	C_w (drag coefficient)	0.26	-
	ρ (fluid density)	1.204	air, 20°C
	g (gravity)	9.8	kg/m.s^2
	v (speed)	60	km/hr
	m_l (payload biomass per truck)	16.8 wood 12.0 straw	tones
	m_v (gross weight truck)	44.8 wood 32.0 straw	tones
	A (frontal area)	4.2	m^2
	Life-time truck	7	years
Operation	t_{max} (max driving hours per day & truck)	18	hr/day.truck
	t'_{max} (max driving days per year & truck)	250	day/yr.truck
	Max.working hours per year & driver	2000	hr/yr.driver
	Diesel price (@ 36 MJ/lt)	eurostat	€/lt
	Lubrication oil cost	0.005	€/km [180]
	Tires replacement cost	0.064	€/km [180]
	Fleet maintenance cost	0.096	€/km [180]
	Labor price (administration/drivers)	eurostat	€/hr
	Extra personnel per driver	0.8	-
	Corporative tax rates	eurostat	%
	Local taxes	3	% of FCI
	Insurance	1	% of FCI
	Overheads	50	% maintenance
Others	Life-time project	30	years
	i_F (inflation (diesel, lub.oil, tires))	4	%/year
	i_M , i_L (inflation maintenance, labor)	2	%/year
	i_T , i_I (inflation taxes & insurance)	2	%/year
	Buildings	8	% of fleet
	Contingency	2	% of fleet
	Legal expenses	5	% of fleet
	Working capital	15%	TCI
	Payback time	3	years
	ROI (Return on Investment)	11	%

Appendix B. Operational conditions in Aspen Plus simulations

Table 0-3: *Comparison of the main operational parameters for the five conversion chains*

Section	Parameter	SNG	Methanol	F-T fuels	Hydrogen	Electricity
Drying	Final MC	10%	10%	10%	10%	10%
	Temperature	115 °C	115 °C	115 °C	115 °C	115 °C
Gasifier	Pressure	1 bar	1 bar	1 bar	1 bar	1 bar
	Temperature	700 °C	900 °C	900 °C	700 °C	900 °C
	Heating	Indirect	Direct	Direct	Indirect	Direct
	Agent	Steam	Air	Air	Steam	Air
Cleaning: CO_2 and H_2S removal	T - feed	55 °C	55 °C	55 °C	55 °C	55 °C
	T - solvent	40 °C	40 °C	40 °C	40 °C	40 °C
	T - stripper	105-110 °C	105-110 °C	105-110 °C	105-110 °C	105-110 °C
	P- absorber	1 bar	1 bar	1 bar	1 bar	1 bar
	P- stripper	2 bar	2 bar	2 bar	2 bar	2 bar
	Solvent	MDEA	MDEA	MDEA	MDEA	MDEA
Cleaning: NH_3 removal	Temperature	40 °C	40 °C	40 °C	40 °C	40 °C
	Pressure	1 bar	1 bar	1 bar	1 bar	1 bar
	Solvent	H_2SO_4	H_2SO_4	H_2SO_4	H_2SO_4	H_2SO_4
WGS reactor or Reformer*	Pressure	28 bar	25 bar	25 bar	* 35 bar	-
	Temperature	398°C	330°C	330°C	* 850°C	-
	Catalyst	Ni-based	Cu/Al_2O_3	Cu/Al_2O_3	*Ni-based	-
	H_2: CO ratio	3	2	2.13	-	-
Catalytic reactors	Name	Methanation	Methanol reactor	F-T reactor	HTS &LTS	-
	Nr reactors	4	1	1	2	-
	Pressure	28 bar	77 bar	23 bar	HTS: 30 bar LTS: 25 bar	-
	Temperature	398-300 °C	200 °C	260 °C	HTS: 435 °C LTS: 220 °C	-
	Catalyst	Ni-based	Cu/Zn/Al	Co-based	Fe_3O_4-Cr_2O_3 ZnO-CuO	-
Upgrading	Final stages	H_2O & CO_2 removal Compression	Phase separation Distillation	Distillation Fractioning	CO_2 removal PSA separation	Combined cycle
Final product	Specification	Wobbe index: 43.5 MJ/Nm^3	Methanol purity: $\leq$ 98.6 %	Aliphatic hydrocarbons	H_2 purity: 99 %	-

# Appendix C.   SNG simulation in Aspen Plus
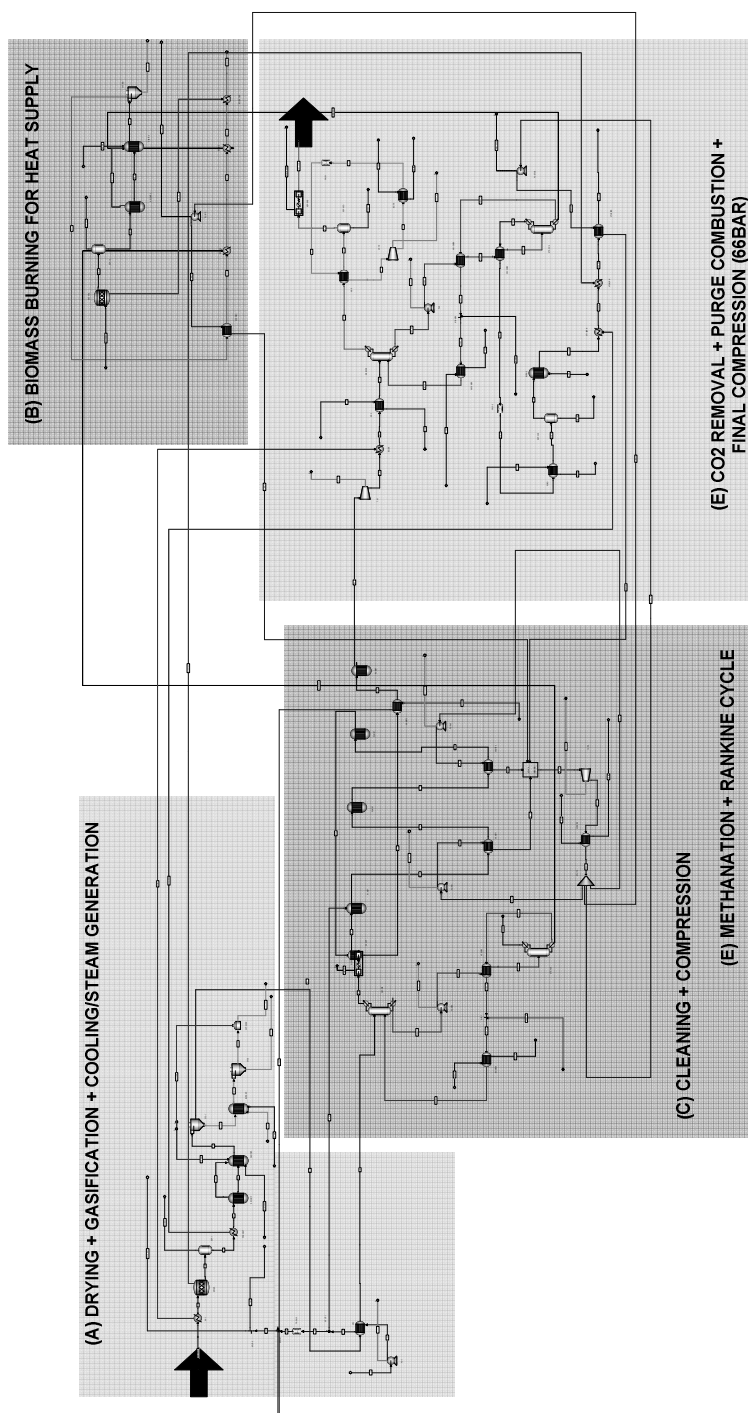
Figure 0.1: *Identification of main sections in the bio-SNG simulation in Aspen Plus.*
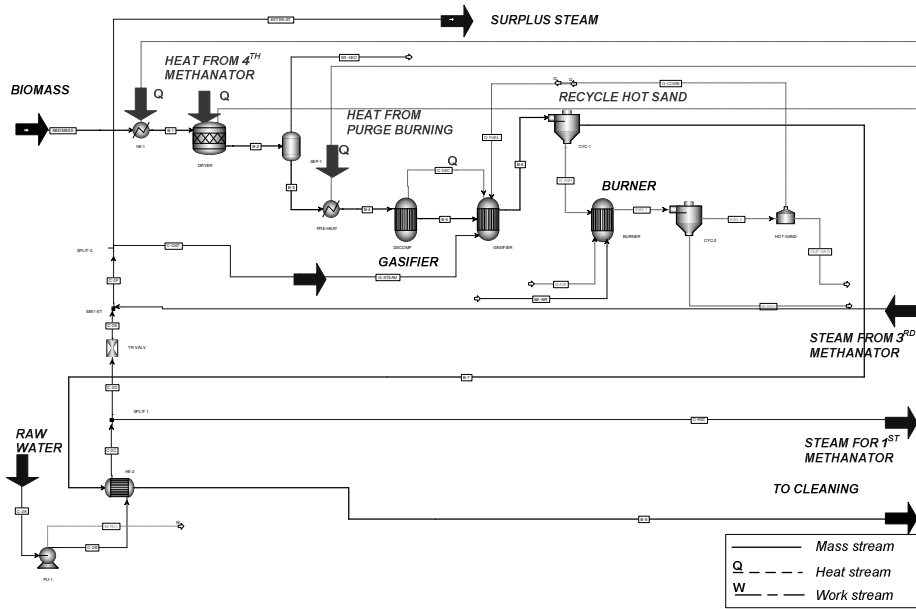
Figure 0.2: Section (A): *Simulation of the drying, gasification and cooling/HRSG for SNG.*
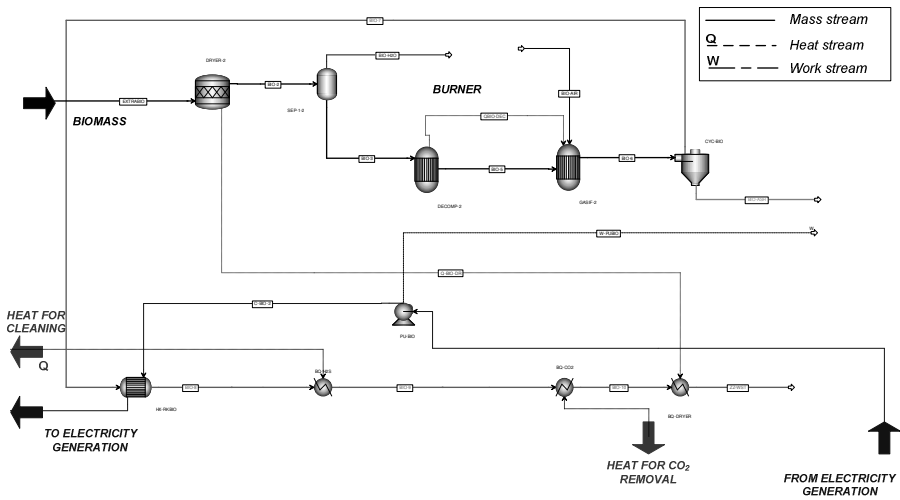
**Figure 0.3: Sections (B):** *Extra biomass burning to supply heat for cleaning & CO$_2$ removal.*
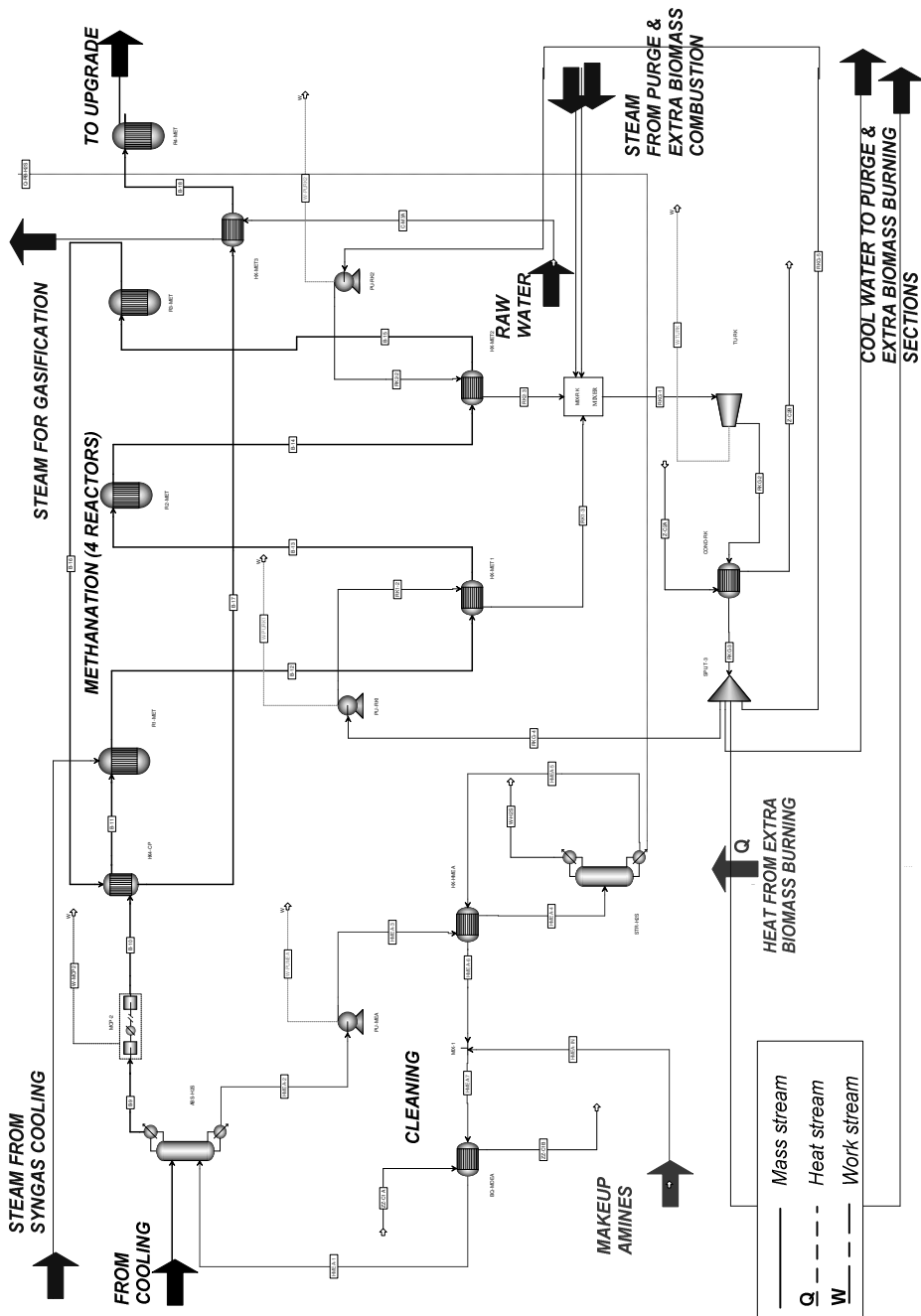
**Figure 0.4: Sections (C/D):** *Simulation of cleaning, compressor, methanation+Rankine cycle.*
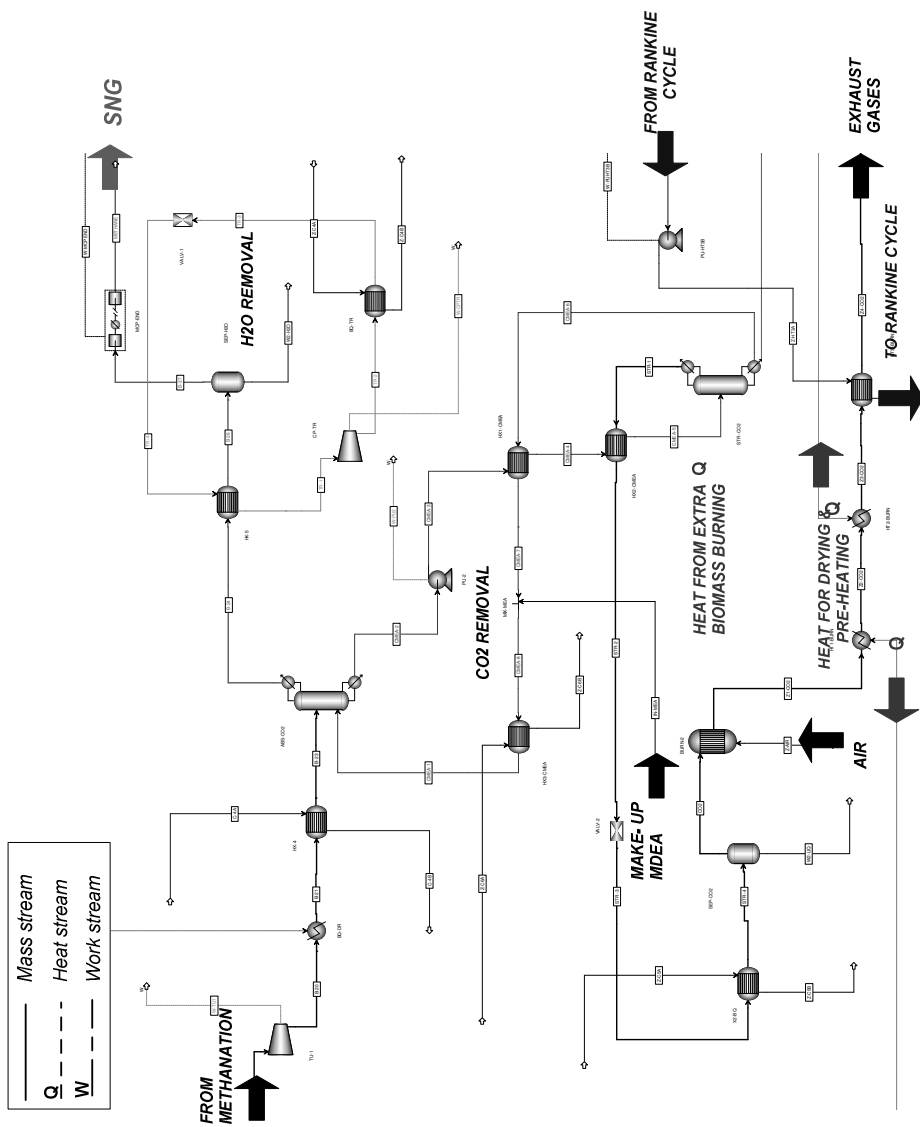
Figure 0.5: Sections (E): *CO_2 and H_2O removal, purge combustion & final compression.*

# Appendix D.   Biomass-to-Methanol simulation in Aspen Plus
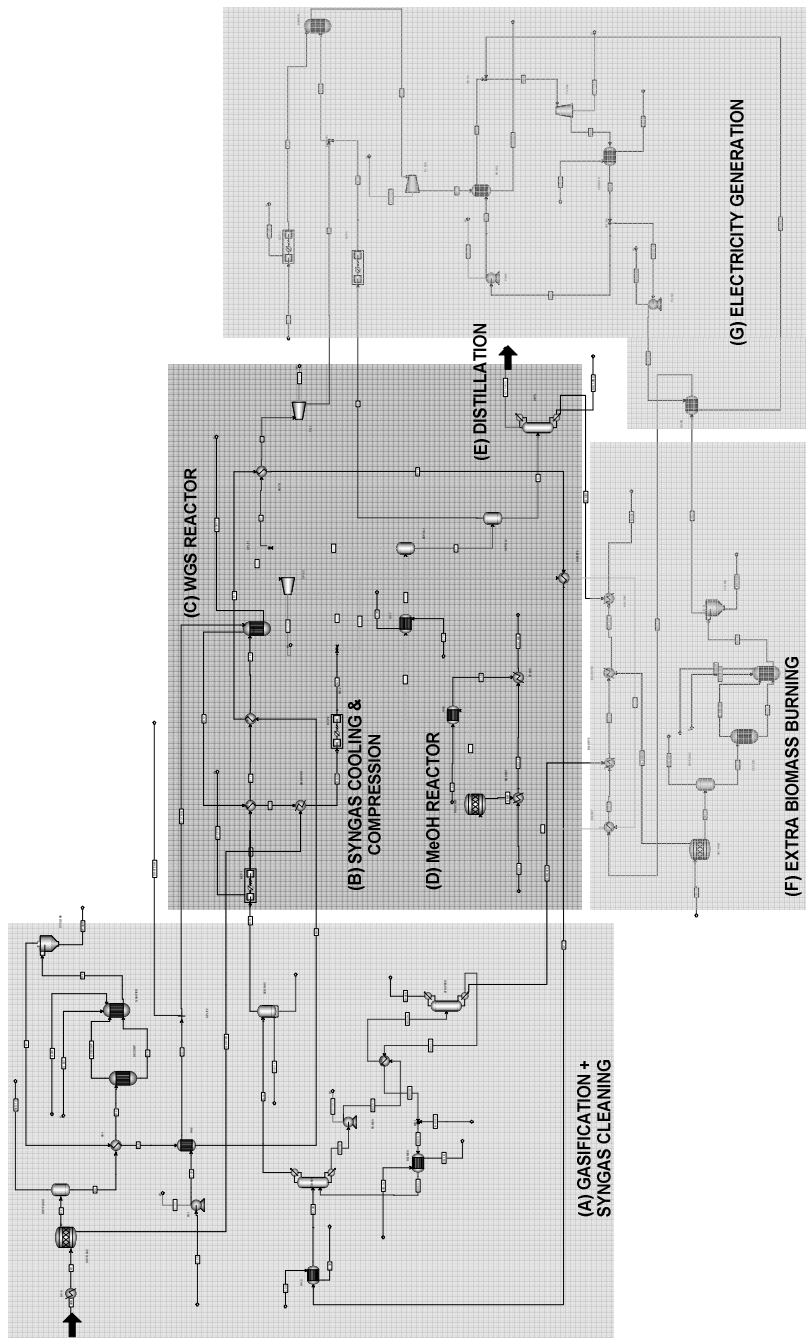
Figure 0.6: Identification of main sections in the bio-MeOH simulation in Aspen Plus.
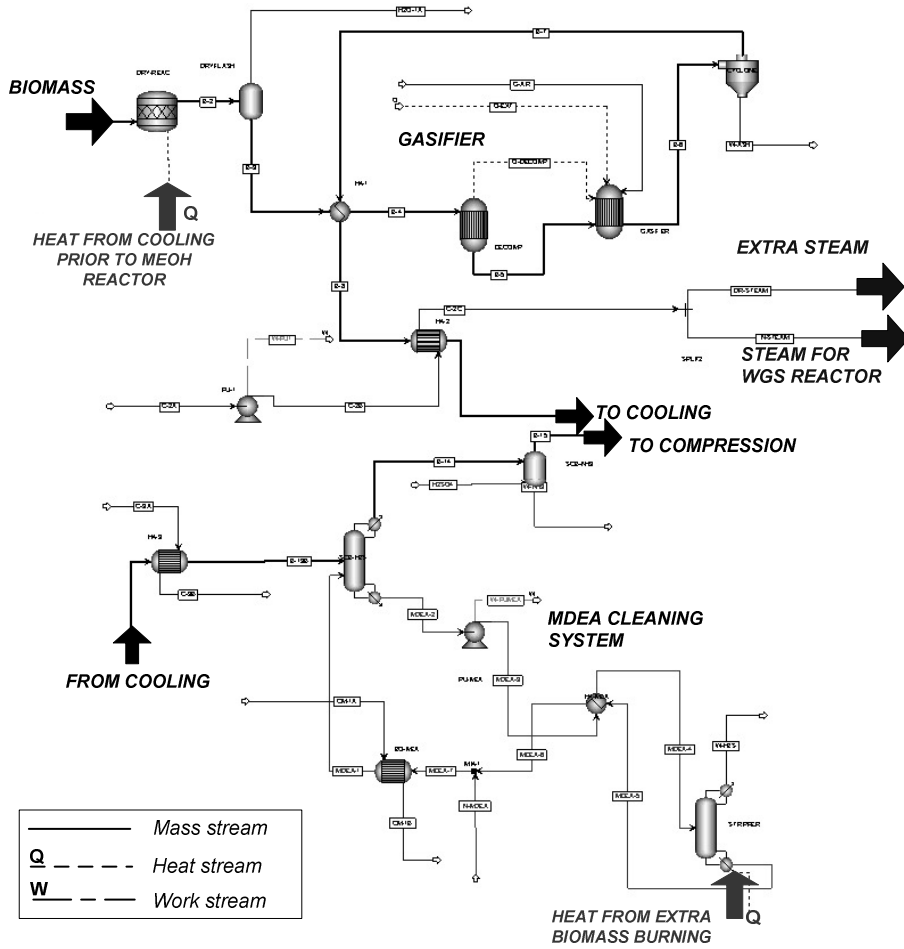
Figure 0.7: Section (A): *Simulation of the drying, gasification, cooling/HRSG and cleaning.*
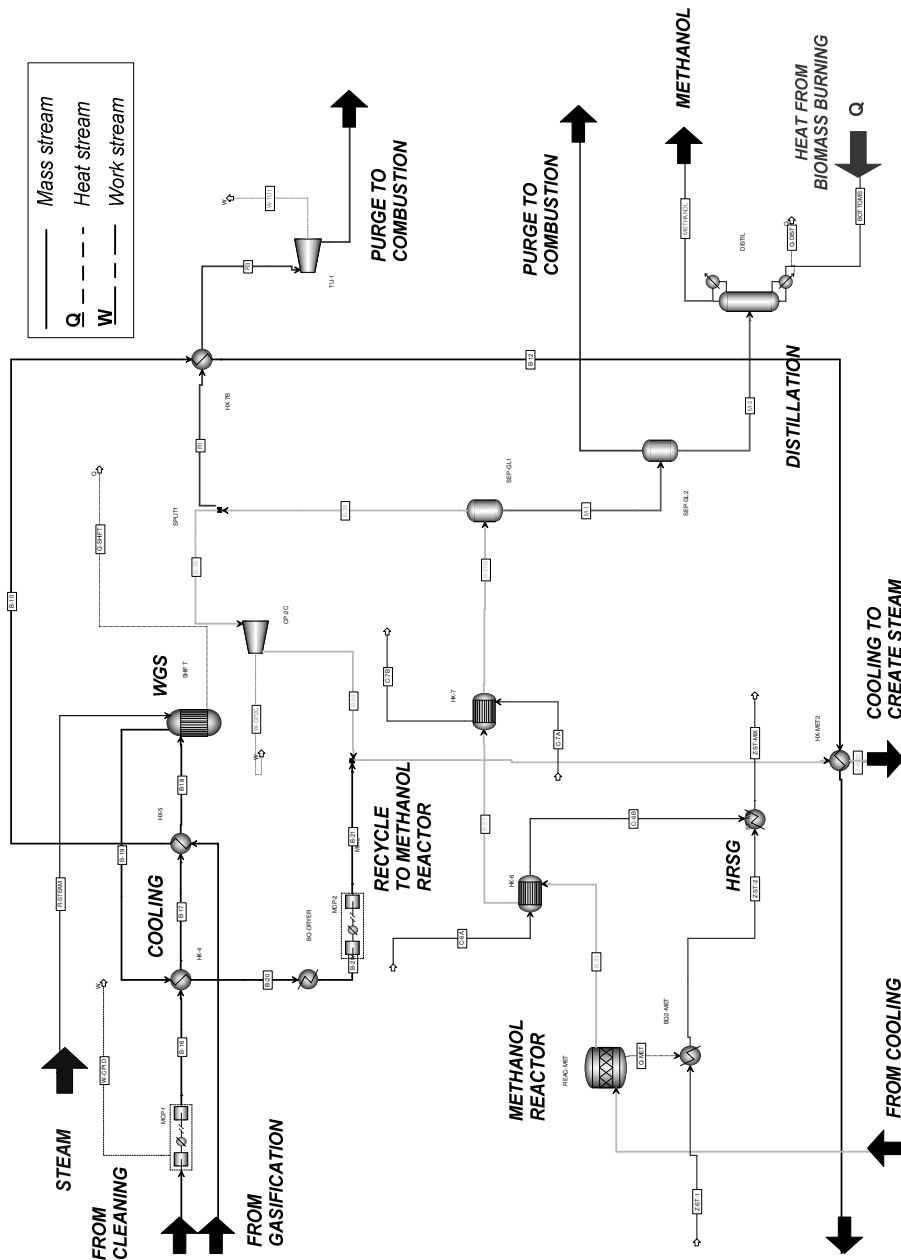
Figure 0.8: Sections (B/C/D/E): *Simulation of syngas cleaning and compression, WGS reactor, MeOH synthesis reactor with recycle, purge separation and final distillation.*
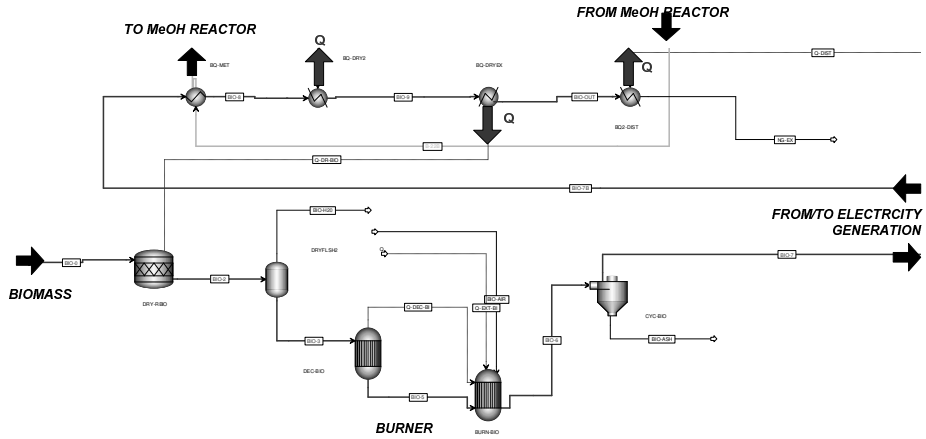
Figure 0.9: Sections (F): *Extra biomass burning to supply heat for the process.*
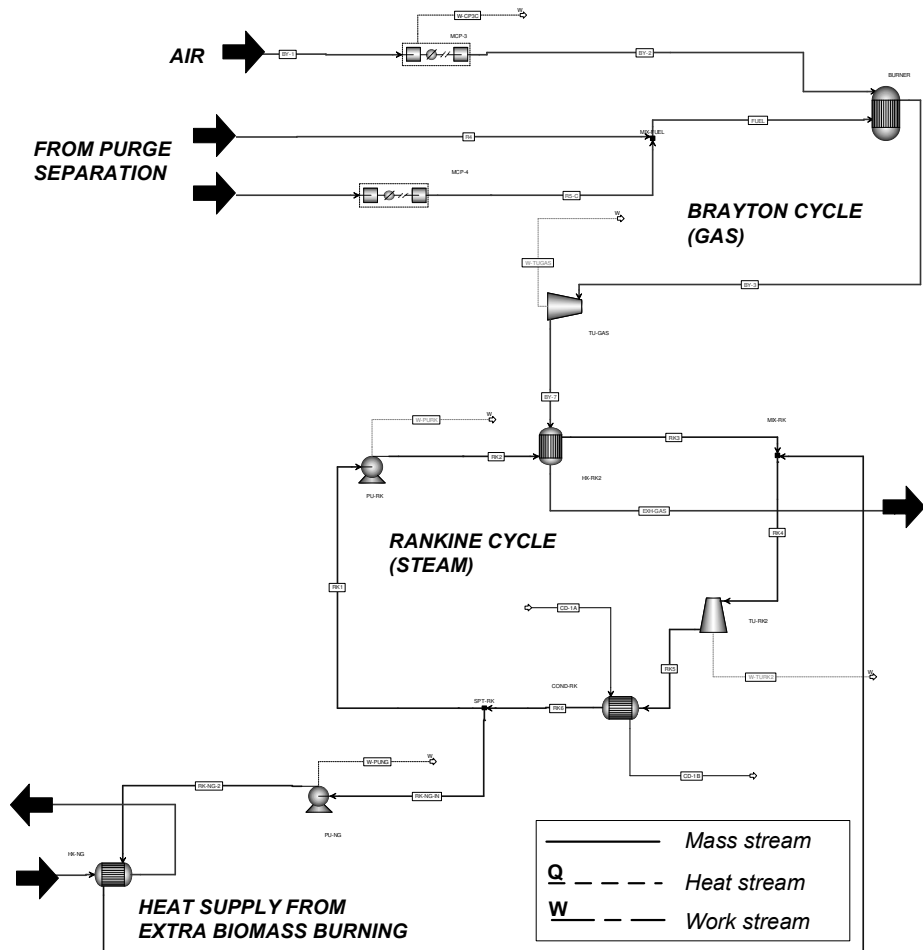

Figure 0.10: Sections (G): *Electricity generation from purge and biomass combustion.*

# Appendix E.   Biomass-to-Fischer Tropsch simulation in Aspen Plus
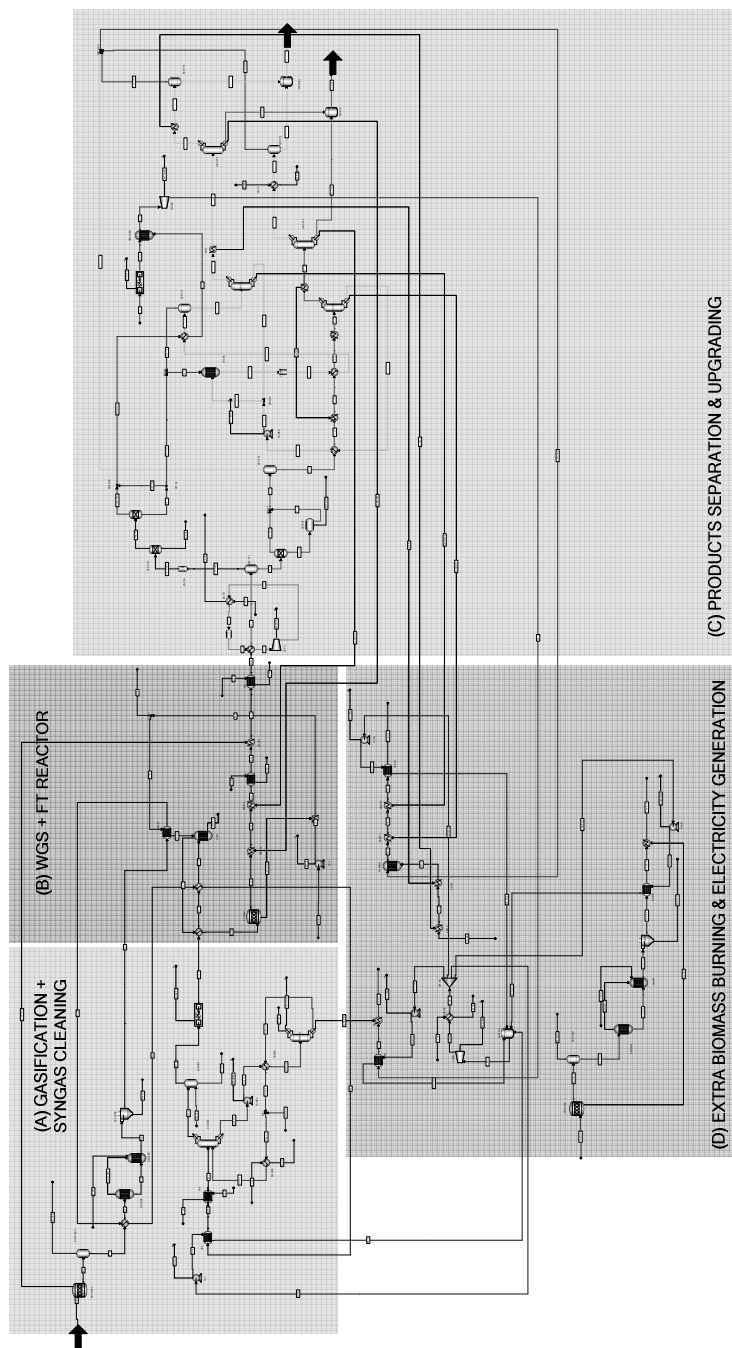
*Figure 0.11: Identification of main sections in the bio-FT simulation in Aspen Plus.*
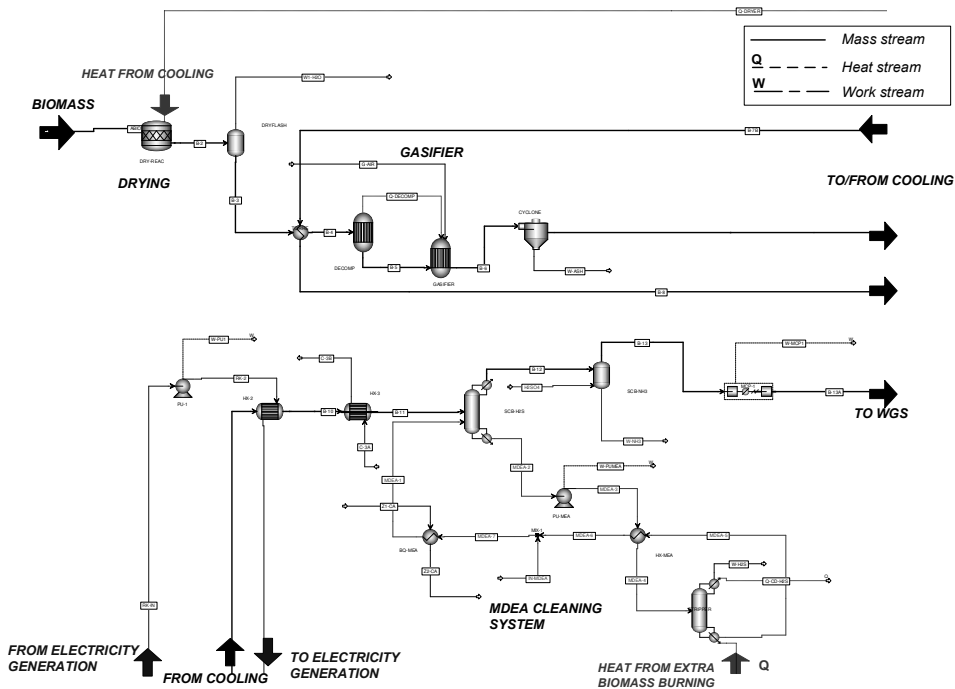
Figure 0.12: *Section (A): Simulation of the drying, gasification, cooling/HRSG and cleaning.*
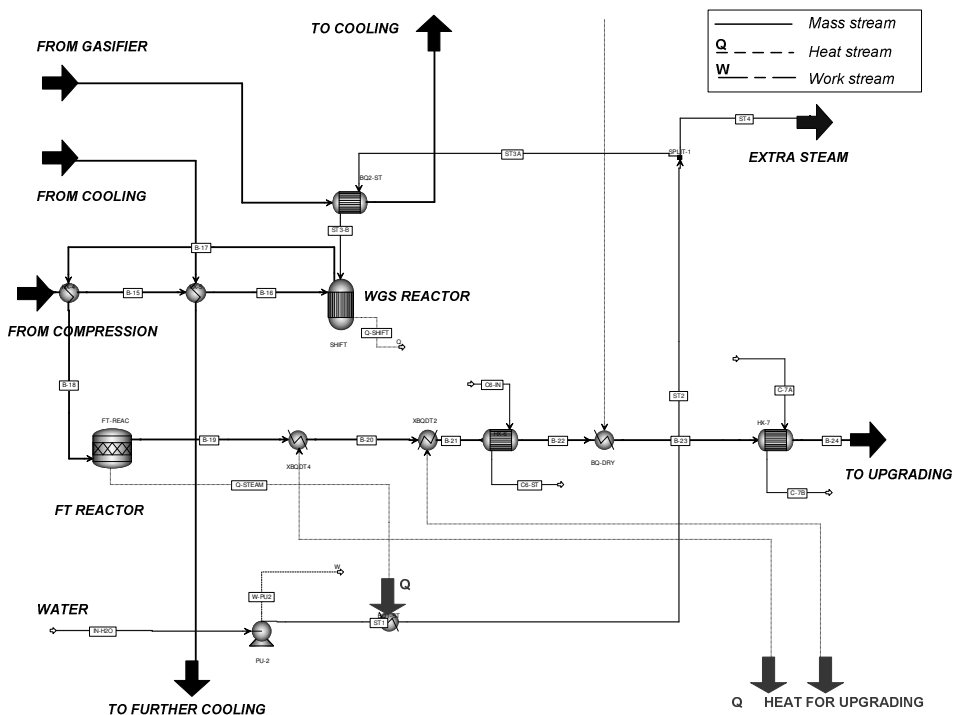

Figure 0.13: Sections (B): *WGS and FT-fuels reactors.*
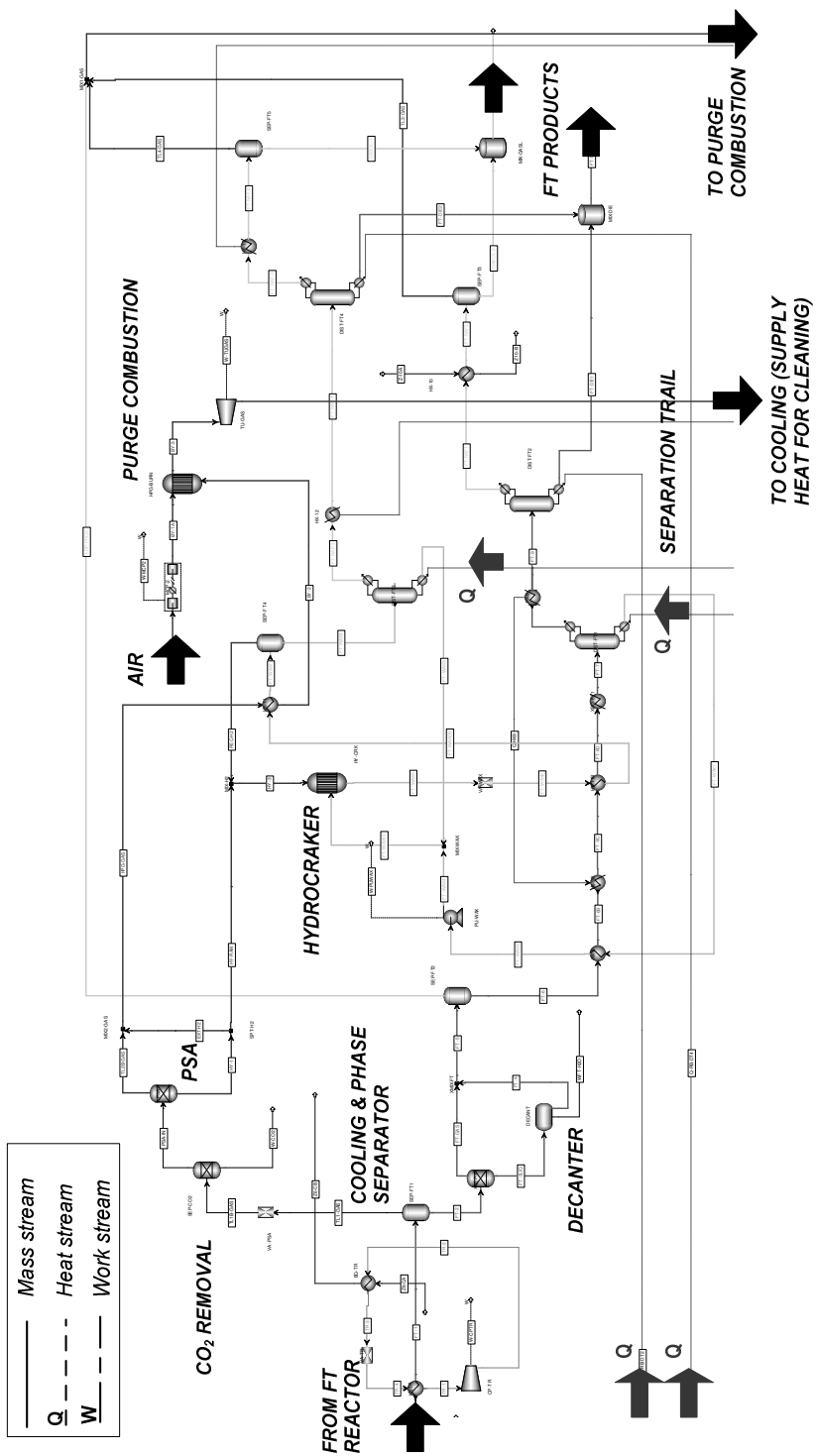
**Figure 0.14: Sections (C):** *Upgrading section of the FT-fuels.*
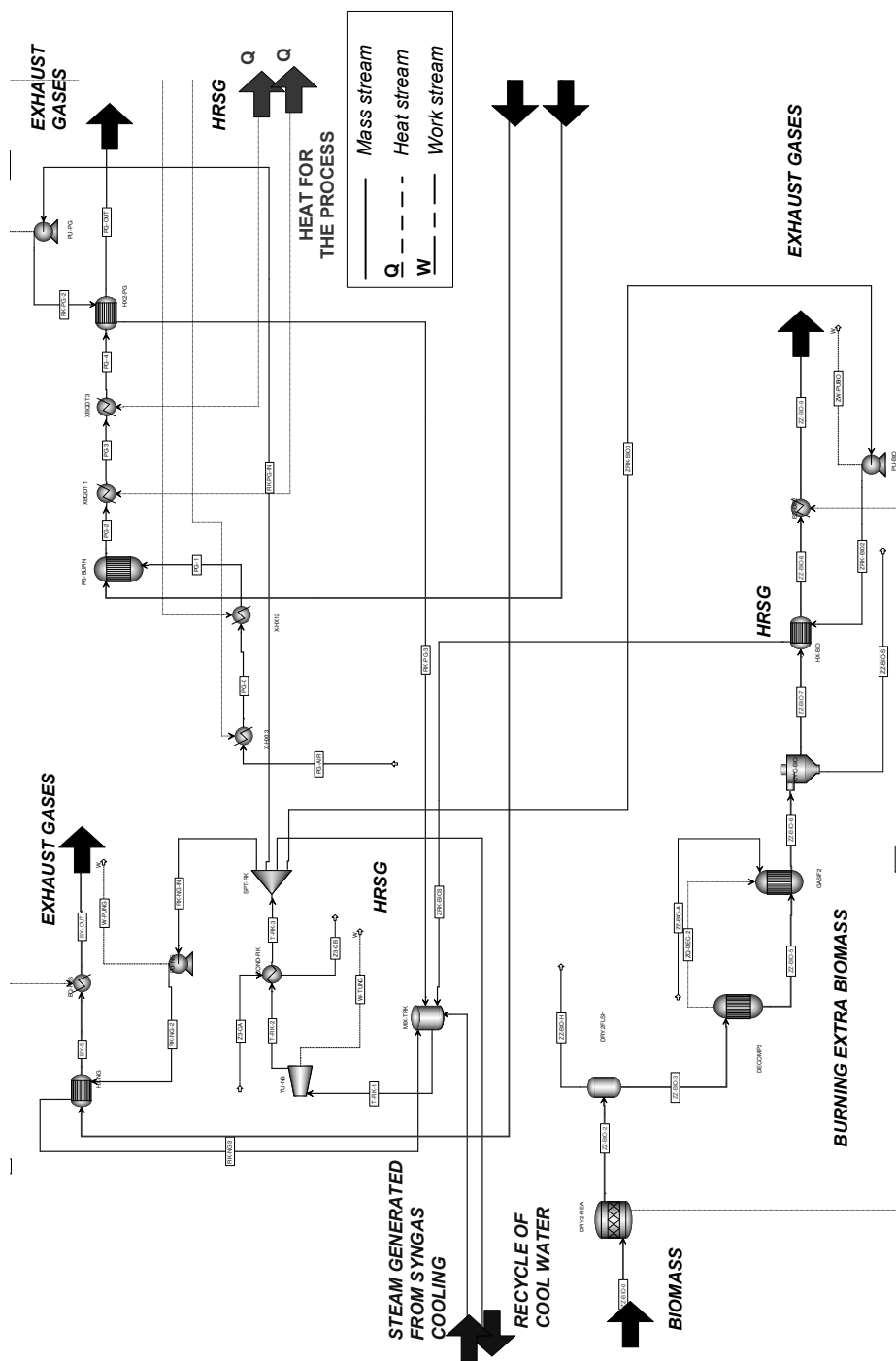
Figure 0.15: Sections (D): *Electricity generation from purge and biomass combustion.*

Appendix F.   Characterization of FT-Diesel

The characterization of the FT-diesel stream has been retrieved from the "*Analysis*" tool of ASPEN PLUS for petroleum products. Parameters obtained from this tool in presented in the following Table 0-4.

Table 0-4: *Diesel properties given by Aspen Plus [39].*

Properties	Description	Values
APISTD	API gravity	52.3
SGSTD	Specific gravity	0.8
WAT	Watson UOP K-factor (K_{UOP})	12.9
MWMX	Molecular weight	206
HMX, MW	Enthalpy	-22.2
HMX, MJ/kg	Enthalpy	-1.4
SMX, kJ/kg-K	Entropy	-6.0
CPMX, kJ/kg-K	Heat capacity	3.1
RHOLSTD, kg/m^3	Standard liquid density (60°F, atmospheric pressure)	0.8
MUMX, kg/s.m	Viscosity	2.2×10^{-4}
KMX, Watt/m-K	Thermal conductivity	0.09
KINVISC, mm^2/s	Kinematic viscosity (@40°C, 1atm)	3.7
SIGMAMX, N/m	Surface tension	0.009

Some other important characterization parameters are estimated by means of numerical correlations. This is the case of the *average boiling point* (BP_{av}), the *standard liquid density* @ 60°F ($d_{60/60}$), the *cetane index* (*CI*), the *Pour Point* (*PP*) and the *Cold Filter Plugging Point* (*CFFP*). Following expressions (0-1) to(0-4) are used to calculate those parameters.

$$BP_{av}(K) = \frac{\left(K_{UOP} \cdot d_{\left(60/60 \right)} \right)^3}{1.8} \tag{0-1}$$

$$d_{\left(60/60 \right)} = \frac{density\ diesel\ \left(60^o F \right)}{density\ water\ \left(60^o F \right)} = \frac{density\ diesel\ \left(60^o F \right)}{1\ g/cm^3} \tag{0-2}$$

$$CI = 454.7 - 1641.4 \cdot d_{\left(60/60 \right)} + 744.74 \cdot \left(d_{\left(60/60 \right)} \right)^2 - 0.554 \cdot BP_{av}\left(^o C \right) + 97.8 \cdot \left(\log\left(BP_{av}\left(^o C \right) \right) \right)^2 \tag{0-3}$$

$$PP(K) = 130.47 \cdot \left(d_{\left(60/60 \right)} \right)^{2.971} \cdot MW^{\left(0.612 - 0.474 \cdot d_{\left(60/60 \right)} \right)} \cdot \eta_{100}^{\left(0.31 - 0.333 \cdot d_{\left(60/60 \right)} \right)} \tag{0-4}$$

where *MW* is the molecular weight and η is the kinematic viscosity @ 40°C in mm^2/s. Generally, the CFPP is a few degrees higher than PP.

Appendix G. Biomass-to-Hydrogen simulation in Aspen Plus
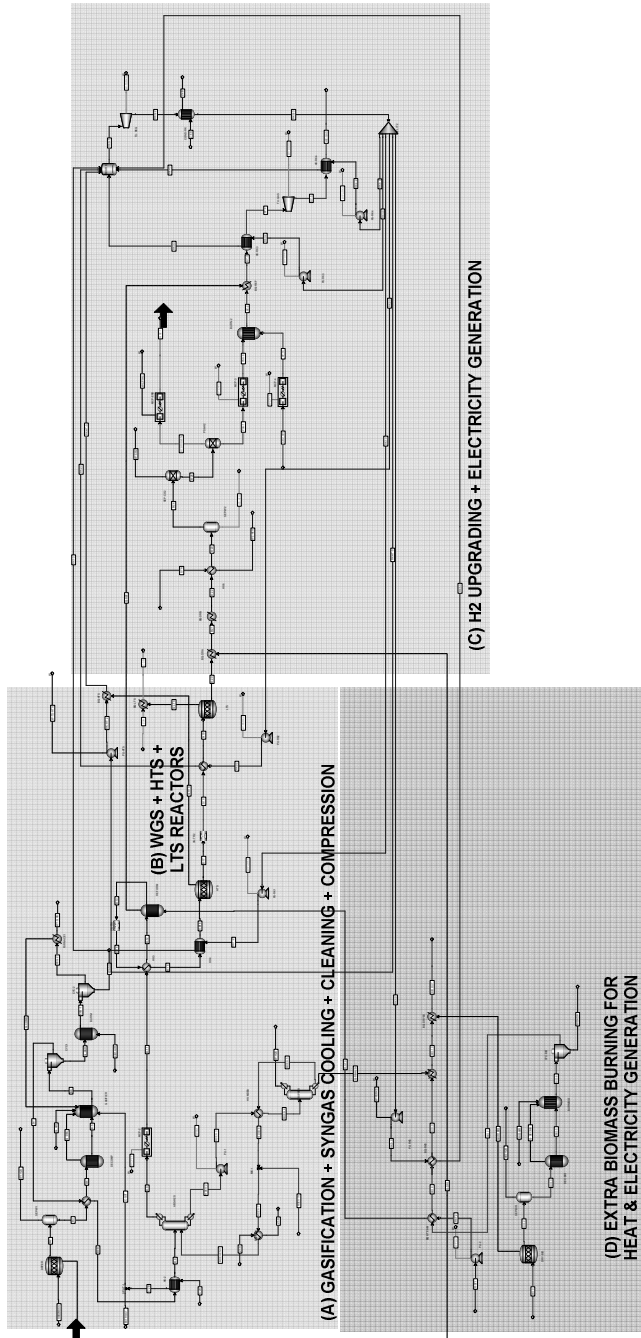
Figure 0.16: *Identification of main sections in the bio-H2 simulation in Aspen Plus.*
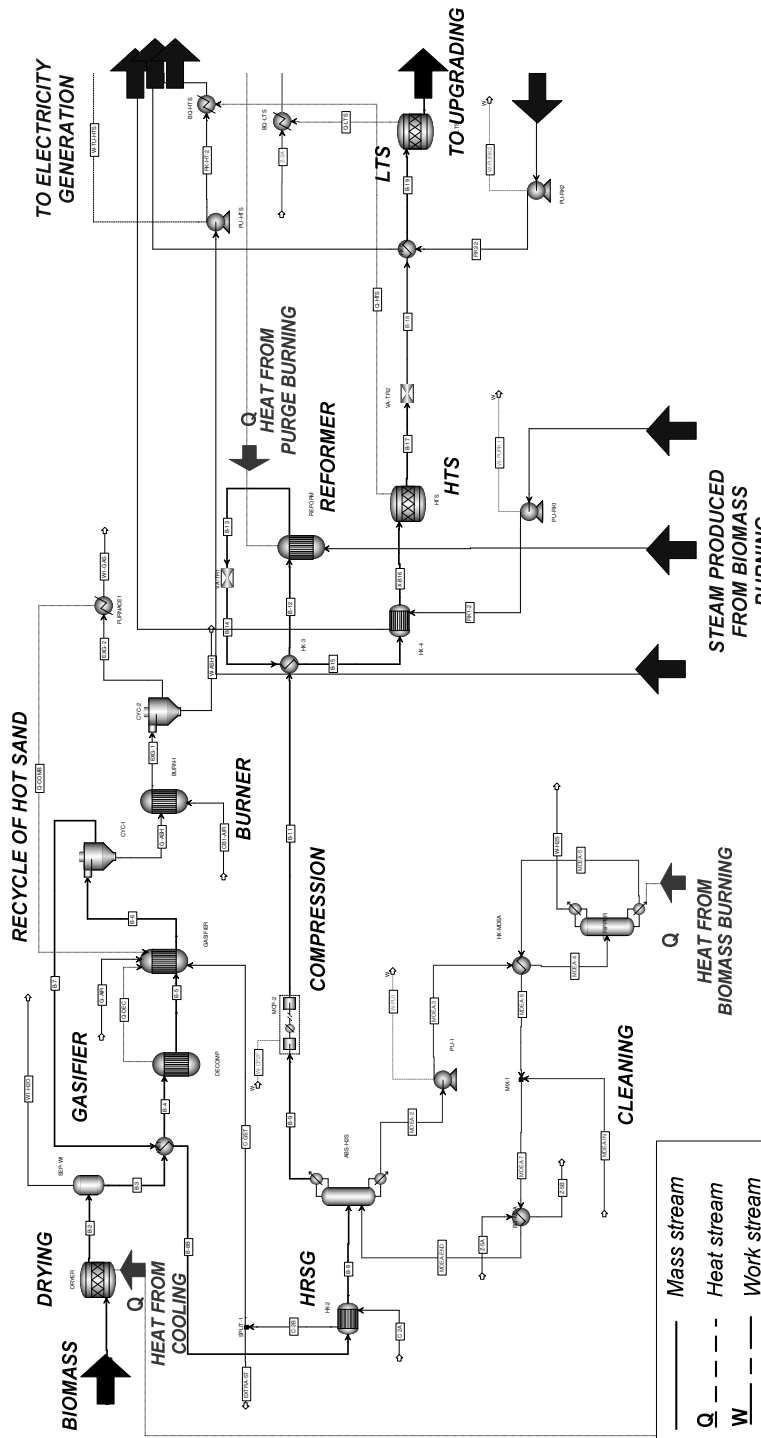
Figure 0.17: *Sections (A/B): Simulation of the drying, gasification, cooling/HRSG, cleaning, Reformer, HTS and LTS reactors .*
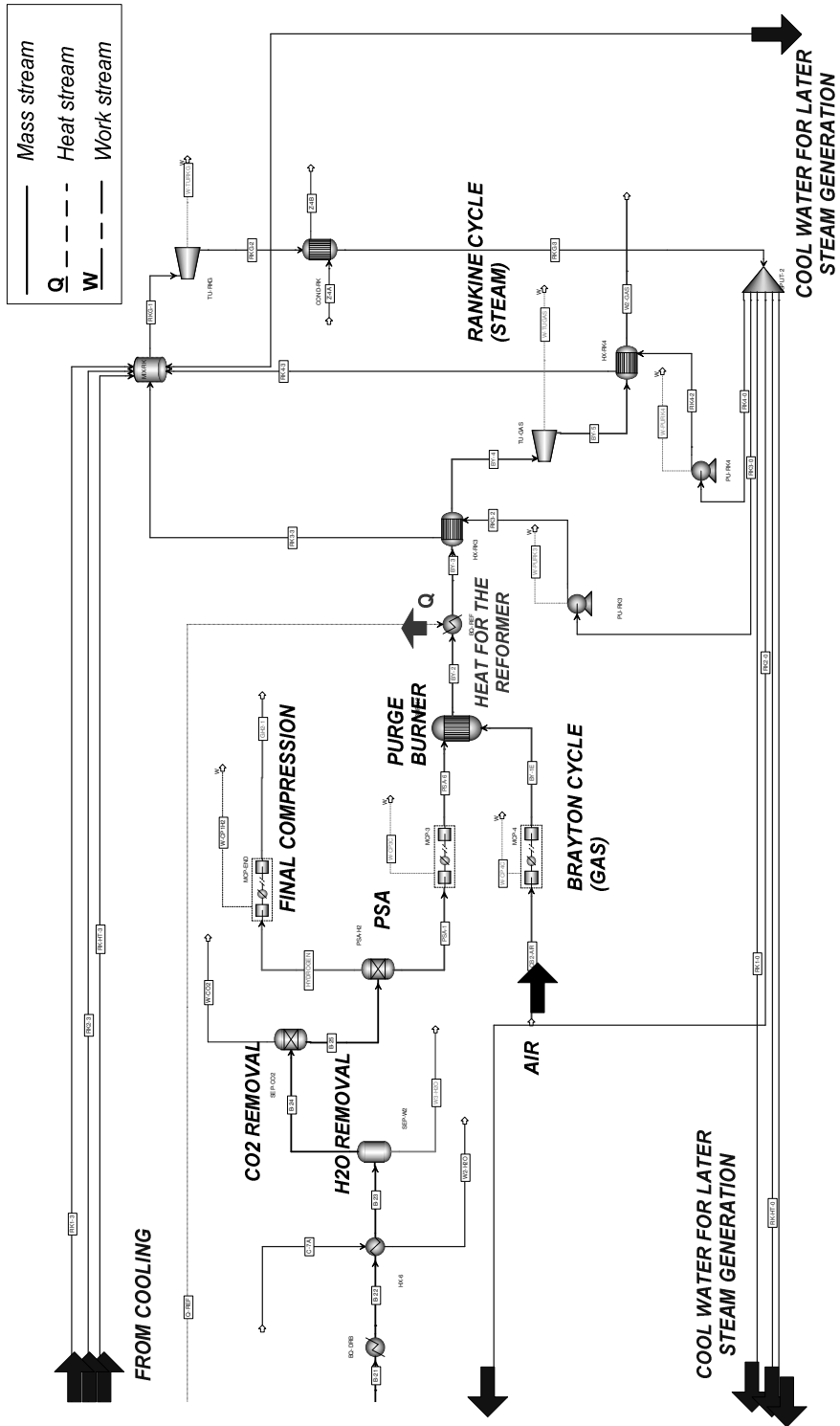
Figure 0.18: *Sections (C): Simulation of the H$_2$ upgrading and electricity generation.*

STEAM TO THE REFORMER

FROM ELECTRICITY GENERATION

EXHAUST GASES

TO ELECTRICITY GENERATION

H2O

BIOMASS
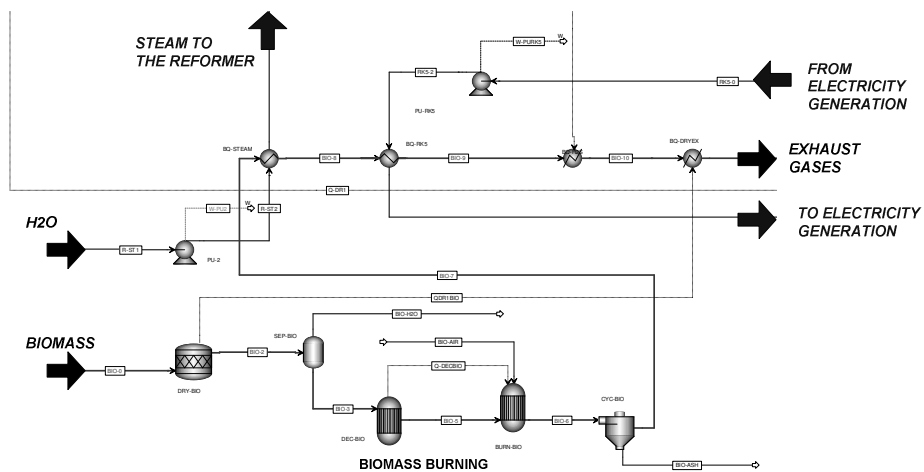
BIOMASS BURNING

Figure 0.19: *Sections (D): Simulation of the extra biomass burning to generate heat for the process and the electricity generation section.*

Appendix H.   Biomass-to-Electricity simulation in Aspen Plus
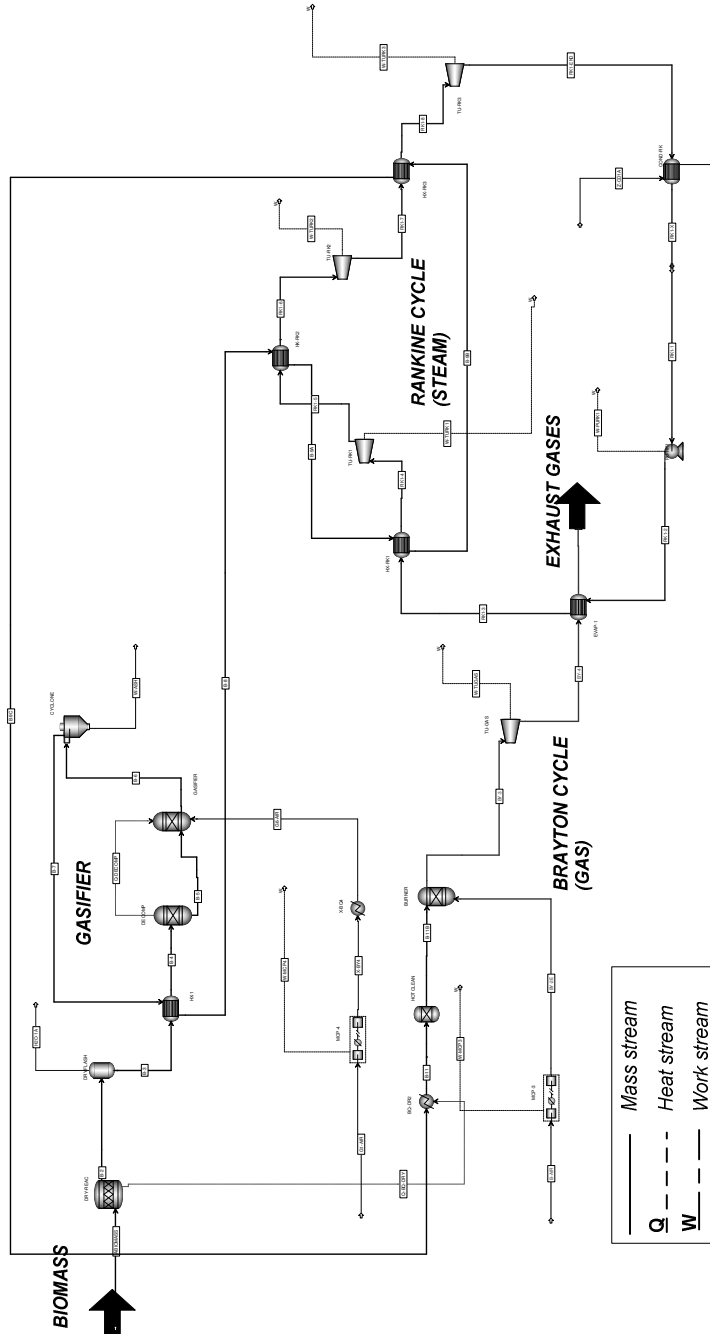
Figure 0.20: *Identification of main sections in the bio-H2 simulation in Aspen Plus.*

Appendix I. Environmental Impact Estimation

I.1.   Equivalence emissions for each compound

Table 0-5: *Characterization factors of different compounds*

| Component	GWP (kg-eq CO_2)	Acidification (kg-eq SO_2)	Eutrophication (kg-eq PO_4)	Summer smog (kg-eq C_2H_4)	Winter smog (kg-eq PM)	Ecotoxicity (kg-eq Pb)	Carciogenesis (kg-eq PAH)
H2O							
N2			0.420				
O2							
NO2		0.700	0.130	0.028	0.127		
NO		0.700	0.130		0.127		
SO2		1		0.048	0.078		
SO3		0.8			0.062		
S							
H2							
CL2							
HCl		0.88					
C							
CO	1.53			0.027	0.001		
CO2	1						
CH4	23						
H2S		1.880					
NH3		1.880	0.350		0.121	0.000	
C2H6				0.123			
C2H4				1		0.001	
C3H8				0.176		0.002	
C4H10				0.352		0.008	
C5H12				0.395		0.054	
C6H14				0.482		0.001	
C7H16				0.494		0.000	
C8H18				0.453			
C9H20				0.414			
C10H22				0.384			
C11H24				0.384			
C12H26				0.357			
H2SO4		0.650					

I.2. Emissions from materials, fuels, and utilities production, distribution and consumption

Table 0-6: Emissions originated during the production, distribution and final consumption of materials and energy. Values are given in kg-eq emission per kg of product. Data from the SimaPro program is used fo this calculation [122].

Material or Fuel	GWP (kgCO$_2$-eq/kg)	Acidification (kg SO$_2$,eq/kg)	Eutrophication (kg PO$_4$,eq/kg)	Summer smog (C$_2$H$_4$ eq/kg)	Winter smog (PM$_{dust}$ eq/kg)	Ecotoxicity (kg Pb eq/kg)	Carciogenesis (kg PAH,eq/kg)
Diesel for tractors:	4.233	0.037	0.006	0.001	0.006	<0.001	<0.001
Lub. oil for tractors:	0.752	0.006	<0.001	<0.001	0.001	<0.001	<0.001
Diesel for trucks:	3.870	0.030	0.005	0.001	0.005	<0.001	<0.001
Coal-electricity[a]:	0.397[b]	0.028[b]	0.001[b]	0.001[b]	0.003[b]	0.001[b]	0.001[b]
Natural gas[a]:	3.719	0.008	<0.001	0.001	<0.001	<0.001	<0.001
N-fertilizer:	3.363	0.014	<0.001	0.001	0.003	<0.001	<0.001
P-fertilizer:	2.070	0.033	0.042	<0.001	0.003	<0.001	<0.001
K-fertilizer:	2.556	0.017	0.011	0.001	0.002	<0.001	<0.001

(a) Average values of the 24 European countries.
(b) Values given in kg-eq emission per MJ.

I.3. Emissions from machinery, trucks and biofuels plant construction

Table 0-7: Emissions originated during the manufacture of one tractor. Specific emissions of each materials (i.e., kg-eq emission/kg) are calculated from [180], whereas specific emissions from fuel and electricity production and use are retrieved from Simapro database [122].

Material and fuels demand (Calculated from [120])		GWP (kgCO$_2$-eq)	Acidification (kg SO$_2$,eq)	Eutrophication (kg PO$_4$,eq)	Summer smog (kg C$_2$H$_4$ eq)	Winter smog (kg PM$_{dust}$ eq)	Ecotoxicity (kg Pb eq)	Carciogenesis (kg PAH,eq)
Aluminum	19kg	231	2	<0.1	<0.1	3	<0.1	<0.1
Copper	5 kg	36	5	<0.1	<0.1	5	<0.1	<0.1
Glass	11 kg	8	<0.1	<0.1	<0.1	<0.1	<0.1	<0.1
Cast iron	3811	1,217	<0.1	8	29	1	<0.1	32
Plastic	48 kg	102	2	<0.1	<0.1	<0.1	<0.1	<0.1
Steel	624 kg	652	3	<0.1	7	3	<0.1	<0.1
Tire rubber	913 kg	1,154	22	2	6	3	<0.1	<0.1
Fuel	201 kg	848	7	1	<0.1	1	<0.1	<0.1
Oil	38 kg	29	<0.1	<0.1	<0.1	<0.1	<0.1	<0.1
Electricity	155 GJ	30,076	71	7	3	10	383	<0.1
Total emissions of 1 tractor		**35,227**	**121**	**19**	**45**	**27**	**383**	**32**

Table 0-8: Emissions originated during the manufacture of one truck. Specific emissions of materials, fuels and electricity (i.e., kg-eq emission/kg) are calculated from [122, 180].

Material and fuels demand (Calculated from [180])		GWP (kgCO$_2$-eq)	Acidification (kg SO$_2$,eq)	Eutrophication (kg PO$_4$,eq)	Summer smog (kg C$_2$H$_4$ eq)	Winter smog (kg PM$_{dust}$ eq)	Ecotoxicity (kg Pb eq)	Carciogenesis (kg PAH,eq)
Aluminum	1,053 kg	10,741	111	2	3	128	<0.1	<0.1
Copper	200 kg	753	108	<0.1	<0.1	106	<0.1	<0.1
Glass	50 kg	37	<0.1	<0.1	<0.1	<0.1	<0.1	<0.1
Plastic	500 kg	1,050	18	1	4	3	<0.1	<0.1
Steel	21,600kg	22,547	110	7	258	99	<0.1	<0.1
Tire rubber	4,300 kg	5,435	105	7	26	12	<0.1	<0.1
Wood	306 kg	89	1	<0.1	1	<0.1	<0.1	<0.1
Fuel	1,618 kg	6,263	48	8	1	7	<0.1	<0.1
Electricity	1,294 GJ	269,160	632	59	25	89	3,431	<0.1
Total emissions of 1 truck		**316,075**	**1,133**	**84**	**319**	**445**	**3,431**	**0**

Table 0-9: Emissions originated during the construction of one H$_2$ plant with a capacity of 120 MW$_{H2}$. Specific emissions of materials, fuels and electricity (i.e., kg-eq emission/kg) are calculated from [122, 180].

Material and fuels demand (Calculated from [123])		GWP (tn CO$_2$-eq)	Acidification (kg SO$_2$,eq)	Eutrophication (kg PO$_4$,eq)	Summer smog (kg C$_2$H$_4$ eq)	Winter smog (kg PM$_{dust}$ eq)	Ecotoxicity (kg Pb eq)	Carciogenesis (kg PAH,eq)
Aluminum	200 tn	1,629	8	0.3	0.9	1	0	0
Copper	150 tn	319	14	<0.1	0.1	2.2	<0.1	<0.1
Glass	1 tn(*)	1	<0.1	<0.1	<0.1	<0.1	<0.1	<0.1
Polyethylene	60 tn	123	0.5	<0.1	<0.1	<0.1	<0.1	<0.1
Nylon	18 tn	164	0.5	<0.1	<0.1	<0.1	<0.1	<0.1
PVC	42 tn	82	0.2	<0.1	<0.1	<0.1	<0.1	<0.1
PET	40 tn	88	0.4	0.1	<0.1	<0.1	<0.1	<0.1
Resines	12 tn	62	0.3	<0.1	<0.1	<0.1	<0.1	<0.1
Silicones	28 tn	75	0.3	<0.1	<0.1	<0.1	<0.1	<0.1
Concrete	10,000 tn	1,979	6	0.3	0.9	1.1	<0.1	<0.1
Steel	3,000 tn	4,644	17	2	6	6	<0.1	<0.1
Firebricks	200 tn[a]	48	0.1	<0.1	<0.1	<0.1	<0.1	<0.1
Wood	1 tn[a]	61	0.4	<0.1	<0.1	0.1	<0.1	<0.1
Rockwool	1 tn[a]	1	<0.1	<0.1	<0.1	<0.1	<0.1	<0.1
Binder(cement)	10 tn[a]	7	<0.1	<0.1	<0.1	<0.1	<0.1	<0.1
Paint	100 tn[a]	293	1.9	0.3	0.1	0.1	<0.1	<0.1
Energy		Included						
Total emissions of 1 plant		**9,576**	**50**	**3**	**8**	**11**	**<0.1**	**<0.1**

(a) This values correspond to own assumptions.

Table 0-10: *Emissions originated during the construction of one power plant with net production of 344 MW$_{el.}$. Specific emissions of materials, fuels and electricity (i.e., kg-eq emission/kg) are calculated from [122, 180].*

Material and fuels demand (Calculated from [124])		GWP (tn CO$_2$-eq)	Acidification (kg SO$_2$.eq)	Eutrophication (kg PO$_4$.eq)	Summer smog (kg C$_2$H$_4$ eq)	Winter smog (kg PM$_{dust}$ eq)	Ecotoxicity (kg Pb eq)	Carciogenesis (kg PAH.eq)
Aluminum	200 tn	1,629	8	0.3	1	1	<0.1	<0.1
Copper	150 tn	319	14	<0.1	0.1	2	<0.1	<0.1
Glass	1tn[a]	0.7	<0.1	<0.1	<0.1	<0.1	<0.1	<0.1
Polyethylene	52 tn	107	0.4	<0.1	<0.1	<0.1	<0.1	<0.1
Nylon	16 tn	142	0.5	<0.1	<0.1	<0.1	<0.1	<0.1
PVC	36 tn	71	0.2	<0.1	<0.1	<0.1	<0.1	<0.1
PET	35 tn	76	0.3	0.1	<0.1	<0.1	<0.1	<0.1
Resines	10 tn	54	0.3	<0.1	<0.1	<0.1	<0.1	<0.1
Silicones	24 tn	65	0.3	<0.1	<0.1	<0.1	<0.1	<0.1
Concrete	56,900 tn	11,261	33	2	5.4	6	<0.1	<0.1
Steel	12,020 tn	18,606	69	9	26	23	0.1	0.1
Firebricks	200 tn[a]	47.5	0.1	<0.1	<0.1	<0.1	<0.1	<0.1
Wood	1 tn[a]	61	0.4	<0.1	<0.1	0.1	<0.1	<0.1
Rockwool	1 tn[a]	2	<0.1	<0.1	<0.1	<0.1	<0.1	<0.1
Binder(cement)	10 tn[a]	7.2	<0.1	<0.1	<0.1	<0.1	<0.1	<0.1
Asphalt	6,000 tn	1,247	4	0.1	0.3	0.3	<0.1	<0.1
Rubber	213 tn	566	2	<0.1	0.1	0.3	<0.1	<0.1
Cast iron	196 tn	288	1	<0.1	0.3	0.4	<0.1	<0.1
Paint	100 tn[a]	293	2	0.3	0.1	0.1	<0.1	<0.1
Energy		Included						
Total emissions of 1 plant		**34,842**	**135**	**12**	**33**	**34**	**0.2**	**0.1**

Appendix J. Calculations for the Economic Evaluation & Profitability Analysis (Chapter 6)

J.1.   Total Capital Investment (TCI) calculation

Total Capital Investment' (**TCI**) has been calculated by means of factored estimation [45]. The application of this method requires the determination of the purchased equipment cost (PE) of all the components units of the conversion system. The rest of the direct (DFC) and indirect fixed costs (IFC) are estimated as percentages of this PE. Table 0-11 also summarizes the corresponding percentages of the Fixed Capital Investment (FCI), whose values lies in the range proposed by several authors [45, 162]

Table 0-11: Calculation of the Total Capital Investment (TCI).

I		(DFC) Direct Fixed Costs		**DFC = A + B + C + D + E**	
	A	(EA) Equipment and assembly		EA = A1 +A2 + A3 + A4 + A5	
		A1	(PE) Purchased equipment	Aspen Icarus, [83, 84, 150, 181, 182]	
		A2	Installation (incl. insulation and painting)	Aspen Icarus, [83, 84, 150, 181, 182]	
		A3	Instrumentation and Control, installed	Aspen Icarus, [83, 84, 150, 181, 182]	
		A4	Piping, installed	Aspen Icarus, [83, 84, 150, 181, 182]	
		A5	Electrical, installed	Aspen Icarus, [83, 84, 150, 181, 182]	
	B	**Buildings, process and auxiliary**		10% FCI	22% PE
	C	**Yard improvements**		2-5% FCI	12% PE
	D	**Service facilities**		8-20% FCI	33% PE
	E	**Land**		Not applied[a]	Not applied
II		(IFC) Indirect Fixed Costs = F + G + H + I		**IFC = F + G + H + I**	
	F	**Engineering and Supervision**		8% FCI	16% PE
	G	**Legal expenses**		2% FCI	2% PE
	H	**Construction expense and contractor's fee**		1.5-6% FCI	4% PE
	I	**Contingency**		5-15% FCI	5% PE
III		**(FCI) Fixed Capital Investment**		**FCI = Direct + Indirect**	
IV		**(WC) Working Capital**		**WC = 0.15 x TCI**	
V		(TCI) Total Capital Investment		TCI = FCI + WC	

(a): It is assumed that the land is given by the municipalities at no cost.

Purchased equipment costs of specific equipment (i.e., gasifiers, catalytic reactors, tar cracker, ASU, Selexol, PSA) are calculated by scaling literature values with Eq.(6-1). Those references are summarized in Table 0-12, together with the scaling factor R_f.

Table 0-12: *Purchased equipment costs for specific equipments (without installation).*

Ref	Equipment	Base cost	R_f	Install. factor	Base scale	Maximum scale
[150]	Steam-blown gasifier	16.3 M$_{2001}$	0.65	1.69	68.8 dry tn/hr	83.0 dry tn/hr
[150]	Air-blown gasifier	38.1 M$_{2001}$	0.70	1.69	68.8 dry tn/hr	75.0 dry tn/hr
[150]	Feeding system[a]	0.41 M$_{2001}$	1.00	1.86	33.5 dry tn/hr	110 dry tn/hr
[150]	Cyclones	2.6 M$_{2001}$	0.70	1.86	34.2 m^3 gas/s	180 m^3 gas/s
[83]	ASU	Eq.(0-5)[b]	1.00	1.75	-	n.a.
[150]	Tar cracker	3.1 M$_{2001}$	0.70	1.86	34.2 m^3 gas/s	52.0 m^3 gas/s
[84]	Selexol	14.3 M$_{1993}$	0.70	1.87	810 kmol/hr (CO_2)	n.a.
[181]	Methanation reactors	2.6M€$_{2003}$	0.70	1.00	23.4 dry tn/hr	n.a.
[104]	FT-fuels reactors	6.7M$_{1996}$	0.72	1.73	131 MW$_{FT}$	133 MW$_{FT}$
[150]	Methanol reactor	7.0 M$_{2001}$	0.6	2.10	87.5 tn/hr (MeOH)	n.a.
[150]	WGS, LTS, HTS reactors	9.02 M$_{1995}$	0.85	1.81	8819 kmol/h (H_2+CO)	n.a.
[150]	Steam reformer	9.40 M$_{2001}$	0.60	2.30	1390 kmol/h (CH_4)	n.a.
[182]	Hydrocracker	6.51M$_{1998}$	0.70	1.73	8.984 lb/hr (waxes)	n.a
[150]	PSA	28.0 M$_{2001}$	0.70	1.69	9.600 kmol/hr (total feed)	n.a.

(a): Two double screw feeders with rotary valves.
(b): ASU capital cost is calculated from the William's expression, where "C" is O_2 consumption (tn/day):

$$PE_{ASU} (M\$_{1991}) = 0.260 \cdot C^{0.712} \tag{0-5}$$

Purchased equipment costs breakdown for each operational unit and biofuel system in given in subsequent Figure 0.21 to Figure 0.25. SNG, H_2 and Methanol production can be done following 4 different configurations (see Figure 3.1), depending on how heat and electricity demand of the plant is covered. Since heat demand of the Fischer-Tropsch plants is covered by heat integration, there are only 2 possible configuration for this process, i.e., "bio&grid" and "bio-100" (see Figure 3.1). By definition, only one configuration is viable for electricity generation as heat and electricity demand is fully covered by the process itself.

PE and assembly (Direct Fixed Costs "A") breakdown for SNG production
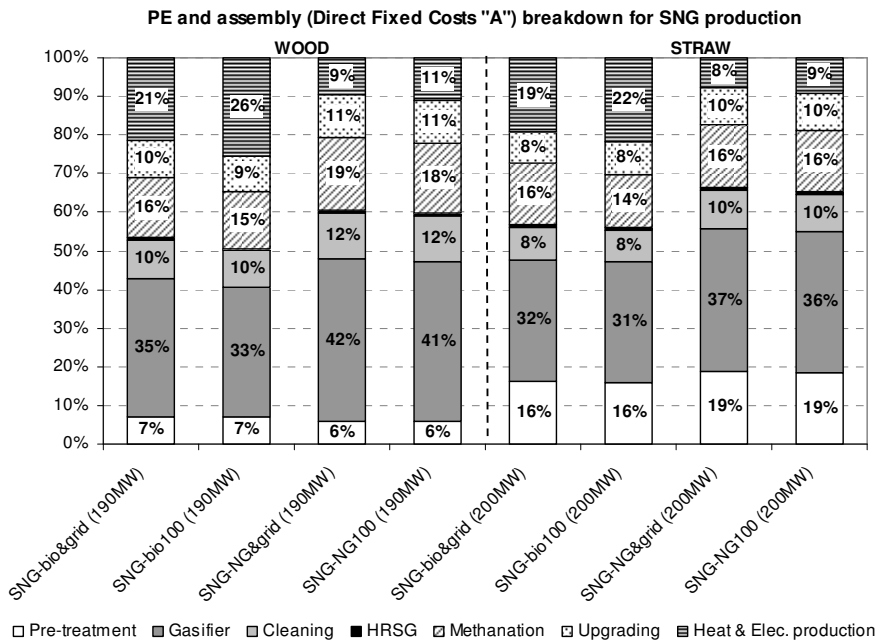
Figure 0.21: Purchased equipment (PE) and assembly costs (Direct Fixed Costs in Table 6-2) breakdown for SNG production under the 4 configurations of Figure 3.1 (see Chapter 3). Values for wood and straw- fuelled plants are given in the left and right side respectively.

PE and assembly (Direct Fixed Costs "A") breakdown for MeOH production
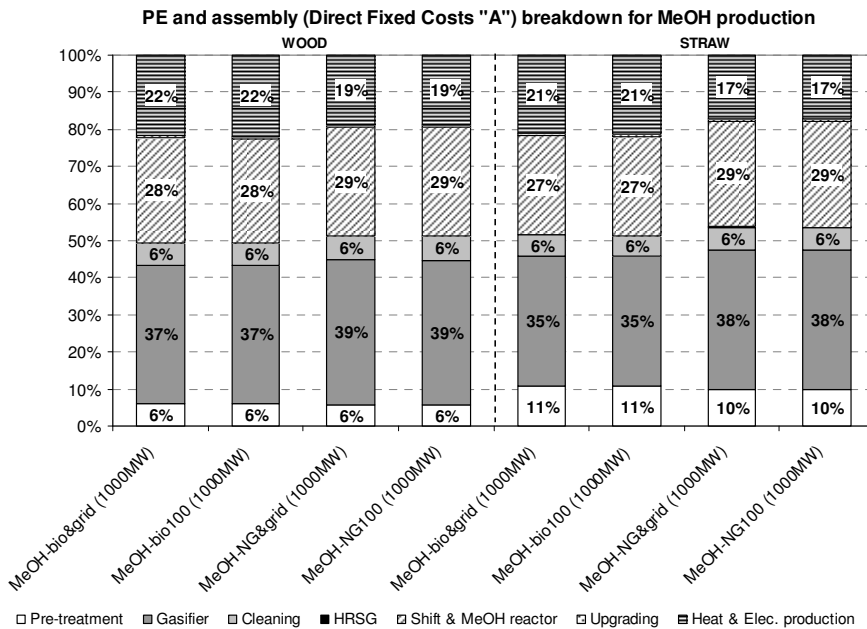
Figure 0.22: Purchased equipment (PE) and assembly costs (Direct Fixed Costs in Table 6-2) breakdown for MeOH production under the 4 configurations of Figure 3.1 (see Chapter 3). Values for wood and straw- fuelled plants are given in the left and right side respectively.

PE and assembly (Direct Fixed Costs "A") breakdown for H₂ production
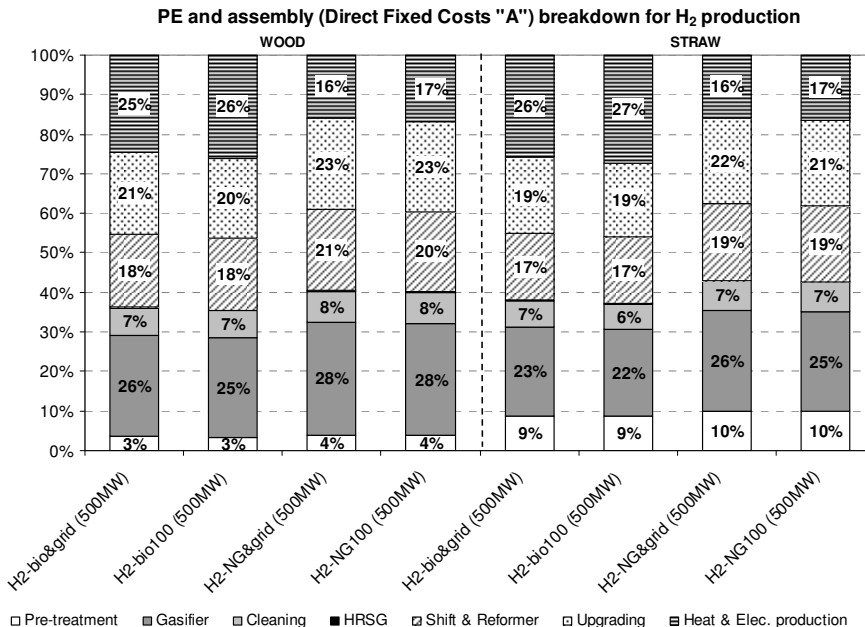
Figure 0.23: Purchased equipment (PE) and assembly costs (Direct Fixed Costs in Table 6-2) breakdown for H₂ production under the 4 configurations of Figure 3.1 (see Chapter 3). Values for wood and straw- fuelled plants are given in the left and right side respectively.
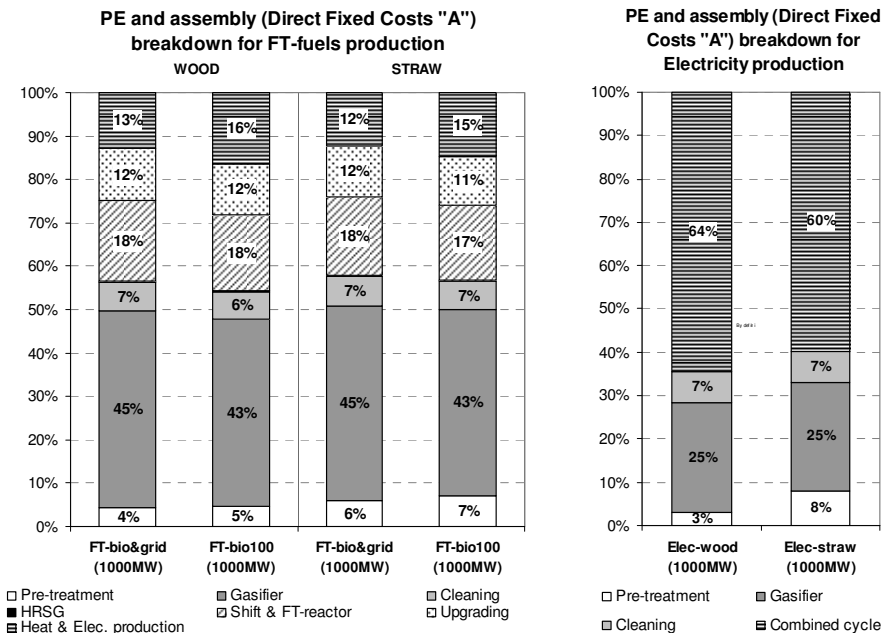
*Figure 0.24: Purchased equipment (PE) and assembly costs for FT-fuels production under 2 configurations.For wood (left) and straw (right) fuelled plants.*

Figure 0.25: Purchased equipment (PE) and assembly costs for electricity generation.

J.2. *Total Production Cost (TPC) estimation*

Analogous to the TCI calculation, some parameters of the TPC are also calculated by factored estimation, as shown in following Table 0-13.

Table 0-13: *Calculation of the annual Total Production Costs (TPC).*

I				
I	**(COM) Manufacturing costs = (A) + (B) + (C)**			**COM = A + B +C**
	A	**(DPC) Direct Production Costs = (A1) to (A10)**		**DPC = A1 to A10**
		A1	Raw Materials	Aspen Plus
		A2	Utilities	Aspen Plus
		A3	Ash disposal	Scaled from [162]
		A4	Waste water treatment	Scaled from [162]
		A5	Operating Labor[a]	Calculated from [45]
		A6	Supervision operating labor	Calculated from [45]
		A7	Maintenance and Repair	7% FCI
		A8	Operating supplies	15 % Maintenance
		A9	Laboratory charges	15% Operating labor
		A10	Patents and Royalties	1% TPC
	B	**(FXC) Fixed charges**		**FXC = (B1) to (B5)**
		B1	Depreciation	Linear, 10 years
		B2	Financing (interest)	50% leverage
		B3	Local taxes	2% FCI
		B4	Property insurance	1% FCI
		B5	Rent	0.5% FCI
	C	**Overheads**		**50% (A5 + A6 + A7)**
II	**(GE) General Expenses**			**GE = G1 + G2 + G3**
	G1	Administration costs		15% Operating labor
	G2	Distribution and marketing		2% TPC
	G3	R & D costs		4% TPC
III	**(TPC) TOTAL PRODUCT COST**			**TPC = COM + GE**

(a): The number of workers and supervisors per shift are calculated based on the number and type of components units (see Table 6.13 in the book of Peters et al, fifth edition [45]).

J.3.   *Biofuels production price for an IRR of 12%*

Following subsequent Table 0-14 and Table 0-15 summarizes the biofuels production costs for a 12% IRR (Internal Rate of Return), whose values are also represented in subsequent Figure 0.26 and Figure 0.27 for a better overview.

Table 0-14: *Production costs including 12% IRR for wood-based biofuels. Logistics and distribution costs are not included. Those values are used in Chapter 6 to determine biofuel 'end-user' price per country in section 6.2.3, as well as in section 8.10.4 to calculate average total costs for each scenario of Chapter 8.*

wood	SNG scale: 190 MW			Methanol scale: 1000 MW			Fischer-T 1000 MW		Hydrogen scale: 500 MW			Electricity ~ 100 MW
Country	bio-100	bio-grid	NG-grid	bio-100	bio-grid	NG-grid	bio-100	bio-grid	bio-100	bio-grid	NG-grid	New plant
AU	13.7	13.5	15.9	19.6	19.4	21.9	20.3	19.7	16.1	16.0	19.3	22.8
BE	14.7	14.4	16.0	20.6	20.4	22.3	21.4	20.8	17.0	16.9	19.3	24.2
BU	11.0	10.8	11.4	17.3	17.2	18.2	17.8	17.2	13.7	13.7	14.9	19.9
CZ	13.2	12.9	14.1	19.8	19.6	21.1	20.5	19.8	16.0	15.9	17.7	22.7
DK	18.9	18.7	18.9	25.6	25.2	26.3	26.5	25.9	21.6	21.2	22.3	29.2
EE	10.5	10.2	11.2	16.6	16.5	17.7	17.1	16.5	13.2	13.1	14.6	19.4
FI	14.0	13.6	15.1	19.8	19.7	21.4	20.7	19.9	16.3	16.2	18.3	23.2
FR	25.2	24.4	23.6	33.2	33.4	32.9	35.2	32.9	28.2	27.5	26.8	37.7
DE	18.6	18.2	19.6	25.3	25.2	26.7	26.5	25.3	21.1	21.1	22.9	28.9
GR	11.8	11.6	9.8	17.7	17.5	16.8	18.3	17.7	14.3	14.2	12.7	20.7
HU	13.3	13.1	14.7	20.0	19.7	21.5	20.6	20.0	16.2	16.0	18.4	22.8
IE	14.6	14.4	15.4	20.6	20.4	21.8	21.3	20.7	17.1	16.9	18.6	23.7
IT	14.9	14.6	15.8	21.3	21.1	22.6	22.1	21.3	17.4	17.4	19.2	24.8
LV	11.5	11.2	13.2	17.7	17.6	19.7	18.3	17.7	14.1	14.1	16.9	20.5
LT	11.6	11.4	12.6	18.0	17.8	19.3	18.5	17.9	14.4	14.3	16.2	20.8
NL	12.3	12.1	14.5	17.9	17.7	20.1	18.5	18.1	14.7	14.5	17.8	21.0
PL	14.1	13.8	14.8	20.8	20.7	22.0	21.6	20.7	16.9	16.8	18.4	23.8
PT	11.6	11.4	12.3	17.8	17.6	18.9	18.3	17.8	14.3	14.2	15.8	20.7
RO	9.5	9.4	11.9	15.6	15.3	17.9	15.9	15.6	12.4	12.1	15.7	18.1
SK	12.6	12.4	14.3	19.2	18.9	21.0	19.7	19.2	15.5	15.3	18.0	22.0
SI	17.1	16.6	17.6	24.1	24.1	25.3	25.2	24.0	19.9	19.7	21.2	27.5
ES	13.0	12.8	14.2	19.4	19.2	20.9	20.0	19.4	15.7	15.6	17.8	22.6
SE	17.4	16.9	22.6	23.6	23.7	28.3	24.9	23.6	19.8	19.5	26.3	27.5
UK	17.0	16.9	17.0	23.4	23.4	23.7	24.6	23.4	21.4	21.3	21.6	29.4
Price	14.3	14.0	15.3	20.6	20.5	22.0	25.6	24.3	17.0	16.8	18.8	27.5
range	±5.5	±5.5	±5.5	±6.2	±6.2	±5.6	±6.6	±6.2	±5.5	±5.3	±5.6	±6.5

Table 0-15: Production costs including 12% IRR for straw-based biofuels. Logistics and distribution costs are not included. Those values are used in Chapter 6 to determine biofuel 'end-user' price per country in section 6.2.3, as well as in in section 8.10.4 to calculate average total costs for each scenario of Chapter 8.

| straw	SNG scale: 190 MW			Methanol scale: 1000 MW			Fischer-T 1000 MW		Hydrogen scale: 500 MW			Electricity ~ 100 MW
Country	bio-100	bio-grid	NG-grid	bio-100	bio-grid	NG-grid	bio-100	bio-grid	bio-100	bio-grid	NG-grid	New plant
AU	20.7	20.6	21.8	27.4	27.4	33.3	27.5	26.7	22.7	22.0	23.6	31.4
BE	19.5	19.5	20.3	25.9	25.9	32.0	25.9	25.4	21.4	20.9	22.0	30.2
BU	12.7	12.8	13.3	19.0	19.0	23.5	18.5	18.2	15.2	14.7	15.6	21.9
CZ	13.2	13.4	14.8	19.6	19.5	25.3	19.0	19.1	15.7	15.3	17.2	22.7
DK	18.6	19.0	19.6	24.9	24.7	30.3	24.6	25.7	20.5	20.4	21.4	28.8
EE	13.1	13.3	13.8	19.5	19.5	24.6	19.1	18.5	15.7	15.1	16.0	22.7
FI	16.4	16.5	17.6	22.5	22.5	28.3	22.3	21.7	18.5	17.9	19.5	26.4
FR	18.9	18.9	19.7	25.6	25.6	31.7	25.5	24.6	21.1	20.3	21.5	29.7
DE	17.9	18.0	19.8	24.1	24.1	30.2	24.0	23.9	19.9	19.5	21.8	27.9
GR	14.4	14.5	15.9	20.6	20.6	26.4	20.2	19.9	16.7	16.2	18.0	24.1
HU	13.0	13.3	15.2	19.4	19.3	25.3	18.8	19.2	15.5	15.3	17.7	22.4
IE	23.1	23.0	22.3	30.1	30.0	34.0	30.3	29.5	25.0	24.3	23.7	33.9
IT	15.9	16.1	17.3	22.3	22.3	28.9	22.0	21.8	18.2	17.8	19.4	26.3
LV	12.9	13.0	15.0	19.2	19.2	25.2	18.7	18.3	15.4	14.9	17.4	22.3
LT	13.0	13.2	14.4	19.5	19.4	24.9	18.9	18.7	15.6	15.2	16.7	22.6
NL	19.0	19.0	20.1	25.5	25.4	31.3	25.4	25.0	21.0	20.5	22.0	29.4
PL	13.1	13.3	14.8	19.5	19.4	25.1	18.9	18.9	15.6	15.2	17.1	22.6
PT	11.6	11.9	13.1	17.7	17.7	23.5	17.1	17.2	14.1	13.8	15.4	21.0
RO	12.9	13.1	15.1	19.3	19.3	25.3	18.8	18.8	15.4	15.1	17.6	22.3
SK	13.1	13.4	15.3	19.5	19.4	25.6	18.9	19.2	15.6	15.4	17.9	22.5
SI	14.1	14.3	16.2	20.4	20.4	26.7	20.0	19.9	16.5	16.1	18.6	23.7
ES	14.5	14.7	16.1	20.9	20.9	27.4	20.5	20.4	16.9	16.5	18.3	24.6
SE	18.6	18.5	24.2	24.8	24.8	34.6	24.8	23.8	20.5	19.8	26.5	29.0
UK	16.1	16.3	17.1	22.2	22.2	27.9	21.9	22.0	18.2	17.9	19.0	26.1
Price range	15.8 ±7.4	15.7 ±7.2	17.2 ±7.0	23.9 ±6.2	23.9 ±6.2	29.1 ±5.6	23.7 ±6.6	23.4 ±6.2	19.6 ±5.5	19.1 ±5.3	21.0 ±5.6	27.5 ±6.5
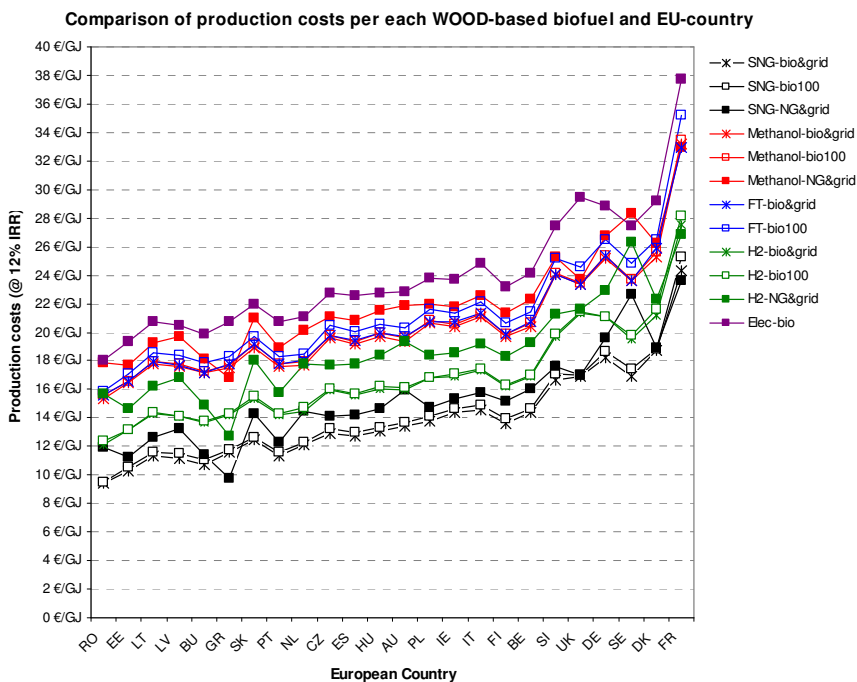
Figure 0.26: *Production costs including 12% IRR for wood-based biofuels. Logistics and distribution costs are not included.*
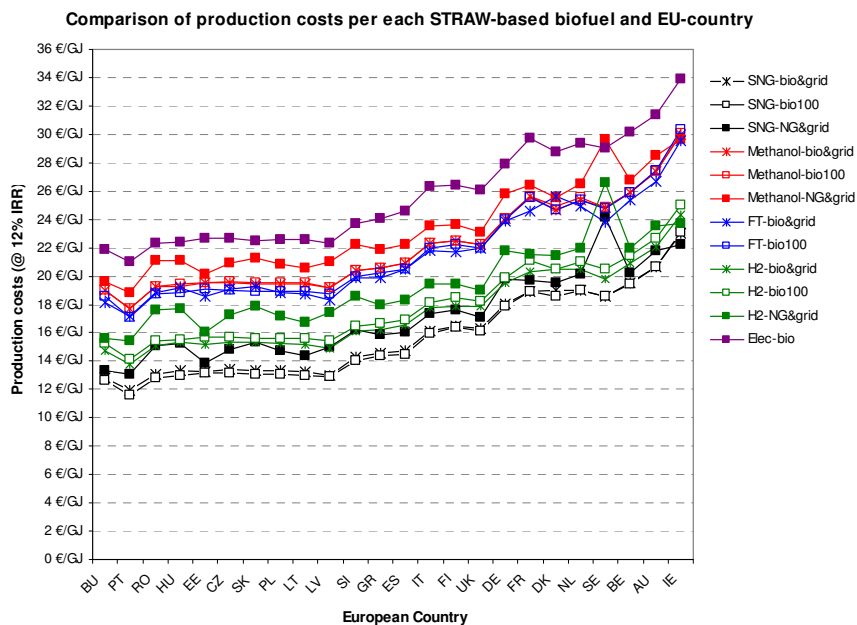
Figure 0.27: *Production costs including 12% IRR for straw-based biofuels. Logistics and distribution costs are not included.*

J.4. *Fuels taxation to equalize biofuel and fossil prices*

Tha aim of this section is to calculate new fossil fuel (TD_{new}) and biofuel taxes (TB) for different fossil fuels replacement (λ) and for any energy sector.

A) Current scenario: Biofuel are not mixed in the energy market

Price fossil diesel (i.e., excluding taxes) = α_{fossil}	(0-6)
Fossil diesel taxation = TD (in %)	(0-7)
Fossil diesel price for consumers (i.e., including taxes) = $\alpha_{fossil} \cdot (1 + TD)$	(0-8)
Fossil Diesel consumption = DC	(0-9)
Actual income from fuel taxation = $CI_{actual} = \alpha_{fossil} \cdot TD \cdot DC$	(0-10)

B) Future scenario: Introduction of biofuels in the energy market

Biofuel replacement = λ	(0-11)
Price fossil diesel (i.e., excl. taxes) = α_{fossil}	(0-6)
Extra taxes for fossil diesel = τ	(0-12)
New fossil diesel taxation = $TD_{new} = TD + \tau$ (in %)	(0-13)
Price fossil diesel for consumers (i.e., incl. taxes)= $\alpha_{fossil} \cdot (1 + TD_{new})$	(0-14)
Fossil Diesel consumption = $(1 - \lambda) \cdot DC$	(0-15)
Biofuel consumption = $\lambda \cdot DC$	(0-16)
Biofuel price (i.e., excl. taxes) = $\alpha_{biofuel}$	(0-17)
Biofuel taxation = TB (in %)	(0-18)
Biofuel price for consumers (i.e., incl. taxes) = $\alpha_{biofuel} \cdot (1 + TD_{new})$	(0-19)
New income from fuel taxation = CI_{new}	(0-20)
$CI_{new} = \alpha_{fossil} \cdot TD_{new} \cdot (1 - \lambda) \cdot DC + \alpha_{biofuel} \cdot TB \cdot \lambda \cdot DC$	(0-21)

In any case, two conditions must be fulfilled: (1st) Income from fuel taxation should remain the same, and (2nd) final end-user biofuel and fossil fuel prices should also be equal. Both conditions are expressed for Eqs.(0-22) and (0-23), which are combined to calculate new extra fossil fuels taxes (TD_{new}) and biofuel taxes (TB), as shown in Eqs.(6-2) and (6-3). As observed, new taxation (TD_{new} or TB) is independent of the global diesel consumption (DC).

$$\alpha_{fossil} \cdot TD \cdot DC = \alpha_{fossil} \cdot TD_{new} \cdot (1 - \lambda) \cdot DC + \alpha_{biofuel} \cdot TB \cdot \lambda \cdot DC \qquad (0\text{-}22)$$

$$\alpha_{fossil} \cdot (1 + TD_{new}) = \alpha_{biofuel} \cdot (1 + TB) \qquad (0\text{-}23)$$

$$TD_{new} = TD + \lambda \cdot \left(\frac{\alpha_{biofuel}}{\alpha_{fossil}} - 1 \right) \qquad (6\text{-}2)$$

$$TB = \frac{\alpha_{fossil} \cdot (1 + TD_{new})}{\alpha_{biofuel}} - 1 \qquad (6\text{-}3)$$

J.5.   Biofuel prices including Ecocosts at country level

Table 0-16: *Final 'integrated; fuel prices per country (i.e., $\alpha_{biofuel,int} = \alpha_{biofuel}(1+TB)+\alpha_{CO2}$) and forest wastes as feedstock.*

Forest wastes	SNG scale: 190 MW			Methanol scale: 1000 MW			Fischer-T 1000 MW		Hydrogen scale: 500 MW			Electricity ~ 100 MW
Country	bio-100	bio-grid	NG-grid	bio-100	bio-grid	NG-grid	bio-100	bio-grid	bio-100	bio-grid	NG-grid	New plant
AU	30.7	30.7	31.0	31.6	31.5	31.8	31.5	31.5	31.7	31.7	32.0	31.4
BE	30.3	30.3	30.5	31.3	31.3	31.4	31.2	31.2	31.3	31.3	31.5	31.0
BU	30.7	30.6	30.7	31.6	31.6	31.6	31.5	31.4	31.6	31.6	31.8	31.3
CZ	29.4	29.4	29.5	30.3	30.3	30.5	30.3	30.2	30.4	30.4	30.6	30.1
DK	33.0	33.0	33.0	34.1	34.1	34.1	34.1	34.0	34.1	34.0	34.1	33.7
EE	25.3	25.3	25.3	26.3	26.3	26.3	26.2	26.1	26.3	26.3	26.3	26.7
FI	29.7	29.7	29.8	30.8	30.8	30.9	30.8	30.7	30.8	30.8	30.9	29.9
FR	33.1	33.0	32.9	34.1	34.1	34.1	34.2	34.0	34.1	34.0	33.9	32.6
DE	34.4	34.3	34.5	35.3	35.3	35.4	35.3	35.2	35.3	35.3	35.5	34.6
GR	28.4	28.4	28.2	29.2	29.2	29.1	29.2	29.1	29.3	29.3	29.2	30.7
HU	30.9	30.9	31.1	32.0	31.9	32.1	31.9	31.8	32.0	32.0	32.2	31.4
IE	31.9	31.9	32.0	32.9	32.9	33.0	32.8	32.7	33.0	32.9	33.0	32.6
IT	33.7	33.7	33.8	34.6	34.6	34.7	34.6	34.5	34.6	34.6	34.8	34.2
LV	25.9	25.9	26.1	26.8	26.8	27.0	26.7	26.7	26.9	26.9	27.1	27.0
LT	25.6	25.6	25.7	26.5	26.5	26.6	26.4	26.4	26.6	26.6	26.8	26.2
NL	31.9	31.9	32.2	32.8	32.8	33.0	32.7	32.7	32.9	32.9	33.2	32.4
PL	28.8	28.8	28.9	29.7	29.7	29.9	29.7	29.6	29.8	29.8	29.9	29.3
PT	31.3	31.3	31.4	32.3	32.3	32.4	32.3	32.2	32.4	32.3	32.5	32.2
RO	30.6	30.6	30.8	31.4	31.4	31.6	31.3	31.3	31.6	31.5	31.9	31.5
SK	32.4	32.3	32.5	33.3	33.2	33.4	33.2	33.1	33.3	33.3	33.6	32.7
SI	29.1	29.1	29.2	30.0	30.0	30.2	30.0	29.9	30.1	30.1	30.2	30.1
ES	28.6	28.5	28.7	29.6	29.5	29.7	29.5	29.4	29.6	29.6	29.8	29.6
SE	33.0	32.9	33.5	34.1	34.1	34.5	34.1	33.9	34.0	34.0	34.6	32.9
UK	41.5	41.5	41.5	42.4	42.4	42.5	42.4	42.3	42.7	42.6	42.7	42.5

Table 0-17: *Final 'integrated; fuel prices per country (i.e., $\alpha_{biofuel,int} = \alpha_{biofuel}(1+TB)+\alpha_{CO2}$) and straw as feedstock.*

straw	SNG scale: 190 MW			Methanol scale: 1000 MW			Fischer-T 1000 MW		Hydrogen scale: 500 MW			Electricity ~100 MW
Country	bio-100	bio-grid	NG-grid	bio-100	bio-grid	NG-grid	bio-100	bio-grid	bio-100	bio-grid	NG-grid	New plant
AU	31.7	31.7	31.8	32.7	32.7	32.8	32.5	32.5	32.6	32.5	32.7	32.5
BE	30.9	30.9	31.0	32.0	32.0	32.0	31.8	31.8	31.9	31.8	31.9	31.7
BU	30.8	30.8	30.9	31.7	31.7	31.8	31.5	31.5	31.7	31.7	31.8	31.4
CZ	29.5	29.5	29.7	30.5	30.5	30.6	30.3	30.3	30.4	30.4	30.6	30.1
DK	32.9	32.9	33.0	33.9	33.8	33.9	33.7	33.8	33.8	33.8	33.9	33.6
EE	25.5	25.5	25.5	26.4	26.4	26.4	26.2	26.1	26.5	26.4	26.4	26.1
FI	30.1	30.1	30.2	31.2	31.2	31.2	31.0	30.9	31.1	31.0	31.1	30.7
FR	32.5	32.5	32.6	33.5	33.5	33.6	33.4	33.3	33.5	33.4	33.5	33.3
DE	34.4	34.4	34.6	35.5	35.5	35.6	35.3	35.3	35.4	35.3	35.5	35.1
GR	28.8	28.8	28.9	29.8	29.8	29.9	29.6	29.5	29.7	29.7	29.8	29.5
HU	30.8	30.9	31.1	31.8	31.8	31.9	31.6	31.6	31.8	31.7	32.0	31.5
IE	33.1	33.0	32.9	34.4	34.4	34.2	34.2	34.1	34.1	34.0	33.9	33.9
IT	33.9	33.9	34.1	34.9	34.9	35.0	34.7	34.7	34.9	34.8	35.0	34.6
LV	26.5	26.5	26.6	27.8	27.8	27.9	27.6	27.5	27.6	27.6	27.7	27.2
LT	26.0	26.1	26.1	27.1	27.1	27.1	26.9	26.8	27.1	27.0	27.1	26.7
NL	32.7	32.7	32.8	33.8	33.8	33.9	33.6	33.6	33.7	33.6	33.8	33.5
PL	28.7	28.8	28.9	29.7	29.7	29.8	29.5	29.5	29.7	29.7	29.9	29.4
PT	31.4	31.4	31.5	32.4	32.4	32.4	32.1	32.1	32.4	32.4	32.5	32.0
RO	30.8	30.8	31.1	31.7	31.7	31.9	31.5	31.5	31.8	31.7	32.0	31.6
SK	32.5	32.5	32.7	33.5	33.5	33.6	33.3	33.3	33.5	33.5	33.7	33.1
SI	29.1	29.1	29.3	30.2	30.2	30.3	30.0	30.0	30.1	30.1	30.3	29.7
ES	28.8	28.9	29.0	29.9	29.9	30.0	29.7	29.7	29.8	29.7	29.9	29.5
SE	33.2	33.2	33.7	34.3	34.3	34.7	34.1	34.0	34.2	34.1	34.7	33.9
UK	41.6	41.6	41.7	42.8	42.8	42.8	42.6	42.5	42.6	42.5	42.6	42.3

Appendix K.   Multidimensional 3E Program

USER INPUT DATA

Biofuel selection

↓Select biofuel from list
SNG

↓Select plant configuration from list
bio100

bio100 : heat and electricity demand of the plant is covered by buring more biomass
bio&grid : heat demand is covered by buring more biomass, elec is taken from grid
NG100 : heat and electricity demand of the plant is covered by buring NG
NG&grid : heat demand is covered by buring more NG, elec is taken from grid

Options
Gaseous (SNG or H2)
Liquid (FT-fuels or MeOH)
Bioelectricity

Biomass parameters

↓Select source from list
Forest residues

Introduce required data   ↓

Biomass amount	kton/yr (dry basis)
Moisture	%
Availability per area	ton/ha
Biomass price	€/ton (dry basis, logistics excluded)

Options
Forest residues
Straw residues
Lignocellulosic energy crops

Transport parameters

Introduce required data   ↓

		Default values	
Truck capacity biomass	payload (ton biomass/truck)	16.8	tn biomass truck
Truck weight biomass	empty truck (tn)	28.0	tn truck
Truck capacity biofuel	payload (ton biofuel/truck)	20.4	tn biofuel truck
Truck weight biofuel	empty truck (tn)	30.0	tn truck
Distribution distance	km	200	km
Distribution cost	€/GJ$_{biofuel}$		

Regional parameters

↓Select country from list
NEW LOCATION

For 'NEW LOCATION'
Introduce required data   ↓

		Default values
		Eurostat
Diesel price	€/GJ	*Eurostat*
Natural gas price	€/GJ	*Eurostat*
Grid electricity price	€/kWh	*Eurostat*
Labour cost - plant operator	€/hr.person	*Eurostat*
Labour cost - plant truck driver	€/hr.person	*Eurostat*
Corporate taxes	%	*Eurostat*
Biomass price	€/GJ	

Options
EU-25 countries
NEW LOCATION

Economic parameters

Introduce required data   ↓

|		Default values
Inflation rate	%	2 %
Bank interest rate	%	5 %
Reference year	-	2010 year

Figure 0.28: *List of the required user data for the 3E Multidimensional program (Multi_model.xls).*

Appendixes

Figure 0.28 [Continuation]: List of the required user data for the 3E program.

FIXED INPUT DATA

Economic parameters

Do not change values ⊠

Parameter		Units
Nr. shifts:	5	shifts per day
Load factor:	8000	h/year

Biomass COLLECTION

Do not change values ⊠

Parameter		Units
Amount N-fertilizer used:	100	kg/ha
Amount P-fertilizer used:	22.4	kg/ha
Amount K-fertilizer used:	39.2	kg/ha
Tractor plough width (wplough):	2.2	m
Tractor speed ($v_{tractor}$):	7.5	km/hr
Tractor lifetime ($l_{tractor}$):	12000	hr
Project lifetime ($l_{project}$):	30	years
Farmer (or tractor) working hours per year ($h_{tractor}$):	2000	hr
Tractor efficiency ($\eta_{tractor}$)	85%	%

Biomass TRANSPORT

Do not change values ⊠

| Parameter		Units
η_t (truck efficiency)	0.4	-
f_r (rolling resistance model)	0.01	-
C_w (drag coefficient)	0.26	-
ρ (fluid density)	1.204	air, 20°C
g (gravity)	9.8	kg/m.s²
v (speed)	60	km/hr
A (frontal area)	4.2	m²
Life-time truck	7	years
t_{max} (max driving hours per day & truck)	18	hr/day.truck
t'_{max} (max driving days per year & truck)	250	day/yr.truck
Max.working hours per year & driver	2000	hr/yr.driver
Lubrication oil cost	0.005	l/km
Tyres replacement cost	0.064	l/km
Fleet maintenance cost	0.096	l/km
Extra personnel per driver	0.8	-
Local taxes	3%	% of FCI
Insurance	1%	% of FCI
Overheads	50	% maintenance
Life-time project	30	years
i_f (inflation (diesel, lub.oil, tyres))	4%	%/year
i_M , i_L (inflation maintenance, labour)	2%	%/year
i_T , i_I (inflation taxes & insurance)	2%	%/year
Buildings	8%	% of fleet
Contingency	2%	% of fleet
Legal expenses	5%	% of fleet
Working capital	15%	TCI
Payback time	3	years
ROI (Return on Investment)	11%	%

Figure 0.29: List of the fixed data for the 3E Multidimensional program (Multi_model.xls).

Appendix L.   Logistics, production costs and final price at optimal biofuels plant scales at European level (Chapter 8)

Logistics costs for the different scenarios presented in Chapter 8 are divided in two items. The first one ("*Log-1*") corresponds to the collection and transport of biomass to a central point of the NUTS-2 region. The second term ("*Log-2*") refers to the transport of biomass from each NUTS-2 region to the biofuel processing plant. Both items are calculated by means of Eqs.(2-3) and (2-1) respectively. The first logistic cost ("*Log-1*") is equal for each scenario as all biomass has to be collected (see Table 0-18). Conversely, the second cost ("*Log-2*") is dependent on each scenario (see Table 0-19), as the driven distance are difference for larger plants (e.g., Fischer-Tropsch and methanol) than the smaller ones (e.g., electricity, hydrogen, SNG). Logistics, production and distribution costs are summed up in general Figure 6.7 and Figure 6.8. Those average costs are calculated based on specific national costs and weighted by the number of plants built in each country.

Table 0-18: First term of the logistics costs ("Log-1") that refers to the collection and transport of biomass to a central location on each NUTS-2 region. Those values are used in in section 8.10.4 to calculate average total costs for each scenario of Chapter 8.

Country	wood	straw
AU	1.5 €/GJ	1.9 €/GJ
BE	1.6 €/GJ	2.7 €/GJ
BU	0.7 €/GJ	0.8 €/GJ
CZ	0.7 €/GJ	1.0 €/GJ
DK	2.0 €/GJ	4.2 €/GJ
EE	1.6 €/GJ	0.6 €/GJ
FI	2.0 €/GJ	1.4 €/GJ
FR	1.7 €/GJ	2.8 €/GJ
DE	1.7 €/GJ	2.7 €/GJ
GR	1.0 €/GJ	1.3 €/GJ
HU	0.8 €/GJ	1.4 €/GJ
IE	0.9 €/GJ	2.2 €/GJ
IT	1.6 €/GJ	2.3 €/GJ
LV	1.7 €/GJ	1.8 €/GJ
LT	1.5 €/GJ	2.2 €/GJ
NL	1.6 €/GJ	3.6 €/GJ
PL	0.9 €/GJ	1.5 €/GJ
PT	0.8 €/GJ	1.0 €/GJ
RO	0.9 €/GJ	1.3 €/GJ
SK	0.7 €/GJ	0.9 €/GJ
SI	1.5 €/GJ	1.5 €/GJ
ES	1.4 €/GJ	2.3 €/GJ
SE	2.2 €/GJ	1.5 €/GJ
UK	1.0 €/GJ	2.5 €/GJ

Table 0-19: *Second term of the logistics costs ("Log-2") that refers to the transport of biomass from a central location to biofuel processing plants. Those values are used in in section 8.10.4 to calculate average total costs for each scenario of Chapter 8.*

Scenario	Logistic cost (Log-2) wood	Logistic cost (Log-2) straw
I-bio100-A1	1.2	1.0
I-bio100-A2	0.9	1.7
I-bio100-A3	0.9	1.0
II-bio100-A1	3.8	3.7
II-bio100-A2	3.6	3.4
II-bio&grid-A1	3.8	3.1
II-bio&grid-A2	3.5	3.1
III-bio100-A3	3.6	3.7
III-bio&gtid-B3	3.5	3.1
IV-bio100-A3	3.2	2.5
IV-bio&grid-B3	2.9	2.6
V-bio100-A3	1.1	1.2
V-bio&grid-B3	1.1	1.1
V-NG&grid-C3	1.0	0.9
VI-bio100-A1	1.1	1.2
VI-bio100-A2	1.1	1.1
VI-bio&grid-B1	1.1	1.1
VI-bio&grid-B2	1.1	1.3
VI-NG&grid-C1	1.2	0.9
VI-NG&grid-C2	1.0	1.1
VII-bio100-A3	1.9	2.0
VII-bio&grid-B3	2.1	2.0
VII-NG&grid-C3	1.9	1.5
VIII- bio100-A3	2.6	3.3
VIII-bio&grid-B3	3.2	3.3
VIII-NG&grid-B3	3.0	2.9

Table 0-14 and Table 0-15 in previous Appendix J.2 summarizes the biofuels production costs for a 12% IRR (Investor's Rate of Return).

Table 0-20: *Final final electricity prices per country (see Chapter 8, section 8.10.4).These values correspond to the application of a new taxation system of section 6.4 and they do not include ecocosts (i.e., $\alpha_{bioelectricity}(1+TB)= \alpha_{coal-electricity}(1+TD_{new})$).*

↓ COUNTRY	I-bio100-A1	I-bio100-A2	I-bio100-A3	II-bio100-A1	II-bio100-A2	II-bio&grid-B1	II-bio&grid-B2	III-bio100-A3	III-bio&grid-B3	IV-bio100-A3	IV-bio&grid-B3	V-bio100-A3	V-bio&grid-B3	V-NG&grid-C3
AT	36,6	39,1	35,1	27,1	27,1	27,1	27,1	27,1	27,1	27,1	27,1	27,1	27,1	27,1
BE	29,9	28,6	29,6	28,3	28,4	28,4	28,4	28,3	28,3	28,4	28,4	28,4	28,4	28,3
BG	21,2	21,1	21,6	22,0	16,9	16,9	16,9	16,9	16,9	16,9	16,9	8,4	8,4	8,4
CZ	26,3	26,2	26,1	27,0	25,7	25,7	25,7	25,7	25,7	25,7	25,7	12,8	12,8	12,8
DK	64,1	62,2	62,2	37,2	57,5	57,5	57,4	57,4	57,4	57,5	57,5	28,7	28,7	28,7
EE	14,9	16,1	16,0	20,2	14,7	14,7	14,7	14,7	14,7	14,7	14,7	7,4	7,4	7,4
FI	22,2	23,0	23,3	38,2	19,0	19,0	19,0	19,0	19,0	19,0	19,0	9,5	9,5	9,5
FR	52,8	53,2	53,6	16,2	17,6	17,6	17,5	17,5	17,5	17,5	17,5	8,8	8,8	8,8
DE	34,7	34,6	34,5	26,3	33,6	33,6	33,6	33,6	33,6	33,6	33,6	16,8	16,8	16,8
GR	21,5	21,4	21,6	19,0	20,5	20,5	20,4	20,4	20,4	20,5	20,5	10,2	10,2	10,2
HU	32,0	32,1	31,7	33,4	33,1	33,1	33,1	33,1	33,1	33,1	33,1	16,6	16,6	16,6
IE	33,5	33,5	33,3	26,9	33,4	33,3	33,4	33,3	33,3	33,3	33,3	16,7	16,7	16,7
IT	33,2	33,2	33,0	32,0	30,9	30,8	30,8	30,8	30,8	30,8	30,8	15,4	15,4	15,4
LV	22,5	22,7	22,6	24,8	16,3	16,3	16,3	16,3	16,3	16,3	16,3	8,2	8,2	8,2
LT	23,4	23,0	23,6	25,7	20,6	20,6	20,6	20,6	20,6	20,6	20,6	10,3	10,3	10,3
NL	30,6	30,8	30,3	22,6	28,9	28,9	28,9	28,9	28,9	28,9	28,9	14,4	14,4	14,5
PL	24,1	24,1	24,1	22,0	23,5	23,5	23,5	23,5	23,5	23,5	23,5	11,8	11,8	11,8
PT	22,9	22,9	22,9	25,8	22,7	22,7	22,7	22,7	22,7	22,7	22,7	11,4	11,4	11,4
RO	28,1	28,2	27,8	24,9	26,2	26,2	26,2	26,2	26,2	26,2	26,2	13,1	13,1	13,1
SK	31,1	31,0	30,7	27,2	31,7	31,7	31,7	31,7	31,7	31,7	31,7	15,8	15,8	15,8
SI	25,2	39,4	39,2	25,6	24,9	24,9	24,9	24,9	24,9	24,9	24,9	12,5	12,5	12,5
ES	28,2	28,1	28,1	29,2	26,7	26,7	26,7	26,7	26,7	26,7	26,7	13,3	13,3	13,4
SE	23,0	23,0	23,4	20,6	16,2	16,2	16,2	16,2	16,2	16,2	16,2	8,1	8,1	8,1
UK	31,4	31,2	31,1	28,8	30,9	30,8	30,9	30,8	30,8	30,8	30,8	15,4	15,4	15,4

↓ COUNTRY	VI-bio100-A1	VI-bio100-A2	VI-bio&grid-B1	VI-bio&grid-B2	VI-NG&grid-C1	VI-NG&grid-C2	VII-bio100-A3	VII-bio&grid-B3	VII-NG&grid-C3	VIII-bio100-A3	VIII-bio&grid-B3	VIII-NG&grid-C3
AT	27,1	27,1	27,1	27,1	27,1	27,1	27,1	27,1	27,1	27,1	27,1	27,1
BE	28,4	28,4	28,4	28,4	28,4	28,4	28,4	28,4	28,4	28,4	28,4	28,4
BG	16,9	16,9	16,9	16,9	16,9	16,9	16,9	16,9	16,9	16,9	16,9	16,9
CZ	25,7	25,7	25,7	25,7	25,7	25,7	25,7	25,7	25,7	25,7	25,7	25,7
DK	57,5	57,5	57,5	57,5	57,5	57,5	57,4	57,5	57,5	57,5	57,5	57,5
EE	14,7	14,7	14,7	14,7	14,7	14,7	14,7	14,7	14,7	14,7	14,7	14,7
FI	19,0	19,1	19,0	19,1	19,0	19,1	19,1	19,1	19,0	19,1	19,1	19,1
FR	17,6	17,6	17,6	17,6	17,6	17,6	17,5	17,5	17,5	17,5	17,6	17,6
DE	33,7	33,7	33,7	33,7	33,7	33,7	33,6	33,6	33,6	33,6	33,6	33,6
GR	20,5	20,5	20,5	20,5	20,5	20,5	20,5	20,5	20,4	20,5	20,5	20,5
HU	33,1	33,1	33,1	33,1	33,1	33,1	33,1	33,1	33,1	33,1	33,1	33,1
IE	33,3	33,4	33,3	33,4	33,3	33,4	33,3	33,3	33,3	33,4	33,4	33,3

COUNTRY ↓	VI-bio100-A1	VI-bio100-A2	VI-bio&grid-B1	VI-bio&grid-B2	VI-NG&grid-C1	VI-NG&grid-C2	VII-bio100-A3	VII-bio&grid-B3	VII-NG&grid-C3	VIII-bio100-A3	VIII-bio&grid-B3	VIII-NG&grid-C3
IT	30,9	30,9	30,9	30,9	30,9	30,9	30,8	30,8	30,8	30,8	30,8	30,9
LV	16,3	16,3	16,3	16,3	16,3	16,3	16,3	16,3	16,3	16,3	16,3	16,3
LT	20,6	20,6	20,6	20,6	20,6	20,6	20,6	20,6	20,6	20,6	20,6	20,6
NL	28,9	28,9	28,9	28,9	28,9	28,9	28,9	28,9	28,9	28,9	28,9	28,9
PL	23,5	23,5	23,5	23,5	23,5	23,5	23,5	23,5	23,5	23,5	23,5	23,5
PT	22,7	22,7	22,7	22,7	22,7	22,7	22,7	22,7	22,7	22,7	22,7	22,7
RO	26,2	26,2	26,2	26,2	26,2	26,2	26,2	26,2	26,2	26,2	26,2	26,2
SK	31,7	31,7	31,7	31,7	31,7	31,7	31,7	31,7	31,7	31,7	31,7	31,7
SI	25,0	24,9	25,0	24,9	25,0	24,9	24,9	24,9	24,9	24,9	24,9	24,9
ES	26,7	26,7	26,7	26,7	26,7	26,7	26,7	26,7	26,7	26,7	26,7	26,7
SE	16,2	16,2	16,2	16,2	16,2	16,2	16,2	16,2	16,2	16,2	16,2	16,2
UK	30,9	30,9	30,9	30,9	30,9	30,9	30,9	30,8	30,9	30,8	30,8	30,8

Table 0-21: *Final final gas prices per country (see Chapter 8, section 8.10.4).These values correspond to the application of a new taxation system of section 6.4 and they do not include ecocosts (i.e., $\alpha_{bioSNG}(1+TB)= \alpha_{fossil\text{-}gas}(1+TD_{new})$).*

COUNTRY ↓	I-bio100-A1	I-bio100-A2	I-bio100-A3	II-bio100-A1	II-bio100-A2	II-bio&grid-B1	II-bio&grid-B2	III-bio100-A3	III-bio&grid-B3	IV-bio100-A3	IV-bio&grid-B3	V-bio100-A3	V-bio&grid-B3	V-NG&grid-C3
AT	10,3	10,3	10,3	10,3	10,3	10,6	10,9	10,3	10,6	10,3	10,3	13,0	12,9	14,6
BE	8,7	8,7	8,7	8,8	8,7	8,7	8,7	8,8	8,7	8,7	8,7	8,7	8,7	8,8
BG	5,5	5,5	5,5	6,4	5,5	6,4	5,5	5,5	5,5	5,5	5,5	9,1	9,0	10,6
CZ	7,6	7,6	7,6	7,6	7,9	7,6	7,6	7,6	7,6	7,6	7,6	8,3	8,4	8,9
DK	7,9	7,9	7,9	8,6	8,6	7,9	8,6	8,6	7,9	7,9	7,9	8,6	8,6	9,0
EE	5,7	5,7	5,7	5,7	5,7	5,7	5,7	5,7	5,7	5,7	5,7	5,7	5,7	5,7
FI	8,2	8,2	8,2	8,7	8,2	8,7	8,2	8,7	8,7	8,2	8,2	11,1	11,5	13,0
FR	8,8	8,8	8,8	8,8	8,8	8,9	8,8	8,8	8,8	8,8	8,8	13,3	13,1	14,4
DE	10,3	10,3	10,3	10,4	10,4	10,4	10,4	10,4	10,3	10,3	10,3	11,2	11,4	11,5
GR	7,8	7,8	7,8	8,2	8,4	7,8	8,7	8,4	8,0	7,8	7,8	9,1	9,1	9,6
HU	8,5	8,5	8,5	8,5	8,5	8,5	8,5	8,5	8,5	8,5	8,5	9,8	9,9	10,4
IE	7,5	7,5	7,5	7,5	7,5	7,5	7,5	7,5	7,5	7,5	7,5	7,5	7,5	7,5
IT	8,1	8,1	8,1	8,1	8,1	8,1	8,1	8,1	8,1	8,1	8,1	8,8	8,8	9,2
LV	8,7	8,7	8,7	9,7	10,7	10,6	8,7	10,7	8,7	8,7	8,7	10,7	10,6	12,2
LT	6,9	6,9	6,9	7,8	7,8	7,8	6,9	7,8	6,9	6,9	6,9	8,5	9,2	9,1
NL	9,3	9,3	9,3	9,3	9,3	9,3	9,3	9,3	9,3	9,3	9,3	9,4	9,3	9,4
PL	7,7	7,7	7,7	7,8	7,8	7,8	7,7	7,8	7,9	7,7	7,7	8,6	8,6	9,0
PT	6,1	6,1	6,1	6,3	6,1	6,1	6,1	6,3	6,1	6,1	6,1	6,4	6,4	6,4
RO	8,8	8,8	8,8	9,0	8,9	9,1	8,8	8,9	9,0	8,8	8,8	10,2	10,3	11,0
SK	8,8	8,8	8,8	9,0	8,8	9,0	8,8	8,8	9,0	8,8	8,8	9,5	9,8	9,9
SI	9,1	9,1	9,1	9,1	11,9	9,1	9,1	11,9	9,1	9,1	9,1	13,0	13,0	15,3

COUNTRY	I-bio100-A1	I-bio100-A2	I-bio100-A3	II-bio100-A1	II-bio100-A2	II-bio&grid-B1	II-bio&grid-B2	III-bio100-A3	III-bio&grid-B3	IV-bio100-A3	IV-bio&grid-B3	V-bio100-A3	V-bio&grid-B3	V-NG&grid-C3
ES	7,8	7,8	7,8	7,9	7,8	7,9	7,8	7,8	7,8	7,8	7,8	8,3	8,4	8,7
SE	19,3	19,3	19,3	19,8	19,6	20,1	19,9	20,2	20,5	19,3	19,3	22,9	22,8	26,0
UK	7,2	7,2	7,2	7,2	7,3	7,2	7,2	7,2	7,2	7,2	7,2	7,4	7,4	7,5

COUNTRY	VI-bio100-A1	VI-bio100-A2	VI-bio&grid-B1	VI-bio&grid-B2	VI-NG&grid-C1	VI-NG&grid-C2	VII-bio100-A3	VII-bio&grid-B3	VII-NG&grid-C3	VIII-bio100-A3	VIII-bio&grid-B3	VIII-NG&grid-C3
AT	12,4	11,8	12,6	11,7	14,0	13,0	10,3	10,3	10,3	10,3	10,3	10,3
BE	8,7	8,7	8,8	8,7	8,8	8,7	8,7	8,7	8,7	8,7	8,7	8,7
BG	7,9	8,1	7,9	8,1	8,8	9,4	5,5	5,5	5,5	5,5	5,5	5,5
CZ	7,9	8,0	7,9	8,1	8,3	8,4	7,6	7,6	7,6	7,6	7,6	7,6
DK	8,3	8,6	8,4	8,6	8,6	9,0	7,9	7,9	7,9	7,9	7,9	7,9
EE	5,7	5,7	5,7	6,2	5,7	6,3	5,7	5,7	5,7	5,7	5,7	5,7
FI	10,9	9,5	10,9	9,7	11,5	10,6	8,2	8,2	8,2	8,2	8,2	8,2
FR	12,1	12,2	12,2	12,3	13,3	13,3	8,8	8,8	8,8	8,8	8,8	8,8
DE	10,7	10,7	10,7	10,7	10,8	10,8	10,3	10,3	10,3	10,3	10,3	10,3
GR	8,3	8,6	8,3	8,6	8,7	8,9	7,8	7,8	7,8	7,8	7,8	7,8
HU	9,2	9,6	9,2	9,8	9,7	10,4	8,5	8,5	8,5	8,5	8,5	8,5
IE	7,5	7,5	7,5	7,5	7,5	7,5	7,5	7,5	7,5	7,5	7,5	7,5
IT	8,6	8,6	8,7	8,6	8,9	8,9	8,1	8,1	8,1	8,1	8,1	8,1
LV	10,7	9,6	10,6	9,5	10,9	9,9	8,7	8,7	8,7	8,7	8,7	8,7
LT	8,1	7,4	8,1	7,4	8,8	7,8	6,9	6,9	6,9	6,9	6,9	6,9
NL	9,4	9,3	9,4	9,4	9,4	9,4	9,3	9,3	9,3	9,3	9,3	9,3
PL	7,9	8,0	8,0	8,0	8,1	8,2	7,7	7,7	7,7	7,7	7,7	7,7
PT	6,2	6,1	6,2	6,4	6,3	6,5	6,1	6,1	6,1	6,1	6,1	6,1
RO	9,6	10,0	9,7	10,1	10,2	10,7	8,8	8,8	8,8	8,8	8,8	8,8
SK	9,3	9,3	9,5	9,4	9,6	9,6	8,8	8,8	8,8	8,8	8,8	8,8
SI	13,0	11,7	12,9	11,6	14,2	13,3	9,1	9,1	9,1	9,1	9,1	9,1
ES	8,1	8,2	8,1	8,2	8,4	8,3	7,8	7,8	7,8	7,8	7,8	7,8
SE	22,2	21,0	22,1	20,8	25,1	23,2	19,3	19,3	19,3	19,3	19,3	19,3
UK	7,3	7,3	7,3	7,3	7,3	7,3	7,2	7,2	7,2	7,2	7,2	7,2

Table 0-22: *Final final diesel prices per country (see Chapter 8, section 8.10.4).These values correspond to the application of a new taxation system of section 6.4 and they do not include ecocosts (i.e., $\alpha_{bioFT\text{-}fuels}(1+TB)= \alpha_{fossil\text{-}diesel}(1+TD_{new})$).*

↓ COUNTRY	I-bio100-A1	I-bio100-A2	I-bio100-A3	II-bio100-A1	II-bio100-A2	II-bio&grid-B1	II-bio&grid-B2	III-bio100-A3	III-bio&grid-B3	IV-bio100-A3	IV-bio&grid-B3	V-bio100-A3	V-bio&grid-B3	V-NG&grid-C3
AT	29,1	29,1	29,1	30,3	31,7	31,7	31,6	31,7	31,6	31,7	31,6	29,1	29,1	29,1
BE	28,6	28,6	28,6	28,6	28,6	28,6	28,6	28,6	28,6	28,6	28,6	28,6	28,6	28,6
BG	29,4	29,4	29,4	31,4	33,8	31,3	33,4	33,7	33,4	33,7	33,4	29,4	29,4	29,4
CZ	27,9	27,9	27,9	29,3	27,9	29,3	29,2	29,3	29,3	29,3	29,3	27,9	27,9	27,9
DK	30,7	30,7	30,7	30,7	30,7	30,7	30,7	30,7	30,7	30,7	30,7	30,7	30,7	30,7
EE	23,6	23,6	23,6	23,6	23,6	23,6	23,6	23,6	23,6	23,6	23,6	23,6	23,6	23,6
FI	27,9	27,9	27,9	30,6	30,7	30,4	30,5	30,7	30,5	30,7	30,5	27,9	27,9	27,9
FR	30,3	30,3	30,3	34,1	34,4	34,5	34,8	34,5	34,8	34,5	34,8	30,3	30,3	30,3
DE	32,3	32,3	32,3	32,8	32,9	33,3	33,1	33,2	34,0	33,2	34,0	32,3	32,3	32,3
GR	27,1	27,1	27,1	27,1	27,1	28,4	27,1	27,1	28,4	27,1	28,4	27,1	27,1	27,1
HU	29,4	29,4	29,4	32,9	33,0	31,0	32,7	32,9	31,0	32,9	31,0	29,4	29,4	29,4
IE	30,2	30,2	30,2	30,2	30,2	30,2	30,2	30,2	30,2	30,2	30,2	30,2	30,2	30,2
IT	32,1	32,1	32,1	33,5	33,3	33,5	33,2	33,6	33,5	33,6	33,5	32,1	32,1	32,1
LV	24,5	24,5	24,5	24,5	24,5	24,5	24,5	24,5	24,5	24,5	24,5	24,5	24,5	24,5
LT	24,2	24,2	24,2	24,2	24,2	24,2	29,2	24,2	29,2	24,2	29,2	24,2	24,2	24,2
NL	30,5	30,5	30,5	30,5	30,5	30,5	30,5	30,5	30,5	30,5	30,5	30,5	30,5	30,5
PL	27,1	27,1	27,1	27,7	27,8	27,7	27,8	28,4	28,3	28,4	28,3	27,1	27,1	27,1
PT	29,9	29,9	29,9	29,9	29,9	29,9	29,9	29,9	29,9	29,9	29,9	29,9	29,9	29,9
RO	29,4	29,4	29,4	31,0	31,0	31,7	31,0	31,0	31,7	31,0	31,7	29,4	29,4	29,4
SK	30,9	30,9	30,9	34,3	34,1	30,9	34,3	34,1	34,3	34,1	34,3	30,9	30,9	30,9
SI	27,2	27,2	27,2	34,6	27,2	34,7	34,2	27,2	34,2	27,2	34,2	27,2	27,2	27,2
ES	27,0	27,0	27,0	27,3	27,6	27,6	27,6	27,6	27,9	27,6	27,9	27,0	27,0	27,0
SE	30,7	30,7	30,7	32,9	32,8	32,8	32,7	32,8	32,7	32,8	32,7	30,7	30,7	30,7
UK	39,5	39,5	39,5	39,8	39,8	39,8	39,9	40,0	40,0	40,0	40,0	39,5	39,5	39,5

↓ COUNTRY	VI-bio100-A1	VI-bio100-A2	VI-bio&grid-B1	VI-bio&grid-B2	VI-NG&grid-C1	VI-NG&grid-C2	VII-bio100-A3	VII-bio&grid-B3	VII-NG&grid-C3	VIII-bio100-A3	VIII-bio&grid-B3	VIII-NG&grid-C3
AT	29,1	29,1	29,1	29,1	29,1	29,1	33,0	33,2	36,3	32,9	32,7	34,7
BE	28,6	28,6	28,6	28,6	28,6	28,6	28,6	28,6	28,6	28,6	28,6	28,6
BG	29,4	29,4	29,4	29,4	29,4	29,4	34,4	33,0	36,0	34,1	34,1	35,0
CZ	27,9	27,9	27,9	27,9	27,9	27,9	29,5	29,5	30,5	29,6	29,6	30,1
DK	30,7	30,7	30,7	30,7	30,7	30,7	32,4	32,4	32,5	30,7	30,7	35,9
EE	23,6	23,6	23,6	23,6	23,6	23,6	23,6	23,6	23,6	23,6	23,6	23,6
FI	27,9	27,9	27,9	27,9	27,9	27,9	30,7	30,6	32,5	30,7	30,7	30,9
FR	30,3	30,3	30,3	30,3	30,3	30,3	35,5	35,9	37,3	34,5	34,5	35,6
DE	32,3	32,3	32,3	32,3	32,3	32,3	33,7	33,6	34,3	33,3	33,3	33,6
GR	27,1	27,1	27,1	27,1	27,1	27,1	27,9	28,6	29,5	27,1	27,1	29,2
HU	29,4	29,4	29,4	29,4	29,4	29,4	33,1	33,2	34,6	33,3	33,5	31,9
IE	30,2	30,2	30,2	30,2	30,2	30,2	30,2	30,2	30,2	30,2	30,2	30,2

↓ COUNTRY	VI-bio100-A1	VI-bio100-A2	VI-bio&grid-B1	VI-bio&grid-B2	VI-NG&grid-C1	VI-NG&grid-C2	VII-bio100-A3	VII-bio&grid-B3	VII-NG&grid-C3	VIII-bio100-A3	VIII-bio&grid-B3	VIII-NG&grid-C3
IT	32,1	32,1	32,1	32,1	32,1	32,1	33,8	33,9	34,7	33,4	33,4	34,0
LV	24,5	24,5	24,5	24,5	24,5	24,5	24,5	24,5	29,0	24,5	24,5	24,5
LT	24,2	24,2	24,2	24,2	24,2	24,2	26,5	26,4	26,6	24,2	29,5	30,0
NL	30,5	30,5	30,5	30,5	30,5	30,5	30,5	30,5	30,5	30,5	30,5	30,5
PL	27,1	27,1	27,1	27,1	27,1	27,1	28,9	28,9	30,2	28,5	28,5	28,8
PT	29,9	29,9	29,9	29,9	29,9	29,9	29,9	30,5	29,9	29,9	29,9	29,9
RO	29,4	29,4	29,4	29,4	29,4	29,4	32,6	33,0	34,9	31,3	31,3	32,3
SK	30,9	30,9	30,9	30,9	30,9	30,9	34,8	36,5	37,2	34,5	34,2	40,2
SI	27,2	27,2	27,2	27,2	27,2	27,2	36,3	31,1	35,8	27,2	35,3	35,5
ES	27,0	27,0	27,0	27,0	27,0	27,0	27,8	27,8	28,4	27,6	27,6	28,3
SE	30,7	30,7	30,7	30,7	30,7	30,7	32,8	34,1	36,4	32,8	32,9	33,2
UK	39,5	39,5	39,5	39,5	39,5	39,5	39,9	39,9	40,2	39,8	40,1	40,2

Table 0-23: Final final electricity prices per country (see Chapter 8, section 8.10.4).These values correspond to the application of a new taxation system of section 6.4 and they include ecocosts (i.e., $\alpha_{bioelectricity}(1+TB)+\alpha_{CO2} = \alpha_{coal-electricity}(1+TD_{new}) +\alpha_{CO2}$).

↓ COUNTRY	I-bio100-A1	I-bio100-A2	I-bio100-A3	II-bio100-A1	II-bio100-A2	II-bio&grid-B1	II-bio&grid-B2	III-bio100-A3	III-bio&grid-B3	IV-bio100-A3	IV-bio&grid-B3	V-bio100-A3	V-bio&grid-B3	V-NG&grid-C3
AT	36,6	39,2	35,1	32,1	32,2	32,1	32,2	32,4	32,4	32,3	32,3	32,3	32,3	32,3
BE	34,4	33,7	34,4	33,4	33,4	33,4	33,5	33,6	33,6	33,6	33,6	33,6	33,6	33,6
BG	23,7	23,6	24,0	27,0	21,9	21,9	21,9	22,2	22,2	22,1	22,1	13,7	13,7	13,7
CZ	30,6	30,6	30,5	32,0	30,7	30,7	30,7	31,0	31,0	30,8	30,9	18,1	18,1	18,1
DK	67,0	65,5	65,2	42,2	62,5	62,6	62,5	62,7	62,7	62,7	62,7	34,0	34,0	34,0
EE	19,9	20,7	20,7	25,2	19,9	19,8	19,9	20,0	20,0	20,0	20,0	12,6	12,6	12,6
FI	26,1	26,7	27,1	43,2	24,2	24,1	24,2	24,3	24,3	24,3	24,3	14,8	14,8	14,8
FR	52,8	53,2	53,6	21,2	22,6	22,6	22,6	22,8	22,8	22,7	22,7	14,0	14,0	14,0
DE	39,3	39,2	39,2	31,3	38,7	38,7	38,7	38,9	38,9	38,8	38,8	22,1	22,1	22,1
GR	26,1	26,0	26,2	24,0	25,6	25,5	25,5	25,7	25,7	25,7	25,7	15,5	15,5	15,5
HU	34,9	35,2	34,8	38,4	38,2	38,2	38,2	38,4	38,4	38,3	38,3	21,8	21,8	21,8
IE	38,7	38,7	38,6	31,9	38,6	38,5	38,6	38,6	38,6	38,6	38,6	22,0	22,0	22,0
IT	33,3	33,2	33,0	37,0	35,9	35,9	35,9	36,1	36,1	36,0	36,0	20,7	20,7	20,7
LV	24,2	24,6	24,5	29,8	21,6	21,4	21,6	21,6	21,6	21,6	21,6	13,4	13,4	13,4
LT	26,2	26,3	26,7	30,7	25,7	25,6	25,7	25,9	25,9	25,8	25,8	15,5	15,5	15,5
NL	35,0	35,3	35,0	27,6	34,0	33,9	34,0	34,2	34,2	34,1	34,1	19,7	19,7	19,7
PL	28,8	28,9	28,9	27,0	28,6	28,5	28,5	28,8	28,8	28,7	28,7	17,0	17,0	17,0
PT	27,7	27,7	27,7	30,8	27,8	27,8	27,8	28,0	28,0	27,9	27,9	16,6	16,6	16,6
RO	28,2	28,3	27,9	29,9	31,3	31,3	31,3	31,5	31,5	31,4	31,4	18,4	18,4	18,4
SK	34,8	34,7	34,4	32,2	36,7	36,7	36,7	37,0	37,0	36,8	36,9	21,1	21,1	21,1
SI	30,2	39,4	39,2	30,6	30,0	29,9	30,0	30,2	30,2	30,1	30,1	17,7	17,7	17,7

ES	31,7	31,6	31,7	34,2	31,8	31,7	31,8	32,0	32,0	31,9	31,9	18,6	18,6	18,6
SE	26,4	26,5	27,0	25,6	21,3	21,2	21,3	21,5	21,5	21,4	21,4	13,4	13,4	13,4
UK	35,7	35,5	35,4	33,8	35,9	35,9	35,9	36,1	36,1	36,0	36,0	20,7	20,7	20,7

COUNTRY	VI-bio100-A1	VI-bio100-A2	VI-bio&grid-B1	VI-bio&grid-B2	VI-NG&grid-C1	VI-NG&grid-C2	VII-bio100-A3	VII-bio&grid-B3	VII-NG&grid-C3	VIII-bio100-A3	VIII-bio&grid-B3	VIII-NG&grid-C3
AT	32,1	32,3	32,1	32,3	32,1	32,3	32,3	32,3	32,3	32,2	32,2	32,3
BE	33,4	33,5	33,4	33,5	33,4	33,5	33,6	33,6	33,6	33,5	33,5	33,6
BG	21,9	21,9	21,9	21,9	21,9	21,9	22,1	22,1	22,1	22,1	22,1	22,1
CZ	30,7	30,7	30,7	30,7	30,7	30,7	30,9	30,9	30,9	30,8	30,8	30,8
DK	62,7	62,6	62,7	62,6	62,7	62,6	62,7	62,7	62,7	62,7	62,7	62,7
EE	19,8	19,9	19,8	19,9	19,8	19,9	20,0	20,0	20,0	19,9	19,9	19,9
FI	24,1	24,2	24,1	24,2	24,1	24,2	24,3	24,3	24,3	24,3	24,3	24,3
FR	22,6	22,6	22,6	22,6	22,6	22,6	22,7	22,7	22,7	22,7	22,7	22,7
DE	38,7	38,7	38,7	38,7	38,7	38,7	38,8	38,8	38,8	38,8	38,8	38,8
GR	25,5	25,6	25,5	25,6	25,5	25,6	25,7	25,7	25,7	25,6	25,6	25,6
HU	38,2	38,2	38,2	38,2	38,2	38,2	38,3	38,3	38,3	38,3	38,3	38,3
IE	38,5	38,6	38,5	38,6	38,5	38,6	38,6	38,6	38,6	38,6	38,6	38,6
IT	35,9	35,9	35,9	35,9	35,9	35,9	36,0	36,0	36,0	36,0	36,0	36,0
LV	21,4	21,6	21,4	21,6	21,4	21,6	21,6	21,6	21,6	21,6	21,6	21,6
LT	25,6	25,7	25,6	25,7	25,6	25,7	25,8	25,8	25,8	25,8	25,8	25,8
NL	33,9	34,0	33,9	34,0	33,9	34,0	34,1	34,1	34,1	34,1	34,1	34,1
PL	28,6	28,6	28,6	28,6	28,6	28,6	28,7	28,7	28,7	28,7	28,7	28,7
PT	27,8	27,8	27,8	27,8	27,8	27,8	28,0	28,0	28,0	27,9	27,9	27,9
RO	31,3	31,4	31,3	31,4	31,3	31,4	31,5	31,5	31,5	31,4	31,4	31,4
SK	36,7	36,7	36,7	36,7	36,7	36,7	36,9	36,9	36,9	36,8	36,8	36,8
SI	30,0	30,0	30,0	30,0	30,0	30,0	30,1	30,1	30,1	30,1	30,1	30,1
ES	31,7	31,8	31,7	31,8	31,7	31,8	31,9	31,9	31,9	31,9	31,9	31,9
SE	21,3	21,3	21,3	21,3	21,3	21,3	21,4	21,4	21,4	21,4	21,4	21,4
UK	35,9	35,9	35,9	35,9	35,9	35,9	36,1	36,0	36,1	36,0	36,0	36,0

Table 0-24: Final final gas prices per country (see Chapter 8, section 8.10.4).These values correspond to the application of a new taxation system of section 6.4 and they include ecocosts (i.e., $\alpha_{bioSNG}(1+TB)+\alpha_{CO2} = \alpha_{fossil\text{-}gas}(1+TD_{new})+\alpha_{CO2}$).

COUNTRY	I-bio100-A1	I-bio100-A2	I-bio100-A3	II-bio100-A1	II-bio100-A2	II-bio&grid-B1	II-bio&grid-B2	III-bio100-A3	III-bio&grid-B3	IV-bio100-A3	IV-bio&grid-B3	V-bio100-A3	V-bio&grid-B3	V-NG&grid-C3
AT	11,5	11,5	11,5	11,5	11,5	11,8	12,1	11,5	11,8	11,5	11,5	14,0	13,9	15,6
BE	9,9	9,9	9,9	10,0	9,9	9,9	9,9	10,0	9,9	9,9	9,9	9,9	9,9	10,0
BG	6,7	6,7	6,7	7,5	6,7	7,5	6,7	6,7	6,7	6,7	6,7	10,1	10,0	11,5
CZ	8,8	8,8	8,8	8,8	9,0	8,8	8,8	8,8	8,8	8,8	8,8	9,5	9,5	10,0
DK	9,1	9,1	9,1	9,8	9,8	9,1	9,8	10,5	9,1	9,1	9,1	10,6	9,8	10,2
EE	6,9	6,9	6,9	6,9	6,9	6,9	6,9	6,9	6,9	6,9	6,9	6,9	6,9	6,9
FI	9,4	9,4	9,4	10,0	9,4	10,0	9,4	10,6	10,0	9,4	9,4	12,8	12,7	14,2

FR	10,0	10,0	10,0	10,0	10,0	10,1	10,0	10,0	10,0	10,0	10,0	14,2	14,1	15,4
DE	11,5	11,5	11,5	11,6	11,6	11,6	11,5	11,6	11,5	11,5	11,5	12,3	12,5	12,7
GR	9,0	9,0	9,0	9,4	9,6	9,0	9,8	9,7	9,1	9,0	9,0	10,4	10,2	10,8
HU	9,7	9,7	9,7	9,7	9,7	9,7	9,7	9,7	9,7	9,7	9,7	11,1	11,0	11,5
IE	8,7	8,7	8,7	8,7	8,7	8,7	8,7	8,7	8,7	8,7	8,7	8,7	8,7	8,7
IT	9,3	9,3	9,3	9,3	9,3	9,3	9,3	9,3	9,3	9,3	9,3	10,0	10,0	10,4
LV	9,9	9,9	9,9	10,8	11,7	11,6	9,9	12,3	9,9	9,9	9,9	12,3	11,6	13,2
LT	8,1	8,1	8,1	8,9	8,9	8,9	8,1	9,1	8,1	8,1	8,1	9,9	10,3	10,2
NL	10,5	10,5	10,5	10,5	10,5	10,5	10,5	10,5	10,5	10,5	10,5	10,6	10,5	10,6
PL	8,9	8,9	8,9	9,0	9,0	9,0	8,9	9,0	9,0	8,9	8,9	9,7	9,8	10,1
PT	7,3	7,3	7,3	7,5	7,3	7,3	7,3	7,7	7,3	7,3	7,3	7,8	7,6	7,5
RO	10,0	10,0	10,0	10,2	10,1	10,3	10,0	10,2	10,2	10,0	10,0	11,4	11,4	12,1
SK	10,0	10,0	10,0	10,1	10,0	10,2	10,0	10,0	10,2	10,0	10,0	10,7	10,9	11,0
SI	10,3	10,3	10,3	10,3	12,9	10,3	10,3	13,1	10,3	10,3	10,3	14,1	13,9	16,2
ES	9,0	9,0	9,0	9,1	9,0	9,1	9,0	9,1	9,0	9,0	9,0	9,5	9,6	9,9
SE	20,5	20,5	20,5	21,0	20,8	21,3	21,1	21,8	21,6	20,5	20,5	24,5	23,9	27,1
UK	8,4	8,4	8,4	8,4	8,4	8,4	8,4	8,4	8,4	8,4	8,4	8,5	8,5	8,6

COUNTRY	VI-bio100-A1	VI-bio100-A2	VI-bio&grid-B1	VI-bio&grid-B2	VI-NG&grid-C1	VI-NG&grid-C2	VII-bio100-A3	VII-bio&grid-B3	VII-NG&grid-C3	VIII-bio100-A3	VIII-bio&grid-B3	VIII-NG&grid-C3
AT	13,5	12,8	13,6	12,8	15,0	14,0	11,5	11,5	11,5	11,5	11,5	11,5
BE	9,9	9,9	10,0	9,9	10,0	9,9	9,9	9,9	9,9	9,9	9,9	9,9
BG	8,9	9,1	8,8	9,1	9,8	10,4	6,7	6,7	6,7	6,7	6,7	6,7
CZ	9,2	9,2	9,1	9,2	9,5	9,5	8,8	8,8	8,8	8,8	8,8	8,8
DK	10,3	9,8	9,5	9,8	9,8	10,2	9,1	9,1	9,1	9,1	9,1	9,1
EE	6,9	6,9	6,9	7,6	6,9	7,6	6,9	6,9	6,9	6,9	6,9	6,9
FI	12,7	10,7	12,1	10,9	12,7	11,8	9,4	9,4	9,4	9,4	9,4	9,4
FR	13,1	13,2	13,2	13,3	14,3	14,3	10,0	10,0	10,0	10,0	10,0	10,0
DE	11,8	11,8	11,8	11,8	12,0	12,0	11,5	11,5	11,5	11,5	11,5	11,5
GR	9,6	9,8	9,5	9,8	9,9	10,1	9,0	9,0	9,0	9,0	9,0	9,0
HU	10,4	10,7	10,3	10,9	10,8	11,5	9,7	9,7	9,7	9,7	9,7	9,7
IE	8,7	8,7	8,7	8,7	8,7	8,7	8,7	8,7	8,7	8,7	8,7	8,7
IT	9,8	9,7	9,8	9,8	10,1	10,1	9,3	9,3	9,3	9,3	9,3	9,3
LV	12,3	10,6	11,6	10,6	12,0	11,0	9,9	9,9	9,9	9,9	9,9	9,9
LT	9,5	8,5	9,3	8,5	10,0	8,9	8,1	8,1	8,1	8,1	8,1	8,1
NL	10,6	10,5	10,6	10,6	10,6	10,6	10,5	10,5	10,5	10,5	10,5	10,5
PL	9,1	9,2	9,1	9,2	9,3	9,4	8,9	8,9	8,9	8,9	8,9	8,9
PT	7,6	7,3	7,4	7,6	7,4	7,7	7,3	7,3	7,3	7,3	7,3	7,3
RO	10,9	11,1	10,8	11,2	11,4	11,9	10,0	10,0	10,0	10,0	10,0	10,0
SK	10,5	10,4	10,6	10,5	10,7	10,7	10,0	10,0	10,0	10,0	10,0	10,0
SI	14,1	12,7	13,8	12,6	15,1	14,2	10,3	10,3	10,3	10,3	10,3	10,3
ES	9,3	9,3	9,3	9,3	9,6	9,5	9,0	9,0	9,0	9,0	9,0	9,0
SE	23,8	22,1	23,2	22,0	26,2	24,4	20,5	20,5	20,5	20,5	20,5	20,5
UK	8,5	8,5	8,5	8,5	8,5	8,5	8,4	8,4	8,4	8,4	8,4	8,4

Table 0-25: *Final final diesel prices per country (see Chapter 8, section 8.10.4).These values correspond to the application of a new taxation system of section 6.4 and they include ecocosts (i.e., $\alpha_{bioFT\text{-}fuels}(1+TB)+\alpha_{CO2} = \alpha_{fossil\text{-}diesel}(1+TD_{new}) +\alpha_{CO2}$).*

COUNTRY	I-bio100-A1	I-bio100-A2	I-bio100-A3	II-bio100-A1	II-bio100-A2	II-bio&grid-B1	II-bio&grid-B2	III-bio100-A3	III-bio&grid-B3	IV-bio100-A3	IV-bio&grid-B3	V-bio100-A3	V-bio&grid-B3	V-NG&grid-C3
AT	30,4	30,4	30,4	31,5	32,8	32,8	32,7	32,8	32,7	32,8	32,7	30,4	30,4	30,4
BE	29,8	29,8	29,8	29,8	29,8	29,8	29,8	29,8	29,8	29,8	29,8	29,8	29,8	29,8
BG	30,6	30,6	30,6	32,6	34,9	32,5	34,5	34,8	34,5	34,8	34,5	30,6	30,6	30,6
CZ	29,1	29,1	29,1	30,6	29,1	30,5	30,5	30,6	30,5	30,6	30,5	29,1	29,1	29,1
DK	31,9	31,9	31,9	31,9	31,9	31,9	31,9	31,9	31,9	31,9	31,9	31,9	31,9	31,9
EE	24,8	24,8	24,8	24,8	24,8	24,8	24,8	24,8	24,8	24,8	24,8	24,8	24,8	24,8
FI	29,1	29,1	29,1	31,9	32,0	31,8	31,8	32,0	31,8	32,0	31,8	29,1	29,1	29,1
FR	31,5	31,5	31,5	35,2	35,5	35,6	35,9	35,6	35,9	35,6	35,9	31,5	31,5	31,5
DE	33,5	33,5	33,5	34,0	34,1	34,5	34,4	34,5	35,2	34,5	35,2	33,5	33,5	33,5
GR	28,3	28,3	28,3	28,3	28,3	29,6	28,3	28,3	29,6	28,3	29,6	28,3	28,3	28,3
HU	30,6	30,6	30,6	34,1	34,2	32,2	33,8	34,1	32,2	34,1	32,2	30,6	30,6	30,6
IE	31,4	31,4	31,4	31,4	31,4	31,4	31,4	31,4	31,4	31,4	31,4	31,4	31,4	31,4
IT	33,3	33,3	33,3	34,7	34,5	34,7	34,4	34,7	34,7	34,7	34,7	33,3	33,3	33,3
LV	25,7	25,7	25,7	25,7	25,7	25,7	25,7	25,7	25,7	25,7	25,7	25,7	25,7	25,7
LT	25,5	25,5	25,5	25,5	25,5	25,5	30,3	25,5	30,3	25,5	30,3	25,5	25,5	25,5
NL	31,8	31,8	31,8	31,8	31,8	31,8	31,8	31,8	31,8	31,8	31,8	31,8	31,8	31,8
PL	28,4	28,4	28,4	28,9	29,1	28,9	29,0	29,6	29,5	29,6	29,5	28,4	28,4	28,4
PT	31,1	31,1	31,1	31,1	31,1	31,1	31,1	31,1	31,1	31,1	31,1	31,1	31,1	31,1
RO	30,6	30,6	30,6	32,1	32,1	32,8	32,1	32,1	32,8	32,1	32,8	30,6	30,6	30,6
SK	32,2	32,2	32,2	35,4	35,2	32,2	35,4	35,2	35,4	35,2	35,4	32,2	32,2	32,2
SI	28,5	28,5	28,5	35,5	28,5	35,7	35,1	28,5	35,1	28,5	35,1	28,5	28,5	28,5
ES	28,2	28,2	28,2	28,5	28,8	28,8	28,8	28,8	29,1	28,8	29,1	28,2	28,2	28,2
SE	31,9	31,9	31,9	34,1	34,0	34,0	33,9	34,0	33,9	34,0	33,9	31,9	31,9	31,9
UK	40,8	40,8	40,8	41,0	41,0	41,0	41,2	41,3	41,2	41,3	41,2	40,8	40,8	40,8

COUNTRY	VI-bio100-A1	VI-bio100-A2	VI-bio&grid-B1	VI-bio&grid-B2	VI-NG&grid-C1	VI-NG&grid-C2	VII-bio100-A3	VII-bio&grid-B3	VII-NG&grid-C3	VIII-bio100-A3	VIII-bio&grid-B3	VIII-NG&grid-C3
AT	30,4	30,4	30,4	30,4	30,4	30,4	34,0	34,2	37,3	34,1	34,0	36,0
BE	29,8	29,8	29,8	29,8	29,8	29,8	29,8	29,8	29,8	29,8	29,8	29,8
BG	30,6	30,6	30,6	30,6	30,6	30,6	35,2	34,0	36,9	35,4	35,4	36,3
CZ	29,1	29,1	29,1	29,1	29,1	29,1	30,6	30,7	31,7	30,9	30,9	31,4
DK	31,9	31,9	31,9	31,9	31,9	31,9	33,6	33,6	33,7	31,9	31,9	37,2
EE	24,8	24,8	24,8	24,8	24,8	24,8	24,8	24,8	24,8	24,8	24,8	24,8
FI	29,1	29,1	29,1	29,1	29,1	29,1	32,0	31,9	33,8	32,1	32,1	32,3
FR	31,5	31,5	31,5	31,5	31,5	31,5	36,6	37,0	38,3	35,6	35,7	36,8
DE	33,5	33,5	33,5	33,5	33,5	33,5	34,9	34,8	35,4	34,5	34,5	34,9
GR	28,3	28,3	28,3	28,3	28,3	28,3	29,1	29,8	30,7	28,3	28,3	30,5
HU	30,6	30,6	30,6	30,6	30,6	30,6	34,1	34,1	35,5	34,6	34,8	33,1
IE	31,4	31,4	31,4	31,4	31,4	31,4	31,4	31,4	31,4	31,4	31,4	31,4

↓ COUNTRY	VI-bio100-A1	VI-bio100-A2	VI-bio&grid-B1	VI-bio&grid-B2	VI-NG&grid-C1	VI-NG&grid-C2	VII-bio100-A3	VII-bio&grid-B3	VII-NG&grid-C3	VIII-bio100-A3	VIII-bio&grid-B3	VIII-NG&grid-C3
IT	33,3	33,3	33,3	33,3	33,3	33,3	34,9	35,1	35,9	34,6	34,6	35,2
LV	25,7	25,7	25,7	25,7	25,7	25,7	25,7	25,7	30,1	25,7	25,7	25,7
LT	25,5	25,5	25,5	25,5	25,5	25,5	27,6	27,5	27,8	25,5	30,6	31,2
NL	31,8	31,8	31,8	31,8	31,8	31,8	31,8	31,8	31,8	31,8	31,8	31,8
PL	28,4	28,4	28,4	28,4	28,4	28,4	30,1	30,0	31,3	29,7	29,7	30,0
PT	31,1	31,1	31,1	31,1	31,1	31,1	31,1	31,8	31,1	31,1	31,1	31,1
RO	30,6	30,6	30,6	30,6	30,6	30,6	33,6	34,0	35,9	32,4	32,4	33,5
SK	32,2	32,2	32,2	32,2	32,2	32,2	35,9	37,4	38,3	35,7	35,4	41,5
SI	28,5	28,5	28,5	28,5	28,5	28,5	37,1	32,1	36,7	28,5	36,3	36,6
ES	28,2	28,2	28,2	28,2	28,2	28,2	29,0	29,0	29,6	28,9	28,8	29,5
SE	31,9	31,9	31,9	31,9	31,9	31,9	34,0	35,3	37,6	34,1	34,1	34,5
UK	40,8	40,8	40,8	40,8	40,8	40,8	41,2	41,1	41,4	41,1	41,3	41,4

Acknowledgements

During my last four years, I had the opportunity to work in close cooperation with a great number of people whose contribution to the research and the writing phase of the thesis deserved special mention. It is a pleasure to convey my acknowledgment to all of them in this section.

In the first place, I would like to show my gratitude to my promotor Prof.dr. H.J. Veringa whose experience, guidance and support enabled me to deepen my understanding of the subject. I especially want to thank his critical remarks and interesting suggestions during the last years of the project, as well as the long discussions about the future of bioenergy. The knowledge I gained from him will surely help me boost my career. I also would like to thank my daily supervisor Dr.ir. K.J. Ptasinski who made possible getting this PhD position at TU/e. I am also grateful for his guidance through discussions during the course of this project, and his suggestions for improving my articles and presentations from the early stage of the research. His extensive knowledge about Thermodynamics, the exergy concept and multidimensional models also helped me understand the importance of having proper evaluation methods, which I hope I have successfully applied in this thesis.

I owe my sincere gratitude to the Cartesius Institute in Leeuwarden for their financial support. I would like to make a special reference to Dr.ir. Y. Krozer and Hilde van Meerendonk for organizing appealing workshops with researchers from other universities and industries, as well as making our stay in Friesland more friendly and enjoyable. Many thanks Hilde for our cheerful conversations about any topic. I also address my acknowledgement to ECN (Energy Research Center of the Netherlands) for inviting me at inspiring workshops about biomass gasification and torrefaction, and for making me aware of the challenges of industrial facilities.

I would like to acknowledge ir. J.G. Wijers for his interesting point of view about biofuels and its applications in the energy market, as well as his willingness to take part in the committee of Master students. My appreciation also goes to Dr.ir. M. Prins whose extensive knowledge about Aspen Plus truly helped me troubleshoot the endless list of errors in my early simulations.

Many thanks to Dr. M. Jurascik with whom I shared the first two years of my doctorate. He made available his support in a number of ways, especially during the enduring phase of modeling biofuels chains and building massive excels for efficiency calculations. I also want to thank him for our humorous chats during the long trips to Friesland and conferences.

In my daily work, I was pleased to share most of my time with my workmates Michiel and Carlos, whom I am in debt for the great atmosphere in our office, as well as for sharing the experience of changing office three times. Thanks Carlos for your funny jokes and good sense of humour, and for your valuable comments on my reports and thesis. Many thanks to Michiel for our hilarious conversations about any matter, as well as for your tips and support during the frenetic phase of looking for a job. I had

great fun learning more about the Dutch culture and your jokes to other members of the SCR group! I also appreciate your commitment to read this thesis and your very constructive comments. During last years I also had the opportunity to meet other people at SCR, and I owe my gratitude to all of them for making my stay more enjoyable. I want to send my special regards to the 'mafia ladies' of the department (Christine, Lida, Dulce, Fernanda, Ivana, Maria, Paola, Qi and Nopi) with whom I share delicious meals and funny stories.

I would like to acknowledge Denise for arranging all administrative matters from the beginning until the end of the project and always guiding me with all regulations. The several nice New Year parties and summer excursions with the SCR group are truly memorable.

During the last years, I had the opportunity to coach few master students in their graduation projects (Kubra, Esayas, Cecilia, Laura, Fernanda and Mesele). I am much indebted for your valuable commitment and quality reports, which are reflected in this thesis.

Finally, I owe my greatest gratitude to my family for their tender support during this doctorate and for always supporting me through the critical decisions. My most affectionate mention goes to my brother Jaume who is my best inspiration. I would like to dedicate my dearest words to my uncle who could not see the end result.

Lastly, I offer my regards and blessings to all of those who were not mentioned here but supported me in any respect during the completion of the project and my stay in the Netherlands.

Many thanks to you all
Anna, 1st March 2011

About the Author

Anna Sues was born in Barcelona on 3rd July, 1979. She finished secondary education at '*Institució La Miranda*' (Sant Just Desvern, Barcelona) in 1998. After graduating high school, she decided to pursue Chemical Engineering at the *University of Barcelona*, where she obtained her master degree in 2003. Her graduation project was performed at *Chalmers University of Technology* (Göteborg, Sweden) under supervision of Prof.dr.ir. Mohammad Taherzadeh. The topic of the research was '*Optimization of Ethanol and Biomass Production from Wood Hydrolyzates by Mucor indicus (rouxii)''*, which was later published in the specialized Journal of FEMS Yeast Research. After her master defense, she worked in several chemical and food companies such as Hempel A/S, Akzo Nobel and Grupo Damm. During the first year of industrial experience, she also performed a Postgraduate Master program at the *Insititut Català de Tecnologia* (Barcelona) in the field of '*Operations and Production Management in Chemical and Pharmaceutical Industries*'. In 2006, she decided to further her interest in Thermodynamics and renewable energy and applied for a PhD position at the Environmental Technology group, a subgroup of the Chemical Reaction Engineering department of the Eindhoven University of Technology. The research project has been carried out under supervision of Prof.dr. H.J. Veringa and Dr.ir. K.J. Ptasinski, and focus on the modeling of bioenergy production from lignocellulosic sources to reduce the consumption of fossil fuels.

Communication with the author can be done via email: anna.sues@hotmail.com